An Engineering Geological Investigation of Waikawa Bay and Whatamango Bay, Marlborough Sounds, New Zealand.

A thesis
submitted in partial fulfillment
of the requirements for the Degree
of
Master of Science in Engineering Geology
at the
University of Canterbury
by
Sonia T. McManus

University of Canterbury
1996

FRONTISPIECE

An aerial view looking south over the Marlborough Sounds.

ABSTRACT

The Waikawa area is a rapidly expanding urban centre within the Marlborough Sounds and as such there is an increasing need for a better understanding of the engineering geological constraints for urban development. The objectives of this study are twofold; firstly to assess the structural characteristics of the area and the nature and extent of the Waikawa Bay Fault, and secondly to complete an engineering geological and hazard assessment in order to determine the development constraints to future urbanisation. The field area extends from Waikawa township to Green Bay and includes The Snout in Picton, Karaka Point and Whatamango Bay. The geology is dominantly Pelorus Group greywacke and weakly foliated Marlborough Schist, which are in faulted contact along the Waikawa Bay Fault.

Structural mapping in the field area identified three distinct deformation phases following the completion of metamorphism. Additionally the area is dominated by a series of reverse thrust faults which generally dip shallowly (approx. 30°) to the west in Picton and steeply (60°-80°) to the east from Waikawa to Green Bay. The Waikawa Bay Fault, an easterly dipping reverse thrust with a dextral strike-slip component, represents a significant structural boundary between the Picton Domain and the eastern rocks of the field area, and is thought to overthrust the Picton Thrust system creating a fault wedge in the Picton area. The Waikawa Bay Fault is also thought to be related to the Green Bay Fault, and tentative correlations are made with the inferred presence of the Waipapa Terrane rocks which may be in contact with Pelorus Group rocks along the Waikawa Bay Fault. Reassessment of the geomorphology of the field area indicates that the age of last rupture of the Waikawa Bay Fault took place between 18-12ka BP, the age estimate being determined from the relative ages of alluvial terraces (W_0-W_5) in Waikawa Stream, the Rimu Terrace alluvial fan and the Maori Cemetery debris fan complex.

Engineering geological investigations involved the use of field mapping, aerial photograph interpretation, hydrological monitoring and limited laboratory testing to determine the geotechnical properties and extent of the bedrock and surficial units in the field area. The principal active geomorphic processes are assessed and the data is presented on an engineering geology map at 1:5,000. The data obtained confirmed that the strength of rock material decreases with increasing weathering grade, and that schist at a maximum of 46MPa is noticeably weaker than the maximum strength for greywacke of 71MPa. Problems were encountered with grainsize determinations for regolith and colluvial material due to the presence of clay aggregates which cannot be resolved using the present methods. The principal clay minerals identified

using XRD methods are kaolinite and illite together with the presence of an illite-chlorite interstratified clay, while imogolite was identified in the red weathered regolith.

The hazard assessment quantifies the hazard potential of the landscape modification processes identified and is also presented in map form as a hazard assessment map at 1:5,000. The processes of slope failure, flooding, stream bank erosion and debris deposition are represented on the map using a colouring system for degree of hazard and a lettering system identifying the principal processes in each area. Hazards are quantified on the basis of their magnitude, their frequency, and the area affected by the process. The final stage in the hazard assessment was the production of a development constraints map, also at 1:5,000, which delineates the degree of geotechnical limitations and the type of investigation required for future urban development. The development constraint map is designed to be used to assess the expected conditions at a site, but does not replace extensive individual site investigations for subdivision planning or for housing construction.

ACKNOWLEDGMENTS

This thesis was completed only with the assistance and generous time of many individuals all of whom deserve my sincere thanks.

My supervisors, David Bell and Joclyn Campbell, who lent support during field work, thinking, write up and to thesis related and un-related incidents. Their help and guidance will always be considered a godsend in the completion of this thesis. Dr. David Nobes also provided valuable advice, particularly in regard to the geophysical aspect and his enthusiasm is much appreciated.

Thanks also to other members of the academic staff, Dr. Doug Lewis, Dr. Jarg Pettinga and Professor Stephen Weaver for their discussion and advice regarding a range of topics from chapter layout to tracking down elusive clay minerals.

This thesis could not have been completed, or in fact started, without the help of the technical staff in the Department of Geological Sciences at the University of Canterbury. Thanks to Rob Spires for thin sections, Steven Brown for XRD analysis of samples, Kerry Swanson for advice regarding clay minerals and SEM and Craig Jones and Neil for their expertise on the SEM. Special thanks goes to Cathy Knight who helped slave over the ring shear machine, set up the Atterberg equipment, field equipment and without whom all the grain size data would be completely wrong (thanks for those last minute pipette analyses - hope the OOS improves soon).

Many of the staff at the Marlborough District Council in Blenheim also enlisted time and effort crucial in the production of this thesis. Thanks to Fraser McRay for getting the whole thing up and running, Neil Morris for his unparalleled enthusiasm and support and Val Wadsworth for all the time he spent in the Graham River. Thanks also to Jen and Diane who made sure the photocopier was working and who kept an eye on me in the filling room in case I got squashed.

Throughout the course of this project several people provided help and company in the field. Thanks to Mark Armstrong who aided with setting out 80m TEM loops in gorse swamped paddocks where even David Nobes feared to tread. Thanks to Tod 'Peter Blake' Waight who shared with me his superb sailing skills even in the monster waves of Queen Charlotte Sound. And thanks to Jane Edgar (Ms Scale) who, after a very wet week in the Sounds, became my expert tunnel gully and batter collapse 'sniffer outer'.

So many friends lent much needed support, both personally and professionally, during this thesis and all deserve a box of roses (Whoops sorry - I'm broke). Thanks again to Jane who kept me entertained during hours of dull and boring (I mean, stimulating and rewarding) lab work and together with Fran Muckle and Jonny McNee, got me through some small crises near the end. Thanks guys for

holding the proverbial hand because I couldn't have done it without you. Thanks to my colleges in Room 213 who so thoughtfully vacated the premises for a conference during my final weeks of write up. Sorry about the grumpy moods. And thanks to Goosie - although you were miles away this time the fax machine and the telephone kept you nearby - you're a groovy friend even if you are a plonker!

Mum and Dad, of course, who endured me moving home for the final months and didn't complain about the bizarre hours I kept. Thanks also to the cat for absolutely nothing, but at least you were there.

The people of the Marlborough Sounds were wonderful. Thank you for your friendship and company particularly during all those weeks spent in my wee tent. The dinner offers, morning and afternoon teas, and roadside chats make the Marlborough Sounds one of my favourite places on earth - pity about the rocks though... Special thanks to Kerry and John at the Waikawa Bay Holiday Park who unfailingly gave me a dry place to stay when I got flooded out of my tent.

Finally, thanks a million to Fudge, without whom none of this would have been possible.

☺☺☺

TABLE OF CONTENTS

LIST OF FIGURES

LIST OF TABLES

CHAPTER 1 INTRODUCTION

1.1. BACKGROUND

1.1.1. Engineering Geology

The south eastern Marlborough Sounds have been the focus of considerable attention regarding urban expansion in the region. Picton, a township of approximately 3,500 people is the centre of development and is located near the head of Queen Charlotte Sound (Figure 1.1.). Picton is surrounded by steep and potentially unstable hill slopes, typical of the south eastern Marlborough Sounds, and consequently expansion has moved north east towards Waikawa. Additional expansion has also tentatively been suggested for the western slopes of Whatamango Bay (Figure 1.1.).

At present the catchments of Whatamango Bay are vegetated by both native beech forest and exotic pine forest. The pine forests are near maturity and will be progressively milled. However, there are no plans to replant the area and residential subdivision is thought to be the intended future development for this land.

Under the requirements of both the Resource Management Act (1991) and the Building Act (1991) (Appendix E2 and E3), local and regional authorities are bound to record any areas of actual or potential natural hazard. The types of natural hazard include inundation, land instability, erosion and seismic hazards, as defined by the Resource Management Act (1991) (Appendix E2). This thesis is, therefore, a continuation of a series of reports aimed at documenting unstable areas in the Marlborough Sounds for future reference. Previous reports were centered on the Havelock area (Kingsbury, 1987), Picton, Waikawa and Shakespere Bay (Horrey, 1989), and a detailed study of Waikawa Bay (McManus, 1994).

1.1.2. Structural Geology

The geology and inter-relationships of bedrock units is related to the engineering geology of the Waikawa-Whatamango Bay areas; schistose slopes being potentially more unstable than those composed of unfoliated greywacke. Generally, structural relationships of bedrock units, schists and greywacke-argillites, are poorly understood in the Marlborough Sounds. Previous studies in the Picton and Waikawa area have established the presence of a low angle thrust system (Nicol, 1988; Horrey, 1989; McManus, 1994). In Picton, intraformational folding of the earlier thrust faults and related structures has produced a basin and dome fold pattern exposing Oligocene sediments in erosional windows (Nicol, 1988). The Waikawa Bay Fault, which has been interpreted as a steeply dipping or vertical oblique thrust fault with the eastern side upthrown (McManus, 1994), is an anomalous feature in the overall

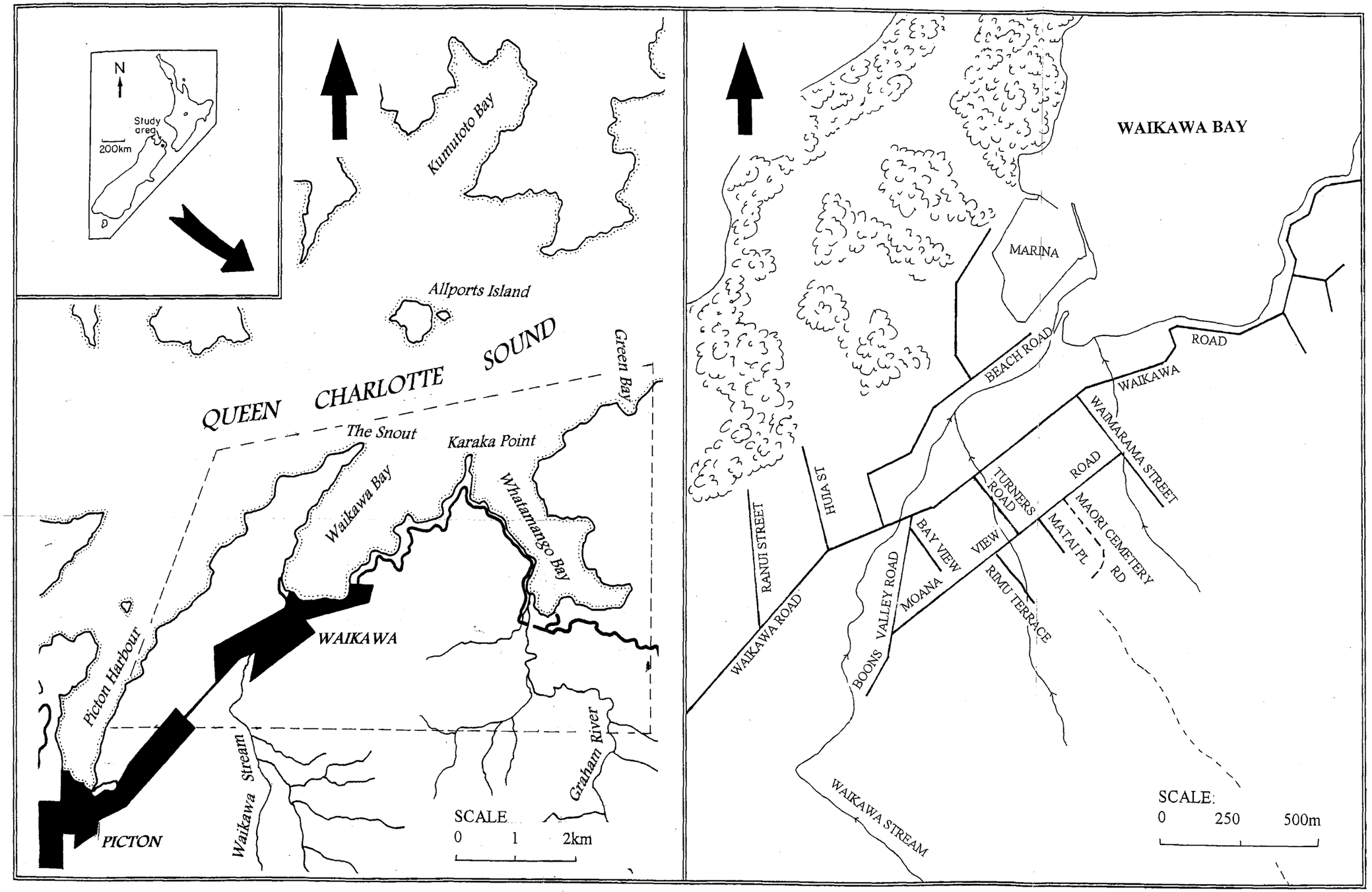

FIGURE 1.1.: Location map showing the position of the field area within the Marlborough Sounds and the principal landmarks of the study area

west to east thrust regime proposed by Nicol (1988). This study investigates the Waikawa Bay Fault and related structures to determine the nature and extent of the fault zone to the north and south of Waikawa and estimate the age of last rupture along the fault. Additionally, the regional implications of the Waikawa Bay Fault in relation to Cenozoic tectonism in New Zealand are discussed, particularly in relation to the possibility of identifying Waipapa Terrane rocks in the field area proposed by Mortimer (1993).

1.2. THESIS OBJECTIVES

The principal objectives of this thesis are two fold; one influenced by the engineering geological characteristics of the Whatamango Bay area and the other concerned with the structural geology and geomorphology of the field area in relation to the Waikawa Bay Fault. The objectives are outlined below.

a) The identification of geological hazards affecting the field area including landslides and potentially unstable slopes, erosion, and flooding. As a part of the geological hazard evaluation, the geotechnical properties of selected surficial units have been determined. Finally, land use planning maps are produced using the information obtained from the engineering geological and hazard evaluations.

b) Structural geological studies of the field area divided into The Snout, Karaka Point and Green Bay Domains and the assessment of the geomorphic evolution of Waikawa with the principal objective being an assessment of the extent, nature and activity of the Waikawa Bay Fault. Additionally, mapping of accompanying structures such as shear zones, folds and faults has allowed further assessment of the overall structure of the field area.

1.3 STUDY AREA

1.3.1. Location and Description

The study area encompasses approximately 30 km^2 of land between The Snout in the west and Green Bay to the east (Figure 1.1.). Waikawa Bay is the main residential settlement in the study area located 7km north east of Picton. Other smaller communities are located at Wharetekura Bay, Sunshine Bay, and Whatamango Bay.

The Snout is a long and narrow peninsular which divides Picton Harbour and Waikawa Bay. At present the Snout is a scenic reserve, with the exception of 4 or 5 houses and batches near the Waikawa marina. Lying approximately half way between Waikawa Bay and Whatamango Bay is Karaka Point. The small low relief peninsular was the site of a Maori Pa 300 years ago and now is preserved as an historic and scenic reserve.

The geology of the study area is dominated by two bedrock units, the Marlborough Schist and the unfoliated greywackes and argillites of the Pelorus Group and possibly the Waipapa Terrane. Subsurface investigations have determined the occurrence of schist west of the Waikawa Bay Fault (Bell, 1993; McManus, 1994) which is interpreted as being part of the Waikawa Bay Fault zone. Schist is the dominant rock type east of the Waikawa Bay Fault and greywacke is present to the west. The schist in Waikawa is restricted to TZ IIa and IIb (Bishop, 1972) and is in both faulted and gradational contact with the unfoliated greywacke (Chapter 2). The unfoliated rocks have a wide distribution within the field area, identified in both Waikawa and Whatamango Bays. Argillite is interbedded with greywacke as fine lamellar beds and some areas are massive greywacke sandstone devoid of any marker horizons. Additionally, there are extensive deposits of colluvium, fan debris, and alluvium. The field area has also been subject to the intense late Quaternary weathering typical of the Marlborough Sounds creating a deep weathering profile at most locations.

Structurally the Waikawa Bay Fault dominates the field area, with other faults identified in Green Bay and across The Snout. Ambiguity exists regarding the activity of the Waikawa Bay Fault, with the last movement inferred to be both pre-Holocene (McManus, 1994) and Late Holocene (Horrey, 1989). Multi- phase folding has also occurred, further complicating the structural history of the field area (Chapter 2).

1.3.2. Land Use and Vegetation

The first inhabitants of the Marlborough Sounds were the Maori. Their use of agriculture as well as hunting facilitated the need for land clearance which, in turn, decreased the stability of the land. Removal of vegetation was principally by fire and charcoal remains in loess and colluvium may be dated back to this era (McManus, 1994). The first Europeans in the Sounds noted the occurrence of several human-generated fires scattered over the hills in the Sounds.

European settlement dates back to the 1850's and these people also used fire as a means of clearing the land. The addition of stock for grazing further increased the instability of many slopes. Farming was not a successful venture in the Sounds however, and had dramatically declined by the 1930's. At present, land use is principally for forestry and recreation, with Waikawa Bay being the only progressive urban centre within the field area. Whatamango Bay is currently dominated by forestry interests. Following the milling of these trees, it is thought that the area will be subdivided for residential development. Presently several applications for land zonation changes between Karaka Point and Waikawa are being processed, the primary interest being urban development.

Vegetation in the field area is dominated to the west by secondary growth of gorse and bracken which has replaced the original podocarp broad leaf and beech podocarp vegetation (Horrey, 1989). To the east of Waikawa, including Wharetekura, Sunshine, and Whatamango Bays the vegetation has reverted back to the original native growth with the beech forest having effectively outgrown the gorse and bracken.

1.3.3. Climate and Precipitation

The Marlborough region is well known for its sunshine and low rainfall. The Sounds however, have a distinctly higher precipitation than the rest of Marlborough. The annual rainfall for Picton is approximately 1200 mm/yr, while Blenheim experiences only 700 mm/yr (McManus, 1994, Figure 1.2.). October through to November are typically the driest months, with the highest rainfall occurring between June and August (Figure 1.3.). Short high-intensity rainstorms are also typical of the Sounds and occur frequently in the field area, for example in April 1995, a storm occurred in the Picton-Whatmango area and 80 mm of rain was reported over a 24 hour period (Chapter 5).

1.4. PREVIOUS WORK

Due to the lack of good unweathered exposure in the Marlborough Sounds, there has been relatively little work done in the field area compared to other locations in New Zealand. Interest in the Sounds was heightened in the 1870's due to the discovery of coal in Picton and subsequent work was principally exploration related. In 1964 Beck produced a geological map of the Marlborough Sounds region at 1:250,000. Beck was followed by Vitaliano (1968) who attempted a detailed petrological and structural study of the south eastern Marlborough Sounds and his work formed the basis for further studies in the area. Conversely more literature exists regarding the western Marlborough Sounds boundary and the geology south of the Wairau Fault (Lauder, 1969; Kingma, 1974).

More recently a number of theses have provided valuable information regarding both the engineering geology and structure of the Marlborough Sounds. The engineering geology of the Havelock area was covered by Kingsbury (1987) while Picton and Waikawa were investigated by Horrey (1989) and McManus (1994). The geological structure of the Picton and Shakespere Bay region was studied by Nicol (1988) and aspects of the Quaternary development of the Sounds was studied by Esler (1984). Additionally, a number of unpublished engineering reports to the Marlborough District Council and other local authorities have provided valuable information regarding the geology of the south eastern Marlborough Sounds.

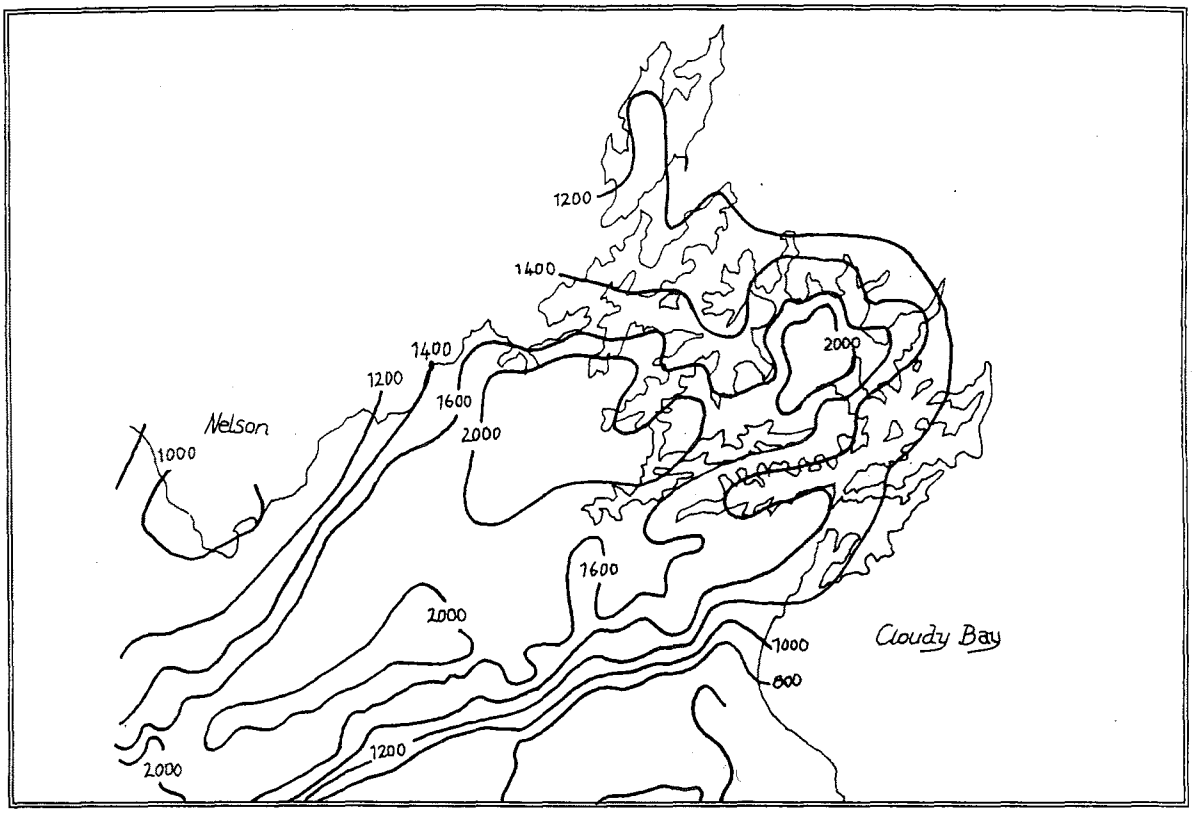

FIGURE 1.2.: Annual rainfall data for the Marlborough region including the Marlborough Sounds (From Kingsbury, 1987).

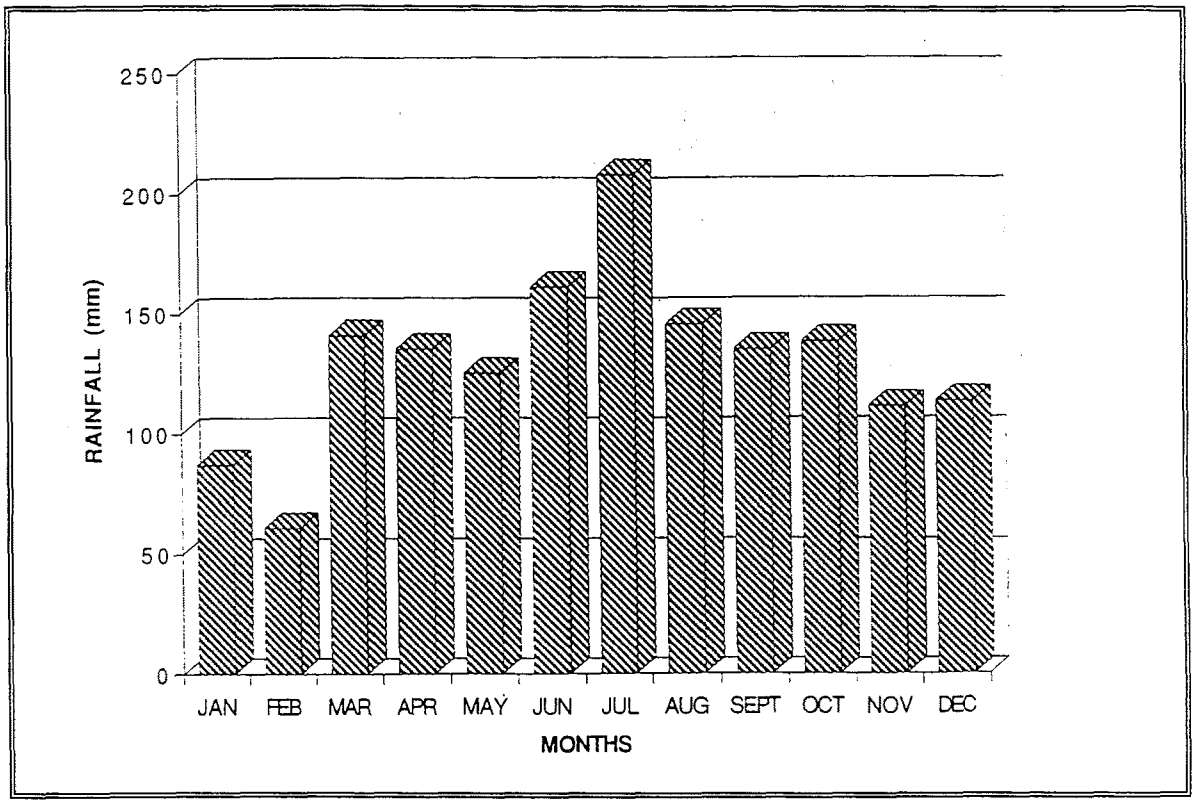

FIGURE 1.3.: The average monthly rainfall(mm) for the Picton/Waikawa area from 1980-1989 (After McManus, 1994).

1.5. INVESTIGATION METHODOLOGY

1.5.1 Engineering Geology Methodology

The methods used in this study follow those presented by Bell and Pettinga (1983) and used by Horrey (1989) and McManus (1994). These methods are used in detail in the Whatamango Bay area, and more generally over the whole study area.

a) Engineering Geological Mapping

Using aerial photographic interpretation of photographs dating from 1959-1994 and site specific investigations, engineering geological maps were compiled as follows:-

A map at a scale of 1:5,000 covers the area between Waikawa Bay and Whatamango Bay. The map depicts the detail of bedrock and surficial unit distribution and the smaller geomorphic features. Maps at 1:5,000 scale also include hazard assessment maps and land use suitability maps.

All grid referenced were obtained from NZMS 260 series sheet P27.

b) Laboratory Testing

From field investigations, samples of schist and greywacke regolith and colluvium, red weathered material and bedrock units were collected. Using the engineering geological method outlined by Bell and Pettinga (1983) limited laboratory testing is required to determine the geotechnical properties of these units. Tests performed included grain size analysis, Atterberg limits, shear strength testing, XRD and SEM for clay mineral identification, pin hole erosion and the Crumb dispersion test, and point load and cone indenter for rock strength determinations.

c) Hazard Assessment

Work completed in the Waikawa urban area by Horrey (1989) and McManus (1994) formed the basis of the hazard assessment at Whatamango Bay. At a scale of 1:5000 the following geological constraints were identified and analysed.

- ☺ Slope Movements: Areas of past, present, and possible movement were documented. Such areas were mainly gullies although some movement was identified on slope faces.
- ☺ Erosion: Principally restricted to stream bank erosion in gullies and the Graham River and Waikawa Stream.
- ☺ Flooding: Flood potential of the Graham River is very high as the river catchment is the largest emptying into Queen Charlotte Sound. Recent flooding is testimony to the rapid changes of which this river is capable. A hydrological study of the Graham River at the Port Underwood Bridge assisted in a flooding hazard assessment.

1.5.2 Structural Methodology

The field area was divided up into a number of fault bounded domains and the structural characteristics of each domain was investigated then compared to neighbouring domains. The domains used in this study included The Snout Domain which borders the Picton Domain studied by Nicol (1988), the Karaka Point Domain and the Green Bay Domain. The principal faulted boundaries identified in relation to the domains include the Picton Thrust System and in particular the Old Freezing Works Fault, the Waikawa Bay Fault, the Whatamango Bay Fault and the Green Bay Fault. Detailed recording of bedding, faulting, shearing and foliation was undertaken on coastal exposures from The Snout to Green Bay (Figure 1.1.). Further information was gained from road and ridge exposures from throughout the field area.

The activity of the Waikawa Bay Fault was assessed using geomorphic evidence of the last rupture event and geophysical methods, transient electromagnetism and ground penetrating radar, to determine the nature of the fault at depth.

1.6. CHAPTER ORGANISATION

The organisation of this thesis is as follows:-

☺ *Chapter 2: Stratigraphy and Structural Geology*

Within this chapter the nature and extent of the schist and greywacke bedrock is investigated and discussed in relation to the principal structural features identified in the field area.

☺ *Chapter 3: Geomorphology*

A description of the nature and origin of the surficial units identified is given and the relative ages of geomorphic deposits and surfaces are discussed in order to develop a geomorphic chronology of events for the field area.

☺ *Chapter 4: The Waikawa Bay Fault*

The information presented in Chapter 3 regarding the age of deposits and surfaces in relation to the last rupture of the Waikawa Bay Fault is assessed and combined with geophysical investigations and subsurface data to determine the activity of the fault.

☺ *Chapter 5: Engineering Geology*

This chapter presents the field and laboratory test results which are discussed and synthesised to produce geotechnical parameters for surficial units and weathered bedrock units.

☺ *Chapter 6: Hazard Assessment and Land Use Planning*

The information presented in the previous chapters is synthesised to produce a hazard assessment of the field area which is presented on a 1:5,000 map. As a continuation of the hazard mapping, this chapter also introduces and details the development of land use planning maps for the purposes of urban development suitability in the field area.

☺ *Chapter 7: Summary and Conclusions*

Finally a synthesis of all the information presented in the previous chapters and recommendations for future studies.

CHAPTER TWO STRATIGRAPHY AND STRUCTURAL GEOLOGY

2.1. INTRODUCTION

This chapter provides a description of the lithologic units comprising the south eastern Marlborough Sounds and an introduction to the distribution of structural elements affecting the field relationships of the units. The objective of the structural component of this chapter is to establish the setting and character of the Waikawa Bay Fault and possible age constraints for fault rupture. Much of the information presented for the structure of the field area is severely restricted by the poor exposure and the lack of marker horizons in the rock material. Almost all of the measurements and observations from which the structural analysis were made were taken from the shore platform which yielded only slightly weathered outcrops. Onshore extrapolation of geological structures was made using geomorphic information from aerial photographs because there are few exposures upslope and those which are observed, for example roading cuts, are extensively weathered. Connections between structures on opposing shorelines could not be made around the head of the major bays because of the alluvial flats occupying valley floors.

2.2. TECTONIC SETTING

2.2.1. Location within the Plate Boundary

South of the Marlborough Sounds the Wairau Fault is traditionally shown as the extension of the Alpine Fault and therefore is the surficial representation of the Indo-Australian and Pacific plate boundary. Oblique movement across the broad deformation zone of the plate boundary has had significant effects on the formation of the Marlborough Sounds. The plate boundary is expressed as westward dipping subduction forming the Hikurangi Trench; movement is reversed into easterly dipping subduction of the Indo-Australian plate in Fiordland. Generally, movement along faults between these two areas takes the form of a broad zone of active deformation accomodated on a complex of oblique thrusts and dextral transfer faults including the Sounds block (Figure 2.1.).

2.2.2. Seismicity

There have been few high magnitude (>4 on the Richter Scale) earthquakes centered within the Marlborough Sounds in recorded history, although several have been centred in south Marlborough. Most activity represents the surface

expression of the plate subduction boundary at deep crustal levels (>40 km). Shallower earthquakes are generally related to the fault systems in southern Marlborough. These faults are thought to take up strain in crustal rocks imposed by the subduction of the Pacific Plate (Reyner, 1989).

Seismic studies show the possibility of both deep and shallow earthquakes beneath the Marlborough Sounds. Reyner (1989) showed the distribution of such earthquakes during the period 1964-1987 which possibly delineates the western edge of the subducting slab (Figure 2.2.). Clustering of focal depths around the Marlborough Sounds makes the region as a whole potentially very seismically active. Further studies by Anderson and Webb (1994) for the period 1990-1993 confirm Reyner's data, particularly with regard to focal depths >40 km (Figure 2.3.). Anderson and Webb (1994), however, identify what they term an aseismic corridor within which the Marlborough Sounds lie (Figure 2.4.). A distinct lack of earthquakes with focal depths less than 40 km confirms the corridor first identified by Hatherton (1970) and later re-identified (1980) as stretching as far south as the Awatere Fault. The aseismic nature of the Marlborough Sounds (Figure 2.4.) is difficult to explain. Pettinga (pers comm, 1995) suggests the corridor reflects a south westward transfer of the current movement on the subducting plate boundary. Tectonic stress which was once taken up by faults in the Marlborough Sounds has now moved south and is accommodated by the south Marlborough/northern Canterbury fault systems, thus leaving the faulted pattern of the Marlborough Sounds a remnant of a more active tectonic period.

2.3. REGIONAL STRATIGRAPHY AND STRUCTURE

2.3.1. Mesozoic Terranes

Within the South Island of New Zealand there have been nine tectonostratigraphic terranes identified which range in age from the Paleozoic to the Late Mesozoic (Bishop et al.,1985). Figure 2.5. is the provisional terrane map from Bishop et al. (1985) and shows the relative distribution of the terranes and their apparent offset across the Alpine Fault. In the Marlborough Region, the distribution of the terranes to the west is considerably less than their counterparts in the south eastern part of the South Island (Figure 2.5.) and extend from the Brook Street and Murihiku Terranes in the west to the Caples Terrane in the east. The east Nelson Regional Sequence is separated from the Marlborough Sounds by the Putaki Melange and the rocks of the Sounds are dominated by the presence of the Caples Terrane correlatives, the Pelorus Group. The age of accretion of the Caples Terrane is commonly believed to have occurred during the Permian to

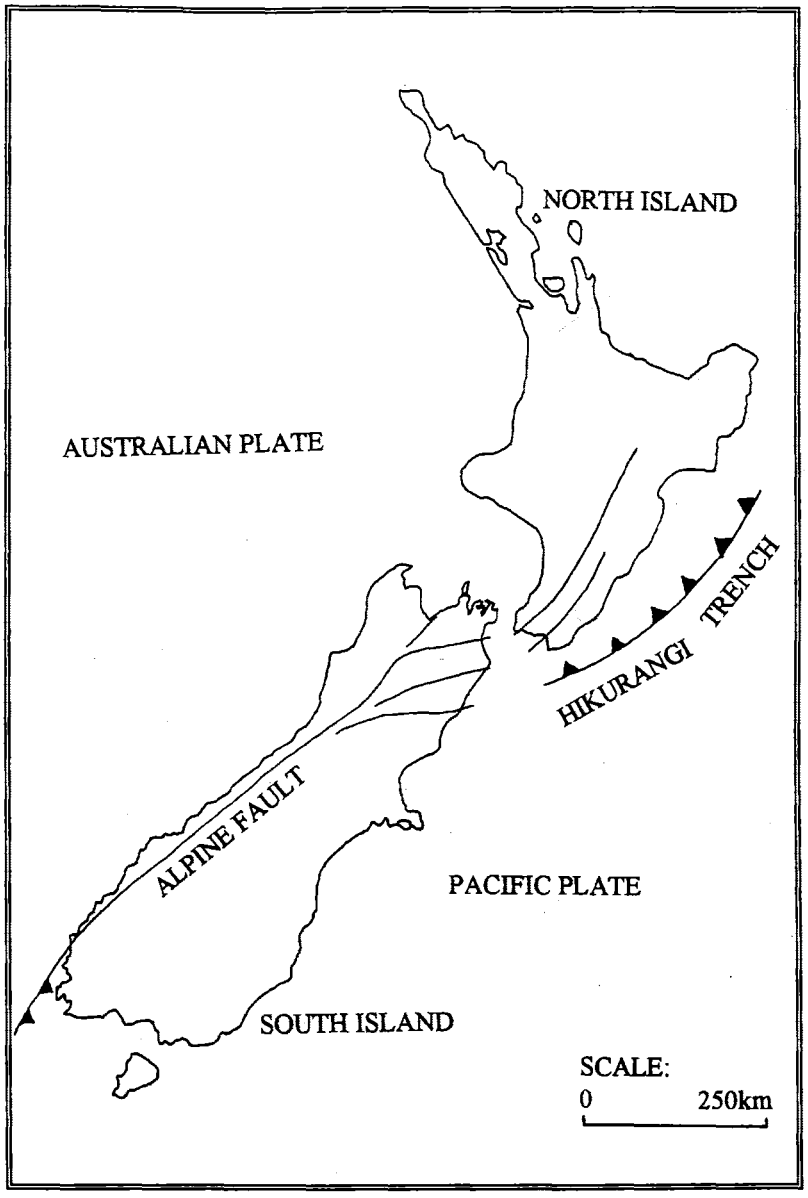

FIGURE 2.1.: A schematic representation of the plate boundary in New Zealand

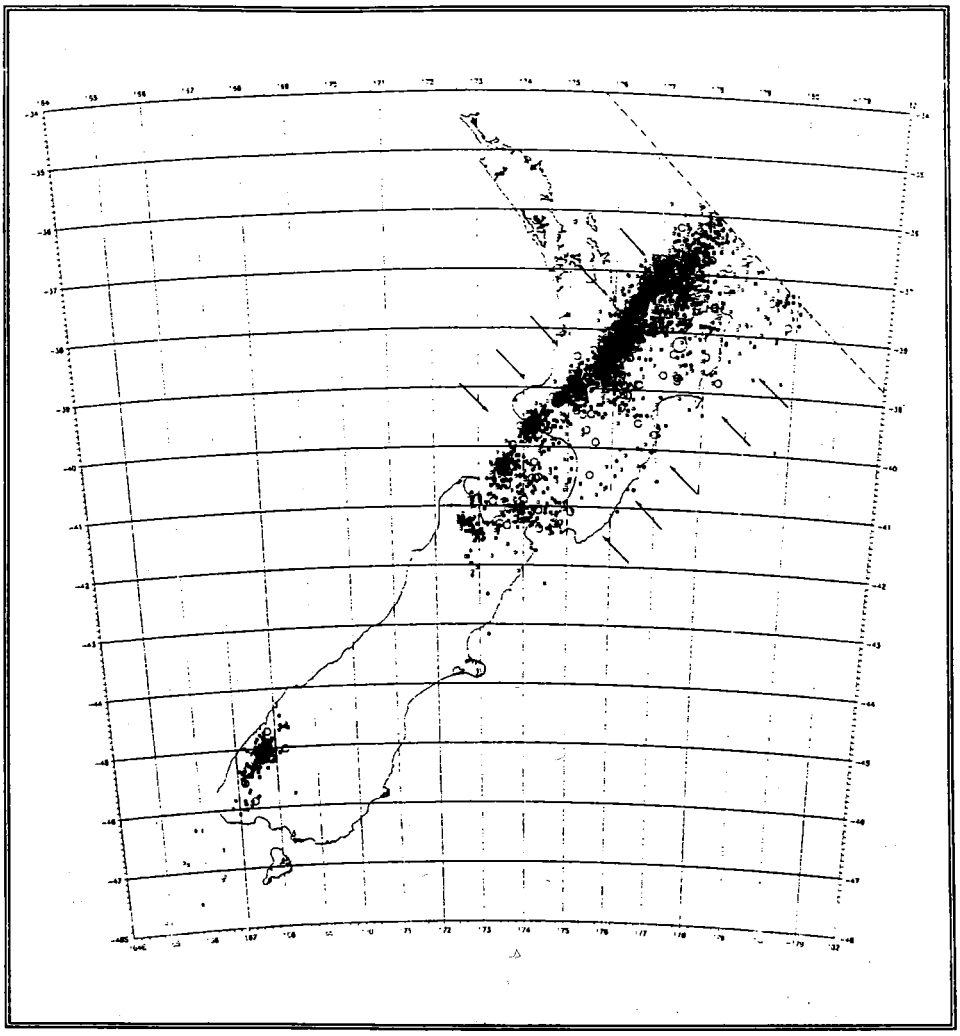

FIGURE 2.2.: The location of earthquakes in New Zealand with magnitudes of 4 or greater and focal depths in excess of 40km for the period 1964-1987 (After Reyner, 1989).

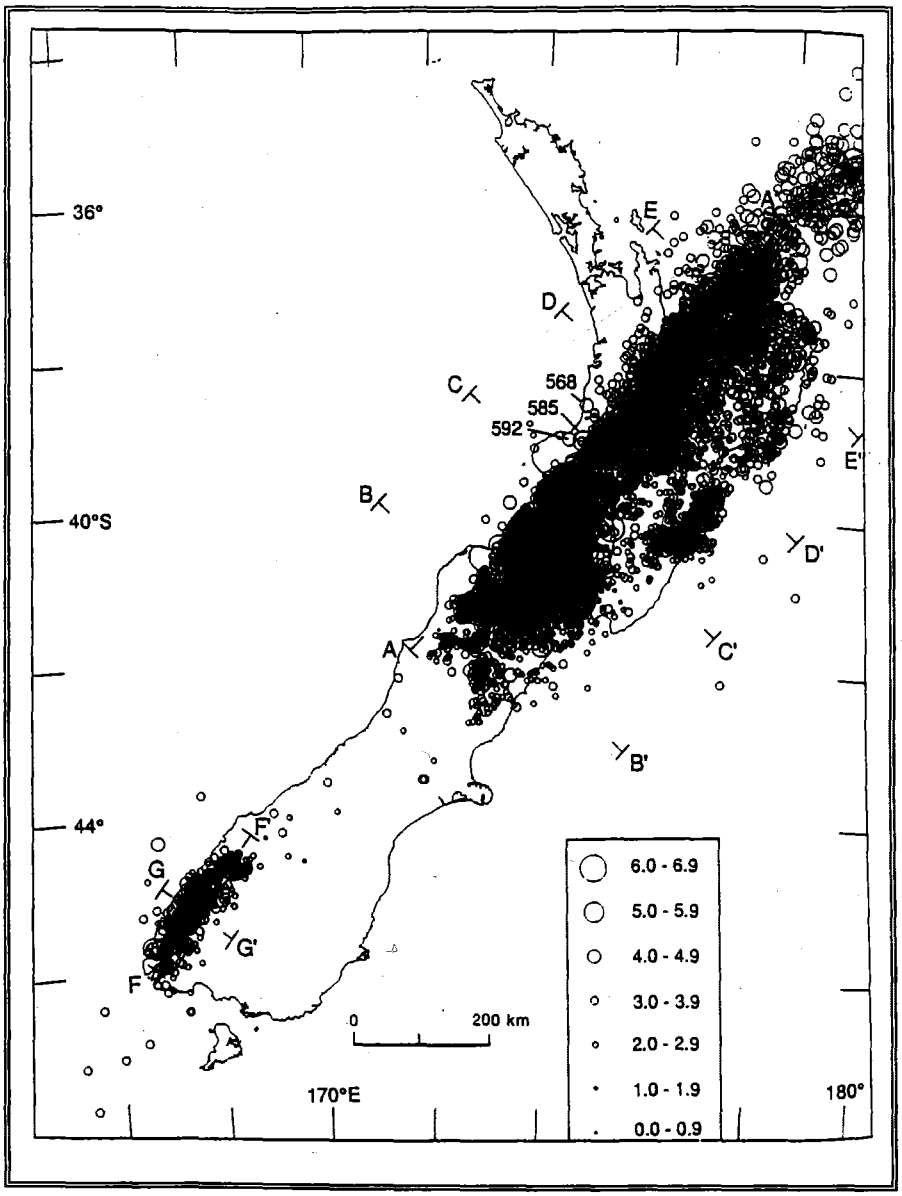

FIGURE 2.3. Earthquakes in New Zealand with focal depths in excess of 40km for the period 1990-1993 (After Andersson and Webb, 1994).

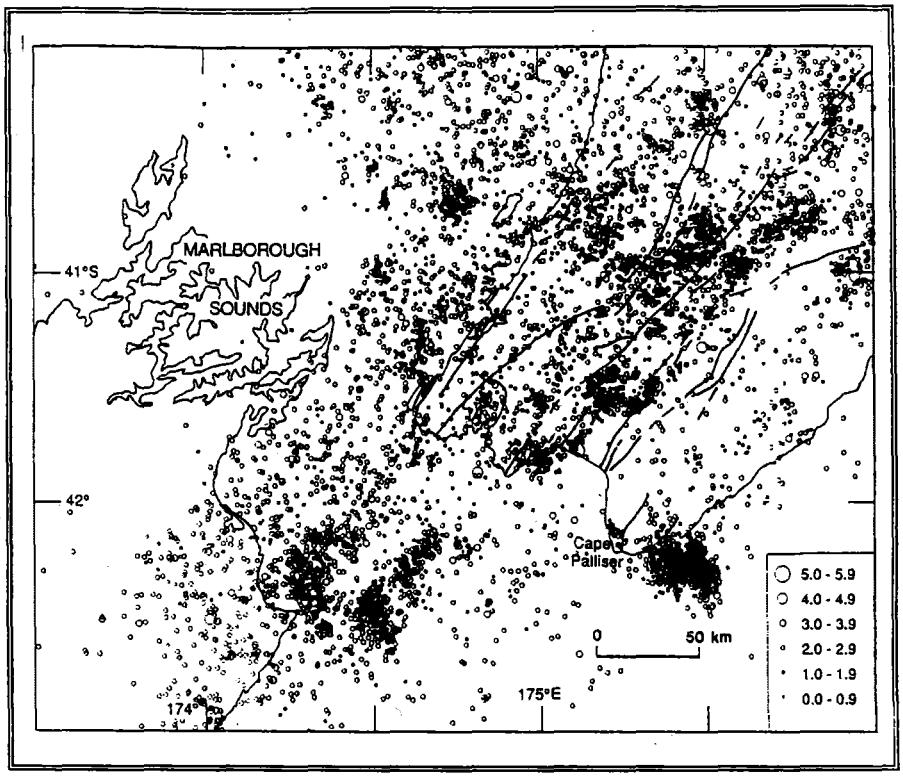

FIGURE 2.4.: A diagram showing the seismic activity in the Wellington and Marlborough region. The Marlborough Sounds area is conspicuous because of the aseismic corridor within which it is located (Andersson and Webb, 1994).

Triassic and later collision with the older Torlesse Terrane (Rakaia) is inferred in Otago. The collision of the two terranes is thought to have occurred in the early Jurassic and resulted in significant metamorphism however, Torlesse Terrane rocks are not commonly believed to be present in the Marlborough Sounds (Section 2.5.)

Pelorus Group rocks are predominantly volcanogenic sandstones and mudstones which are now considerably indurated to produce 'greywackes' and 'argillites', which are terms in common usage and can embrace a wide variation in clastic composition. These rocks are thought to have originated as sediments laid down as a series of fan deposits in a deep sea trough (Johnston, 1983). Pelorus Group rocks are principally volcanically derived sediments and conventionally believed to be the eroded remains of the Brook Street volcanic arc (Suggate, 1978). Close similarity of age and composition makes the Pelorus Group rocks a correlative of the Caples Terrane rocks in Otago and Southland.

The Pelorus Group was originally considered to be of Late Carboniferous-Early Permian age (Suggate, 1978). However, now the more accepted age is Late Permian-Mid Triassic and equivalent to the Caples Terrane on the basis of poorly preserved plant remains which are the only fossiliferous age indicators for the Marlborough Sounds (Nicol, 1988). The thickness of the Pelorus Group remains uncertain as the lower boundary is gradational with schist and the upper boundary is tectonic (Vitaliano, 1968), though the apparent thickness is generally accepted to be in the order of 10 km (Kingma, 1974, Johnston, 1983).

Although the Pelorus Group rocks have previously been subdivided (Nicol, 1988; Suggate, 1978; Bell, 1992) poor outcrop exposure makes mapping of subdivisions difficult. Therefore, for the purposes of this study, the rocks are defined as greywacke and argillite only. Greywackes are dark grey-greenish grey and contain a large number of angular lithic fragments. These rocks are generally poorly sorted with a very fine grained matrix. Sixty percent of the lithic fragments are composed of sandstone, siltstone, and mudstone. Minor fragments of volcanics, granite, and schist also occur (Vitaliano, 1968). The argillites are most commonly interbedded with the greywacke and occur as fine lamellar bedding. Some massive argillite also crops out within the field area and is dark grey-blue grey in colour. Vitaliano (1968) identified that 60% of the argillite which he analysed was siltstone; the remainder being mudstone. These rocks are uniform in their mineral composition with equigranular texture and are well sorted.

2.3.2. Metamorphism and Protoliths of the Marlborough Schist

The Marlborough Schist is the largely more metamorphosed equivalent of the Pelorus Group rocks (Figure 2.6.), with metamorphism generally increasing progressively towards the south east although faulted boundaries complicate the bedrock relationships. The term Marlborough Schist was introduced by Hector (1872) and internal boundaries were delineated by MacKay (1886). Further divisions were made by Turner (1935) and Hutton and Turner (1936) as Chlorite Zone I-Chlorite Zone IV, which introduced textural zones reflecting increasing foliation. More textural subdivisions were made by Bishop (1972) who proposed Textural Zone I-Textural Zone IV (Table 2.1.). Kingsbury (1987) subdivided TZ II rocks in the Havelock area into St I and St II on the basis of erosional features and landscape development. For the purposes of this study, the classification proposed by Bishop (1972) will be used.

The total thickness of the Marlborough Schist is undetermined and reasons for the uncertainty are outlined by Vitaliano (1968) as follows:

1. The upper contact is gradational;
2. The base of the unit is not exposed;
3. Key repeated horizons are not present;
4. The unit is modified by extensive faulting.

The type of schist is dependent on the mineralogy of the original rock. Four schist types are recognisable in the Marlborough Sounds; quartzo-feldspathic, micaceous, ferruginous, and greenschist (Bell, 1992; Vitaliano, 1968).

Sedimentary younging has been identified in the direction of increasing metamorphism, indicating significant pre-metamorphic folding (Kingma, 1974; Beck, 1964; Suggate, 1978). Sedimentary bedding has generally been identified roughly parallel to schistosity (Beck, 1964; Kingma, 1974), however this is not true for much of the schistose rock in the eastern part of the field area, and where they are sub-parallel it is clear that bedding is strongly transposed.

The age of metamorphism of the Marlborough Schist was thought by Kingma (1974) to be Devonian. However, the more commonly accepted age of metamorphism is Late Jurassic-Early Cretaceous, or the Rangitata Orogeny (Nicol, 1988; Horrey, 1989; Grindley et al., 1959), mainly determined indirectly by dating of schistose correlatives in Otago and Southland.

Difficulties arise with terrane affiliations particularly in relation to the presence or absence of the Torlesse Terrane and the Waipapa Terrane. The schists in the Marlborough Sounds have traditionally been correlated with the Caples Terrane rocks observed in Otago and the presence of the Torlesse Terrane is

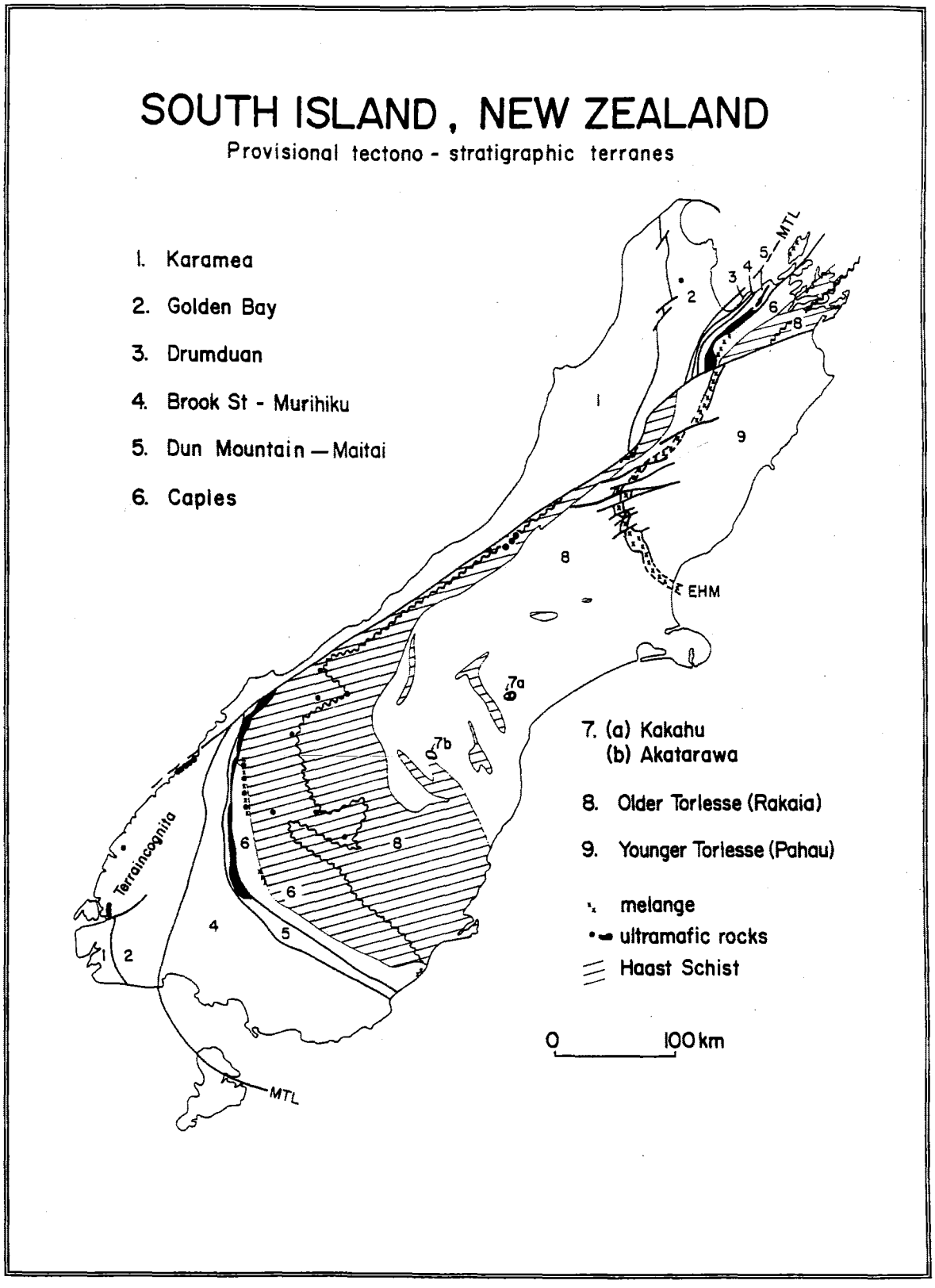

FIGURE 2.5. Provisional Terrane Map of the South Island of New Zealand showing the nine identified tectonostratigraphic terranes (From Bishop et al., 1985).

TABLE 2.1.: Textural zonations of schist developed in greywacke rock and siltstone defined by Bishop (1972).

Textural Zonations in Greywacke and Siltstone Derived Schist		
Textural Zones	Descriptions	
	Greywacke	Siltstone
Textural Zone I	Indurated, non-foliated, massive and blocky outcrops, no fissility.	Faint Phyllitic sheen parallel to bedding or cleavage.
Textural Zone II A	Slight foliation, fissility parallel to foliation, faint micaceous sheen on foliation surfaces. Bedding recognisable, relatively undisturbed.	Distinct micaceous sheen, fissility pronounced. Bedding generally still visible.
Textural Zone II B	Penetrative foliation which shapes outcrops. Fissility dominant parallel to foliation. Smooth micaceous sheen on hand specimen. Discontinuous bedding.	Quartz and feldspar segregation with some chlorite development. Microcrenulation lineation common. Bedding sheared out along foliation.
Textural Zone III A	Strongly foliated. Segregation lamination beginning to develop. Mineral or lithologic lineation common producing a rippled foliation.	Thin quartz albite segregation lamellae well developed. Individual lamellae persistent for several centimetres along foliation.

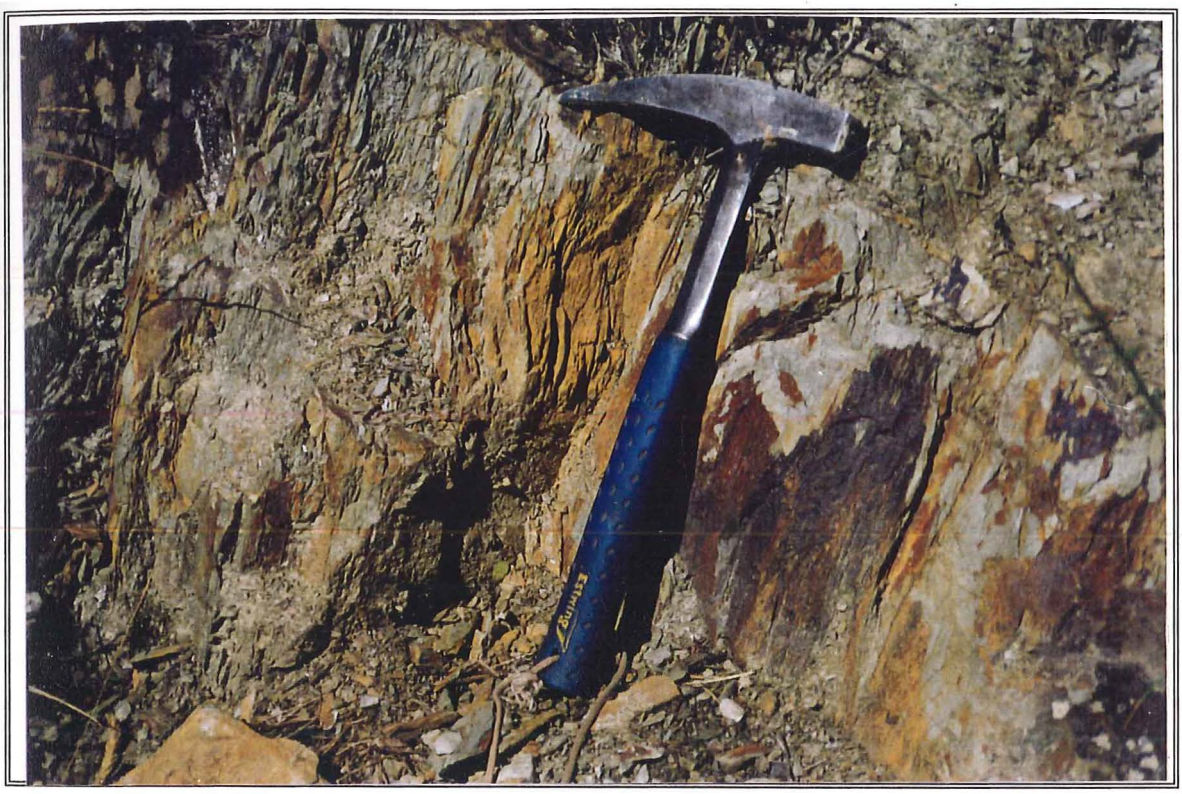

FIGURE 2.6. Field exposure of the Marlborough Schist TZIIa in Whatamango Bay near the Waipuna Headland (GR 2699990 599335).

uncertain. Crustal shortening of up to 60% (May, 1989) could account for the absence of Torlesse rocks in the Marlborough Sounds which, when using paleogeographic reconstructions of displacement along the Alpine Fault, should occur near Picton (Nicol and Campbell, 1990). Miocene thrusting may have caused the Torlesse rocks to be underthrust beneath the Caples Terrane rocks and it is also thought that Miocene thrusting may also account for problems in correlation of geological features across Cook Strait (Nicol and Campbell, 1990). Nicol (1989) proposed a west to east thrusting direction of faults in the Picton region (Section 2.3.4.) which are thought to be Miocene in age or possibly younger, and the presence of a Torlesse protolith was not observed in the Picton region. Mortimer (1993) however proposes a different terrain assemblage to that favoured by Nicol (1989) and Nicol and Campbell (1990) in which he recognises the presence of Waipapa terrane rocks in the south eastern Marlborough Sounds as the Arapawa Block which is separated from the Kaituna Block, comprising Caples and possibly Torlesse Terranes, by the Picton Fault Zone (Figure 2.7.). Mortimer (1993) uses textural and mineralogical characteristics to delineate the presence of the Waipapa Terrane in the Marlborough Sounds and the higher grade TZIV schists being derived from a Torlesse Group protolith. The implications for Miocene thrust tectonics previously recognised in the south eastern Sounds (Nicol, 1989). This re-evaluation of the distribution of the terrane sourced protoliths affects the interpretation of thrust geometry and transport. The possibility that the TZIV block of schist immediately west of Picton places Torlesse protoliths between Pelorus and Waipapa rocks which cannot be produced by simple west to east imbrication. Mortimer has based this interpretation on the composition of two specimens from the northern margin of the block and general observations of the abundance of quartz in segregation lamellae and veins. Given the tectonic problemsraised by such a correlation, it is beyond the scope of this study either to accept this revised correlation unequivocally or to explore that problem further.

The proposed distribution of Waipapa rocks is founded on a much more comprehensive sample base and the possibility that par or all of the rocks in the Picton/Waikawa Bay area could be Waipapa Terrain rather than Pelorus, does affect the interpretation of structure in the study area. The presence of the Waipapa Terrane implies that thrusting has occurred in an east to west direction to keep Waipapa rocks tectonically above Pelorus Group and this assumption constrains the role of the Waikawa Bay Fault which must be either a roof thrust over a fault wedge created by the Picton Thrust stack (Nicol, 1989), or a younger discordant structure with dominantly strike slip motion. Although confirmation of

the presence of the Waipapa Terrane is outside the scope of this study, the inferred presence of the terrane has significant implications for thrusting models in the field area and is discussed in detail in Section 2.6.

2.3.3. Late Cretaceous and Early Tertiary Basin Formation

A sedimentary basin forming during the Late Cretaceous and Early Tertiary is inferred by the presence of sedimentary rocks such as the Elevation Mudstone, the Picton Conglomerate and the Shakespeare Bay Sandstone which outcrop in the Picton region. The sedimentary material is considered to be Tertiary in age on the basis of forminifera samples obtained from each of the sediment types (Nicol, 1988). The age of the basal unit, the Picton Conglomerate is thought to be Landon while the overlying units, the Elevation Mudstone and the Shakepeare Bay Sandstone are also given a Landon age (Nicol, 1988). The depositional environment of the Tertiary rocks in the Picton area is thought to have been a marginal marine or lagoonal to an inner shelf environment and the sequence presently preserved in Picton is believed to be the basal sequence of a much more extensive Tertiary succession which has now been removed (Nicol, 1988). The presence of high volatile bituminous coal seams within the Elevation Mudstone implies that the coal was buried by several kiolmeters of sediments and the sedimentary basin was tectonically active following the deposition of the parent materials for the coal seams. Nicol (1988) estimates that the tectonic influences, inferred to be an extensional regime, continued after the Landon.

2.3.4. Miocene to Recent Convergent Deformation

a) Introduction

The structure of the south eastern Marlborough Sounds is dominated by the presence of the major shear zones which have led to the formation of the main valleys such as Queen Charlotte Sound. The strike-slip Queen Charlotte Fault Zone and correlatives such as the Kenepuru Fault Zone, are thought to have developed in relation to the formation of the plate boundary which is presently defined by the Wairau Fault south of the Marlborough Sounds (Figure 2.8.), and the influence of a compressional tectonic regime operational since the Miocene. Movement along these principal shear zones within the Marlborough Sounds has caused the dislocation of schist and greywacke bedrock in a dominantly dextral strike slip motion to the north east.

Within the Picton region the principal structural elements which have influenced the distribution of bedrock are the Miocene are younger thrust

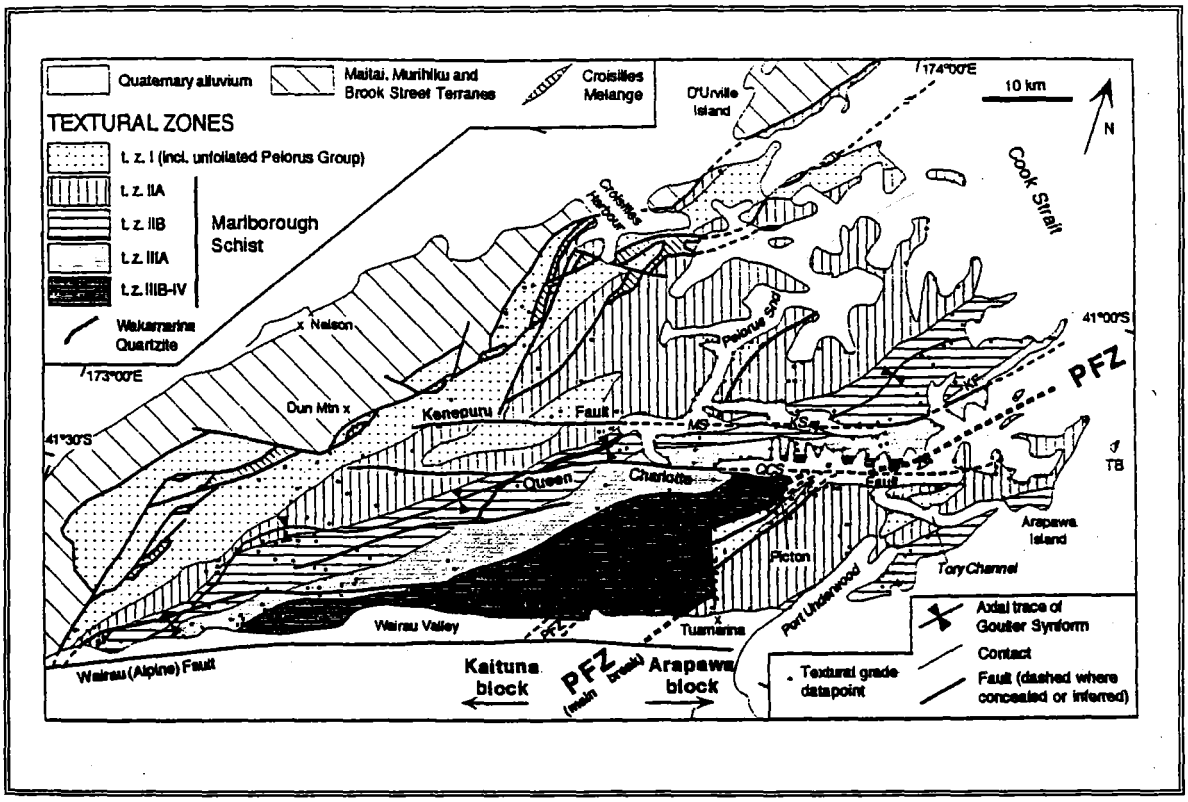

FIGURE 2.7. The distribution of the Marlborough Schist within the Kaituna Block and the Arapawa Block defined by Mortimer (1993). The Arapawa Block contains the Waipapa Terrane.

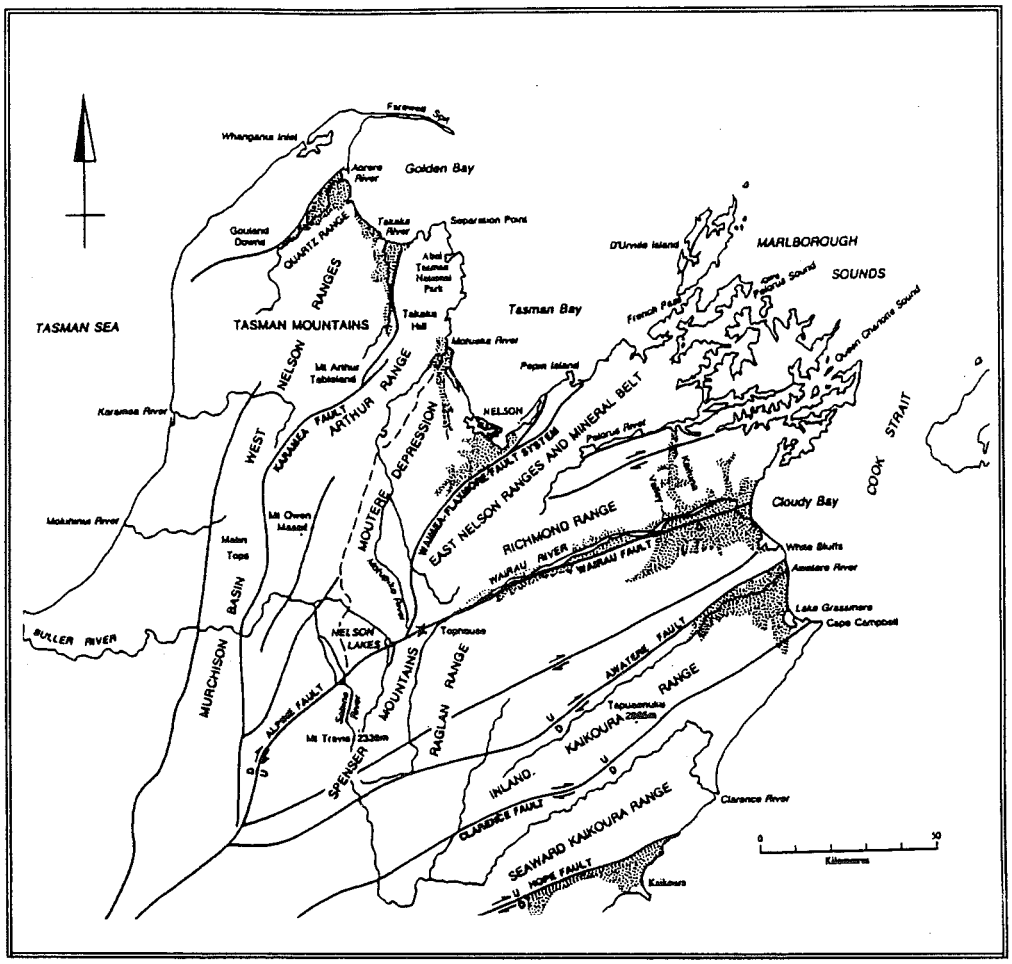

FIGURE 2.8.: Nelson and Marlborough regions showing the tectonic features of the region. The Marlborough Sounds Blocks is defined by the Wairau Fault to the south, the east Nelson sequence to the west and Cook Strait to the east and north. (Campbell and Johnston, 1992).

complexes described by Nicol (1988) and Nicol and Campbell (1990) and summarised below.

b) The Picton Thrust System

The tectonic regime operating in the Picton area was studied extensively by Nicol (1988) and summarised by Nicol and Campbell (1990). The Picton Thrust system (Figure 2.9.) is dominated by the Shakespeare Bay Thrust which strikes approximately NNE and separates TZ IV schist to the west from Pelorus Group rocks and Oligocene sediments to the east. The thrust dips to the west at approximately 50°-70° and it represents the most recent thrusting movement in the Picton Domain (Figure 2.9 .).

Older thrust faults in the Picton region include the Old Freezing Works Thrust and the Picton Thrust (Figure 2.9.). The Picton Thrust has a variable strike due to folding of the thrust surface, and dips moderately (40°-50°) to the east. The Old Freezing Works Thrust dips more shallowly eastward and northward (20°-35°), has a variable strike, and separates the TZ II and III schists from the unmetamorphosed
Pelorus Group and unconformable Oligocene inliers beneath (Figure 2.9.).

Nicol (1988) estimated the age of thrusting to be no older than Miocene, with thrusts becoming younger towards the top of the thrust stack (Figure 2.10. cross section). Evidence was in the form of coal rank obtained from the Oligocene sediments (Section 2.3.3.) exposed by thrusting and erosion in Picton. Development of the Picton thrust system was thought to have been associated with an east-west compressional regime during the Miocene. This regime allowed considerable crustal shortening and subsequent thickening of the basement rock in the south eastern Marlborough Sounds.

Folding of sediments and the overlying thrust sheets in the Picton region indicates a classical basin and dome type interference folding pattern. Nicol identified a set of isoclinal and steeply inclined folds which he interpreted as pre-dating the metamorphic events. The subsequent folding events included a north trending set which resulted from east-west compression and a cross folding event with a north easterly trend creating the basin and dome structures.

The direction of thrusting identified by Nicol (1988) was a west to east direction in which the age of the thrusts becomes younger from east to west and from the bottom to the top of the thrust stack, the Shakespeare Bay Fault being the youngest thrust (Figure 2.10.; Nicol, 1988). As previously mentioned the west to

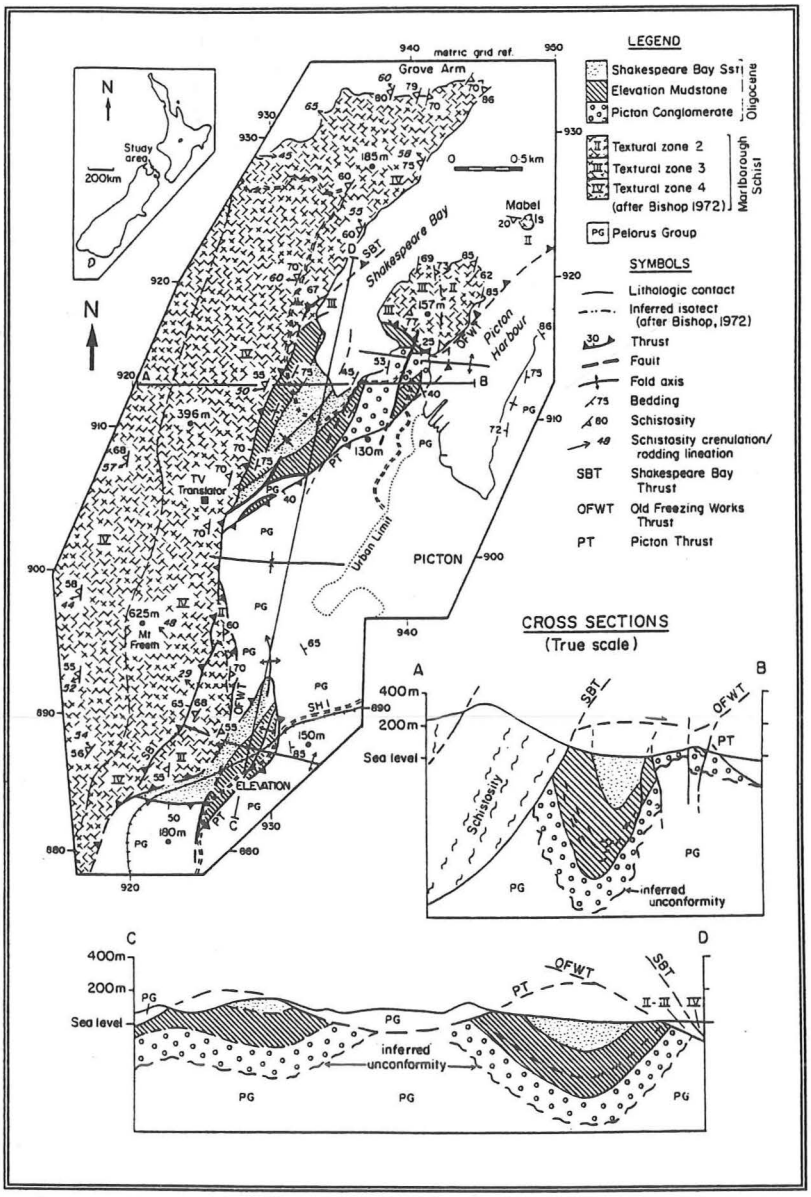

FIGURE 2.9.: The structural components of the Picton Thrust System (After Nicol and Campbell, 1990).

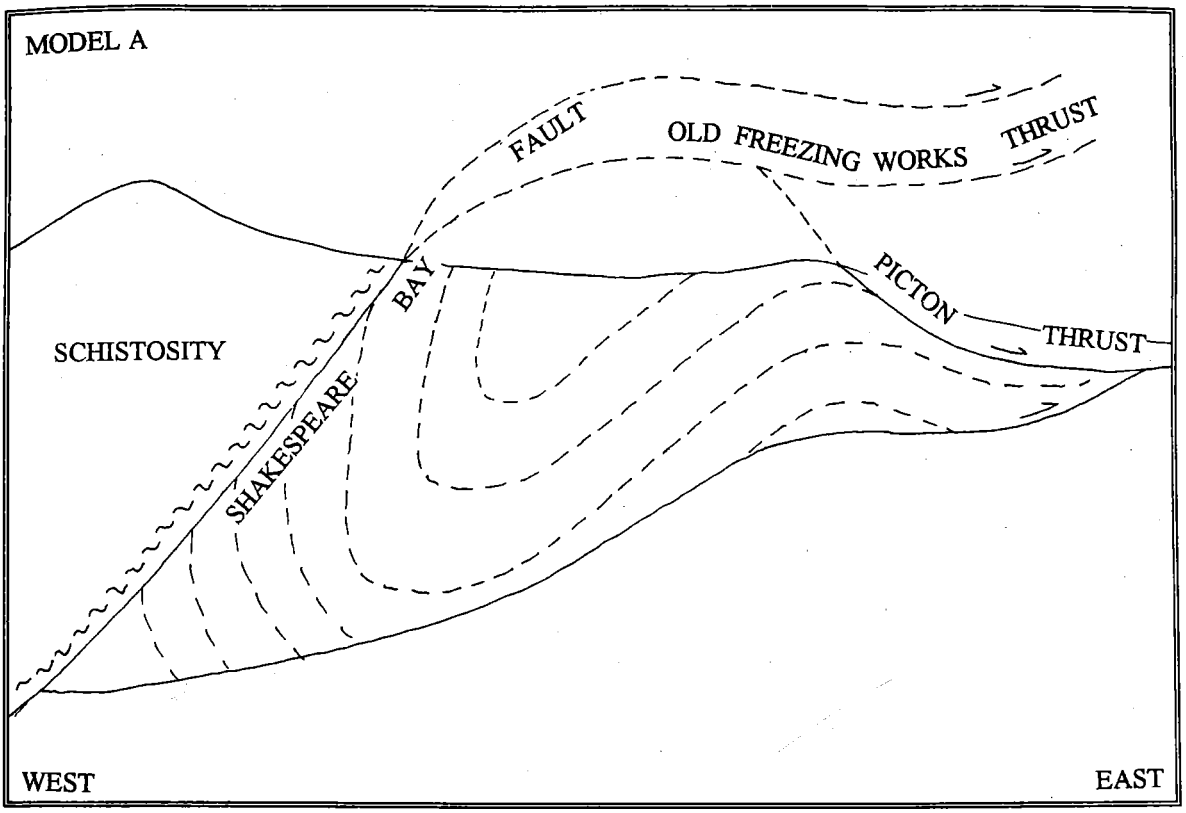

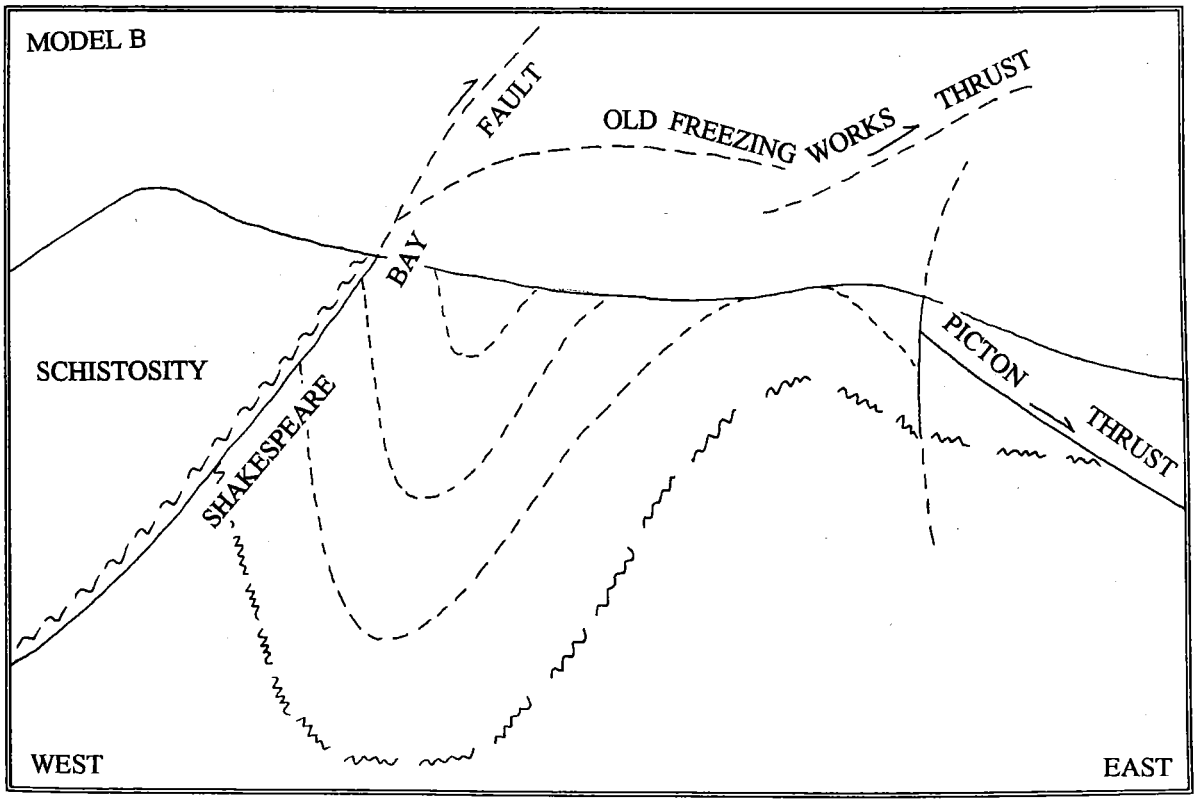

FIGURE 2.10.: The two structural models developed by Nicol (1988) showing a) the antiformal stack incorporation model , and b) the overthrusting model. The overthrusting model was favoured by Nicol or the Picton Thrust System.

east thrusting direction has implications for the terrane model presented by Mortimer (1993).

c) The Waikawa Bay Fault

The influence of the Waikawa Bay Fault which has an easterly dip direction and is anomalous to the structures identified in Picton by Nicol (1988) may be important in understanding the implications posed by the presence of the Waipapa Terrane. The inferred presence of Waipapa Terrane in the south eastern Marlborough Sounds requires the presence of a significant fault boundary separating Pelorus schists above the Old Freezing Works Thrust and probable Pelorus basement from Waipapa Rocks. Such a contact is constrained because Pelorus must either pass beneath or be truncated vertically. Mapping of the area dominated by the Waikawa Bay Fault adjacent to the Picton Thrust system is completed in order to provide some constraints for the following issues:

1) What happens to the eastern extensions of the Picton and Old Freezing Works Thrusts identified by Nicol (1988) in the Picton region?

2) What is the relationship of the Waikawa Bay Fault, which has an opposing dip and contrasting style to the thrusts identified in the Picton Thrust System?

3) What is the location and extent of the Waikawa Bay Fault north of the obvious topographic expression in Waikawa (Chapter 3) as the fault trace appears to stop abruptly?

The problems associated with the Waikawa Bay Fault outlined above are addressed in this study using a number of methods. This chapter attempts to clarify the above points in the following manner:

1) Identifying and describing the internal structure of each fault bounded domain within the field area (Section 2.4.).

2) Comparison of the structures between the domains identified in Section 2.4. (Section 2.5.).

3. A specific study of the Waikawa Bay Fault and its location north of the observed fault trace from evidence of shearing etc. in the basement rocks and the geomorphic expression of the fault.

Additionally, the evidence for Quaternary activity of the Waikawa Bay Fault is addressed using geomorphic and geophysical expression of the fault for potential seismic hazard evaluation and is detailed in Chapter 4.

2.4. STRUCTURAL DOMAINS OF THE WAIKAWA BAY AREA

2.4.1. The Snout

An early phase of folding on the Snout (F1) may be evident from the presence of overturned bedding on the western side of The Snout (Figure 2.11.) and the F1 structures form an overturned anticline syncline pair which strike NE-SW as seen on Figure 2.11. The presence of these overturned beds may simply indicate that the folding is of a mesoscopic scale only, although stereographic information (Figure 2.12.) appears to show consistent clustering of points for the overturned folding, and mapped zones of consistent face implies that the F1 is macroscopic in scale. Figure 2.11. includes a cross section of the overturned F1 folds along the A-B cross section line showing the fanning of cleavage associated with the folding. The F1 folding appears to be tight and variably dipping from moderate to steep (Figure 2.12.) which is reflected by the absence of discordant bedding and schistosity and the folds have a moderate south east plunge.

Further folding may be observed which trends approximately NW-SE (Figure 2.11.) and cross cuts the F1 folds. The result of the cross folding is a gentle change in both the strike and dip of the schistosity from the north to the south of the peninsula. Figure 2.12. is a stereoplot of the schistosity showing the change in schistosity from the north to the south thus indicating the presence of the folding. The effect of this cross folding on bedding would produce a basin and dome structure, and the wave length and location of the synform is compatable with the wave length of cross folds recognised by Nicol (1988).

Along the western edge of The Snout is evidence for a shear zone trending parallel to the coast line, approximately NE-SW (Figure 2.11.). Shearing of the bedrock is apparent only on the westen most headlands indicating that if the shearing is associated with a major fault, the location of the structure would be off shore. However, there is no indication as to the direction of dip for the shear zone and therefore correlation of the shearing with a particular fault in Picton Harbour is not possible. Shearing is represented as sheared zones on the headlands without any implications as to the character of the associated faulting (Figure 2.11.).

Further shearing may be present cross cutting The Snout and related to a significant change in topography along the crest of The Snout. North east of the topographic change, where the ridge crest is elevated, the presence of TZIIa schist appears to have been thrust over the Pelours Group greywacke which outcrops to the south west (Figure 2.11.) extending into Picton. Evidence of a shear zone on the shore platform in Picton Harbour is obscured at Pine Beach as there is no bedrock cropping out at the head of the bay. The eastern extent of the fault is also

A. LOCATION DIAGRAM

PICTON HARBOUR

WAIKAWA BAY

TZIIa

PINE BEACH

TZI

MARINA

POSSIBLE LOCATION OF
THE OLD FREEZING WORKS THRUST

SCALE
250 0 250 500m

B.

C. CROSS SECTIONS

200m

PROJECTED FAULT PLANE
OLD FREEZING WORKS THRUST
APPROX. DIP 30°

KEY TO MAP

- RIDGE TRACK
- BEDDING
- OVERTURNED BEDDING
- FOLIATION
- THRUST FAULT SHEAR ZONE
- F1 OVERTURNED SYNCLINE
- F1 OVERTURNED ANTICLINE
- F2 SYNCLINE AXIS
- FOLIATION FORM LINES
- ISOTECT BOUNDARY

FIGURE 2.11.: The Structural Characteristics of The Snout Domain

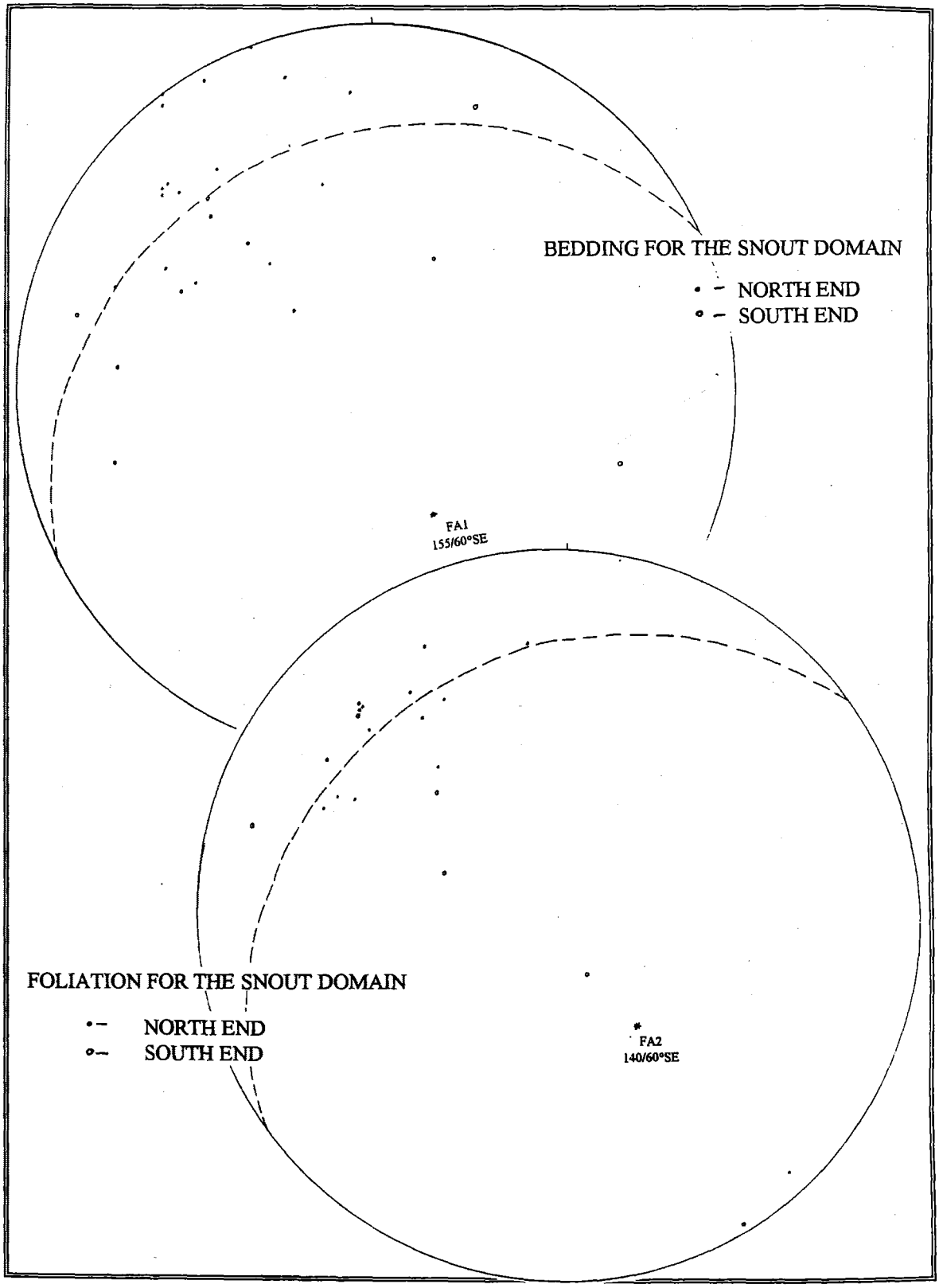

FIGURE 2.12.: Stereographic projections for The Snout Domain.

unknown (Figure 2.11.). The location and character of this discordance indicates that the structure may be the north eastern extension of the Old Freezing Works Thrust identified in Picton on the opposite side of the harbour (Nicol, 1988). As previously mentioned (Section 2.3.4.), the Old Freezing Works Thrust in Picton separates the TZII and TZIII schists from Pelours Group greywacke, has a variable strike and dips at approximately 20°-25° towards the north.

The structures identified on the Snout, including the F1 and younger phases of folding and the change in textural zone along the inferred location of the Old Freezing Works Thrust may be correlated with the structural characteristics of the Picton region (Nicol, 1988). The Picton region is dominated by the presence of north east trending pre-thrusting folds and Miocene thrusts which have been refolded by easterly trending, sub-horizontal upright and open folds (Nicol and Cambell, 1990) and which have resulted in an open basin and dome interference folding pattern. Therefore, it appears that The Snout may be included within the Picton Thrust System due to the similarity of structures with the western side of Picton Harbour.

2.4.2. Karaka Point

The western shore of Whatamango Bay shows the presence of multiple folding events influencing the character of the Karaka Point Domain which incorporates exposures between Waikawa Bay and western Whatamango Bay (Figure 2.13.). In addition to the information obtained along the shore platform from Whatamango Bay to Waikawa, correlation could be made with exposures along the Port Underwood Road approximately 20m upslope. However, data were limited along road exposures due to the intense weathering observed in the cut faces by comparison with slight weathering on the shore platform.

The rock material exposed from Whatmango Bay to Waikawa Bay ranges from weakly foliated greywacke (TZI) in the south eastern and south western sections increasing in metamorphic grade (TZIIa and TZIIb) towards Karaka Point while the cleavage is most intense in the finely laminated sandstone/mudstone lithologies and in more massive mudstone. The rock at karaka Point is dominantly schistose material (TZIIa) and grades in and out of more foliated material on what appear to be a lithologically controlled basis. Foliated rock is most pronounced between Wharatekura and Sunshine Bays (Figure 2.13.) and appears to grade into incipiently foliated greywacke material south of Wharetekura Bay. Schistose material is observed on the uppermost ridges which extend south into the Boons Valley catchment of Waikawa Stream, including the upper slopes east of Waikawa

township (McManus, 1994), but the relationship to either bedding locally or the shore exposures cannot be determined because of the limitations of the outcrop.

Mapping of bedding and younging directions indicate the presence of an F1 folding event which is evident as a series of anticlines and synclines whose axial traces may be identified along the coastal platform of western Whatamango Bay (Figure 2.13.). Bedding along the coast line is essentially vertical and strikes consistently towards the east. The Karaka Point Syncline, located to the south east of Karaka Point (Figure 2.13.), is an isoclinal fold with a steeply plunging fold axis while the axial plane dips moderately to steeply to the south, shown in the cross section along the foreshore of Whatamango Bay (Figure 2.13). South of the Karaka Point Syncline the next antiform, the Karaka Point Antiform, crops out and is also a plunging isoclinal fold with a northerly dipping axial plane (Figure 2.13.). The Karaka Point Antiform is thought to represent refolding of the F1 Karaka Point Syncline by later folding on the basis of younging directions indicating that the syncline is antiformal (Figure 2.13.). Further south is the Waipuna Synformal Anticline located just north of the Waipuna Headland (Figure 2.13.) which is also an F1 fold defined as a steep northerly dipping, steeply plunging isoclinal fold (Figure 2.13.).

The influence of the post metamorphic F2 phase of folding responsible for inverting these macroscopic folds has caused the transposition of the F1 fold axial planes (Figure 2.13.) and resulted in a series of kink fold associated with changes in cleavage dip directions. Figure 2.13. shows the position of the F2 folds in the Karaka Point Domain associated with cleavage directions. The F2 folds are steeply dipping towards the north with a shallow to moderate plunge (Figure 2.14.) and the F1 Karaka Point Syncline becomes refolded about the F2 folds reversing the dip of the axial plane and creating the Karaka Point Antiform (Figure 2.13.). The projected strike of the Waikawa Bay Fault north east of Waikawa may be related to the presence of kink folding south of Karaka Point. Althought there is no shear zone observed which may be related to the Waikawa Bay Faulttrace, the intense kink folding on a mesoscopic scale in Fault Bay is thought to represent the presence of faulting at depth which has not propogated to the surface. The faulting is therefore interpretated as being a blind thrust which is a splay of the main trace of the Waikawa Bay Fault inferred to be located off shore in Waikawa Bay (Figure 2.13.).

The stereoplots of foliation show that there is a significant scatter of all data points including the F2 structures which indicates that foliation is influenced by an F3 cross folding event (Figure 2.14.) however the lack of data restricts

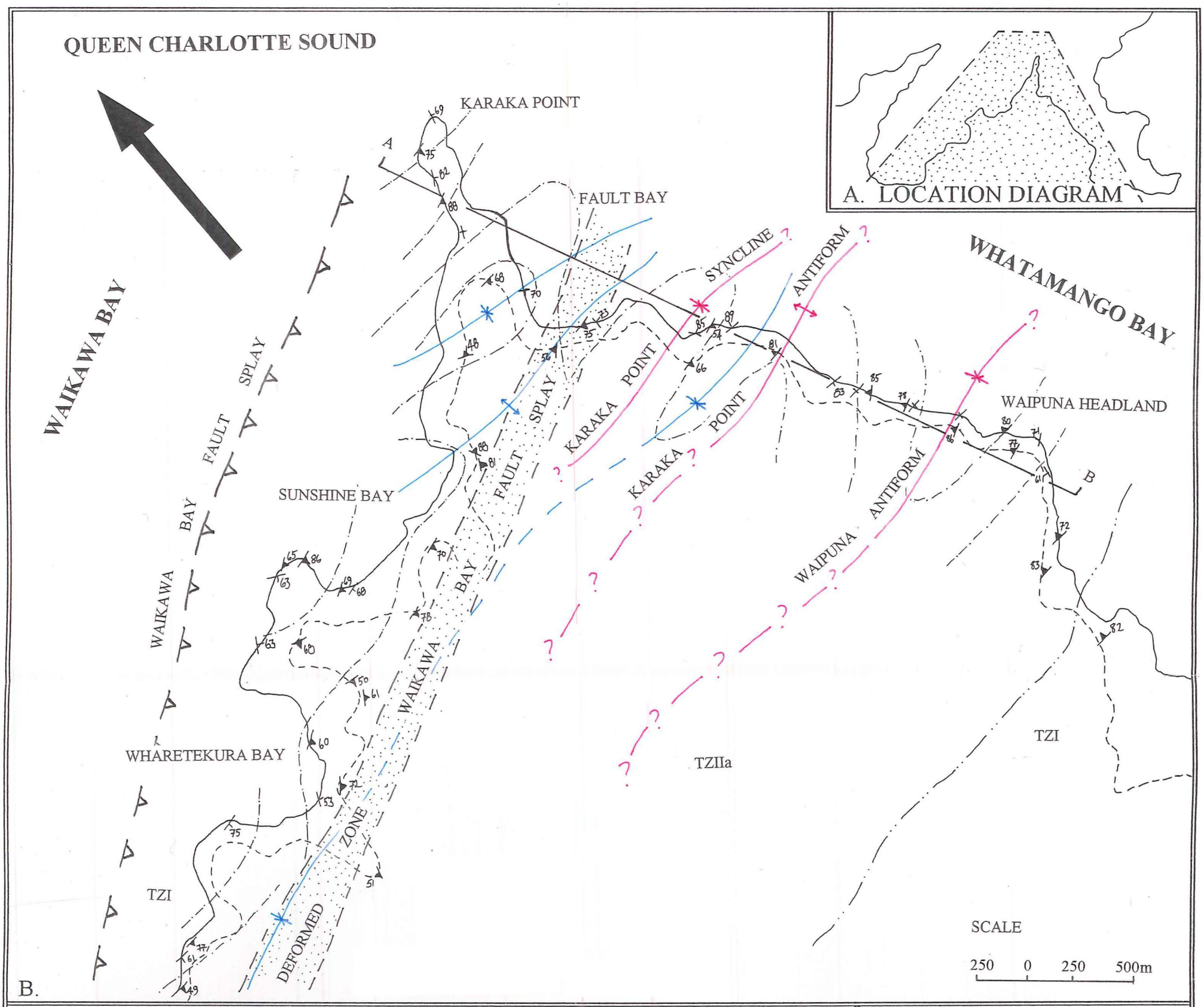

FIGURE 2.13.: The Structural Characteristics of The Karaka Point Domain

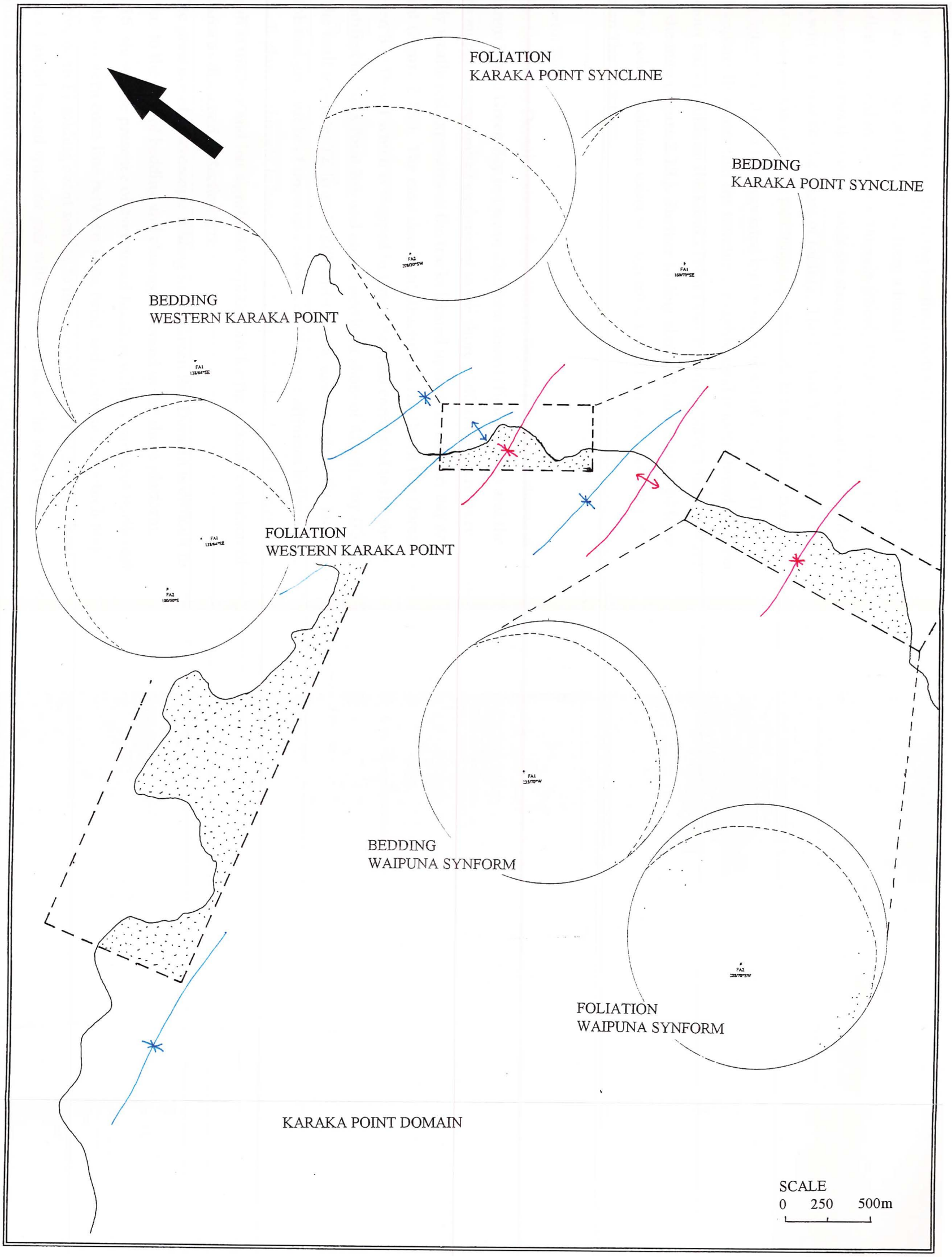

FIGURE 2.14.: Stereographic projections for the Karaka Point Domain

interpretation of the F3 structures in this study. It is important to note the disimilarity of the structural characteristics identified in the Karaka Point Domain with those of The Snout (Section 2.4.1.). The F1 structures on The Snout are dominantly overturned north east trending isoclinal folds which have been gently refolded by an open set of later folds to form a broad basin and dome formation similar to that observed in the Picton Domain (Nicol, 1988). The Karaka Point Domain however shows that the F1 folds are strongly refolded about east trending kink folds which define the F2 phase of folding. The F2 structures have caused significant transposition of the F1 fold hinges, particularly for the Karaka Point Syncline (Figure 2.13.) and the associated kink folding is not observed on The Snout. It appears therefore that the trends are roughly similar to the broad synform on The Snout but the folds on the Karaka Point Domain appear have a shorter wave length on the map (Figure 2.13.). Further folding about F3 axes is inferred from the scatter of poles to foliation using stereographic projection which is also not observed on The Snout.

2.4.3. Green Bay

The Green Bay Domain extends from Ahuriri Bay on the eastern shores of Whatamango Bay to Green Bay in Queen Charlotte Sound (Figure 2.15.) and the exposures mapped were limited exclusivley to the shore platform as there were only highly weathered exposures in the tracks located upslope of Ahuriri Bay and Tuna Point (Figure 2.15.). The most dominant structure of the Green Bay Domain is the Green Bay Thrust which is mapped in Green Bay and correlated to the shear zones identified in Tuna Point Bay and on the northern shore of Ahuriri Bay (Figure 2.15.). The fault separates TZIIb and TZIII schist on the eastern side of the fault from unfoliated greywacke of uncertain Pelorus or Waipapa affinities to the west and the fault plane is thought to have an easterly dip. The direction of movement on the fault is unclear and has significant implications for the tectonic evolution of the field area as discussed in Section 2.5.

The presence of macroscopic folding in the Green Bay Domain is difficult to identify due to the lack of bedding and cleavage exposed in the shore platform. Figure 2.15. shows the presence of overturned bedding with a consistent north east strike on the western coast line between Tuna Point and Motueka Bay which may be indicative of an F1 folding event similar to that identified on The Snout. There may be an F1 anticline and syncline pair with the anticline to the west (Figure 2.16.) which seem to have subhorizontal fold axes with axial planes dipping moderately to the SE and striking roughly towards the north east however the

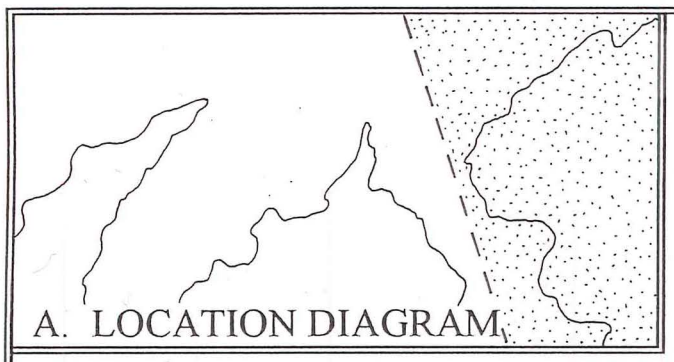

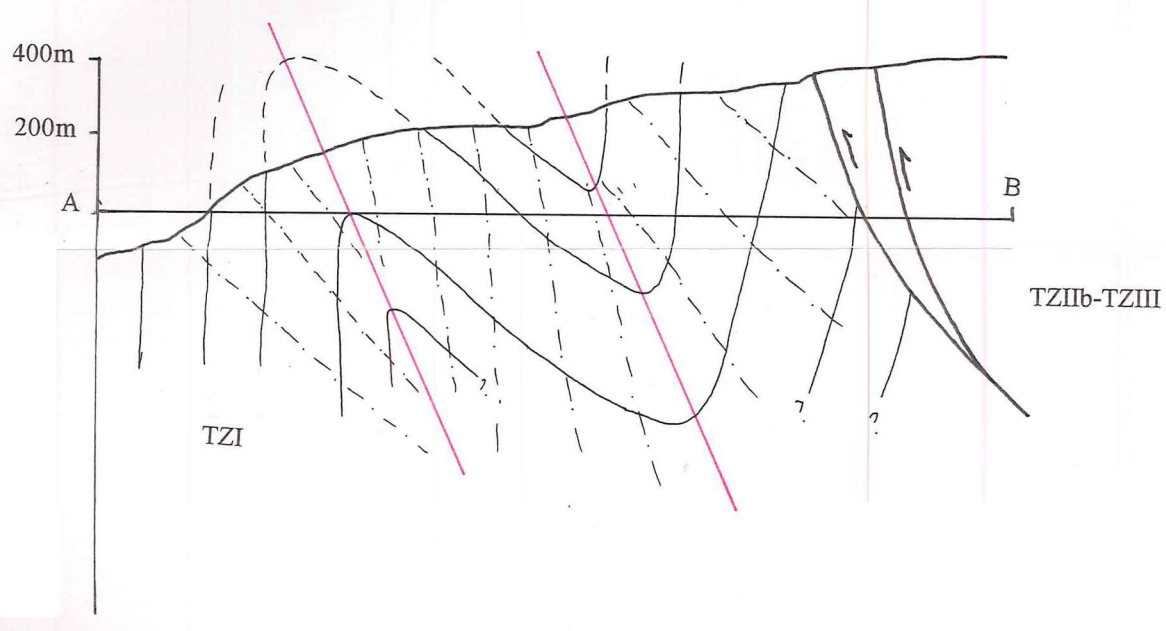

C. CROSS SECTIONS

KEY TO MAP

- BEDDING
- OVERTURNED BEDDING
- FOLIATION
- FOLIATION FORM LINES
- THRUST FAULT (INFERRED)
- SYNFORM AXIS
- ANTIFORM AXIS
- F1 FOLDING EVENT

FIGURE 2.15.: The Structural Characteristics of The Green Bay Domain

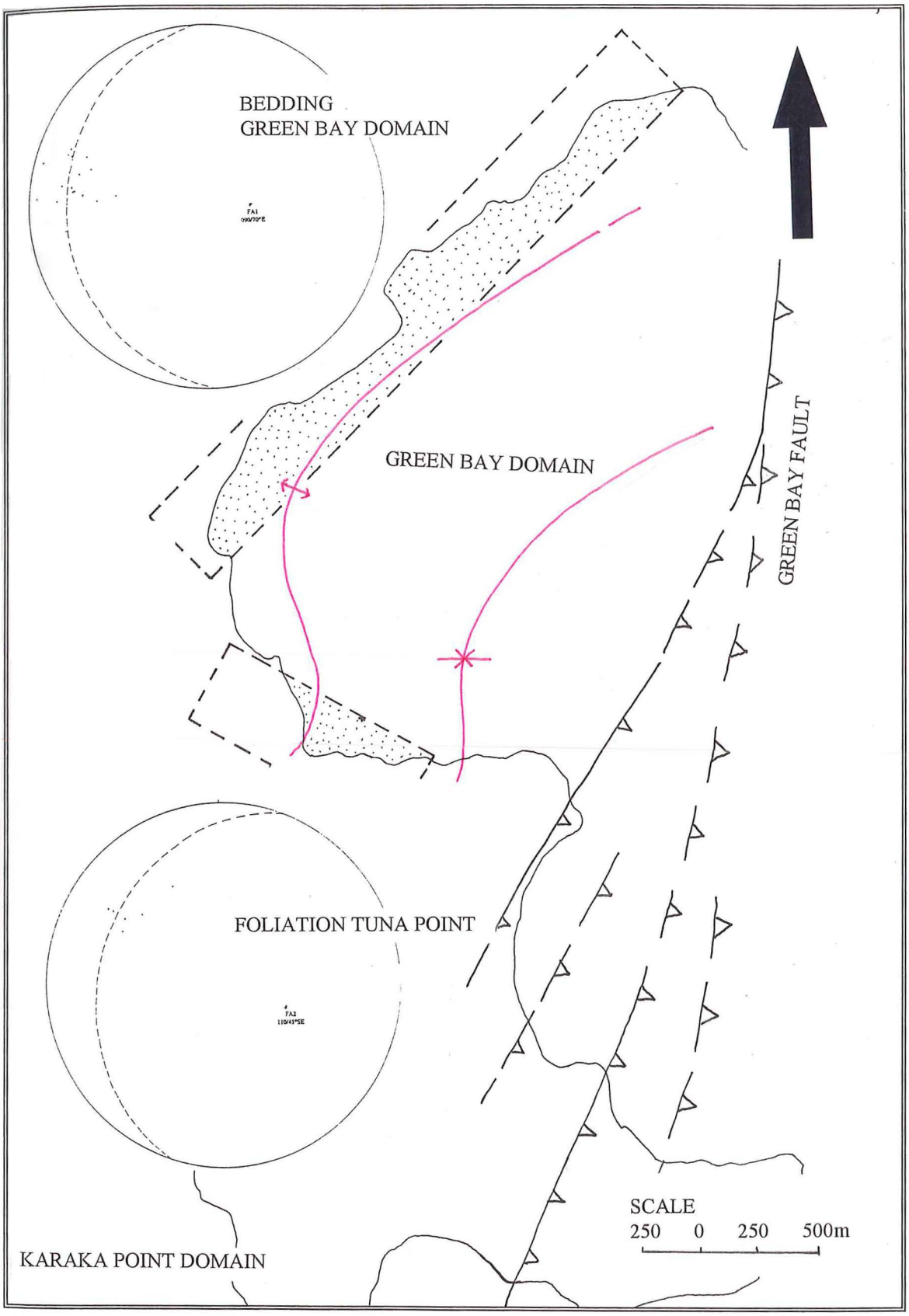

FIGURE 2.16.: The stereographic projections for the Green Bay Domain

majority of measured younging directions indicate that a syncline is present to the west and there are geometric difficulties in accounting for these smaller scale folds. It is thought therefore that the folding in the Green Bay Domain is dominated by a syncline to the west and a dominantly overturned sequence (Figure 2.15.) and the few anomalous younging directions measured indicate mesocsopic folding associated with the main folds.

Evidence for F2 folding is difficult to find as there is little difference between the trends of bedding and cleavage in the Green Bay Domain and the cleavage development is considered to be synchronous with F1.

The Green Bay Domain is noticibly different from the Karaka Point Domain due to the absence of the intense post metamorphic F2 folding events, and the nature the F1 axial planes. In the Karaka Point Domain, the axial planes are sub-vertical with steep northerly and southerly dips and steep fold plunges, while F1 axial planes in the Green Bay Domain are principally moderately inclined with overturned limbs, moderate easterly dips and sub-horizontal fold axes. The correlation of the Green Bay Domain with the structures identified on the Snout however may indicate that these two Domains are related because the F1 structures on the Snout are also sub horizontal folds which dip towards the east (Section 2.5.1.).

2.5. COMPARISONS BETWEEN DOMAINS

2.5.1. Folding

The comparison of folded strucures between the domains presented in this study and the Picton Domain (Nicol, 1988) indicates that there is possibly two distinctly different types of folding within the field area. In the Picton Domain and The Snout Domain, mapping identified an F1 fold pattern which has a north east trend and the folds themselves are generally moderately inclined isoclinal folds with moderate south west plunging fold axes (Figure 2.11.) and similar folding may be observed in the Picton Domain (Nicol, 1988). Furthermore the influence of later folding creating a broad basin and dome structure can be identified in both domains and the later folds trend NW-SE (Figure 2.11.). Cleavage development in The Snout Domain displays a similar orientation to bedding and therefore the cleavage is thought to have developed in relation to F1 development.

As previously mentioned (Section 2.4.3) the Green Bay Domain appears to display F1 structures similar to those identified in Picton and on The Snout. Although there are difficulties in ascertaining the relationship of younging directions to macroscopic folding, the folds present are north east trending

moderately inclined folds with overturned limbs (Figure 2.15.). The development of cleavage in the Green Bay Domain, like cleavage development in The Snout Domain, is thought to have been synchronous with F1 as there are no locations where bedding and cleavage are strongly discordant. Any minor discordance is thought to be the result of cleavage fanning in relation to F1.

The F1 fold patterns in the Karaka Point Domain are similar to those observed in The Snout and Green Bay Domains as the folds trend consistently east with steeply-moderately inclined axial planes although the fold axes in the Karaka Point Domain are more steeply plunging than those in the other domains which are sub-horizontal to gently plunging.

The presence of F2 structures in the field area are variable between domains with the Karaka Point Domain being the only location where F2 folding can be readily observed. The F2 structures are north east trending kink folds which have a shallow plunge and they are thought to be related to thrust movement of the Waikawa Bay Fault. The F2 folds refold the cleavage (S1) which developed in relation to the F1 structures and F2 is not clearly observed in either the Picton, The Snout or the Green Bay Domains although thrusting is identified in each domain.

Identification of an F3 folding event may be observed in all of the domains except the Green Bay Domain however, the presence of F3 folding in the Green Bay Domain is absent, however cannot be discounted as the data obtained from the domain was limited and may simply not represent the presence of gentle F3 structures. In the Picton and The Snout Domains the F3 folding resulted in a broad synformal feature which plunges moderately towards the east south east and is defined by a gentle swing in the strike of S1 cleavage (Figure 2.11). The F3 folding creates a broad basin and dome interference fold pattern. In the Karaka Point Domain the F3 folds have a shorter wave length than those observed elsewhere in the field area and all structures associated with the F3 folding phase are thought to post-date the thrusting events.

Table 2.2. summarises the nature of folding events for each domain identified in the field area.

2.5.2. Faulting

A number of faults and sheared zones have been identified in the field area and correlation of these faults across domains may provide some constraint on the possible origin of the individual domains.

Within the Snout Domain there is one inferred fault which crosses the Snout approximately at the position of the topographic break identified along the crest of

TABLE 2.2.: Summary of the folding events and the folding styles identified for each domain in the field area.

SUMMARY OF FOLDING STYLES			
DOMAIN	***F1***	***F2***	***F3***
Picton	• NE strike • Moderate-steep dip • Moderate plunge to the SW	• Not observed • Associated with thrusting	• Broad synform • Moderate plunge to the ESE
The Snout	• NE strike • Moderate-steep dip • Moderate plunge	• Not observed • Associated with thrusting	• Broad synform • Moderate plunge to the ESE
Karaka Point	• NW-SE strike • Moderate-steep dip • Steep plunge	• Kink folds striking to the NE • Shallow plunge • Thrust related	• Cross folding with a shorter wave length than other domains
Green Bay	• NE strike • Moderate dip to the SE • Low plunge • Overturned	• Not observed • Possible thrust associations	• Not expressed

the Snout. The fault appears to separate TZIIa schists to the north east from the Pelorus Group greywacke rocks present to the south west and extending into Picton. Although the fault was not observed, it is thought to pass through Pine Beach on the western side of the Snout and the location on the eastern side is undetermined (Figure 2.11.). The fault is thought to be the continuation of the Old Freezing Works Thrust identified by Nicol (1988) in Picton which also separates TZII and TZIII schists from the Pelorus Group Greywacke and the Oligocene sedimentary inliers in the Picton Domain (Figure 2.9.). The Old Freezing Works Thrust has a northerly dip between 20°-35°, striking across Picton Harbour, and it appears that the fault may have been folded down to the east which accounts for its presence across on the Snout. The presence of a sheared zone to the West of the Snout implies the influence of a significant fault which probably is located in Picton Harbour. The identiy of this fault is unknown however it is possible that faulting may be related to a strand of theWaikawa Bay Fault which has not broken to the surface. Similarly, the fault may be an as yet unidentified fault associated with the Picton Thrust Zone incorporating a west to east movement. However, without information as to the sense of dip on the shear zone identified on the western shores of the Sout, the identiy of possible contributing faults remains unclear.

The previous discussions (Section 2.5.1) has indicated that there are significant differences between the structure of the Karaka Point Domain and the Green Bay Domain which are located either side of Whatamango Bay. The differences indicate that there is a major discontinuity within Whatamango Bay and the nature of this feature is thought to be a faulted zone. The strike of this inferred fault is approximately NW-SE althought the dip of the feature is unknown and movement of the fault is believed to be dextral strike slip on account of possible dislocation of the Waikawa Bay Fault and the Green Bay Fault (See discussion below). The fault is not known to be observed on shore; further mapping of the Graham River catchment, the inferred position of the structure, would be necessary assess the onshore extent of any faulting. Figure 2.17. shows the inferred position of the Whatamango Bay Fault and the displacement of structures across it.

The Green Bay Fault separates the TZII and TZIII schists to the east from the unfoliated Pelorus Group greywacke to the west (Figure 2.15.) and the fault is a thrust structure which is believed to dip steeply towards the east. The direction of thrusting is uncertain although if the Green Bay Fault is correlated to the Waikawa Bay Fault (See below) then thrusting would be from the east to the west. The Green Bay Fault appears to splay at the southern end into Whatamango Bay and there is evidence for one of the splays on the southern coast of Ahuriri Bay (Figure 2.15.)

and the fault is thought to be influenced by later faulting which defines Whatamango Bay as the Whatamango Bay Fault (Figure 2.17.).

The Waikawa Bay Fault appears to be a major discontinuity in the field area as it separates the Snout and Picton Domains from the Karaka Point Domain, previously identified as a structurally separate domain (Section 2.5.1.). The Waikawa Bay Fault, where it is observed in Waikawa is a steep east dipping thrust fault with the eastern side being upthrown and a component of dextral strike slip motion. The fault strikes approximately NE and is inferred to splay at the north eastern end with the main fault trace heading off shore into Waikawa Bay (Figure 2.13.). Splays of the Waikawa Bay Fault which have not broken to the surface may be inferred south of Karaka Point in Whatamango Bay due to the intense kink folding in this area (Section 2.4.2.). The extension of the Waikawa Bay Fault into Whatamango Bay from the Karaka Point splay is thought to be offset by the Whatamango Bay Fault and may possibly be correlated with the Green Bay Fault on the eastern side of Whatamango Bay (Figure 2.17.). However this inference is tentative as the structure east of the Green Bay Fault is unknown and is only assumed to be similar to that identified in the Karaka Point Domain although correlation of structural characteristics west of both the Waikawa and Green Bay Faults indicates that they may both be the same structure. Such a correlation would suggest that the Whatamango Bay Dault may function as a shallow strike-slip transfer fault separating the Waikawa Bay Fault as a more westerly advancing lobe of the whole thrust system. If so there is no requirement that this fault either extends into the lower plate or strikes far into either Queen Charlotte Sound or the Graham Valley. Further mapping is needed to confirm this theory and is considered to be outside the scope of this thesis.

2.6. CONCLUSIONS AND REGIONAL CROSS-SECTION

The structural characteristics of the field area indicate that there are two distinct types of deformation which have occurred and the areas which are affected by the deformation are separated by significant faulting represented by the Waikawa Bay and possibly the Green Bay Faults. The field area can therefore be separated into two zones incorporating domains which encompass similar types of deformation; Zone 1 represents the Picton Domain, The Snout Domain and the north western portion of the Green Bay Domain, while Zone 2 incorporates the Karaka Point Domain and tentative correlation with the eastern portion of the Green Bay Domain. The deformational phases identified for Zone 1 and Zone 2 are summarised in Table 2.3.

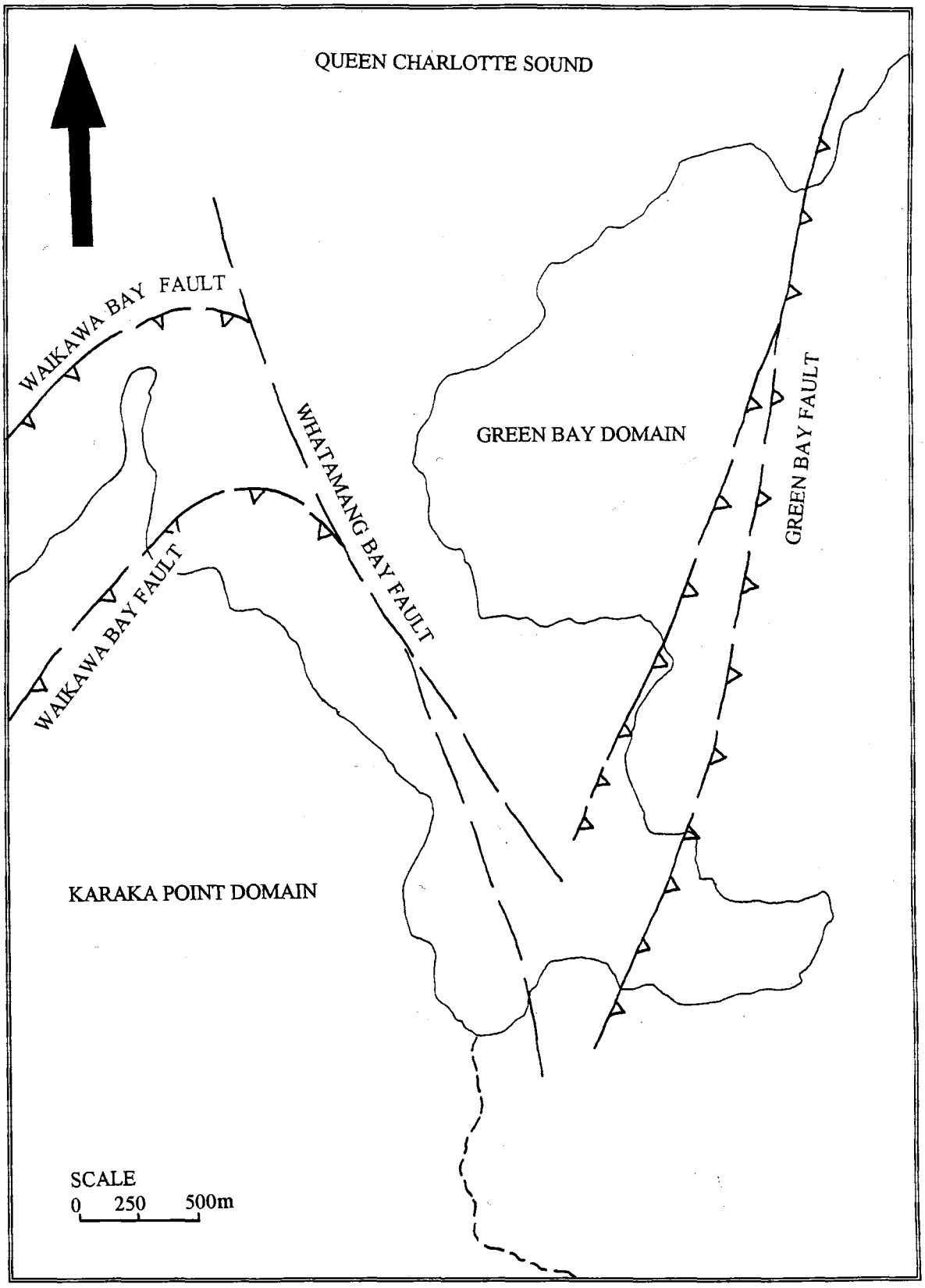

FIGURE 2.17.: The inferred location of the Whatamango Bay Fault separating the Green Bay and Karaka Point Domains. The fault is thought to be a transfer fault bewtwwn the Waikawa Bay Fault and the Green Bay Fault.

TABLE 2.3.: Summary of the deformational phases identified in the field area separated into two separate zones reflecting different types of deformation.

SUMMARY OF DEFORMATION EVENTS				
ZONE	***DOMAINS***	***D1***	***D2***	***D3***
ZONE 1	Picton The Snout NW Green Bay	• Syn-metamorphic folding (F1) • Axial planar cleavage development (S1)	• Thrust faulting during the Miocene	• Cross-folding into broad open folds • Basin and dome structures: post-metamorphic
ZONE2	Karaka Point [East Green Bay ?]	• Syn-metamorphic folding (F1) • Axial planar cleavage development (S1)	• Development of kink folds	• Cross-folding about NE-SW axes • Folded F2 axes

The first deformational episode, D1, is associated with a syn-metamorphic folding event F1, which saw the development of a set of steep-moderate dipping, sub-horizontal isoclinal folds whose axial traces strike in a north easterly direction in Zone 1. In Zone 2 however the F1 folding was a syn-metamorphic event producing a moderate to steeply dipping, steeply plunging isoclinal fold set which strike in a NW-SE direction. D1 is assumed to be Mesozoic, possibly Late Jurassic deformation and regionally can be expected to involve more complex deformation which could affect the orientation of F1 from place to place thus accounting for differences between Zone 1 and Zone 2. The development of S1 cleavage is also associated with D1 as an axial planar cleavage.

The principal event for both Zones in D2 is the onset of Miocene thrust faulting of the Old Freezing Works Thrust, the Waikawa Bay Fault and the Green Bay Fault. During this period the Whatamango Bay Fault is also thought to have developed in response to thrusting along the Waikawa Bay and Green Bay Faults. Thrust faulting in Zone 2 is expressed by the development of kink folds which have folded the S1 cleavage. The influence of thrust faulting along the Waikawa Bay Fault is thought to have caused the overthrusting of the Zone 2 rocks over the Domains composing Zone 1.

D3 is a post metamorphic and post thrusting deformation event which is principally defined by the development of cross folding in both Zone 1 and in Zone 2. The cross folding in Zone 1 is represented by broad open folds which have produced a basin and dome interference pattern extending throughout the Picton and The Snout Domains. The presence of such folding in the western Green Bay Domain, as previously discussed, cannot be discounted due to the limited data. Cross folding in Zone 2 displays a considerably shorter fold wave length than that observed in Zone 1 and results in the folding of F2 structures about NE-SW axes.

The regional tectonic implications of the faulting and folding identified in the field area are affected by the current theories regarding terrane analysis in the south eastern Marlborough Sounds discussed by Nicol (1988) and Mortimer (1993) and summarised in Section 2.3. The Waikawa Bay Fault is an important constraint on the structural development of the field area as the fault is apparently anamolous to the structure identified by Nicol (1988) were the transportation direction for thrust movement in the Picton region is from the west to the east with faults dipping towards the west (Figure 2.9.). The Waikawa Bay Fault however has an easterly dip and thrust movement on the fault implies an east to west transport direction and may provide the necessary structure for Mortimer's theory (1993) for east to west emplacement for the Waipapa Terrane (Section 2.3.2.). The Mortimer

model would require overthrusting of the Waipapa Terrane over the Caples Terrane rocks to the west and if the Waikawa Bay Fault represents the base of the Waipapa Terrane, the west to east thrusting identified in Picton would constitute a faulted wedge underneath the roof thrusts of the Waipapa Terrane. Figure 2.18. shows the location and sense of movement on all of the faults identified in the field area and the cross section shows a schematic reconstruction of the fault relationships assuming that the Waikawa Bay Fault has overthrust Waipapa Terrane over the adjacent rocks to the west.

Problems are encountered with the overthrusting model presented in Figure 2.18. with regard to the time required to complete the amount of movement implied by the model. Nicol (1988) associated thrust faulting in the Picton Domain with Miocene tectonism and any movement of the Waikawa Bay Fault would have been after the emplacement of the Picton thrust wedge. Significant erosion is also necessary following thrust movement to remove evidence of the roof thrusts from the Picton region and it is unknown if the deposition of such large amounts of sediment into sedimentary basins adjacent to the Marlborough Sounds region has occurred.

An alternative solution to account for the presence of the Waikawa Bay Fault is that the fault is considerably younger than the faults identified in Picton and a dominance of strike slip movement, combined with oblique thrusting has transported the Karaka Point Domain into its present position and the structure of the domain may be related to Waipapa Terrane rocks from another location but still within the Marlborough Sounds Region. Evidence for this hypothesis is scarce and requires substantial mapping across Queen Charlotte Sound to find correlatives of the Karaka Point Domain structure. Therefore, the overthrusting model of the Karaka Point Domain, a possible correlative for the Waipapa Terrane, over the Caples Terrane to the west creating a fault wedge in the Picton region, is tentatively favoured in this study.

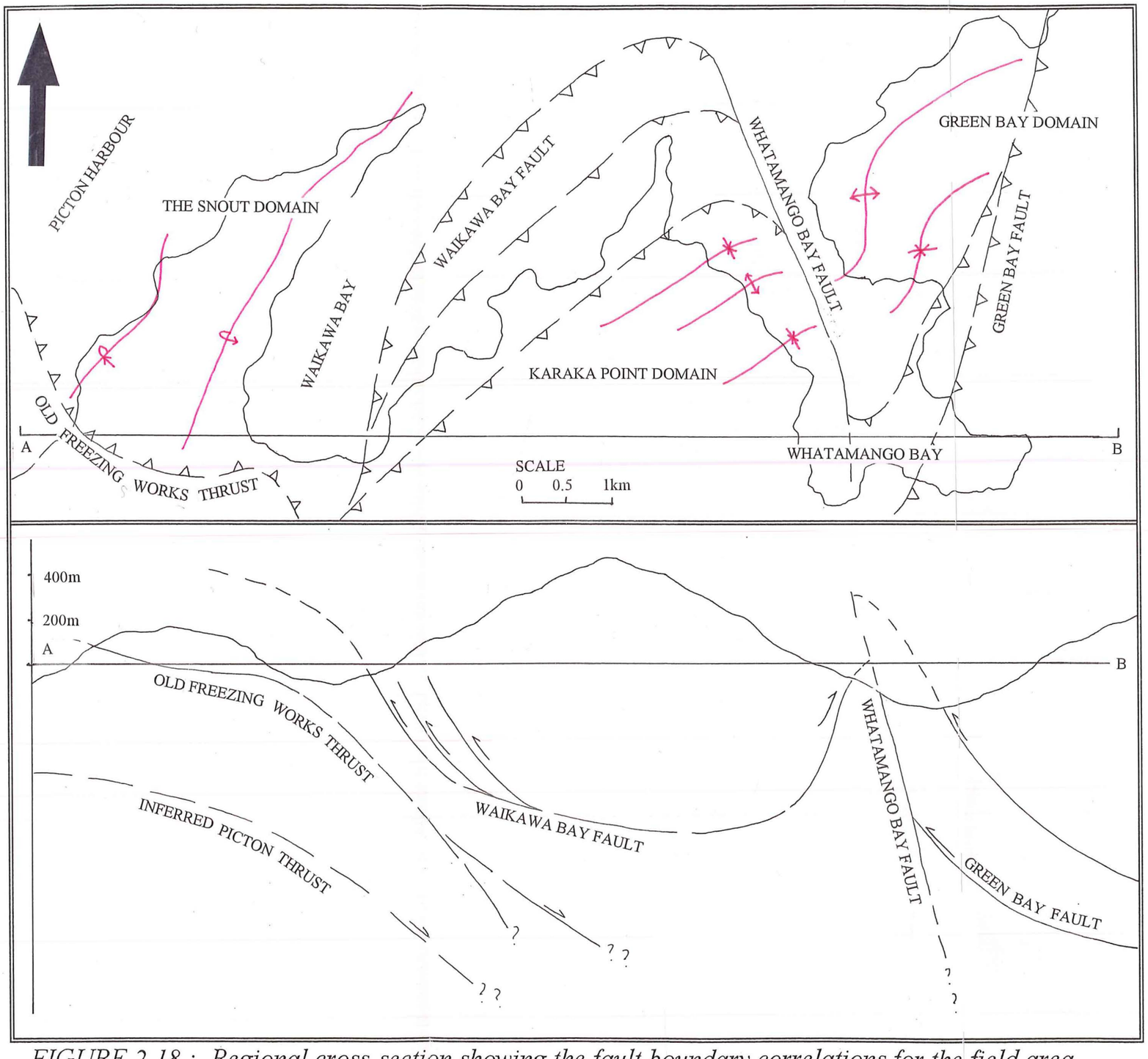

FIGURE 2.18.: Regional cross-section showing the fault boundary correlations for the field area

CHAPTER THREE GEOMORPHOLOGY

3.1. INTRODUCTION

This chapter is concerned with the evolution of the present landscape within the field area and the processes which have modified, and continue to modify, the landscape, the deposits produced by the processes and their relative distribution. The geomorphic history of the field area is studied from the Pleistocene through to the present day and concentrates specifically on the periglacial and interglacial climates and their influence on the distribution and type of surficial deposits found in the field area at present.

An engineering geological assessment of an area requires knowledge of the relative ages of geomorphic surfaces and the geological processes which have shaped the landscape in order to assess the activity and subsequent hazard potential of any given process at a particular site. Therefore a study of the geomorphology of the field area will provide age constraints for the development of alluvial terraces and fans, debris deposits and slope failures in addition to an estimate for the age of last rupture of the Waikawa Bay Fault. Furthermore, the distribution of regolith and surficial deposits such as alluvium, colluvium and debris deposits will indicate those areas which have remained relatively stable or insitu during landscape development and those areas which have been subject to substantial alteration as a result of the active geomorphic processes. This chapter identifies the surficial materials in the field area, their distribution and characteristics, the nature of the processes which have formed the surficial deposits and the order of the principal geomorphic events in the field area.

3.2. WEATHERING PROCESSES

3.2.1. Mechanisms of Weathering

a) Processes

The periglacial and interglacial climatic fluctuations during the late Quaternary have had a significant effect on the development of the Marlborough Sounds, principally due to deep weathering produced during warm interglacial climates. The Marlborough Sounds are geologically well known for the high degree of weathering of bedrock units which is a combination of chemical, mechanical, and biological processes acting in response to tectonic and climatic influences (Section 3.6. and 3.7 respectively). The processes involved in weathering may be classified as endogenetic; those which relate to the mineralogy and structure of the rocks, and exogenetic factors; climate, vegetation, and other external influences (Small and Clarke, 1985).

In the Marlborough Sounds the endogenetic factors are seen most clearly in the preferential weathering of fine grained rocks and zones of weakness such as shear

zones. Mudstones have considerably more mineral grain boundaries and planes of weakness due to the small size of the constituent minerals in mudstones and thus weather much more easily than sandstone. The mineralogy of the rocks is also important as minerals such as feldspar will weather more quickly than the resistant minerals such as quartz. Additionally, foliation surfaces in schistose material, faults and fractures, at macroscopic and microscopic scales, are planes of preferential chemical and mechanical weathering again because of the smaller grain size in mudstones than in sandstones and because of multiple shear planes in the mudstones. As foliation and shear zones develop, the material being metamorphosed or sheared may undergo a grain size reduction in response to the new geological conditions imposed. For example, tectonic influences on the landscape prior to or during the early Quaternary have produced major shear zones presently defined by the alignment of the major valleys such as Queen Charlotte Sound, which have developed partially from grainsize reduction of material within the shear zone and the movement of water through the zone, and partially from preferential weathering of these structures. Weathering of sheared zones occurs macroscopically at outcrop scale, and can also be seen in hand specimen and thin section.

Exogenetic factors in the Marlborough Sounds generally involve late Quaternary climatic fluctuations. Although the major glacial ice advances of the Pleistocene did not reach to the Marlborough Sounds, the region was subjected to periglacial climates in response to the major glaciations occurring to the south and south west. The intervening periods between the major glacial advances saw the temperatures rise and in the Marlborough region, as elsewhere, there was a return to interglacial climates. Both periglacial and interglacial climates have contributed to the mechanical and chemical weathering of bedrock since the Late Tertiary. Freeze and thaw weathering action combined with mineral decomposition has led to the development of significant deposits of residual soils or regoliths overtop of the bedrock.

Almost all of the bedrock exposed in the Marlborough Sounds has undergone some degree of weathering during the Quaternary. Fresh rock outcrop is very limited and therefore, from an engineering and planning perspective, analysis of the geotechnical properties and extent of weathered rock which forms the foundation material is very important. The weathering front in the Marlborough Sounds can be up to 30m deep from fresh, unweathered bedrock at the base to completely weathered regolith near the surface. Typically 15 m thick weathered outcrops are observed in the field area along road cuttings and generally range from slightly weathered rock material at the base to a completely weathered regolith overlain by colluvium deposits. Figure 3.1. shows a weathered bedrock batter cut in greywacke displaying the gradation of weathering from the top of the batter in regolith to the base of the batter which is moderately weathered bedrock. The influence of rock

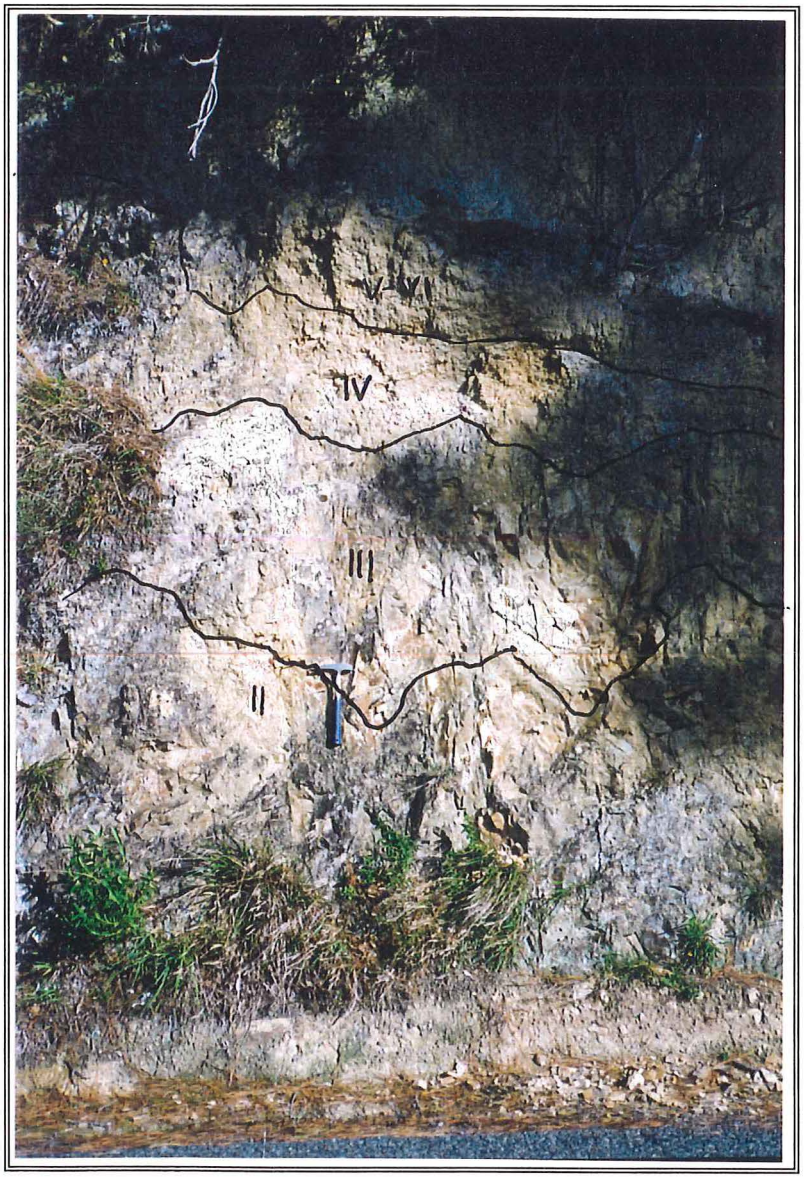

FIGURE 3.1.: *Weathered greywacke bedrock showing the gradation of weathering grades from Grade II through to Grades V-VI.*

defects is observed by the increased weathering along the joint and fracture surfaces. In schistose bedrock the influence of lithology on weathering is similar to that of jointing and fracturing where the pelitic or mud rich layers are often more easily weathered than the quartz rich or psammitic layers.

b) Rock and Soil Terminology

There is a great deal of literature dealing with definitions of weathered materials, however it is difficult to find consensus regarding what constitutes rock and soil. The definitions of rock and soil in this study follow the engineering geological descriptions introduced by Bell and Pettinga (1983; Appendix C1). The engineering geological descriptions are principally concerned with the strength and coherence of materials to define the boundary between rock and soil for engineering purposes. In contrast the geological definitions presented by Bell and Pettinga (1983; Appendix C1) deal with mode of origin of the material, for example sedimentary, igneous or metamorphic, and the distinction between rock and soil uses the position of the modern weathering front rather than the strength or coherence of the material. In this study the classification of rock and soil use the field classification scheme from Bell and Pettinga (1983) which includes weathering, strength, colour and fabric to describe rock (weathering grade I-VI; Appendix C2) and weathering, water content, strength, colour and fabric to describe soil (weathering grade V-VI; Appendix C2).

Weathering zones and grades must also be defined. Zones of weathering have received extensive coverage in the literature (Saunders and Fookes, 1970; Deere and Patton, 1971; Grainger and Harris, 1986) and are summarised by Kingsbury (1987). The zonation of weathering adopted in this study and shown in Table 3.1. follows that presented by Kingsbury (1987) and is modified from Deere and Patton (1971). The weathering zones in Table 3.1. cover both soil and rock material and can be identified in the field area in greywacke and schistose rock or soil. Summarised in Table 3.1. are the unit descriptions for this study as introduced by McManus (1994) as well as a graphical representation of the soil and bedrock units identified.

c) Weathering Grades

Bell and Pettinga (1983) developed a weathering classification which allowed the identification of individual weathering zones by way of simple visual characteristics and the principal features for identification of each zone are presented in Table 3.2. In the field area weathering Grade I is fresh greywacke or schistose rock material which has not undergone any identifiable alteration due to weathering and is found in areas such as deeply incised streams where weathered material is often removed. The greywacke and schistose materials in the field area are comprised of greenish grey sandstone and darker grey mudstone layers which display foliation in the schist. The only visual change in the rock as weathering increases from Grade I to Grade II is a slight medium brown discolouration of the rock mass produced by iron oxide alteration on the defect surfaces while the rock strength remains

TABLE 3.1.: A description of the typical profile identified in the field area combined with a graphic log (McManus, 1994) and correlated with weathering zones from Kingsbury (1987).

BEDROCK PROFILE AND WEATHERING ZONES			
Unit Description		Depth	Graphic log
This Study (After McManus, 1994)	**Kingsbury** (1987)		
TOPSOIL Usually dry-moist, light-dark brown/black extensive rootlets with some lithic content		0 to 0.2m	
LOESS Light yellow-white sandy silt, dry-moist, non-plastic with highly weathered clasts		0.2-0.4m	
COLLUVIUM **Top:** Highly-completely weathered gravely clay. Disorientated lithics of mixed lithological origin. Matrix is mottled yellow/white or blue clay, moist-wet, moderately plastic.	**A. Colluvium**	0.4 to 1.4-3.4m	
Base: Coarse mod-highly weathered, blocky, clayey gravel. Angular clasts in yellow/white or blue clay matrix. Clast supported with disorientated clasts. Irregular and sharp basal contact, gradational upper contact.			
BEDROCK **Regolith:** Completely weathered and mottled clays, yellow/white or blue, moderately plastic.	**B. Regolith** Ba Horizon (Eluviation) Bb Horizon (Illuviation) Bc Horizon (Saprolite)	1.4-3.4 to 7.0m	
Weathered bedrock: Highly weathered, moist-wet, gravely clay. White veining represents weathered joint surfaces. Clasts have orientation of insitu bedrock.	**C. Weathered Rock** Ca Horizon (Transition Zone)	7.0 to 15m	
Moderately-unweathered rock, original structures intact. Joint surfaces have iron oxide staining and some white clay formed.	Cb Horizon (Partly weathered) **D. Unweathered Rock**	15+m	

TABLE 3.2.: Desriptions of the weathering grades used in this study to describe weathered rock material (After Bell and Pettinga, 1983).

ROCK WEATHERING		
TERM	GRADE	ROCK DESCRIPTION
Residual Soil (RW)	VI	Discoloration and complete transformation to soil, original fabric destroyed.
Completely Weathered (CW)	V	Discoloration and transformation to soil, original fabric largely preserved.
Highly Weathered (HW)	IV	Material pervasively altered with discoloration and loss of strength, fabric preserved, lithorelicts.
Moderately Weathered (MW)	III	Penetrative discoloration and alteration of rock material with some loss of strength.
Slightly Weathered (SW)	II	Slight discoloration of rock fabric, no loss of material strength.
Unweathered (UW)	I	No discoloration or loss of strength or any other effects due to weathering.

unaltered. Rock defects such as joint surfaces and foliation planes display higher weathering due to the water being transported along these features and therefore within Grade II weathered rock there may be zones of Grade III or IV along these surfaces.

Weathering Grade III, however, begins to show a brown discolouration which penetrates the rock fabric, although the original colour of the rock is still evident. The rock begins to lose strength due to alteration of the rock fabric as minerals such as feldspar begin to weather to sericite and other clay minerals (Chapter 5). As the rock material becomes more highly weathered and changes to Grade IV, the rock looses all of its original colour and becomes a medium to light brown. The rock strength continues to deteriorate but the rock fabric, although highly altered, is still evident. Weathering, as previously mentioned, is accentuated by fracturing and foliation within the rock mass and these relict features can be seen, particularly in the higher grades of weathering.

As the degree of weathering increases to Grades V and VI the rock material is progressively altered to soil material which is termed regolith in this study and is described in Section 3.2.2. Regolith material is an unconsolidated unit which has a uniform strength despite the presence of relict planes of weakness such as bedding, foliation and joint surfaces. Additionally the grain size of the regolith varies with weathering grade ranging from a gravelly silty clay (Grade V) to a clast-free clay with some silt (Grade VI). Figure 3.2. shows the gradation of weathering in jointed schistose bedrock from Grade II at the base to Grade V, regolith, at the top, a total depth of approximately 15m.

3.2.2. Regolith Deposits

The definition of regolith in this study is insitu weathered bedrock and in the field area regolith deposits are often caused by chemical weathering prevalent during interglacial periods. The original fabric of the bedrock material, bedding, jointing or foliation, are still discernible in the regolith in the form of lithorelics, this being the principal distinction from fine grained colluvium which displays complete disorientation of the clasts with regard to their original bedrock orientation. Because the bedrock structures retained in the regolith material are relict and are completely weathered they do not influence the strength of the regolith material, for example there is no reduction of strength associated with joint surfaces in regolith as would be expected in unweathered bedrock. Regolith material, although being defined as weathered bedrock, displays the characteristics of an engineering soil (Section 3.2.1.) and therefore the boundary between weathered rock and soil is transitional.

Using the weathering classification of Bell and Pettinga (1983; Section 3.2.1.) regolith material in the field area includes weathering grades V (completely weathered) and VI (residual soil; Table 3.2.). Both weathering grades indicate the

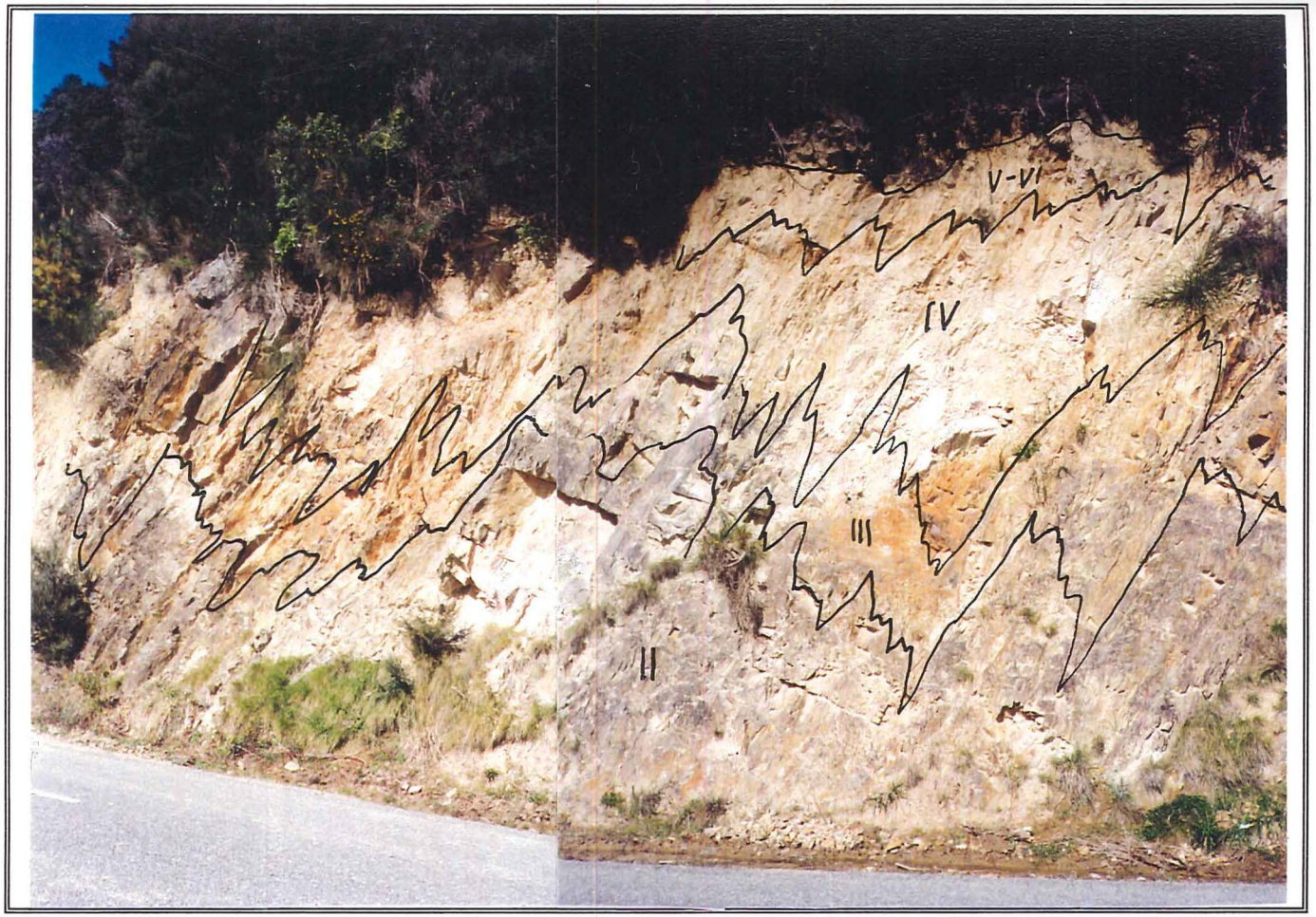

FIGURE 3.2.: *Weathered schist outcrop showing the influence of foliation on weathering grades. The outcrop is approximately 15m high and ranges from Grade II at the bottom to Grade V-VI at the top.*

complete weathering to 'soil' material, with the principal difference between weathering grades being the preservation of the original rock fabric in completely weathered rock (Grade V) and its absence in Grade VI (Table 3.2.). Table 3.1. shows the typical profile of weathered bedrock in the field area, including the distinction between regolith and weathered rock, while Figure 3.1. shows a weathered bedrock profile in which the gradation is moderately weathered rock (weathering grade III) through to regolith material (weathering grade V-VI). Within the field area the development of regolith within the overall weathering profile reaches a maximim thickness of 4m on the more gentle slopes (<15°) where the regolith has not been modified by slope wash processes, and on the very steep slopes (>35°) has been stripped off as a result of slope wash and gravity to become incorporated into colluvium deposits.

3.2.3. Red Weathering

Red weathering is widespread throughout the Marlborough Sounds, recognised from at least Havelock (Kingsbury, 1987) to Waikawa (Horrey, 1989, McManus, 1994), and is believed to correlate to red regolith development in the Wellington region (Te Punga, 1964). The age of red weathering has been tentatively correlated with interglacial climates during which times chemical weathering of exposed surfaces dominated over the freeze/thaw mechanical weathering principally associated with periglacial climates. According to Te Punga (1964) red weathering development requires a tropical or sub-tropical climate including a mean annual temperature in excess of 15.5° C, an annual rainfall of more than 1020mm/yr and a hot and dry season (Te Punga, 1964). As discussed by Kingsbury (1987) the present conditions in the Marlborough Sounds are not suitable for the development of red weathered profiles because although the annual rainfall is higher than that required (Chapter 1) and the Sounds do experience a hot and dry season the mean annual temperature is only 11° C and considerably lower than that required.

Although the youngest phase of red weathering is associated with the Oturian Interglacial (120-80ka BP), the main phase of red weathering is thought to be associated with the 250ka BP Terangian Interglacial (Kingsbury, 1987; Te Punga, 1964) and red weathering is also possibly correlated to surfaces as old as Late Pliocene (1.8Ma BP; Te Punga, 1964). Hematite (Fe2O3), which is anhydrous ferric oxide, has been identified as the mineral which causes the red colour in the red weathered surfaces (Te Punga, 1964).

The preservation of instu red weathered profiles (Figure 3.3.) in the field area is restricted to remnant spurs and ridges similar to profiles identified in Havelock (Kingsbury, 1987) and the older (Pre-Otiran) alluvial surfaces in Waikawa (Horrey, 1989). A red weathered ridge is present on the eastern side of Whatamango Bay (Figure 5.3. Map Volume) and the Wo alluvial terrace in Waikawa Stream displays a

red weathered profile (Section 3.7.1.) which may be correlated with a corresponding alluvial terrace on the eastern slopes of Waikawa township (Section 3.7.1.). Using X-Ray diffraction the mineralogy of the red weathered regolith material (Chapter 5) in the field area indicated the presence of imogolite ($Al_2O_3.SiO_2.2.5H_2O$; Brindley and Brown, 1980) which was not observed in any material not subjected to red weathering. Imogolite is thought to be the weathered remains of volcanic glass and its presence in the field area may represent a volcanic ash deposit possibly related to volcanic eruptions in the North Island. Red weathering may therefore be used to estimate minimum ages of these surfaces rather than the deposits because if the last phase of red weathering occurred during the Oturian interglacial (120-80ka BP) then the age of the red weathered surfaces may be considered 80ka BP or older (Section 3.7.).

3.3. SLOPE DEPOSITS AND PROCESSES

3.3.1. Mass Wasting and Colluvium

In the field fine-grained matrix-rich colluvium may be difficult to distinguish texturally from insitu weathered bedrock, however the method of emplacement differs markedly because colluvium is the product of weathered bedrock which has been transported downslope by gravity and/or slope wash processes. Regolith is here defined in comparison as insitu weathered bedrock which has not been subject to any transportation downslope. The clasts in regolith thus reflect the original orientation of features such as bedding and jointing in unweathered bedrock. In contrast to regolith clasts, all clastic fragments in colluvium are angular to sub-angular and have a distinctly random orientation (Figure 3.4.). Figure 3.5. is a diagrammatic representation of the orientation of clasts within colluvium compared to those present in regolith deposits showing the random orientation of clasts in the colluvial material. Due to the slope wash mechanism of transportation, colluvium varies in texture reflecting proximity to the original weathered surface. Coarse and poorly sorted blocky colluvium contains angular clasts 30-40 cm in diameter, which indicates that the material has not been transported far from the original source area, and because these deposits occur on the higher slopes (above 200m) they are thought to represent periods of mass wasting during periglacial climates in the field area (Kingsbury, 1987). The blocky slope failure deposits have subsequently undergone chemical weathering during the interglacial periods to produce a silty clay matrix. Additionally the size of the clasts in the blocky colluvial material reflects the joint spacing and degree of fracturing within the original bedrock material.

Colluvium may be considerably more matrix-rich and depleted in lithic content towards the base of slopes, indicating the deposition of fine materials by slope wash processes and greater distance from source material. Generally the coarse-grained and clast supported deposits on the lower slopes are related to slope failures

FIGURE 3.3.: Red weathering along the Port Underwood Road east of Whatamango Bay. The red weathering has occurred in greywacke regolith and indicates a minimum age for the surface of 80ka BP.

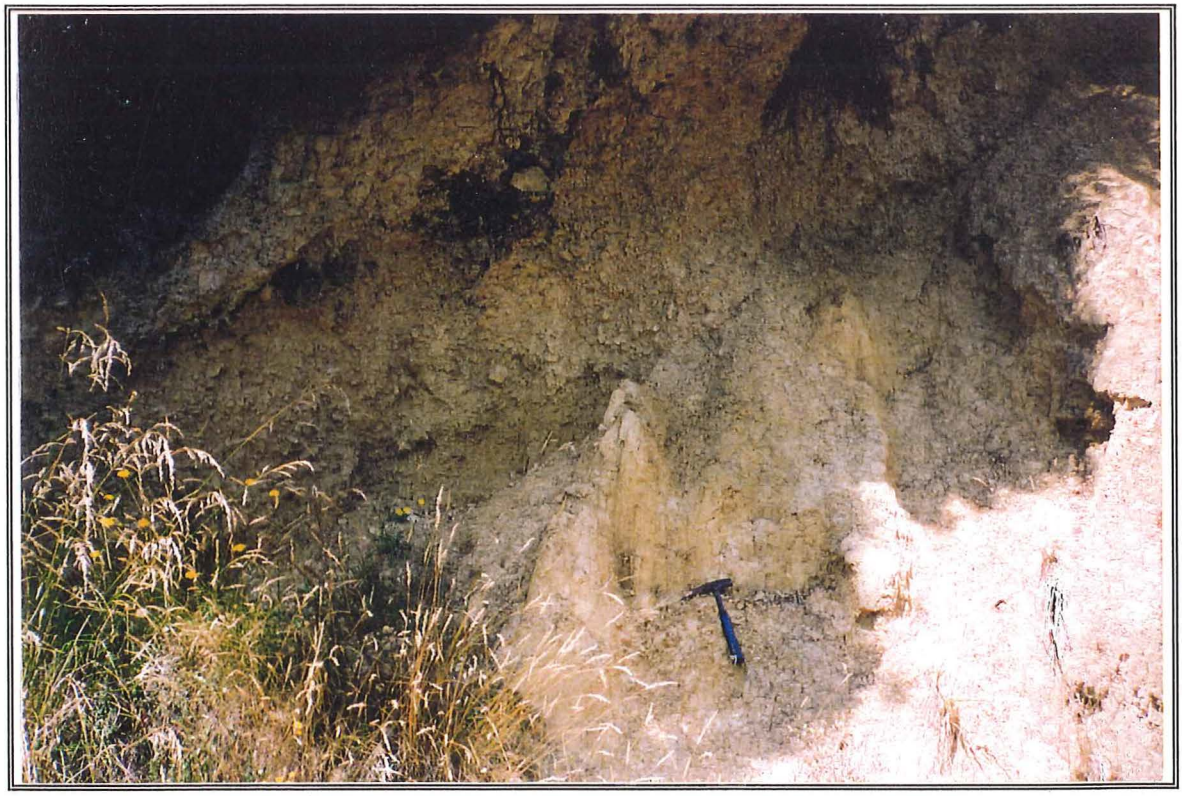

Figure 3.4.: *A colluvial profile over bedrock showing the random orientation of colluvial clasts and the uneven contact of colluvium over bedrock.*

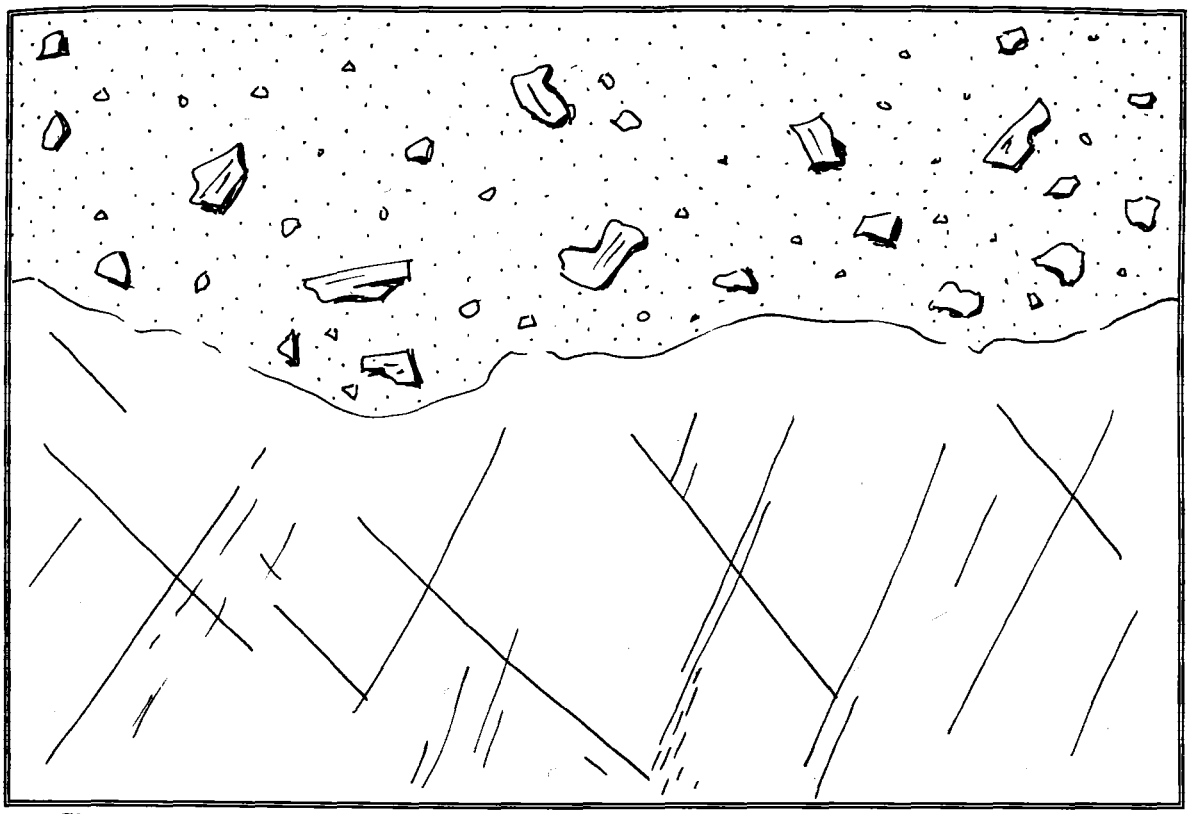

a) Clast orientation within colluvium showing random orientation relative to bedrock structures such as jointing and bedding.

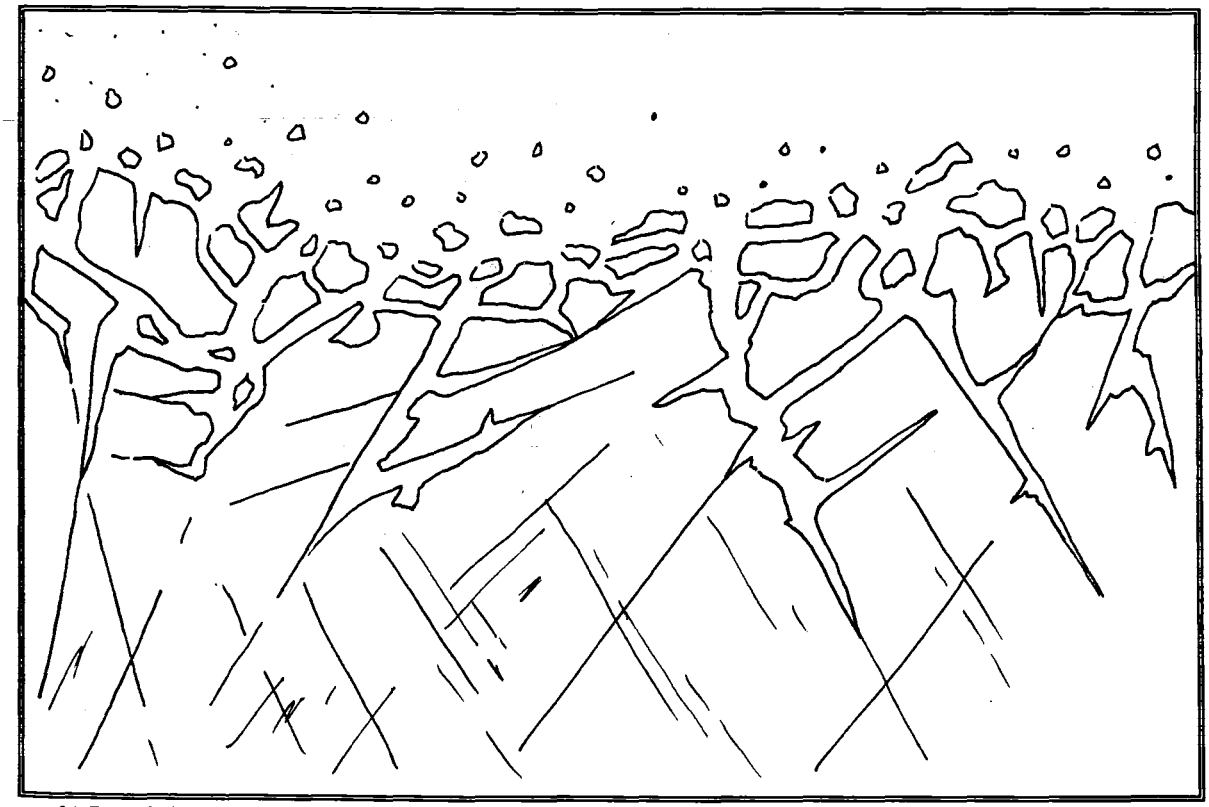

b) Regolith material showing the relationship of clasts to the bedrock structures such as jointing and bedding where clast orientation is dictated by such features.

FIGURE 3.5.: *Comparison of clast orientation relative to bedrock structure such as jointing in both colluvium (a) and regolith (b).*

which are described in Section 3.3.2. Colluvial deposits have a maximum thickness of 3-4m on the lower slopes of the field area, with less than 1m deposited on those slopes exceeding 35°. In the Marlborough Sounds at the present time the widespread vegetation cover significantly reduces the effects of slope wash transportation and because most weathering is of a chemical nature, colluvial production is limited. Additionally, the deposition of blocky colluvium is most intense during periglacial climates when the vegetation is reduced and the bedrock subjected to freeze/thaw processes. Both schist and greywacke bedrock produce colluvial deposits and the distinction of bedrock sources is made predominantly by clast composition, and to a lesser degree by the geotechnical properties of the matrix material (Section 5.5).

3.3.2. Slope Failures

Landscape modification by slope movement processes has been extensive in the Marlborough Sounds during the Quaternary. Regolith development and the deposition of colluvium have been substantial, and it is within these deposits that many of the the surficial slope movements related to the Last Glaciation (80-10ka BP) have taken place. Large deep seated bedrock failures have also occurred throughout the Marlborough Sounds, especially by foliation-controlled movements in schists,but they are not present within the study area.

This study uses the Varnes Classification system for slope failures (Varnes, 1978) to categorise the slope failures within the field area. The Varnes system (Table 3.3.) is useful because not only does it base the classification on the type of slope movement but also on the engineering geological material within which the slope failure occurs (Justice, 1994). Furthermore, the Varnes Classification system identifies the existence of 'complex failures' which involve two or more of the slope failures within the classification system. The complex failure category is particularly useful within the field area as failures within the surficial material typically involve combinations of rotational, translational and flow mechanisms, and are in fact the most prevalent type of slope failure. In addition to the type of failure and nature of the failed material, the Varnes classification system includes a rate of slope failure which is also presented in Table 3.3. The rate of movement scale identifies 'extremely rapid' movements which are in excess of 3m/s, and range to 'extremely slow' movements of less than 0.06m/year. The scale is open-ended, allowing for failures of any rate (Table 3.3.) When describing a failure using the Varnes Classificaion the speed of the movement is described first and followed by the slope failure type, for example 'slow rock block slide' (Justice, 1994).

a) Complex Failures

Using the Varnes Classification (1978), the failures which occur in unconsolidated regolith and colluvium are complex slide failures which combine rotational or translational headscarps, translational motion in the body of the

movement and flow mechanisms at the terminal extent of the failure (Figure 3.6.). Failures which occur on the steep (>35°) slopes of the upper catchment areas are primarily translational in the headscarp and main body regions and become flow failures at the foot of the slope. Translational failures will occur in deposits of limited thickness (<1m), as rotational failures require significant thicknesses (>1m) of material. The failure surface of slope movements in the field area is the colluvium/bedrock interface, which represents a permeability barrier which creates a zone of seepage flow and/or elevated pore pressures, and a significant change in the coherence of material with the colluvium, an unconsolidated unit, overlying the indurated bedrock material. Regolith is not a component of these steep slope failures because due to the removal of regolith during slope wash processes it is not preserved on slopes in excess of 35 degrees (Section 3.2.1.). The rate of movement for these complex steep slope failures is generally rapid (0.03m/min to 3m/sec) and therefore the failures are classified as being rapid complex translational flow failures.

On the lower, more moderate (15°-35°) slopes in the field area, failures tend to be complex movements combining rotational, translational and flow elements (Figure 3.6.). Due to the thicker (up to 4 m) deposits of colluvium on the lower slopes the head scarp region commonly fails in a rotational manner. The material is then transported downslope by means of translation, with failure occurring along the bedrock/colluvium interface. The zone incorporating the failure surface is often the site of increased pore pressures which reduce the normal stress imposed by the weight of the overlying material. The failures become earth and debris flows at the base of the slope due to the water entrained within the material, and often lateral scarps may be observed at the edges of the flow. The rate of movement for these complex failures is varied, with rapid to very rapid failures (0.03m/min - 3m/s) through to very-extremely slow (1.5m/yr-0.06m/yr) failures observed within the field area. Therefore the lower slope failures may be defined as very rapid to extremely slow complex rotational, translational and flow failures.

b) Triggering Mechanisms

i)Rainfall

One of the principal factors in slope failure is a high antecedent soil water content and in the Marlborough Sounds this is commonly the case in winter months due to the high rainfall and low evapotranspiration rates (Section 1.3.3.). Failure is most likely to occur when rainfall of particularly high intensity or long duration occurs in combination with high antecedent soil water conditions. For example the rainfall event of 2-6 August 1995,when219mm rain fell in 5 days,caused six moderate sized (<300m^3) road batter failures along the Port Underwood Road between Waikawa and Karaka Point,and one failure in excess of 300m^3 in Wharetekura Bay.

TABLE 3.3.: A summary table of the Varnes Classification for slope failures including the rate of movement scale (Redrawn from Varnes, 1978.; After Justice, 1994).

Type of Movement			Type of Material		
			Bedrock	Engineering Soils	
				Predominantly coarse	Predominantly fine
Falls			Rock fall	Debris fall	Earth fall
Topples			Rock topple	Debris topple	Earth topple
Slides	Rotational	Few units	Rock slump	Debris slump	Earth slump
			Rock block slide	Debris block slide	Earth block slide
	Translational	Many units	Rock slide	Debris slide	Earth slide
Lateral Spreads			Rock spread	Debris spread	Earth spread
Flows			Rock flow (deep creep)	Debris flow	Earth flow (soil creep)
Complex	Combination of two or more principle types of movement				

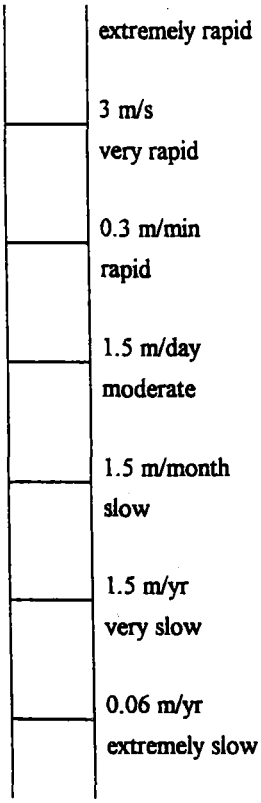

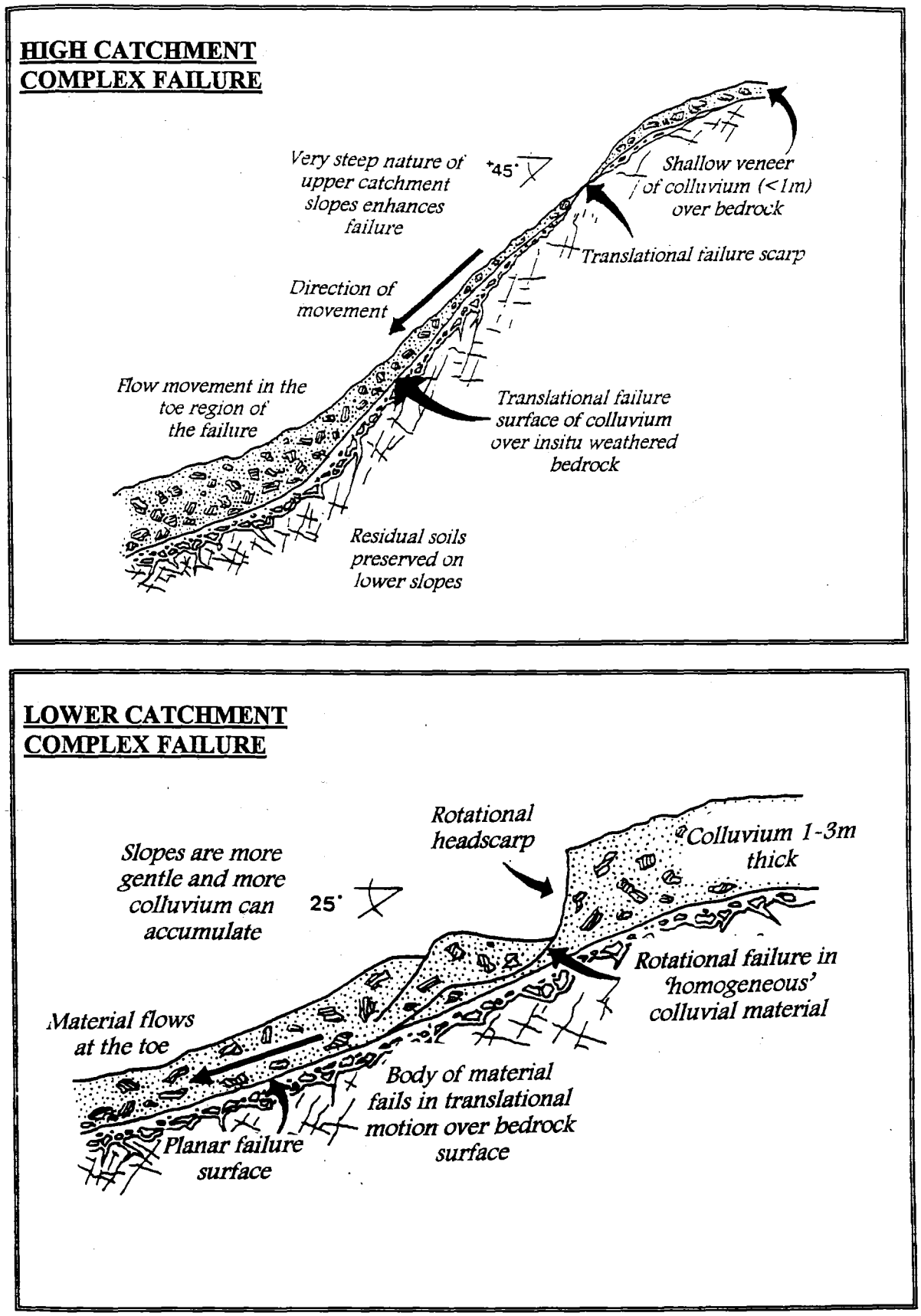

FIGURE 3.6.: Schematic cross-sections of the principal slope failure types in the field area. Complex failures may be divided into the high catchment complex failures involving translational and flow failure mechanisms, and the lower catchment complex failures which display rotational, translational and flow failure mechanisms.

ii) Vegetation Removal

Vegetation removal often plays an important role in slope instability as the growth of shallow rooting plants such as gorse and native bracken serves to bind the unconsolidated surficial materials, and instability problems may be observed where such vegetation has been removed (Figure 3.7.). Vegetation removal also affects the stability of colluvial slopes by exposure of the colluvium to direct rainfall and subsequent erosion. Furthermore, surface water can infiltrate into the colluvium on unvegetated slopes and percolates down to the bedrock/colluvium interface. Water which reaches the interface between the two units can cause destabilisation of the surficial material by causing uplift pressures which reduce the frictional resistance to sliding along the interface. Devegetated slopes are therefore more susceptible to sliding failure than vegetated slopes within the field area.

3.4. EROSIONAL PROCESSES

3.4.1. Stream Bank Erosion and Debris Deposition

Stream bank erosion is prevalent within the field area, occuring both in the major rivers (the Graham River and Waikawa Stream) and in the smaller streams within gully systems. The erosion occurs when the stream flow is turbulent and removes material from the sides of the stream or river. The erosional power of the stream is dependent on the nature of the material being eroded, the amount of sediment entrained within the flow, and the velocity of the stream during the flood event. As can be seen in Figure 3.8. the size of the particles moved by the water is an important parameter on the velocity required for erosion, however there is very little difference in the required velocity for erosion of unconsolidated clays and silts and sand sized particles, indicating that in the field area any weathered material which is not gravel sized or larger will be equally suceptible to stream bank erosion.

The material which is eroded by the stream is often the product of slope movements within the stream catchment or unconsolidated stream bed or bank material which has been transported downstream by an earlier flooding event. Erosion of these materials, which are unconsolidated colluvial and regolith mixes or unconsolidated alluvium, may be so extensive that the material becomes a debris flow where the sediment is the principal component and water acts as a buoyancy aid or reduces the internal friction of the particles. These debris flows are common in the field area and the remains of the flows can be seen at the base of most of the streams as fan shaped debris deposits. As more material becomes entrained in the stream flow by erosion upstream and the stream flow become a dense slurry, the capacity of the stream to transport larger and larger particles increases so that many of the debris flows identified in the field area contain clasts which measure 0.5m in diameter and larger.

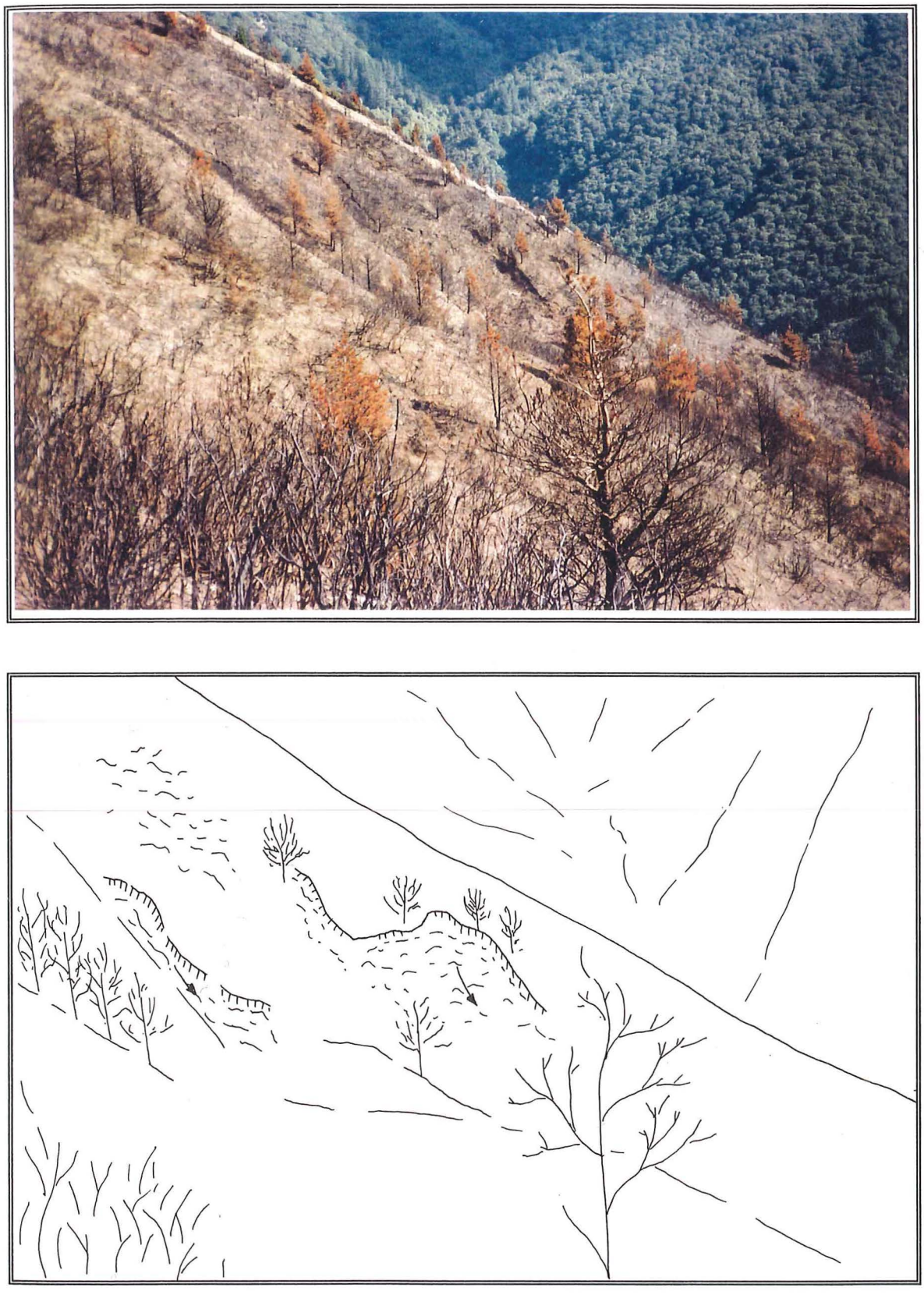

FIGURE 3.7.: The influence of vegetation removal on slope stability in the field area. This slope at the head of Whatamango Bay was cleared by burning in mid 1995 and subsequently numerous surficial failures have occurred within the colluvial material.

Figure 3.9. shows a debris deposit located on the western shores of Whatamango Bay which is associated with a small catchment and gully system upslope. The deposit is located at the base of the slope where the stream reaches the ocean and the largest size clast exposed in the deposit measures approximately 0.4m in diameter. The material is dominantly matrix supported and at this location is 2-3m thick. As can be seen in Figure 3.9. the debris deposits are poorly sorted and there are no recognisable sedimentary structures within the mass which is the principal distinction from alluvial fans which display sedimentary features such as imbrication of clasts (Section 3.5.). The remobilisation of debris deposits is common in the field area, both in the middle and lower reaches of the streams while the upper and middle reaches of the stream are often identified as being the areas of principal erosion.

3.4.2. Tunnel Gully Erosion

Tunnel gullying is a shallow subsurface erosional feature and because of their subsurface nature the tunnels are very difficult to locate until their roofs collapse and rilling occurs. The tunnels observed in the field area will form in both greywacke and schist-derived colluvium of any thickness, although they appear to be restricted to the top 1m of colluvial material (Figure 3.10.). The size of the tunnels in the field area can reach up to 0.5m in diameter and although rates of formation are unknown, tunnel development is thought to be a slow and progressive process often taking years for tunnels to develop. The tunnel shown in Figure 3.10. was observed during a single rainstorm event in the field area during April, 1995 and measures approximately 0.5m in diameter. The tunnel, which formed within 1m of the ground surface in a schistose colluvial soil is thought to have developed as the result of seasonal wet and dry periods over several years until it exited in the cut face seen in Figure 3.10.

Tunnel gully formation requires specific conditions which include a high and/or seasonally variable rainfall, a soil which is subject to desication cracking, reduced vegetation, an impermiable profile within the soil and often the presence of a dispersive clay mineral in the soil (Selby, 1993). The presence of high proportions of Na^+ in the soil is also recognised as possibly being a contributing factor for the formation of tunnel gully erosion, as sodium disperses the clay minerals because of the higher repulsive forces and may also increase the osmotic potential of the soil, thus increasing the amount of water contained in the void spaces of the soil (Holmgren and Flanagan, 1977; Selby, 1993; Chapter 4). The process of tunnel development involves the infiltration of rain water into cracks, or in some cases around dead tree roots, and the water then moves laterally into the soil and begins to

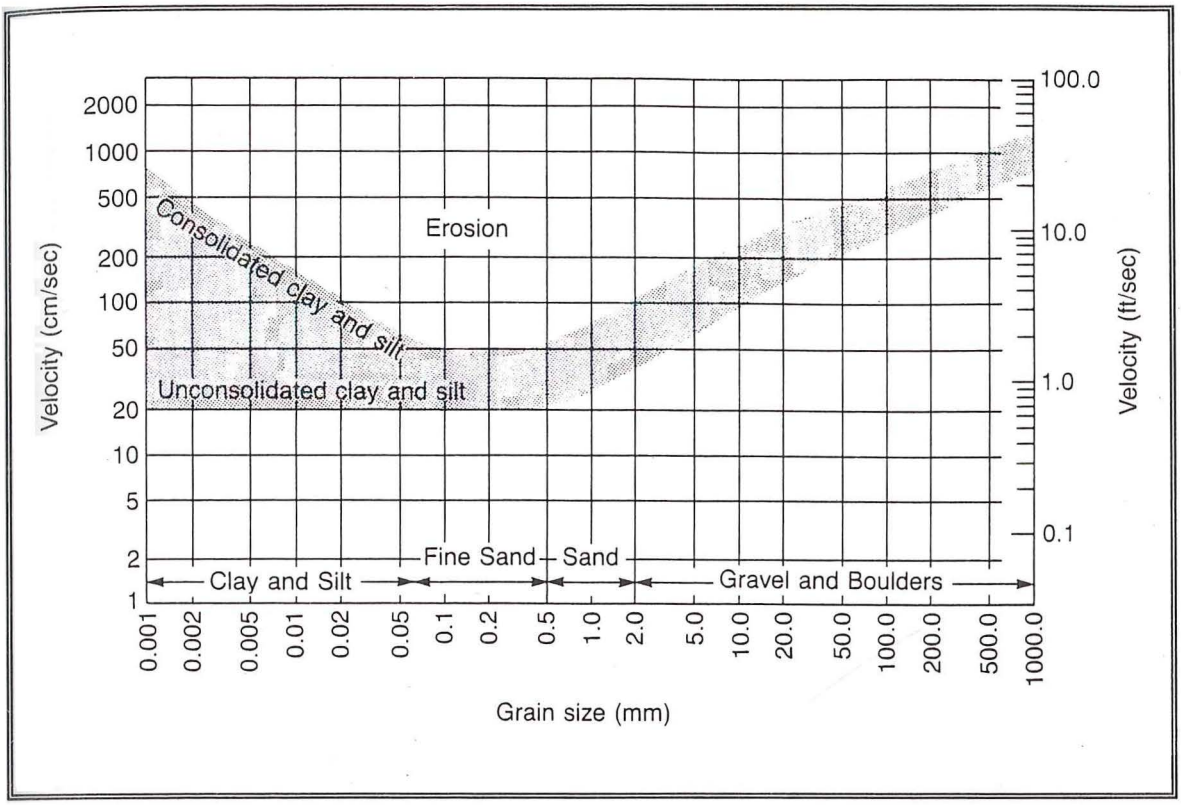

FIGURE 3.8.: *The Hjulstrom Diagram showing the relationship between grainsize and water velocity in 1m or water to cause the movement of quartz grains on a planar river bed and the influence of cohesion and consolidation on erosion (After Boggs, 1987).*

FIGURE 3.9.: *A debris flow deposit at the base of a gully in Whatamango Bay. The deposit shows complete disorientation of clasts within the matrix and the largest clast measures >30cm in diameter (GR P27 259995 599320).*

FIGURE 3.10.: A tunnel gully which has formed in the top 1m of a schistose colluvial deposit in Wharetekura Bay. The tunnel measures approximately 0.4m in diameter.

seep downslope and the movement of water is often constrained by impermeable layers within the soil. Once the water finds a pre-existing exit from the soil further downslope, for example shrinkage cracks, the water can then flow and remove soil particles to form a tunnel which the tunnel can then become enlarged and accommodate a greater volume of water. The tunnel will remain as a tunnel until the roof of the structure collapses and the tunnel becomes a rill. Figure 3.11. is a diagramatic sketch showing the formation and development of tunnel gullying in shallow soil situations from Bell and Trangmar (1987).

The development of tunnel gullying in the field area is difficult to ascertain because any tunnel collapse is obscured by the extensive vegetation of the slopes, however, tunnels are observed particularly in road cuts (Figure 3.10.) and in cut batters behind houses. The presence of dispersive clays in the soils of the field area is uncertain (Chapter 5), although many of the soil samples analysed in this study were high in sodium which may be significant for erosional processes. Tunnel gullying in the field area is observed in the top 1m of the soils in the field area which are subject to desiccation cracking during the summer months allowing access for rain water into the subsurface soil horizons, and additionally water is thought to enter the soil through dead and decaying tree roots.

3.5. DEPOSITIONAL PROCESSES AND MATERIALS

3.5.1. Alluvium

Alluvium is the product of fluvial action of streams and rivers and is defined as an unconsolidated gravel to silty clay deposit. Within the field area alluvium fills in the lower reaches of the major river valley systems, the Graham River Valley and Boons Valley, and forms alluvial fans such as the Rimu Terrace fan. Alluvium forms when material entrained within a stream is deposited due to a reduction in the velocity of the stream, generally in response to a decrease in stream gradient. During a flood event the grain size of material entrained is larger than for normal flow due to the increase in stream velocity, and the largest alluvial clasts observed within the field area are approximately 0.3m-0.4m and are rounded to sub-rounded which indicates that older material has been reworked sufficently to round the clasts.

Sedimentary structures such as grainsize sorting and vertical graded bedding within alluvium indicates the nature of the depositional environment. Gravel beds which contain the largest alluvial clasts, gravels and boulders, are associated with high velocity flows which often occur during flood events. Silts and clays are associated with overbank flows which have a lower velocity than the channel flow and thus allow the finer material to drop out of suspension. Figure 3.12. shows the variation in alluvium grain size from gravel sized clasts of the channel deposits to silty overbank deposits exposed in a degradation terrace in the Graham River. Channel alluvium in the field area is generally composed of the coarse grained

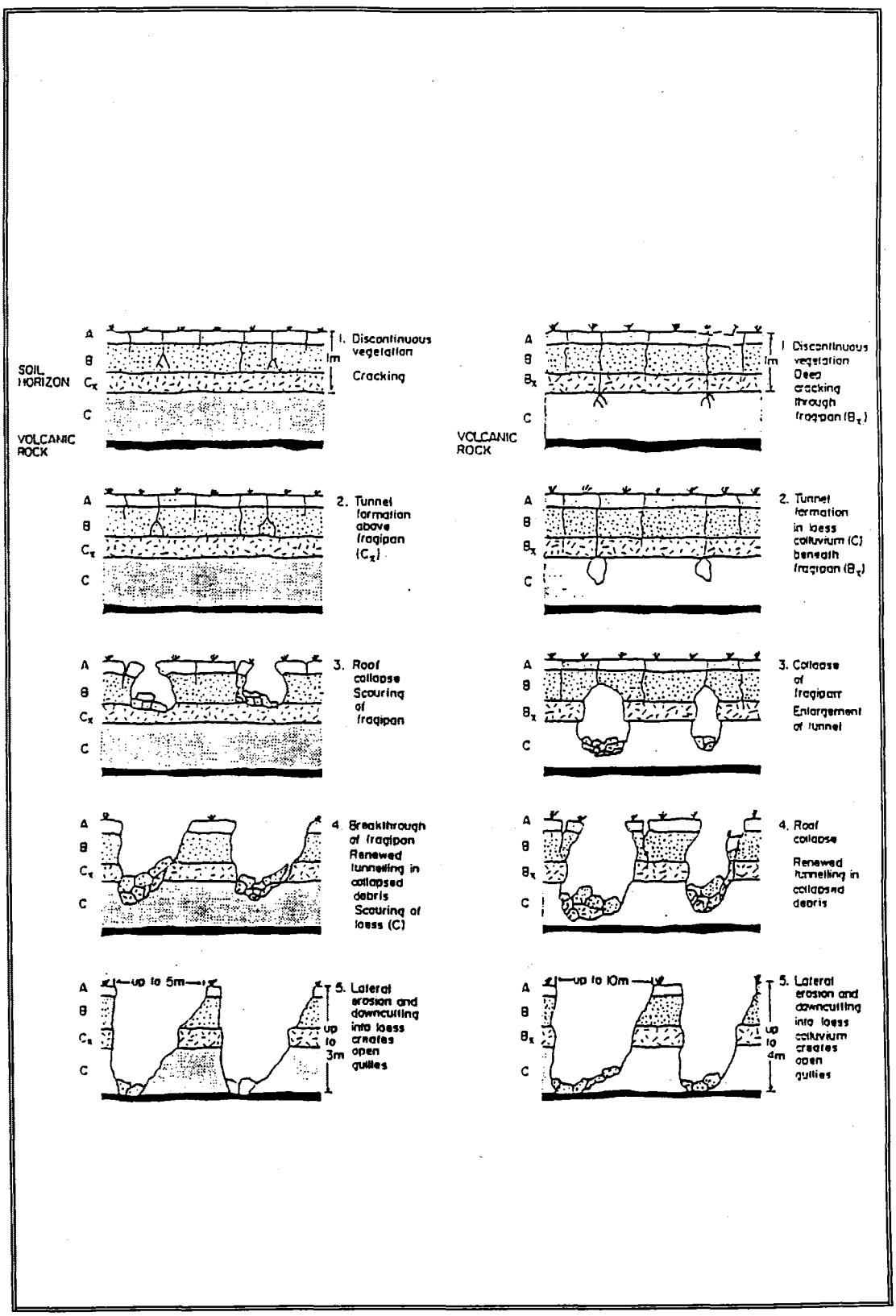

FIGURE 3.11.: A schematic representation of shallow tunnel gully development. For comparison deep tunnel gully development is also included (After Bell and Trangmar, 1987).

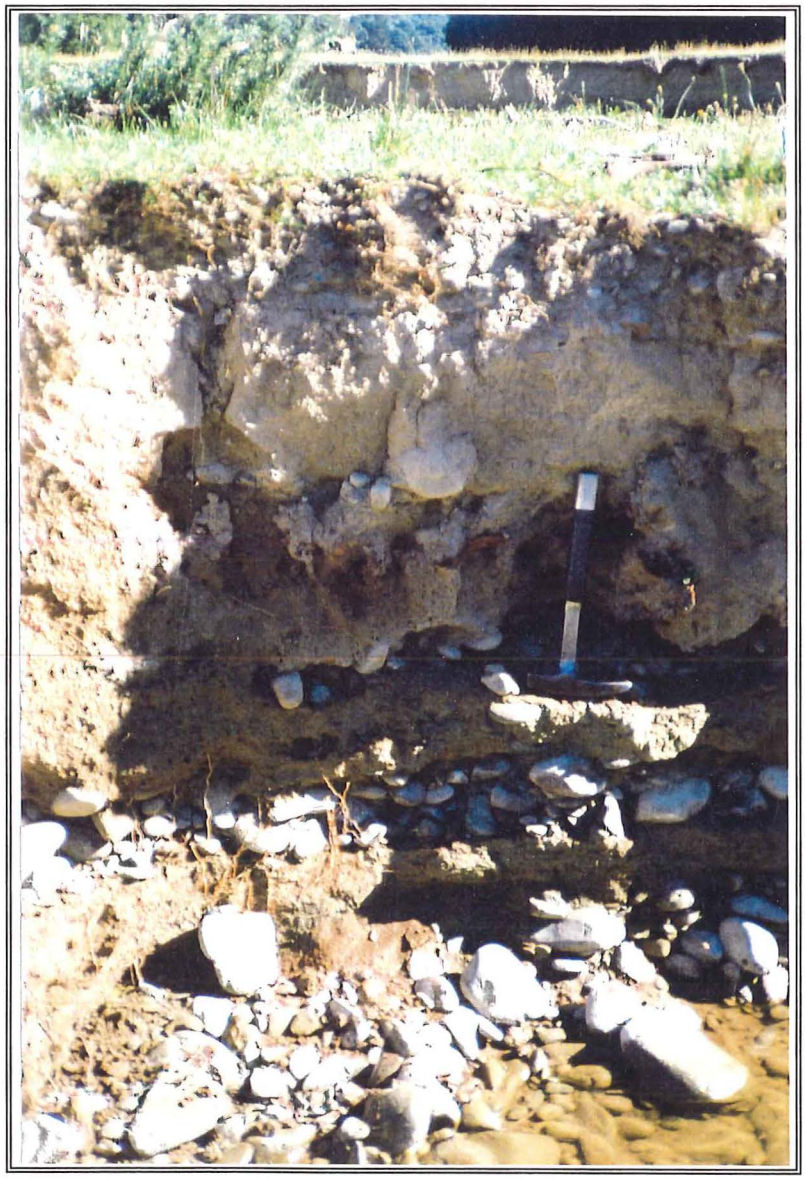

FIGURE 3.12.: *Flood plain alluvium in the Graham River showing different episodes of deposition reflected in grainsize changes. Coarse gravels indicate channel deposits while silty clay material represents overbank deposits. Note the imbrication of the gravels in the terrace alluvium.*

material which does not display obvious bedding, and the predominant sedimentary structure is imbrication of clasts with the long axes of the gravels orientated parallel to the flow direction (Boggs, 1987). Cross bedding and ripples may be observed in the finer grained sediments, sand and silts and are associated with reduced stream discharge rates.

3.5.2. Alluvial Terraces and Fans

Alluvial fans are shaped as a segment of a cone in plan view and develop when a river or stream encounters a significant decrease in gradient and the material entrained or transported by the stream is deposited. Alluvial fans are commonly confused with debris fans which are composed of debris flow material (Section 3.4.1.), however the debris fan deposits are devoid of sedimentary structures such as grainsize sorting while the alluvial fans are distinguished by pronounced imbrication of gravel sized clasts within the deposit. Alluvial fans are generally associated with periods of sparse vegetation and high rates of sediment supply and areas of steep topography which are prone to high intensity rain storm events (Boggs, 1987). Therefore, because the sediment supply in the field area is limited by the extensive vegetation of the catchment slopes, substantial alluvial fan deposition is not presently occurring.

Alluvial terraces represent periods of stream aggradation and degradation relative to external factors such as sediment supply and base sea level changes (McManus, 1994; Horrey, 1989; Kingsbury, 1987). The terraces themselves are comprised of sub-angular to subrounded gravels up to 0.4m diameter within a silty matrix interbedded with some silty clay layers representing a lower velocity flow of water and sediment from the stream channel onto the fan surface (Figure 3.12.). Alluvial terraces in the field area are found in both the Waikawa Stream and the Graham River, and the terraces of both rivers are attributed to sedimentation and erosion during the Late Quaternary. Aggradation terraces represent a phase of increased sediment supply compared to the present day situation and are generally associated with periglacial climates (Section 3.7.1.).

In the field area there are two aggradation alluvial terraces identifed in Waikawa Stream relating to different periglacial climatic events, and only one aggradation terrace in the Graham River (Section 3.7.1.). Degradation surfaces are terraces which have been cut into the aggradated alluvium in response to a reduction in the sediment supply in the catchment area and are generally also associated with a rising sea level. In the field area the degradation terraces in Waikawa Stream and the Graham River are thought to be associated with the present interglacial period, the Aranuian (Section 3.7.1.), and it is thought that small scale fluctuctations in present day sea level and/or tectonic uplift east of the Waikawa Bay Fault may account for the degradation terraces. Certainly Gibbs (1979) identifies that the sea level has

periodically risen above the current level within the last 10,000 years during which the degradation surfaces are thought to have developed (Figure 3.13.; Section 3.7.1.).

3.6. ACTIVE TECTONIC INFLUENCES

The Marlborough Sounds have been extensivelly modified by tectonic influences since the Tertiary (65Ma BP-recent) because the region is geographically close to the surficial expression of the Pacific/Australian plate boundary, the Wairau Fault (Figure 2.1.). Significant thrusting since the Miocene has resulted in faulted contacts between schistose and greywacke bedrock due to the compressional regime active during this period while folding of bedrock, development of cleavage (Chapter 2) and the continuation of faulting into the Quaternary has created the dissected landscape seen in the Marlborough Sounds at the present time. Within the field area there is one principal fault zone identified which has had a significant influence on the geomorphology and geology of the area. Vertical and dextral strike slip movement along the Waikawa Bay Fault, which can be observed from Milton Terrace in Picton to Waimarama Street in Waikawa (Figure 1.1.), is responsible for the presence of schist to the east of the fault and greywacke bedrock in faulted contact to the west. Movement of the fault during the Quaternary has caused the diversion of Waikawa Stream and probably caused substantial slope failures in the field area. Rupture of the fault may have also influenced the downcutting of alluvial terraces and created changes in slope gradient which may have caused the deposition of alluvial fans such as the Rimu Terrace alluvial fan. The age of the last movement along the Waikawa Bay Fault is important to determine the minimum activity of the structure and its potential activity in the future. Detailed discussion regarding the movement and age of last rupture along the Waikawa Bay Fault is presented in Chapter 4.

3.7. LANDSCAPE EVOLUTION

3.7.1. Introduction

This study of geomorphic landscape modification is restricted to the Pleistocene and Recent periods and is principally governed by climatic events and late Quaternary faulting of the Waikawa Bay Fault. Evolution of the landscape prior to the Pleistocene was presented in Chapter 2, which discussed the influence of pre and post metamorphic folding and faulting observed in the field area. The distribution and inter-relationship of regolith and the surficial units described in this chapter (Sections 3.2.2. and 3.3-3.5 respectively) are further analysed in order to determine a sequence of geomorphic events which have led to the present day landscape in the field area. The time frame investigated in this study is from the Late Quaternary through to the present day, because any geomorphic events prior to the Late

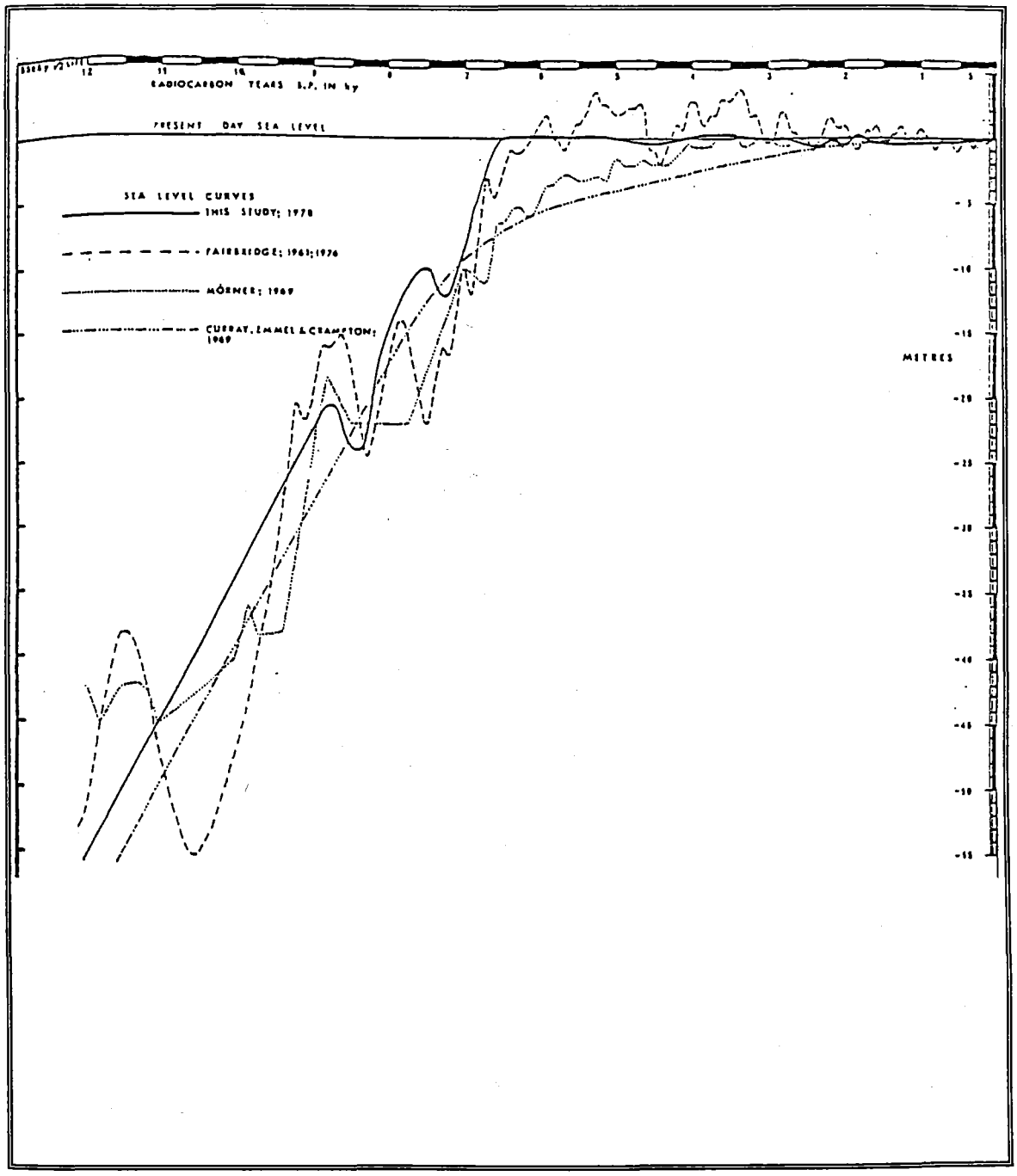

FIGURE 3.13.: A composite diagram from Gibbs (1979) showing the fluctuations in sea level since the Pleistocene (approx. 12ka BP). Of particular interest are the sea level rises in the last 10ka BP which are thought to correlate to degradation of terrace alluvium in Waikawa Stream and the Graham River.

Quaternary are not preserved in the field area due to subsequent landscape modification.

3.7.2. Climatic Influences and Alluvial Deposition

Quaternary climatic conditions have had a considerable effect on the landscape in the field area, particularly with respect to alluvial deposition and erosion. Global climatic change in the Quaternary led to glacial advances to the southwest of the Marlborough Sounds region which resulted in periglacial climates in the field area. The change from interglacial to periglacial climates meant that the dominant weathering process was freeze/thaw weathering which contributed to the extensive mass wasting of the bedrock material forming blocky colluvial deposits. The periglacial climates were also responsible for the extensive alluvial terraces and alluvial fan identified in the field area because of the increased sediment supply and reduced vegetation cover (Figure 3.14.). The alluvial terraces in Waikawa Stream were studied by Horrey (1989), who identified a relict aggradation terrace (W_o) on the south western side of the present Waikawa Stream channel. The age of this deposit is thought to correlate with the pre-Otiran glaciations during which periglacial climates in the field area would have provided the necessary conditions for the deposition of large quantities of sediment. The W_o surface has been modified by red weathering and therefore the minimum age of the surface developed on the aggradation gravels is related to the Oturian interglacial (120,000-80,000 yrs BP), which is thought to represent the last phase of red weathering in the field area (Horrey, 1989). The age of the surface may be older than Oturian and could be correlated to a Terangian interglacial age, which is thought to be the principal period of red weathering as determined by Te Punga (1964) in Wellington and extrapolated into the field area (Horrey, 1989). A remnant of the Wo alluvial terrace is also identified on the eastern side of Waikawa Stream (Figure 3.12.) as a red weathered surface preserved beneath the Rimu Terrace alluvial fan and thought to have been uplifted by the Waikawa Bay Fault (Chapter 4.).

Further alluvial aggradation occurred during the Otiran Glaciation (80-10ka BP), which is considered by Burrows et al (1988) to have extended to 10ka BP in the Marlborough Sounds, and is represented in Waikawa Stream by the W_1 alluvial terrace (Horrey, 1989). The W_1 alluvial gravels (Figure 3.14.) were also deposited in periglacial conditions similar to those which produced the Wo alluvial terrace. The age of the W_1 deposit is thought to be Otiran (80-10ka BP) due to the lack of red weathering and the development of a thin (<300mm) loess cover on the surface of the deposit which, therefore, means the gravels were deposited following the last phase of red weathering associated with the Oturan interglacial (120-80ka BP). The Maori Cemetery debris fans and the Rimu Terrace alluvial fan were deposited following the Otiran interstadial period in the later part of the Otiran Glaciation(25-

10ka BP) and these deposits interfinger with the upper parts of the W_1 alluvial deposit in Waikawa Stream (Section 3.7.3.). The oldest of the Maori Cemetery debris fans shows displacement from movement of the Waikawa Bay Fault, while the younger debris fans and the younger Rimu Terrace alluvial fan do not show any displacement. The inferred age of faulting for the Waikawa Bay Fault is thought to have occurred before the end of the Late Otiran glaciation (18-12ka BP) on the basis of the debris fan displacement and is discussed in detail in Chapter 4.

The formation of the degradation surfaces within alluvium inWaikawa Stream is associated with the Aranuian interglacial period (10ka BP-present in the field area) and represent the progressive incision of Waikawa Stream into the W_1 alluvial terrace gravels (80-10ka BP). Horrey (1989) identified a decrease in present day fluvial incision of the W_1 gravels towards the coast line due to a decreasing channel gradient. Erosion of the W1 gravels is related to sea level rising to a peak approximately 6.5ka BP and fluctuations from the present day level, and a decreasing sediment supply as the catchment slopes became more vegetated in response to the warmer interglacial climate. The W_2, W_3, and W_4 degradation terraces are only preserved on the western side of Waikawa Stream (Figure 3.14.) and the amount of downcutting from the W_1 terrace to the present day channel reaches a maximum of 10m (GR P27 259640 599150). As previously mentioned (Section 3.5.2.) degradation is generally associated with a rising sea level and the degradation terraces in the field area are thought to indicate small fluctuations in sea level during the present interglacial period. Gibbs (1979) identified periods of higher sea level compared to the present day height within the last 10,000 years (Figure 3.13 .), and combined with the decrease in sedimentation rate due to vegetation of the catchment areas, degradation terraces were formed in both the Graham River and Waikawa Stream.

Correlation of the alluvial terraces in Waikawa Stream with the terraces of the Graham River is difficult due to the lack of datable material. Charcoal material has been found in the gravels of both rivers and previous work (Horrey, 1989) showed that the maximum age of charcoal in Waikawa Stream was $250^{\pm}150$ yrs BP and is associated with Polynesian or early European burning. However, financial and time limitations in this study meant that radiocarbon dating of material in the Graham River was not possible. In the Graham River only one aggradation terrace is identified which forms a small remnant on the western edge of the flood plain (Figure 3.15.) and the age of this surface is tentatively correlated with the W_1 alluvial terrace in Waikawa Stream because there were no red weathered profiles observed. Therefore, because aggradation of alluvium required increased sediment supply and devegetation of the catchment area, the formation of the deopsit is restricted to periglacial climates which have not been subjected to red weathering and thus the age of the aggradation terrace in the Graham river is considered to be associated with

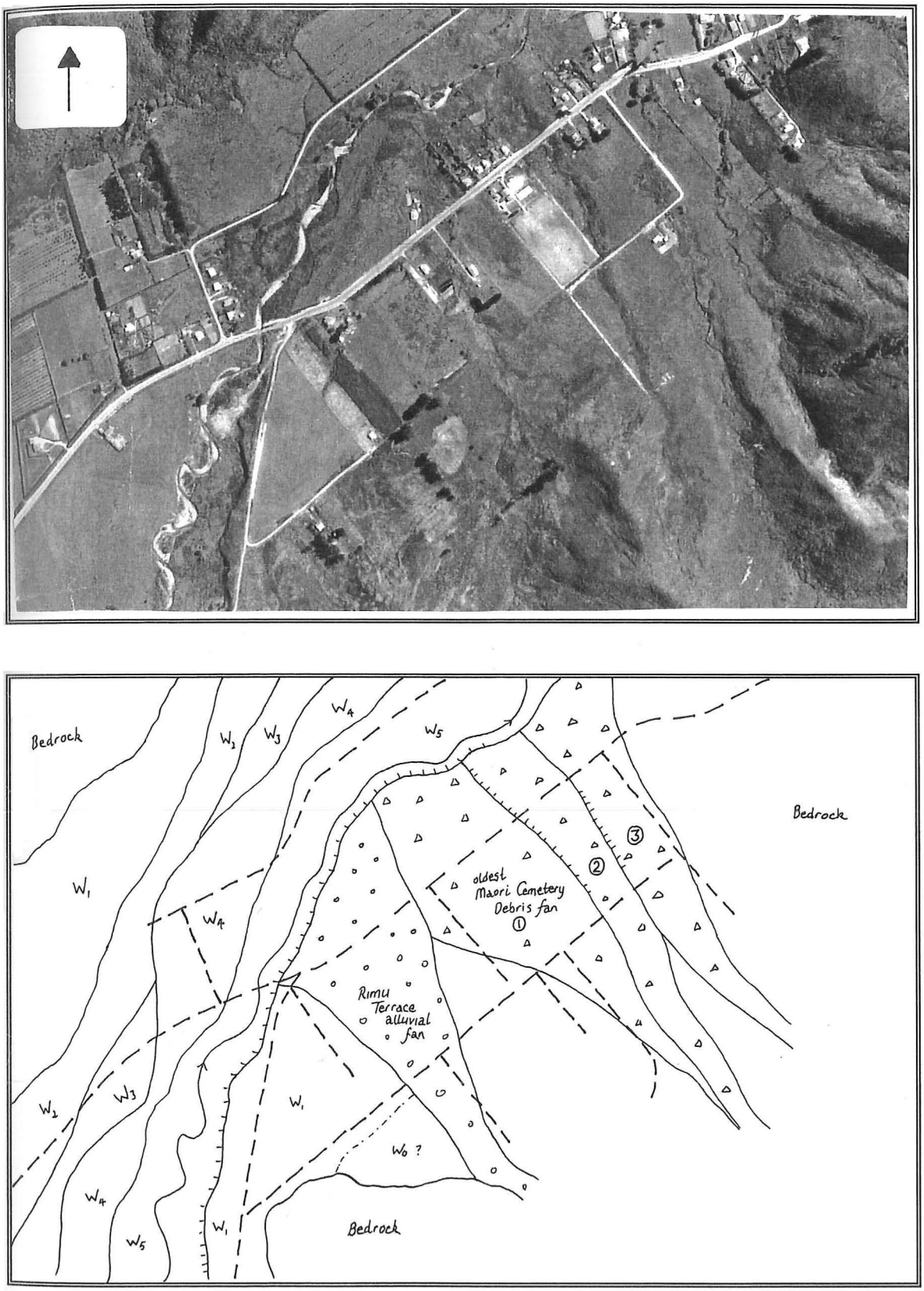

FIGURE 3.14.: An aerial photograph and sketch showing the relationships of the Rimu Terrace alluvial fan (18-10ka BP) to the Maori Cemetery debris fans which range in age from 25ka BP to 10ka BP. Note also the relationship of the fans to the alluvial terraces in Waikawa Stream.

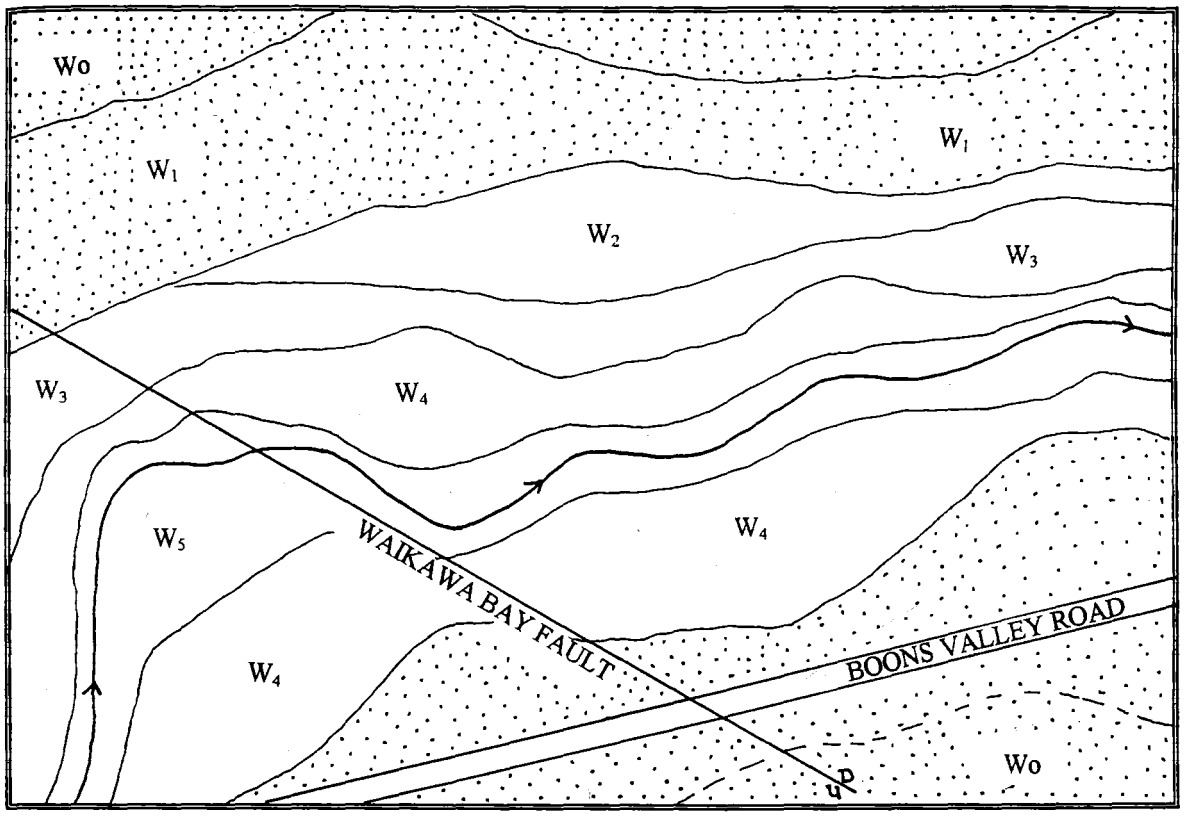

Alluvial terraces in Waikawa Stream (After Horrey, 1989)

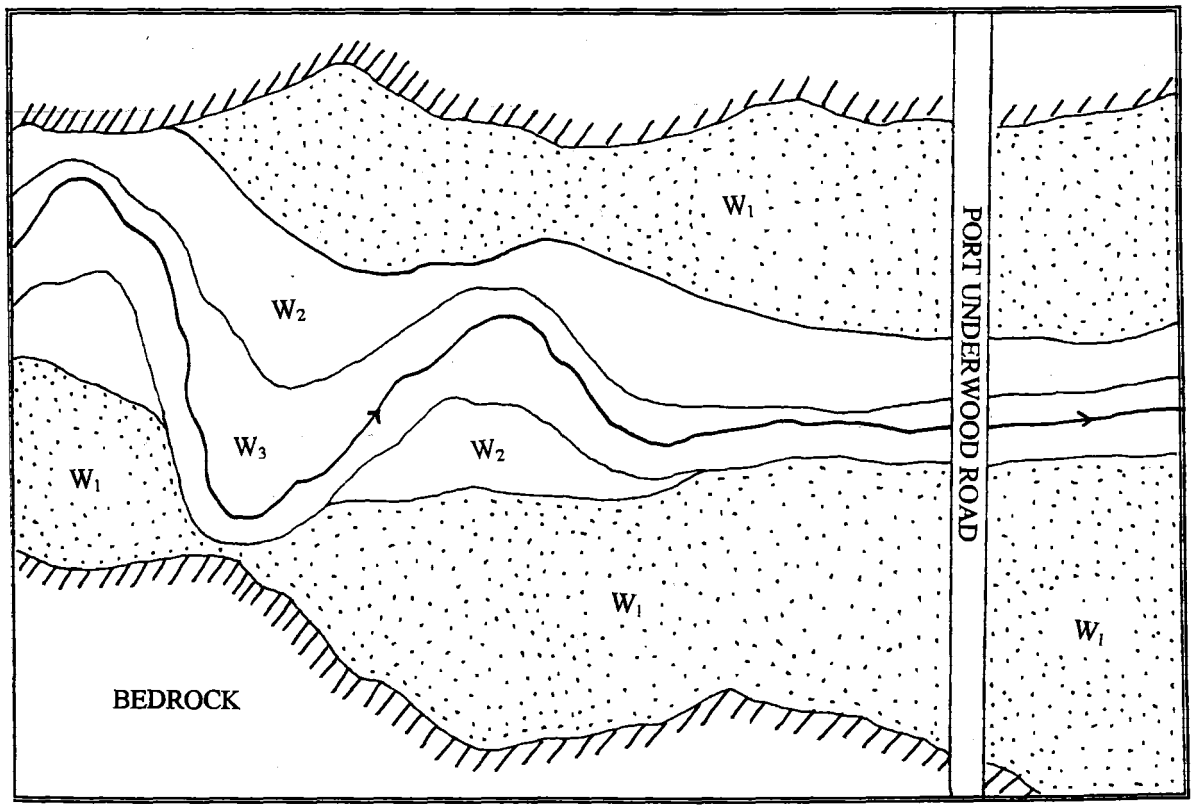

Alluvial terraces in the Graham River

FIGURE 3.15.: *Correlation of the alluvial terraces in Waikawa Stream and in the Graham River. Stippled terraces represent aggredational phases.*

the Otiran glaciation (80-10ka BP in the field area) and most probably the Late Otiran (<25ka BP).

A similar sequence of alluvial degradation may be observed in the Graham River and the amount of downcutting into the aggradation terrace is significantly less (<5m) than in Waikawa Stream (up to 10m). Two degradation surfaces may be identified in the Graham River which are thought to be correlatives of the W_2 and W_3 surface in Waikawa Stream, with the younger surface being the present day river channel. The reason for greater down cutting in Waikawa Stream compared to the Graham River is unknown but may be related to the absence of active faulting in the Graham River catchment. Figure 3.15. shows the proposed correlation between the alluvial terraces of Waikawa Stream and those identified in the Graham River.

3.7.3. Surficial Slope Failures

Although the Marlborough Sounds landscape has been continually modified by slope movement processes since the Late Quaternary, the only failures which have been preserved in the field area are those which are associated with the last glaciation, the Otiran (80-10ka BP). Slope movements are more prevalent during periglacial periods due to the development of significant thicknesses (up to 4m) of coluvium in the field area as a result of mechanical freeze/thaw weathering. The onset of chemical weathering meant the development of finer grained colluvium and also regolith profiles over bedrock and slope failures since the Otiran glacial period have occurred within all of these deposits. The relict features of the Otiran slope failures are still apparent in the form of degraded headscarps which define the bedrock ridges in the field area. Slope failures were more frequent during the periglacial climates due to the lack of vegetation on the slopes because vegetation increases the binding of surficial materials and reduces the potential instability (Section 3.3.2.). It is difficult to determine the exact age of these older slope failures because the material which was displaced during the original failures has since been modified by slope wash and gravity in addition to subsequent slope failures, and there is also no datable material contained within the slope movement material which implies a lack of vegetation.

Since the return to a warmer interglacial climate (Aranuian 10ka BP-present) vegetation has been re-established and large slope failures within colluvium have become less frequent in the field area. Seismic activity from sources outside of the Marlborough Sounds have undoubtedly had an influence on the slope stability in the field area within the last 10,000 years, however it is impossible to determine whether a seismic origin has been responsible for any particular slope failure.

Vegetation removal due to fire, both natural and human induced, has caused slope failures in the field area within the last 5,000 years. During historical times(<500 years) the slopes in the field area have been systematically cleared using

fire for agricultural purposes by both Maori and European inhabitants and many of the landslide deposits identified in the field area are related to slope failures during this time. Charcoal found in a landslide deposit in Waikawa township (GR P27 259730 599220) was radiocarbon dated (McManus, 1994) and returned an age of $270^{\pm}180$ yrs BP and is probably related to Polynesian modification of the slopes.

3.7.4. Fan Surfaces

Fan surfaces in the field area are derived from either debris depositional events or alluvial deposition, with the largest of these fans found to the east of Waikawa township and smaller, principally debris fans identified throughout the field area. The oldest fan surfaces identified in the field area are the Rimu Terrace alluvial fan and the Maori Cemetery debris fans (Figure 3.14.), and these fans are thought to have been deposited during the last glaciation (Otiran, 80-10ka BP). During the Otiran glaciation a periglacial climate was prevalent over warmer climatic fluctuations causing devegetation and mass wasting of the slopes within the field area. The fan surfaces have not been modified by red weathering and therefore the fans were deposited since to the last phase of red weathering during the Oturian interglacial period (120-80ka BP) as determined by Te Punga (1964).

The Maori Cemetery debris fans form a fan complex of three distinguishible surfaces with the oldest surface being the southern-most fan and progressive downcutting of the younger fan surfaces towards the north (Figure 3.14.). The oldest debris fan surface has been modified by movement of the Waikawa Bay Fault and a 1m scarp with the eastern side upthrown may be determined across the fan. The younger debris fans are though to have been deposited since fault movement and have eroded away any evidence of fault movement (Chapter 4). Similarly the Rimu Terrace alluvial fan, which is located south of and adjacent to the oldest Maori Cemetery debris fan, shows no evidence of displacement by the fault and thus the age of the alluvial fan is thought to be similar to that of the younger debris fans.

The remaining fan surfaces within the field area are associated with the present interglacial period and devegetation of the slopes from both natural and human-induced burning. These surfaces are considerably smaller than the large debris and alluvial fans deposited during periglacial intervals due to the decreasing sediment supply as vegetation in the field area becomes re-established.

3.8. CHRONOLOGY OF GEOMORPHIC EVENTS

The geomorphic evolution of the field area during the Quaternary is dominated by the influence of periglacial and interglacial climates. The chronology of events which have led to the formation of the present day landscape in the field area is summarised in Table 3.4. The earliest recognisable event during the Quaternary period is a the deposition of a pre Otiran alluvial terrace in Waikawa

Stream which is thought to be associated with a periglacial climatic period. The alluvial terrace surface (Wo) has experienced at least one period of red weathering which constrains the age of the surface to at least 120ka BP, as the last phase of red weathering is thought to have occurred during the Oturian interglacial (120-80ka BP; Te Punga, 1966) and the age could be considerably older. The age of terrace deposition is thus considered to be Waimean (250-120ka BP) or older (Table 3.4.).

During the Otiran glaciation (approximately 80-10ka BP) periglacial climates prevailed in the field area contributing to reduced vegetation and mass wasting of the slopes, and it is thought that periglacial climates may have persisted in the field area untill approximately 10ka BP (Burrows et al, 1976; Horrey, 1989). During the lowered sea levels in the Otiran (Gibbs, 1979) substantial deposition of alluvium in Waikawa Stream began to form the W1 alluvial terrace (Horrey, 1989). Coincident with the deposition of the W1 terrace alluvium was the formation of the Maori Cemetery debris fans and the Rimu Terrace alluvial fan which interfinger with the W1 surface on the eastern side of Waikawa Stream. The age of these fans is thought to be Late Otiran as the deposits interfinger with the upper part of the W1 alluvial terrace and fault movement during the Late Otiran has also modified the oldest fan surface. The younger fan deposits to the north and south of the oldest Maori Cemetery debris fan have not been displaced by faulting and therefore are thought to have been deposited since fault rupture.

During the Otiran glacial period there was substantial landscape modification by slope movements within the colluvium in the field area, and the relict headscarp regions define the present day bedrock ridges. Slope failures were more prevalent during periglacial periods due to the lack of vegetation and the development of up to 4m of colluvium as a result of freeze/thaw weathering processes. The slope failures which can be observed in the field area at the present time are thought to obscure evidence of any failures older than the last glaciation.

With the onset of the present Aranuian interglacial (approximately 10ka BP - present) the climate became warmer, native vegetation became re-established, and mechanical weathering was predominantly replaced by chemical weathering. Degradation of the W1 alluvial terraces in both the Graham River and Waikawa Stream occurred in relation to the rise in sea level to the present day level, and vegetation has been periodically removed by natural and, during historic times, human induced burning causing instability of the slopes within the field area.

TABLE 3.4.: The geomorphic chronology of the field area from the pre-Waimean glaciations to the present day

GEOMORPHIC EVOLUTION

Pre-Waimean Glaciations

- Periglacial climates lead to predominantly mechanical weathering.
- Mass wasting forming thick colluvial deposits.
- Possible deposition of the Wo alluvial terrace in Waikawa.

Terangian Interglacial (250ka BP)

- Change to mainly chemical weathering.
- Main phase of red weathering occurs approx. 250ka BP (Te Punga, 1963).

Waimean Glaciation (250-120ka BP)

- Change to periglacial climates and mass wasting of the slopes due to mechanical weatheing.
- Significant slope failures continue to modify the slopes in the field area.
- Youngest possible age for the deposition of the Wo alluvial terrace.

Oturian Interglacial (120-80ka BP)

- Last red weathering phase approximately 100ka BP (Te Punga, 1963).
- Chemical weathering dominates over mechanical weathering.
- Red weathering occurs on the surface of the Wo alluvial terrace.
- Possible deposition of ash deposits from volcanic eruptions in the North Island which also become modified by red weathering.

Otiran Glaciation (80-10ka yrs BP)

- Periglacial climates thought to exist in the Marlborough Sounds until 10ka BP (Burrows et al, 1976).
- Lowering of sea level (-140 m present sea level; Gibbs, 1979).
- Alluvium deposited out towards Cook Strait (Horrey, 1989).
- Deposition of the W1 alluvial terrace in Waikawa Stream and Graham River.
- Deposition of the Maori Cemetery debris fans in Waikawa (25-10ka BP)
- Deposition of the Rimu Terrace alluvial fan (18-10ka BP).
- Last movement of the Waikawa Bay Fault (approx. 18-12ka BP) which disrupts gravels in the oldest of the Maori Cemetery debris fans.
- Headscarps of slope failures define the bedrock ridges.

Aranuian Interglacial (10,000 yrs BP - recent)

- Sea level reaches approximately the same level as the present day with minor fluctuation causing degradation of the W1 alluvial terraces in Waikawa Stream and the Graham River.
- A return to interglacial climates and dominantly chemical weathering.
- Continuation of slope movements.
- Removal of vegetation by fire and urban development during historical times (<500 yrs BP) causes slope modification by landsliding in surficial deposits.

CHAPTER FOUR THE WAIKAWA BAY FAULT

4.1. INTRODUCTION

The Waikawa Bay Fault is observed to the east of Waikawa township upslope of Moana View Road, where it strikes approximately 050° and has a steep (60°-80°) easterly dip. Movement along the fault has involved considerable reverse thrust motion from an easterly direction (Chapter 2) and right lateral strike slip movement. Therefore, the fault may be considered as an oblique reverse thrust/dextral strike slip fault. Strike slip movement can be observed in the dislocation of watercourses such as Waikawa Stream, while the vertical component of the most recent activity is evident along Maori Cemetery Road where the eastern side of the fault has been upthrown by approximately 1m over the western side. To the north the faule is thought to splay rather than be represented as a single trace, and the width of the faulted zone is considered to be at least 100m wide. This chapter details the information regarding the timing of the last movement of the Waikawa Bay Fault and attempts, using geophysical techniques, to further constrain the northern and southern extents of the fault. Subsurface data obtained in the field concerns the nature and extent of the fault and is integrated with the geophysical and geomorphic information in order to constrain the timing of the last movement and the activity of the Waikawa Bay Fault.

4.2. PREVIOUS WORK

2.2.1. Horrey's (1989) Hypothesis

Horrey (1989) identified the displacement of W1 alluvial gravels, which he considered to have a depositional age of 10-6.5 ka BP, within 100m of the inferred fault trace in Waikawa Stream, and small scale reverse faulting upthrown on the eastern side was exposed in the W4 degradation surface (<6.5ka BP). A seismic refraction survey was performed across the only observable trace of the fault along Cemetery Road (Figure 4.1.), but identified no appreciable vertical displacement of the bedrock surface despite a 1m vertical offset in the gravels at the ground surface. Horrey therefore inferred that the last rupture of the Waikawa Bay Fault had occurred within the last 6,000 years based on the observed disturbance of the late Holocene W4 degradation terrace. On the basis of this information, Horrey (1989) estimated a class III activity of the Waikawa Bay Fault (Table 4.1.) which classifies the fault as the 'least active of those faults expected to move again' (NZGS, 1966). Horrey considered this a minimum activity classification because although there was no conclusive evidence, repeated faulting within the 50-5ka BP time frame was thought to be likely.

FIGURE 4.1.: A location map which shows the relationships between the geomorphic surface and the Waikawa Bay Fault in the field area. The Maori Cemetery debris fans are represented in decreasing age of deposition; ① being the oldest fan, ② the next youngest, and ③ the youngest fan.

TABLE 4.1.: The New Zealand Geological Survey active fault classification Scheme (NZGS, 1966). The Waikawa Bay Faultis classified as a Class III active fault, having moved once in the 5,000-50,000 year period with no movements identified in the last 5,000 years

FAULT ACTIVITY		Movement in the last 5,000 yrs		
		REPEATED	SINGLE	NONE
Movement in 5,000-50,000 yrs	REPEATED	I	I	II
	SINGLE	I	II	III
	NONE	I	III	-
Movement in 50,000-500,000 yrs	REPEATED	I	II	III
	SINGLE	I	III	Not active*
	NONE	I	III	-

* May be mapped as a 'Late Quaternary fault trace'

The above table implies the following definitions:

A CLASS I ACTIVE FAULT is principally one that has shown repeated movement over the last 5,000 years, but the category also includes those with a single movement and repeated movement in the last 50,000 years.

A CLASS II ACTIVE FAULT is considered less active than one shown in CLASS I. It is principally one that has shown, as a minimum, repeated movement over the last 50,000 years, but the category also includes those with a single movement in the last 5,000 years and repeated movement in the period of 50,000-500,000 years ago.

A CLASS III ACTIVE FAULT is the least active of those faults that are expected to move again. It is principally one that has shown, as a minimum, a single movement in the last 50,000 years, but also includes those showing repeated movements in the period of 50,000-500,000 years ago.

Horrey' (1989) estimate for the age of last rupture of the Waikawa Bay Fault is now thought to be too young based on inaccuracies in dating the age of the geomorphic surfaces and deposits in the field area.

4.2.2. McManus' Hypothesis (1994)

McManus (1994) used geomorphic evidence from the inferred ages of alluvial terraces and both alluvial and debris fan surfaces to produce an estimate of the age of last fault rupture. The only trace of the fault cuts the southernmost of the Maori Cemetery debris fans (Figure 4. .) which had an estimated age of 10-6.5ka BP, the age postulated by Horrey (1989), and is equivalent in age to the W1 alluvial terrace in Waikawa Stream. The oldest fan surface in the field area, then thought to be the Rimu Terrace alluvial fan which was given an age of >80ka BP on the basis of an extensive red weathered profile, is not displaced by the trace of the Waikawa Bay Fault. The age of last faulting was considered to be older than the the Rimu Terrace alluvial fan because deposition of the fan alluvium would have destroyed any trace of the fault. The oldest debris fan adjacent to the Rimu Terrace fan was believed to have been 'draped' over the original fault scarp and subsequent episodes of debris deposition would have progressively removed any trace of the fault rupture. The rupture of the gravels in Waikawa Stream was though to possibly be related to movement of a fault other than the Waikawa Bay Fault and consequently, the fault was thought to have last ruptured no less than 80ka BP. The activity of the Waikawa Bay Fault was also defined as Class III (Table 4.1.) on the basis that the fault had experienced at least one rupture within 50-500ka BP, and this classification was also considered to be a minimum activity rating due to the possibility of repeated movements within this time frame.

As with the estimate presented by Horrey (1989) the age of last rupture proposed by McManus (1994) is thought to be incorrect and again is due to inaccuracies in dating the geomorphic events in the field area. The age of >80ka BP for the last faulting is thought to be an overestimation and faulting is considered to be considerably younger than this estimate (Section 4.2.).

4.3. GEOMORPHOLOGY

4.3.1. Introduction

Due to the fact that there are no marker horizons which can be traced across the fault to indicate movement rates or time of movement, the geomorphic indicators such as the relative ages of faulted deposits and surfaces are considered the most valuable tool in assessing the activity of the Waikawa Bay Fault. The Waikawa Bay Fault trace is observed cutting across several of the geomorphic surfaces in the field area, namely fan surfaces and alluvial gravels, and an assessment of the possible age

of these surfaces and their relationships to the fault and other surfaces provide an estimate of the time of last rupture. In Chapter 3 the ages of the geomorphic surfaces in the field area were revised, and below is a discussion of the relationship of these surfaces to the age of faulting. The following discussion is divided into a description of the ages of the relevant geomorphic features in the field area as detailed in Chapter 3, and a sequence of events which preceded faulting and modified the fault trace following the last rupture event.

a) The Age of Geomorphic Features.

The Waikawa Bay Fault trace can be seen cutting the Maori Cemetery debris fans on the eastern side of Waikawa Stream (Figure 4.1.). The origin of these debris fans is now thought to be associated with mass wasting and erosion during the last glaciation, the Otiran which occurred approximately 80-10ka BP (Section 3.7.4.). Because the fans are seen to aggrade to the top of the W1 alluvial gravels deposited during the same period, their depositional age is further constrained to the latter period of aggradation during the Otiran glaciation (25-10ka BP). A thin (approx. 300mm) layer of loess mantles the debris fans which is associated with periglacial climates and is thought to have been deposited near the end of the Otiran Glacial period (approx 14-10ka BP). The fault trace is observable only in the oldest of these fans, which was probably deposited between 25-18ka BP (Section 3.7.4.), and the younger Maori Cemetery debris fans are thought to have been deposited between 15-10ka BP as they are downcut into the original fan surface and represent subsequent depositional events.

The fault is inferred south of the debris fans although there is no observable surface trace. The Rimu Terrace alluvial fan is located immediately south of the Maori Cemetery debris fans and the age of the fan is thought to be equivalent to the age of the younger Maori Cemetery fans, approximately 15-10ka BP (Section 3.7.4.) as the fan also erodes into the oldest Maori Cemetery debris fan. Red weathering, which was observed in the stream channel is not now thought to relate to the deposition of the fan material as described by McManus (1994) but rather the fan is believed to cover, and be eroded into, an older alluvial terrace correlated with the red weathered Wo surface which is also found on the western side of Waikawa Stream (Horrey, 1989).

The small scale reverse faults observed in the W1 alluvial gravels in Waikawa Stream by Horrey (1989; Section 4.2.1.) are now thought to represent a rupture event along the Waikawa Bay Fault following deposition of the gravels. Although the disruption of gravel described by Horrey (1989) was exposed in the W4 degradation terrace, the faulting is not necessarily associated with the age of the degradation surface (<6.5ka BP) as Horrey proposed. Instead it is thought that the disruption of the gravels is related to their depositional age and because faulting is observed

propagating to within 1m from the surface, rupture is believed to have occurred near the end of the depositional period (18-10ka BP).

b)Geomorphic Chronology of the Waikawa Bay Fault

Although there have undoubtedly been repeated movements along the Waikawa Bay Fault (Chapter 2) the events constraining the last movement of the fault are indicative of only one movement since the Last Glaciation. During the Otira Glaciation significant thicknesses of alluvium were deposited in Waikawa Stream which are presently named the W1 alluvial terrace. Coincident with the deposition of alluvium in Waikawa Stream during the later part of the Otira Glaciation (25-10ka BP) was the formation of the large Maori Cemetery debris fans and the Rimu Terrace alluvial fan on the eastern side of Waikawa Stream. Following, or possibly during, the deposition of the oldest of these debris fans (Chapter 3), faulting occurred along the Waikawa Bay Fault. Displacement at depth would have been distributed over a greater area within the debris fan gravels as rupture propogated to the surface and it is thought that rupture was accommodated along a number of smaller splays of the Waikawa Bay Fault resulting in a disturbed zone at the surface now seen in the form of a 1m vertical offset over a 100m wide zone. Subsequent debris deposition of the younger Maori Cemetery fans to the north (Figure 4.1.) progressively eroded the fault scarp and thus, as observed at the present time, the scarp is only seen in the portion of the oldest fan deposit preserved from later erosion and deposition. To the south of the debris fans the Wo alluvial terrace, which was subjected to red weathering, was displaced by possibly multiple fault movement raising the eastern side to the present day level (Figure 4.1.). Following rupture, the WO terrace was progressively eroded by stream action, which was followed by the deposition of the Rimu Terrace alluvial fan obscuring the trace of fault rupture south of the Maori Cemetery debris fans. In addition, slope movements identified on the northern edge of the Rimu Stream (Figure 4.1.) would have contributed to removing any trace of rupture as landslide deposits would have covered the fault scarp. Displacement of the W1 gravels in Waikawa Stream as observed by Horrey (1989) is thought to be related to this phase of faulting, and the displacement of gravel has been exposed by subsequent degradation of the W_1 gravels to form the W_2, W_3 and W_4 surfaces.

Faulting therefore, based on the age of geomorphic features, deposits and surfaces in the field area, is thought to have occurred during the later period of aggradation during the Otira Galciation. Rupture occurred after the deposition of the oldest Maori Cemetery debris fan (<18ka BP) and before the deposition of the remaining fans to the north which occurred between approximately 15-10ka BP, constraining rupture to between approximately18-12ka BP.

4.4. GEOPHYSICAL INVESTIGATIONS

4.4.1. Introduction

During February 1995 geophysical investigations were performed in an attempt to determine the nature of the Waikawa Bay Fault and the extent of the fault north of the present day fault scarp. Both Transient Electromagnetism (TEM) and Ground Penetrating Radar (GPR) were used and the survey locations are shown in Figure 4.2. The following discussion outlines the results obtained using both methods, and also integrates the geophysical data with the geomorphic information. The methodology of each of the geophysical techniques used in the field area is detailed in Appendix B1, and the results from the investigations are also presented in Appendix B1.

4.4.2. Transient Electromagnetism (TEM)

a) Theory

Electromagnetic methods involve the use of a primary magnetic field which is transmitted into the ground and which induces a response from the earth. The secondary electrical response is measured by a receiver antenna and the strength of the field is determined by the ground conductivity (McNeill, 1990). Transient (or time domain) electromagnetic methods are slightly different from standard EM methods because the primary magnetic field is introduced into the ground as a series of short pulses. The secondary current produced by the earth cannot turn off as fast as the primary pulse, and therefore because they take longer to decay than the primary currents, it is the secondary current which is measured. Appendix B1 details the methodology of transient electromagnetic survey methods.

b) Results

The TEM survey performed in the field area involved 4 TEM stations and used a approximately 80mx80m square or rectangular transmitter loop and a central loop configuration (Appendix B1) orientated in three dimensions relative to the strike of the fault; X is parallel to strike, Y is perpendicular to strike and Z is orientated to give the vertical component (Figure 4.3.). The location of the TEM stations relative to the trace of the Waikawa Bay Fault is shown in Figure 4.2. The TEM information was also used to determine the thickness of the unsaturated surficial material above bedrock based on the conductivity of the materials. Table 4.2. shows the results of the soundings for depth to bedrock which indicate that the depth of the fan materials is between 22 and 30m, and that the water table is relatively consistent at approximately 5m.

i) Station WAIK100

Figure 4.4. shows the time vs voltage plots for both the X and Y orientations for station WAIK100 and both display significant signal reversals, indicating the

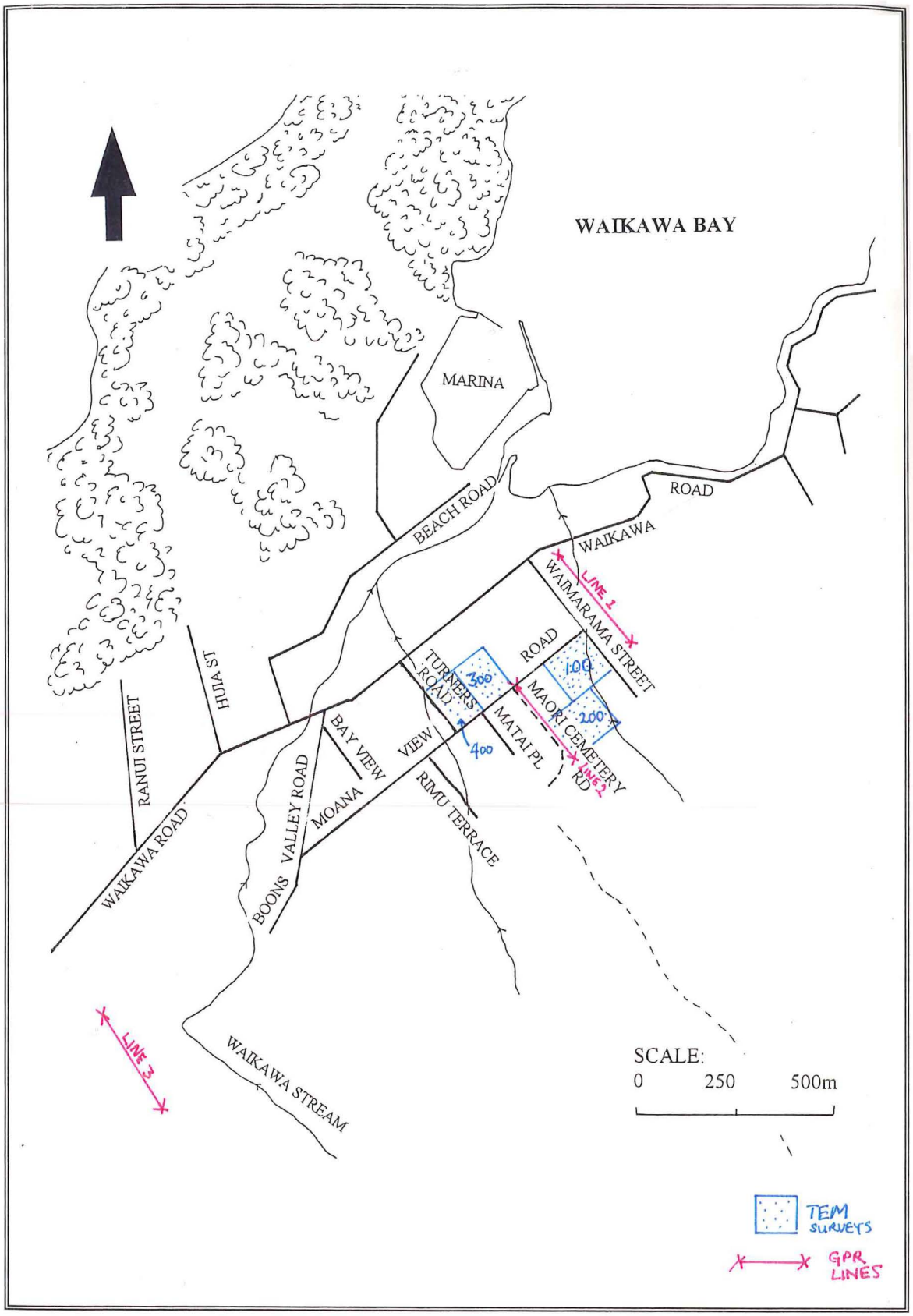

FIGURE 4.2.: The location of the geophysical investigations relative to the strike of the Waikawa Bay Fault and showing possibly splaying at the northern end.

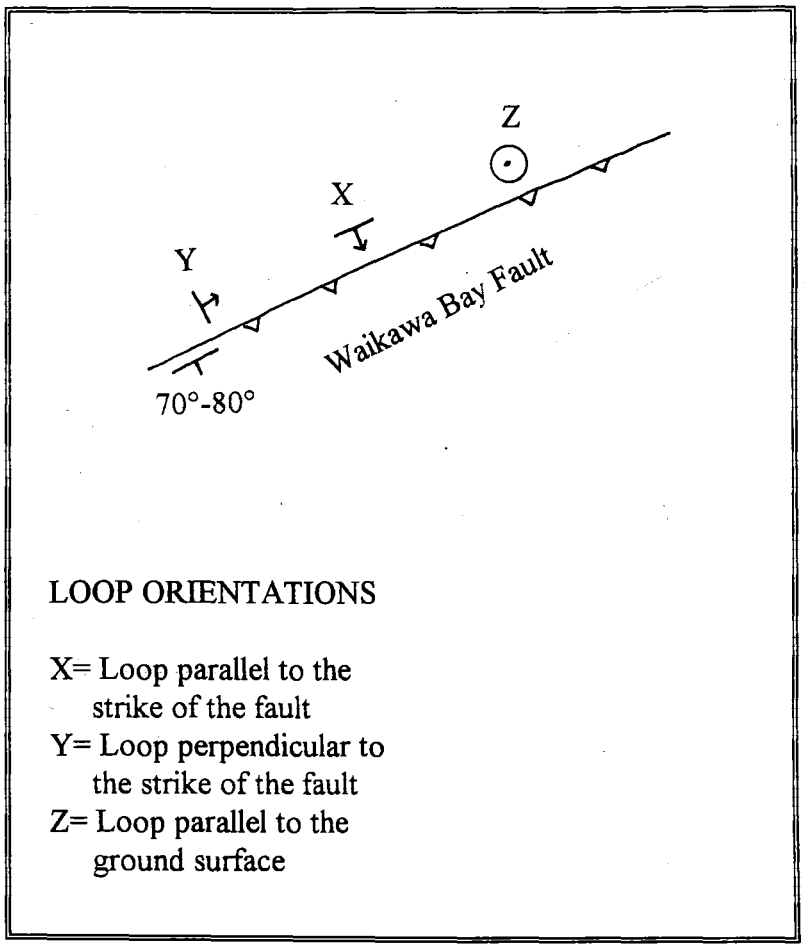

FIGURE 4.3. A schematic diagram to show the relative orientations of the TEM receiver loop and the strike of the Waikawa Bay Fault.

presence of a more highly conductive feature. The decay of the secondary field will be slowed down by the presence of a conductive body or layer because the signal becomes concentrated in that zone, while in resistive layers the signal will decay quickly. In WAIK100/X the reversal begins at approximately 0.04ms and, because of the orientation of this window parallel to the strike of the fault trace, is thought to indicate the presence of a shear zone the depth of which is not able to be determined. WAIK100/Y also shows a signal reversal at approximately 0.01ms and similarly to WAIK100/X station, indicating that there is a subsurface feature concentrating current orientated perpendicular to the trace of the fault. It is thought that the reversal observed in WAIK100/Y may represent the edge of the debris fan surface because the receiver coil is orientated perpendicular to the fault trace and parallel to the inferred edge of the debris fan. As observed in Figure 4.4. the fan gravels are moderately resistive and therefore the decay of the secondary field is still relatively quick.

ii) Station WAIK200

The location of WAIK200 was on the eastern side of the fault and it was expected that because the fault is thought to dip towards the east, some indication of the shear zone associated with the fault would be detected. The station which was orientated parallel to the fault, WAIK200/X (Figure 4.5.), shows a distinct signal reversal at approximately 0.06ms which is similar to the response recorded in WAIK100/X (Figure 4.4.), and is also thought to represent a higher conductivity zone associated with the fault shear zone parallel to the receiver coil direction. Additionally, the edge of the fan may have also been detected in WAIK200/Y (Appendix B1) which shows a signal reversal at approximately 0.07ms.

iii) Station WAIK300

Due to the considerable influence of cultural detail such as power lines and fences at this station located within the grounds of the local school (Figure 4.2.) the data obtained was not considered as reliable as the previous stations which were on relatively unmodified land. A possible signal reversal may be present in WAIK300/X (Appendix B1) at approximately 0.1ms, although it is also possible that the 'reversal' may be due to the cultural contamination at the site. If the reversal is real it may represent a splay of the fault to the west of the main trace. WAIK300/Y did not show any detail and the signal was seen to decay rapidly into noise (Appendix B1).

iv) Station WAIK400

Due to problems related to the influence of cultural detail only one station was attempted at this location adjacent to WAIK300 (Figure 4.2.). WAIK400/X (Figure 4.6.) showed no geological detail and there was considerable noise at this site.

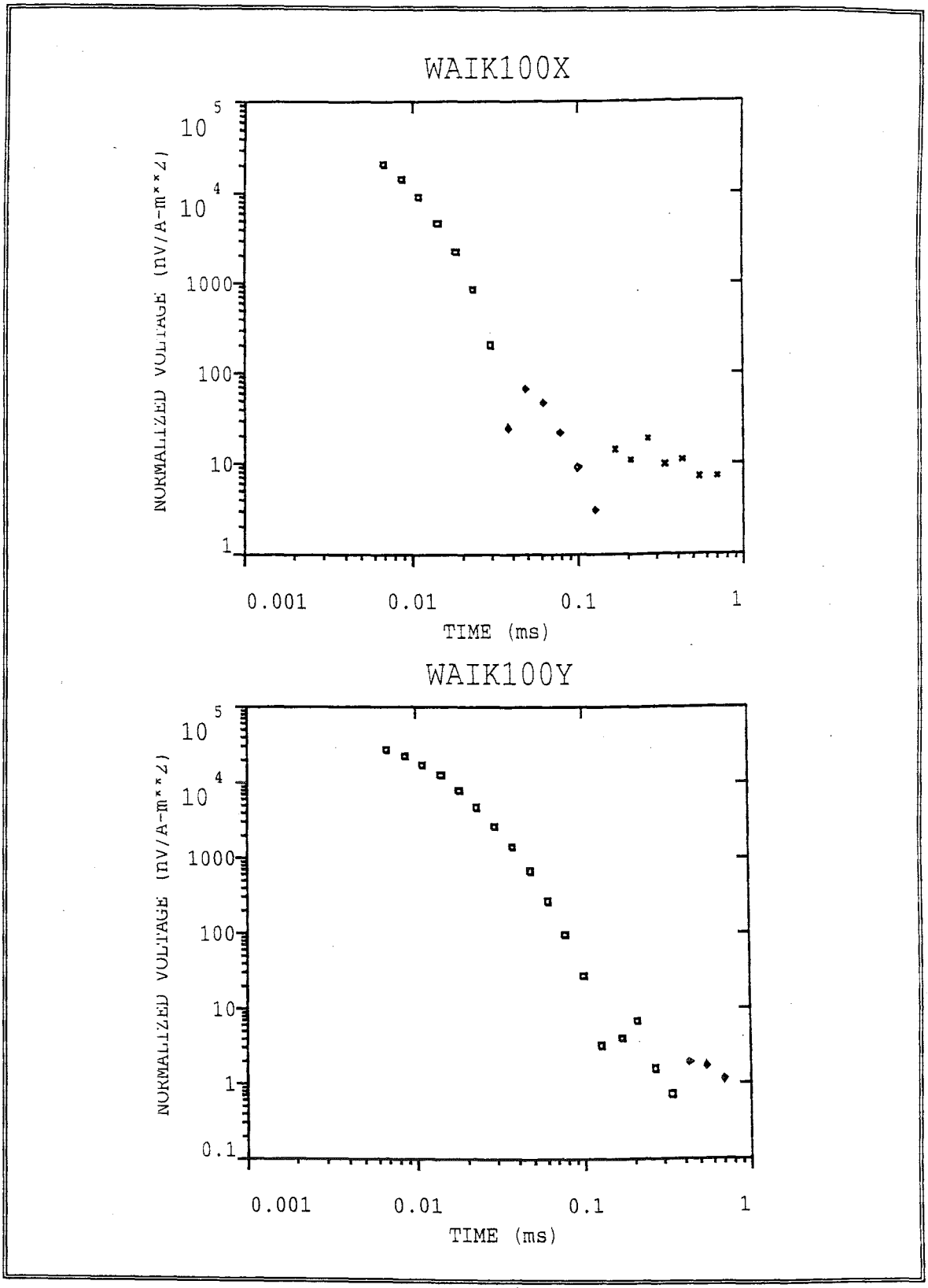

FIGURE 4.4. TEM soundings both parallel (WAIK100/X) and perpendicular (WAIK100/Y) to the strike of the Waikawa Bay Fault. Both profiles show reversals indicating the presence of more conductive structures. WAIK100/X is thought to show the location of the Waikawa Bay Fault

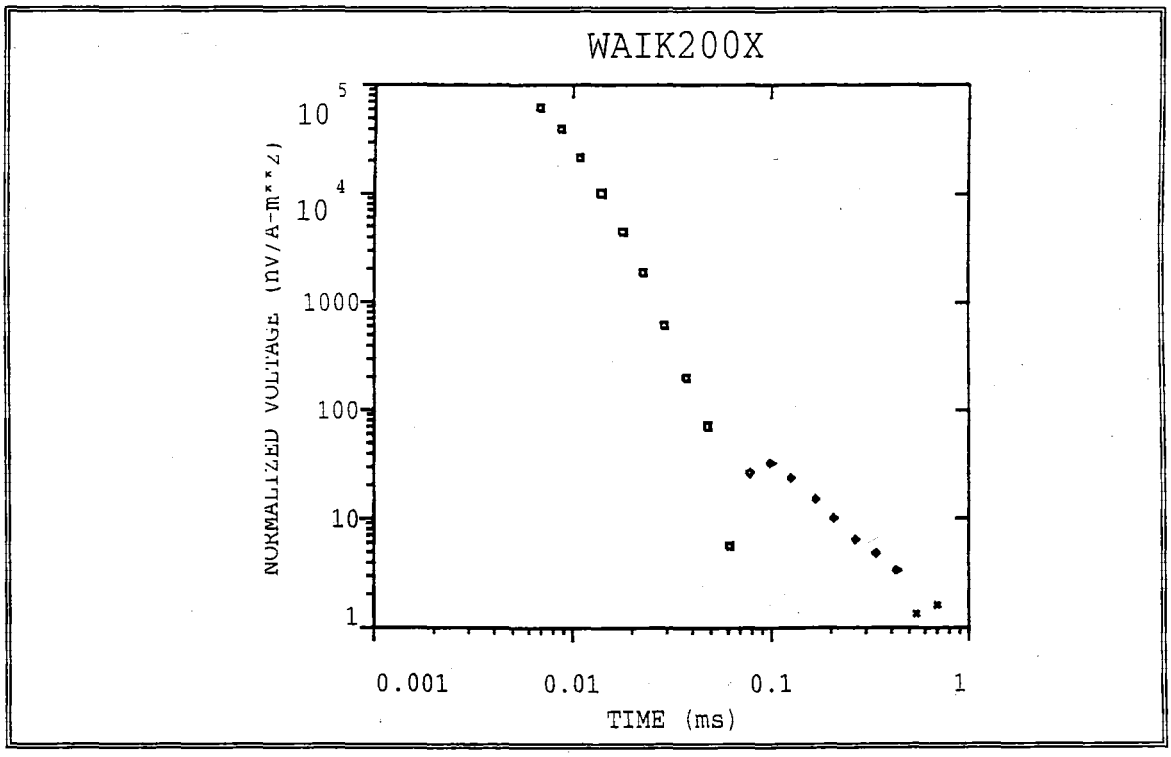

FIGURE 4.5.: TEM sounding showing a signal reversal at approximately 0.07ms which is thought to indicate the presence of a conductive shear zone.

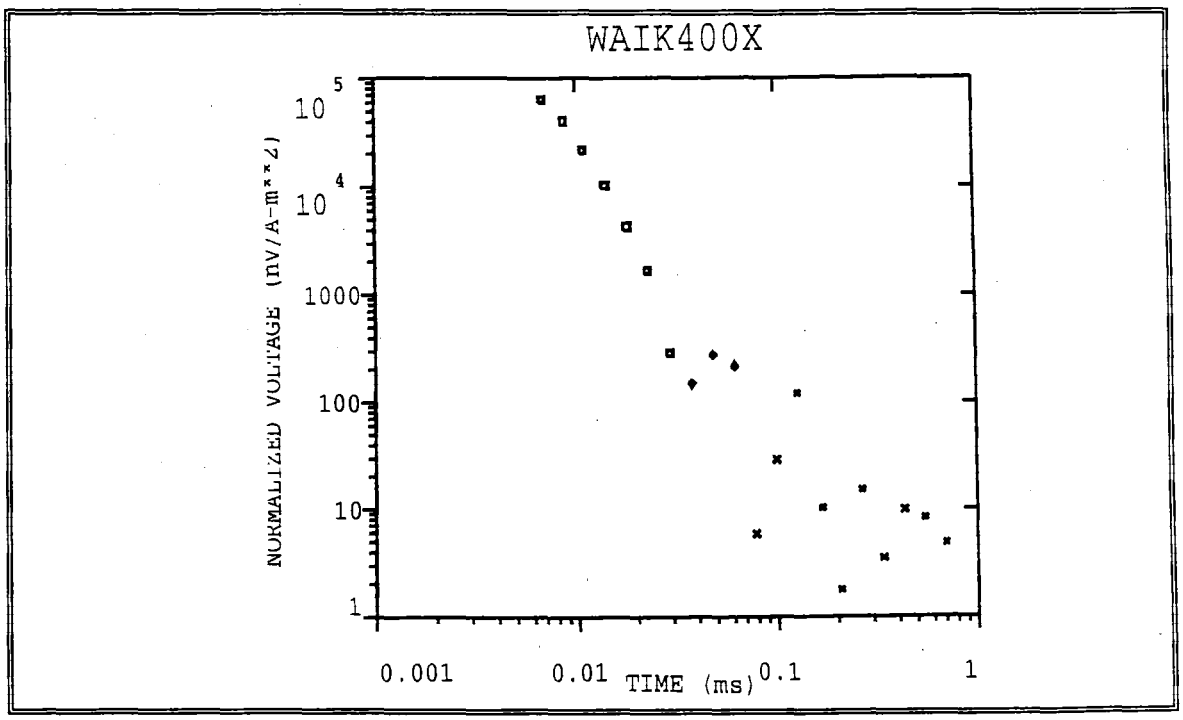

FIGURE 4.6.: TEM sounding for WAIK400/X showing the influence of considerable noise at this location.

4.4.3. Ground Penetrating Radar (GPR)

a) Theory

Ground penetrating radar (GPR) is similar to seismic reflection because it records the response of the earth to a high frequency pulse transmitted into the ground. Any feature in the ground which causes the pulse to be reflected back to the receiver is recorded. GPR data are commonly presented as wiggle traces with the positive part of the trace shaded. Figure 4.7. is a diagrammatic representation of the concept of GPR methods and an example of the way in which the ground may respond. The details of GPR are presented in Appendix B1 and the results obtained are presented below.

b) Results

GPR was used in order to determine the nature and extent of the Waikawa Bay Fault in the near-surface materials, and three survey lines were used at various locations along the observed and inferred position of the fault. Figure 4.2. shows the locations of the GPR lines in this study relative to the strike of the Waikawa Bay Fault.

i) Line One: Waikawa Bay North

The position of Line 1 is shown on Figure 4.2. and the site was selected because the trace of the Waikawa Bay Fault is unknown north of the Maori Cemetery fan and the fault is inferred to splay at its northern end. The location of line 1 is the youngest of the Maori Cemetery debris fans at the far north of the fan complex, and the most recent trace of the Waikawa Bay Fault is thought to have been eroded away during deposition of the fan during the late Otiran (15-10ka BP; Section 4.3.). Radar profiling along line one was conducted in two sections due to the fact that a stream cuts the paddock, and therefore GPR profiles were obtained for both parts of the paddock. Figure 4.8. shows the GPR wiggle trace obtained for both of the sections. Several continuous reflectors can be identified in the profile, which are thought to relate to phases of fan deposition or possible alluvial channels within the fan. The most prominent feature of the profile is a large diffraction which occurs in the centre of the line and is observed either side of the break in the line marking the position of the small stream cutting the fan surface, while the reflectors mentioned above appear to be disrupted at approximately 6m depth (Figure 4.8.). Disruption of structures can be seen to a depth of approximately 10m. Apparent diffractions are also seen at either end of the section, these features are related to interference from fences at the boundary of the paddock.

ii) Line 2: Maori Cemetery Road

The location of Line 2 was chosen because it is the only place in the field area where there is a definite fault scarp related to the Waikawa Bay Fault. The survey was conducted along the Maori Cemetery Road (Figure 4.2.) which runs up the oldest of the Maori Cemetery debris fans (Section 4.2.). As seen in the profile from Line 1,

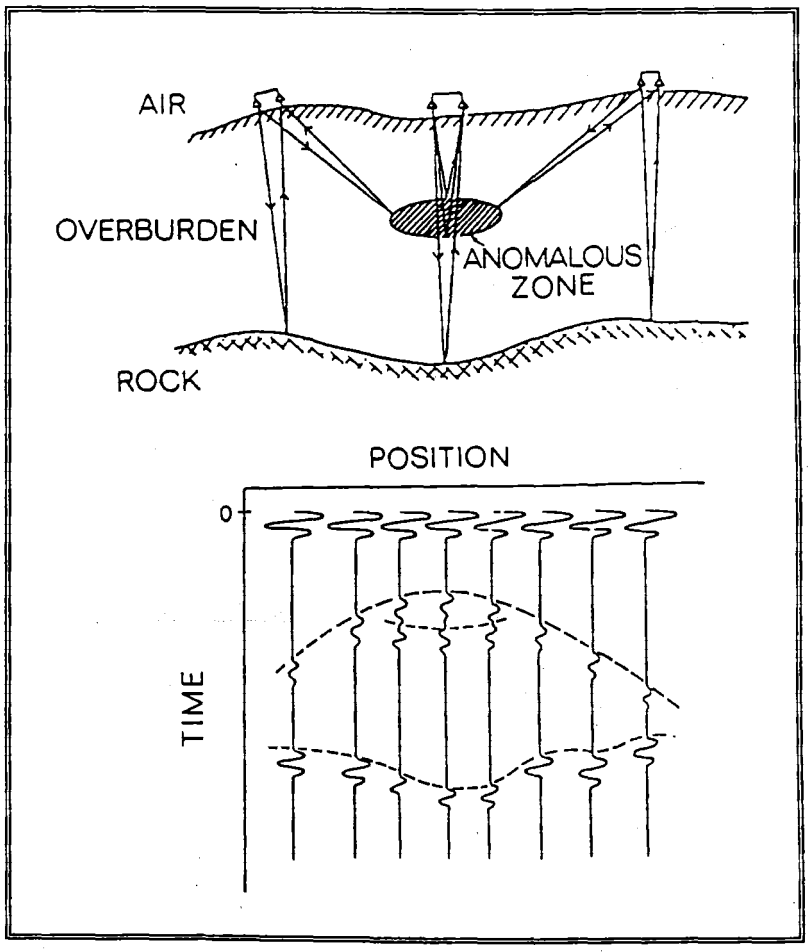

FIGURE 4.7.: The concepts of ground response for Ground Penetrating Radar (Davis and Annan, 1989).

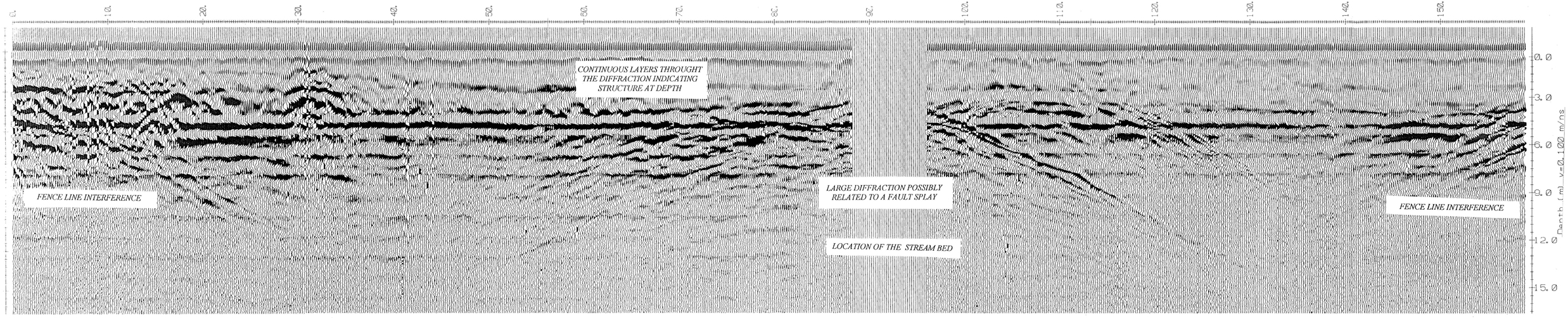

98

FIGURE 4.8.
WAIMARAMA STREET PROFILE: LINE 1

there are several small discontinuous reflectors observed (Figure 4.9.) which are believed to represent small scale modification of the fan by streams during formation of the fan, and the most prominent reflector is interpreted as the water table at approximately 5m. Up to three diffractions may be seen in the profile (Figure 4.9.) which do not appear to cause disruption of the near surface reflectors at the western end of the profile (15m and 14m respectively), but there is a large diffraction at approximately 75m which appears to cause disruption of the overlying material. The water table passes through the structure, which indicates that it is a diffraction and not a sedimentary structure related to the deposition of the fan. It is possible that another diffraction may be present at the eastern extreme of the profile (approx. 100m), although this may be caused by interference by a boundary fence at this end of the survey line rather than any geological structure within the fan material.

iii) Line 3: Waikawa Bay Saddle

The inferred position of the fault south of the Maori Cemetery debris fans is a trend southwards to Milton Terrace in Picton and on to the Elevation, and passes across Waikawa Stream close to where the stream is diverted by almost 90°. Between Waikawa Stream and Milton Terrace there is a relict bedrock spur which has a prominent depression forming a saddle through which the fault is inferred. Line 3 was located parallel to the ridge across the inferred fault trace (Figure 4.2.).

A number of strong reflectors were found in the Line 3 profile which were inferred to represent gross bedding planes, while the most interesting part of the profile is the disruption of bedding observered at approximately 20m, 50m and again at approximately 90m, and there also appears to be a large multiple diffraction associated with the 50m disruption (Figure 4.10.). There is a complete absence of cultural interference at this location as there were no fences, power lines etc. near the survey line and therefore the features observed in the profile (Figure 4.10.) are considered to be of a geological origin. At the eastern end of the profile (approximately 5m) there is a very large dipping reflector and the origin of this feature is uncertain as it may represent another diffraction, although there are no horizontal marker horizons which would assist in determining the nature of the structure.

c) Discussion

The major diffraction observed in Line 1, which is associated with the location of the stream cutting the paddock (Figure 4.8.), is thought to represent one of the splays of the Waikawa Bay Fault north of the observed fault scarp along Maori Cemetery Road. The presence of the stream may also be indicative of the location of faulting as the stream in plan view appears to follow a small depression which may well represent the fault trace. The GPR profile shows that fault displacement does occur at depth and the upper part of the profile indicates a lack of displaced

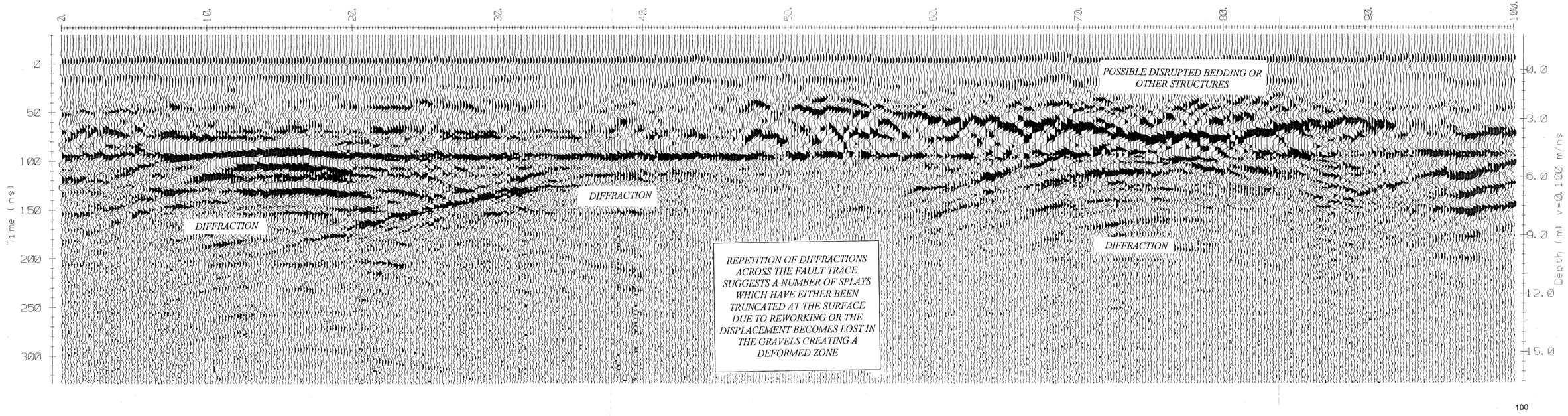

FIGURE 4. 9.
MAORI CEMETERY ROAD PROFILE: LINE 2

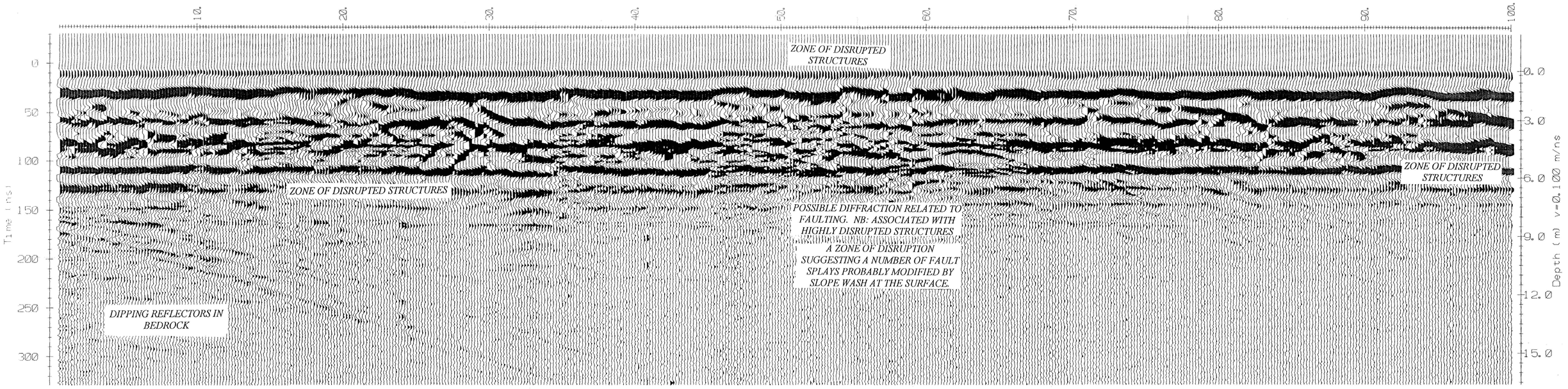

FIGURE 4.10.
WAIKAWA SADDLE PROFILE: LINE 3

structures. This feature is thought to represent the presence of a younger debris fan which was deposited following rupture and which has eroded into and subsequently covered any surface trace of the fault at this location.

The presence of numerous diffractions in Line 2, which appear to terminate consistently at approximately 6m depth, possibly reflects the presence of a number of small fault splays constituting a faulted zone and along which fault movement has been dissipated resulting in the warping of the fan surface. An alternative explanation is that the top 6m of material has been reworked since rupture and the reworking of the debris gravels has modified the fault scarp resulting in the gentle warping observed at the present day surface. The diffraction which occurs at approximately 75m is related to disruption of the upper fan surface (Figure 4.9.) and this is tentatively correlated to the main trace of the Waikawa Bay Fault which also does not rupture to the surface of the fan. The nature of the fault, as determined by McManus (1994) and as summarised in Section 4.1. is that of a faulted zone with numerous splays from the main trace and this is possibly represented in this survey line. The main trace of the fault occurring at approximately 75m along the survey line is complemented by up to 2 other fault splays however it is equally possible that the diffractions may be caused by buried material within the fan.

The Line 3 profile, which was the only line completed directly over insitu bedrock, showed considerable disruption of the bedrock material which is thought to correspond to the inferred location of the fault. As observed in the preceding profiles, the trace of the Waikawa Bay Fault does not have a single line of rupture but appears to be a zone of faulting which may be up to 100m wide. The presence of the saddle on the bedrock ridge also correlates with the fault line as can be seen in the profile at approximately 50m (Figure 4.10.).

4.4.4. Fault Character from Geophysical Investigations

The geophysical investigations in this study provided limited information on the nature of the Waikawa Bay Fault, and also on the age constraints of the debris fan material within which the only observable trace of the fault may be found. The TEM survey was inconclusive due to the problems associated with cultural noise in the field area in the form of power lines, fences and fill material, particularly at the WAIK300 and WAIK400 stations. The GPR, however, yielded considerably more information regarding the nature of rupture and the extension of the Waikawa Bay Fault to the north and south of the observed trace. The Waikawa Bay Fault was suspected to have last ruptured immediately following the deposition of the oldest Maori Cemetery debris fan (Section 4.3.) and the information from Line 2 indicates that the gravels themselves have possibly experienced displacement at depth. The disruption of the gravels near the surface may indicate that displacement of the

material became dissipated along numerous smaller splays within the gravels causing warping of the surface. An alternative explanation may be that there was a significant fault rupture creating a surficial scarp which has since been modified by erosion and subsequent debris deposition. Faulting is thought to have occurred following the deposition of the fan material, thus enabling the entire fan to have been disturbed by fault movement which at the surface was accommodated by several smaller splays of the fault.

The lateral extent of the Waikawa Bay Fault has also been constrained as the fault may be observed south of Waikawa Stream passing through the saddle of the bedrock ridge, and is inferred to continue along Milton Terrace to Picton (Figure 4.1.). The northern extent of the fault remains uncertain but it appears that the fault splays to the north, resulting in a number of traces all of which are difficult to identify due to substantial modification of the fault traces. One splay of the main fault is thought to have been located in GPR Line 1 (Figure 4.8.) defined at the surface by a small stream north of Waimarama Street. The trace possibly continues out into Waikawa Bay and may form the frontal edge of a thrust system to the south east (Chapter 2) however, evidence for faulting in Waikawa Bay is limited to some shearing observed along the coast line from Waikawa to Karaka Point (Chapter 2, Figure 2.13.).

The geophysical investigations support the theory that the Waikwa Bay Fault is not a single fault line which forms a number of splays at the northern end. Rather the Waikawa Bay Fault is more accurately defined as a fault zone which is at least 100m wide and any one of the faults in the zone has the potential to rupture and the identification of a fault zone further complicates the nature of the Waikawa Bay Fault north of the observed trace.

4.5. SUBSURFACE INVESTIGATIONS

4.5.1. Trenching

Subsurface data was obtained in the field area during 1994 (McManus, 1994) to determine the nature of the bedrock material either side of the inferred fault trace south of the Rimu Terrace alluvial fan and also in an attempt to identify rupture within the debris fan gravels across the observed fault trace. The results of trenching are reproduced from McManus (1994) in this study and the trench logs are presented in Appendix B2. Figure 4.11. shows the inferred position of the Waikawa Bay Fault, the nature of the fault zone relative to the bedrock types identified during trenching and the position of the test pits as presented in Appendix B2. The test pit data are discussed below and Table 4.3. summarises the nature of the bedrock material identified in each test pit.

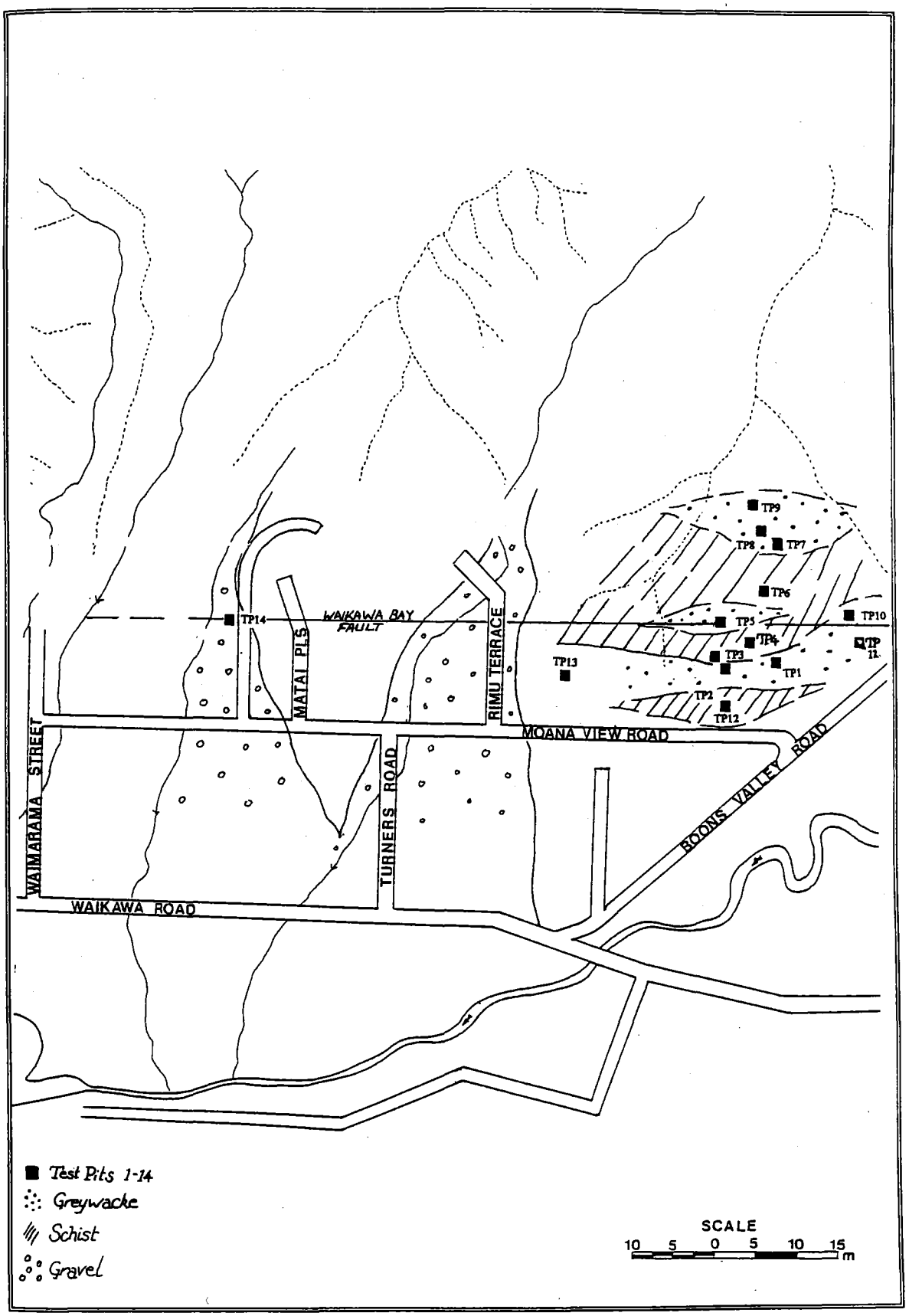

FIGURE 4.11.: Location of test pits 1-14 from McManus (1994) and the inferred position of greywacke and schist bedrock in the faulted zone

TABLE 4.2.: TEM soundings for the depth to bedrock in the Maori Cemetery debris gravels. Layer 1 represents the depth to the water table, Layers 1 and 2 represent the thickness of the gravels and Layer 3 represents the top of the more resistive bedrock units. The thickness of bedrock cannot be resolved

TEM SURVEY RESULTS FOR ELECTRICAL PROPERTY OF CONSTITUENT UNITS.											
WAIKAWA 100			WAIKAWA 200			WAIKAWA 300			WAIKAWA 400		
Layer	Ohm-m	Thick	Layer	Ohm-m	Thick	Layer	Ohm-m	Thick	Layer	Ohm-m	Thick
1	112	3	1	92	7	1	138	25	1	109	10
2	75	23	2	78	20	2	6	6	2	57	12
3	1,836	-	3	1,945	-	3	2,300	-	3	1,100	-

TABLE 4.3.: Summary of the nature of bedrock identified in test pits relative to the inferred trace of the Waikawa Bay Fault (McManus, 1994).

SUMMARY OF TEST PIT DATA (McManus, 1994)		
TRENCH NUMBER	Position relative to Inferred Fault Trace	Description of Bedrock
Test Pit 1	West	Greywacke bedrock
Test Pit 2	West	Greywacke Bedrock
Test Pit 3	West	Schistose bedrock
Test Pit 4	West	Schistose bedrock
Test Pit 5	On the Fault	Greywacke bedrock
Test Pit 6	East	Schistose bedrock
Test Pit 7	East	Greywacke bedrock
Test Pit 8	East	Greywacke bedrock
Test Pit 9	East	Greywacke bedrock
Test Pit 10	East	Greywacke bedrock
Test Pit 11	West	Greywacke bedrock
Test Pit 12	West	Schistose bedrock
Test Pit 13	West	Greywacke bedrock
Test Pit 14	On the Fault	Debris fan gravels

Trenching across the Waikawa Bay Fault was attempted in TP 14 (GR P27 259715 599210) which was 3m deep, 1m wide and 10m in length. The gravels exposed in the trench face, as described in Appendix B2, did not display any faulting or apparent disruption associated with faulting, thus it was assumed that any rupture of the surface gravels was dissipated across a faulted zone at least 100m wide, and may not have been seen over a distance of 10m represented by trenching. Additional trenching was completed south of TP14 (Figure 4.11.) and the trench logs are presented in Appendix B2. The trenching either side of the inferred fault trace determined the presence of schistose material (TZIIa-TZIIb; Chapter 2) and unfoliated greywacke bedrock. McManus (1994) inferred that greywacke existed to the east of the fault, while schist occured to the west. Trenching indicated that within the shear zone associated with the Waikawa Bay Fault greywacke and schist bedrock occur in a discontinuous manner with lenses of both rock types present. Much of the material which was trenched was landslide debris which post-dates the rupture event covering the fault scarp, and the identification of schist and greywacke bedrock was made on the basis of schistose or greywacke clasts within regolith material underlying the landslide deposits (Appendix B2).

4.5.2. Hand Augering

Hand augering was used by McManus (1994) in order to complement the test pit data, and 32 holes were drilled to a maximum of 2.2m and averaging approximately 1.0m deep, extending from Boons Valley Road to Waimarama Street and the locations of the drill holes are shown in Figure 4.12. The information from the augering is presented in Appendix B2 and is reproduced from McManus (1994).

The results of the hand augering in the field were limited in relation to identification of the Waikawa Bay Fault Trace. However augering indicated that the Waikawa Bay Fault is more accurately defined as a faulted zone extending at least 100m either side of the inferred and observed trace of the fault. Augering was able to be performed on a smaler scale than the trenching and indicated that the relationship of schist and greywacke within the shear zone is complicated, with lenses of each bedrock type possibly being as small as 1m wide. Difficulties were encountered in drilling at many locations due to the presence of gravel material and some landslide deposits which restricted the depth of some of the holes to less than 1m.

4.6. CONCLUSIONS

Investigation of the Waikawa Bay Fault using geomorphic information, geophysical techniques and subsurface data indicates that the fault is more likely to be a wide (a minimum of 100m) zone of ground deformation which has experienced

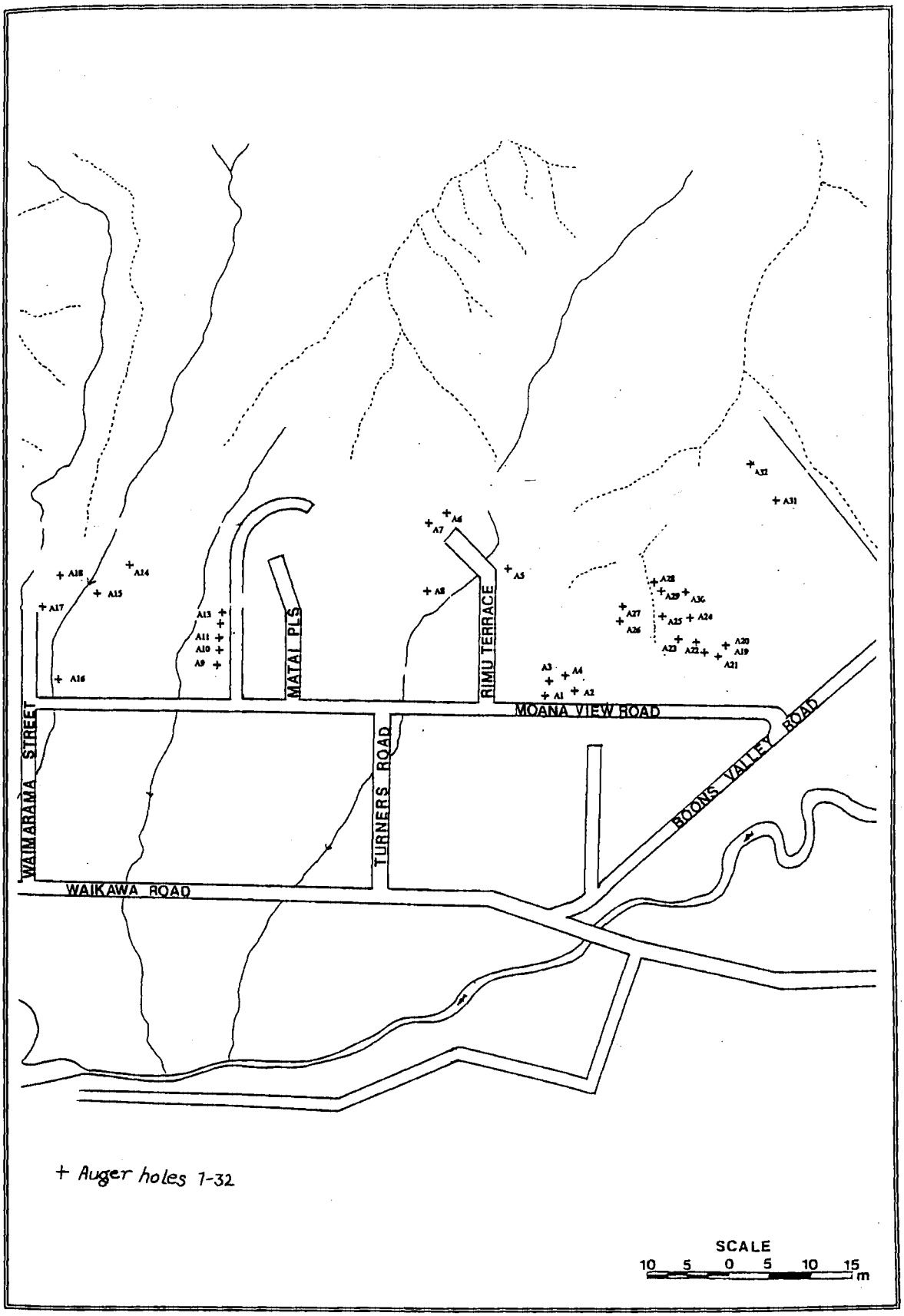

FIGURE 4.12.: The location of auger hole drilling from McManus (1994).

repeated fault movement. Schist bedrock is observed on the eastern and upthrown side of the fault and greywacke is found to the west. Within the shear zone augering suggested that schist and greywacke bedrock occurs in discontinuous lenses. Trenching and augering across the trace of the Waikawa Bay Fault throughout the field area showed the highly disrupted nature of the bedrock material and the extent of the zone which is at least 100m wide.

The extent of the Waikawa Bay Fault north and south of the observed trace (Figure 4.1.) is believed to pass through the Waikawa Saddle to the south, and to splay considerably to the north. Geophysical information indicates that the Waikawa Saddle has been extensively modified by faulting, which accounts for the lower topographic expression, and GPR also shows a wide (up to 100m) zone of faulting across the saddle. The fault can be followed north across the Maori Cemetery debris fans to north of Waimarama Street where the fault is thought to splay. One trace of the fault passes through the youngest debris fan just north of Waimarama Street and is observed in GPR profile for Line 1 (Figure 4.8.). A large diffraction associated with a small depression filled by a stream is thought to mark the location of the fault splay.

The age of last faulting has been constrained by both geomorphic and geophysical information. The fault is observed as a scarp across the oldest of the Maori Cemetery debris fans which is thought to have been deposited between 25 and 18ka BP. The fault rupture at the surface forms a disrupted zone which is a minimum of 100m. GPR, Line 2 indicates that most of the fan gravels in the oldest Maori Cemetery debris fan have been disrupted by subsurface faulting and movement has become dissipated within the gravels near the surface (Figure 4.9.). Erosion and subsequent deposition of the younger debris fans to the north and the Rimu Terrace alluvial fan to the south (approximately 15~10ka BP) has removed any trace of the faulting at the surface further constraining the estimated age of last rupture to approximately 18~12ka BP.

Fault activity is considered to be Class III which means that the fault has moved at least once between 50~5ka BP and with no evidence of movement within the last 5,000 years. Class III faults are those which are least active of the faults expected to move in the future. Repeated movements have undowbtedly occurred along the Waikawa Bay Fault which are older than 50ka BP and are represented by the faulted contact between the schistose and greywacke bedrock in the field area.

CHAPTER FIVE ENGINEERING GEOLOGY

5.1. INTRODUCTION

The investigation methodology used in this study follows that developed by Bell and Pettinga (1983) and concentrates principally on the pre-feasibility/feasibility and design stages of an investigation (Figure 5.1.). The principal aim of such an engineering geological investigation has been to provide a terrain analysis and a database for the production of both hazard and development constraint maps. Analysis of natural landscape processes and hazard evaluation follows methods previously developed in the Marlborough Sounds by Kingsbury (1987) in Havelock, Horrey (1989) in Picton and Waikawa, and McManus(1994) at Waikawa.

The objectives of the engineering geological aspects of this study are therefore:

1. Analysis of rock and soil properties from data obtained during field investigations.
2. Characterisation of rock and soil materials using limited laboratory testing.
3. Presentation of rock and soil distribution and the geomorphic features onto a 1:5000 engineering geological map of the field area.

This chapter divides the investigation programme used in this study into field and laboratory investigations and integrates the information obtained from both studies into discussions about the processes and geotechnical parameters of soil and rock in the field area. The details of the laboratory tests used in this study are presented in Appendices D4-11, and the results of each test are discussed separately in the text.

5.2. FIELD INVESTIGATION PROGRAMME

5.2.1. Methodology

The methodology of Bell and Pettinga (1983), outlined in Figure 5.2., has been used in this study to provide an engineering geological assessment of the field area. Published maps and reports, unpublished theses, engineering reports for the Marlborough District Council, and aerial photographs since 1959 formed the available data base. Presentation of the data was on an engineering geological map at a scale of 1:5000 (Section 5.2.3.) which showed the extent of surficial and bedrock units including colluvium, regolith and alluvium, the location of slope failures both active and inactive, areas of erosion and deposition, and principal structural features such as the Waikawa Bay Fault.

5.2.2. Aerial Photograph Interpretation

Aerial photography remains one of the most effective techniques for land assessment in areas such as the Marlborough Sounds because, due to the steep topography and dense vegetation in much of the field area, access to many locations is

SITE INVESTIGATION STAGES AND OBJECTIVES

PROJECT STAGE	SITE INVESTIGATION OBJECTIVES
I Pre-Feasibility and/or Feasibility	1. Selection of a geotechnically suitable site (or sites) 2. Assessment of the environmental impact of the project
II Design	3. Design and specification of foundations and associated earthworks, and of compatible engineering structures 4. Design of temporary engineering works to permit project construction
III Construction	5. Construction monitoring to confirm satisfactory design performance of the structure 6. Construction logging to provide a record of foundation conditions for future reference
IV Operation and/or Maintenance	7. Investigation of existing engineering structures to evaluate safety or long-term performance 8. Design and implementation of remedial works as required

FIGURE 5.1. The principal objectives for each stage of a site investigation (After Bell and Pettinga, 1983).

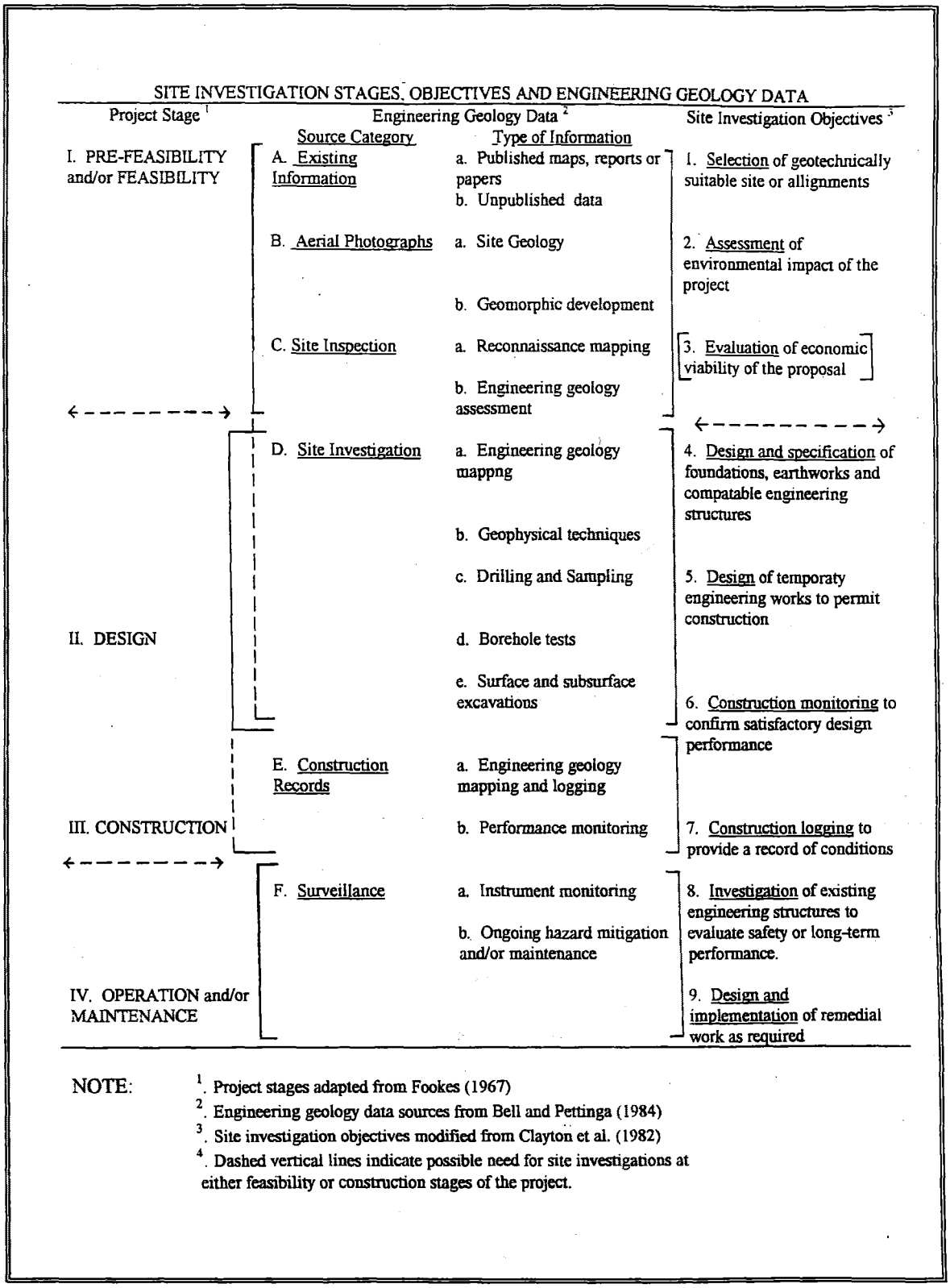

FIGURE 5.2. The relationship between the stages, objectives and data for an engineering geology site investigation (Bell, 1990).

limited. Aerial photography proved to be a very valuable remote sensing technique for the identification of previously unstable areas where field verification was impractical. Furthermore, the aerial photography allowed the interpolation of features such as the extent of fault lines identified during field work.

A number of aerial photographic runs were made available through the Marlborough District Council covering a time span of 36 years (1959-1995), thus allowing assessment of various features over time. Additionally, infra-red and colour photographs were available which allowed further analysis of vegetation changes. The earliest photographs available of the field area were the 1959 run which formed the basis of the aerial photograph data base used in this study. The photographic runs used for this study are presented in Table 5.1.

5.2.3. Engineering Geological Mapping

Preliminary mapping of the entire field area was undertaken between December 1994 and February 1995. Engineering geological investigations concentrated on the area between Waikawa township and Whatamango Bay, incorporating Karaka Point (Figure 1.1) and including all land between sea level and the ridge tops because of the possibility of urban development in these areas. Field mapping was completed at a scale of 1:5000 using aerial photographic base maps. The information which is presented on the engineering geology map includes the extent of surficial units such as colluvium, alluvium, debris and landslide deposits in areas where those materials have a thickness in excess of 1m. Bedrock lithologies of schist and greywacke are represented on the map and the only differentiation between weathering grades in bedrock is the division between regolith material and less weathered rock, defined in Chapter 3. Geomorphic information such as active and inactive headscarp regions of slope failures, areas of landslide and debris deposition, areas of alluvial deposition, and significant erosional features such as tunnel gullies and eroded stream banks are also differentiated on the engineering geology map. Additionally, gross structural features such as the Waikawa Bay Fault, are shown. The engineering geology map is presented as Figure 5.3. (Map Volume).

5.2.4. Insitu Percolation Tests

a) Introduction

The objective of insitu percolation assessment is to determine the range of infiltration rates which may be obtained in the field area and the relationship between percolation rate and geology. Due to the lack of available percolation test sites within the field area, previous test results used for the evaluation of sites for septic tank disposal were obtained from the Marlborough District Council. The percolation test follows NZS 758, and measures the rate at which water drains from a standard diameter (100mm) bore hole following a period of hole swelling of

approximately 12 hours. The test also requires a description of the soil at the site to determine the extent and nature of the material which will support the septic system. In general a minimum of 4 holes are recommended for any one site.

Percolation testing is necessary to ascertain the suitability of a site for septic tank installation and additionally, septic tank systems require sufficient land for an evapotranspiration (ETS) field adjacent to the tank (Figure 5.4.). The nature of the soil in which the ETS field is located is important because the effluent must be able to drain sufficently slowly so that the liquid may be treated by aerobic bacteria and purification occurs, but soils high in clay will restrict the movement of effluent through the soil and subsequent purification of the liquid because of the small grainsize and lack of interparticle pore spaces. Conversely, thin soil cover overlying highly fractured or jointed bedrock, or material with high percolation rates such as gravel, will allow effluent to quickly move directly to the watertable without purification having occurred which can then pollute ground water and has the potential to reach surface water. ETS fields must also be located some distance from any natural drainage or water courses.

The size of the ETS field is relative to the capacity of the septic tank. Table 5.2. shows the specified tank capacity for the number of bedrooms in the residence (NZS 758) and Table 5.3. show the relation between the percolation rate and the total length of piping required for evapotranspiration (after Lough, 1952). The following discussion concerns two sites showing favourable and unfavourable percolation rates which have been obtained in the field area and Appendix D1 presents all of the percolation data obtained in this study.

b) Discussion

As previously mentioned, the soils of the Marlborough Sounds are typically up to 4m on the mid to lower slopes, becoming considerably thinner (<1m) on the upper slopes. The regolith material is predominantly a silty clay with some sand, although the red weathered regolith deposits are high in clay (up to 90%, Section 5.3.2.) while the colluvial soils have a gravel component up to 40% (Section 5.3.2.) and the matrix material is generally a silty clay. The occurrence of large amounts of clay or gravel will cause the percolation rates of the soils to be low or high respectively and therefore will generally be unsuitable for an the installation of an ETS. Underlying the soil cover is fractured, and in some places foliated, bedrock and the percolation rates of such bedrock is generally high particularly if the soil cover is thin (<1m). Additionally, the land available for an ETS field is limited by the steep topography and the frequent occurrence of water-courses, as the ETS requires a flat or gently sloping site which is removed from surface water influences.

The percolation data for the field area are variable and all of the results are presented in Appendix D1, while a representative selection of sites showing the variability is presented in the following discussion. Figure 5.5 shows the cumulative

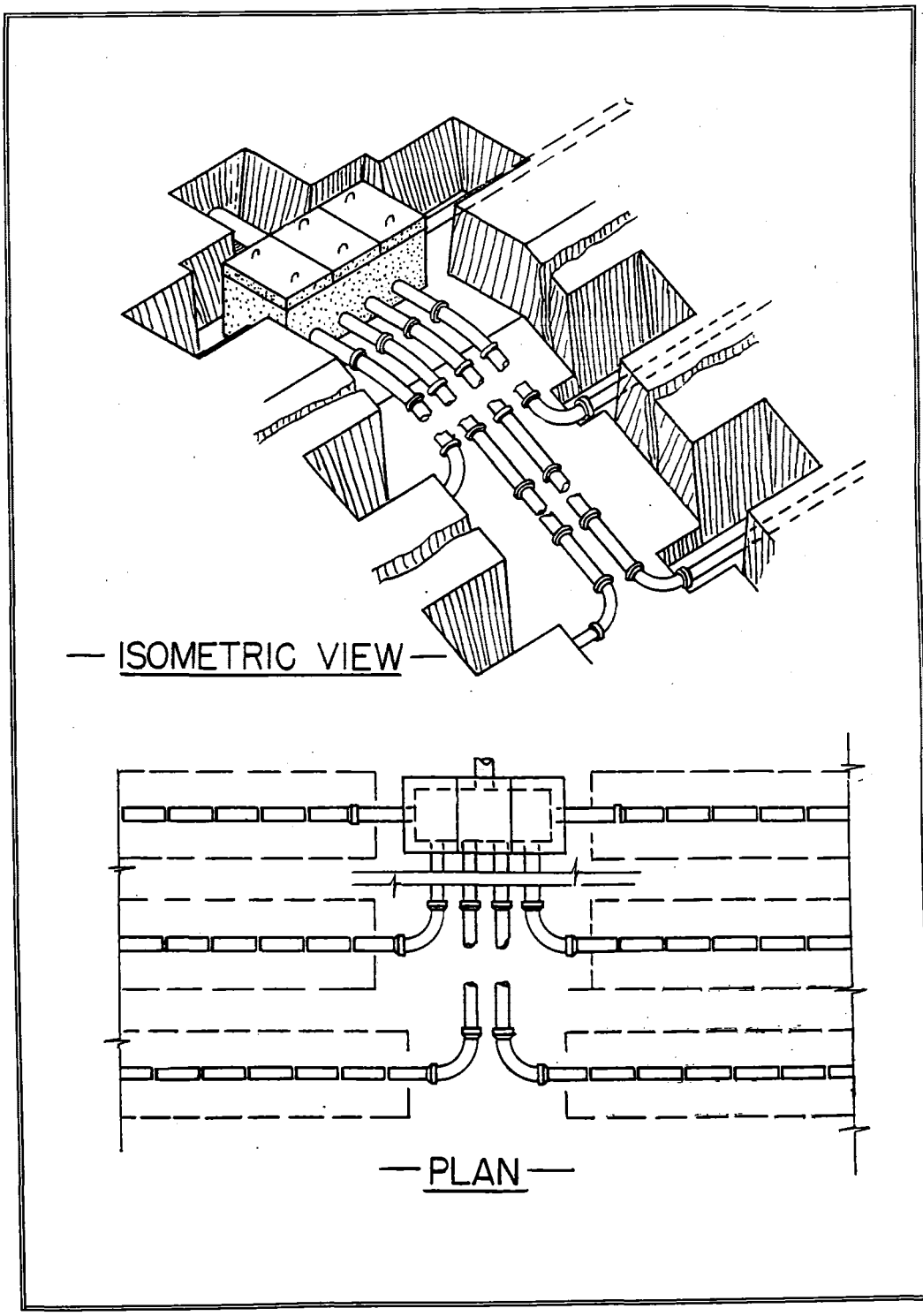

FIGURE 5.4.: The standard trenching and piping layout for an evapotranspiration system on sloping ground shown in both isometric and plan view (From Lough, 1952).

Table 5.1. The aerial photographic runs since 1959 used for engineering geological assessment in this study.

Photograph run number	Scale	Date
2191/41-43	1:20,000	1959
2190/41-43	1:20,000	1959
SN 10786 70505-70507	1:50,000	1979
WSO 63 A/1-5	1:10,000	1983
WSO 63 C/1-6	1:10,000	1983
WSO 63 D/4-7	1:10,000	1983
SN 12077 J/18-20	1:45,000	1993

Table 5.2. Showing the relationship between the size of the house served and the size of the septic tank required (After Lough, 1952).

Max. No. Bedrooms	Liquid Capacity of Tank (Gals)
2	300
3	400
4	500
5	600
6	700

Table 5.3. The relationship between the percolation rate and the length of tile line required for septic disposal (After Lough, 1952).

Time required for water to fall 2.5 cm. (mins.)	Length of tile needed for houses ≤2 bedrooms (m).	Additional length for each bedroom over 2 (m).
2 or less	21	10.5
5	30	15
10	39	19.5
15	51	25.5
30	72	36
60	96	48

PERCOLATION DATA FOR SITE (A) IN WHATAMANGO BAY

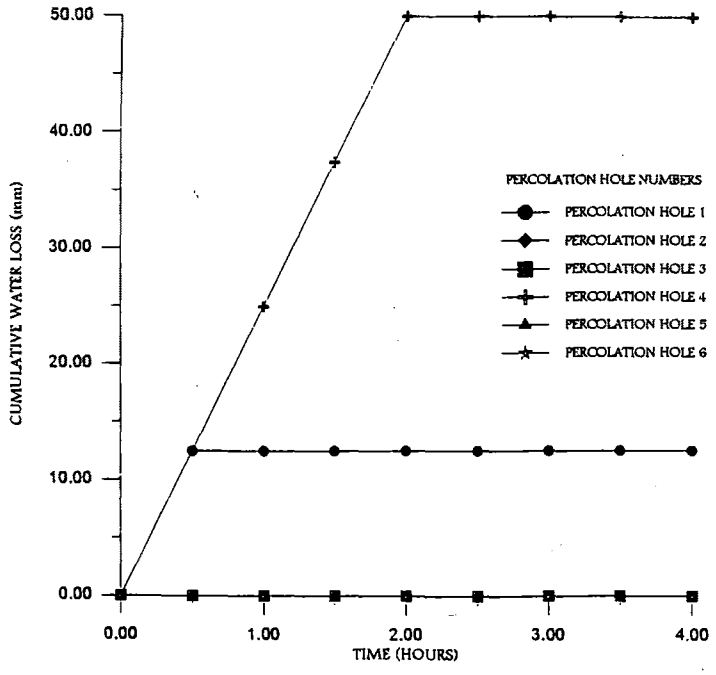

PERCOLATION DATA FOR WHARETEKURA BAY SITE

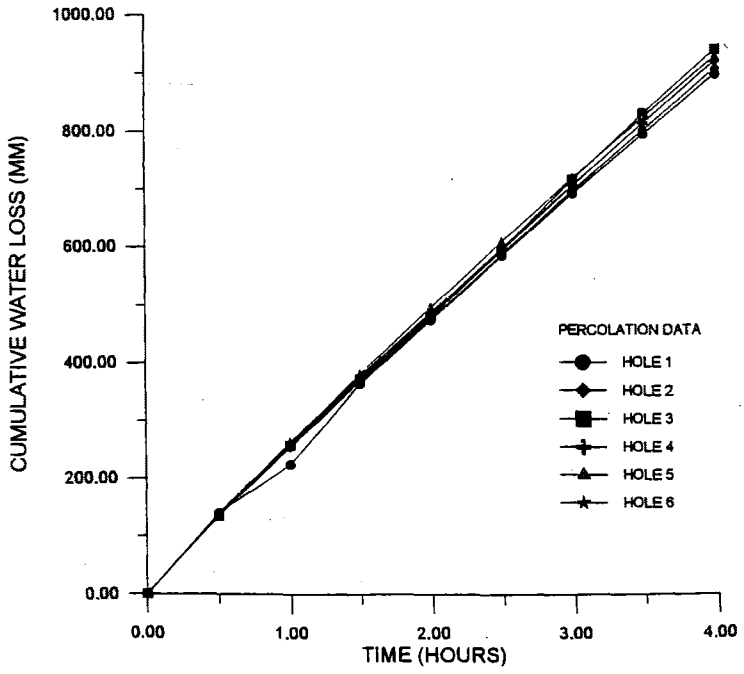

FIGURE 5.5.: Percolation data for Site A in Whatamango Bay with percolation rates of 0mm/hr for all holes. Note: data from holes 2,3,5 and 6 plot along the X-axis as all percolation rates are zero. Percolation data for Site B in Wharetekura Bay showing consistent percolation rates of approx. 200mm/hr for all holes.

water loss recorded in the holes for each site plotted against time. The percolation rates for each of the holes is determined by the the slope of the flattest portion of the percolation curve. The percolation rates for each of the holes at the locations described below are given on each graph and averaged to estimate the percolation rate the site.

One particular site (a) located at the head of Whatamango Bay (GR P27 260025 599245) recorded extremely low percolation rates of less than 25mm per hour for 5 of the six holes tested (Figure 5.5.). The soil is recorded as being predominantly clay which would account for these low and unfavourable percolation rates. As introduced above, an ETS requires soil which allows the effluent to drain slowly enough for the liquid to be purified by aerobic bacteria, however drainage rates which are too slow will cause the liquid effluent to swamp the ETS field without purification. In addition to the unfavourable soil conditions at this particular site, the proposed ETS field was close to a surface waterway and there was very little gently sloping or flat ground which could be used to expand the effluent disposal system. As a result the proposal for installation of a septic tank was not approved.

Figure 5.5. also shows the percolation data obtained from a house site (b) in Wharetekura Bay (GR P27 259833 599340) which was favourable for a septic tank design because the percolation rates indicate that the infiltration is quick enough (approximately 200mm/hr) to allow for purification of the effluent and yet not so slow as to inhibit drainage such as was observed at site a). Figure 5.6. shows the location of the system and the size of the evapotranspiration field given the percolation measurements obtained (MDC, 1988).

5.2.5. Hydrological Investigations

a) Monitoring Programme

The Graham River was monitored for approximately six months from March to September 1995 to assess the response times of flood events compared to rainfall in the catchment area. A Kainga 1000 Series pressure transducer was installed on the upstream side of the Port Underwood Road bridge on the Graham River to measure the water level using changes in water pressure. Accuracy is in the order of 0.25% of the full scale pressure range and the range is additionally calibrated to temperature fluctuations within the maximum ranges of -5 to +50° C. The pressure transducer was interfaced to an Aquitel 2 data acquisition and flood protection system using a WRSC analogue data converter. Figure 5.7. shows the frame used to hold and protect the Aquitel 2 system, which was powered by a rechargeable NiCd battery and solar panels. The rainfall was measured by a previously installed system in the Boons Valley catchment which feeds the Waikawa Stream and is adjacent to the Graham River catchment. The installation of a rainfall recorder in the Graham River was precluded by funding restrictions and therefore the Boons Valley rainfall recorder

had to be used. The readings obtained therefore are not ideal, although they are considered suitable for a preliminary assessment of the nature of the Graham River's response to rainfall.

b) Results

Both rainfall and stream level were measured for the period March 23 1995 to September 18 1995, and the data are presented in Appendix D2 and D3. The rainfall was measured in millimetres and each day ended at midnight. Table 5.4. lists the twelve maximum rainfall events occurring at two, three and six hourly intervals to show the nature of rainstorm events in this part of the Marlborough Sounds. The range of rainfall intensities are consistent regardless of the storm duration. The range for 2 hour rainfall events is from 15 to 25.5mm, with an average intensity of 9.75mm/hr, while for a 3 hour event the range is from 19 to 32.5mm with an average intensity of 8.2mm/hour. The average intensity drops with longer duration rainstorm events, although the ranges are similar indicating that the greatest intensities are obtained from the shorter duration rainstorm events. The figures for the 6 hour storm events range from 28-51mm and have an average intensity of 5.9mm/hour.

Stream flow data are presented in Appendix D3 and the relationship of rainfall in the Boons Valley catchment to the stream flow in the Graham River at the Port Underwood Road bridge is discussed below. The maximum flow obtained in the Graham River was 17,120 l/sec^{-1} which occurred on April 5, 1995 while the minimum flow was 20 l/sec^{-1} also recorded in April on the 27th and the average flow rate for the period 24 March to 17 September 1995 was 88 l/sec^{-1}. Figure 5.8. shows the relationship between the rainfall data (mm) and the stream flow data (l/sec^{-1}).

c) Discussion

Flows in the Graham River showed seasonal variation over the six months of data collection, with most of the peak flows occurring during the winter months as opposed to autumn and spring flows (Figure 5.8.). From the raw rainfall and stream flow data several important parameters may be derived which assist understanding of the nature of the Graham River. Firstly, the base flow may be measured directly from the flood hydrograph (Figure 5.8.) and for the Graham River is calculated at approximately 0.35 cumecs, or 350 l/sec. Secondly the quick flow response of the Graham River, which is the overland flow component that quickly moves into the main channel or watercourse via surface runoff and interflow (Allaby and Allaby, 1991), may be calculated using the equation:

$$D = 1.25\ K^{0.2}$$

where: D= the number of days between storm peak and the end of the quick (overland) flow

K= drainage basin area (catchment area) in km^2 (Fetter, 1980)

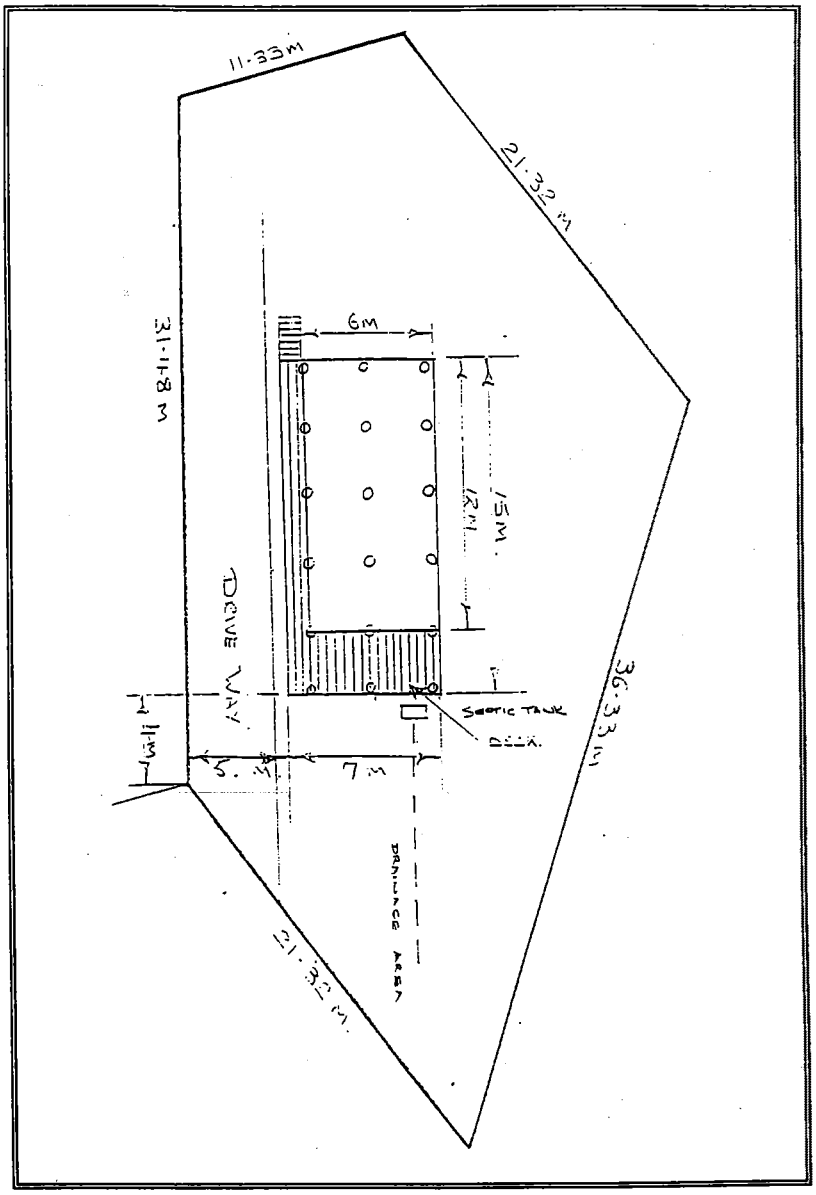

FIGURE 5.6.: The location of a septic tank and evapotranspiration system at site b) in Wharetekura Bay, and is the system installed using the data in Figure 5.5.b.

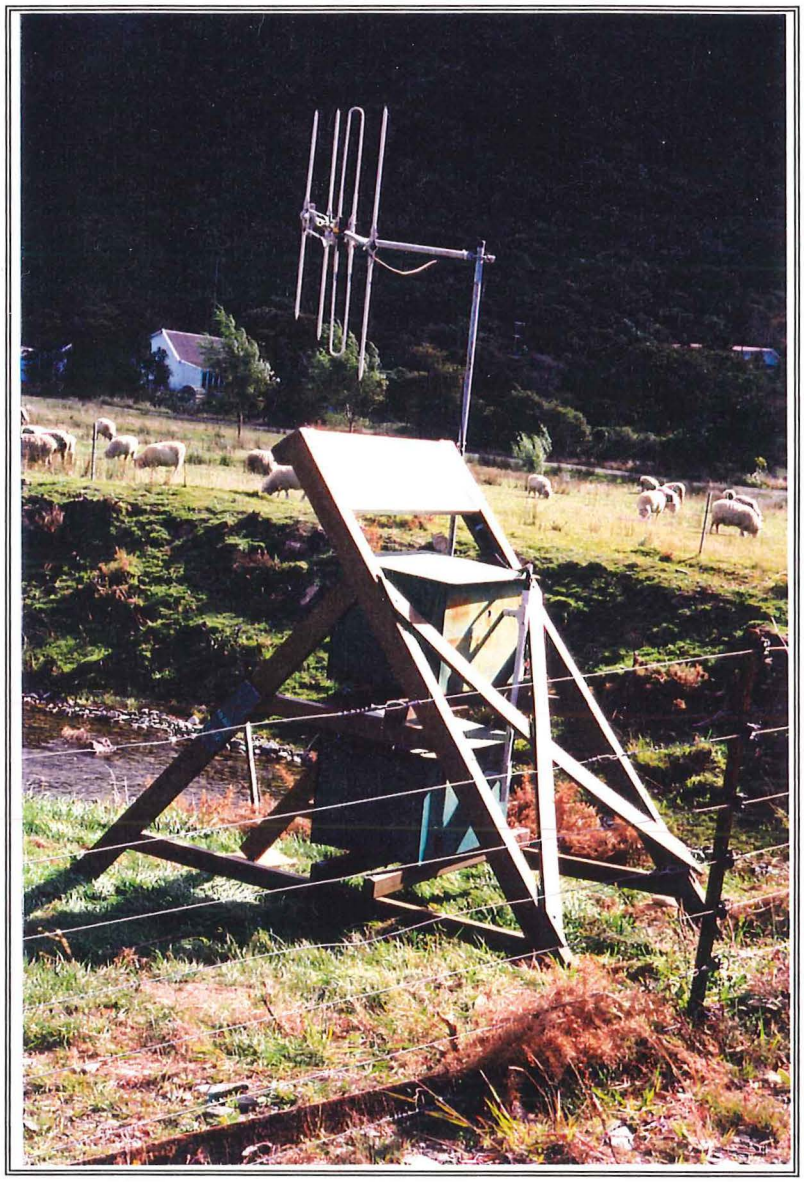

FIGURE 5.7.: The Aquitel 2 data acquisition and flood protection system and protective frame. The system is powered by a rechargeable NiCd battery and solar panels. The system was located at the Port Underwood Road Bridge in Whatamango Bay.

The quick flow response for the Graham River is D = 2.2 days given a total catchment area of approximately 18.0 km^2. Therefore, the time for the stream to return to base flow following a storm event, that is the time for all the overland flow to drain from the catchment, is approximately 2 days.

Thirdly, the runoff percentage may be estimated. This parameter requires the total base flow and the total quick flow in cumecs. Base flow equates to 52,810 l/sec^{-1} or 52.8 cumecs over the 178 day period. Quick flow is 130,590 l/sec^{-1} (130.59 cumecs). Therefore, the run off percentage (Base flow/Quick flow x 100) is calculated at 40.5%. However it is important to remember that these calculations do not adequately take into account the factors of slope angle, vegetation, drainage density and other catchment characteristics (Fetter, 1980) and thus the final figure is approximate. For instance, a steeper slope angle will increase runoff percentage while vegetation of the catchment will similarly reduce runoff and therefore the calculations are a simplification of the range and diversity of conditions which may exist in the catchment area.

Additional information may be derived from the flood hydrograph when rainfall information is also plotted (Figure 5.8.). From this graphical representation of the data, the lag time between each rainfall event and the associated stream flow peaks may be estimated. The flood hydrograph in Figure 5.8. shows a lag time of approximately 12 hours between each rainfall and flood event. An important factor when interpreting such information is the antecedent soil water conditions, because water runoff will be greater when the catchment soils are saturated as less water can infiltrate into the ground. Therefore during winter months when the rainfall is higher the soils will be wetter than during the dry summer months and the infiltration is less, which in turn creates a shorter lag time between the rainfall and flood events. One can observe on the flood hydrograph (Figure 5.8.) that, although there is a delay in the response time of the flow compared to the rainfall at the beginning of each event, the maximum flow and rainfall peaks occur at the same time. Additionally maximum flow peaks related to a period of consistent rainfall prior to the maximum flow event do not display a delay in response time at the beginning of the event as can be seen at the end of April, 1995. Significant trends are not obvious, however, because flow data for summer months is absent and continued monitoring would be required to confirm this trend. The presence of vegetation in the catchment area can also affect the runoff of water during a storm event because the vegetation absorbs much of the water falling onto the ground, and therefore vegetated catchments will have smaller flood peaks compared to devegetated catchment areas. The implications for the Graham river which has a heavily vegetated catchment, is that the flood peaks would be expected to increase should the catchment become devegetated.

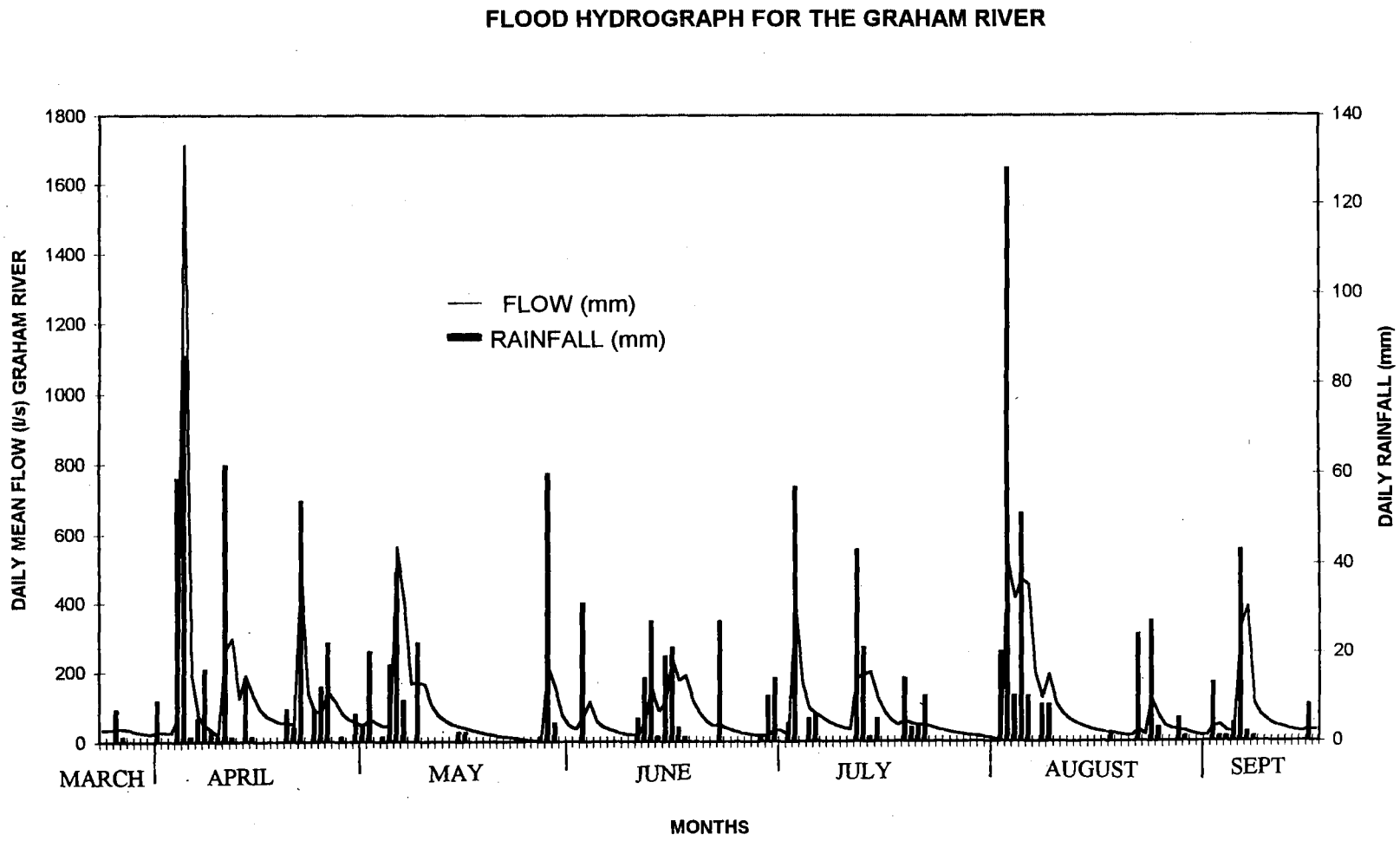

FIGURE 5.8.: The flood hydrograph for the Graham River from March to September, 1995 incorporating rainfall data from the Boons Valley Catchment.

The recurrence intervals for flooding events, defined as flows which will overtop the stream banks, in the Graham River are difficult to accurately predict with the limited amount of rainfall and flow data. However flood events which will overtop the road at the Port Underwood Road bridge have occurred in the recent past, with the last flood occurring in November 1994. Rough estimations of floods of this stage indicate that these events have recurrence intervals of a minimum of 10 years however the flow rate during an event of this size could not be measured as there were no events of this size during the monitoring period. The stream flow data obtained during the six months of monitoring indicate that high flow events of 50-60 l/sec^{-1} will occur at least once a year, with two events of this size occurring during the winter of 1995.

One of the most interesting features shown by the flood hydrograph (Figure 5.8.) is the occurrence of a flood event with a peak of 1,712 l/sec^{-1} during the autumn of 1995. The flood occurred on April 5 in response to a rainfall of approximately 80mm in 24 hours, and followed a dry period in the Marlborough Sounds. Therefore the antecedent soil moisture conditions were not saturated indicating that the runoff rate should have been lower than the flood peak indicates. It appears therefore that the soils within the Graham River catchment may have low infiltration rates in summer contributing to sudden flooding events during the summer and autumn, and this hypothesis is supported by the occurrence of the flood event previously mentioned during November 1994 which occurred during a dry summer period. However, the patterns shown on the flood hydrograph may be considerably influenced by the lack of a rainfall recorder within the Graham River catchment and possibly indicates that rainstorm events which have led to the floods in the Graham River are localised events not accurately recorded by the recorder in Boons Valley.

5.3. LABORATORY DATA

5.3.1. Introduction

During the course of field work samples of rock and soil material were collected for laboratory testing. The samples obtained were mainly disturbed bulk samples, although some insitu tube samples were collected for specific index tests. Both the sampling program and the laboratory analysis were based around two specific objectives

1) engineering characterisation of surficial deposits for the purposes of foundation stability and geological hazard assessment.

2) identification of weathering grades within bedrock types and further characterisation of these grades.

Generally therefore, the testing was divided into rock and soil analysis and Table 5.5. shows the tests performed in this study and the materials tested in each analysis.

Table 5.4. Rainfall events measured in Boons Valley catchment.

Rainfall (mm) 2 hrs	Date	Rainfall (mm) 3 hrs	Date	Rainfall (mm) 6 hrs	Date
25.50	22/04	32.50	22/04	51.00	04/04
25.00	11/04	32.00	11/04	50.50	22/04
23.50	27/01	30.50	04/04	45.00	23/02
23.50	23/02	26.50	23/02	40.50	03/08
21.00	04/04	25.00	12/07	40.00	03/08
18.50	12/07	23.50	27/01	37.50	05/04
17.50	09/05	23.50	05/04	36.50	12/07
17.00	22/08	21.50	03/08	35.50	11/04
16.00	23/02	21.00	03/08	32.50	28/05
16.00	05/04	20.00	09/05	32.00	27/01
15.50	07/04	19.50	28/05	30.00	06/09
15.00	03/08	19.00	07/04	28.00	03/08
Average intensity 9.75mm/hr		Average intensity 8.2mm/hr		Average intensity 5.9mm/hr	

Table 5.5. Summary of the laboratory testing program and the material tested.

Laboratory Test	Rock Material*	Soil Material*
Grain Size Analysis	NT	RR, GR, SR, GC, SC
Atterberg Limits	NT	RR, GR, SR, GC, SC
Dispersion Testing	NT	RR, GR, SR, GC, SC
Point Load Strength Index	WS III, IV, V, WG III, IV, V	NT
NCB Cone Indenter	WS III, IV, V, WG III, IV, V	NT
X-Ray Diffraction Analysis	WS III, IV, V, WG III, IV, V	RR, GR, SR, GC, SC
Scanning Electron Microscope	WS III, IV, V, WG III, IV, V	RR, GR, SR, GC, SC
Ring Shear Testing	NT	RR,SR,

Rock Material* WS III - weathered schist grade III, WS IV-weathered schist grade IV, WS V-weathered schist grade v; WG III-weathered greywacke grade III, WG IV-weathered greywacke grade IV, WG V-weathered greywacke grade V.
Soil Material* RR-red weathered regolith, GR-greywacke regolith, SR-schistose regolith, GC-greywacke colluvium, SC-schistose colluvium
NT-not tested.

5.3.2. Grainsize Analysis

a) Introduction

The objective of the grainsize analysis programme was to identify variations between sample sets which possibly reflect the origin of the material, and to produce grading curves to characterise the various materials identified by field mapping. The samples selected for grainsize analysis were divided into five soil types depending on their original bedrock source. Five samples were chosen from schistose colluvium, while six each were selected from greywacke colluvium, greywacke regolith and schistose regolith. Additionally, four samples of red weathered regolith of greywacke origin were tested. Test methodology followed NZS 4402 and is described in Appendix D4.

b)Results

Problems were encountered during the grainsize testing program regarding the presence of clay aggregates appearing as both sand and silt sized particles. Clay aggregates were identified initially by the production of anamolous grainsize results and their presence was confirmed using a binocular microscope following sieving. The clay aggregate problem was most prevalent in the red weathered soils which, in hand specimen, appeared to be slightly silty clay soils but which on sieve analysis produced up to 15% sand and over 70% silt. The clay fraction, using the pipette method as outlined in NZS 4402, produced no more than 17% clay which would reclassify the red weathered soils as clayey silts with some sand. All of the other soil types identified in the field and tested in the laboratory were subject to the same clay aggregate problems, although to lesser degrees than the red weathered soils. Errors in the measurement of the clay % in the soils tested estimates that up to 90% of the red weathered soils may be composed of clay, while for the other regolith and colluvial soils tested there is thought to be up to 50% more clay than presently estimated. The clay aggregates in the silt fraction were estimated using the texture and plasticity of samples in hand specimen, which indicated that the soils are predominantly silty clays rather than clayey silts.

The results obtained from the grainsize analysis are from direct testing of the samples and these results have variable degrees of error associated with the influence of sand and silt sized clay aggregates. The grainsize proportions of each soil type were averaged to show the general trends in grainsize relative to the soil type and original bedrock type. The proportions of gravel, sand, silt and clay are presented in Table 5.6. which also indicates the range of measurements and the number of samples tested for each soil type. Figure 5.9 is a plot of phi size versus cumulative percent for the same averages to show relationships between the different soil materials and trends are discussed below. Schistose soils appear to be consistently lower in sand and gravel than greywacke soils, with 6% and 52.5% gravel and sand respectively for schist regolith compared to 9.7% and 55.9% for greywacke regolith.

For colluvial soils there is 16.2% and 42.0% gravel and sand in schistose colluvium, while greywacke colluvium has 18.7% gravel and 44.2% sand. Conversely, the schistose soils are consistently higher in silt percentages than the greywacke material, while clay percentage is consistently higher in greywacke soils. Schistose regolith has 25.2% and 12.1% silt and clay respectively compared to 21.1% and 13.3% in greywacke regolith, while schistose colluvium contains 31.3% silt and 10.5% clay compared to 24.7% silt and 12.0% clay in greywacke colluvium. Red weathered regolith does not correlate to any of the other soils tested and contains no gravel, 12.8% sand, 71.3% silt and 15.9% clay.

The trends observed between regolith and colluvium indicate that although the gravel percentages in colluvium are consistently higher than for regolith, the sand percentages are higher in regolith. Similarly the regolith material has a higher percentage of clay compared to colluvium but has a lower percentage of silt sized particles. There was a considerable range of values obtained for each soil type with a range of greater than 30% obtained for gravel in greywacke colluvium, the range being 8.9%-40.3%, and an average of 18.7%.

c) Discussion

Figure 5.9. shows the grainsize plots of cumulative percent versus phi size for the averaged samples presented in Table 5.6. above. The plot indicates that the regolith soils, both greywacke- and schist-derived, have approximately 10% less gravel, although trends in sand, silt and clay sized materials do not show any distinction between soil types. Red weathered regolith material shows a significantly higher percentage of silt compared to the other samples and a correspondingly lower sand percentage. The percentage of clay sized particles appears to be similar to those of the other soil types. However, due to the problems with disaggredation outlined above, the trends shown in Figure 5.9. are not to be treated with any confidence. The grainsize analysis in this study followed the procedure set out in NZS 4402 for sieve and pipette analysis and the difficulties encountered indicate that there is a weakness with the method for analysis of these particular soils. The red weathered soils analysed in this study showed that after sieving up to 80% of the sand and silt fraction were composed of clay aggregates leading to up to 90% clay for these materials. Because the silt fraction, which was analysed using the pipette method, was identified as containing up to 50% of the total clay content in the form of aggregates which did not disperse with the introduction of calgon, the pipette analysis also gave incorrect percentages of clay and silt. Although 20 ml of calgon was added to the column prior to testing in order to disaggregate the sample it is thought that the amount used was not sufficient to completely disperse the clay aggregates.

Significantly more work is required to produce an accurate grainsize analysis of these soils, centered principally to obtain true proportions of clay from the

Table 5.6. Summary of grain size data showing percentages of constituent particle sizes and averaged values for each soil type. Clay percentages are to be considered as minimum values due to difficulties arising from clay aggregates in the samples.

GRAIN SIZE ANALYSIS				
**SAMPLE*	*GRAVEL %*	*SAND %*	*SILT %*	*CLAY %*
R B1	-	12.8	70.6	16.6
R B2	-	13.4	70.8	15.9
R B8	-	9.4	74.7	16.0
R B9	-	15.5	69.3	15.3
AVERAGE	0.0	12.8	71.3	15.9
SC B4	10.5	52.0	27.8	9.8
SC B10	29.2	54.9	12.5	3.4
SC B11	21.6	33.6	33.3	11.5
SC B14	13.5	27.7	41.7	17.2
SC B17	10.0	29.6	45.8	14.6
SC WH5	12.2	54.4	26.9	6.5
AVERAGE	16.2	42.0	31.3	10.5
SR B3	2.4	62.0	24.2	11.5
SR B12	2.6	52.8	30.9	13.7
SR B13	6.9	67.7	18.6	6.8
SR B15	2.2	50.8	31.2	17.5
SR B16	5.9	45.1	31.6	17.5
SR B23	16.2	63.5	14.5	5.8
AVERAGE	6.0	52.5	25.2	12.1
GC B5	26.7	47.4	19.2	6.8
GC B6	40.3	31.1	21.1	7.6
GC B7	13.3	46.0	30.1	10.7
GC B20	10.0	40.7	29.1	20.3
GC B21	8.9	37.6	30.1	20.4
GC WH3	13.4	61.5	18.7	6.4
AVERAGE	18.7	44.2	24.7	12.0
GR B18	9.2	50.9	23.4	16.8
GR B19	0.3	41.2	31.1	27.4
GR B22	11.9	59.2	20.7	8.2
GR WH4	10.8	64.8	18.4	6.1
GR WH6	16.5	63.9	11.8	7.8
AVERAGE	9.7	55.9	21.1	13.3

*Sample: R=Red regolith, SC=Schistose colluvium, SR=Schistose regolith, GC=Greywacke colluvium, GR=Greywacke regolith

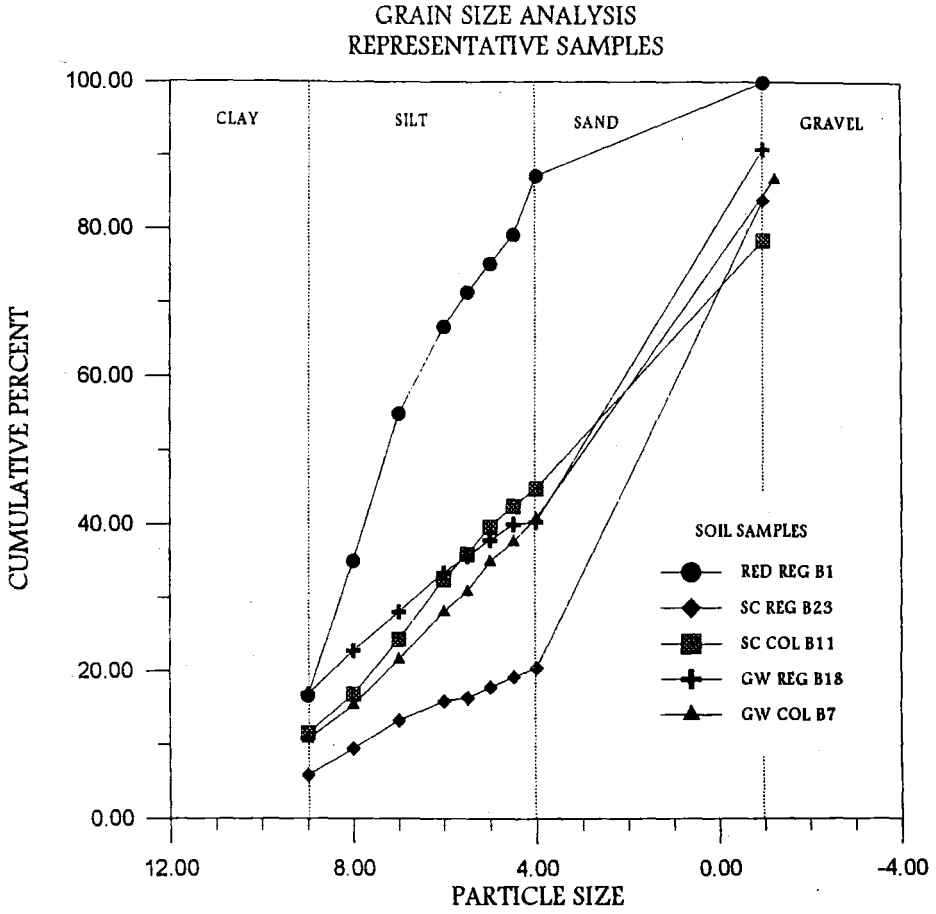

FIGURE 5.9.: Average grainsize analysis for each of the soil types identified in the field area. The number of samples for each soil is indicated on the graph. Values for all clay samples are to be considered as minimum values due to the problems associated with clay aggregates.

aggregates in order to perform the pipette analysis of the mud fraction. Due to time restrictions during this study a more detailed analysis of the problems associated with grainsize analysis could not be completed. It appears that the amount of dispersant used, 20 ml of calgon, is insufficent to fully disperse the clay minerals in the soil samples and further work is needed to determine the amount of calgon required. A detailed analysis of the type of clay minerals present in the soils may also be necessary to determine the nature of the bonding between soil particles, as the disaggregation of the soils is important for Atterberg Limits and shear strength determinations as well as grainsize analysis (Chapter 7.).

5.3.3. Atterberg Limits

a) Introduction

The samples tested for grainsize were also tested for Atterberg limits (Table 5.7.), and the objectives of the Atterberg Limit analysis were two-fold. Firstly, the soil samples were tested in order to further characterise their geotechnical properties in relation to an overall engineering geological assessment. Secondly, Atterberg limit testing was used in an attempt to correlate information regarding the clay mineralogy of the samples by comparing activity with X-Ray Diffraction (Section 5.3.7.) and scanning electron microscopy (Section 5.3.8.). The Activity of a particular soil is dependent on the percentage of clay sized particle in the material, and Skempton (1953) provided an analysis of soil activity for four types of clay mineral (namely kaolinite, illite and Na and Ca montmorillonite), later confirmed by Pandian and Nagaraj (1990), which allows correlation of Activity (Plasticity Index versus clay %) with the principal clay mineral groups. Additionally clay mineralogy may be estimated by plotting Plasticity Index and Liquid Limit according to Grim (1962), who also determined the approximate trends of the major clay mineral groups, namely kaolinite, illite and and montmorillonite. Difficulties arose, however, with regard to assessing clay mineralogy from Activity because of the problems in obtaining accurate clay percentages as a result of clay mineral aggregation (Section 5.3.2.).

The methodology and test procedures for both the Liquid Limit (cone penetration test) and the Plastic Limit tests follow the guide lines set out in NZS 4402 and are detailed in Appendix D5.

b) Results

The soils were tested and subdivided as colluvial and regolith samples, and further subdivided on the basis of their bedrock parent. Table 5.7. shows the Atterberg Limit data and related parameters, Plasticity Index and Activity, again averaged for all of the soil samples tested and divided on the basis of soil type and bedrock origin, as was described for grainsize analysis (Section 5.3.2.). Four samples of red weathered regolith were tested , five of greywacke regolith and six each of the

Table 5.7. Atterberg Limit data and related parameters showing trends in soil behavior relative to the soil type and the original bedrock origin. Clay percentages used to determine the Activity are those presented in Table 5.6. and are considered as minimum values only due to clay aggregates.

	ATTERBERG LIMITS			
*SAMPLE**	*PLASTIC LIMIT*	*LIQUID LIMIT*	*PLASTICITY INDEX*	*ACTIVITY DATA*
R B1	25	52	27	1.6
R B2	25	52	27	1.7
R B8	23	48	25	1.6
R B9	24	51	27	1.8
AVERAGE	24	51	27	1.7
SC B4	26	40	14	1.4
SC B10	21	35	14	4.1
SC B11	25	34	9	0.8
SC B14	18	31	13	0.8
SC B17	17	32	16	1.1
SC WH5	19	35	17	2.6
AVERAGE	21	35	14	1.8
SR B3	26	32	6	0.5
SR B12	25	41	16	1.2
SR B13	26	34	8	1.2
SR B15	22	37	15	0.9
SR B16	22	45	23	1.3
SR B23	28	49	21	3.6
AVERAGE	25	40	15	1.2
GC B5	23	35	12	1.8
GC B6	24	36	12	1.6
GC B7	21	36	15	1.4
GC B20	23	36	13	0.6
GCB21	17	34	16	0.8
GC WH3	31	39	8	1.3
AVERAGE	23	36	13	1.3
GR B18	23	38	14	0.8
GR B19	24	39	15	0.6
GR B22	20	29	9	1.1
GR WH4	24	40	16	2.6
GR WH6	25	49	24	3.1
AVERAGE	23	39	16	1.6

SAMPLE* : R=Red Regolith, SR=Schistose Regolith, SC=Schistose Colluvium, GC=Greywacke Colluvium, GR=Greywacke Regolith

schistose colluvium and regolith and the greywacke colluvium. The Liquid Limits and Plastic Limits show that the schistose colluvium is markedly lower than the regolith material with 21 and 35 respectively for Plastic and Liquid Limit in schistose colluvium compared to 25 and 40 for the schistose colluvium. The greywacke materials indicate that although there is no difference between Plastic Limits for regolith and colluvium (23) the colluvium is distinctly lower in Liquid Limit with 36 for greywacke colluvium compared to 39 for the greywacke regolith (Table 5.7). Red weathered regolith is consistent with the Plastic Limits of the other regolith samples at 24, however the Liquid Limit for the regolith material is considerably higher at 51 than for any of the other samples tested.

Plasticity Index of red weathered regolith material is significantly higher than that of the remaining samples with 27 obtained for red weathered regolith, and between 13-16 for the other soils tested. When Plasticity Index is plotted against the liquid limit on the Casagrande Plasticity Diagram (Figure 5.10.) an estimate of the plasticity of the soil may be obtained. The most significant trend observed is the clustering of the red weathered regolith samples which consistently plot towards the high plasticity subdivision and away from most of the other samples tested. The majority of the remaining samples cluster together and are all classified as soils of intermediate plasticity. There are no observable trends associated with individual soil types or with lithologic variation (Figure 5.10).

Determination of the clay mineralogy of the soil samples was estimated using both Activity data and mineralogical trends from Skempton (1953), and the estimated mineralogical content derived from the relationship between Plasticity Index and Liquid Limit (Grim, 1962). Activity data is represented on Figure 4.11. with the major clay mineral trends determined by Skempton (1953) superimposed. The Activity plot suggests that the regolith samples, excluding red weathered regolith, are dominated by illite clays while the colluvial samples display a large scatter across the clay mineral trends in the Activity diagram. The scatter in data points of colluvial material is believed to indicate that the soils are derived from both greywacke and schistose sources. Red weathered material, due to the high Plasticity Index (Table 5.7.), is apparently dominated by montmorillonite clay minerals (Figure 5.11.).

Clay mineralogy as determined from the data of Grim (1962) is presented in Figure 5.12. and the averaged Atterberg Limit data for each soil type is also plotted. The Grim diagram shows that all of the soil types, other than red weathered regolith, cluster along the kaolinite line, while the red weathered material is intermediate between kaolinite and illite.

c) Discussion

The principal problem identified with Atterberg Limit analysis in this study is the use of clay percentage to assess the Activity and clay mineralogy of the samples tested because, as discussed in Section 5.3.2., the estimates of clay percentage are

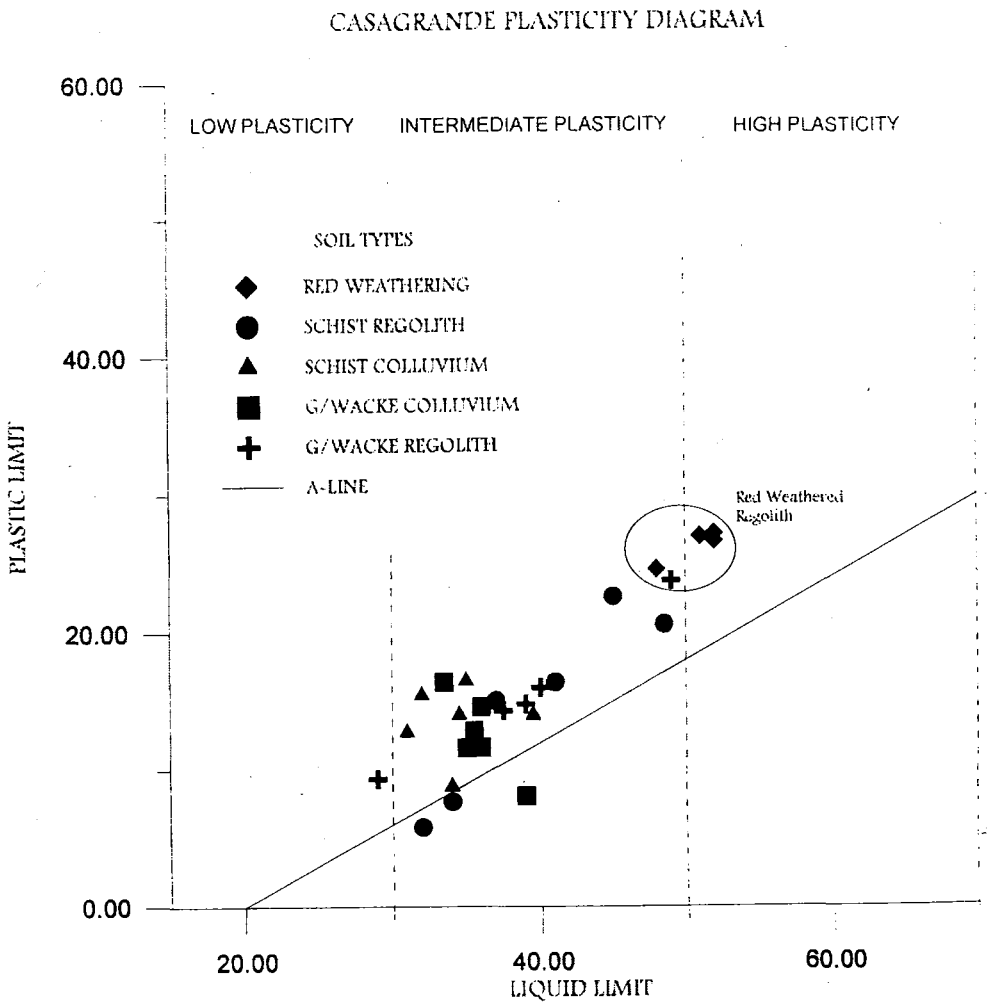

FIGURE 5.10.: *The Casagrande Plasticity diagram which shows the Plastic Limit values versus Liquid Limit indicating the Plasticity of each soil type. Note the clustering of the red weathered samples in the high Plasticity category. All samples plot near to or above the A-line which indicates clays or silts of moderate to low plasticity.*

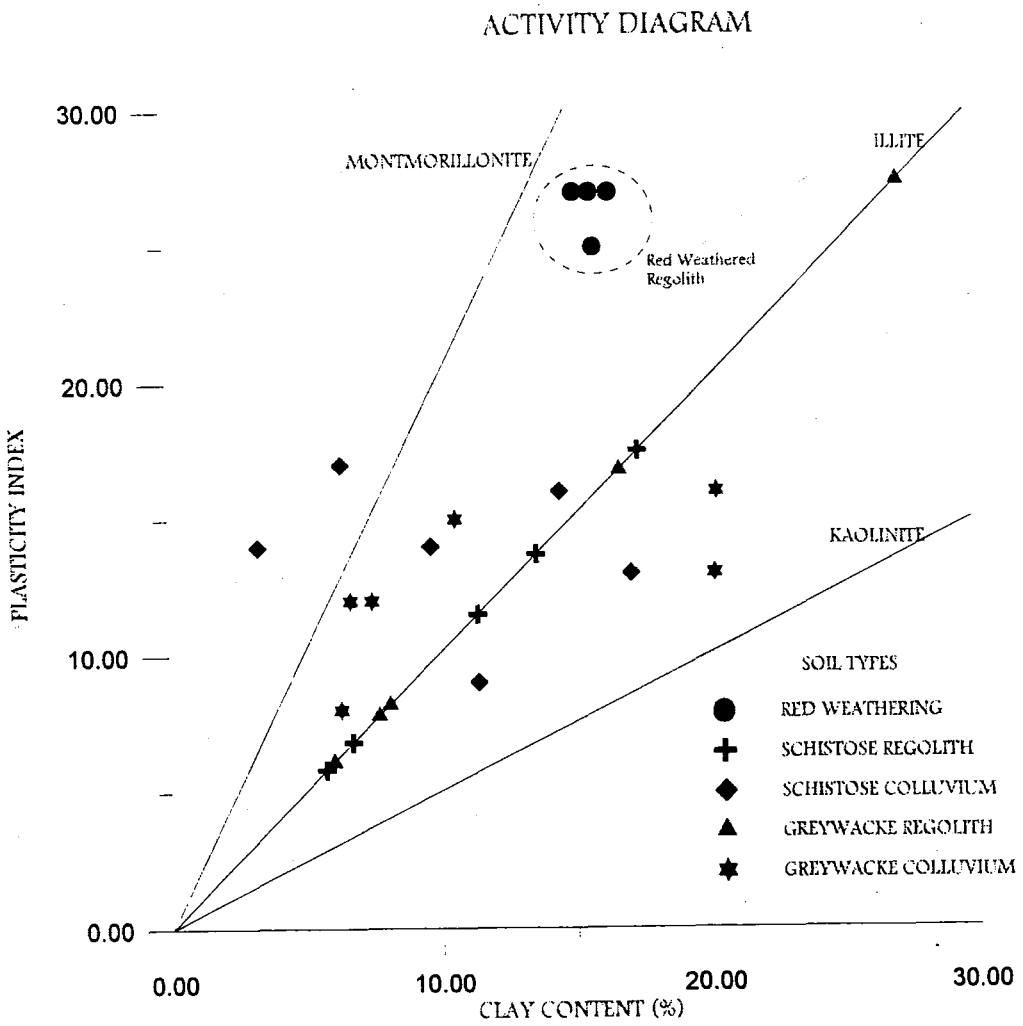

FIGURE 5.11.: *Activity diagram (After Skempton, 1953) showing the inferred clay mineralogy of soil samples tested for Atterberg Limits. Note the clustering of red weathered samples, consistency of regolith samples which plot on the illite line, and the scatter associated with colluvial samples.*
Problems with interpretation arise from inaccurate clay% values due to clay aggregates. Clay% for each sample may be up to and exceeding 50% (See Figure 5.13.).

minimum values only. The problems are illustrated in the different clay mineralogy estimates derived from two separate classification schemes, Skempton (1953; Figure 5.11.) and Grim (1962; Figure 5.12.). The analysis used by Grim (1962) does not require any estimate of grainsize percentages and uses Plasticity Index and Liquid Limit values only. As described above, the estimated clay mineralogy of the samples using the Grim Classification shows a dominance of kaolinite in all samples other than red weathered regolith, which plots close to the illite field (Figure 5.12.). Clay mineralogy from Activity data as defined by Skempton (1953), does require an estimate of clay percentage for each soil type and therefore, because of the difficulties associated with clay aggregates (Section 5.3.2.), the clay mineralogy using the Skempton method is not thought to be accurate. Section 5.3.2. indicates that up to 90% clay may be present in some samples, and if these estimated clay percentage values are used to determine clay mineralogy from Activity, the results are more consistent with those obtained using the Grim Classification. Figure 5.13. shows the Activity data using the estimated clay percentages estimated in Section 5.3.2. and the results indicate that the soils are dominated by kaolinite and illite, including the red weathered regolith material. Clay mineralogy data are presented in Section 5.3.7. and Section 5.3.8., and further discussion is presented in association with the data obtained using XRD and SEM methods.

5.3.4. Erosion Tests

a) Introduction

Testing for dispersion of the soils in the field area used both the pinhole erosion test and the crumb test. The tests were performed in order to determine the erodibility of the soils in their natural state. For this purpose, therefore, undisturbed 35mm diameter tube samples were taken of the constituent soils. The crumb test used material obtained as bulk samples and was the same material used in the grainsize analysis and for Atterberg limit testing. The methodology and procedures are presented in Appendix D6.

b) Results

Pinhole erosion tests were performed using two samples each of grey wacke regolith, greywacke colluvium, schistose regolith and schistose colluvium. The crumb test was performed on one sample of each soil type including red weathered regolith. The results of both tests are presented in Table 5.8. and a description of the erodibility of the soil samples is also given following NZS 4402. The Pinhole erosion test indicates that all of the soils tested were classified as being ND 2-ND 4 which indicates that the soils are non-dispersive. The Crumb Dispersion test identified a slight reaction in all soils other than the schist regolith material, which showed no dispersive reaction.

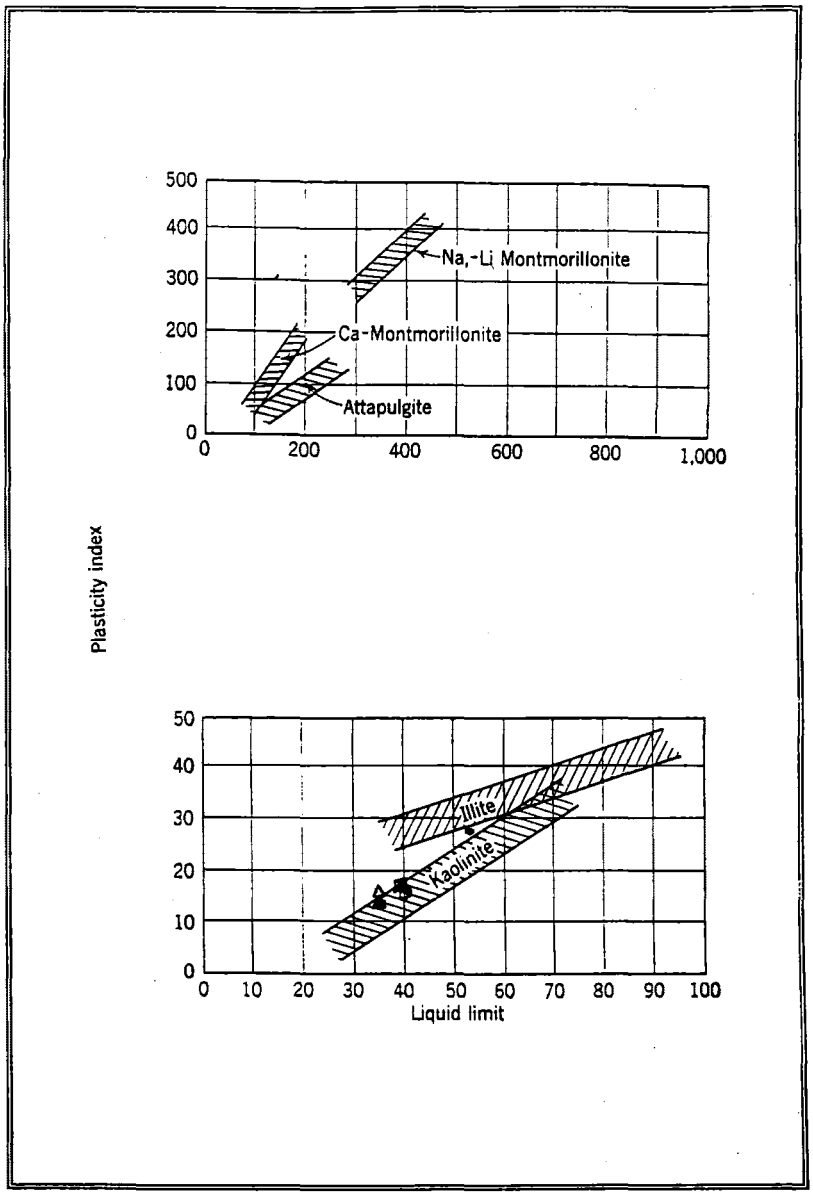

FIGURE 5.12.: The Grim Classification (Grim, 1962) which shows the relationships between clay mineralogy and Plasticity Index versus Liquid Limit. Compare to Figures 5.11. and 5.13.

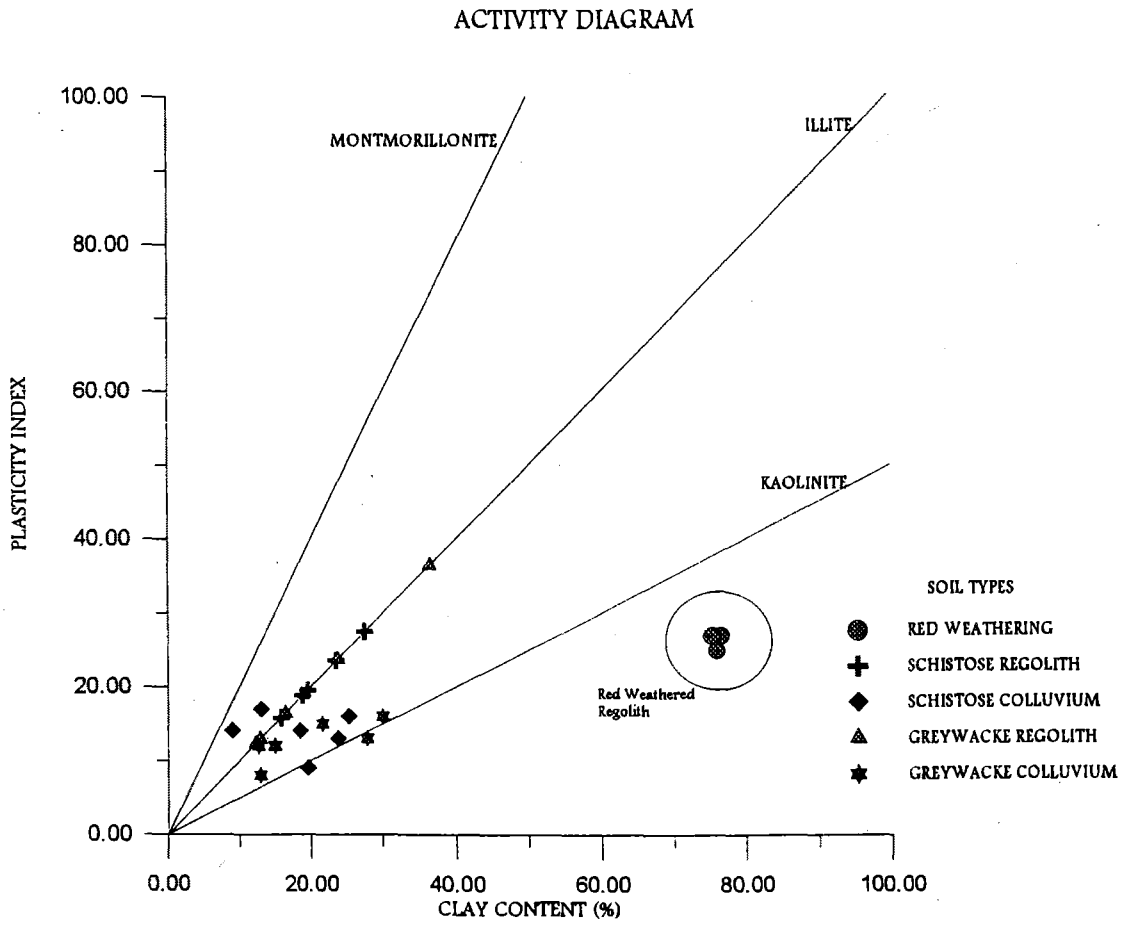

FIGURE 5.13.: Amended Activity data with clay percentages estimated from grain size analysis problems. All samples other than red weathered regolith have up to 50% more clay than shown in FIGURE 5.11. Samples all cluster near the kaolinite line and illite line which is consistent with Grim (1962) and the XRD information.

c) Discussion

The lack of highly dispersive soils is the most prominent feature of the erodibility tests because field observations such as rilling and tunnel gullying indicate that erosion of the soils is actively occurring. However, from the erodibility results in Table 5.8. which indicates that the soils non-dispersive but slightly erodible, it appears that erosion is not dependent on the presence of dispersive clay minerals in the soils and the steep slopes may be modified by tunnel gullying which is not related to dispersion (Chapter 3). The tube samples used in the pinhole erosion test were taken during the height of summer, therefore the soils had a low natural water content which may also contribute to the low erosive nature as soils require time to equilibrate with water. The water introduced to essentially dry soils during the pinhole erosion test may cause initial swelling and only partial saturation therefore providing anomalous results to naturally wetted soils. Field observations confirm that accelerated erosion such as tunnel gullying and stream bank erosion within the field area occurs predominantly during the wetter winter months.

5.3.5. Point Load Test

a) Introduction

The point load test and the cone indenter test (Section 5.3.6) were used to confirm field observations regarding the strength of weathered greywacke and schist. Using the weathering classification scheme presented by Bell and Pettinga (1983; See Chapter 3) various weathering grades of both bedrock lithologies were tested to provide further constraints for the classification system. The objective of the point load testing programme was to determine the change in strength characteristics with an increase in weathering, and also to compare the strength of greywacke and schist. The schistose samples were tested both perpendicular and parallel to foliation in order to determine the anisotropy index of schistose material. The 'irregular lump' test was used because core samples were unavailable for testing. The procedure and methodology of the point load test is presented in Appendix D7.

b) Results

Because the point load test was performed on irregular shaped lumps of rock material, the results presented are calibrated to a standard 50mm diameter lump size. The uniaxial compressive strength (UCS) of each sample may be calculated from the point load number $Is_{(50)}$ using the formula:-

$$\sigma_c = 24\ Is_{(50)}$$

where: Is is the point load strength calibrated to 50mm diameter.

Table 5.9. shows the average measured point load strength $Is_{(50)}$ and the UCS values calculated from $Is_{(50)}$. The greywacke material showed mean strengths of 3MPa($Is_{(50)}$) and 71 MPa(UCS) for weathering grade II, 0.3MPa($Is_{(50)}$) and 7 MPa(UCS) for grade

III and 0.08MPa($Is_{(50)}$) and 1MPa(UCS) for grade IV. Weathered schist was tested both parallel and perpendicular to foliation and the strengths for both orientations are given in Table 5.9. The schist weathered to grade II showed an $Is_{(50)}$ strength of 1.1MPa parallel to foliation and 1.9MPa perpendicular, while for grade III the $Is_{(50)}$ was 0.2MPa parallel and 0.8MPa perpendicular to foliation. For weathering grade IV, the $Is_{(50)}$ was 0.02MPa parallel and 0.6MPa perpendicular to the foliation while calculated UCS values in MPa indicated that grade II schist was 27MPa parallel and 45MPa perpendicular, for Grade III was 5.4MPa parallel and 19.6MPa perpendicular and 0.5MPa parallel and 8.6MPa perpendicular to foliation for weathering grade IV schist. The range of values obtained for $Is_{(50)}$ showed that considerable variation could be expected in test results for weathered rock material, both schist and greywacke and ranges possibly reflected the gradational contacts between different weathering grades. Because the schistose material was tested both parallel and perpendicular to the foliation surfaces the variability of strength within anisotropic material and the Strength Anisotropic Index (Bieniawaskie and Franklin, 1972) was also determined. The Strength Anisotropy Index ($Ia_{(50)}$) is the ratio of point load strength perpendicular to foliation to the strength parallel to foliation. In this study $Ia_{(50)}$ is calculated as 1.7 for Grade II schist, 4.0 for Grade III and 15.0 for the schist weathered to Grade IV.

c) Discussion

The results obtained (Table 5.9.) show a decrease in point load strength and uniaxial compressive strength (UCS) with increasing weathering. Figure 5.14. and Figure 5.15. show the decreasing point load strength ($Is_{(50)}$) as the weathering grade increases in both greywacke and schistose material. There is considerable overlap between samples of each weathering grade which is thought to represent the gradational nature of the weathering front, but nevertheless a significant trend may be seen. The samples show a large scatter of data points in both the greywacke and schist samples, which in schistose samples is thought to result in part from the irregular nature of the failure surface when loading is perpendicular to foliation (Kingsbury, 1987) the influence of jointing and bedding in greywacke samples. Additionally, the scatter in the schistose and greywacke samples is attributed to the insensitivity of the point load equipment at low compressive strengths. As expected, the schistose material was considerably weaker than greywacke, particularly when the load was applied parallel to the foliation (Figure 5.15.); when the Strength Anisotropy Index is plotted (Figure 5.16.) a linear relationship can be derived between the point load strength parallel and perpendicular to foliation with an increase in weathering grade. This trend indicates that there is a gradation between the strength of anisotropic rock material between each weathering grade.

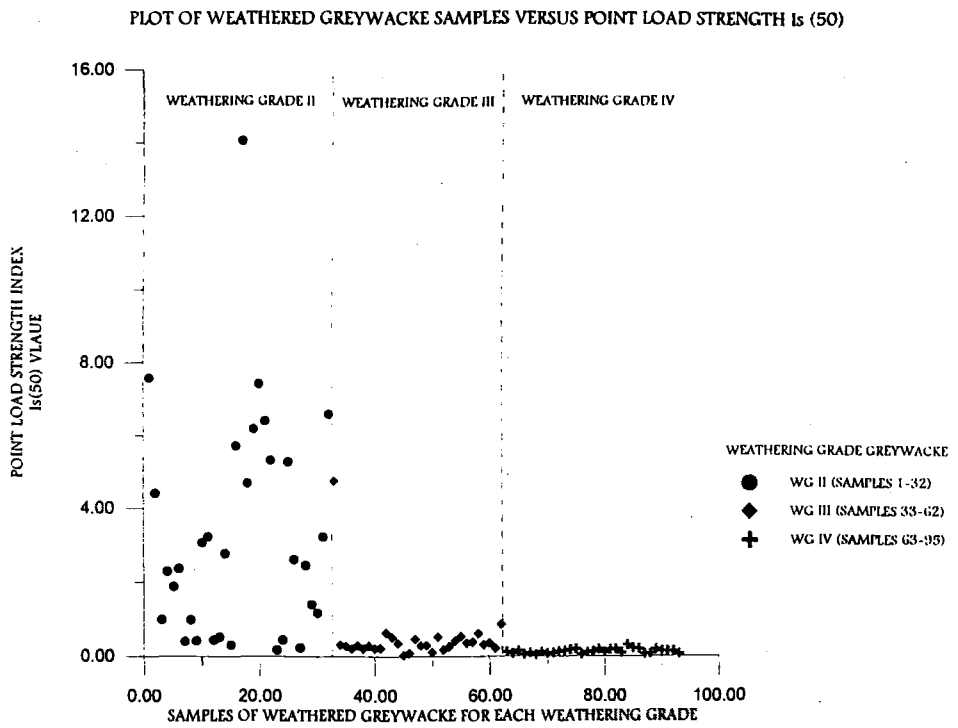

FIGURE 5.14.: *Plot of Point Load Strength ($Is_{(50)}$) for weathered greywacke samples (WG) showing the increase in strength with decreasing weathering grade. X-axis represents individual samples tested in each weathering grade arranged in the sequence tested for each grade.*

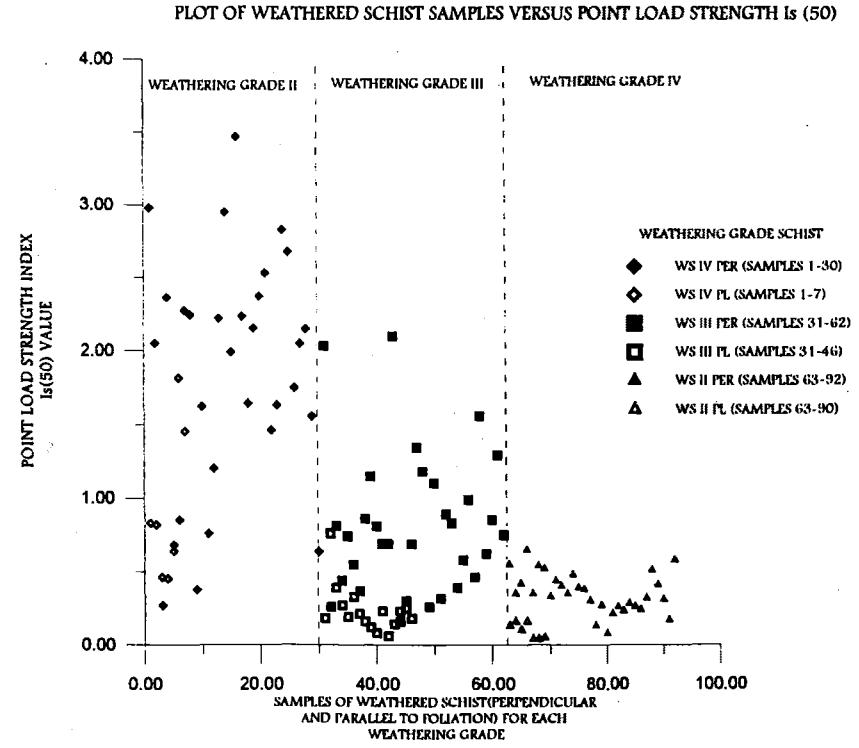

FIGURE 5.15.: *Plot of Point Load Strength ($Is_{(50)}$) for weathered schist samples (WS) tested both parallel (PL) and perpendicular (PER) to foliation showing changes in rock strength with increasing weathering grade. X-axis represents individual samples tested in each weathering grade arranged in the sequence tested for each grade.*

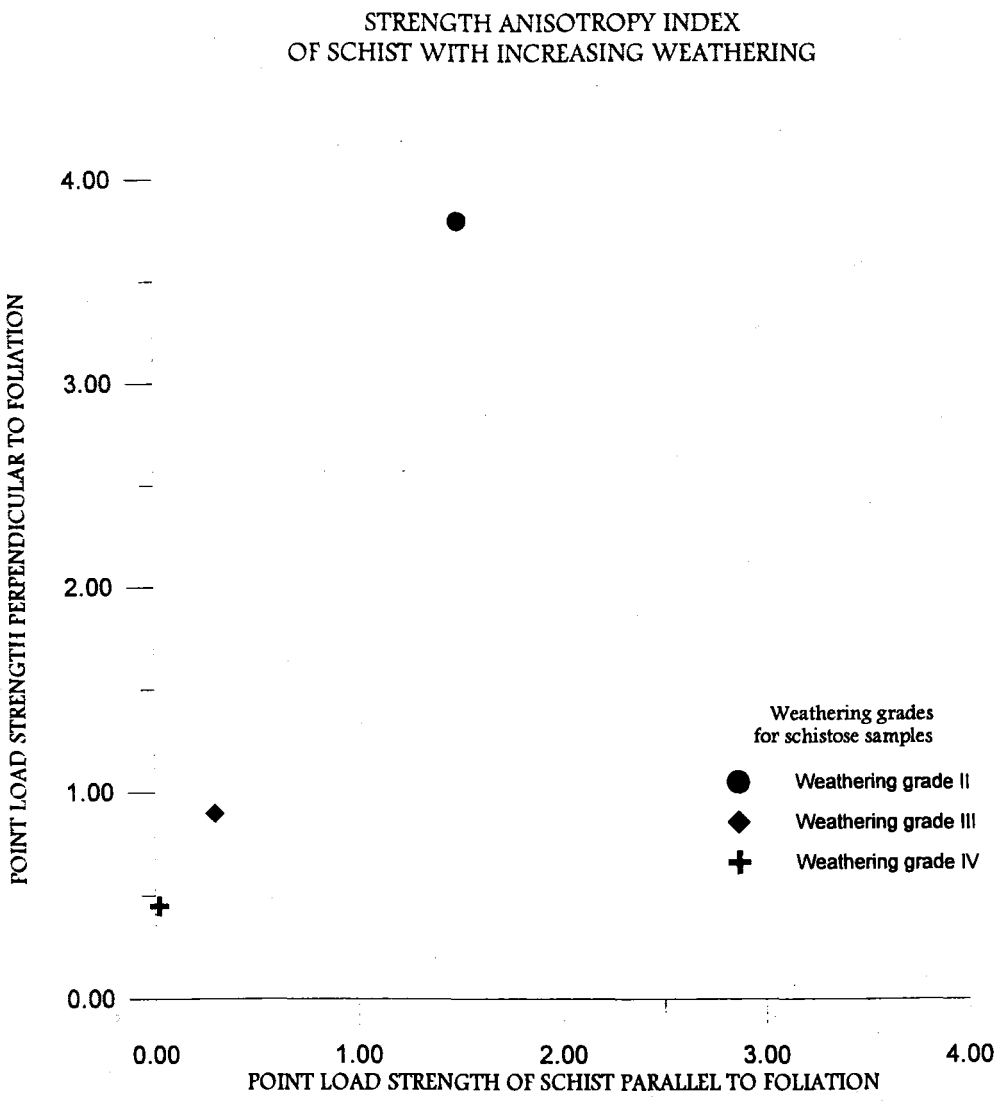

FIGURE 5.16.: *The Strength Anisotropy Index for schist tested parallel and perpendicular to foliation using the Point Load test. Mean data for the Point Load tests were used.*

5.3.6. NCB Cone Indenter Test

a) Introduction

The principal objective of the NCB cone indenter tests was to provide strength values of the weathered bedrock to be correlated with the results obtained from the point load test (Section 5.3.5). The cone indenter test measures the deflection of a metal strip by a small chip of rock material which is loaded by a metal cone (Figure 5.17.), and the samples used for the cone indenter test were the same as for the point load tests. The MRDE cone indenter handbook does not specify the number of tests required or the number of samples to be tested and therefore each weathering grade was tested in excess of 20 times following Kingsbury (1987) in order to provide a correlation with tests elsewhere in the Marlborough Sounds. The size of the samples tested, approximately 12 x 12 x 6mm, also followed Kingsbury (1987) and due to the small size of the samples tested and the difficulty in orientating the samples adequately, schistose material was not able to be tested parallel to the foliation surfaces. Therefore, all schist samples were tested perpendicular to foliation. The test procedure and methodology are presented in Appendix D8.

b) Results

The cone indenter number (CIN) was measured for each weathering grade and averaged to identify trends (Table 5.10). CIN values were obtained using the weak rock test for highly weathered material (Appendix D8) and the uniaxial compressive strength (UCS) in MPa was calculated (Appendix D6). The averaged CIN for greywacke material ranged from 3.2CIN for weathering Grade II, 2.0CIN for Grade III and 1.3CIN for greywacke weathered to Grade IV while the averaged calculated UCS values were 52MPa for Grade II, 33MPa for Grade III and 22MPa for weathering Grade IV. The schistose material was weaker than the greywacke and CIN values for schist were 1.8 for Grade II, 0.7 for Grade III and for schist weathered to Grade IV, CIN was 0.6. The UCS values for schist were 34.9 MPa, 21.1 MPa and 10.1 MPa for weathering Grades II, III and IV respectively. There was a wide range of CIN values measured for each weathering grade, for example 0.2-7.7CIN, 2.0-5.1CIN and 0.2-15-5CIN for greywacke weathered to Grades II, III, and IV respectively, while schist ranged from 0.1-3.3CIN, 0.2-3.8CIN and 0.3-1.5CIN for each weathering Grade II, III and IV. Table 5.10. shows both the CIN and the UCS values for weathered schist and greywacke of grades II, III, and IV. Problems were encountered with the weakest rock material, as even the weak rock test caused some of the samples to crush. Therefore, in order to obtain representative CIN and UCS averages, the number of failed tests were also taken into account.

c) Discussion

The data obtained from the cone indenter test showed a trend similar to the point load test whereby an increase in weathering grade correlates to a decrease in rock strength. The decrease in strength with weathering is gradual and there is

Table 5.8. Soil dispersion testing using both Pinhole Erosion test and the Crumb Dispersion test.

SOIL DISPERSION TESTS			
PIN HOLE EROSION			
SAMPLE		*CLASSIFICATION*	*DESCRIPTION*
Schist regolith	T1/A	ND3	Non-dispersive
	T1/B	ND3	Non-dispersive
Schist colluvium	T2/A	ND3	Non-dispersive
	T2/C	ND3	Non-dispersive
G/wacke regolith	T3/A	ND2	Non-dispersive
	T3/B	ND3	Non-dispersive
G/wacke colluvium	T4/A	ND4	Non-dispersive
	T4/C	ND2	Non-dispersive
CRUMB DISPERSION			
SAMPLE		*CLASSIFICATION*	*DESCRIPTION*
Schist regolith	T1/C	Grade 1	No reaction
Schist colluvium	T2/B	Grade 2	Slight reaction
G/wacke regolith	T3/C	Grade 2	Slight reaction
G/wacke colluvium	T4/B	Grade 2	Slight reaction
Red weathering	B1	Grade 2	Slight reaction

Table 5.9. Mean Point Load results and calculated Uniaxial Compressive Strength with the range of values measured.

POINT LOAD ROCK STRENGTH RESULTS				
Sample	Point load strength Is (50)		Uniaxial compressive strength (MPa)	
Greywacke Grade II	3.0 *(0.2-7.6)*		70.8 *(4.0-182)*	
Greywacke Grade III	0.3 (0.1-*0.6)*		7.06 *(2.4-15.4)*	
Greywacke Grade IV	0.08 *(0.04-0.19)*		1.9 *(1.1-4.8)*	
*Schist Grade II	// 1.1 *(0.01-5.2)*	⊥1.9 *(0.3-3.5)*	// 26.8 *(0.3-124.9)*	⊥ 45.4 *(6.5-83.2)*
Schist Grade III	// 0.8 *(0.08-0.4)*	⊥0.8 *(0.2-2.1)*	// 5.4 *(1.5-18.3)*	⊥ 19.6 *(3.8-50.4)*
Schist Grade IV	// 0.02 *(0.04-0.2)*	⊥0.3 *(0.1-0.7)*	// 0.5 *(0.9-3.9)*	⊥ 8.6 *(2.0-15.6)*

*Schist tested parallel to Foliation (//) and perpendicular to foliation (⊥)

Table 5.10. Mean Cone Indenter results (CIN) and calculated uniaxial compressive strength with range of values indicated in brackets.

NCB CONE INDENTER ROCK STRENGTH RESULTS		
SAMPLE	CONE INDENTER NUMBER (CIN)	UNIAXIAL COMPRESSIVE STRENGTH UCS (MPa)
Greywacke Grade II	3.2 *(0.2-7.7)*	52.3 *(3.1-108.4)*
Greywacke Grade III	2.0 *(0.3-5.1)*	32.9 *(5.4-84.3)*
Greywacke Grade IV	1.3 *(0.2-15.3)*	21.7 *(2.8-253.0)*
Schist Grade II	1.8 *(0.1-3.3)*	34.9 *(2.5-189.8)*
Schist Grade III	0.7 *(0.2-3.8)*	21.1 *(3.4-63.3)*
Schist Grade IV	0.6 *(0.3-1.5)*	10.1 *(5.8-25.3)*

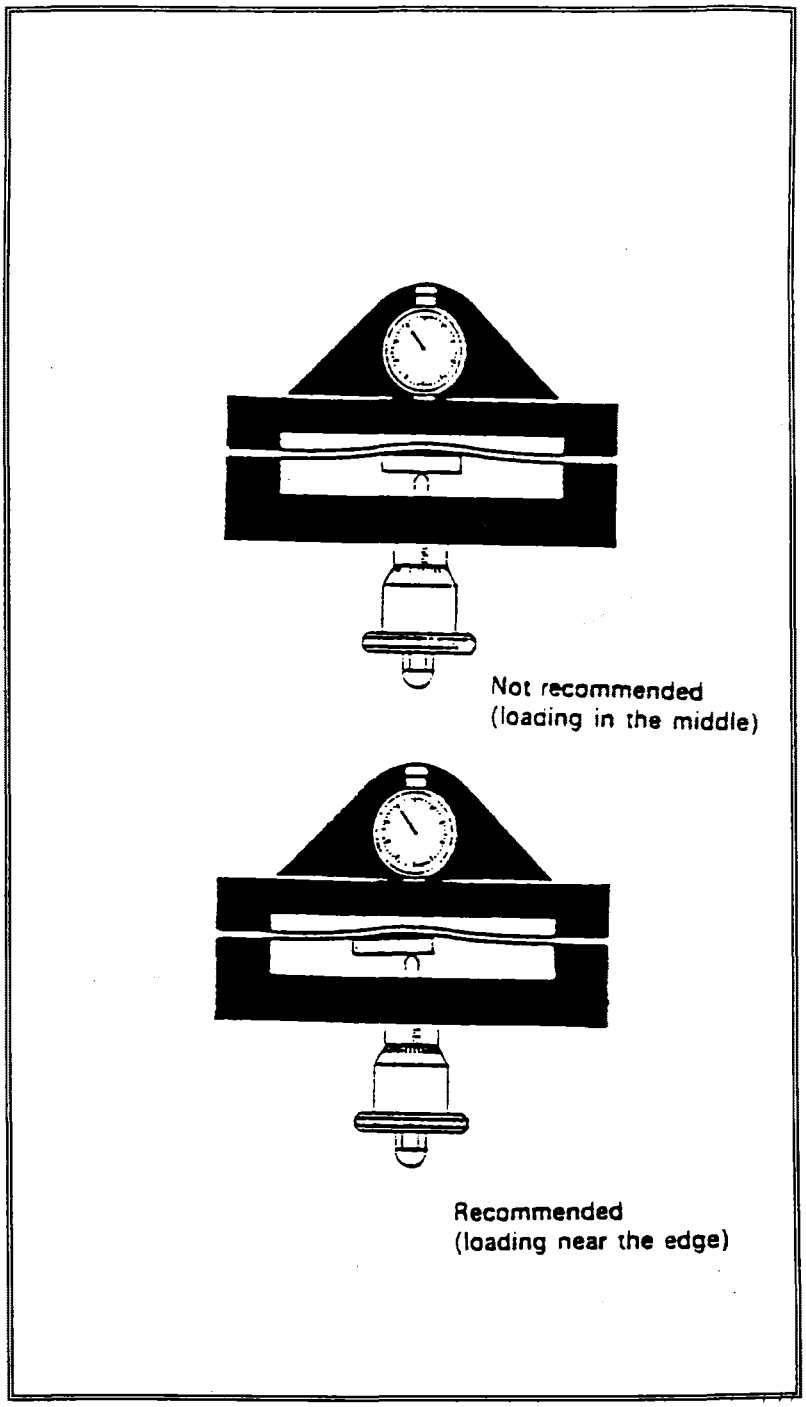

FIGURE 5.17:. A diagram of the Cone Indenter device for the measurement of compressive rock strength.

considerable overlap between the weathering grades (Figures 5.18. and 5.19.). Following Kingsbury (1987) a linear regression analysis of the cone indenter number versus the equivalent UCS values should show a line which passes through the origin. This is true for plots of the measured CIN and the calculated UCS (Figure 5.20.) which is expected as UCS is calculated from the CIN.

Comparison of the calculated UCS values from the cone indenter tests with those obtained from the point load test was favourable, as the UCS values for both point load and cone indenter are similar. Similar trends between the point load number ($Is_{(50)}$) and the cone indenter strength (CIN), which showed a decrease in strength with an increase in weathering grade, could be correlated with the UCS values for point load and cone indenter (Tables 5.9. and 5.10.). Kingsbury (1987) comments that the insensitivity of the cone indenter will result in inaccuracies which reduce the application of the test for the calculation of UCS in highly weathered rocks, however UCS values for the weakest rock material in this study, the weathered schist, were more closely correlated to point load UCS values than the stronger greywacke material. The greywacke material showed considerable difference between the calculated UCS values for point load and for CIN ranging from 20MPa to 26MPa, while the calculated UCS values for schistose material tested perpendicular to foliation showed no more than 10MPa difference. The differences between the Point load and CIN derived UCS values is thought to be partially due to the limited number of samples which were able to be tested. It is uncertain why there were greater correlation of the UCS values for schistose material compared to the greywacke samples and it is thought that a more detailed study is required which is outside the scope of this thesis. Figure 5.21 shows the comparison of UCS values calculated from both point load testing and cone indenter tests for each weathering grade in both schist and greywacke.

5.3.7. X Ray Diffraction

a) Introduction

X-ray diffraction (XRD) was used on the same samples tested for grainsize and Atterberg Limits in order to determine the clay mineralogy of each soil type. XRD is also used to provide a correlation with clay mineral determinations using the scanning electron microscope (Section 5.3.8.) and Atterberg Limit Activity data (Section 5.3.3.). Furthermore whole rock XRD analysis was performed on samples of schist and greywacke from each weathering grade to identify constituent minerals and for comparison with thin section analysis (Section 5.4.3.). Quantative analysis of whole rock mineralogy or clay mineralogy was not performed in this study due to a lack of a definitive method for analysis (Thorez, 1976) and therefore percentages of clay minerals identified were not estimated. The methods used for both clay mineral XRD analysis and whole rock XRD are presented in Appendix D9.

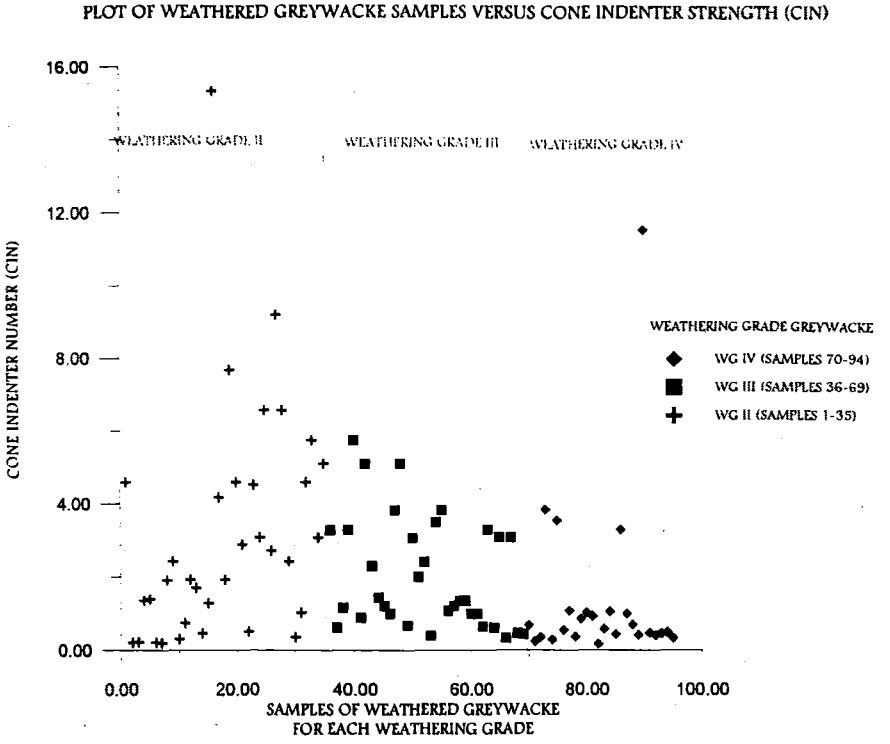

FIGURE 5.18.: *Plot of Cone Indenter Number (CIN) for weathered greywacke samples (WG) showing an increase in strength with a decrease in weathering grade.*
X-axis represents individual samples tested in each weathering grade arranged in the sequence tested for each grade.

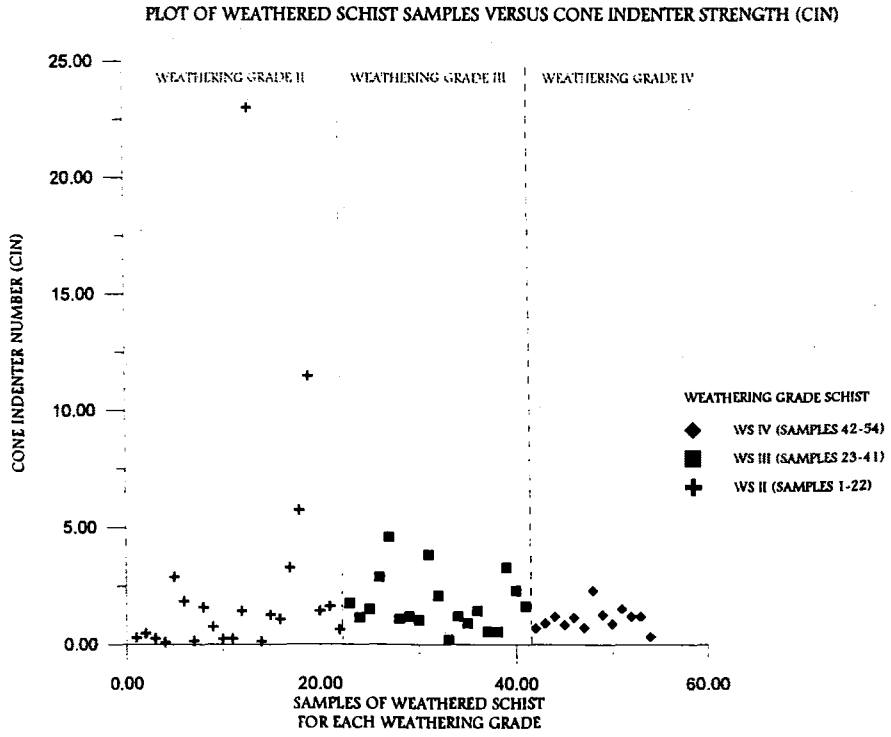

FIGURE 5.19.: *Plot of Cone Indenter Number (CIN) for weathered schist samples (WS) showing an increase in strength as weathering grade decreases.*
X-axis represents individual samples tested in each weathering grade arranged in the sequence tested for each grade.

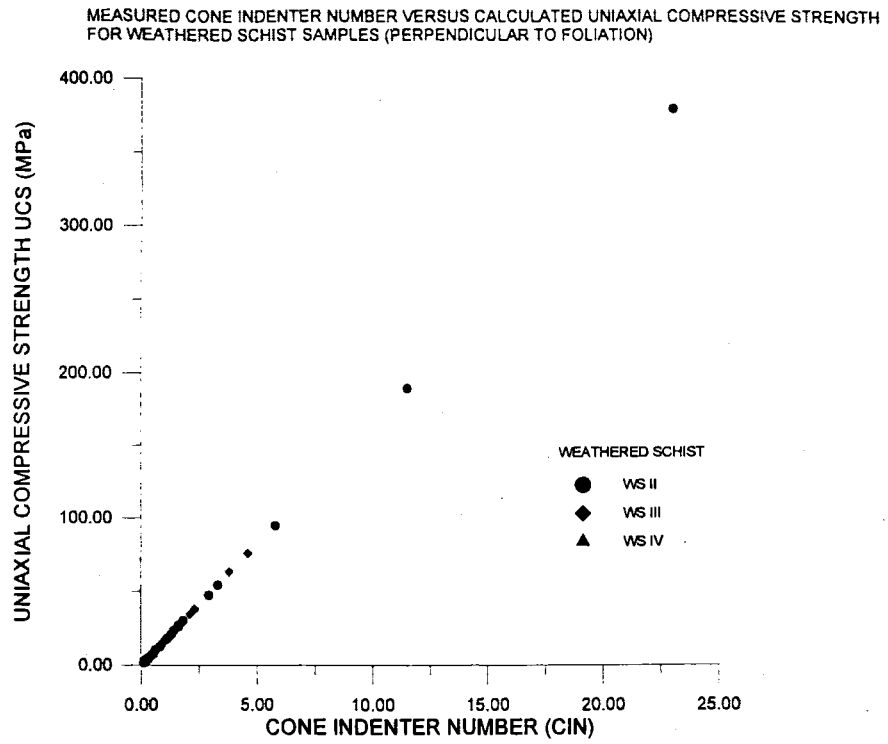

FIGURE 5.20.: *a) Linear regression from CIN versus the calculated UCS (Mpa) for schist of each weathering grade.*
**[Calculations for UCS follow those presented by MRDE and are described in Appendix D8].*

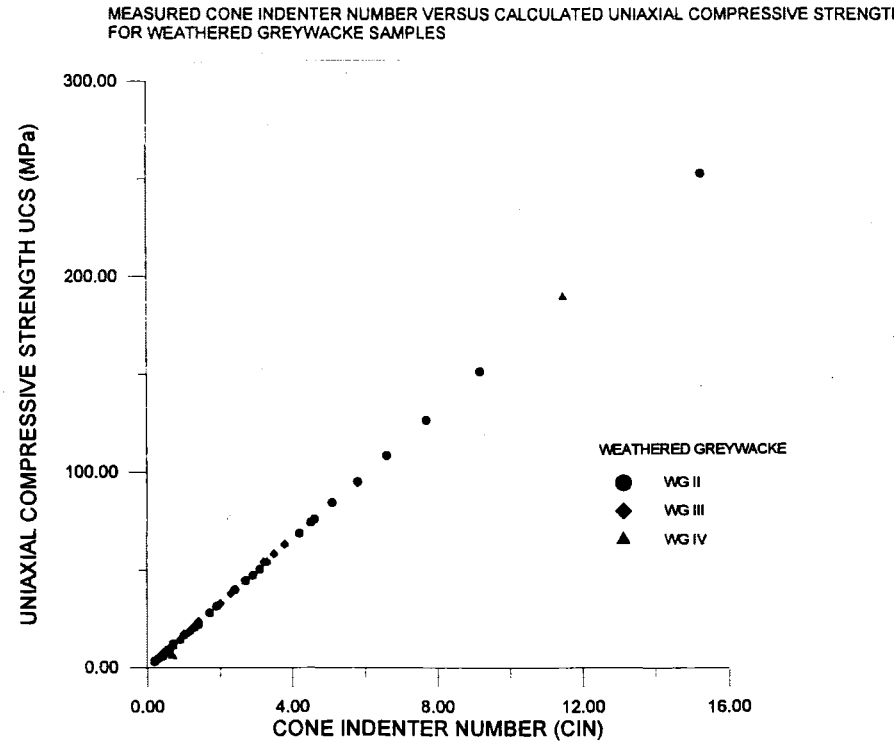

FIGURE 5.20.: *b) Linear regression from CIN versus the calculated UCS (Mpa) for weathered greywacke.*
**[Calculations for UCS follow those presented by MRDE and are described in Appendix D8].*

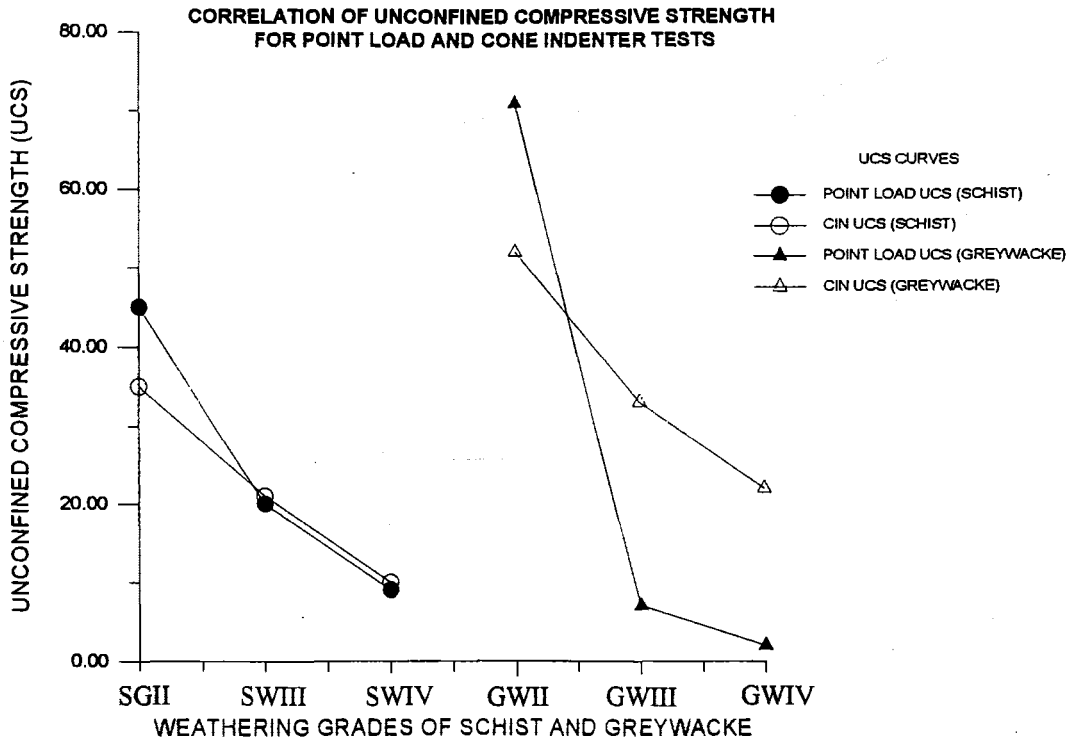

FIGURE 5.21.: A comparison of the calculated UCS values for each weathering grade of schist and greywacke from Point load measurements and the Cone Indenter.

b) Results

Table 5.11. shows the constituent clay minerals found for each sample and the minerals identified in whole rock XRD analysis. The results indicated the presence of kaolinite and illite in all samples, while a complex illite-chlorite interstratified clay was present in predominantly schist-derived samples although some of the greywacke material also included the illite-chlorite clay. Other important clay mineral constituents were chlorite, muscovite and clay sized quartz. The clay mineral imogolite, a poorly crystalline clay mineral generally found in soils containing volcanic glass (Brindley and Brown, 1980), was present only in the red weathered soils.

c*) Discussion*

There are no significant trends identified with the whole rock XRD analysis to define the differences between weathering grades or between lithology. Clinochlore, a close relative of chlorite, was the only mineral which had a variable occurrence identified in the whole rock analysis and was most common in the schistose rocks of higher weathering grades III and IV (Table 5.11.). Although not performed in this study, quantative mineral analysis may be useful in determining the proportions of minerals relative to weathering grade, for example an increase in sheet silicate minerals in the schists such as muscovite.

Clay mineral analysis detected some interesting trends between the schistose and greywacke bedrock materials. A complex interstratified illite-chlorite clay is present in all schist derived samples but is not exclusively limited to these materials. The presence of this clay is expected as the schistose rocks are derived from the chlorite schist zone (Chapter 2). The greywacke-derived regolith samples which contain the illite-chlorite clay probably reflect a gradational contact between TZI unfoliated greywacke and TZIIa foliated schist. Greywacke colluvial samples which contain the illite-chlorite clay are thought to represent colluvium of mixed greywacke and schistose sources but with a dominance of greywacke material. The other clay minerals present are considered to be indicative of a common parent rock with a quartz and feldspar present. The quartz, which is more resistant to erosion than feldspar, is present in the diffractograms while the feldspar weathers to kaolinite and illite.

As with the whole rock analysis, further work is required concerning quantative analyses of the clay mineralogy in order to identify the relative abundance of kaolinite, illite and the illite-chlorite clays to determine the original bedrock material. As introduced with the Atterberg Limit analysis (Section 5.3.3.), the clay mineralogy confirmed the nature of the original bedrock material with a dominance of kaolinite being indicative of unfoliated greywacke material, while illite and smectite clays represent a schistose origin (Kingsbury, 1987; Horrey, 1989).

Table 5.11. Summary of X-Ray Diffraction analysis for both whole rock and clay minerals

*WHOLE ROCK ANALYSIS				
*SAMPLE	ALBITE	QUARTZ	MUSCOVITE	CLINOCHLORE
G II	☺	☺	☺	☺
G III	☺	☺	☺	X
G IV	☺	☺	☺	X
S II	☺	☺	☺	X
S III	☺	☺	☺	☺
S IV	☺	☺	☺	☺

*CLAY MINERAL ANALYSIS						
*SAMPLE	QUARTZ	KAOLINITE	CHLORITE	ILLITE	ILLITE-CHLORITE	IMOGOLITE
RED B1	☺	☺	X	☺	X	☺
RED B2	☺	☺	X	☺	X	☺
RED B8	☺	☺	X	☺	X	☺
RED B9	☺	☺	X	☺	X	☺
SC B4	☺	☺	☺	☺	☺	X
SC B10	☺	☺	☺	☺	☺	X
SC B11	☺	☺	☺	☺	☺	X
SC B14	☺	☺	X	☺	☺	X
SC B17	☺	☺	X	☺	☺	X
SC WH5	☺	☺	X	☺	☺	X
SR B3	☺	☺	☺	☺	☺	X
SR B12	☺	☺	☺	☺	☺	X
SR B13	☺	☺	☺	☺	☺	X
SR B15	☺	☺	X	☺	☺	X
SR B16	☺	☺	X	☺	☺	X
SR B23	☺	☺	X	☺	☺	X
GC B5	☺	☺	☺	☺	X	X
GC B6	☺	☺	☺	☺	??	X
GC B7	☺	☺	☺	☺	X	X
GC B20	☺	☺	X	☺	☺	X
GC B21	☺	☺	X	☺	☺	X
GC WH3	☺	☺	X	☺	☺	X
GR B18	☺	☺	X	☺	X	X
GR B19	☺	☺	X	☺	X	X
GR B22	☺	☺	X	☺	X	X
GR WH4	☺	☺	☺	☺	☺	X
GR WH6	☺	☺	☺	☺	??	X

*Whole Rock Analysis: ☺=mineral present, X=mineral absent, ??=uncertainty in identification
*Sample: G= Greywacke samples, S=Schist samples
*Clay Mineralogy: ☺=mineral present, X=mineral absent, ??=uncertainty in identification
*Sample: RED=red regolith, SC=Schistose colluvium, SR=Schistose regolith, GC=Greywacke colluvium, GR=Greywacke regolith

Red weathered material has a distinctive mineralogy showing the exclusive presence of imogolite, a clay mineral which is generally seen in soils with high quantities of volcanic glass (Brindley and Brown, 1980). Imogolite is thought to represent volcanic glass incorporated within ash deposits probably derived from volcanic eruptions in the North Island (Chapter 3) which has been subsequently weathered. However it is uncertain to what extent the ash deposits affected the development of red weathering and it may be that both the ash deposits and the underlying bedrock material have been subjected to red weathering. The parent material of the red weathered regolith tested in this study is greywacke and XRD analysis of the red weathered material confirms this origin because of the complete absence of the illite-chlorite clay associated with schistose material. Red weathered regolith is composed of kaolinite and illite and has no interstratified illite-chlorite clay, and also shows a complete lack of chlorite which may indicate that the parent material was a massive sandstone rather than a layered sandstone/mudstone material (Figure 5.22.). Figures 5.23. and 5.24. show the diffractograms of schist derived samples compared to greywacke derived samples and the diffractogram of red weathered regolith which indicates the greywacke parent material which may have a thin covering of ash.

Correlation of the XRD clay mineralogy with the estimates determined using Atterberg Limit data are possible given the amended clay percentage estimates. As described in Section 5.3.3. the original estimates were significantly affected by the clay mineral aggregates which caused a lower clay percentage estimate and therefore Figure 5.13. represented the ammended Activity data which showed a dominance of kaolinite and illite clays with a complete absence of montmorillonite. Additionally, the XRD data can be correlated with the Grim Classification (1962; Figure 5.12.) which plots Plasticity Index against Liquid Limit and the clay mineralogy is estimated to be dominantly kaolinite and illite.

5.3.8. Scanning Electron Microscope

a) Introduction

Scanning electron microscope (SEM) photomicrographs were analysed in an attempt to correlate the clay mineralogy identified by XRD analysis and suggested by activity data from Atterberg limits. The SEM facilities also provided the use of energy dispersive system (EDX) analysis which allowed further correlation with XRD determinations. Appendix D10 presents both the visual data from the SEM and the EDX graphs identifying clay minerals from each sample. Clay mineralogy was determined using diluted samples from grainsize analysis at 9ϕ in an attempt to isolate individual clay crystals on the slide rather than a collection of clay minerals which are more difficult to identify. Clay mineralogy was determined both visually

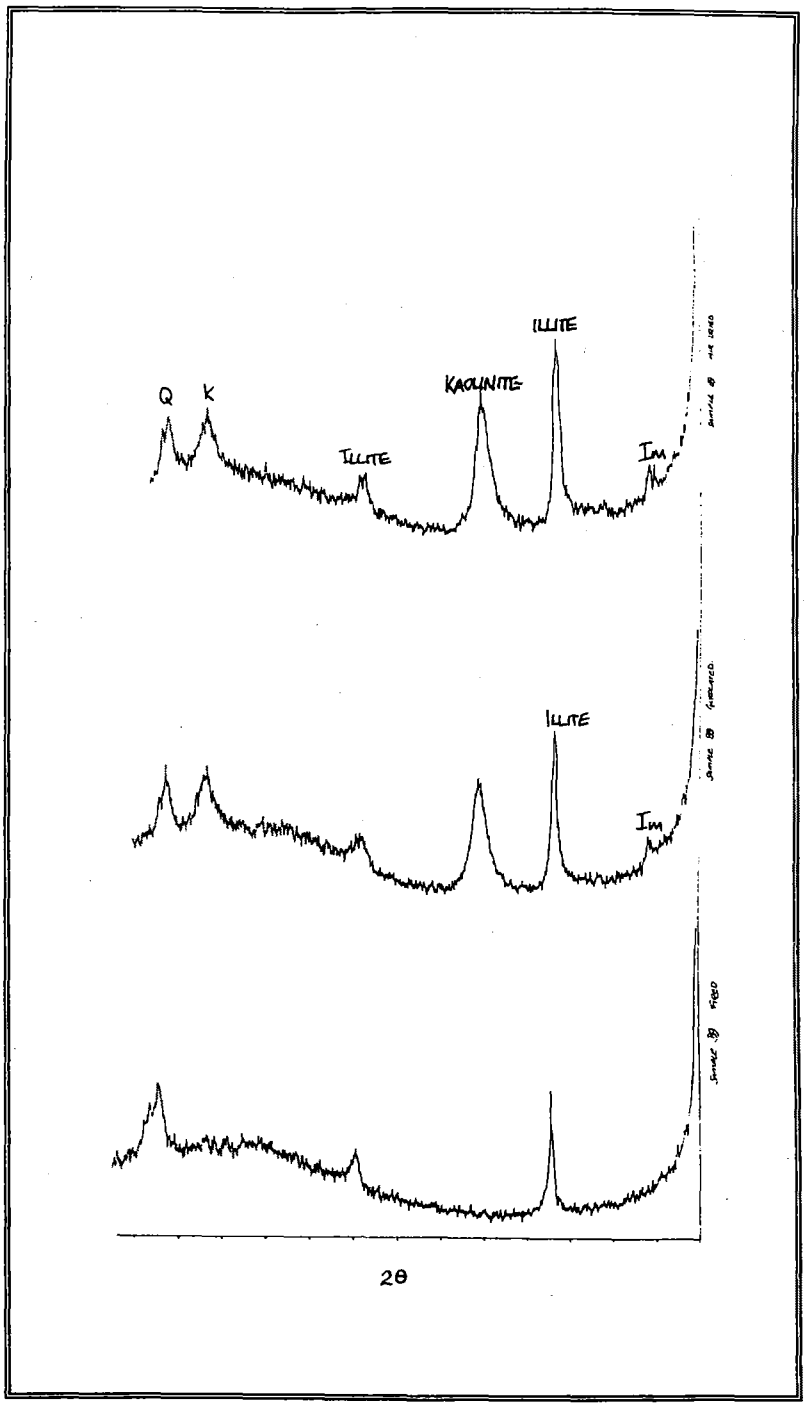

FIGURE 5.22.: X-ray diffractograms for red weathered regolith.

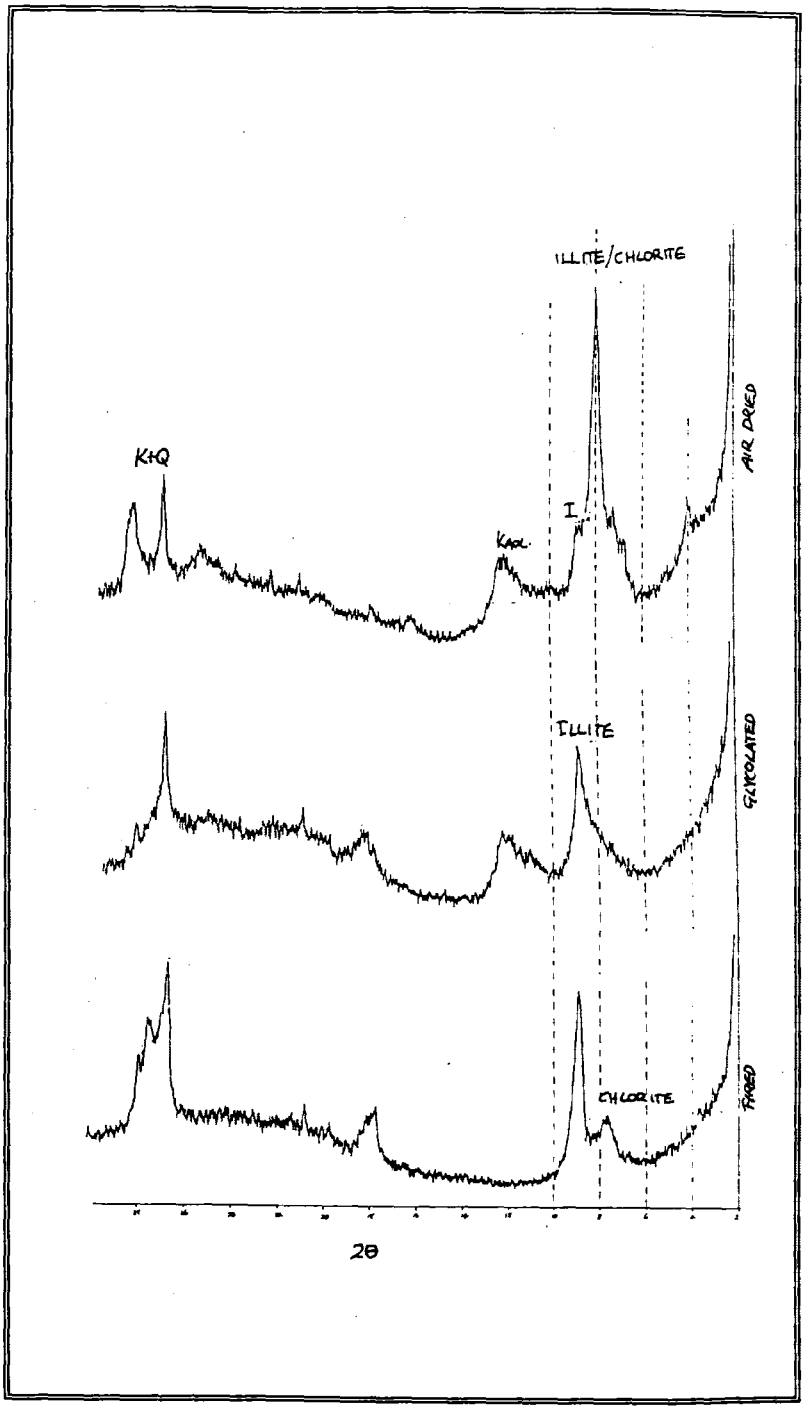

FIGURE 5.23.: X-ray diffractograms for schistose colluvium

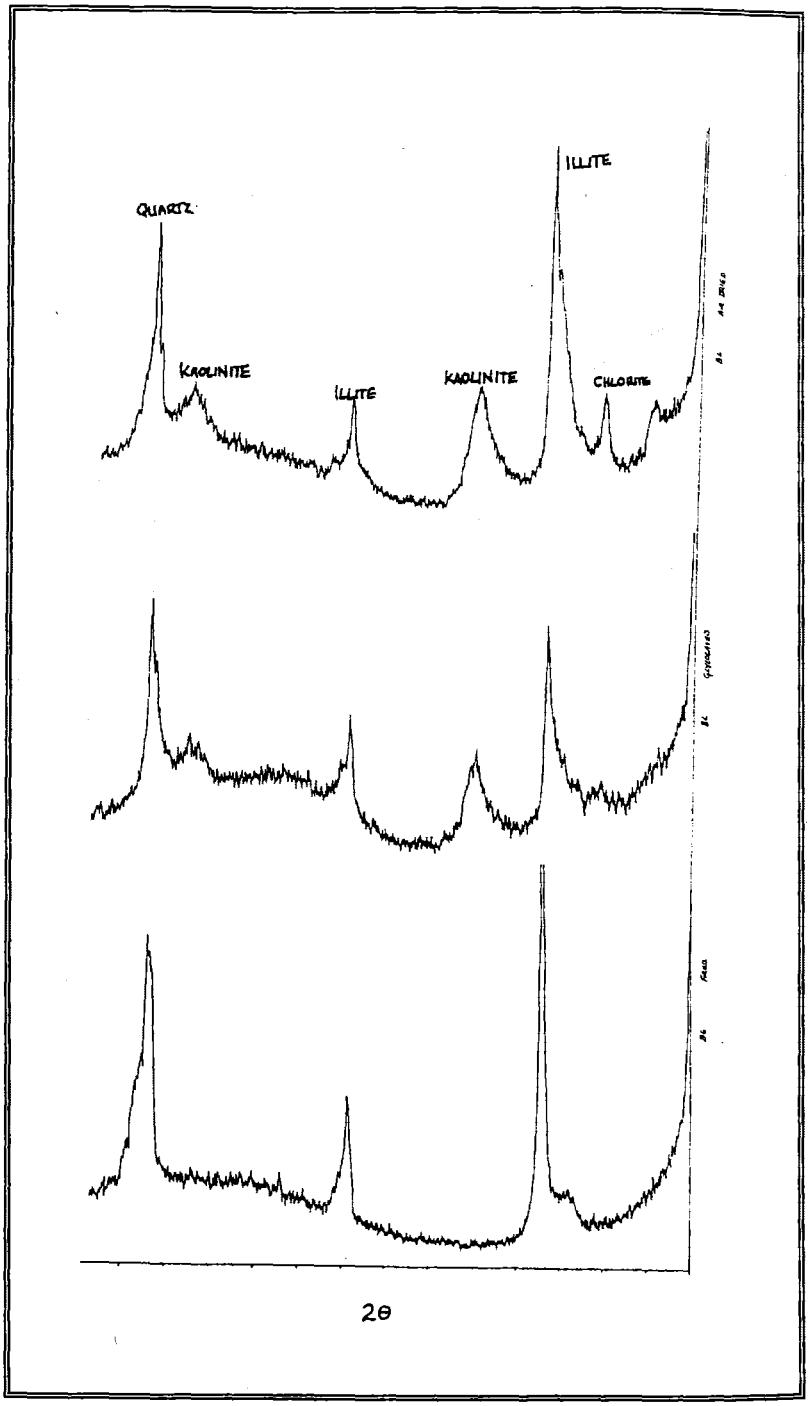

FIGURE 5.24.: X-ray diffractograms for greywacke colluvium.

and chemically using EDX and the minerals chosen for analysis were considered to be representative of the clay mineralogy of the sample as a whole on a visual basis.

b) Results

Analysis of the clay suspension samples showed the dominant presence of illite minerals and reduced amounts of kaolinite. Primarily the identification of different clay minerals was made using the EDX data because typically both illite and kaolinite have hexagonally shaped crystals (Figure 5.25.) when viewed under the SEM and thus are difficult to distinguish. Equal peaks of Si and Al indicate kaolinite clays (Figure 5.26.), while illite is shown by the presence of major elements of Si, Al and K with the K peaks generally less than the Al peaks (Figure 5.27.). Both the photomicrographs of constituent clay mineralogy and the corresponding EDX graphs for each sample are presented in Appendix D10.

c) Discussion

The main difficulty using the SEM for clay mineral analysis is that the principal component clays identified in this study, kaolinite and illite, are very similar in shape when viewed under the SEM as both are hexagonal. Furthermore, the use of the EDX system is limited to only one mineral at a time, and it is purely chance that in any one sample two different minerals are studied using EDX if they look alike. Therefore the SEM data is presented as an attempt to correlate the data obtained using XRD which is a more accurate assessment of clay mineralogy. Nevertheless, the EDX analysis has shown the presence of kaolinite and illite, although it failed to identify the presence of any chlorite clays and this may simply be because they are combined with illite clays. Additionally the EDX analysis of each sample identified that there is a high Na content in the soils which may be influential on their erosive properties (Section 5.3.4.). Excess sodium in soil material causes the soil particles to repulse, which makes the material more easily eroded, and sodium creates an increased osmotic pressure which allows more water into the soil void spaces which also may enhance erosion (Holmgren and Flanagan, 1977). The origin of the high Na content in the soil samples is thought to be due to salt spray from the ocean as high Na may be observed in coastal soils elsewhere in New Zealand, for example the Port Hills in Christchurch (Bell, pers comm. 1995).

5.3.9. Ring Shear Testing

a) Introduction

In order to calculate the residual friction angle (ϕ_r) and the cohesion (c_r)of the soils in the field area ring shear testing was attempted. Problems arose in obtaining residual values which were related to both the ring shear machine and the soils being tested such that two samples were sent to the University of Auckland for comparative testing. The internal friction angle represents the soil's resistance to slide failure on a slope (Figure 5.28.) and is related to the moisture content of the soils because

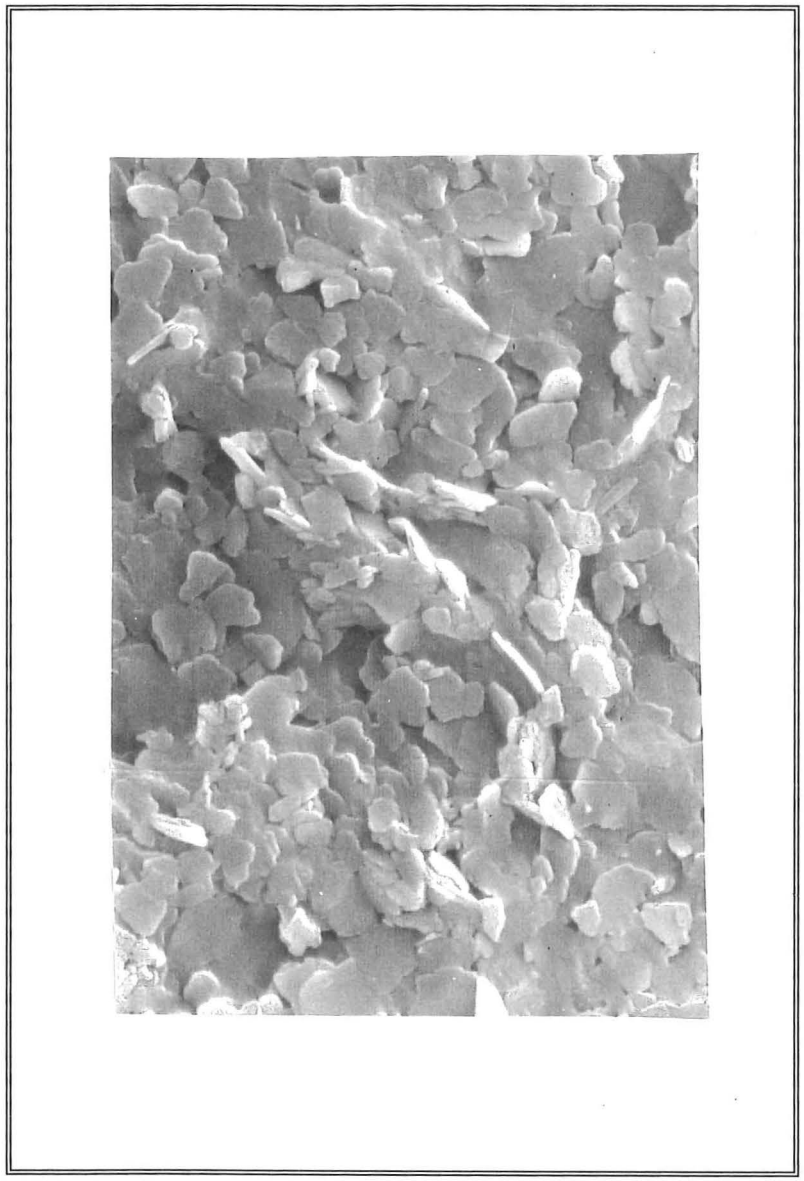

FIGURE 5.25.: A photograph of kaolinite and illite clay crystals using the Scanning Electron Microscope. Notice the almost identical shape of the illite and kaolinite which are essentially impossible to distinguish visually in oriented sections.

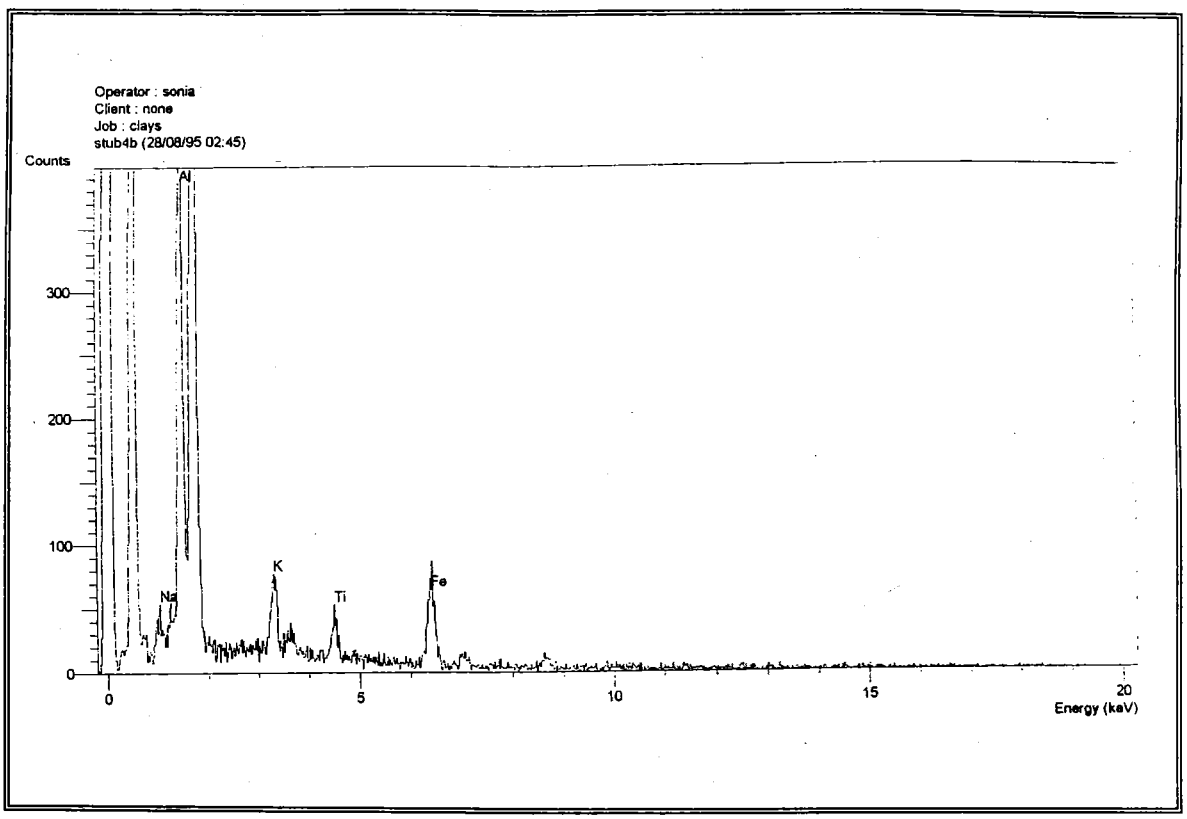

FIGURE 5.26.: A characteristic EDX graph of kaolinite showing the essentially equal peaks of silica (Si) and aluminum (Al).

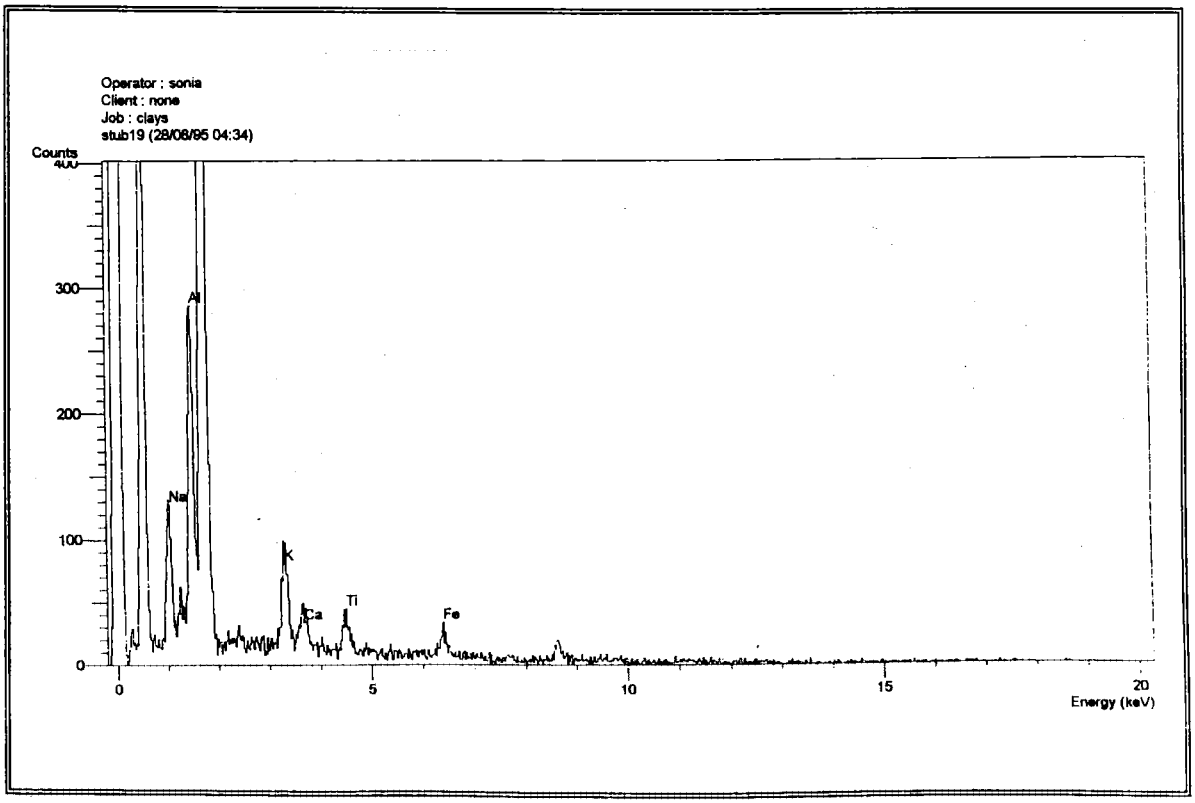

FIGURE 5.27. A characteristic EDX graph of an illite clay showing the major elements of silica (Si), aluminum (Al) and potassium (K). Notice the Al peak is greater than the K peak, indicative of illite.

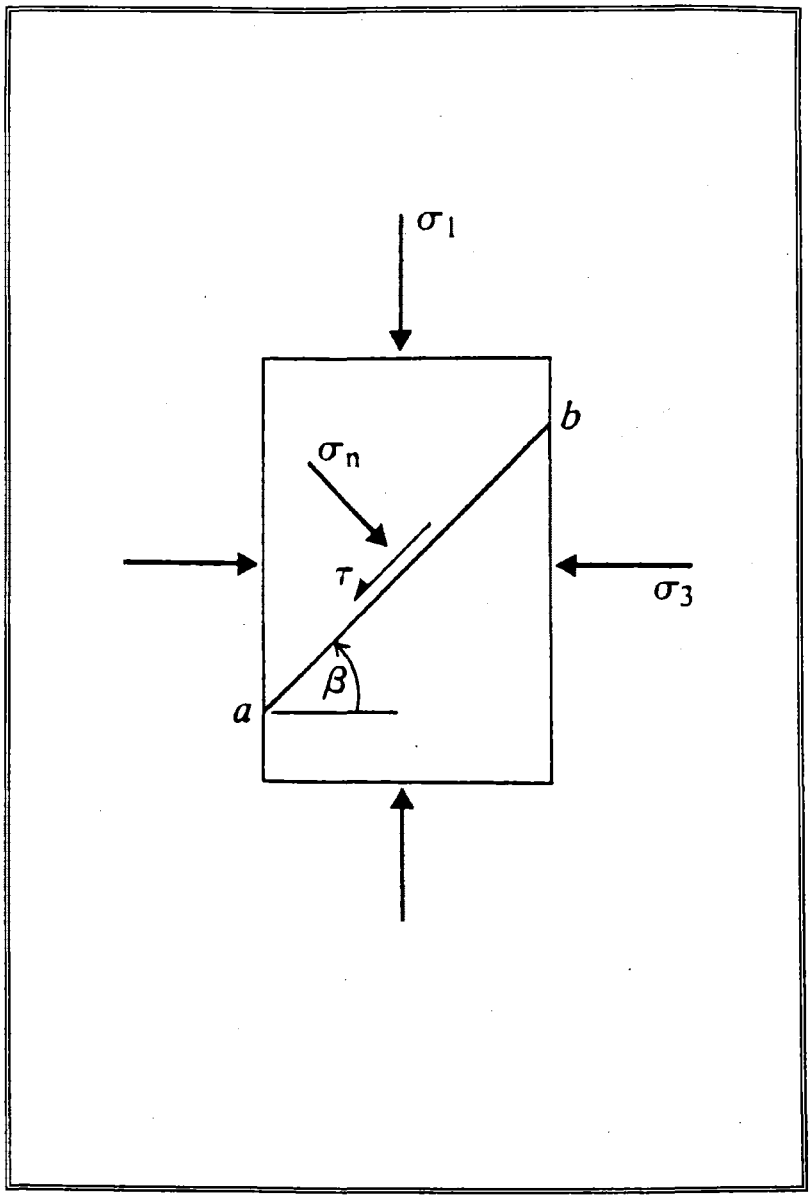

FIGURE 5.28: A diagrammatic representation showing the angle of internal friction ϕ_r (β) in relation to the principal stresses (σ_1 and σ_3), the normal stresses (σ_n) and the frictional resistance (τ) along the shear plane (a-b) (From Brady and Brown, 1985).

moisture reduces friction along a shear plane. The influence of increasing normal stresses on the failure plane is also important as an increase in the normal stress will contribute to an increase in friction along the failure plane and can increase the residual friction angle. Clays are generally assumed to have an average friction angle of approximately 13° (Rahn, 1986), although this value may range from 3°-4° for pure clays and depending on the clay content may be as high as 25° (Lambe and Whitman, 1979) . The methodology and test procedure is presented in Appendix 11.

b) Results

Due to the problems associated with testing at the University of Canterbury, the tests performed by Auckland University are analysed in this study and compared to the results obtained at the University of Canterbury. The high friction angles obtained during initial testing were confirmed by the University of Auckland results. The ϕ_r value for the red weathered material was 23°, with 21° for the schistose regolith tested in Auckland, while the Christchurch tests indicated the internal friction angle for the red weathered material was 24°. The soils were tested at water contents slightly over their Plastic Limits and with a variety of normal stresses ranging from 1Kg to 6Kg representing between 2-6m of soil above the shear plane respectively. Figure 5.29. shows the plot of shear strength versus normal load for the red weathered greywacke-derived regolith, while Figure 5.30. shows the shear strength plot for the schistose regolith sample. The samples are classified as mainly silty clays with up to 90% clay estimated for the red weathered material (Section 5.3.2.), although more than 50% of the clay is bound as sand and silt sized aggregates (Section 5.3.2.).

c) Discussion

Although the average value for clay soils is accepted as being approximately 13°, the friction angle depends on the clay mineralogy, percentage of clay and the amount of non-clay minerals present in the sample. The clay mineralogy was determined by XRD as being dominantly kaolinite, illite and chlorite and the presence of kaolinite and illite was confirmed by Activity analysis using amended clay percentage estimates (Section 5.3.3.) and the Grim Classification (Section 5.3.3.). Using the mineralogy information, Figure 5.31. shows the relationship between mineralogy, Plasticity Index and the internal friciton angle. For the friction angles determined in this study, 20°-25°, Plasticity Index values of between 25-28 will be accounted for by the presence of kaolinite clays (Figure 5.31.; Grim, 1962).

The presence of clay aggregates within the samples tested for internal friction angle are also thought to contribute to the results obtained. Clay aggregates were identified during grainsize analysis (Section 5.3.2.) and were most prevalent in the red weathered material, where up to 90% clay was estimated for the soils from hand specimen analysis although using grainsize testing less than 17% clay was identified. The aggregates appear to act as a granular material which generally are assumed to

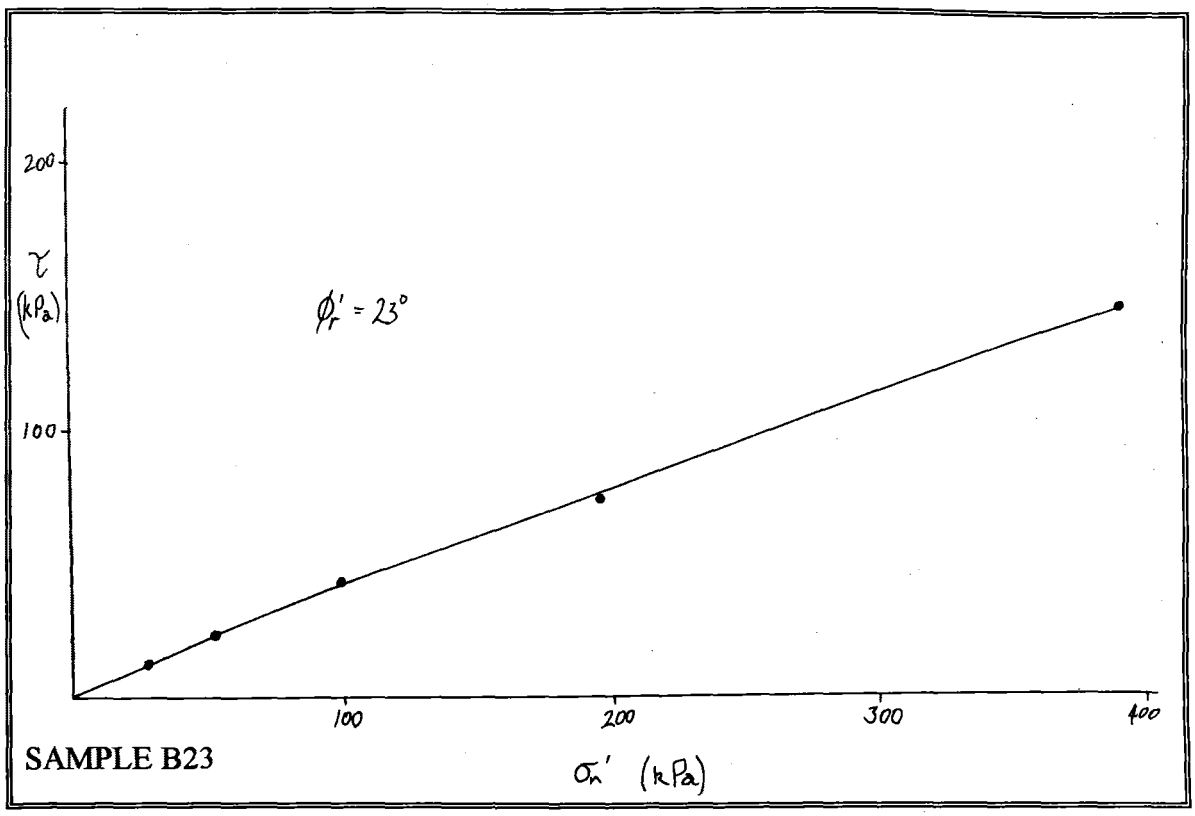

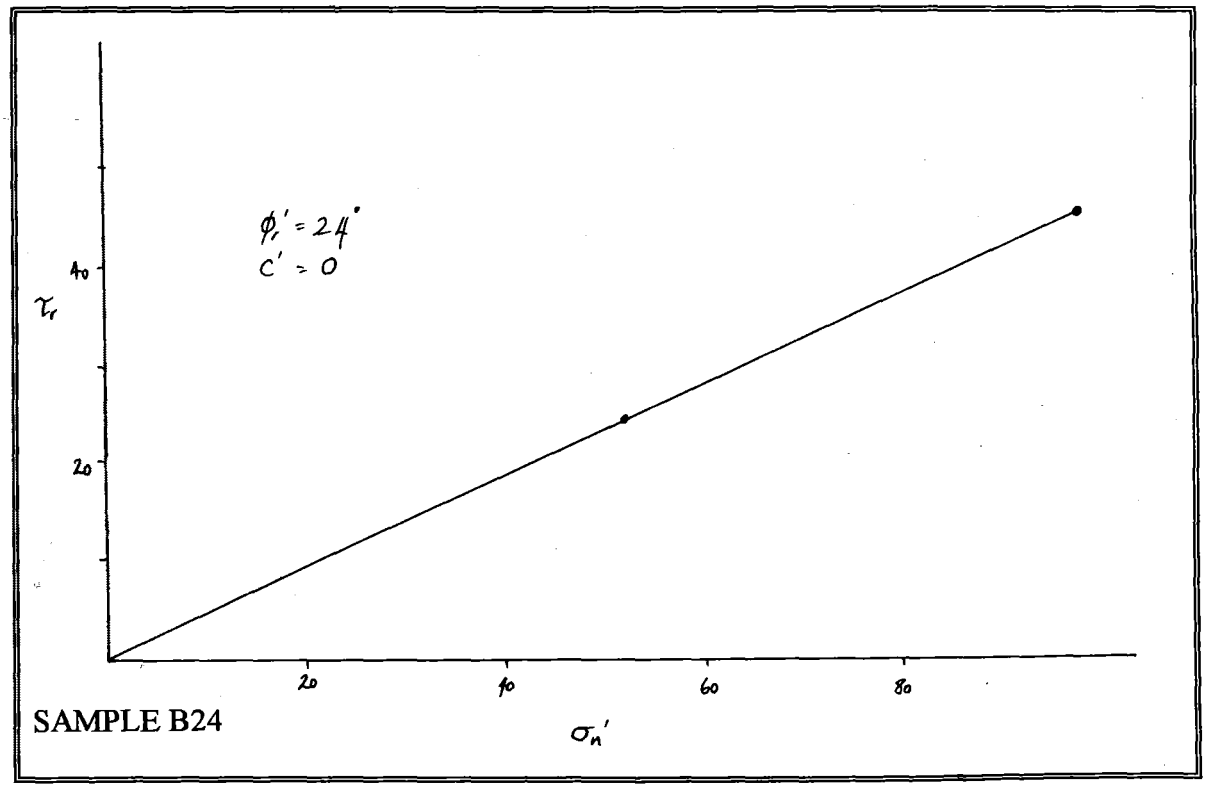

FIGURE 5.2 9. A plot of normal stress (σ_n) versus shear strength (τ) for samples B1 and B2, red weathered regolith which have a (ϕ_r) of 23°and 24° respectively.

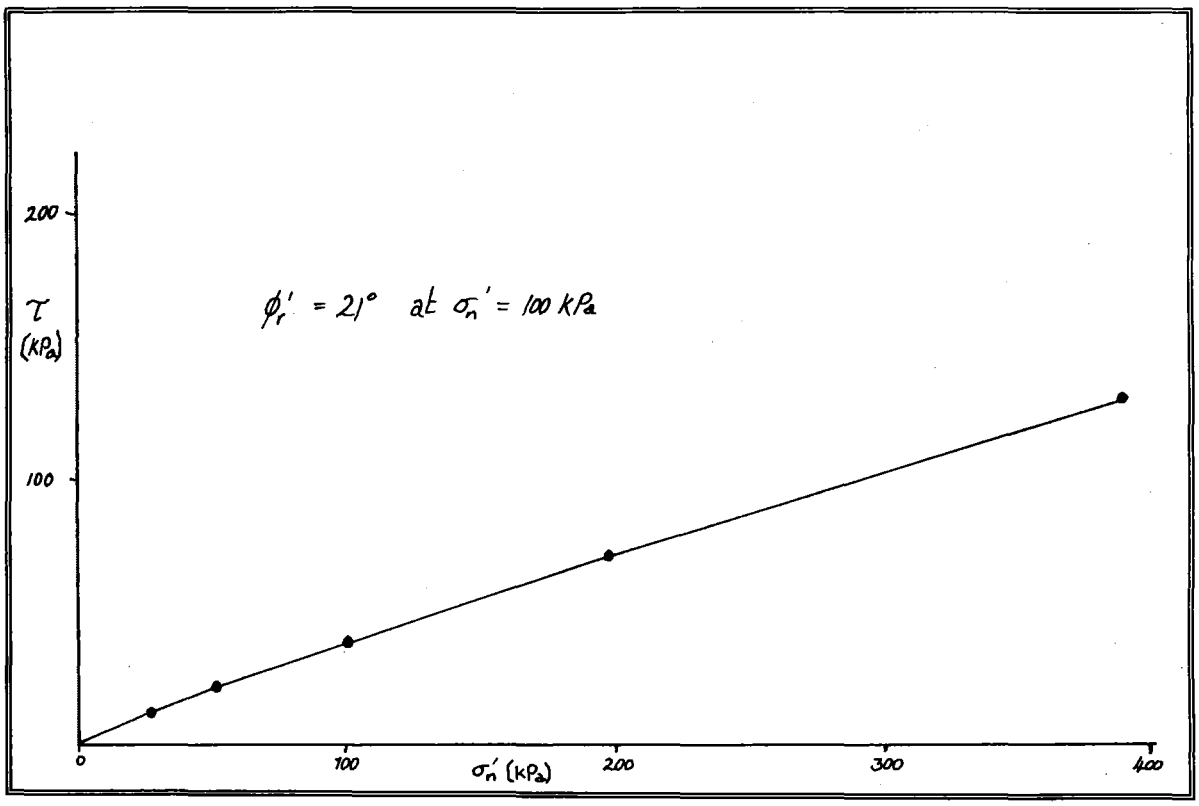

FIGURE 5.30.: A plot of normal stress (σ_n) versus shear strength (τ) for sample B23, a schistose regolith sample which has a ϕ_r of 21°.

have a higher angle of internal friction compared to soils dominated by clay; sands for example can have phi r values up to 35° (Lambe and Whitman, 1979). Additionally, the presence of clay sized quartz particles in these soil samples may impart a higher shear strength on the soil material because the quartz minerals are granular in nature in comparison to the sheet silicate nature of many true clay minerals such as kaolinite (Lambe and Whitman, 1979). Figure 5.32. shows the influence of quartz on the shear strength of soils and those soils with clay contents up to 70% may still have internal friction angles up to 30° (Lambe and Whitman, 1979).

5.4. WEATHERING GRADES

5.4.1. Introduction

Schist and greywacke weathered to grades II, III and IV (Bell and Pettinga, 1985) were analysed for their relative strengths using the point load test and the NCB cone indenter test (Section 5.3.5. and 5.3.6.). This discussion integrates the laboratory information on the strength of individual weathering grades in order to determine geotechnical parameters for different degrees of weathering in both schistose and greywacke rock. Thin sections were made of each grade to analyse the mineral constituents and the mineralogy was integrated with the information from whole rock XRD analysis in order to determine any mineralogic changes with weathering. The petrographic analysis (Section 5.4.3.) was also used to study the microstructure of the rocks with increased weathering.

5.4.2. Rock Strength

Commonly it is observed that rock strength will decrease with increased weathering, irrespective of the mode of weathering (chemical, mechanical or biological) and the original rock type. Additionally, in the Marlborough Sounds schistose rock is generally assumed to have a significantly reduced strength compared to greywacke, particularly when load is applied parallel to foliation. Both point load testing and NCB cone indenter tests confirmed the loss of strength due to weathering and further showed the greater strength of greywacke over schist (Section 5.3.5 and 5.3.6).

Point load testing showed that the calculated UCS values were higher for the greywacke than the schist with an average value of 71MPa for weathering grade II in greywacke compared to 45MPa for schist loaded perpendicular to foliation. The results obtained for lower weathering grades in greywacke however indicate that the schistose rock has a greater strength, for example for weathering grade III greywacke yielded 7.1MPa while the corresponding schist was 20MPa. Similar results were observed in the Grade IV greywacke and schist samples. When compared to the average UCS values calculated from the CIN testing, which provided strength results consistent with those expected, the anomalous nature of the point load results for weathered greywacke becomes obvious. The CIN testing calculated 52MPa for Grade

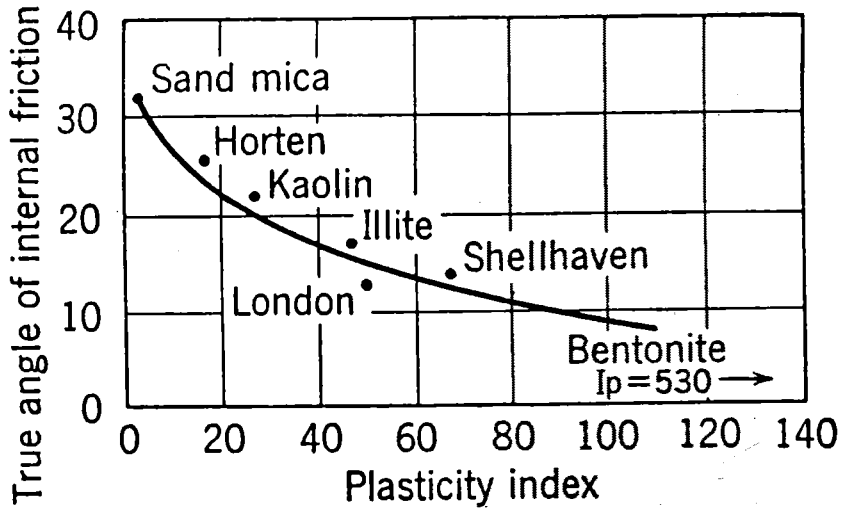

FIGURE 5.31: The relationship between Plasticity Index and ϕ_r *with respect to clay mineralogy (Grim, 1962).*

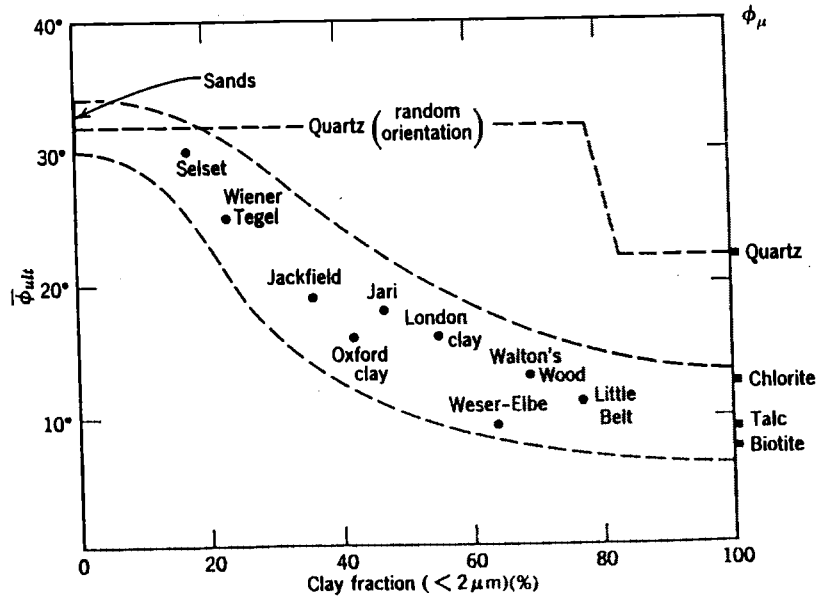

FIGURE 5.32.: The relationship between the residual friction angle ϕ_r [ϕ_{ult}] and the clay fraction. Also the influence of quartz, which has a higher shear strength (From Lambe and Whitman, 1979; After Skempton, 1964)

II greywacke compared to the 71MPa from the point load tests while for schist weathered to the same degree CIN calculated 35MPa compared to the 45MPa for point load. Figure 5.21. shows the range of UCS values calculated from both point load and CIN testing which confirms that there is a closer correlation between the calculated UCS values for schist between the two test methods than for the greywacke samples. The reasons for the trends is unclear, however the problems concerning sensitivity of the point load test instrumentation for measurement of low rock strengths previously identified (Section 5.3.6.) may be significant. Because the schistose material is considered to be weaker than the greywacke material the point load test may overestimate the strengths of these very weak rocks. It is evident that the CIN method also overestimates the strengths of both schist and greywacke at higher weathering grades compared to the values calculated for point load. As identified by Kingsbury (1987) the anamolous results may be influenced by the unsuitability of the CIN method for testing of weathered rock as the test was originally designed for the testing of coal samples. Table 5.12. summarises the average strength characteristics of schist and greywacke using both the point load and CIN test methods

The Strength Anisotropy Index from the point load test indicated that there is a linear decrease in strength in schistose material for each weathering grade (Figure 5.16.). The linear relationship between perpendicular and parallel strength of schistose rock shown in Figure 5.16. represents the gradational changes between strength and weathering grade and provides parameters for estimating the maximum and minimum strengths of schist at any degree of weathering.

5.4.3. Mineralogy and Structure

Whole rock X-ray diffraction analysis of weathering grade failed to determine any mineralogical changes with weathering grade. The schist and greywacke were principally composed of quartz, albite feldspar and muscovite with some samples containing clinochlore. Clinochlore, a close relative of the clay mineral chlorite, was the only mineral which was not present in all samples but it was not observed to occur exclusively with increased weathering of either rock type. Petrographic studies of weathered rock did show, however, changes in mineralogy as weathering increased, with chlorite being the dominant clay mineral identified for schist. The abundance of clay minerals in greywacke increased with increasing weathering because minerals such as feldspar weather to sericite and other clay minerals (Figure 5.33.). The presence of kaolinite and illite in the weathered rock material is thought to be from the weathering of minerals within the parent rock. There also appears to be a genetic relationship between weathering and rock type. Schist weathers more easily than greywacke because the foliation surfaces within schistose material, which have an abundance of fine grained clay minerals (Figure 5.33.), become zones of

weakness along which the weathering process is accelerated. Although the schist has an abundance of mica minerals for weathering, the presence of silt and clay sized non clay minerals in unmetamorphosed rocks, for example mudstone, will also be easily weathered. The weathering of unmetamorphosed sandstones is principally related to the breakdown of feldspar minerals to illites and kaolinites (Figure 5.33) while chlorite is thought to be one of the original constituent minerals of the schistose rock material.

It is not only the foliation surfaces in schist which display accelerated weathering relative to the unfoliated rock mass, but rock defects such as joint sets and fracture surfaces also provide zones of weakness which are subjected to intensified weathering. The joints and fractures in the rock mass are similar to the foliation surfaces because they allow the movement of water which is a principal component in weathering (Chapter 3) and therefore the joint surfaces often show more intense weathering. Rock defects may be observed in both schist and greywacke bedrock although they are often more closely spaced and intense in fine grained or foliated bedrock compared to massive sandstone units and therefore the weathering along joints is more intense in the schistose rock rather than the greywacke. Table 5.12. summarises the mineralogy of each weathering grade for both schist and greywacke material from XRD and petrographic analyses.

5.5. GEOTECHNICAL PARAMETERS

5.5.1 Introduction

One of the objectives of this study was to determine the geotechnical characteristics of the surficial deposits, regolith and colluvium, in the Marlborough Sounds. The objective was achieved using laboratory characterisation techniques in order to determine the mineralogy, shear strength and texture of the individual units, and the data obtained was then correlated with field information where applicable. The following discussion examines the geotechnical parameters of the constituent soils identified in the field area, namely regolith and colluvium, with an additional discussion for red weathered regolith, and then synthesises the laboratory and field information obtained and presented in the earlier part of this chapter.

Regolith material in the study area was subdivided into schist-derived, greywacke-derived and red weathered regolith. The geotechnical characteristics of each of the regolith types indicated significant differences related to the original bedrock lithology and mineralogy. Due to the unusual geotechnical characteristics of the red weathered regolith, it is discussed separately (Section 5.5.4.).

Colluvial material was also sampled with respect to the bedrock from which it was derived and was sub-divided into samples of greywacke colluvium and schist derived colluvium. As observed with the regolith material, the original bedrock

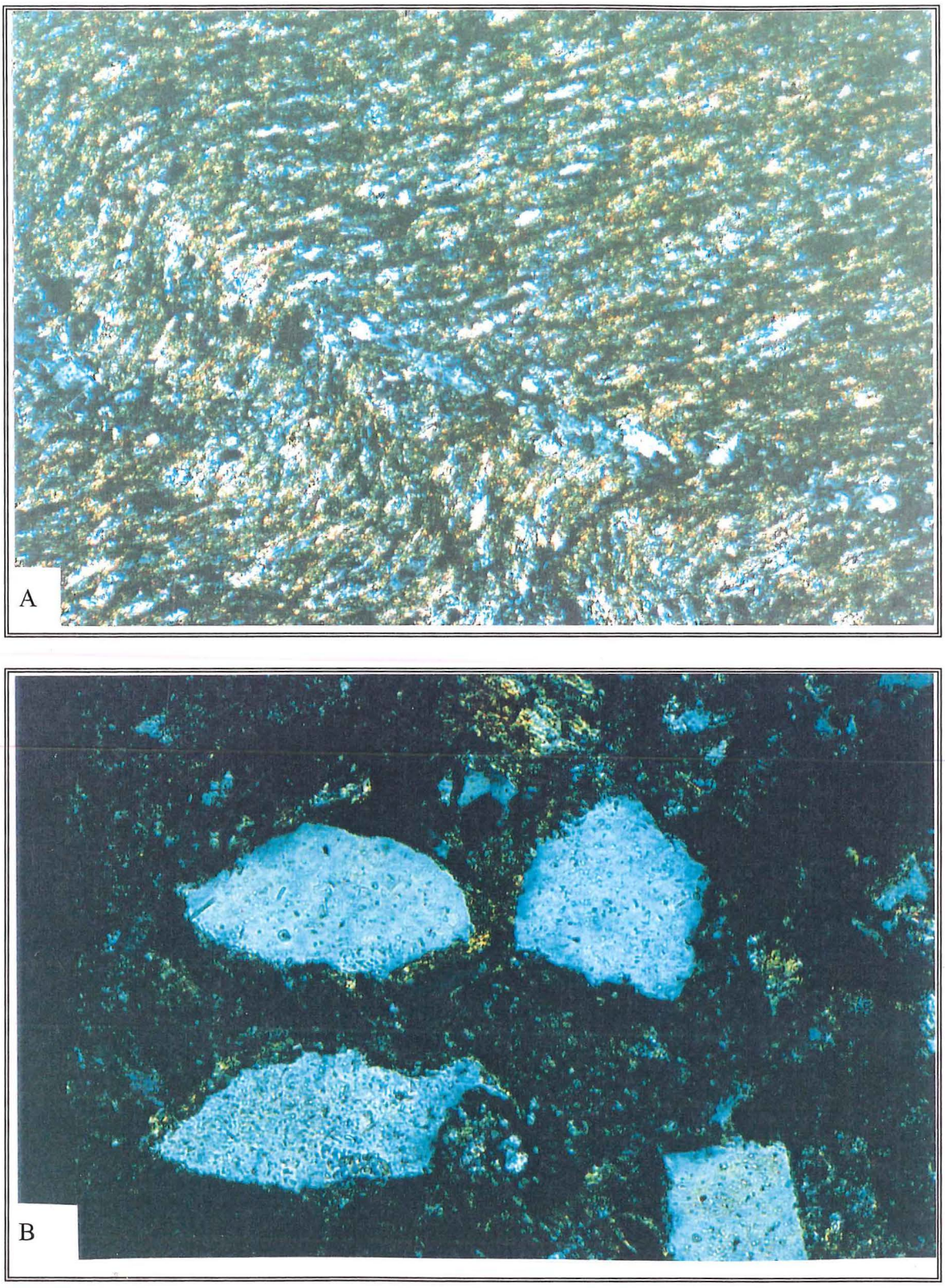

FIGURE 5.33. Photomicrographs of A) weathered schistose material showing the fine grain size and abundance of clay minerals such as chlorite and micas, and B) greywacke sandstone showing the break down of quartz and feldspar to clay minerals.

Table 5.12. A summary of the strength characteristics and the mineralogy of each weathering grade with respect to lithology.

SUMMARY OF CHARACTERISTICS OF WEATHERING GRADES										
SAMPLES		*STRENGTH CHARACTERISTICS						*MINERALOGY (XRD AND PETROGRAPHY)			
Lithology	Weathering Grades	Point Load Is(50)		Point Load UCS		Cone Indenter	CIN UCS	Qtz	Albite	Muscovite	Clinochlore
Schist	II	// 1.1	⊥ 1.9	// 27	⊥ 45	1.8	35	☺	☺	☺	X
	III	// 0.2	⊥ 0.8	// 5.4	⊥ 20	0.7	21	☺	☺	☺	☺
	IV	// 0.02	⊥ 0.3	// 0.5	⊥ 8.6	0.6	10	☺	☺	☺	☺
Greywacke	II	3.0		71		3.0	52	☺	☺	☺	☺
	III0	0.3		7.1		2.0	33	☺	☺	☺	X
	IV	0.08		1.9		1.3	22	☺	☺	☺	X

*Strength Characteristics: //=strength parallel to foliation, ⊥=strength perpendicular to foliation

*Mineralogy: ☺=mineral present, X=mineral absent

lithologies contributed to significant differences between the two colluvial types, schist and greywacke.

The nature of red weathered regolith is different to that of the other soil types in the field area. The red weathered regolith collected for this study is of greywacke origin and its occurrence is sporadic, generally preserved on relict bedrock ridges or spurs. The conditions pertaining to the development of red weathering have been discussed in Chapter 3.

5.5.2. Regolith

a) Grainsize and Atterberg Limits

Grainsize analysis and the determination of Atterberg Limits were used in an attempt to identify textural differences between the regolith derived from schist and greywacke, such as differences in plastic and liquid limit and proportions of sand, silt and clay. One of the principal limitations of the analysis is the presence of clay aggregates within the regolith material which caused problems in accurately assessing the percentages of sand, silt and clay (Section 5.3.2.). The grainsize analysis classifies the regolith soils as sandy silts with some clay, however the field description classifies the soils as silty clays and therefore the clay aggregates are thought to constitute up to 50% of the soil which would alter the clay fraction from 12-13% to approximately 60%. Table 5.13 summarises the textural information obtained from grainsize analysis, but the clay fraction is to be considered a minimum value only. The reason for the presence of the clay aggregates and the problems associated with their disaggregation for grainsize analysis is outside the scope of this study, but certainly more detailed analysis on the nature and mineralogy of the aggregates is required.

Atterberg Limit data showed that the regolith soils had a higher Plastic and iquid Limit than the colluvial soils (Section 5.5.3.) and the regolith data are summarised in Table 5.13. The regolith soils show very little difference between schistose material and greywacke soil, with average Plastic and Liquid Limit values of 25 and 40 respectively for the schistose soils and 23 and 39 for the greywacke material (Table 5.13.). The Plasticity Index values are therefore also similar with 15 for schistose regolith and 16 for greywacke. The Plasticity Index of the regolith samples indicates that the soils are moderately plastic and composed of silts and clays as they plot above the 'A-line' on the Casagrande Plasticity Diagram (Figure 5.10.; Section 5.3.3.). The values obtained for Plastic and Liquid Limit and the Plasticity Index are considered accurate in this study because, unlike the Activity data discussed below, these parameters are not influenced by the problems in obtaining real values for grainsize percents.

b) Mineralogy

X-Ray Diffraction analysis of the regolith samples failed to identify any mineralogical differences between the regolith and colluvium material. Regolith is composed of quartz, kaolinite, illite, some chlorite and the schistose samples included an interstratified illite-chlorite clay mineral. Table 5.13. summarises the mineralogical characteristics of the regolith material as determined by XRD analysis. The presence of chlorite was sporadic and did not appear to be restricted by soil type, either regolith or colluvium, nor was it restricted by bedrock lithology (Table 5.11.). The illite-chlorite clay identified in all of the schistose regolith samples and only one of the greywacke regolith samples is thought to represent the original mineralogy of the parent rock, because the schistose material is classified as chlorite schist and the illite component is thought to be the result of weathering of minerals such as feldspar. The identification of the illite-chlorite mineral in greywacke samples is considered to represent the gradational contact between greywacke material and low grade schists (TZIIa-TZIIb) in the field area.

SEM failed to identify the presence of the illite-chlorite interstratified clay however, using EDX analysis the presence of both kaolinite and illite were confirmed (Section 5.3.8.). Additionally, the EDX analysis of the regolith samples identified that all of the soils in the field area have a high or moderate sodium content which may have a significant effect on the erodibility of the soils in the field. The positive ionic charge of Na will increase the particle repulsion of the soil and also increases the potential for water movement within the inter-particle voids in the soil, giving the soils a higher erosive potential than soils without Na^+ (Chapter 3.). The origin of the sodium in the soils is believed to result from the influence of sea spray which contains high quantities of sodium (Section 5.3.4.). There was no difference in the occurrence of Na between greywacke- and schist-derived regolith soils and similarly no difference between regolith and colluvium.

Activity data obtained from the Atterberg Limit testing was used to complement the mineralogical information obtained from both XRD and SEM testing, however problems were encountered in obtaining accurate Activity data because of the presence of clay aggregates which caused the clay percentages to be anomalously low (Section 5.3.3). As discussed in Section 5.3.3. the clay aggregates may account for an additional 40-50% of the original clay percent in addition to the clay percentages actually obtained. The Activity data obtained was reassessed using amended estimates for clay percent and the results showed favourable correlation with the mineralogical information determined by XRD and SEM. The amended Activity data (Figure 5.13.) suggest that the dominant clay minerals in the regolith soils are kaolinite and illite, which is consistent with the results obtained from XRD.

c) Shear Strength

Shear strength analysis of soils in the field area was limited due to problems with equipment and the difficulty in obtaining a residual shear strength for many of the soils tested. Schistose regolith was tested using the ring shear device and an angle of internal friction (ϕ_r)was determined to be 21° (Figure 5.29., Table 5.13.). The 21° obtained was consistent with a clay mineralogy dominated by kaolinite (Figure 5.31.) and the presence of quartz which imparts a higher shear strength on the soil. Quartz acts as a granular material and will increase the shear strength of the soil compared to a soil which is composed completely of clay minerals which are sheet silicates (Figure 5.32). The influence of clay aggregates may also be important in the shear strength of the regolith material as the aggregates may also act as granular components in the clay soil and therefore increase the shear strength of the material.

5.5.3. Colluvium

a) Grainsize and Atterberg Limits

Colluvial soils have a wide range of textures from a blocky clast supported, matrix depleted gravel, to a matrix supported gravelly silty clay. The material tested in this study was the matrix material in the gravelly silty clay, which was more extensive in the field area than the blocky gravel.

Grainsize analysis of the matrix material of colluvium showed that the soils were dominated by between 15-20% gravel and almost 45% sand, classifying the colluvium matrix as gravelly silty sands with some clay which was anamolous with the soil textures and plasticity observed in the field . In hand specimen the matrix of colluvial material is a gravelly silty clay with some sand and the differences in soil description is due to the clay aggregate problem identified in Section 5.3.2. Up to 50% clay aggregates in the sand and silt sized fraction of colluvial matrix material is estimated to account for the variation between laboratory classification and hand specimen observations. The colluvial material does not show any variation in grainsize in relation to different bedrock origins, as both the greywacke and schist derived colluvium have similar proportions of gravel, sand, silt and clay. The original grainsize data are summarised in Table 5.14. while the ammended data is discussed below in Section 5.3.3.

Atterberg Limit testing of the colluvial soils showed that both the greywacke and schist colluvium had lower Plastic and Liquid Limits compared to the regolith soils. Schistose regolith Plastic and Liquid Limits were 25 and 40 respectively compared to 21 and 35 respectively for the schistose colluvium while greywacke regolith showed 23 and 39 for Plastic and Liquid Limits compared to 23 and 36 for the colluvium. The reason for the differences are thought to simply reflect the statistical error associated with testing small numbers of samples because, as previously mentioned (Section 5.3.4., Table 5.14.), the range of values for both Liquid

and Plastic Limit is significant (Table 5.7.). The Plasticity Index of the colluvial samples shows that the average plasticity of the schistose colluvium is lower (13) than the greywacke colluvium (14; Table 5.14.) which is also thought to be due to statistical error resulting from limited samples for testing. However, when all of the samples are plotted on the Casagrande Plasticity Diagram (Figure 5.10.) the soils are classified as being of moderate plasticity and in general plot on or above the 'A-line' indicating that they are soils composed of silts and clays (Figure 5.10.). The variablility of the data obtained from Atterberg Limit testing indicates that the number of tests performed was inadequate to reliably determine the plastic and liquid limits of the soils in the field area and more work is required to identify if there are any significant trends related to lithology and mineralogy. Such detailed analysis of the soils was outside the scope of this thesis.

b) Mineralogy

XRD and SEM analysis were used in an attempt to identify the mineralogy of the colluvial soils for comparison with regolith material and to identify any mineralogical trends between greywacke and schistose parent material.

The XRD data identified similar mineralogical trends to the regolith samples (Section 5.5.2.) with the principal minerals being quartz, kaolinite, illite, some chlorite and again the presence of an interstratified illite-chlorite clay. However there were differences between the greywacke-derived and schist-derived colluvial samples with the schistose material showing the presence of the mixed layer illite-chlorite clay which was also present in some of the greywacke colluvium material. The presence of illite-chlorite clay in some of the greywacke derived colluvial samples may indicate that there is a gradational contact between greywacke and the metamorphosed schist material at some locations within the field area. Table 5.14. summarises the mineralogical characteristics of the colluvium samples tested in this study.

SEM analysis, as with the regolith material (Secion 5.5.2.), did not identify any smectite clays however the presence of illite and kaolinite was determined using the EDX facilities (Figures 5.26.and Figure 5.27.) and the results of the EDX and SEM analyses of clay mineralogy are summarised in Table 5.14. Sodium was identified in both the schist derived and greywacke derived colluvial samples and this is believed to influence the erodibility of the soils in the field area. As discussed with the regolith samples (Section 5.5.2.) the presence of Na^+ in a soil can increase the repusion of soil particles and increase the osmotic movement of water in the voids of the soil thereby accentuating the erosive nature of the soil. Pinhole erosion and Crumb testing (Section 5.3.4.) did not classify the soils as erosive however, there is field evidence for substantial erosion (Chapter 3) within the field area which, although perhaps principally due to physical erosion, may be due to dispersion and accentuated by the presence of Na^+ in the soils. As previously mentioned (Section 5.3.4.) the origin of

the Na in the soils is thought to be from the influence of sodium rich salt spray from the ocean.

The Activity data was used to complement the mineralogical assessment of the XRD and SEM analyses of the colluvial soils. As discussed in Section 5.5.2. the principal limitation of the Activity data is the influence of clay aggregates which constrain the estimation of clay percentages to minimuim values only as the Activity of a soil is critically dependent on the clay content of the material. With up to 50% of the soil materials thought to be composed of clay aggregates the amended Activity data incorporates the estimated clay percentages and is shown in Figure 5.13. The mineralogical characteristics of the colluvial soils using the amended Activity data can be correlated with the XRD and SEM analyses and the principal clay minerals identified are kaolinite and illite.

5.5.4. Red Weathered Regolith

a) Grainsize and Atterberg Limits

Red weathered regolith material is analysed separately due to the unusual nature of the soil compared to the other regolith samples and also compared to the colluvial material. Conventional grainsize analysis of the red weathered regolith indicates that the material is completely devoid of gravel and is classified as a clayey silt with some sand, with an average silt component of 70% and clay contributing only 16% of the soil. In hand specimen however, the red weathered soil is classified as a slightly silty clay with up to 90% of the material estimated to be clay (Section 5.3.2.), and the variation between hand specimen and grainsize analysis is attributed to the presence of clay aggregates. Clay aggregates were observed in the sand fraction using a binocular microscope and were interpreted in the silt fraction by the textural differences between hand specimen and the grainsize analysis. Although all of the soils tested in this study are affected by clay aggregates, the red weathered regolith is particulary susceptible to aggregation of clay minerals into sand and silt sized particles and the reasons for increased aggregation in red weathered soils are not clear and were not investigated.

The Atterberg Limits of the red weathered regolith material showed differences compared to the colluvial and remaining regolith soils, particularly with respect to the Liquid Limit. Red weathered material has a Liquid Limit of 51 compared to between 35 and 39 for other regolith and colluvial samples (Table 5.7.). The average Plastic Limit value of 25 is comparable to the Plastic Limits of the other samples which are between 21-25 (Table 5.7.), but the range of values is limited which indicates consistency for the determination of Plastic Limit. As mentioned for the regolith soils (Section 5.5.2.) the reason for the higher liquid limit may be due to mineralogical differences compared to the other soils in the field area. Plasticity Index values for the red weathered regolith were also different to those obtained for

the other soils in the field area with 27 obtained for the red weathered material and between 13 and 16 for the remaining soils (Section 5.3.3.). The red weathered regolith, when plotted on the Casagrande Plasticity Diagram (Figure 5.10.), clusters apart from the other soils and is classified as high plasticity silts or clays which is a reflection of the higher liquid limit values obtained. Table 5.15. summarises the grainsize data and the Atterberg Limit data obtained for the red weathered regolith material in this study.

b) Mineralogy

The XRD diffractograms indicated that the mineralogy of the red weathered material was almost identical to that of greywacke-derived regolith and colluvium (Sections 5.5.2. and 5.5.3.). Indeed, the red weathered regolith tested in this study is insitu weathered greywacke and therefore, the presence of quartz, kaolinite and illite were confirmed. The presence of imogolite, a clay mineral which is generally associated with soils high in volcanic glass, was identified exclusively in the red weathered regolith material and is thought to represent the influence of ash deposits from North Island volcanic eruptions prior to or during the development of the red weathered surfaces (Chapter 3). The illite-chlorite interstratified clay found in some of the greywacke derived samples was absent from the red weathered material. Table 5.15. summarises the clay mineralogy of the red weathered regolith soil derived from XRD analysis.

SEM and EDX analysis of the red weathered material identified the dominance of kaolinite and illite clay minerals, and also showed the high to moderate content of Na in the soils. As with the other soil samples tested in this study, the presence of sodium creates a potentially erosive soil which when combined with the physical erosional mechanisms, may contribute to a highly eroded landscape (Chapter 3). The origin of the Na^+ in the soil material is thought to be derived from salt rich sea spray (Section 5.3.4.).

Activity values for the red weathered regolith were also significantly influenced by the presence of clay aggregates which are believed to contribute to a clay percentage of up to 90% for the red weathered soils (Section 5.5.3.). The measured clay percent (average 16%) was amended in Figure 5.13. to account for the clay aggregates and the Activity values were assessed accordingly. The Activity diagram indicates that the red weathered material is dominantly composed of kaolinite (Figure 5.13.) which is consistent with the mineralogy determined by both the XRD and SEM analyses.

c) Shear strength

Shear strength testing of the red weathered regolith material provided residual ϕ^r values of 23° and 24° tested in Auckland and also in Christchurch (Section 5.3.9.). As with the other regolith samples, a ϕ_r value of 23° or 24° for the red weathered regolith indicates that the mineralogy is dominated by kaolinite

Table 5.13. A summary of the textural characteristics, mineralogy and internal friction angles for regolith samples.

SUMMARY OF LABORATORY DATA FOR REGOLITH SAMPLES																
*SAMPLES		Textural chatacteristics								*Mineralogy						Strength
		Grain Size (%)				*Atterberg Limits				X-Ray Diffraction					SEM	
Lith.	No.	Gravel	Sand	Silt	Clay	PL	LL	PI	ACT	Q	K	C	I	IC	Na	ϕr
SR	B3	2.4	62.0	24.2	11.5	26	32	6	0.5	☺	☺	☺	☺	☺	H	
	B12	2.6	52.8	30.9	13.7	25	41	16	1.2	☺	☺	☺	☺	☺	H	
	B13	6.9	67.7	15.6	6.8	26	34	8	1.2	☺	☺	☺	☺	☺	H	
	B15	2.2	50.8	31.2	17.5	22	37	15	0.9	☺	☺	X	☺	☺	H	
	B16	5.9	45.1	31.6	17.5	22	45	23	1.3	☺	☺	X	☺	☺	H	
	B23	15.2	63.5	14.5	5.8	28	49	21	3.6	☺	☺	X	☺	☺	H	21°
	AVG	6.0	52.5	25.2	12.1	25	40	15	1.2							
GR	B18	9.2	50.6	23.4	16.8	23	38	14	0.8	☺	☺	X	☺	X	H	
	B19	0.3	41.2	31.1	27.4	24	39	15	0.6	☺	☺	X	☺	X	H	
	B22	11.9	59.2	20.7	8.2	20	29	9	1.1	☺	☺	X	☺	X	H	
	WH4	10.8	64.8	18.4	6.1	24	40	16	2.6	☺	☺	☺	☺	☺	H	
	WH6	15.5	63.9	11.8	7.8	25	49	24	3.1	☺	☺	☺	☺	??	VH	
	AVG	9.7	55.9	21.1	13.3	23	39	16	1.6							

*Samples: SR=Schistose regolith, GR=Greywacke regolith
*Atterberg Limits: PL=Plastic Limit (%), LL=Liquid Limit (%), PI=Plasticity Index, ACT=Activity
*Mineralogy: ☺=mineral present, X=mineral absent, ??=difficulty in identification, H=high concentration, VH=very high concentration

Table 5.14. A summary of the textural characteristics and mineralogy for colluvial samples.

SUMMARY OF LABORATORY DATA FOR COLLUVIAL SAMPLES															
*SAMPLES		Textural chatacteristics								*Mineralogy					
		Grain Size (%)				*Atterberg Limits				X-Ray Diffraction					SEM
Lith.	No.	Gravel	Sand	Silt	Clay	PL	LL	PI	ACT	Q	K	C	I	IC	Na
SC	B4	10.5	52.0	27.8	9.8	26	40	14	1.4	☺	☺	☺	☺	☺	M
	B10	29.2	54.9	12.5	3.4	21	30	14	4.1	☺	☺	☺	☺	☺	VH
	B11	21.6	33.6	33.3	11.5	25	34	9	0.8	☺	☺	☺	☺	☺	VH
	B14	13.5	27.7	41.7	17.1	18	31	13	0.8	☺	☺	X	☺	☺	M
	B17	10.0	29.6	45.8	14.6	17	32	16	1.1	☺	☺	X	☺	☺	H
	WH5	12.2	54.4	26.9	6.5	19	35	17	2.6	☺	☺	X	☺	☺	H
	AVG	16.2	42.0	31.3	10.5	21	35	14	1.8						
GC	B5	26.7	47.4	19.2	6.8	23	35	12	1.8	☺	☺	☺	☺	X	H
	B6	40.3	31.1	21.1	7.6	24	36	12	1.6	☺	☺	☺	☺	??	H
	B7	13.3	46.0	30.1	10.7	21	36	15	1.4	☺	☺	☺	☺	X	M
	B20	10.0	40.7	29.1	20.3	23	36	13	0.6	☺	☺	X	☺	☺	VH
	B21	9.9	37.6	30.1	20.4	17	34	16	0.8	☺	☺	X	☺	☺	H
	WH3	13.4	61.5	18.7	6.4	31	39	8	1.3	☺	☺	X	☺	☺	H
	AVG	18.7	44.2	24.7	12.0	23	36	13	1.3						

*Samples: SC=Schistose colluvium, GC=Greywacke colluvium, AVG=Average values

*Atterberg Limite: PL=Plastic Limit (%), LL=Liquid Limit (%), PI=Plasticity Index, ACT=Activity

*Mineralogy: ☺=Mineral present, X=mineral absent, ??=difficulty in identification, M=moderate concentration, H=high concentration, VH=very high concentration.

Table 5.15. A summary of the textural characteristics, mineralogy and the angle of internal friction for regolith samples.

SUMMARY OF LABORATORY DATA FOR RED REGOLITH SAMPLES																	
*SAMPLES		Textural chatacteristics								*Mineralogy							Strength
		Grain Size (%)				*Atterberg Limits				X-Ray Diffraction						SEM	
Lith.	No.	Gravel	Sand	Silt	Clay	PL	LL	PI	ACT	Q	K	C	I	IC	IM	Na	ϕr
GR	B1	-	12.8	70.6	16.6	25	52	27	1.6	☺	☺	X	☺	X	☺	H	23°
	B2	-	13.4	70.8	15.9	25	52	27	1.7	☺	☺	X	☺	X	☺	H	24°
	B8	-	9.4	74.7	16.0	23	48	25	1.6	☺	☺	X	☺	X	☺	M	
	B9	-	15.5	69.3	15.3	24	51	27	1.8	☺	☺	X	☺	X	☺	M	
	AVG	-	12.8	71.3	15.9	24	51	27	1.7								

*Samples: GR=Greywacke Regolith

*Atterberg Limits: PL=Plastic Limit (%), LL=Liquid Limit (%), PI=Plasticity Index, ACT=Activity

*Mineralogy: ☺=mineral present, X=mineral absent, M=moderate concentration, H=high concentration

(Figure 5.29.), which is consistent with the information obtained using XRD (Section 5.3.8.). The influence of clay-sized quartz particles in the red weathered samples imparts a higher shear strength due to the granularity of the mineral compared to the sheet silicate nature of the clay minerals and the influence of clay aggregates may also impart some increased shear strength on the soil by acting as a granular material (Section 5.3.9.).

5.6. SYNTHESIS

The objectives of this chapter were to provide additional information on the geotechnical parametres of the surficial units identified in the field area (Chapter 3), and to the assess that information with respect to the landscape modification processes introduced in Chapter 3. The information regarding the geomorphic features and the distribution of surficial and bedrock units identified was presented on an engineering geological map of the field area at a scale of 1:5000 (Figure 5.3. map pocket).

Analysis of the field area was divided into two areas of investigation; field observations and testing, and limited laboratory testing. The field investigation programme consisted of engineering geological mapping, insitu percolation testing and hydrogeological investigations of the Graham River. Laboratory testing was divided into two sub-categories, the first concerned with assessing the geotechnical properties of the soil material in the study area and the second involved the characterisation of weathering grades in greywacke and schistose rock material.

The production of an engineering geological map involved the use of information gained during field work, aerial photographic interpretation and the study of previous work in the area. Field work involved a hydrogeological study of the Graham River to determine the relationship between rainfall (measured in the adjacent Boons Valley catchment) and stream flow at the Port Underwood Bridge. The findings indicate that the river responds very quickly, less than 12 hours, to high rainfall in the catchment. The flow is greatest during winter months, but it is known that the Graham River is be prone to 'flash floods' at any time of the year.

Insitu percolation data was collected from records kept by the Marlborough District Council and used to assess the soils in the field area for the suitability of effluent disposal using septic tank systems. The soils in the Marlborough Sounds are very variable with regard to percolation and it appears that site specific investigations are required to assess the soils at any one site. Both thin soils over fractured bedrock and soils high in clay material are generally unfavourable for septic tank systems.

Laboratory investigations uncovered problems with the classification and testing of the soils within the field area. Grainsize analysis found that the soils are silty clays or clayey silts but assessment is approximate due to the presence of clay aggregates of sand and silt size in all soils tested. The aggregates contributed to shear

strength results because the clay particles contained significant proportions of non-clay minerals such as quartz which caused the soils to act as granular materials rather than clay rich soils and thereby imparting a higher shear strength to the samples. Analysis of the clay mineralogy identified the presence of a complex interstratified illite-chlorite clay, which was considered to be dominantly indicative of schistose soils and the nature of which requires additional investigation.

Testing of weathered rock material using point load and cone indenter tests show that there is a decrease in rock strength with an increase in weathering grade. Furthermore, the schistose material is weaker than greywacke of the same weathering grade. The anisotropic nature of schist accounts for the material being considerably weaker when load is applied parallel rather than perpendicular to foliation. The Point Load test and the Cone Indenter tests provided calculated Unconfined Compressive Strength values which showed that strength values were overestimated for the higher weathering grades in CIN and for schist using the point load test. Weathering causes a decrease in the UCS values of the material which is more pronounced in schistose material particularly when schist is loaded parallel to the foliation direction.

CHAPTER SIX HAZARD ZONATION AND LAND USE PLANNING

6.1. INTRODUCTION

6.1.1. General

The importance of hazard assessment and engineering geology for land use planning in New Zealand was highlighted by the Abbotsford Landslip Disaster in 1979 where more than fifty houses were destroyed in a single landslide event. The Commission of Inquiry found that there needed to be a closer collaboration between engineers and geologists prior to and during the investigation of any major civil engineering construction including residential development. The disaster heightened awareness in New Zealand that accurate assessment of active geological processes, foundation conditions and the geomorphic evolution of an area are important for safe construction and urban subdivision practice. This chapter incorporates all of the information presented in the previous chapters concerning geology, geomorphology and geotechnical characteristics of the field area into a hazard zonation map and subsequently a development constraints map. These maps provide data on the degree of hazard associated with particular geological processes and the geotechnical constraints for urban development imposed by the processes and hazards. The methodology and practice of determining the degree of hazard or extent of geotechnical limitations for locations within the field area are detailed and provide the basis for similar studies in the Marlborough Sounds and other areas throughout New Zealand.

6.1.2. Legislation

In New Zealand there are currently two works of legislation, the Resource Management Act 1991 and the Building Act 1991, which identify the importance of natural hazard assessment in the field of urban planning and development. The Resource Management Act (RMA) effectively replaced the Town and Country Planning Act 1977 when it was introduced in 1991, and is primarily concerned with the management of environmental resources, both natural and physical (Bell et al. 1992). Furthermore, the RMA makes Councils responsible for the effects which management policies may have on the environment. With respect to natural processes, development options may be restricted by active processes because of the associated potential hazards. Individual Councils are therefore required to identify and collate information relating to areas which are prone to hazardous processes such as slope instability and flooding. In the Marlborough Sounds this requirement has been developed into a Natural Hazards Register which identifies those areas

throughout Marlborough which are affected or potentially affected by natural hazards, and where further development should be carefully investigated or avoided.

The RMA is primarily concerned with the issuing of Resource Consents which include land use consents, subdivision consents, coastal permits, water permits and discharge permits. Urban development requires the approval of subdivision applications and under the RMA this is only possible if use of the land in question is not likely to initiate, accelerate or worsen specified active geological processes which are falling debris, subsidence, erosion, slippage or inundation, on, or adjacent to the site (Appendix E2). The RMA does not, however, stipulate the use of geotechnical or engineering geological investigations to assess land for subdivision consents, as any such information is provided at the discretion of each council or regional authority.

The Building Act, also introduced in 1991, is seen to complement the RMA at the scale of building construction and thus the requirements of the Building Act concerning natural hazards are similar to those outlined in the RMA. The active geological processes identified in the Building Act are erosion, avulsion, falling debris, subsidence, slippage alluvion or inundation, and The Building Act also requires the identification of hazardous processes under Section 31 (Appendix E3) and gathering of information regarding hazardous processes into the Project Information Memorandum. Section 36 in the Building Act outlines the requirements for the issuing of building consents which parallel the subdivision consent in the RMA and stipulates that land which is subject to hazards such as erosion, falling debris, subsidence etc. (Appendix E3) is not suitable for building work unless the Council is satisfied that development of the land will not initiate, accelerate or accentuate the identified process.

6.1.3. Terminology

This study concentrates on the identification of the active geological processes within the field area and integrates the magnitude, recurrence interval and affected area of the active processes into a hazard assessment. The concept of hazard is outlined in the current literature by several authors, for example Coates (1981) who defines a hazard as "a phenomenon associated with geologic processes that can produce a disaster when a critical threshold is exceeded and can result in significant loss in life or property". A natural geological event or process only becomes a hazard when it threatens something of value, for example monetary, ecological or historical value, including human life, or it puts something or someone at risk. This concept is amplified by Tanaka (1981) who stated that 'an earthquake in the wilderness is a seismic event. When humans clear the land and build by the fault and over a swamp, they have created a seismic hazard. When the earthquake happens and buildings are destroyed and people killed, a seismic disaster has taken place'. One of the most

relevant definitions of hazard for this study is that given by the Resource Management Act 1991 as follows: 'Any atmospheric or earth or water related occurrence[1] the action of which adversely affects or may adversely affect human life, property or other aspects of the environment'. Incorporating the definitions and discussion presented in Appendix E1, the following definition of hazard is proposed for this study.

NATURAL HAZARD

One or more natural or human induced landscape modification processes* of varying duration, which have potential to cause loss of life, injury, or property/infrastructure damage within or adjacent to, a given human community. Natural hazards have a specified magnitude, return period and affected area.

**Earthquakes, tsunami, erosion, volcanism and geothermal activity, landslip, subsidence, sedimentation, wind, drought, fire, flooding, rock fall, and avalanche.*

Related to the concept of hazard is the concept of risk but because this study is only concerned with a hazard analysis, a definition of risk is not necessary. However the most relevant definitions given in the literature, and a discussion on the distinction between hazard and risk, are presented in Appendix E1.

6.2. HAZARD MAPPING

6.2.1. Terrain Analysis

Following the identification of the geological processes which are active in the field area, an assessment of their actual and potential effect on urban development is required. There are two principal analysis systems which provide the basis for the assessment used in this study, the PUCE system from Australia and the GASP system developed in Hong Kong. The method of analysis and the types of information used for both studies are outlined below and then integrated into the hazard and development constraint assessment methodology which is used in this study.

a) The PUCE System

The PUCE system of terrain analysis was developed in Australia to classify areas with similar physical attributes. Generally, an area is evaluated using features

[1] *Earthquakes, tsunami, erosion, volcanism and geothermal activity, landslip, subsidence, sedimentation, wind, drought, fire or flooding'

such as vegetation, bedrock nature, surface morphology and land use and utilises aerial photography and field investigations to determine the physical attributes (Grant and Finlayson, 1978). The study area is subdivided from an original province evaluation (Table 6.1) depending on the type of information and detail of investigation required, and the scale of mapping varies for each type of terrain evaluation as presented in Table 6.1. The Province maps are generally produced from geological maps at a scale of 1:250,000 (Grant and Finlayson, 1978) and from these terrain unit and terrain component maps may then be created at scales of 1:50,000 and 1:5000 respectively.

The PUCE system of terrain evaluation uses a numerical classification to describe the individual components mapped, the numerical nomenclature being adopted primarily for use in computer data systems. Figure 6.1. is an example of a terrain analysis using the numerical classification system. The most useful scale of mapping for hazard assessment is the Terrain Component mapping at 1:5,000 which includes information about the nature of surficial material, slope profiles including failed slopes, and land use of the area.

b) Geotechnical Area Studies Program

In Hong Kong a system of geological hazard identification and geotechnical limitations to urbanisation has been developed along similar, although more detailed, lines to the PUCE system. The Geotechnical Area Studies Program (GASP) terrain analysis is also based on the information obtained from sources such as aerial photography and field investigation to produce a terrain classification map (Brand, 1988). The land in Hong Kong is comprised of steep and deeply weathered granite and volcanic slopes which are prone to landsliding hazards that are similar to those in the Marlborough Sounds. Regional maps are produced at scales of 1:20,000, while the district scale of 1:2,500 allows maps with greater detail. The type of information presented on the district maps includes slope gradient, terrain component, terrain morphology, the nature of erosion and instability, hydrology, vegetation and slope condition (Brand, 1988).

From maps such as the vegetation, erosion and engineering geology maps, terrain classification maps are prepared. These maps can be used for land use planning or further classification of the individual terrain factors. Figure 6.2. shows the relationships and origins of maps under the GASP system and the scales which may be used for each map type, and Figure 6.3. shows the types of maps produced using the GASP technique.

The Geotechnical Land Use Map (GLUM) is used to assess the suitability of land for further urban development. The land, or terrain, is divided into four classes each representing various degrees of geotechnical limitations for urbanisation. Land which is classified as having extreme geotechnical limitations is zoned under the

TABLE 6.1. Using the PUCE system, an example of the type of subdivisions performed and the numerical system used to classify the terrain (After Grant and Finlayson, 1978).

Province	**Terrain Pattern**	**Terrain Unit**	**Terrain Component**
52.009	**22/2**	**1.7.11**	**431 023 01**

MEANS:-

Province	52	Quaternary
	.009	Ninth recognised province of Quaternary age
Terrane Patterrn	2	Relief amplitude to 75m
	2	Drainage density 2 stream-lintes per 1.6km
	/2	Second recognised terrain pattern with the above parameters in the particular porvince
Terrain Unit	1.7	Undulating sloping surface
	.1	Clay soils
	1	Grasslands
Terrain Component	4	Slopes major axis concave, minor axis planar
	3	Major axis to 5°
	1	Minor axis to 1°
	03	Soil profile (Serial within province)
	2	Land use - pasture
	01	Vegetation (Serial within province)

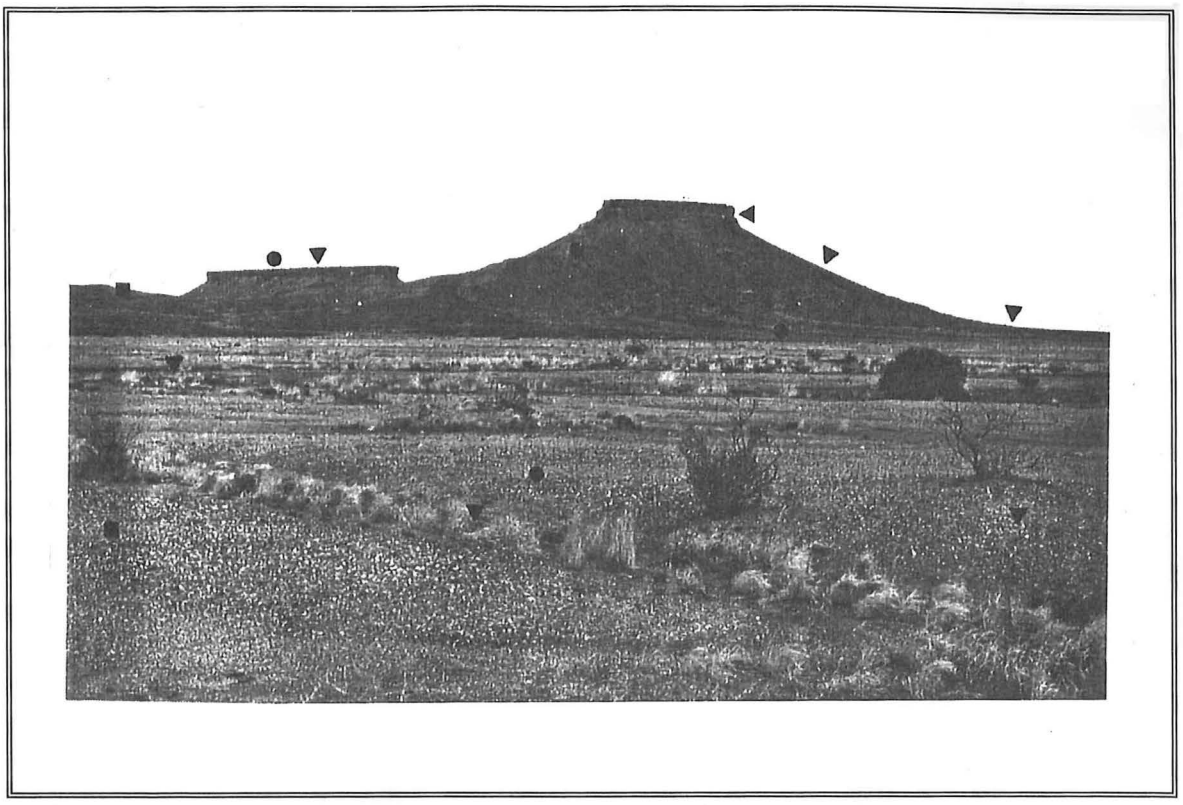

FIGURE 6.1.: An example of the terrain analysis using the PUCE system (After Grant and Finlayson, 1978)

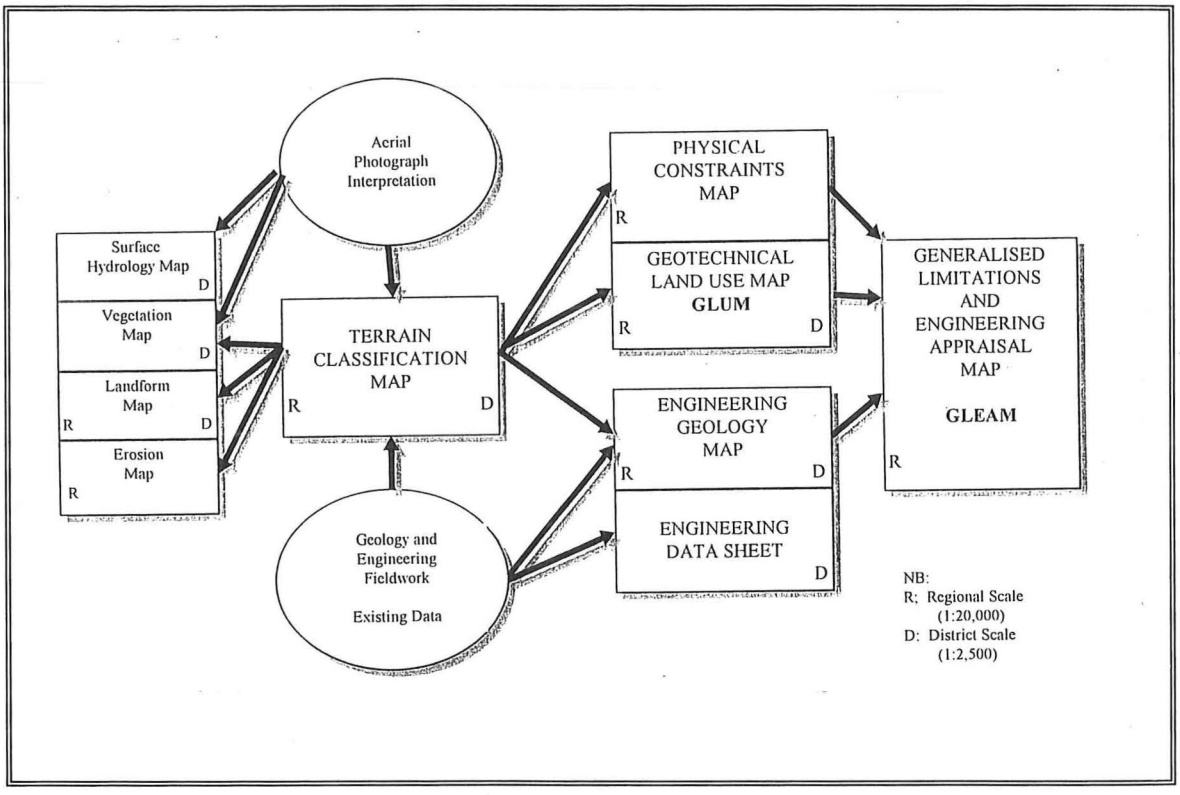

FIGURE 6.2.: A flow chart showing the inter-relationships between the various components of the GASP classification system (Redrawn from Brand, 1988).

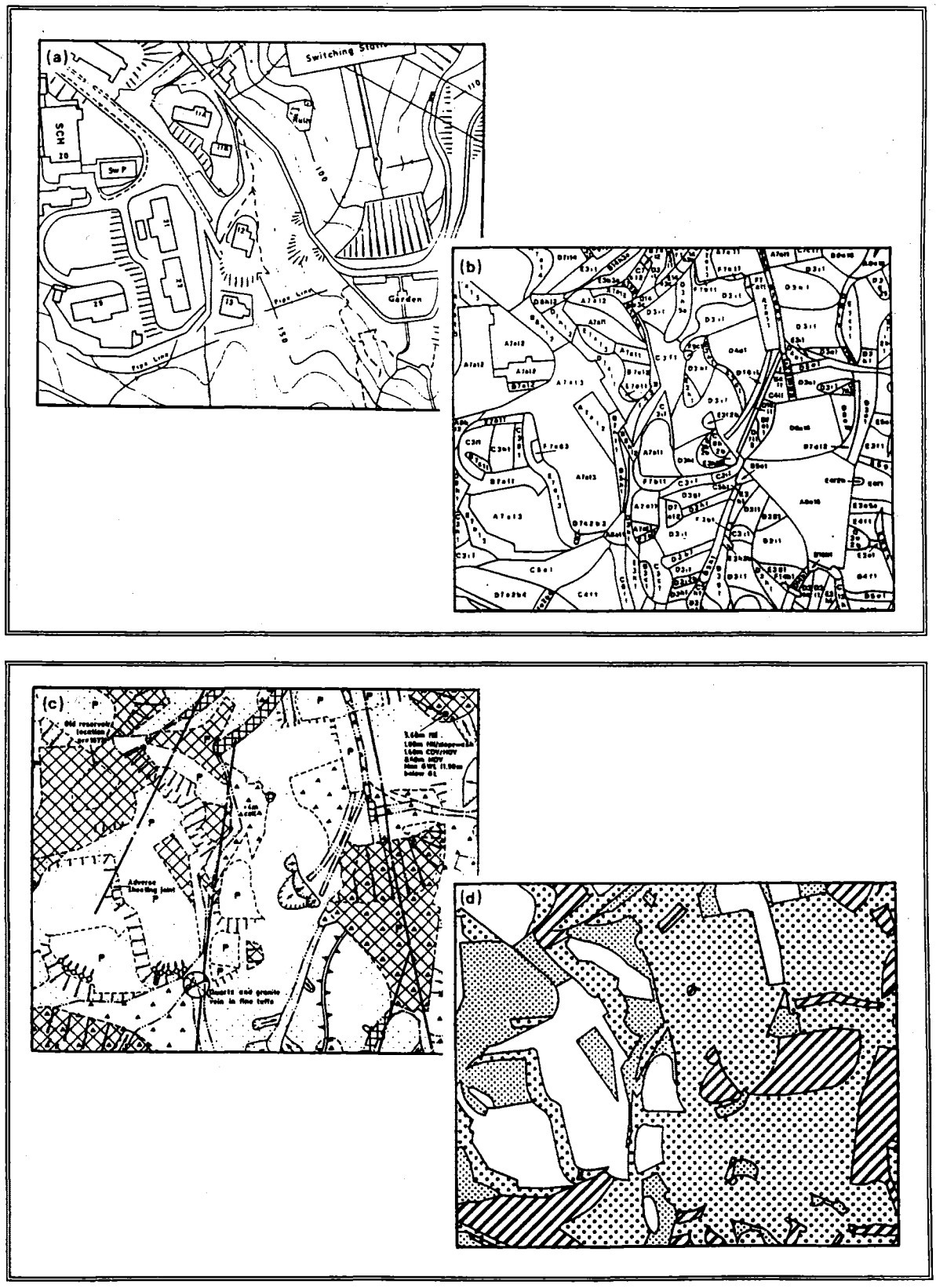

FIGURE 6.3.: Examples of the types of maps produced using the GASP system. Maps include a base map, a terrain classification map, an engineering geology map and a geotechnical land use map (GLUM) (After Brand, 1988).

GLUM class IV. Lesser degrees of limitation are represented by GLUM classes III, II and I, indicating high, moderate and low restrictions for urban development. Those areas of land zoned GLUM class I therefore are most suitable for further urbanisation. GLUM maps may be prepared at both regional and district scales, 1:20,000 and 1:2,500 respectively. In addition to the GLUM classification, a physical constraints map may also be compiled from the original terrain classification mapping. The physical constraints map differs from the GLUM because instead of defining the degree of suitability for urban development, it represents the nature or type of constraint to urbanisation. Generally the physical constraint map is prepared at the regional scale of 1:20,000 and is used to complement the GLUM and the types of constraints identified on the physical constraint map include areas of erosion, slope instability, flood plains and deposits of colluvium.

Finally, at a regional scale of 1:20,000 all of the information from the GLUM and the physical constraints maps is combined onto a General Limitations and Engineering Appraisal Map (GLEAM). The GLEAM is an interpretative map designed for use by planners, civil engineers and geotechnical engineers and is principally used to indicate land which is considered suitability for urban development (Brand, 1988). Figure 6.2. shows the relationship of the GLEAM to the other maps produced in the GASP system and Figure 6.4. is an example of a GLEAM from the Hong Kong area (Brand, 1988).

6.2.2. Engineering Geological Approach

The engineering geological component of a terrain analysis is crucial to the development of a hazard and land use planning assessment for an area as the engineering geological investigations provide information on the types and nature of both surficial and bedrock materials, and the activity of various geological processes in the field area. The engineering geological approach used in this study is based on that introduced by Bell and Pettinga (1983) and expanded upon in (1985) which recognises the importance of a field analysis of geological processes and laboratory analysis of materials for a hazard assessment related to potential urban development. As identified by Bell (1990), and Bell and Pettinga (1985) the input of an engineering geologist is vital at all stages of development from the pre-feasibility/feasibility stage to the operation and/or maintenance stage (Figure 5.2.). Bell and Pettinga (1985) proposed an idealised geotechnical investigation program to apply to residential subdivision of land as follows:

1) Identification of geological hazards to the proposed development (such as flooding, landslip, and seismicity) at the initial planning (or feasibility) stage;

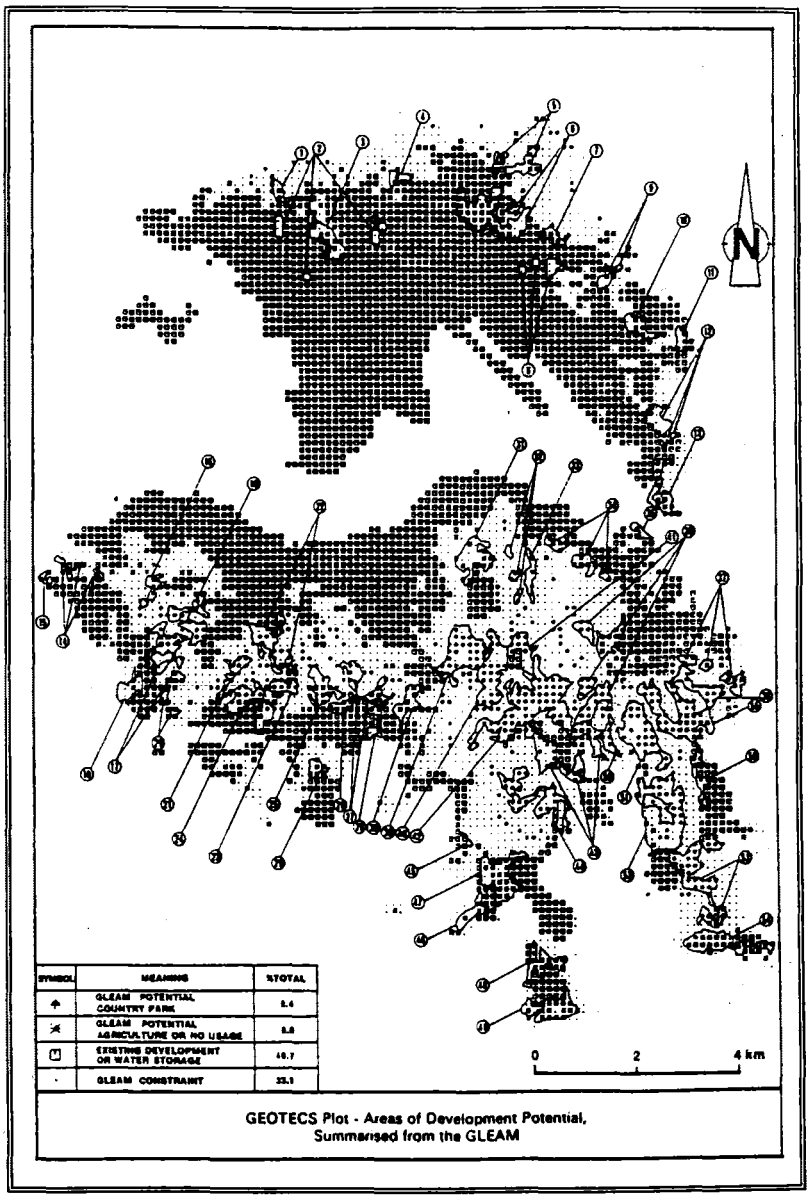

FIGURE 6.4.: An example of a Generalised Limitations and Engineering Appraisal map (GLEAM) from the GASP classification system (After Brand, 1988).

2) Design stage investigations to assess any geological, geomorphological, or geotechnical constraints to development, and to determine a final subdivision layout;
3) Adequate geotechnical control (for example, of earthworks) during site construction; and
4) Provision for long-term monitoring of the completed project, with maintenance as required.

The investigation program outlined above may be used to evaluate any planned subdivision proposals or may be used to assist in the planning of new residential subdivisions in addition to investigations of individual building sites. Additionally the engineering geologist is required to present the scientific data obtained during an investigation in a manner which is easily understood by non-geologists or engineers. Ultimately the information presented in an engineering geological study will be used by land use planners and council staff who may have no background in earth science, and therefore the information must be clear, concise and well presented and preferably in map form with a written explanation.

6.2.3. The Present Study

a) Introduction

The approach to hazard zonation and land use planning which has been used in this study integrates the terrain analysis used in the GASP system with the engineering geological approach presented in Section 6.2.2. above. The GASP system was considered most relevant to the present study because of the detail and scale of mapping, and the types of information used to produce an assessment of development constraints and geological hazards in the field area. Unlike the PUCE analysis the GASP system recognises the need for a detailed analysis (1:2,500) for the terrain classification maps, the GLUM, and the engineering geology maps (Figure 6.2.). The PUCE maps only require a detailed investigation (1:5,000) for individual terrain component maps, for example a soil erosion map, and these maps do not integrate all of the information essential for an adequate hazard and land use planning assessment. This study modifies the scaling system used in the GASP system for a hazard analysis and uses a standard 1:5,000 scale for each of the engineering geology, hazard assessment and development constraints maps. The uniformity of scaling over the entire investigation is important for consistency in the detail of information presented and is considered an adequate scale for planning decisions and from which individual site investigations may proceed.

b) Engineering geology maps

The engineering geology map used in this study is the equivalent of the terrain classification map in the GASP and not the GASP engineering geology map. The difference arises from the fact that in the GASP analysis the terrain classification map is the cornerstone for all other types of assessment because it includes information such as the distribution of surficial units, slope angle, drainage patterns and active geological processes in the field area etc, from which further assessment in the form of hazard maps, development constraint maps and individual component maps may be derived. Thus the GASP terrain classification map is equivalent to the engineering geology map in this study which includes infomation concerning the nature and distribution of the surficial and bedrock units in the field area, the topography, extent and activity of geological processes such as slope failure, structural features such as fault lines, and some cultural detail such as roading and bridges. Figure 6.5. illustrates the differences in the two approaches, GASP and this study, in the form of flow charts. The GASP maps are all derived from the basic terrain analysis which integrates all of the field work, existing data and aerial photographic information obtained about the area, including the engineering geology map. In this study the engineering geology map displays all of the information gained from field work, existing data and API, and also incorporates the information from limited laboratory investigations. The engineering geology map in this study uses the above information to delineate those areas of specific geological units, for example alluvium, which in turn provides information about the types of processes that are currently active, or which may be active given a change in conditions such as additional urbanisation .

As an example, landslide deposits are important to identify because they delineate areas which have experienced previous instability and may have the potential to do so in the future (Section 6.3.). Similarly, alluvium indicates areas of previous inundation and sedimentation which may be important from a hazard and planning perspective. Geomorphic information is also presented on the engineering geology map because an understanding of the age of particular surfaces, such as landslide deposits and alluvial terraces and fans, will provide an indication of the recurrence interval of the contributing geological processes at a particular site. Debris fans, for example, are often good indicators of the activity of gullies directly upslope. Those fans which display deep incision of streams and significant weathering profiles, for instance red weathered surfaces, are less likely to be reactivated than fans which display sparse vegetation and shallow stream beds. Therefore, the engineering geology map shows the extent of surficial geological units and the estimated age of surfaces relative to adjacent surfaces. Additionally geomorphic features resulting from erosion and slope failure such as headscarps and terraces, are illustrated on the engineering geology map.

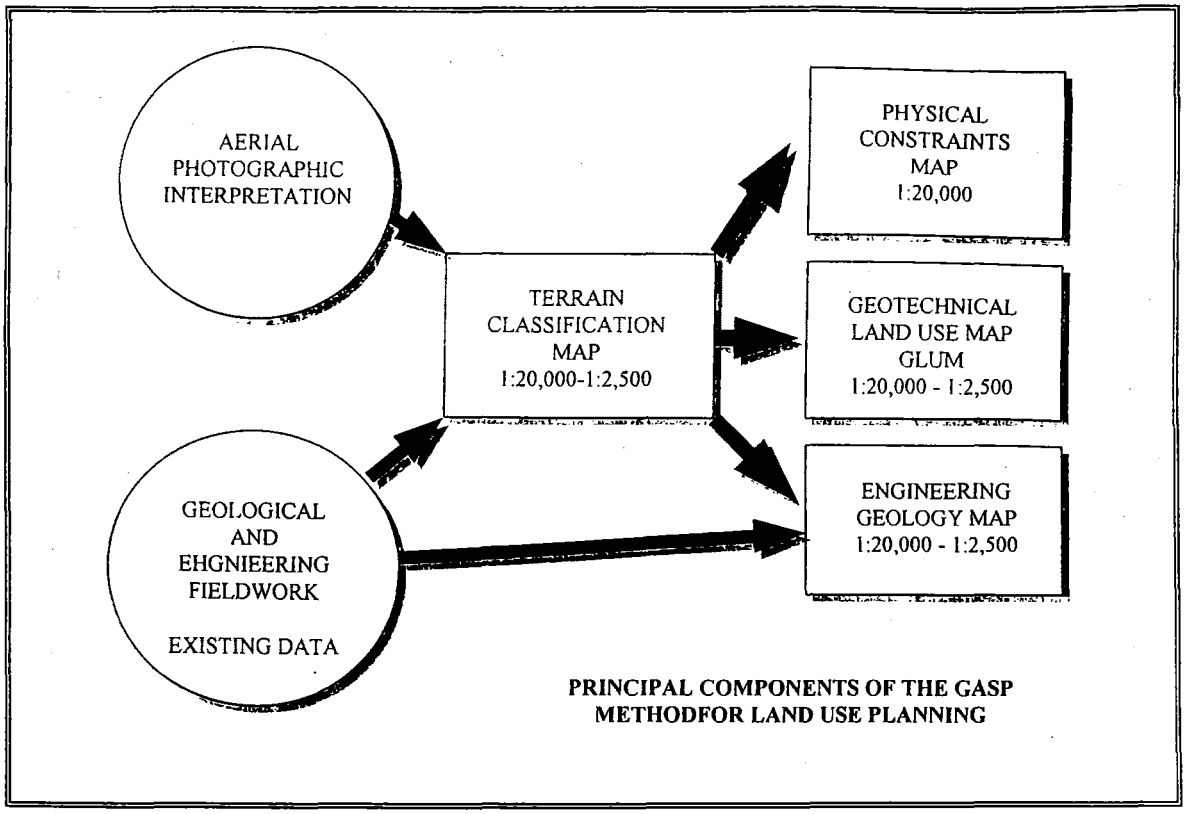

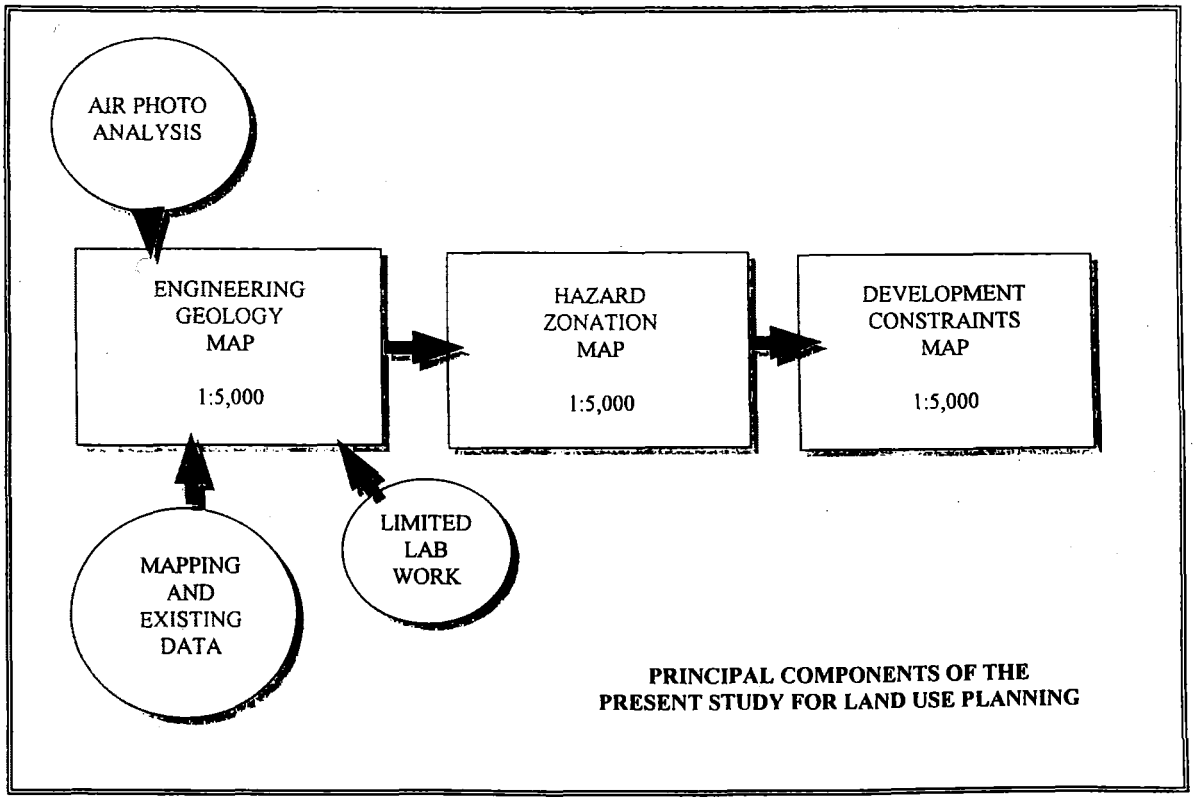

FIGURE 6.5.: Flow diagrams which show the comparative methodology between the GASP classification system and that used in this study. Note in particular the relationship of the engineering geology map to the other maps in both flow diagrams.

c) Hazard Maps

The hazard map produced by this study is similar in content to the physical constraints map of the GASP system. In the GASP system, the physical constraints map uses the information presented in the terrain classification map and delineates the type of constraint to urban development but is not derived from the engineering geology maps as is the case in this study (Figure 6.5.). The hazard map presented in this study is a quantification of the hazard posed by a particular geological process and consequently hazard mapping follows directly from the engineering geology map (Figure 6.5.). There is also a principal difference in the scale used for the two maps as the hazard maps in this study are produced at a scale of 1:5,000, equivalent in scale to the engineering geology map, while the physical constraint maps used in Hong Kong are restricted to regional scales of 1:20,000.

The hazard map in this study is comprised of two sets of information pertaining to the type and degree of hazard identified. Firstly, the degree of hazard is determined in relation to each active process and the highest degree of hazard is represented on the map using a stop light colouring system (Figure 6.6.). The colouring system is used in this study in order to provide clarity and ease of interpretation for those using the maps, as the colouring system reflects the severity of the hazard with red used for high degree of hazard while blue represents negligible hazard. Additionally, yellow is used to represent the areas of moderate hazard and green for low hazard areas. The stoplight colouring system was selected in favour of the use of symbols for hazard zones which, although essential for reproduction in black and white, the maps are generally more difficult to read than colour maps and tend to become complicated. Solid and dashed lines on the hazard map indicate the nature of the the boundary between different hazard zones. Solid lines indicate that the boundary between hazard zones is well defined, for example areas of stream bank erosion in steep and narrow valleys where the the extent of the erosion is limited by the topography etc. Dashed lines are used when the boundary between the hazard zones is gradational and cannot be accurately delineated, for example in the headscarp region of slope failures where the extent of headscarp regression is uncertain and similarly at the base of gully systems the runout zone depends on the slope gradient, the velocity of the failure and the amount of material being transported.

The hazard zones represented by colour on the map are further qualified by a lettering system which represents the type of process which has given rise to the hazard zonation, with uppercase letters indicating the principal geological process involved in the hazard zonation. Additionally, other subordinate hazardous processes operating in the area at the same time are also shown on the hazard map using lower case letters which represent the type of geological process or processes involved.

Table 6.2. defines the letters which have been chosen in this study to represent the individual processes and Figure 6.6. is an example of a hazard zonation map from McManus (1994) to illustrate the way in which the colouring and lettering system is used in this study. Figure 6.7. represents an area on the hazard map which has a high degree of hazard represented by the colour of the zone, red. The geological process which contributes to the high hazard zonation is slope failure which is represented by the upper case 'L', and the secondary process affecting the area is represented by lower case 'e' for stream bank erosion. An upper case 'E' indicates that the principal process has changed to stream bank erosion and at the base of the gully debris deposition 'D' dominates over a subordinate stream bank erosional process 'e'. The hierachy of the lettering system eliminates the problems identified by Horrey (1989) in representing areas which are subjected to two or more processes. The system used in this study is removed from the complicated lettering systems used in other studies (eg. PUCE) and combines the clarity of colour with the information provided by lettering. Provided the number of active processes are kept at a minimum and remain simplified in their classification the system used will adequately represent the degree and type of hazard within the field area.

The hazard mapping in this study is different from that presented in the Picton/Waikawa area by Horrey (1989) because Horrey did not define his hazard zones on the basis of further urban development and the effects which such development may have on the landscape. Rather Horrey based his zonation on the present state of the field area and those processes affecting the field area at that time. This study recognises the potential problems associated with future urban development, however, because as hazard is defined in this thesis (Section 6.1.3.) a geological processes cannot become a geological hazard unless there is some human component associated with it. In other words, if a landslide were to occur in an area where no human activity was taking place, then the event would not be considered a hazard as it does not threaten any thing of value to humans. However should the same landslide occur within an urbanised area and damage the structures, damage industry or agriculture, or threaten lives, the landslide has become hazardous. Because much of the field area is currently not urbanised, many of the processes identified in this study would not be hazardous if a prediction of future development was not made.

The basis for the hazard zonation used in this study is the magnitude, periodicity and affected area of the active process and the zonations are detailed in Section 6.3.

d) Development Constraint Mapping

The final step in this study is an assessment of the development constraints which are imposed by the geological hazards in the field area. Development

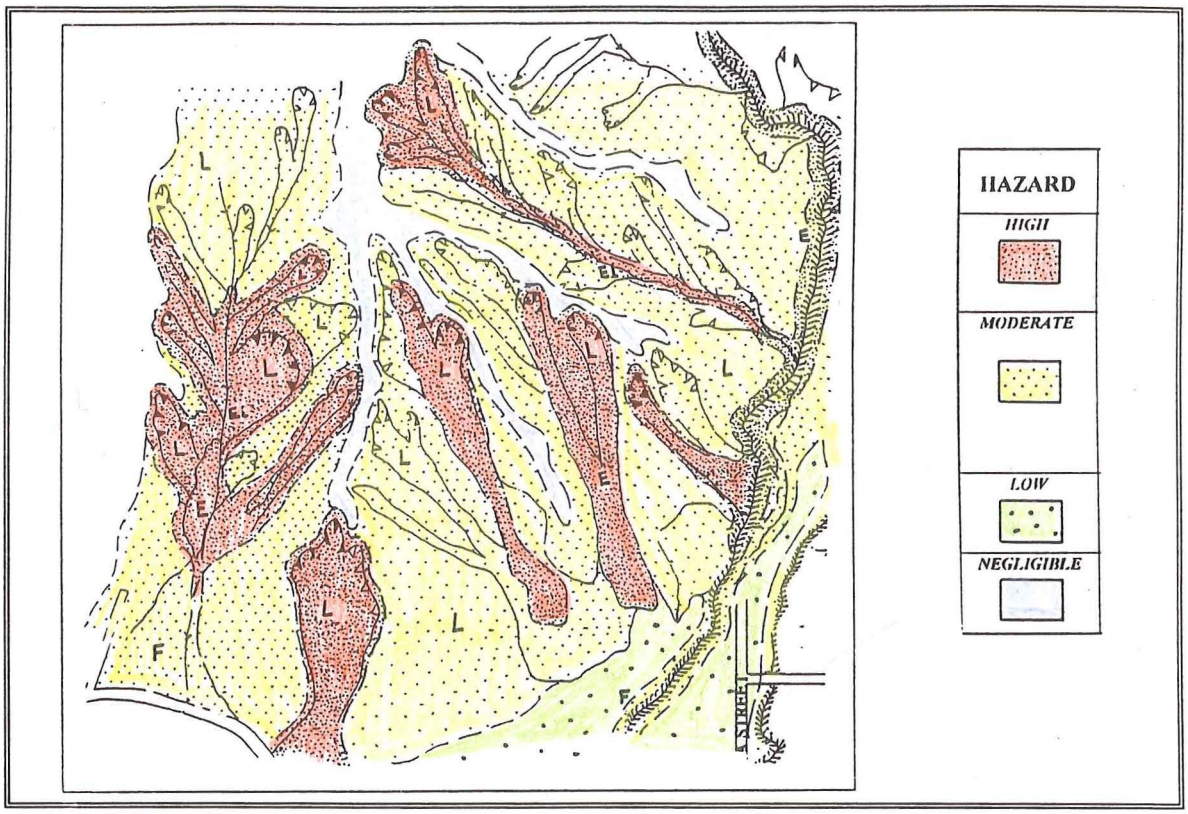

FIGURE 6.6.: An example of a hazard zonation map of part of Waikawa township using the classification system developed in this study (See TABLE 6.2.).

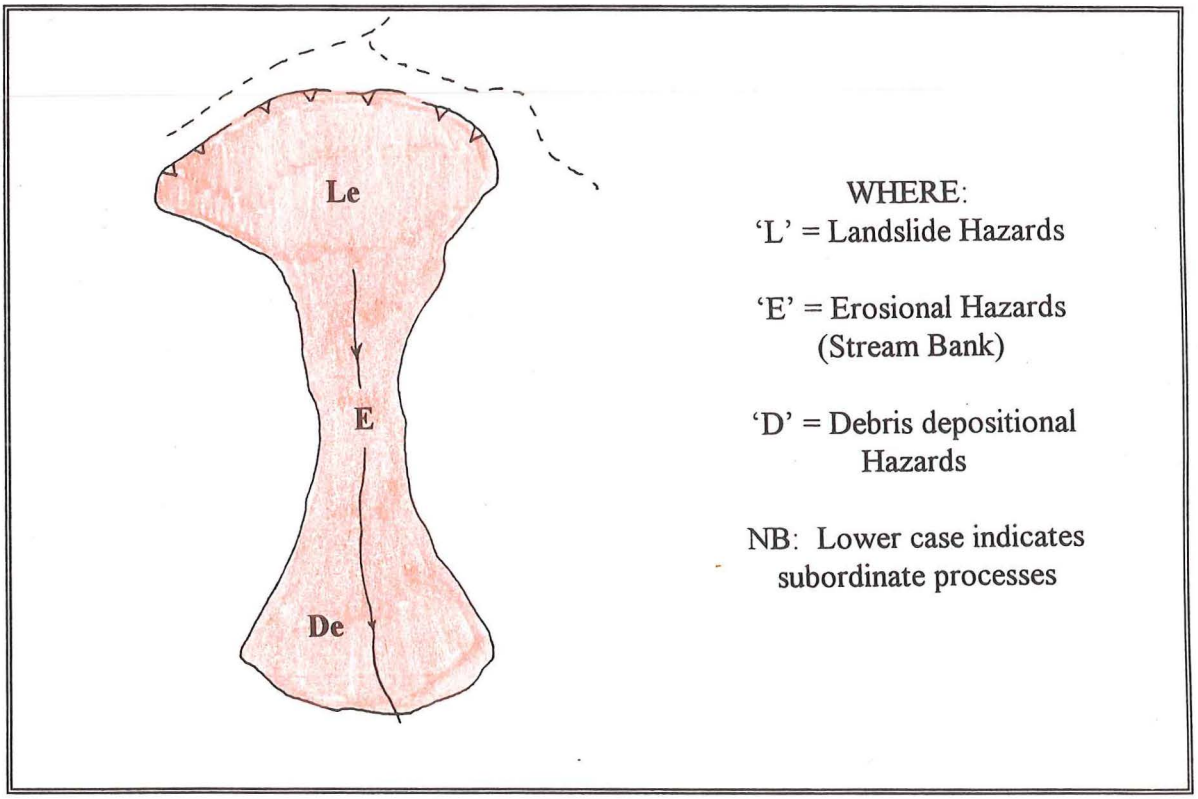

FIGURE 6.7.: A detailed example the information presented on the hazard zonation map in FIGURE 5.3 (Map Volume). The example is a slope failure showing the colouring and lettering system used in this study.

TABLE 6.2.: The hazard zonation used in this study for the production of hazard maps. The hazard map in FIGURE 6.9. (Map Volume) and the example map in FIGURE 6.6. use this classification system.

PROCESS → / HAZARD ↓	SLOPE MOVEMENT L	FLOODING F	STREAM BANK EROSION E	DEBRIS DEPOSITION D
HIGH	* Any slope failures within the last 36 years. * Any failure in excess of $100m^3$ which has occurred in the last 100 years.	* Any areas of flooding and siltation which have occurred within the last 36 years (NB: where no stream protection measures emplaced).	* Any areas of stream bank erosion within gully systems or in major river beds which has occurred within the last 36 years.	* Debris sedimentation which has occurred within the last 36 years.
MODERATE	* Any failure between 10-$100m^3$ which has occurred prior to 36 years ago. * Failures $>100m^3$ which has been active greater than 100 years ago. * Unmodified slopes in excess of 35° with >1m colluvium	* Any areas which are subject to flooding and sedimentation within a 10-100 year time frame.	* Any areas of stream bank erosion within gully systems or in major river beds which has occurred within the last 100 years.	* Debris sedimentation which has occurred within the last 100 years.
LOW	* Unmodified slopes which have greater than 1m of colluvium and are between 15°-35° slope.	* Any areas which will experience flooding and sedimentation only in the event of flood protection measures failing.	* Not enough information to justify a hazard zonation.	* Debris sedimentation which has occurred prior to 100 years ago.
NEGLIGIBLE	* No identifiable hazard associated with this process.	* No identifiable hazard associated with this process.	* No identifiable hazard associated with this process.	* No identifiable hazard associated with this process.

constraint mapping follows logically from the hazard mapping which identified the types of constraint to urban development, while development constraint mapping examines the suitability of an area for urban development and utilises the information presented in both the engineering geology and, more specifically, the hazard maps. The development constraint approach is a correlative of the GLUM method which considers the geotechnical limitations to development in an area. The approach used in this study differs from the GLUM system in that it is derived from the hazard mapping and not directly from the terrain classification maps, as in the GASP system (Figure 6.5.). The methodology used for development constraint mapping in this study is similar to that used by Horrey (1989) and assumes that urbanisation of the field area is a possible future development. Therefore the development constraints zonation in this study is a continuation of the hazard analysis which also assumed the possibility of future urban development of the field area.

The scale of the development constraint mapping (1:5,000) in this study is consistent with that used for both the engineering geology mapping and the hazard map, which provides continuity throughout the entire assessment procedure. The GLUM analysis also recognises the suitability of the method to both regional and district mapping, although it is felt that the information presented is sufficently detailed that regional development constraint mapping is unnecessary. However the scale of development constraint mapping in this study is not sufficient for individual building sites or even small subdivision planning, and it is therefore not intended to replace site specific engineering geological mapping and/or geotechnical analysis. Rather it is to be used to identify those areas which require detailed investigations prior to further development and those areas which are generally suitable for additional urban development and furthermore, the constraint mapping highlights the amount of detail required in the site-specific engineering geological assessments.

The method of representing the development constraint categories parallels that used in the hazard mapping by using both colour and lettering systems to define the individual components for each zone. The degree of constraint to development is identified primarily by using a colouring system to represent areas of varying geotechnical limitations to development. The colours used are different from the hazard zonation in order to eliminate confusion between the maps, and to establish a standard colour system for development constraint mapping similar to the stoplight system used for the hazard mapping. The line types used also differ from those used on the hazard maps because there are no clear boundaries between areas requiring different geotechnical investigations as there were between areas of varying degrees of hazard. The lettering system used for the development constraints map is the same as that used for the hazard zonation and is presented in Table 6.3., while Figure 6.8.

TABLE 6.3.: The development constraint zonation used in this study for the production of development constraint maps. The development constraint map in FIGURE 6.10. (Map Volume) and the example map in FIGURE 6.8. use this classification system.

PROCESS → / CLASSES ↓	SLOPE MOVEMENT L	FLOODING F	STREAM BANK EROSION E	DEBRIS DEPOSITION D
CLASS IV	* Extreme geotechnical limitations. * Urban development unsuitable without intensive investigations and appropriately extensive mitigation measures.	* Extreme geotechnical limitations. * Urban development unsuitable without mitigation of hazards.	* Extreme geotechnical limitations. * Urban development unsuitable without mitigation of hazards.	* Extreme geotechnical limitations. * Urban development unsuitable without mitigation of hazards.
CLASS III	* Significant geotechnical limitations. * Intensive investigations and appropriately extensive mitigation measures.	* Significant geotechnical limitations. * Extensive site investigations essential	* Significant geotechnical limitations. * Extensive site investigations essential	* Significant geotechnical limitations. * Extensive site investigations essential
CLASS II	* Generally favourable for urban development. * Intensive investigations and appropriately extensive mitigation measures.	* Generally favourable for urban development. * Some site investigations required.	* Generally favourable for urban development. * Some site investigations required.	* Generally favourable for urban development. * Some site investigations required.
CLASS I	* Few limitations to urban development. * Residential development recommended.	* Few limitations to urban development. * Residential development recommended.	* Few limitations to urban development. * Residential development recommended.	* Few limitations to urban development. * Residential development recommended.

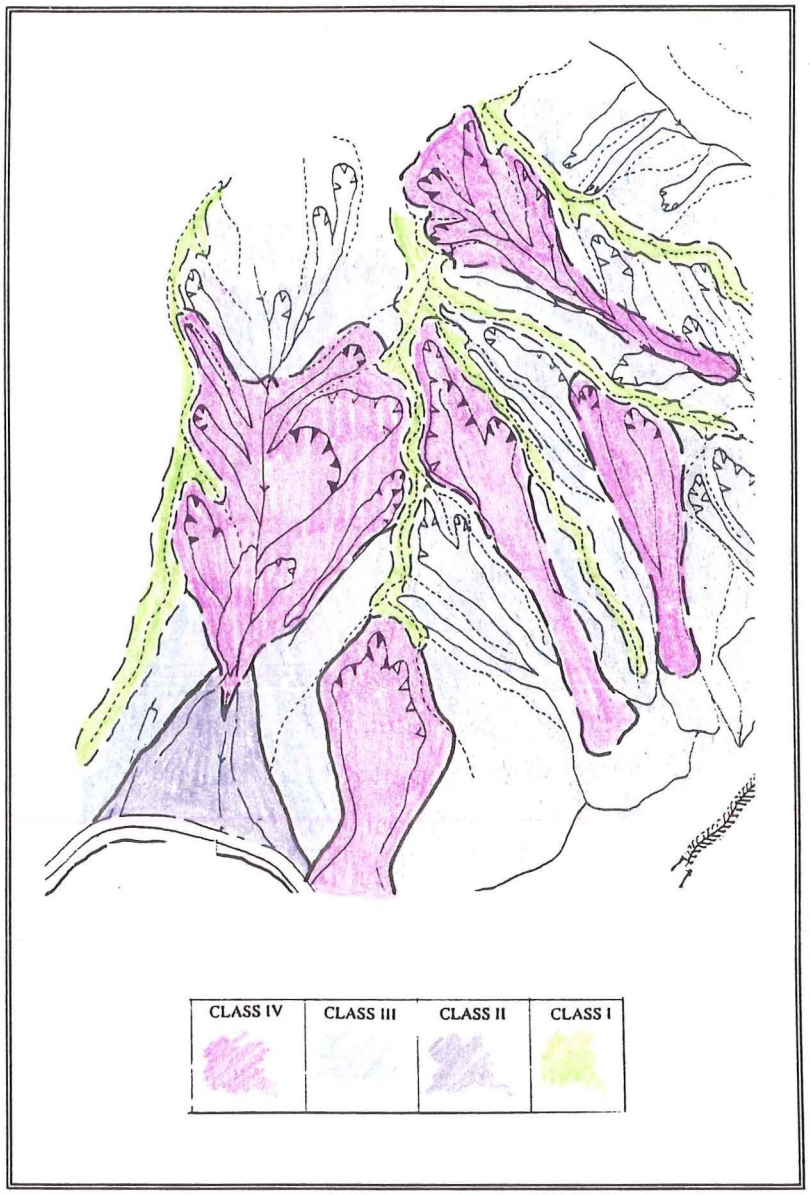

FIGURE 6.8.: An example of a development constraints map showing part of Waikawa township. The classification system is that used in this study and described in TABLE 6.3.

shows the way in which development constraint zones are mapped in this study and is a portion of the development constraint map for Waikawa (McManus, 1994). The use of the colour mauve, for example, indicates that the area is subject to Class IV development constraints and has extreme geotechnical limitations (Section 6.4.), while the upper case letter 'L' indicates that landsliding is the principal process constraining urban development in this area. Further processes operating in the area include stream bank erosion 'e' and debris deposition 'd', although these processes are subordinate to the landsliding as indicated by the lower case letter used as in the hazard mapping (Section 6.2.3.c).

6.3. HAZARD ZONATION

6.3.1. Zoning Approach

As previously mentioned the hazard zonation used in this study is an attempt to quantify the degree of hazard imposed by a particular process in the field area. The quantification of hazards in this study is based on the magnitude, frequency and area affected by the process. The hazard zones adopted in this study are adapted from the zonation used by Horrey (1989), who identified three different hazard zones; high, moderate and low. Negligible hazards have been included as well to identify those areas which are not affected by geological processes posing a significant hazard or threat to future urban development. Although the extent of such zones is limited in the Marlborough Sounds because of the topography and nature of surficial materials etc., it is included for use in other studies which may deal with larger areas of negligible hazard.

The degree of hazard in the field area is based upon three related parameters, the magnitude, return period and area affected by the individual process. The magnitude of an event is a quantification of the size of the event, for example the volume of material involved in a landslide or the stage height of a flood event. Generally it is accepted that large scale events such as major floods will occur more infrequently than small scale events, although they have a greater initial impact and therefore magnitude is related to frequency. The frequency of hazardous events is the time frame between events of a particular magnitude. For example, a landslide which has a large magnitude ($>100m^3$) may occur once in every 20 years however, within that 20 years 40 smaller magnitude events may occur.

Frequency of particular hazardous processes has been the principal method for determining hazard zones in past studies in the Marlborough Sounds (Horrey, 1989), although the use of frequency alone is very simplistic because it is not an independent parameter and is dependant on the magnitude of the event. This study therefore proposes a combination of frequency and magnitude in assessing the degree of hazard associated with each process and location. Additionally, the area affected

by a process of a specific magnitude is incorporated in the assessment, for example the land area affected by flooding or inundation, because it reflects the extent of the hazardous process. The affected area is inherently related to both frequency and magnitude because the land affected by a particular process will vary depending on the size of the event and the frequency with which it occurs. For example, a landslide event which has a large magnitude (involves greater than $100m^3$ material), and therefore a relatively low frequency, will have a widespread affected area due to the size of the event. However, smaller magnitude landslide events will have a smaller affected area than the large event but will occur more frequently and thus, overall, may have a similar sized area affected by the process.

In order to determine the extent of the hazardous processes and the degree of hazard which they impose the aerial photographic data base, from 1959 to present, has been used. The photographs provide a historical review of the processes which have been active in the field area over the last 36 years, since 1959, and provide information on frequency, magnitude and the affected area. This study follows Horrey (1989) in using the photographic data base to estimate the frequency of events, although Horrey did not use the data base to determine the magnitude of events. Horrey (1989) identified any processes active within the then 30 year period defined by the photographs and classified them as being the most frequent and subsequently the most hazardous. However there are problems with this simplistic hazard analysis because events which have a high frequency and corresponding low magnitude may not necessarily be hazardous to urban development, for example small scale gully reactivation occurs during most rainstorm events but is often restricted to the channel. Similarly, a landslide event may be hazardous during failure but after failure there may be no material available for further failure and therefore the process is no longer hazardous. Additionally, the most recent events are not necessarily the largest or most frequent events. However, the identification of large magnitude and low frequency events, for example large scale landslides which have not been active within the last 36 years, may be hazardous to future urban development because the failed material may become reactivated.

This study attempts to integrate both frequency and magnitude into a hazard assessment, and to use these concepts to assess the area affected by the active processes. One limitation of the hazard assessment method used in this study is that the photographic data base has a limited extent of only 36 years, and therefore distinguishing between areas affected by low frequency events and areas which have not been affected by a hazardous process within the last 36 years may be difficult. Thus the use of historical records is also important in assessing the degree of hazard at any particular location, as these provide vital information about the magnitude and frequency of processes which extends beyond the photographic information.

The hazard zonation used in this study is detailed below, describing the criteria for determining the degree of hazard for each geological process identified in the field area. Furthermore, the classification system is summarised in Table 6.2. and an example of a hazard map adapted from McManus (1994) is presented in Figure 6.6. The hazard zonation for this study is presented on a 1:5,000 map of the entire field area and is given in Figure 6.9.(Map Volume).

6.3.2. High Hazard Zones

Land within the field area which is classified as having a high degree of hazard is that which has experienced initiation or reactivation of a geological process within the time frame determined by the aerial photographic data base; ie. since 1959 (Section 6.3.1.). Additionally those processes which have not been identified as active using the aerial photograph data base but which are potentially of large magnitude, and have occurred within the historical time frame (100 years) are also considered as being of high hazard. The basis for these areas being high hazard areas is the notion that high magnitude equates to low frequency but large affected area, and therefore that such magnitude events are potentially hazardous to urban development. Similarly, the low magnitude events have a higher frequency, again defined for each process below, but cause less damage, however it is their frequency which makes them a high hazard to urbanisation. It is important to note that while frequency and magnitude may classify land as having a high hazard zonation this does not necessarily mean the land is unsuitable for urban development (Section 6.4.).

The following discussion identifies the conditions under which each geological process identified in the field area is considered to be a high hazard.

a) Slope Failure

Slope failures considered to pose a high degree of hazard are those which have been active within the time frame of the aerial photographic data base, particularly failures which have been repeatedly active since 1959 (Section 6.3.1.). These failures are generally high frequency, low magnitude events with a limited affected area. The magnitude of slope failures, as mentioned above, is related to the frequency with which they occur and in the field area those slope failures which occur at least once within the limits of the aerial photographic data base and constitute $<100m^3$ of material are considered as low magnitude events and, due to their frequency have high degree of hazard.

Any failures of a high magnitude which have occurred in the past 100 years, the extent of the historical data base, are also classified as high hazard areas. High magnitude failures have a longer recurrence interval, or lower frequency, however the area affected by these events is greater than low magnitude events. High

magnitude slope failures in this study are defined as those failures which have a frequency outside the aerial photographic data base, that is 36 years, and involve in excess of $100m^3$ of material for each event.

Those areas adjacent to, or down slope of, active slope failures which are likely to be affected during failure are also included as high slope failure hazards, for example runout zones. Therefore, actively regressing headscarps, runout zones which are affected by the flow movement at the base of slope failures or areas of lateral spreading are all classified as being of high hazard.

b) Flooding

High flooding hazards are allocated to areas which have experienced inundation or siltation within the last 36 years, particularly in relation to rivers or streams which do not have flood protection schemes in place. In general high flood hazards are restricted to the present day flood plain of the Graham River, and particularly downstream of the Port Underwood Bridge. As mentioned in Chapter 5 the recurrence interval of a high magnitude flood event in the Graham River which will inundate the campground adjacent to the river is approximately 10-15 years. Waikawa Stream has been armoured in the lower reaches through the township to control and restrict flood waters and therefore the flood plain of Waikawa Stream is not given a high hazard zonation (Section 6.3.4.).

c) Stream Bank Erosion

High hazard classification for stream bank erosion is based on the occurrence of events within the time frame of the aerial photograph data base. Those areas which have experienced incision or collapse of stream banks within the last 36 years, as identified on the aerial photographs, are zoned as high hazard areas. The hazard zonation is important because the areas of stream bank erosion indicate that the slopes of the catchment are undergoing erosion of the toe which may possibly lead to slope failure, and therefore the hazards associated with streambank erosion are often related to slope failure hazards.

d) Debris Deposition

The deposition of sediment in the form of debris fans at the base of the catchments in the field area is generally associated with stream bank erosion. Stream bank erosion contributes to a considerable percentage of the material which makes up the debris fans, and therefore the activity of the fans is directly related to the activity of stream bank erosion. Any areas of debris deposition which have occurred within the last 36 years as identified on the aerial photographs are zoned as high stream bank erosion hazards due to the possibility of further sedimentation affecting any urban development on the fan surfaces.

6.3.3. Moderate Hazard Zones

While high hazard zones are intrinsically related to the most recent activity or the highest magnitude events in the field area, moderate hazard zones are defined by less frequent processes which are generally defined as lower magnitude events occurring within the last 100 years, as defined for each process below. Within the field area land which has not been modified by geological processes but which has the potential for such events, for example landsliding in unmodified slopes in excess of 35 degrees is also defined as being of moderate hazard. The following section discusses the application of moderate hazard in relation to the hazardous processes identified in the field area.

a) Slope Failure

Areas which have a moderate degree of slope movement hazard are those which have been subjected to low magnitude events ($<100m^3$) that have not been active within the aerial photographic time frame of 36 years. Furthermore, those high magnitude failures ($>100m^3$) which can be observed in the field or on the aerial photographs, but which have no record of movement within historical times, (ie. the last 100 years) are also zoned as areas of moderate hazard. These failures have a moderate degree of hazard because although the frequency of the event is low (>100 years), the magnitude is high and should the area become developed further failure may occur. The moderate hazard classification for slope failures therefore, also incorporates the frequency and magnitude information which is the basis for high hazard areas, but over different time scales and levels of activity to differentiate between the high and moderate hazard zones. In addition to areas of previously active slope failure, moderate hazard is allocated to some slopes in the field area which have not previously been subject to slope movement processes. The unmodified slopes classified as being of moderate hazard are restricted to those which have a slope angle in excess of 35, and those slopes with 1metre or more of surficial deposits covering the bedrock surface. These slopes are considered the most likely to fail should urban development, including roading and services, proceed because they are similar in nature to slopes which have previously failed.

b) Flooding

Moderate hazard zones also apply to those areas subject to flooding and sedimentation within a 10-100 year period where flood protection schemes are not emplaced. The main flood plain of the Graham River upstream of the Port Underwood Road bridge is zoned as a moderate hazard because the stream has not been subject to any substantial down-cutting events, and therefore the main flood plain is not significantly higher than the present channel. The Waikawa Stream flood plain downstream of the Waikawa Road bridge is also prone to inundation and sedimentation during a 10-100 year period, although the river has a rock armoured

flood protection scheme to restrict erosion of the river banks rather than overtopping. Therefore the main channel and flood plain of Waikawa Stream is also zoned as being moderate hazard. Some of the smaller streams in the field area, for example Rimu Stream in Waikawa, show either significant down-cutting of the channel or have flood protection measures. Only the immediate channel area of these streams is therefore zoned as being moderately hazardous.

c) Stream Bank Erosion

Parts of the gullies within which stream bank erosion has occurred outside of the aerial photographic time frame, but within the last 100 years are defined as having a moderate degree of hazard. Moderate stream bank erosion hazards are difficult to quantify because the erosion in the gullies is not easily identified due to the heavy vegetation in the field area.

d) Debris Deposition

Debris fans which have not been active within the 36 year period defined by the aerial photographic data base, but which have been within historical times are considered to have a moderate degree of hazard. Many of the debris fans which are included in this hazard zonation display geomorphic features which indicate the age of the deposit, such as small surficial streams which have not had sufficient time to downcut into the debris deposits and a natural lack of established vegetation, indicating activity within a 100 year period. Such areas are considered hazardous due to the possibility of reactivation of the streambank erosion in the gully which feeds the debris fan, the possibility of debris deposition on the fan, and the potential damage to any urban development on the fan surface.

6.3.4. Low Hazard Zones

Low hazard zones are those areas within the field area where the geological processes identified pose little threat to actual or potential urban development. Due to the steep slopes and the extent of the main flood plains in the field area low hazard zones are not extensive as most areas are prone to high or moderate hazards from geological processes. In general the low hazard zones equate to areas where the geological processes have been inactive for more than 100 years, or areas where geological processes are potentially active but would not cause substantial impact on the landscape. As with the high and moderate hazard zones the classification is based upon determination of frequency and magnitude of specific geological processes and is detailed below for each of the identified processes.

a) Slope Failure

The slopes within the field area which constitute a low hazard to urban development are those with a moderate slope angle (between 15° and 35°) that have not been modified by slope movement processes. Although these slopes may

experience some form of failure should development proceed, for example the collapse of vertical faces or the development of extension cracks as support is removed from the base of the slope, the failures are not likely to be sudden or damaging to property and these areas may be reinstated by using retaining structures. Failures will require extreme rainfall events combined with high antecedent water conditions and often complete devegetation. The depth of surficial material on these gentle unmodified slopes is approximately 3m of colluvium over regolith. In general, therefore, the slope movement processes are inactive on these slopes, urban development is unlikely to induce slope movement, and thus the slopes are classified as being of low hazard.

b) Flooding

Those areas which will experience inundation and siltation only if the flood protection measures fail in a flood event are zoned as being of low hazard from flooding processes because such flood protection measures are generally designed for a 50 year flood event . In the field area low flooding hazard zones are used to define the flood plain of Rimu Stream which has been culverted to divert flood waters. In Rimu Stream, the flood plain will only experience inundation and siltation if the culvert were to become blocked and flood waters overtop the banks of the stream. There are few areas with in the field area which have low flooding hazard zonation due to the lack of flood protection measures in place (Section 6.3.2. and Section 6.3.3).

c) Stream Bank Erosion

The determination of hazard zones other than high and moderate hazard zones for stream bank erosion processes in gullies cannot be quantified because any stream bank erosion which has occurred outside of the historical data base (>100 years) is not preserved in the field area due to subsequent erosion. Therefore only the high and moderate stream bank erosion hazards are represented in the gully systems of the field area.

d) Debris Deposition

The debris fans in the field area which have not been active within the extent of the historical database (>100 years), are zoned as having a low degree of hazard. These fans are stable features within the field area and are identified by the incision of streams on the fan surfaces and the deep weathering profile observed in stream banks combined with extensive vegetation in undeveloped areas. Urban development of the fan surface is unlikely to cause reactivation of the fan, and thus the area poses little threat or hazard for actual or potential urbanisation. The main area of low deposition hazard is the Maori cemetery fans which make up the central and eastern portion of Waikawa township (Figure 6.9.; Map Volume).

6.3.5. Negligible Hazard Zones

The main problem with assigning a negligible hazard from any one geological process to a location in the field area is that generally there is more than one process modifying a particular location within a given time frame. Therefore the identification of negligible hazard zones in the field area is limited due to the combination of geological processes of different degrees of hazard. Areas of negligible hazard however are defined as locations at which there is no significant hazard associated with a particular geological process. In the field area negligible hazard zones are limited to the uppermost ridges because these areas are not subject to any of the geological processes identified in this study, namely slope failures because the the maximum thickness of colluvium is less than 1m, flooding hazards, stream baank erosion and debris deposition.

The negligible hazard zonation is included in this study in order to complete the range of hazard degrees which may be identified at any location, and potentially also for use in similar studies in the Marlborough Sounds and other areas where hazard zonation is required at a district scale of 1:5,000.

6.3.6. Additional Hazards in the Field Area

In the field area there are two potentially hazardous processes, tunnel gully erosion and seismicity, which cannot be quantified using the hazard zonation method presented in this chapter because the processes cannot be adequately defined in terms of magnitude, frequency or affected area. However both tunnel gully erosion and seismic hazards are important for a complete hazard assessment of the field area and therefore the processes are described in detail below.

a) Tunnel Gully Erosion

Tunnel gully erosion occurs within the top 1m of surficial material in the field area and is observed in both schistose and greywacke colluvium deposits regardless of the thickness of the material and it is possible that tunnel gullies may be restricted to loess rich soils. However, the laterial extent of tunnel gully erosion, even if the tunnels have collapsed is impossible to estimate due to the dense vegetation in the study area. Therefore the magnitude of the tunnel systems, the frequency of their occurrence and the area affected by the process cannot be determined.

Tunnel gully erosion does not constitute a high degree of hazard to urban development in the field area, even though the occurrence of the tunnels may be extensive, because as the tunnels are shallow they are not likely to cause destabilisation of house foundations, for example pole foundations which will extend through the surficial material to the bedrock below. Therefore in this study tunnel

gully erosion is represented in the hazard classification (Table 6.2.) and on the hazards map (Figure 6.9.; Map Volume) with a lower case letter 't' to indicate the presence of tunnels. Due to the difficulties of quantifying areas of tunnel gully development there is insufficent data with which to assign a hazard zonation in the field area.

b) Seismic Hazards

The quantification of seismic hazards within the field area is very difficult due to the difficulties in determining the hazards for earthquake events of varying magnitude in combination with the existing geological processes identified in the field area. The Waikawa Bay Fault east of Waikawa township is classified as having a class III activity rating (Chapter 4) and therefore rupture of the fault is possible which would have serious implications for urban development in the field area. Additionally, the Marlborough Sounds region is in a seismically active part of New Zealand and the influence from earthquake events not directly related to the field area is also important for a complete seismic hazard assessment. Because of the complications associated with assessing seismic hazards in the field area a separate seismic hazard investigation is recommended and was outside the resources of this study. The hazard map for this investigation (Figure 6.9.; Map Volume) simply locates the principal fault lines in the field area and indicates an area either side of the faults which could be immediately affected should fault rupture occur.

6.4. DEVELOPMENT CONSTRAINTS

6.4.1. Approach

The development constraint mapping of the field area is concerned with the suitability of land for urban development and the types of geotechnical limitations which are imposed upon the land by the geological hazards identified and presented on the hazard map (Figure 6.9.; Map Volume). As mentioned in Section 6.2.3.d. the assessment of development constraints in the field area requires the assumption that there is a likelihood of future urban development in the field area. Therefore the constraint analysis correlates with the hazard mapping (Section 6.3.) which also assumes the possibility of urbanisation.

The constraint zones which are used in this part of the study are adapted from Horrey (1989) and the GLUM methodology (Section 6.2.3), and principally define the type and detail of geotechnical investigation required for any location in the field area. The constraint zones are divided into four degrees of geotechnical limitation ranging from Class IV, which represents extreme limitations to urban development, to Class I in which there is no geotechnical limitations to urban development. Furthermore, the development constraints are assessed relative to each of the geological processes identified within the field area because the degree of

geotechnical limitation will vary depending on the type of process it represents. Table 6.3. summarises the development constraint zonation used in this study while Figure 6.8. is a portion of a development constraint map adapted from McManus (1994) of the eastern portion of Waikawa township.

Although the hazard zonation provides the basis of the development constraint mapping it does not represent an exact correlation between the degree of hazard for a particular process and the degree of geotechnical limitations for the same process. Therefore an area which is zoned as being of moderate hazard is not necessarily zoned as having moderate geotechnical limitations on the development constraint map because the two parameters do not represent the same conditions. For example, an area on the hazard map which has been zoned as having a moderate slope failure hazard may represent a slope movement of large magnitude but which has not been active in the last 100 years (Section 6.3.3.a). The geotechnical limitation for this same area is going to be significant (Class III) or extreme (Class IV), due to uncertainty regarding the possibility of reactivation during development. Similarly, a slope failure which has occurred within the time frame of the aerial photograph data base is zoned as being high slope failure hazard. If this event has occurred within shallow (1m) colluvial deposits on the upper slopes, the failure is unlikely to reactivate as most of the potentially unstable material has already failed. Therefore, although such failures constitute a high hazard zonation due to their recent activity, the level of geotechnical limitations imposed would be Class III (high) or Class II (moderate) rather than Class IV (extreme).

The following sections detail the types of development constraint categories identified in the field area and explain how the degree of hazard associated with each geological process affects the type and degree of constraint to urban development. The development constraints for the entire field area are represented in map form at a scale of 1:5,000 so as to be compatible with both the engineering geology and hazard zonation maps. The development constraints map is produced in Figure 6.10. (Map Volume).

6.4.2. Class IV: Extreme Geotechnical Limitations

Detailed site investigations are essential at the subdivision and construction stages of development for any land classified as Class IV, and in general the land is unsuitable for urban development unless extensive geotechnical investigations are performed and suitable remedial or preventative measures are designed. The land included in this class incorporates most of the high hazard areas and some of the land zoned as being moderate hazard. High hazard areas which are excluded from this category are those slope movements which occur in very shallow colluvial deposits

and are not likely to become reactivated or may be easily remedied following urban development. These features have significant rather than extreme geotechnical limitations and the geotechnical investigations required will reflect this zonation.

It is important to note that although it is recommended that land classified as having extreme geotechnical limitations be avoided with respect to urban development, it is not necessarily excluded from development because in many instances remedial measures may mitigate the hazard posed at a locality. However the remedial measures are generally costly and require constant maintenance and observation. Therefore, the cost of developing land in the Class IV zone is high and suitable sites for development can usually be found in other nearby locations.

a) Slope Movements

Any active slope movements which develop in thick colluvium (3-4 m) and areas of intense stream bank erosion which have been active within the last 36 years have extreme geotechnical limitations to development due to the likelihood of further activity. Geotechnical investigations required would be extensive and in general these areas are not considered suitable for urban development, although these areas are not excluded from development because of the possibility of suitable remedial measures being emplaced if sufficent funds are expended.

b) Flooding, Erosion and Deposition

The flood plain of the Graham River, which has experienced inundation and siltation, particularly the camping ground down stream of the Port Underwood Road bridge, is considered subject to extreme geotechnical limitations due to the lack of information regarding return periods for flooding events. The flood plain is generally unsuitable for urban development unless considerable flood protection measures are emplaced.

Debris deposition associated with stream bank erosion which has occurred within the last 36 years is also considered to have extreme geotechnical limitations for urban development due to reactivation of these features during high intensity rainstorm events. Urban development on active fan surfaces would be subject to considerable sedimentation in such an event and therefore significant remedial measures would need to be employed to stabilise such locations.

6.4.3. Class III: Significant Geotechnical Limitations

Both moderate and low hazard zones contribute to the Class III development constraint zonation. Land in Class III requires extensive site investigations including engineering geological mapping, trenching and augering in order to determine the nature of the subsurface, and detailed analysis of geomorphic processes at the site at both the subdivision and construction stages. Limited laboratory testing to determine

the geotechnical characteristics of the geological units on site, including grainsize, Atterberg Limits and XRD for clay mineralogy as the identification of certain clay minerals, ie. smectites, is important to determine the geotechnical parameters of the soils, is also recommended prior to development and planning. Additionally, mitigation of hazards may be required should urban development go ahead, for example retaining walls for unstable slopes.

a) Slope Failure

All of the high hazard slope failures which were not classified under Class IV extreme limitations are included under the Class III development constraints. Although these small shallow failures are not likely to prevent urban development, they are still active features and as such require substantial geotechnical investigations. Similarly, many of the larger inactive slope movements, zoned as being moderate hazard areas, have the potential for reactivation in relation to additional urban development and therefore these areas require significant investigations before development can proceed. Additionally, steep unmodified slopes with >1m of unconsolidated surficial material also comes under Class III, due to the potential for slope failure during development.

The small magnitude inactive slope failures which have been allocated a moderate hazard zonation and have occurred within the shallow colluvial deposits on the upper slopes are not considered to require substantial geotechnical investigations because they have not been recently active (ie. within 36 years). These features are described in Section 6.4.4. below.

b) Flooding, Erosion and Deposition

The flood plains of rivers and streams which are prone to flooding within a 10-100 year interval also have significant geotechnical constraints to development, for example the higher flood plain in the Graham River which is zoned as moderate hazard. The lower Waikawa Stream flood plain is also zoned under the Class III development constraints.

Erosional and depositional features which are of moderate hazard zonation, for example debris fans which have not been active in the last 35 years (Section 6.3.3.c), are classified under Class III due to potential reactivation associated with stormwater disposal and culverting from urban development of the fan surface.

6.4.4. Class II: Low Geotechnical Limitations

In general the land zoned under Class II is favourable for urban expansion and there are few geotechnical limitations to development. Class II land requires detailed site investigations, for example at a scale of 1:500, including engineering geological mapping, trenching and augering, and limited laboratory analysis for geotechnical parameters of the rock and soil materials for individual house sites.

Subdivision planning in areas zoned Class II however require less detailed engineering geological information, for example 1:1,000 because the geotechnical limitations indicate that the area is generally favourable for subdivision. Low hazard zones are commonly included within Class II and some of the areas zoned as moderate hazards are subjected to only moderate geotechnical limitations.

a) Slope Failures

Within the field area, Class II development constraints include all moderate to steep (15-35) slopes which remain unmodified by slope movements and which are covered by unconsolidated surficial material in excess of 1m. These slopes will require detailed site investigations at the construction stage due to the possibility that additional development may initiate slope movements. As mentioned in Section 6.4.3. above, the moderate hazard shallow failures which occur on the upper slopes and have not been active within the last 36 years are zoned under Class II because the geotechnical limitations are not likely to restrict urban development in such areas.

b) Flooding, Erosion and Deposition

Any locations which are prone to flooding in a high magnitude flood event only if protection measures fail, are zoned under Class II development constraints due to the unlikely occurrence of stop bank or culvert failure. The flood plain of the culverted Rimu Stream, for example, is unlikely to inundate the surrounding area unless the culvert becomes blocked, and therefore the zoning equates to the low hazard zone of this area (Figure 6.9.; Map Volume). There is insufficient data concerning the developmental constraints associated with tunnel gully and stream bank erosion. However, debris deposition associated with streambank erosion will be given a Class II zonation if the deposits have not been active within the last 100 years as the likelihood of reactivation is low even with urban development.

6.4.5. Class I: No Geotechnical Limitations

Land identified within Class I is the most favourable land for urban development as essentially there are no active or potentially active geological hazards associated with these areas and the geotechnical investigations required would be minimal. All the land zoned as having negligible hazards on the hazard map is incorporated into the Class I development constraint zonation while some of the low hazard zones are also included. For example, the Maori Cemetery debris fans, which are zoned as low hazard areas, have little or no geotechnical constraints to urban development and therefore are zoned as Class I. The type of investigations required in areas classified as Class I will involve a general walkover inspection while subsurface and laboratory investigations are largely unnecessary.

6.5. SELECTED CASE STUDIES

6.5.1. Introduction

The following case studies are presented to show the interaction of the active geological processes with present urban development in the field area, each case study being an example of a high or moderate geological hazard. As introduced in Section 6.1.3. a geological process cannot become a geological hazard without the influence of human activity and in this study human activity is centered around actual or potential urban development. The case studies presented below are divided up into four areas associated with the active geological processes in the field area which pose the greatest hazard for urban development and indicate the extent of geotechnical investigations or limitations associated with similar sites in the field area.

It should be noted that the current study is based around a design or feasibility/pre-feasibility investigation and does not require the detail of investigation needed for site specific investigations. Therefore the case studies presented below are based on general observations and no attempt has been made to investigate the individual locations at a site specific scale (approximately 1:500).

6.5.2. Surficial Slope Instability

- Manuka Cottage, Wharetekura Bay (GR P27 269805 599330)

The house originally located at this site was destroyed in a failure event in June 1993 (Figure 6.11.). The house was built on a colluvial slope in excess of 35, and the failure scarp appears to have developed initially in road fill beneath the Port Underwood Road. The head scarp measures approximately 10m, long with up to 600m^3 of material becoming mobilised during the failure (Figure 6.11.). The speed of the failure was sufficient to completely destabilise the house foundations such that the house slid into the ocean at the bottom of the slope. The reasons for this particular failure include the nature and origin of the material on which the house was built. Above the house site there is evidence for a relict gully with thick (>4m) colluvial deposits preserved as a wedge approximately 7m wide (Figure 6.12.). It is concluded that the house was built on the downslope remains of this relict gully deposit and the failure occurred along the colluvial/bedrock interface. The triggering mechanism was probably water percolating into the failure surface from the road above the house and reducing friction between the colluvium and the bedrock below (Figure 6.13.). The site was vegetated with some large established trees and there appeared to be no evidence of previous slope movements within the gully deposits. As water is the principal factor for triggering failure sites such as Manuka Cottage must be carefully drained and culverted to avoid additional surficial

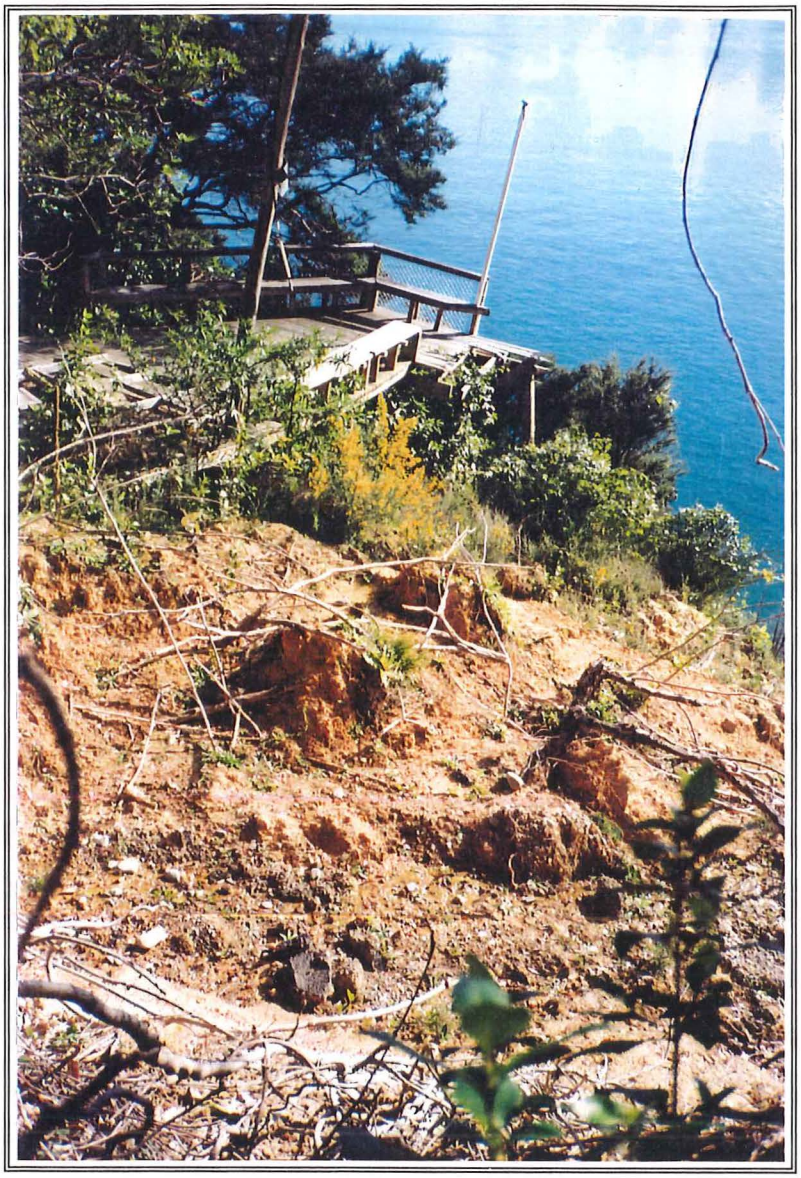

FIGURE 6.11.: A photograph showing the damage to Manuka Cottage following the failure of a relict gully system. Cross-sections (following page) showing the geological profiles before and after failure.

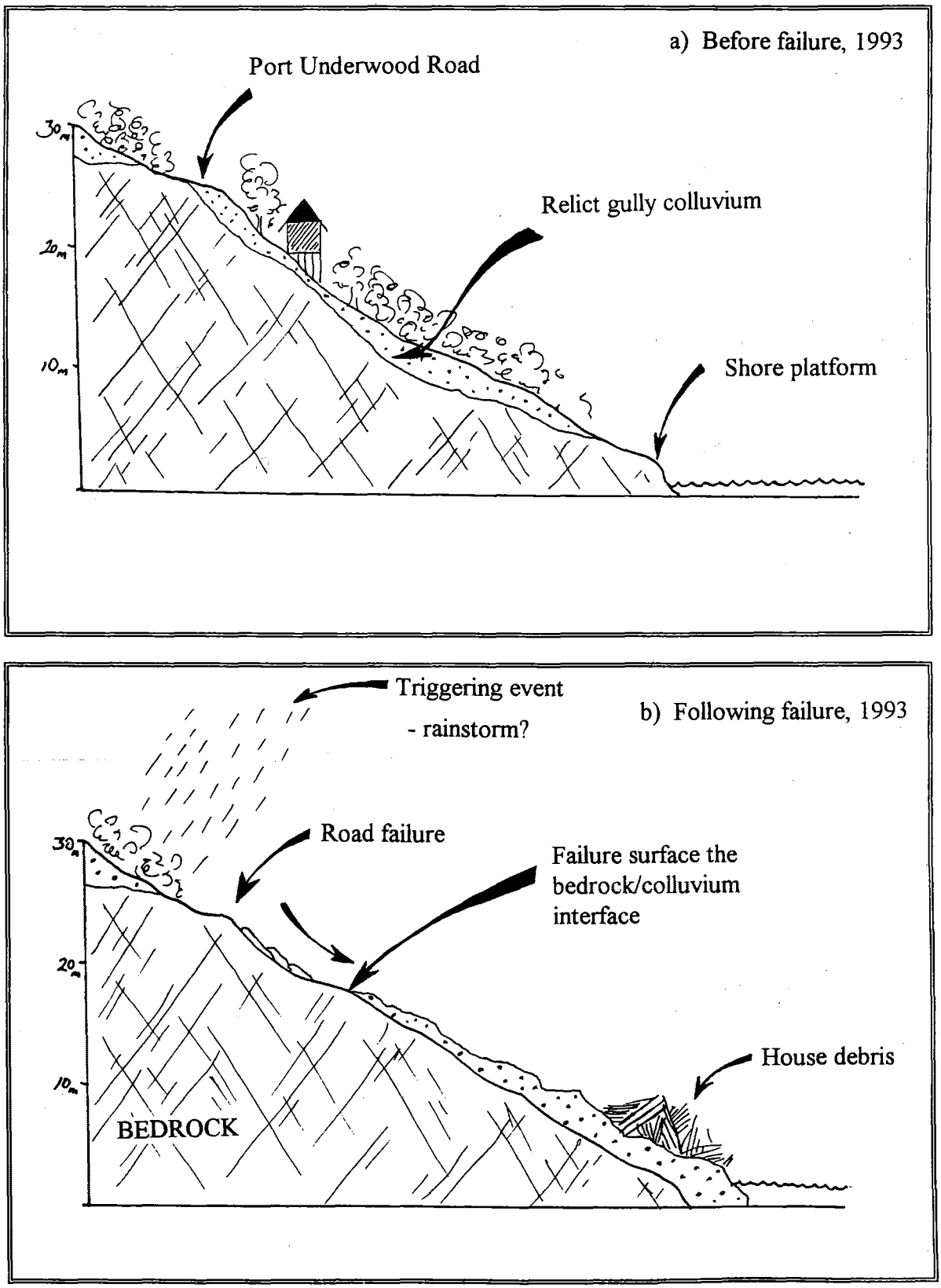

FIGURE 6.11. (ctd.): Cross Sections of the Manuka Cottage failure. Section a) shows the geological profile prior to failure, indicating a 4-5m thickness of colluvial material. Section b) shows the failure surface along the bedrock/colluvium interface. Failure was probably due in part to high antecedent water conditions.

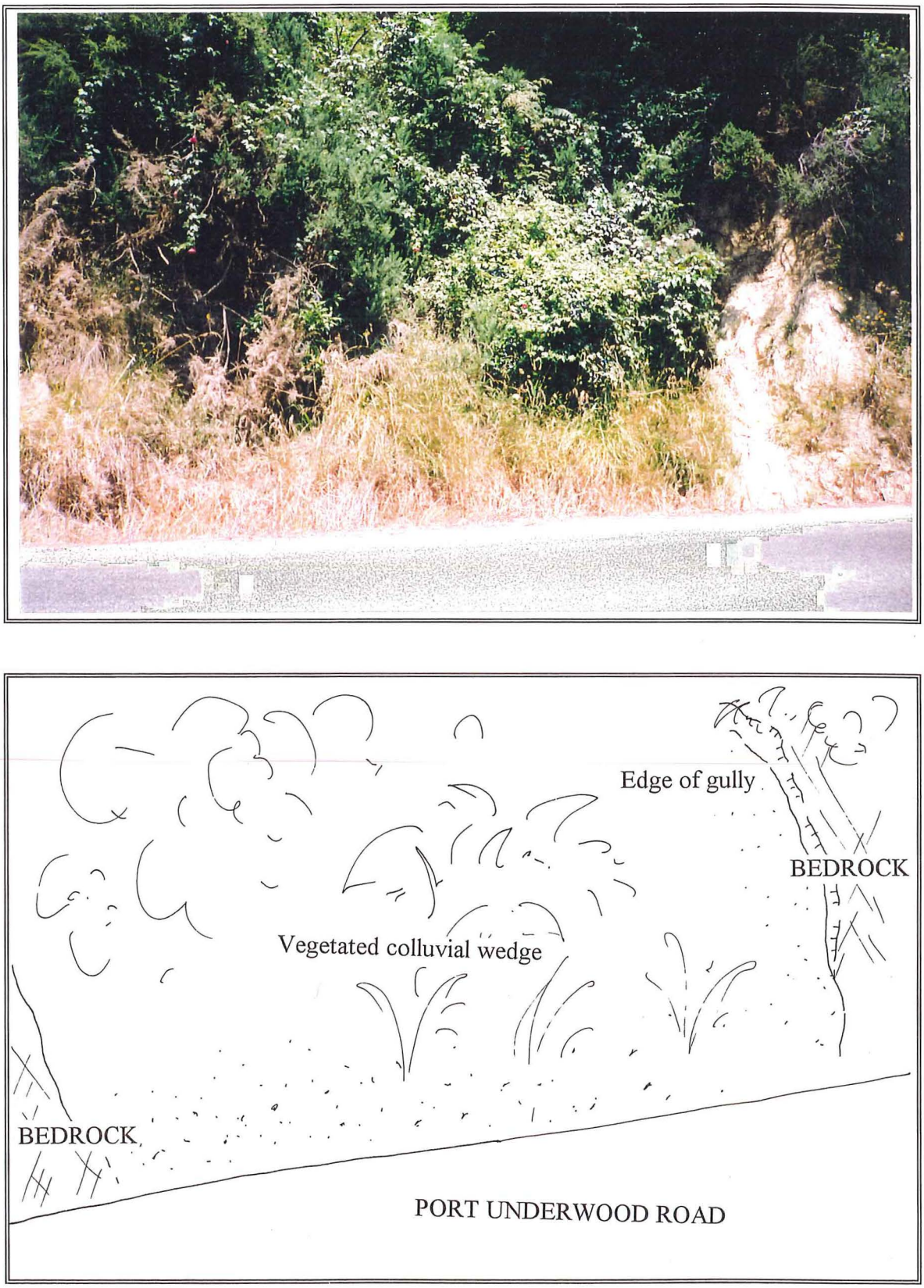

FIGURE 6.12.: A photograph and diagrammatic sketch of the colluvial wedge above the Manuka Cottage site. The wedge is thought to indicate a relict gully system upon which Manuka Cottage was at least partially built.

failures which may damage or destroy property. Failures such as this also pose a danger to human life as, in this case, it was fortunate no one was in the house at the time of failure.

- Port Underwood Road, Waikawa to Whatamango

Much of the outer part of Port Underwood Road between Waikawa township and Whatmango Bay has been constructed on poorly consolidated fill material which is unstable. The locations of failures which occurred during the course of this study are shown on the plan of the road in Figure 6.14. The average size of failure is equivalent to a low magnitude failure (Section 6.3.) and involves a headscarp up to 10m in length, incorporates up to $100m^3$ of material and is generally identified as predominantly colluvium with some road fill material. Cracks occur frequently in the Port Underwood Road and are the first signs of failure in road fill (Figure 6.15.). During the winter of 1995 up to 6 fill and colluvium failures were observed along 3km of road between Karaka Point and Whatamango Bay. The triggering factor for the road fill failures is water from inadequate drainage systems associated with housing above the road, and poorly maintained culverting along the Port Underwood Road. Water percolates through the unconsolidated fill and colluvial material to the colluvium/bedrock interface where water reduces the friction on the bedrock surface. Small movements of the surficial material causes cracks to appear in the road fill material. Once the cracks have developed more water may then quickly enter the road fill material and percolate down to the failure surface. Many of the failures below the road occur in relation to small streams and both active and inactive gully systems. Failures which occur in association with active gullies and streams are generally the result of poor culvert construction or maintenance. Figure 6.16a. shows the effects of poor storm water removal in Whatamango Bay (GR P27 259980 599340) where the house above the road had a storm water culvert designed so that water drained directly onto the rock/soil face below the drive way. However the presence of a relict gully system was not identified and the blockage eventually resulted in the failure of the face (Figure 6.16a.) and required remedial measures to ensure no further failure occurred (Figure 6.16b.)

6.5.3. Bedrock Batter Failures

Although there are no large scale bedrock landslide failures in the field area the failure of cut batters in weathered rock material above and below roads occurs frequently. Failure is influenced by the orientation of joint and fracture sets combined in places with foliated rock material and may be hazardous both upslope of, and beneath house sites. The following case studies show some of the bedrock batter failures which occur within the field area.

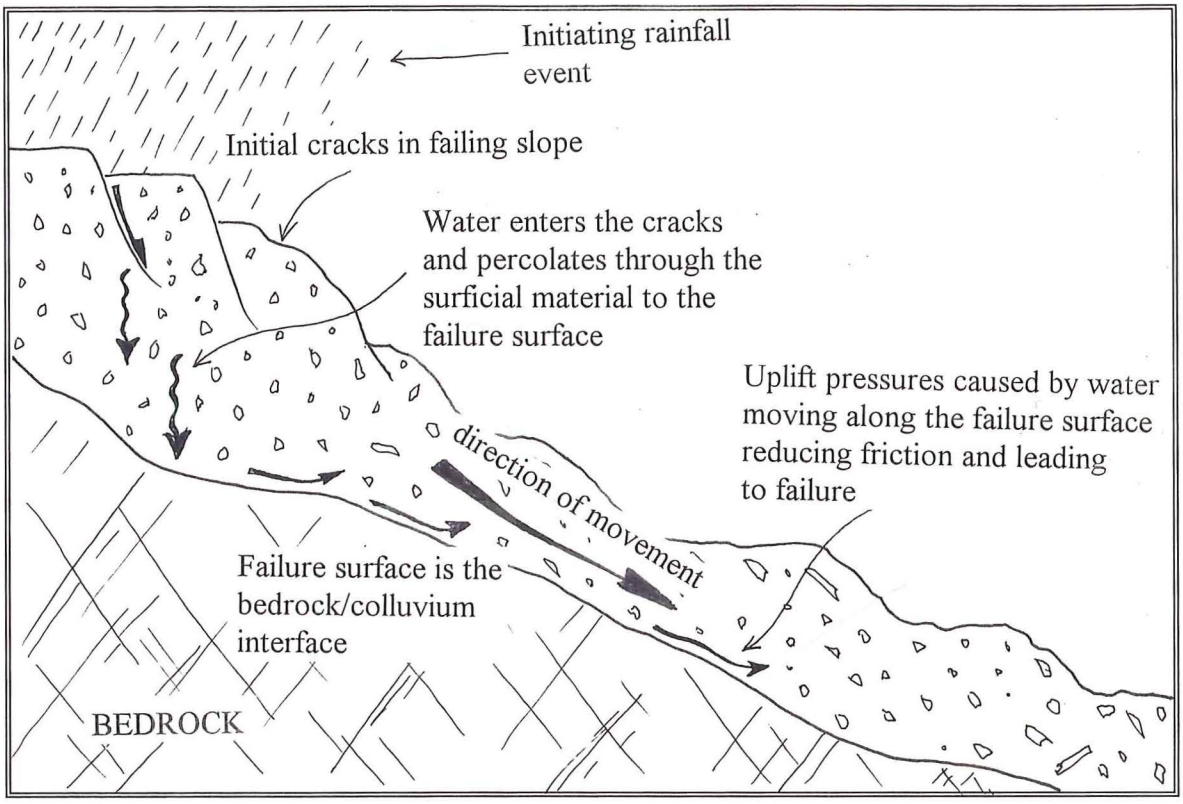

FIGURE 6.13.: A diagrammatic sketch which shows the influence of water on the movement of slope failures.

FIGURE 6.14.: Cracks which have formed in the Port Underwood Road following a rainstorm in November 1994. Approximately 20cm of slumping is related to failure in road fill and colluvial material down slope. Note, hammer for scale.

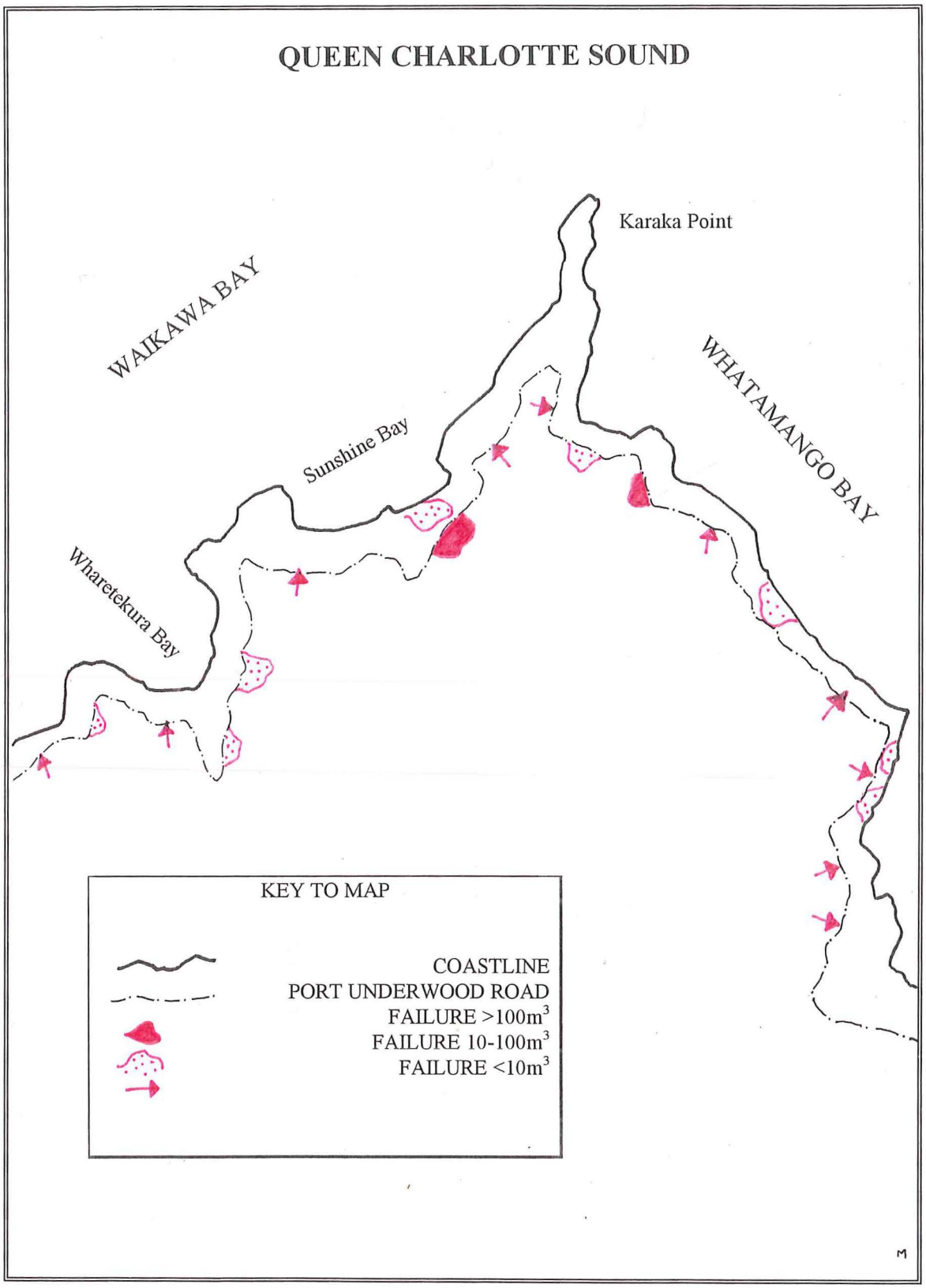

FIGURE 6.15.: The locations of slope failures related to the Port Underwood Road which have occurred during the coarse of this study. Note in particular the higher frequency of failures on the eastern portion of the road between Karaka Point and Whatamango Bay.

FIGURE 6.16.: Poor storm water removal has lead to the failure of a relict colluvium filled gully below the access road to the house above. Photograph a) shows the damage caused by storm water disposal directly onto the rock/soil face.

FIGURE 6.16 (ctd.). Photograph b) shows the remedial measures which were employed and include re-culverting storm water under the Port Underwood road and replanting of the failure surface.

- Port Underwood Road.

The section of the Port Underwood Road between Waikawa and Whatamango Bay is regularly subjected to batter failures in both jointed greywacke and schistose rock masses above the road, especially during winter months when the wet conditions lead to high antecedent water conditions which can destabilise the rock faces. During the course of this study a number of storm events and one earthquake event highlighted the instability of cut faces above the road in relation to jointing patterns and foliation. On 23 March 1995 an earthquake measuring 5.2 on the Richter scale and centered in the Marlborough Sounds northwest of Waikawa occurred. Figure 6.17. shows the extent of rock batter failure along the Port Underwood Road during the earthquake. The failure in this example occurred along jointed and weathered greywacke bedrock. The fact that the earthquake occurred at the end of summer when the rock and soil materials were dry is an important factor. The hazard potential of rock faces in an earthquake would be significantly increased should the earthquake have occurred during the wetter winter months. During winter both rock and soil material have a higher moisture content and water can destabilise the rock faces due to a reduction in friction between the joint or foliation surfaces. The hazard potential therefore is greatest when the rock faces are subject to high antecedent water conditions during winter, particularly when the joint or foliation surfaces dip steeply (>45°) down slope.

There were a total of 8 batter failures observed along the Port Underwood road between Waikawa and Karaka Point during the winter of 1995 with the average volume of each failure being less than $100m^3$ and the failure dimensions were approximately 5m high and 5-10m across the headscarp. Two larger failures were observed during the same storm event on the 5 August. The largest of these failures was a planar rock failure in jointed schistose material north of Wharetekura Bay (GR P27 269848 599346). The initial headscarp measured approximately 20m in length and the height was approximately 10m above the surface of the road. This particular failure (Figure 6.18.) displayed progressive failure over a period of 1 month. The rock face first failed on the 5 August during a 4 day rainstorm during which over 200mm of rain fell in the 5 days prior to failure. The rock face failed a second time on the 7th September following 43mm of rain in a 24hr period. Over $300m^3$ of rock and soil failed during the second event and an additional scarp approximately 2m high and 15m along the face appeared adjacent to the first (Figure 6.19.). Both failures occurred in jointed rock where the joints were orientated subparallel to the face and dipping steeply downslope (Figure 6.20.). Water percolates down into the joints increasing the water pressures on the rock face and therefore reduces the effective normal stress between the joint surfaces initiating batter failure.

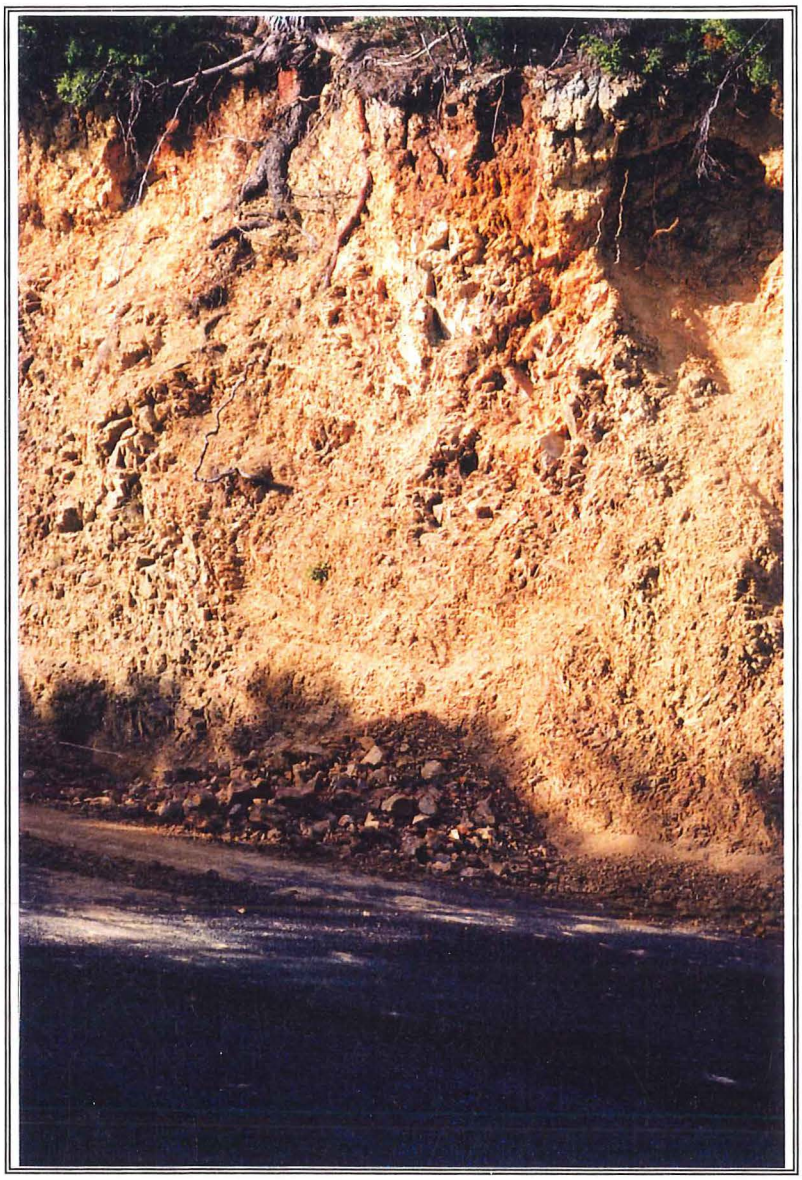

FIGURE 6.17.: The failure of a road batter in greywacke material following the earthquake during March 1995.

FIGURE 6.18.: One of the road batter failures following heavy rain during August 1995.

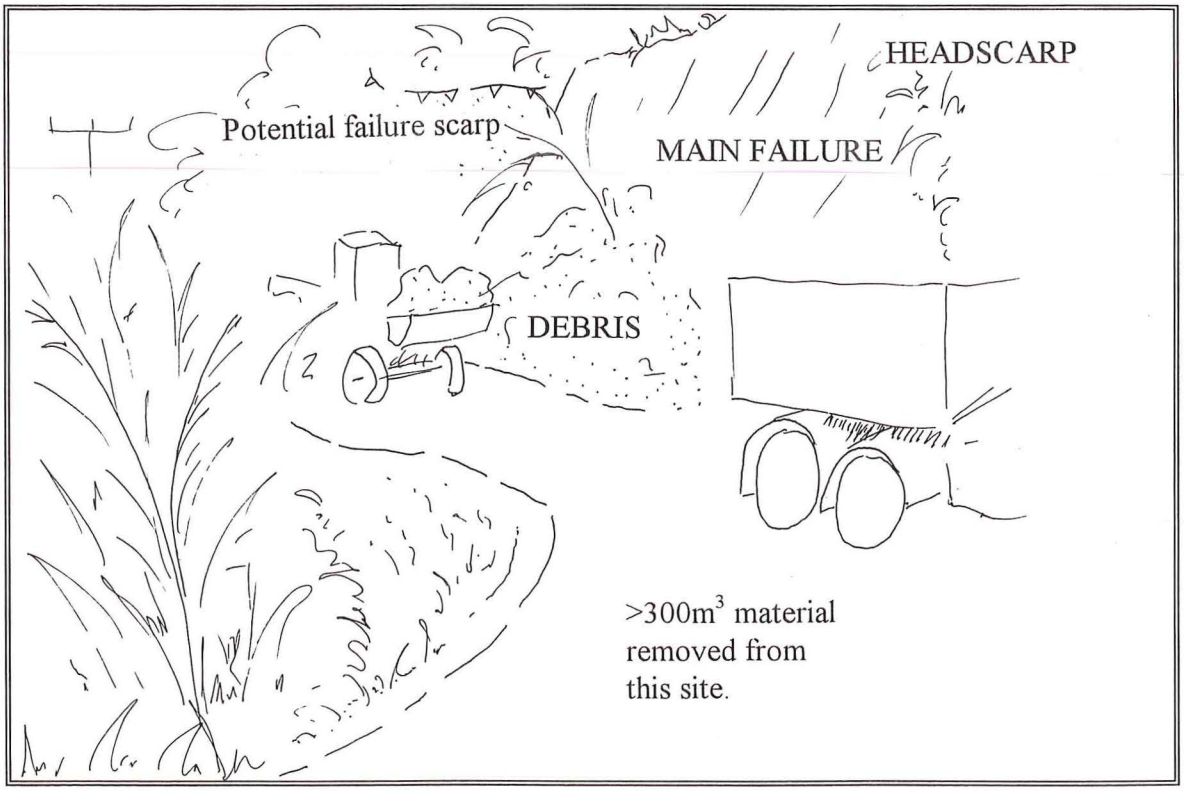

FIGURE 6.19.: The second failure of the slide in Figure 6.18. This failure shows another scarp developing north west of the main failure and is likely to fail during future rain storm events. Over 300m^3 of rock and soil were removed from this location and the failure measures approximately 15-20m high.

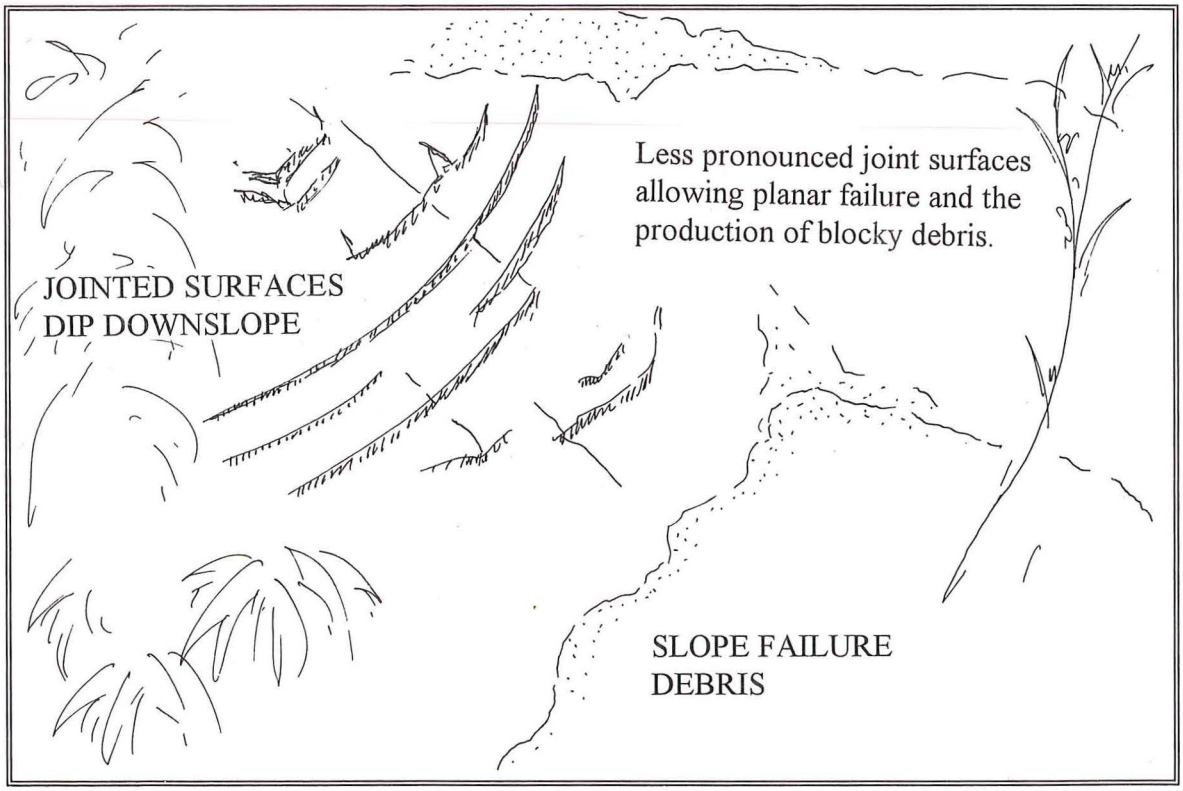

FIGURE 6.20.: The failure surface of the batter failures in FIGURE 6.18. and FIGURE 6.19. Note the steeply dipping joint surfaces along which planar failure has occurred.

- Forestry track, Whatamango Bay (GR P27 259949 599340)

A wedge failure 10m wide and approximately 15m high was observed on the forestry track upslope of the Port Underwood Road on the western side of Whatamango Bay. The failure occurred along two joint sets intersecting a rock face orientated at 160.

Set 1: 165/54NE

Set 2: 127/85N

Figure 6.21. shows the actual failure and a schematic diagram with stereographic projection and wedge orientation sketch (Figure 6.22) showing the failure surfaces relative to the rock face. The largest failed block from the failure was in the order of 5m, while most debris was less than 1m in diameter. The failure occurred in schistose rock, although schistosity was not a principal factor in this particular location. However, other localities within the field area are subjected to failure along both foliation surfaces and open joint sets.

6.5.4. Inundation Considerations

Both Waikawa Stream and the Graham River are capable of flooding events which threaten property and services. The steep topographic nature of both catchment areas allows significant runoff in a rainstorm event. Both rivers have moderately sized catchment areas (between 12-18km^2) and relatively narrow channels, which means that storm events can result in overtopping of the river banks. The flow response time of the rivers to rainfall events in the catchment area is small, with less than 12 hours between the storm event and the flood event. Flood recurrence intervals are difficult to estimate due to the lack of recorded data, particularly in the Graham River, but overtopping of the bank of the Graham River is thought to have a 10 year recurrence interval.

The problems associated with development of the flood plains of the Graham River and Waikawa Stream involve both inundation and siltation, and could be significantly reduced with the construction of stop bank systems. Such flood control measures are particularly important in Waikawa Stream where the flood plain in the lower reaches below the Waikawa Road Bridge has already undergone urban development. In the Graham River, however, urban development is minimal on the flood plain as the river floods easily, the last overtopping event occurring in November 1994. The camping ground managed by the Department of Conservation located downstream of the Port Underwood Road bridge has been zoned as a high hazard area with regard to flooding and siltation. The zoning will remain high until stop banks are constructed to restrict and control the flow of water during high magnitude flood events.

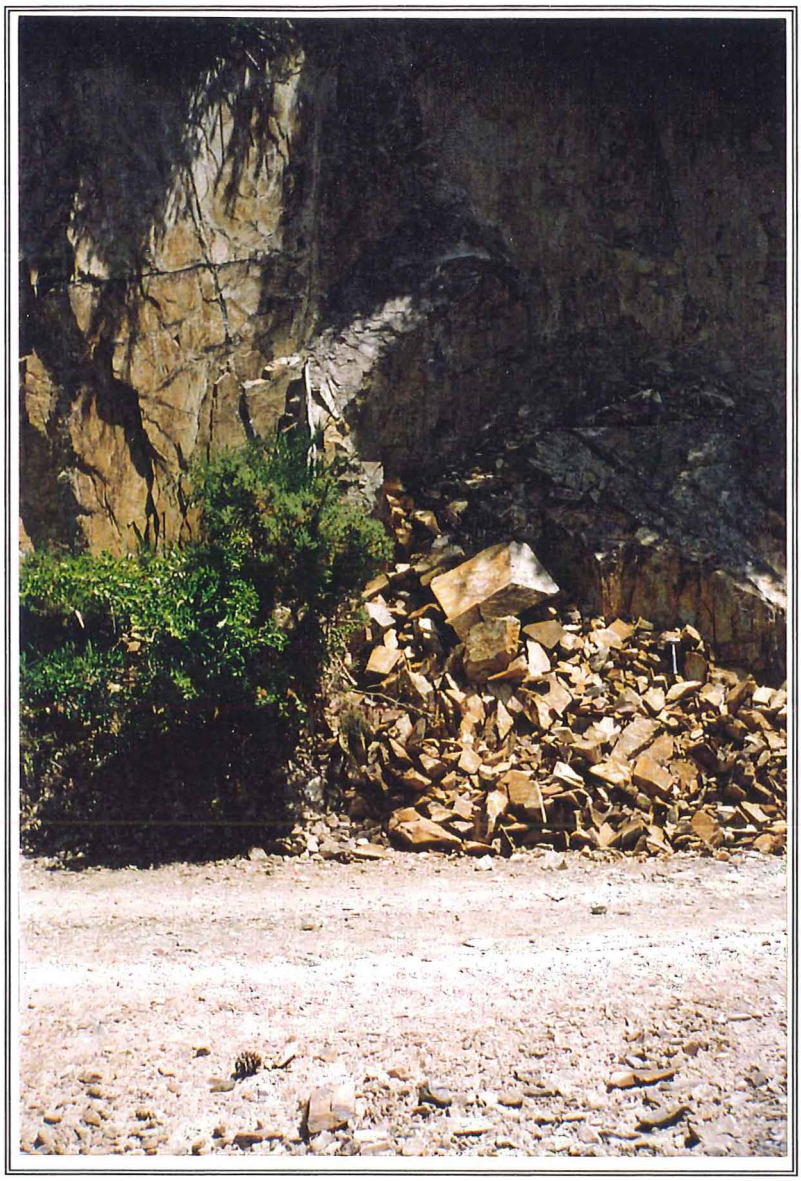

FIGURE 6.21. A Photograph and sketch of a wedge failure on the forestry road above the Port Underwood Road in Whatamango Bay. Stereographic interpretation in given in FIGURE 6.22.

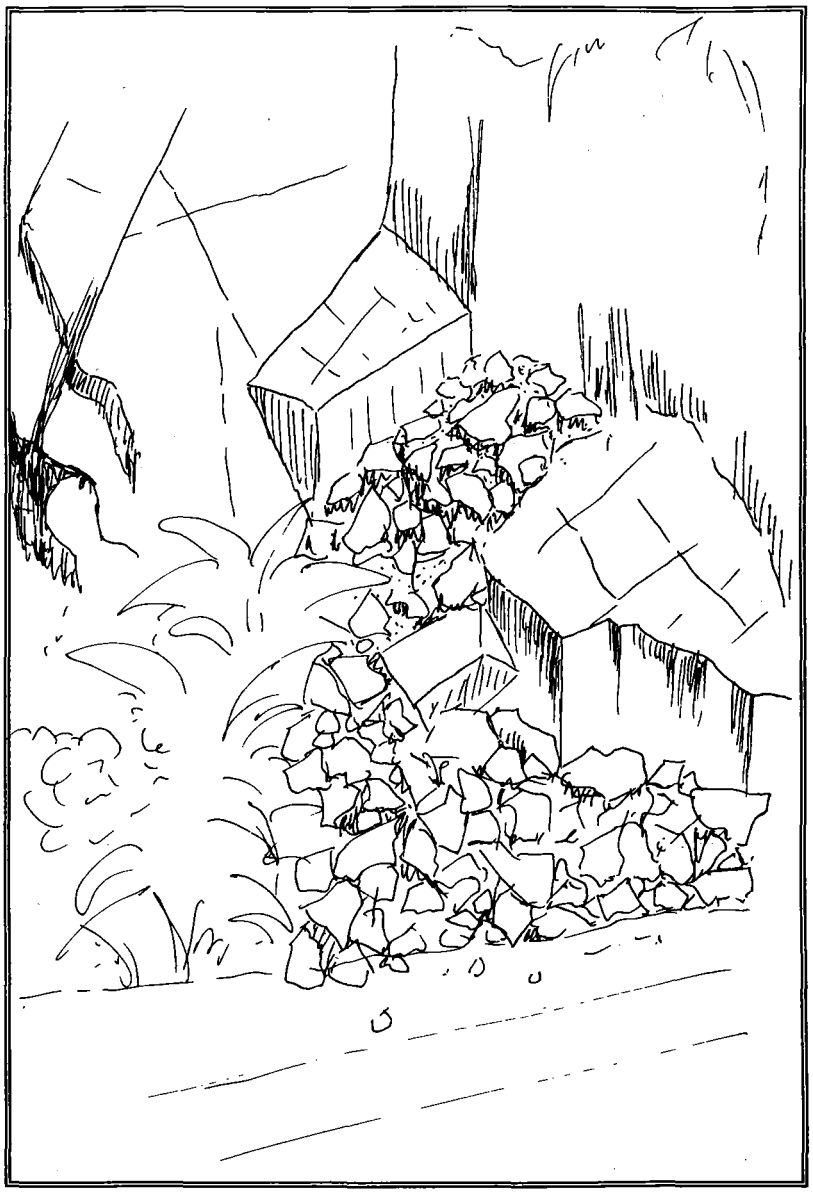

FIGURE 6.21 (ctd.).: Schematic representation of wedge failure.

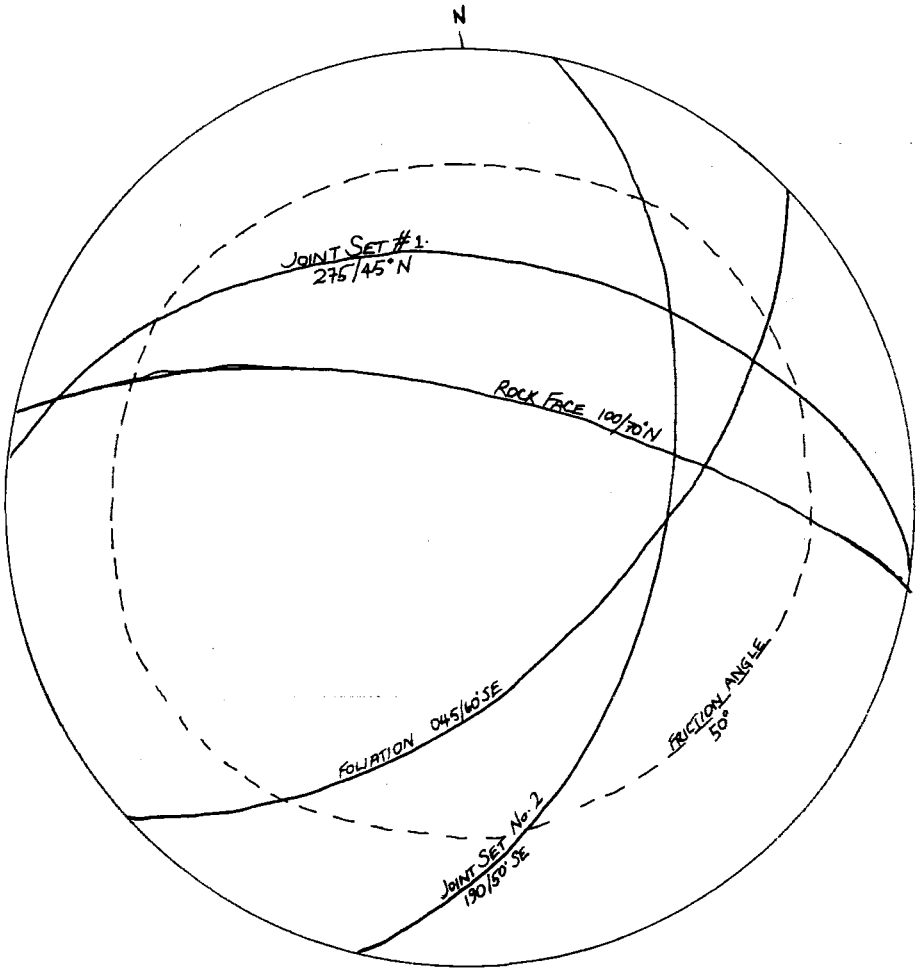

FIGURE 6.22. The failure of blocks in heavily jointed schistose rock near to Karaka Point along the forestry track. The stereoplot indicates that a failure angle below 50° will result in wedge failure.

6.6. SYNTHESIS

The hazard zonation used in this study is an adaptation of the Geotechnical Area Studies Program (GASP) physical constraints map and the hazard mapping by Horrey (1989). The mapping produced from the hazard zonation studies uses the information presented on the engineering geology map (Figure 5.3.; Map Volume) to assess the degree of constraint to urban development in relation to the active geological processes operating in the field area. The scale of the mapping is the same as the engineering geology map, 1:5,000, which is considered suitable for the feasibility/pre-feasibility or design stages of an investigation, and which provides continuity from the engineering geology to the hazard assessment. The engineering geology map presents the distribution of the bedrock and surfical units in the field area and indicates the geomorphic features which are subsequently quantified by the hazard mapping. The hazard assessment uses four categories of hazard ranging from high hazards through moderate and low hazards, to negligible hazards. The extent of each hazard zone is further qualified by the geological process which imposes the hazard, for example slope failures and inundation/siltation processes. The zonation of the field area is made on the basis of magnitude, frequency and affected area of the geological processes and the degree of hazard is represented by a stoplight colouring system.

The development constraint assessment of the field area uses the hazard mapping to determine the degree of geotechnical limitations imposed at any locality, and the nature of the geotechnical investigations required for further urban development. The development constraints map is also amended from Horrey (1989) and the Geotechnical Land Use Map (GLUM) of the GASP analysis. Unlike the GLUM system, which is derived from the terrain classification map, the development constraint evaluation in this study uses the information from the hazard mapping and as such is similar to the methodology proposed by Horrey (1989). Development constraints are divided into four categories which reflect the geotechnical limitations, for example Class IV includes areas of extreme geotechnical limitation to urban development while Class I is essentially devoid of geotechnical limitations. As with the hazard mapping a colour classification system is used to distinguish between the varying degrees of geotechnical limitations. The development constraint map is also produced at 1:5,000 scale covering the entire field area and correlating with the engineering geology and hazard zonation maps. The types of geological processes which impose the hazard and geotechnical constraint in the field area are represented on the maps using a simple lettering system. Each geological process is assigned a representative letter which is used to identify areas prone to a particular process on the map. The use of upper case letters indicates that the process

corresponds to the highest hazard or constraint in that area. Lower case letters represent processes which have a lesser degree of hazard or a lesser degree of geotechnical constraint.

Both the hazard zonation and the development constraint classification developed in this study are considered to be applicable to other areas within the Marlborough Sounds and throughout New Zealand. The proposed development options for the field area involve substantial areas of further urban development, with several subdivision applications already having been submitted to Council. The field area contains substantial areas of high hazard and also Class IV geotechnical limitations, particularly in relation to surficial slope failures and active debris fans and although these areas are not necessarily impossible to develop, they would certainly require considerable geotechnical investigations and hazard mitigation which are very costly. The areas most suitable for development are those zoned as having Class II geotechnical limitations although many of the Class III areas may also be suitable for urbanisation. Consideration should be given to the density of development, particularly housing in the field area because although many areas may support one or two houses on a potentially unstable slope, greater intensity development would undoubtedly cause slope failures. In all cases vegetation removal should be discouraged and in developed areas the disposal of stormwater must be carefully managed to avoid initiation or aggravation of potentially damaging geological processes. If development of the land in the field area is carefully controlled the area will remain a valuable and productive resource.

CHAPTER SEVEN SUMMARY AND CONCLUSIONS

7.1. PROJECT OBJECTIVES

This study was effectively subdivided into two distinct areas; structural geology and engineering geological investigations leading to hazard assessment and development constraints. The following discussions summarise the main points from each of the areas studied in this investigation and concludes with recommendations for future work and subsequent investigations.

The principal objectives of the structural component of this study were related specifically to the Waikawa Bay Fault located to the east of Waikawa township. The objectives are listed below:

☺ Determination of what happens to the eastern extensions of the Picton and Old Freezing Works Thrusts identified by Nicol (1988) in the Picton region

☺ Determine the relationship of the Waikawa Bay Fault, which has an opposing dip and contrasting style, to the thrusts identified in the Picton Thrust System.

☺ Provide constraint on the location and extent of th Waikawa Bay Fault north of the obvious topographic expression in Waikawa.

☺ Using geomorphic, geophysical and subsurface information attempt to constrain the age and nature of the last rupture of the Waikawa Bay Fault.

The engineering geological component of the study was principally concerned with the formulation of a hazard assessment procedure and the application of the procedure to the field area. Additionally, the production of a development constraint mapping method for potential urban development in the field area was a principal objective. The objectives for the engineering geological study are presented below.

☺ Using aerial photograph interpretation, field mapping and limited laboratory testing, determine the geotechnical properties and the extent of both bedrock and surficial units in the field area. The extent of the bedrock and surficial units combined with geomorphic and major structural features is presented on an engineering geology map at 1:5,000.

☺ From the engineering geology investigations, an assessment of the geological hazards in the field area which are posed by active geological processes in the field area such as erosion, slope failures, and flooding, is represented on a hazards map also at a scale of 1:5,000.

☺ The production of a development constraint map at 1:5,000 for potential urban development in the field area to delineate those areas which are subject to extreme, substantial, moderate and low geotechnical constraints.

7.2. STRUCTURAL GEOLOGY AND GEOMORPHOLOGY

7.2.1. Stratigraphy

The Marlborough Sounds are principally composed of the Pelorus Group greywackes which are unfoliated greywackes and argillites correlated with the Caples Terrane rocks in Otago, and the Marlborough Schist. The Pelorus Group greywackes are Late Permian unfoliated volcanically derived sedimentary rocks and are generally considered to grade into the Marlborough Schist which increases in metamorphism towards the south east. The Marlborough Schist is generally thought to be chlorite zone schist ranging in texture from TZIIa and TZIIb to TZIV. Although the contact between the greywacke and schist is considered to be gradational, the schist is often in faulted contact with the greywacke throughout the Marlborough Sounds. The age of metamorphism is now considered to be Late Jurassic-Early Cretaceous and based on the dating of correlative rocks in the Otago and Southland regions.

Terrane correlations are difficult particularly with respect to the presence or absence of a Torless protolith in the south eastern Marlborough Sounds and there are currently two theories explaining the terrane affilitations in the Sounds. The traditional view was the presence of Caples Terrane correlatives in the Marlborough Sounds with Torlesse Terrane rocks either underthrust beneath the Caples rocks, or being absent altogether. An alternative view was proposed by Mortimer (1993) in which the south eastern Marlborough Sounds are correlated with the Waipapa Terrane and separated from the Caples Terrane rocks by the Picton Fault Zone.

7.2.2. Structural Features

The structural characteristics were studied by dividing up the field area into a set of fault bounded domains which included The Snout Domain, Karaka Point Domain and the Green Bay Domain which in turn were compared with the Picton Domain as studied by Nicol (1988). The Picton Domain is dominated by a series of thrust faults which constitute a west to east transport direction with the Shakespeare Bay Thrust identified as the youngest fault in the thrust stack (Nicol, 1988). Previous studies of the Waikawa Bay Fault had identified the structure as an anomalous feature when compared to the Picton Thrust System and the structural investigations in this study revolved around determining the nature and kinematics of the Waikawa Bay Fault and related structures.

Within the field area there were three deformational phases identified in each of the structural domains. The first phase (D1) involved a syn-metamorphic compressional event which resulted in a set of folded structures (F1) with a consistent strike to the NE and was identified in all domains. In association with the formation of F1 folds was the development of an axial planar cleavage (S1) which indicates that the folding was most likely syn-metamorphic.

of F1 folds was the development of an axial planar cleavage (S1) which indicates that the folding was most likely syn-metamorphic.

The second deformational episode (D2) principally involved the onset of thrust faulting in the field area and is thought to have occurred during the Miocene. Thrust faulting in the Picton Domain and The Snout Domain was dominated by westward dipping thrust faults which transported foliated schistose material over the unfoliated greywacke and Tertiary sediments now exposed in Picton Harbour (Nicol, 1988). D2 thrust faulting in the Karaka Point Domain is seen in the initiation of the Waikawa Bay Fault. Coincident with the development of thrusting along the Waikawa Bay Fault in the Karaka Point Domain was the production of kink folding forming an F2 event. The Green Bay Fault is also thought to have been initiated during the D2 period.

The final deformational phase identified in the field area (D3) is principally concerned with a post thrusting cross folding event (F3), most apparent in the Picton Domain and inferred in The Snout Domain. Cross folding ((F3) is not observed in the Green Bay Domain however it is thought that this may be a function of the limited data rather than an absence of cross folding altogether. In the Karaka Point Domain cross folds have a considerably shorter wavelength than the folds observed in the Picton and The Snout Domains.

Identification of the Waipapa Terrain is not possible given the limited data however there were structural features which suggested that the structure of parts of the south eastern Marlborough Sounds are different either side of the Waikawa Bay Fault. It may be that the Waikawa Bay Fault and the Green Bay Fault represen a thrust system dipping towards the east and over thrusting the rocks in the Picton Domain. The inferred presence of the Whatamango Bay Fault may indicate that transform faults are separating lobes of the easterly dipping thrusts.

7.2.2. Geomorphic Chronology

The geomorphic history of the field area in this study is principally related to climatic changes influenced by glacial advances to the south and south west of the Marlborough Sounds during the Late Quaternary. Periglacial climates in the field area have seen considerable devegetation of the slopes and the development of significant amounts of colluvial material from mass wasting of the slopes during dominantly mechanical weathering. The oldest deposit identified in the field area is the Wo alluvial terrace which has a minimum depositional age equivalent to the Waimean Glaciation (250-120ka BP). The surface of the fan has been modified by red weathering which is thought to have last occurred during the Oturian Interglacial period (120-80ka BP). Remnants of the Wo terrace can be found on both sides of Waikawa Stream, although the terrace has since been substantially eroded

and modified. During the Oturian Interglacial the base sea level rose and the slopes became more vegetated causing downcutting of the alluvial gravels of the Wo terrace and with the onset of the Otiran Glaciation (80-10ka BP) Waikawa Stream began to aggrade once more forming the W1 alluvial terrace which is believed to be present in the Graham River also.

Following the main interstadial period during the Otiran Glaciation the eastern slopes of Waikawa Stream were modified by large debris and alluvial fans aggrading to same level as the W1 terrace. The oldest debris fan of the Maori Cemetery debris fan complex is thought to have been deposited between 25-18ka BP and following its deposition the last movement of the Waikawa Bay Fault is thought to have occurred uplifting the eastern side of the fault relative to the west. Subsequent deposition of debris material and alluvium as fans north and south of the oldest identified fan occurred between approximately18-10ka BP, and the fault scarp was eroded and then covered by the younger Maori Cemetery debris fans and the Rimu Terrace Fan.

During the Otiran Glaciation there was also significant slope failures which have defined the present day ridges observed in the field area and relict headscarps may still be identified. Sea levels began to rise again as the temperature climbed at the beginning of the present interglacial, the Aranuian Interglacial. The slopes in the field area have since been extensivelly re-vegetated and chemical weathering has again become dominant over mechanical weathering processes. Slope failures have occurred and are often related to devegetation of the slopes by natural and human induced burning by both Polynesian and European settlers. Sea level fluctuations have caused periodic degradation of the W_1 alluvial terrace in both Waikawa Stream and in the Graham River and the development of the W_2, W_3 and W_4 terraces with W_5 being the present day stream channel..

7.3. THE WAIKAWA BAY FAULT

7.3.1. Fault Nature

The Waikawa Bay Fault is classified as a vertical or steeply dipping oblique thrust fault which is upthrown on the eastern side. The eastern side of the fault is dominantly composed of schistose bedrock (TZIIa and TZIIb) which is thrust over unfoliated greywacke to the west. The age of thrusting is thought to be Miocene and related to thrusting which occurred in the Picton Thrust System at approximately the same time. The Waikawa Bay Fault is currently only observed in the oldest of the Maori Cemetery debris fans and is inferred to continue south across Waikawa Stream, along Milton Terrace and into Picton where it joins the faults of the Picton Thrust System at the Elevation. To the north the fault is thought to splay, with one splay believed to continue into Waikawa Bay and strike parallel but offshore from the coast

to Karaka Point. Structural analyses indicate that there may be another splay of the fault which has not ruptured the surface and this blind thrust strikes parallel to the offshore splay and is inferred beneath Fault Bay south of Karaka Point.

The age of last rupture along the Waikawa Bay Fault has been previously interpreted as occurring within the Late Holocene (Horrey, 1989), and also not less than 80ka BP (McManus, 1994). This study reassessed the relative ages of all geomorphic surfaces which have been affected by faulting or have modified the fault scarp, and a new age of rupture of 18-12ka BP has been determined. The activity of the Waikawa Bay Fault is therefore considered to be Class III active, the least active of those faults which are expected to rupture again.

7.3.2. Geophysics

Geophysical investigations of the Waikawa Bay Fault were used to determine the northern and southern extent of the fault from the known scarp in the oldest Maori Cemetery debris fan. Both transient electromagnetism (TEM) and ground penetrating radar (GPR) were used with varying degrees of success. The TEM stations, approximate $80m^2$ square and rectangular loops, were located close to and distal from the known fault trace. The two stations located close to or on the trace, WAIK100 and WAIK200 indicated the presence of a structure which is interpretated as being the fault while the other two stations were contaminated by cultural detail causing consideral noise.

GPR traverses across the fault trace were more successful in identifying the Waikawa Bay Fault at depth. Three GPR lines were completed; Line 1 located north of the trace, Line 2 crossed the known scarp and Line 3 was located to the south. The fault was identified in all of the GPR lines although the Waikawa Bay Fault was more accurately described as a faulted zone as splays of the fault were observed in all of the traverses either side of the inferred of actual fault trace. From the GPR survey the Waikawa Bay Fault is thought to be a zone of faulting which is at least 100m wide and possibly considerably more.

7.3.3. Subsurface Investigations

Trenching and augering were used in a previous study (McManus, 1994) and were analysed in this study to determine the nature of the faulted zone associated with the Waikawa Bay Fault. Trenching across the fault identified no obvious disruption of the debris fan gravels, however the depth of the trench was only 3m and possible reworking of the fan or dissipation of displacement at depth within the gravels is thought to be responsible. Trenching further south on a bedrock ridge covered by landslide debris identified the complicated nature of the faulted zone. Discontinuous lenses of both schist and greywacke were observed in the faulted zone

within approximately 100m across the inferred fault trace, although schist was dominant to the east and greywacke to the west of the fault outside of the faulted zone.

Hand augering involved the drilling of 32 holes to a maximum depth of 3m in the vicinity of the inferred fault trace and supported the information obtained from the trenching. Augering was competed in areas which could not be trenched and showed that the lenses of schist and greywacke in the faulted zone were smaller, and that the shear zone is composed of a large number of discontinuous splays which cause dislocation of both schist and greywacke.

7.4. ENGINEERING GEOLOGICAL INVESTIGATIONS

7.4.1. Summary

The methodology for the engineering geological investigations in this study followed those presented by Bell and Pettinga (1983) and was primarly used to produce a terrane annalysis of the field area for the production of subsequent hazard and development constraint maps. The principal objectives of the study were to characterise the surficial and bedrock units from field investigations and the use of limited laboratory testing to determine the geotechnical characterists of the surficial and bedrock units. The terran analysis was presented in the form of an engineering geology map which inclued the distribution of the rock and soil and the geomorphic features identified in the field area. Aerial photographic interpretation, and engineering geological mapping of the field area were primarily used to obtain information for investigation in this study.

As part of the field investigation programme, insitu percolation rates were assessed to determine the range of infiltration rates for the field area. Additionally a hydrological investigation of the Graham River was also performed using a pressure transducer installed a the Port Underwood Road Bridge to determine the variation in flow of the river and compared to rainfall in the adjacent Boons Valley catchment.

Laboratory investigations were divided into tests for weathered bedrock characteristics and tests for the geotechnical properties of regolith and colluvial soils and both sets of tests were further subdivided for schist and greywacke bedrock types. The tests used to determine the properties of bedrock weathered to varying degrees involved the point load and NCB cone indenter strength tests from which unconfined compressive strength (UCS) values were calculated. The weathering grades used for strength testing were Grade II-Grade IV for both schist and greywacke while schistose bedrock was tested both parallel and perpendicular to foliation using the point load test. X-ray diffraction whole rock analyses were also performed and compared to

petrographic studies in order to determine any mineralogical changes in the bedrock material with increased weathering.

Soil material, including colluvium, regolith and red weathered regolith were subdivided into schist-derived and greywacke-derived material for testing of geotechnical characteristics. Grain size testing was performed on all samples in order to determine textural differences between the soil types and between soils from different bedrock origins. Both sieve and pipette analyses were used. Atterberg Limits were determined for the same samples tested for grain size using the cone penetrometre to obtain Liquid Limit values and the related Plasticity Index and Activity parameters were also calculated. The erosive properties of the soils were tested using both the pinhole erosion test and the Crumb test while the strength of selected samples were tested using the ring shear testing device to determine the residual friction angle (ϕ_r). Clay mineralogy of all the soil samples was determined using XRD of orientated samples at 9phi and kaolinite and illite were identified as the principal clay minerals. XRD was compared with the results obtained from the scanning electron microscope and the results determined from Atterberg Limit Activity data.

7.4.2. Conclusions

a)Field Investigations

The percolation data obtained from the Marlborough District Council indicated that there is a considerable range of infiltration rate values for the soils of the field area. Favourable infiltration rates for the installation of septic tank and evapotranspiration systems were obtained from regolith and colluvial soils which had moderate clay percentages and which were of substantial thicknesses (>1m). Other locations in the field area indicated that percolation rates were unfavourable in soils high in clay content which restricts the drainage of effluent, and in thin soils overlying gravels or fractured bedrock which causes the effluent to drain away before purification of the liquid can be completed.

Hydrological investigations showed that the Graham River displays a lag time of less than 12 hours between a rainfall event and a peak flow event at the Port Underwood Road Bridge. The runoff percentage calculated for the catchment area was approximately 40%, while approximately 2days are required for the Graham River to return to base flow level following a high flow event. It appears that the Graham River is also prone to 'flash flood' events which may occur at any time of the year.

b) Weathering Grades

Strength characteristics of greywacke and schist which has been weathered to varying degrees indicates that the greywacke has a higher unconfined compressive

strength than the schist at the same weathering grade while schist which is loaded parallel to foliation is also identified as being weaker than the schist loaded perpendicular to foliation. UCS values calculated from the point load test were overestimated for the schistose material while the UCS values calculated from the cone indenter number overestimated the strength of both greywacke and schist at higher weathering grades.

The mineralogical characteristics of each rock type did not appear to differ with changes in weathering grade. The principal minerals identified using whole rock XRD and petrographic analysis were quartz, albite feldspar and muscovite with some samples containing clinochlore a close relative of chlorite.

c) Regolith

Textural trends identified in regolith samples were complicated by the presence of clay aggregates in all of the samples tested which provided inaccurate grain size calculations, particularly of the clay fraction which has significant implications for the Activity of the soils determined from Atterberg Limit testing. It is thought that regolith soils, which were classified in the field as silty clays and reclassified by grainsize analysis as sandy silts with some clay, may contain up to 50% clay contained principally as clay aggregates in the sand and silt fraction, and therefore the clay percentages determined by grain size analysis are considered as minimum values only.

Atterberg Limit data showed that the regolith samples had higher Liquid and Plastic Limit values compared to colluvial soils with very little difference between greywacke-derived and schsit-derived regolith samples. Calculation of the Plasticity Index for the regolith material classified the soil as moderately plastic silts and clays when plotted on the Casagrande Plasticity Diagram.

The mineralogy of the regolith samples was primarily determined using XRD and complemented by SEM information and Activity values corrected for clay content due to the clay aggregate problems. XRD identified the presence of quartz, kaolinite, illite and some chlorite while the schist-derived samples contained a complicated interstratified illite-chlorite clay. The interstratified clay was identified in one greywacke-derived sample. SEM identified the presence of both the kaolinite and illite clay minerals in the regolith samples and also showed that the samples have a moderate to high sodium content. The origin of the sodium is inferred to be from salt spray and may influence the erosive qualities of the soil in the field. When tested in the laboratory all of the regolith samples were classified as non-erosive to slightly erosive using the pinhole and Crumb tests. Activity data, when ammended for clay aggregate problems identified the presence of kaolinite and illite clay minerals in the regolith samples using the classification of Skempton (1953) rather than illite and

montmorillonite estimated using the unmodified activity data and original clay percentages.

The shear strength of regolith was tested using the ring shear device and a residual friction angle (ϕ_r) of 21° was obtained. The regolith samples are thought to be affected by the presence of clay sized quartz fragments which impart a granular influence on the soil and thus increasing the shear strength. Additionally the presence of clay aggregates is thought to increase the shear strength of the regolith by also acting as a granular influence.

d) Colluvium

The problems encountered in the regolith sample concerning inaccurate grain size analysis due to clay aggregates in the silt and sand fraction were also identified for the colluvial material. Colluvium was texturally different from the regolith material by the presence of up to 20% gravel which was not identified in the regolith samples. Colluvium was classified as gravelly silty clays in the field while laboratory testing classified the material as gravelly silty sands with some clay confirming the influence of the clay aggregates. Up to 50% of the sample is inferred to be composed of clay principally contained in the sand and silt fractions. There did not appear to be any textural variations between greywacke-derived and schist-derived colluvium.

Although Atterberg Limit testing identified that the colluvial soils have lower Plastic and Liquid Limits compared to the regolith material there was little variation between greywacke colluvium and schistose colluvium. Plasticity Index calculations identified the collvuial material as moderately plastic principally composed of silts and clays as defined by the Casagrande Plasticity Diagram. As with the regolith soils, the Activity values were affected by inaccurate clay percent estimates and therefore ammended clay percentages were used to determine the mineralogy of the samples from Activity. Activity was used to compliment the data obtained using XRD and SEM.

The XRD clay mineral analysis of the colluvial samples identified the same trends as seen in the regolith material. The dominant minerals present were quartz, kaolinite, illite, some chlorite and the interstratified illite-chlorite clay present in all of the schist-derived samples and some of the greywacke samples. As identified in the regolith material, SEM studies of colluvium confirmed the presence of kaolinite and illite clay minerals, and high to moderate levels of sodium. Again, the presence of sodium is thought to represent the influence of salt spray. Ammended Activity data identified the presence of kaolinite and illite using the Skempton Classification (1953).

e) Red Weathered Regolith

Due to the unusual properties of the red weathered regolith material in the field area, the soil was analysed separately from the other regolith samples. Red

regolith in this study was derived from greywacke bedrock as there was no schist-derived red weathered regolith identified in the field area.

Red weathered regolith was more severely affected by clay aggregates than the other soil samples in this study with up to 90% of the soil thought to be composed of clay although the grain size analysis yielded only 17% clay. The red soils are classified in the field as slightly silty clays while grain size analysis classified the material as clayey silts with some sand and the red weathered regolith samples were completely devoid of gravel sized clasts.

Atterberg Limits indicated that the red regolith material had different properties to the other soils tested in the field area. Although the Plastic Limit values were similar to those obtained for other samples, the Liquid Limits values were considerably higher. Plasticity Index calculations indicated that the red weathered soils were more plastic than the remaining regolith and colluvial soils and the material was classified as highly plastic using the Casagrande Plasticity Diagram. As with the other samples tested Activity values were estimated using ammended clay percentages as the original values were anomalous with the other characteristics of the soils.

Mineralogy, as for the other regolith and colluvial soils, was determined principally using XRD and complemented by SEM and Activity data. XRD confirmed that the red weathered regolith was greywacke-derived material due to the absence of the interstratified illite-chlorite clay mineral which was previously interpretated as being exclusive to schistose material. Other principal minerals were kaolinite, quartz, illite and also imogolite which is a clay mineral generally associated with soils containing volcanic glass. The regolith samples in this study are thought to represent surfaces which have been modified by a thin layer of volcanic ash most likely derived from volcanic eruptions in the North Island prior to or during the development of red weathered profiles in the field area. SEM identified the presence of kaolinite and illite and the high to moderate sodium content found in the other soil samples. Again, the sodium is believed to be derived from salt spray affecting the soil in the field area. Activity values using ammended clay percentages identified the presence of kaolinite clays rather than the presence of montmorillonite found using the original clay percentage data.

7.5. HAZARD ZONATION

7.5.1. Background

The principal legislation behind the assessment of geological hazards in the Marlborough Sounds are the Resource Management Act 1991 and the Building Act 1991. Both of these pieces of legislation require the identification and collection of information regarding areas of slope instability, erosion, flooding and other

geological hazards for the purposes of issuing resource concents and building permits.

The term hazard is defined in this study as 'one or more natural or human induced landscape modification process* of varying duration, which have the potential to cause loss of life, injury, or property/infrastructure damage within or adjacent to a given human community. Natural hazards have a specified magnitude, return period and affected area. *Earthquakes, tsunami, erosion, volcanism and geothermal activity, landslip, subsidence, sedimentation, wind, drought, fire, flooding, rock fall and avalanche'.

7.5.2. Hazard Mapping

The hazard mapping in this study is a modification of the physical constraints maps developed by the Geotechnical Area Studies Program (GASP) in Hong Kong, and attempts to quantify the information presented in the terrain analysis which is the engineering geological mapping in this study. The scale of mapping is 1:5,000 and covers the same area as the engineering geology map. Quantification of geological processes as geological hazards requires an assessment of the magnitude, frequency and affected area of each process at any given location and in this study assumes future urban development within the field area.

Hazard mapping uses a colouring classification scheme representing the highest degree of hazard imposed on any one area and is qualified by a lettering system representing the type of geological process or processes affecting that area. The colouring system uses a hierachy of colours called the stoplight system which uses red to delineate areas of highest hazard through yellow and green, to blue which represents negligible hazard. The lettering system uses uppercase letters to represent those processes which are dominant in an area and lower case letters for subsiduary geological processes.

The data base used for the hazard zonation in this study involves the use of aerial photographs of the field area the earliest of which is 1959 and extend to 1993. The activity of particular processes is assessed using the aerial photographic data base and in general any process which has been active within the 36 year time frame of the photographs is considered to be high hazard. Those processes which have been active outside of the aerial photographic data base but which have been active within the last 100 years, the historical data base, are considered to be of moderate hazard. Processes which have been active outside the historical data base or which are not considered to have substantial impact on urban development are considered to be of low hazard. Areas of negligible hazard are those which are not subjected to any identifiable threat from any particular geological process.

7.5.3. Hazard Zonation

The hazard zonation approach in this study attempts to quantify the degree of hazard imposed by particular geological processes using the magnitude of the process, the regularity with which a process of a particular magnitude is expected to occur, and the area affected by a particular process of a particular magnitude. Hazard zones are subdivided into high hazard, moderate hazard, low hazard and negligible hazard and these degrees of hazard are assessed for each of the assessed geological processes substantially modifying the field area. The principal active processes identified in this study are slope failures, flooding, stream bank erosion, and debris deposition, with tunnel gullying and seismicity also identified, but due to difficulties in quantification, are not zoned in this study.

7.6. DEVELOPMENT CONSTRAINTS AND LAND USE PLANNING

7.6.1. Development Constraint Mapping

The assessment of development constraints for the field area is the final step in the hazard assessment study and uses the information from the hazard mapping presented earlier in this study. Development constraints in this study are considered to be correlatives of the Geotechnical Land Use Map (GLUM) from the GASP methodology which attempts to assess the land for the suitability of future urban development. However in the GASP system the GLUM is derived from the terrain analysis whereas in this study the development constraints follow on logically from the hazard mapping rather thant the engineering geological investigations. As with both the engineering geology mapping and the hazard mapping the scale of the development constraint map is 1:5,000. However, at a 1:5,000 scale the development constraint assessment is not adequate to replace geotechnical investigations of individual building sites, rather it is to be used as an indication of the expected conditions and the type of investigation which may be necessary.

Mapping of development constraints is similar to that developed for the hazard mapping and uses both the colouring and lettering system. The stoplight colouring system is not used to avoid confusion with the hazard maps, and for consistency the lettering system representing geological processes is the same as that used for the hazard assessment.

7.6.2. Development Constraint Zonation

Four development constraint zones are used in this study and each represents a different degree of constraint and the requirement of a different type of investigation prior to additional urban development. Class IV represents extreme geotechnical limitations for urban development and extensive and detailed site

investigations at both the subdivision and construction stages is recommended. Class IV land is often associated with high hazard zones and the land is generally unsuitable for urban development without substantial hazard mitigation and remedial measures being emplaced. Often the cost of developing Class IV land is high enough to preclude this land from future urbanisation.

Class III development constraints constitute significant geotechnical limitations for urban development and may include areas of both moderate and low hazard. Land zoned as Class III requires extensive site investigations at both the subdivision and construction stages however this land is generally suitable for development following the construction of moderate mitigation measures, for example retaining walls. Both subsurface investigations and limited laboratory testing is recommended for such sites to determine the geotechnical characteristics of the material on site.

Land classified as Class II has low geotechnical limitations to development and is generally favourable for urbanisation. These areas still require extensive site investigations for construction purposes however for subdivision consents the degree of investigation required is less extensive, for example 1:1,000. Land included in Class II zonations is generally of low and moderate hazard zonation.

Class I land, that which has no geotechnical limitations is the most favourable for urban development. Essentially land classified as Class I is not affected by active geological processes and is generally associated with negligible hazard zones. The type of geotechnical investigations for such sites will involve little more than a walkover inspection and remedial or mitigation measures are deemed unnecessary and unfortunately, Class I land in the field area not very extensive.

7.7. FURTHER WORK

7.7.1. Structural and Geomorphic Investigations

The following are recommendations for additional investigations concerning the structural geology and the geomorphic evolution of the field area and the Marlborough Sounds in general.

- ☺ A detailed structural analysis of the Green Bay and Karaka Point Domains is needed to determine any structrual characteristics which may be attributed to the presence of the Waipapa Terrane in the south eastern Marlborough Sounds.
- ☺ Further work is required on the nature and extent of the Waikawa Bay Fault with respect to its inferred nature as a basal thrust for a more extensive thrust system which may involve the Green Bay Fault and the Whatamango Bay Fault as a transfer structure.

☺ More work is necessary on the nature and extent of red weathering as these red weathered surfaces are some of the most important geomorphic time indicators within the Marlborough Sounds.

7.7.2. Engineering Geological Investigations

Several problems were encountered when investigating the engineering geological properties of the bedrock and surficial units in the field area an further work is suggested below.

☺ Detailed analysis of the clay aggregates identified within the sand and silt fractions during grain size analysis is required to accurately determine the proportions of clay in the samples. Red weathered soils in particular appear to be affected by these clay aggregates and further work is suggested to discover why the clay aggregates are present. Furthermore more work may be required on the analytical methods for grainsize determination.

☺ A detailed investigation of the clay mineralogy of the soils in the field area would provide valuable information on the nature of the soils and may assist in assessing the problems associated with clay aggreagates in the samples.

☺ Continued work is recommended on the nature and mineralogy of the red weathered soils which have been identified as having considerably different characteristics to the other regolith and the colluvial soils. In particular an assessment is necessary as to the origin of the clay mineral imogolite in the red weathered samples as this may provide a constraint on the geomorphic development of red weathered surfaces should the mineral be derived for ash fall deposits.

☺ More work using the scanning electron microscope may be useful to delineate the structural characteristics of soil and possibly provide information on the shear strength of the different materials. Further detailed work is necessary regarding the shear strength of soils in the Marlborough Sounds.

7.7.3. Hazard Zonation and Development Constraint Mapping

Althought the hazard zonation and development constraint methodology used in this study has been developed and modified using a number of other methods, there are still several areas which require specific and detailed study.

☺ A detailed assessment of the seismic hazards in the field area, and within the whole Marlborough Sounds, is necessary to provide a complete geological hazard assessment.

☺ Investigation of the nature and extent of tunnel gully erosion may be required as these features are difficult to quantify in the field area. Such a study could be

combined with a detailed analysis of the erodibility and dispersive quality of the soils in the Marlborough Sounds for a complete hazard assessment.

☺ This study concentrated on the hazards and development constraints imposed by urban development in the field area. Further work is recommended on the possible effects of rural and industrial development such as forestry which has become a very important industry for the Marlborough Sounds.

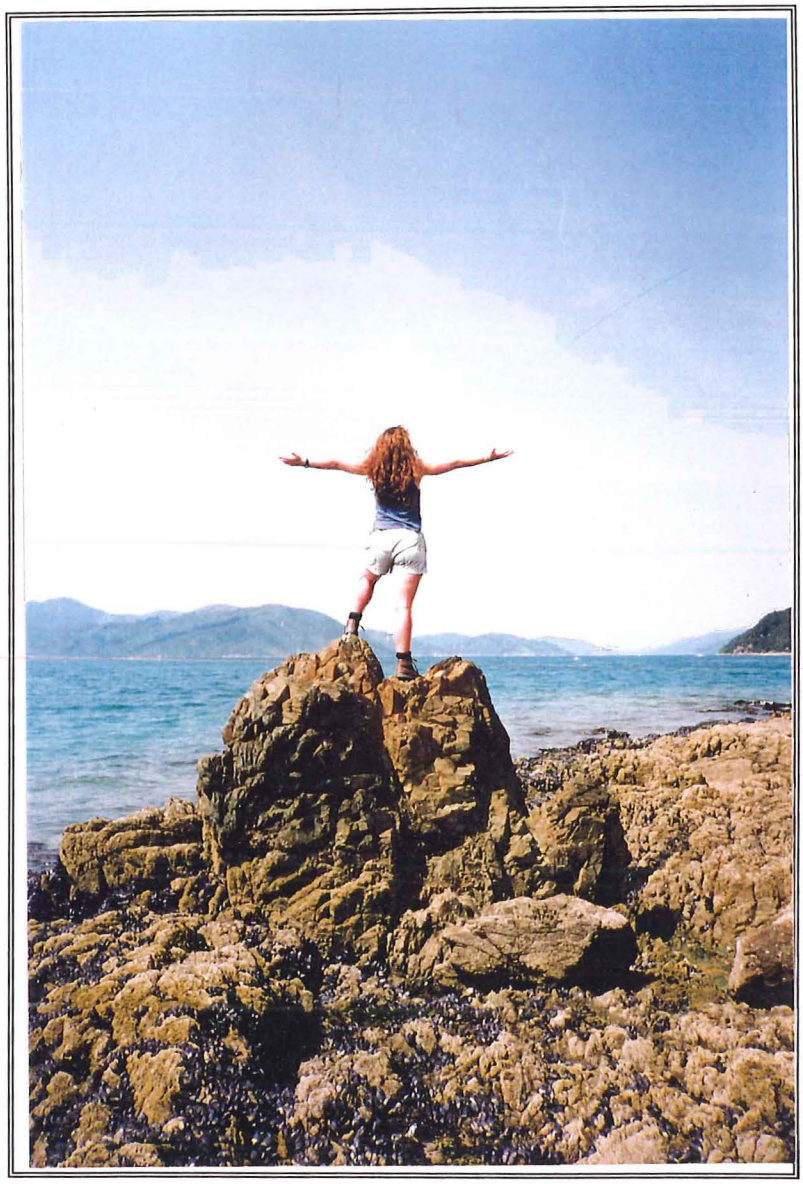

TAILPIECE

TA DAAA.....FINISHED!!!!

HASTA LA VISTA..... BABY!

REFERENCES

Allaby, A. and Allaby, M. (1991) The Concise Oxford Dictionary of Earth Sciences. Oxford University Press, Oxford. p410

Allen, R.E. (ed.) (1985) The Oxford Dictionary of Current English. Oxford University Press, Oxford: p889

Anderson, H. and Webb, T. (1994) New Zealand seismicity: patterns revealed by the upgraded National Seismograph Network. New Zealand Journal of Geology and Geophysics 37:477-493

Beck, A.C. (1964) Geological Map of New Zealand. DSIR. Marlborough Sounds. Map Sheet 14

Bell, (1993) Land Stability Moana View Road, Unpublished consultant report to the Marlborough District Council

Bell, D.H. (1992) Geology and Geomorphology of the Marlborough Sounds Area. IN: Natural Processes and Environmental Hazards in the Marlborough Sounds - Issues and Options. Sutherland, R.D.; Kirk, R.M. and Bell, D.H. (Eds.) Report to the Marlborough District Council

Bell, D.H. (1990) The Role of the Engineering Geologist in Urban Development. New Zealand Geomechanics News 41:22-31

Bell, D.H. and Pettinga, J.R. (1985) Engineering Geology and Subdivision Planning in New Zealand. Engineering Geology 22:45-59

Bell, D.H. and Pettinga, J.R. (1983) Presentation of Geological Data; Philosophy and methods of investigation used in New Zealand. Proceedings of the Symposium on Engineering for Dams and Canals, Alexandra, IPENZ 94(g):4.1-4.36

Bieniawski, Z.T. and Franklin, J.A. (1972) Suggested Methods for Determining the Uniaxial Compressive Strength of Rock Materials and the Point Load Strength Index. International Society for Rock Mechanics, Committee on Laboratory Tests, Document 1:12

Bishop, D.G.; Bradshaw, J.D. and Landis, C.A. (1985) Provisional Terrane Map of South Island, New Zealand. IN Howell, D.G.; Jones, D.L.; Cox, A. and Nur, A. (eds) Proceedings of Circum Pacific Terrane Conference. Stanford University Publications Geological Sciences 18

Bishop, D.G. (1972) Progressive Metamorphism from Prehnite-Pumpellyite to Greenschist Facies in the Dansey Pass area, Otago, New Zealand. Geological Society of America Bulletin 83:3177-3198

Boggs, S. (Jr.) (1987) Principles of Sedimentology and Stratigraphy. Merrill Publishing Company, Ohio. p784

Brand, E.W. (1988) Landslide Risk Assessment in Hong Kong IN Proc. of the 5th International Symposium on Landslides, Switzerland, Vol. 2:

Brindley, G.W. and Brown, G. (1980) Crystal Structures of Clay Minerals and their X-Ray Identification. Spottiswoode Ballantyne Ltd, London. p 495

Burrows, C.J.; Chinn, T. and Kelly, M. (1976) Glacial Activity in New Zealand Near the Pleistocene-Holocene Boundary in the Light of New Radiocarbon Dates. Boreas 5(2):57-60

Coates, D.R. (1981b) Geology and Society. Chapman and Hall, New York, 159p

Costa, J.E. and Baker, V.R. (1981) Surficial Geology - Building Within the Earth J Wiley and Sons, 1st ed. 498p

Deere, D.U. and Patton, F.D. (1971) Slope Stability in Residual soils. IN Proceedings of the 4th Panam. Conf. on Soil Mechanics and Foundation Engineering 1:87-170

Einstein, H.H. (1988) Landslide risk assessment procedure. Proceedings of the Fifth International Symposium on Landslides, 1075-1090

Esler, W.R. (1984) Aspects of the Quaternary Geology of the Marlborough Sounds. Unpublished B.Sc. (Hons) thesis, Victoria University, Wellington. p62

Fetter, C.W. (Jr.) (1980) Applied Hydrogeology. Charles E. Merril Publishing Company, Columbus. p 488

Gardenier, J. and Keey, R.B. (1991) Risk Assessment of Industrial and Natural Hazards. Proceeding of a Workshop for the Centre for Advanced Engineering. 191p

Gibbs, J.G. (1979) Late Quaternary Shoreline Movements in New Zealand. Unpublished Ph.D. Thesis, Geology Department, Victoria University of Wellington, New Zealand

Grainger, P. and Harris, J. (1986) Weathering and Slope Stability on Upper Carboniferous Mudrocks in South West England. Quaternary Journal of Engineering Geology 19:155-173

Grant, K. and Finlayson, A. A. (1978) The Assessment and Evaluation of Geotechnical Resources in Urban or Regional Environments. Engineering Geology 12:219-293

Grim, R.E. (1962) Applied Clay Mineralogy. Mcgraw-Hill Book Company, Inc. New York, p422

Grindley, G.W.; Harrington, H.J. and Wood, B.L. (1959) The Geological map of New Zealand 1:2,000,000. Bulletin of the New Zealand Geological Survey, 66:111

Hatherton, T. (1980) Shallow Seismicity in New Zealand 1956-75. Journal of the Royal Society of New Zealand 10:19-25

Hatherton, T. (1970) Gravity, Seismicity and Tectonics of the North Island, New Zealand. New Zealand Journal of Geology and Geophysics 13:125-144

Hector, J. (1872) Reports on Gold Mines in the Province of Marlborough. New Zealand Geological Survey Report on Geologic Exploration 1871-1872, 7: 119-129

Holmgren, G.G.S. and Flanagan, C.P. (1977) Factors Affecting spontaneous dispersion of Soil Materials as Evidenced by the Crumb Test IN Dispersive Clays, Related Piping and Erosion in Geotechnical Projects (Sherard, J.L. and Decker, R.S. , eds.) ASTM STP 623, American Society for Testing Materials : 218-239

Horrey, P.J. (1989) Engineering Geological Investigations and Hazard Assessment for the Picton, Waikawa and Shakespeare Bay Area, Marlborough Sounds. Masters Thesis, University of Canterbury, Christchurch: p170

Hutton, C.O. and Turner, F.J. (1936) Metamorphic Zones in northwest Otago. Transactions of the Royal Society of the New Zealand Geologic Society :405-416

IPENZ (1983) Engineering Risk; Report of the President's Task Committee on Professional Practice and Risk, Institute of Professional Engineers, New Zealand, Wellington. p95

Johnston, M.R. (1983) Geology of the Marlborough Sounds. Unpublished Report to the Marlborough Catchment Board.

Justice, T.R. (1994) Engineering Geological Investigations of Two North Canterbury Landslide Complexes. Unpublished M.Sc. Thesis, University of Canterbury, Christchurch: p174

Kingma, J.T. (1974) The Geological Structure of New Zealand. J Wiley and Sons, New York, 407p

Kingsbury, P.A. (1987) Engineering Geological Investigations, Havelock Area, Marlborough. Masters Thesis, University of Canterbury, Christchurch, 358p

Lambe, T.W. and Whitman, R.V. (1979) Soil Mechanics. John Wiley and Sons, New York: p553

Lauder, D.W. (1969) The ancient drainage of the Marlborough Sounds. New Zealand Journal of Geology and Geophysics 13:747-749

Lough, R. C. (1952) Disposal of Sewage from Farm Homesteads. New Zealand Department of Agriculture, Bulletin 322. p 14

May, D.; Waters, D. and Chanier, F. (1989) Miocene Thrust Faulting in the Southeastern Portion of the East Coast Deformed Belt. IN Recent Advances in East Coast Geology and Geophysics. A one-day review of current ideas and recent progress; Wednesday 31st May, 1989. New Zealand Geological Survey, Lower Hutt.

McKay, A. (1890) On the Geology of Marlborough and the Amuri District of Nelson. Reports of the Geological Survey, during 1888-1889, 20:85-185

McManus, S.T. (1994) An Engineering Geological Investigation of Waikawa Bay, Marlborough Sounds. Unpublished B.Sc.(Hons) Thesis, University of Canterbury, Christchurch. p169

Mortimer, Nick. (1995) Possible Large Displacements Between Eastern and Western North Island: Constraints from Greywacke Terranes? Geological Society of New Zealand Annual Conference Abstracts, Geological Society of New Zealand Misc. Publication 81A: p147

Mortimer, Nick. (1993a) Metamorphic zones, terranes and Cenozoic faults in the Marlborough Schist, New Zealand. New Zealand Journal of Geology and Geophysics 36:357-368

Mortimer, Nick. (1993b) Jurassic tectonic history of the Otago Schist, New Zealand. Tectonics 12(1):237-244

New Zealand Government (1991) The Building Act. New Zealand Government Publishers, Wellington

New Zealand Government (1991) The Resource Management Act. New Zealand Government Publishers, Wellington

Nicol, A. (1988) The Picton Thrust System. Masters Thesis, University of Canterbury, Christchurch, 125p

Nicol, A. and Campbell, J.K. (1990) Late Cenozoic thrust tectonics, Picton, New Zealand. New Zealand Journal of Geology and Geophysics 33:485-494

New Zealand Standards Association (1989) NZS 4402 Methods of Testing Soils for Civil Engineering Purposes: Part 1 Soil Classification and Chemical Tests

Pandian, N.S. and Nagaraj, T.S. (1990) Critical Reappraisal of colloidal Activity of Clays. Journal of Geotechnical Engineering. 116(2):285-296

Rahn, P.H. (1986) Engineering Geology: An Environmental Approach. Elsevier, New York, p 589

Reyner, M. (1989) New Zealand Seismicity 1964-87: an interpretation. New Zealand Journal of Geology and Geophysics 32:307-315

Saunders, M.K. and Fookes, P.G. (1970) A review of the relationship of rock weathering and climate and it's significance to foundation engineering. Engineering Geology 4:289-325

Selby, M.J. (1993) Hillslope Materials and Processes 2nd Edition. Oxford University Press, Oxford. p451

Skempton, A.W. (1953) The Colloidal 'Activity' of Clays. Proceedings of the 3rd International conference on Soil Mechanics and Foundation Engineering, Switzerland. 1:57-60

Small, R.J. and Clark, M.J. (1985) Slopes and Weathering. Cambridge University Press, London. p112

Stillwell, H.D. (1992) Natural Hazards and Disasters in Latin America. Natural Hazards 6:131-159

Suggate, R.P.; Stevens, G.R. and Te Punga, M.T. (1978) The Geology of New Zealand, Vol. I and Vol. II., Nelson and Marlborough, New Zealand Geological Survey, Wellington: P172-174

Sutherland, R.D.; Kirk, R.M. and Bell, D. (1992) Natural and Environmental Hazards in the Marlborough Sounds - Issues and Options. A report to the Marlborough District Council

Tanaka, J.M.C. (1981) Letters to the editor. Geotimes 26(12):12

Te Punga, M.T. (1964) Relict Red Weathering Regolith at Wellington. New Zealand Journal of Geology and Geophysics 7(2):314-339

Thorez, J. (1976) Practical Identification of Clay Minerals: A handbook for teachers and students in clay mineralogy. Institute of Mineralogy, Liege State University, Belgium: p90

Turner, F.J. (1935) Contribution to the Interpretation of Mineral Facies in Metamorphic Rocks. American Journal of Science, 25:409-421

Varnes, D. J. (1978) Slope Movement Types and Processes. in Landslides - analysis and Control, Chapter 2, (Schuster, R.L. and Krizek, R.J. eds). National Academy of Sciences

Varnes, D.J. (1984) Landslide Hazard Zonation - Principles and Practice. UNESCO, Paris: 63p

Vitaliano, C.J. (1968) Petrography and Structure of the South eastern Marlborough Sounds, New Zealand, New Zealand Geological Survey Bulletin 7: 40p

APPENDIX A.

TIME SCALES

A1 GEOLOGICAL TIME SCALES

Paleozoic

Mesozoic

Cenozoic

A2 QUATERNARY GLACIATIONS

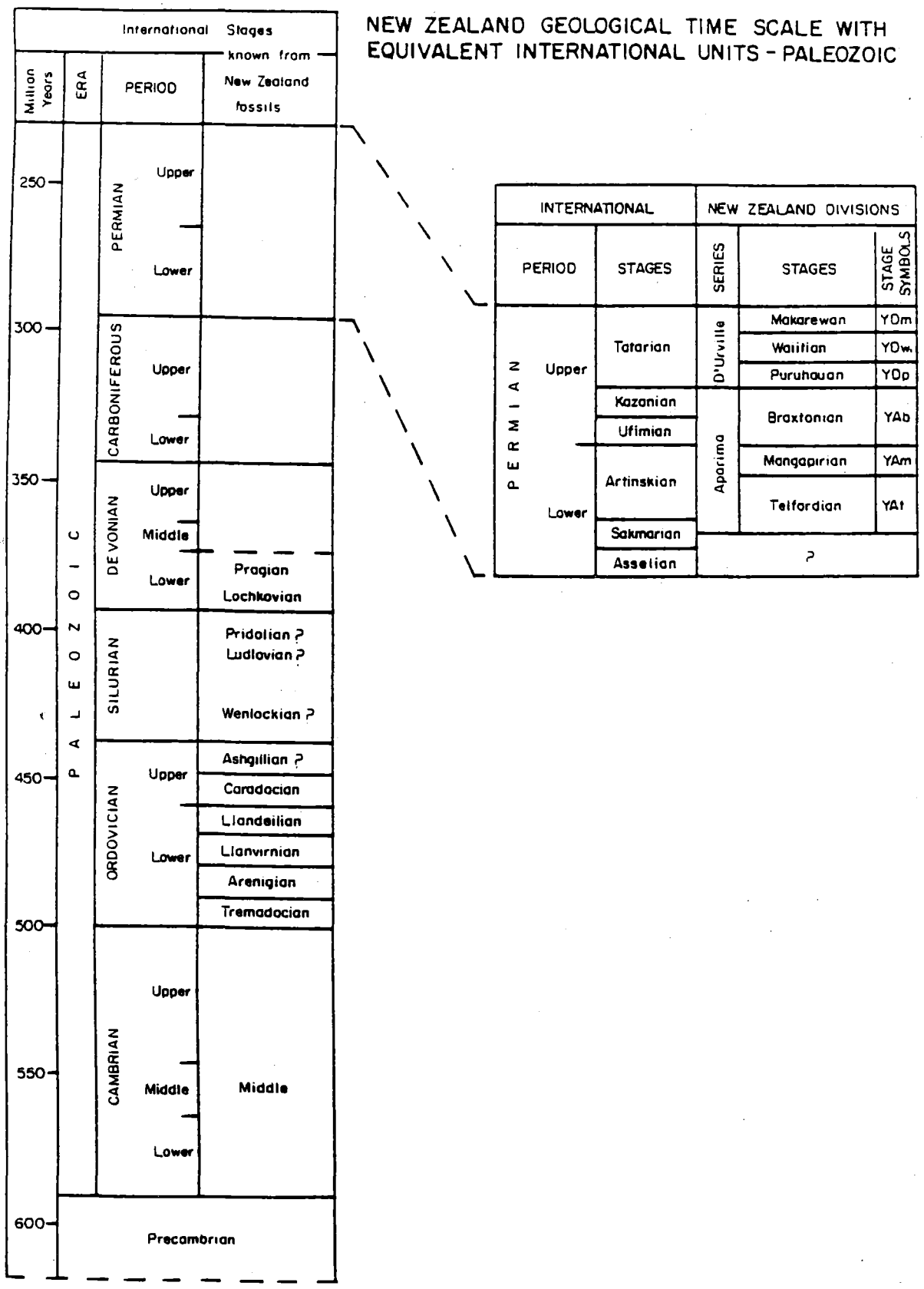
NEW ZEALAND GEOLOGICAL TIME SCALE WITH EQUIVALENT INTERNATIONAL UNITS - PALEOZOIC
International Stages known from New Zealand fossils
Million Years
ERA
PERIOD
250
300
350
400
450
500
550
600
PALEOZOIC
PERMIAN
Upper
Lower
CARBONIFEROUS
Upper
Lower
DEVONIAN
Upper
Middle
Lower
Pragian
Lochkovian
SILURIAN
Pridolian ?
Ludlovian ?
Wenlockian ?
ORDOVICIAN
Upper
Lower
Ashgillian ?
Caradocian
Llandeilian
Llanvirnian
Arenigian
Tremadocian
CAMBRIAN
Upper
Middle
Lower
Middle
Precambrian
INTERNATIONAL
NEW ZEALAND DIVISIONS
PERIOD
STAGES
SERIES
STAGES
STAGE SYMBOLS
PERMIAN
Upper
Lower
Tatarian
Kazanian
Ufimian
Artinskian
Sakmarian
Asselian
D'Urville
Aparima
Makarewan
Waitian
Puruhauan
Braxtonian
Mangapirian
Telfordian
YOm
YOw
YOp
YAb
YAm
YAt
?

NEW ZEALAND GEOLOGICAL TIME SCALE WITH EQUIVALENT INTERNATIONAL UNITS – MESOZOIC

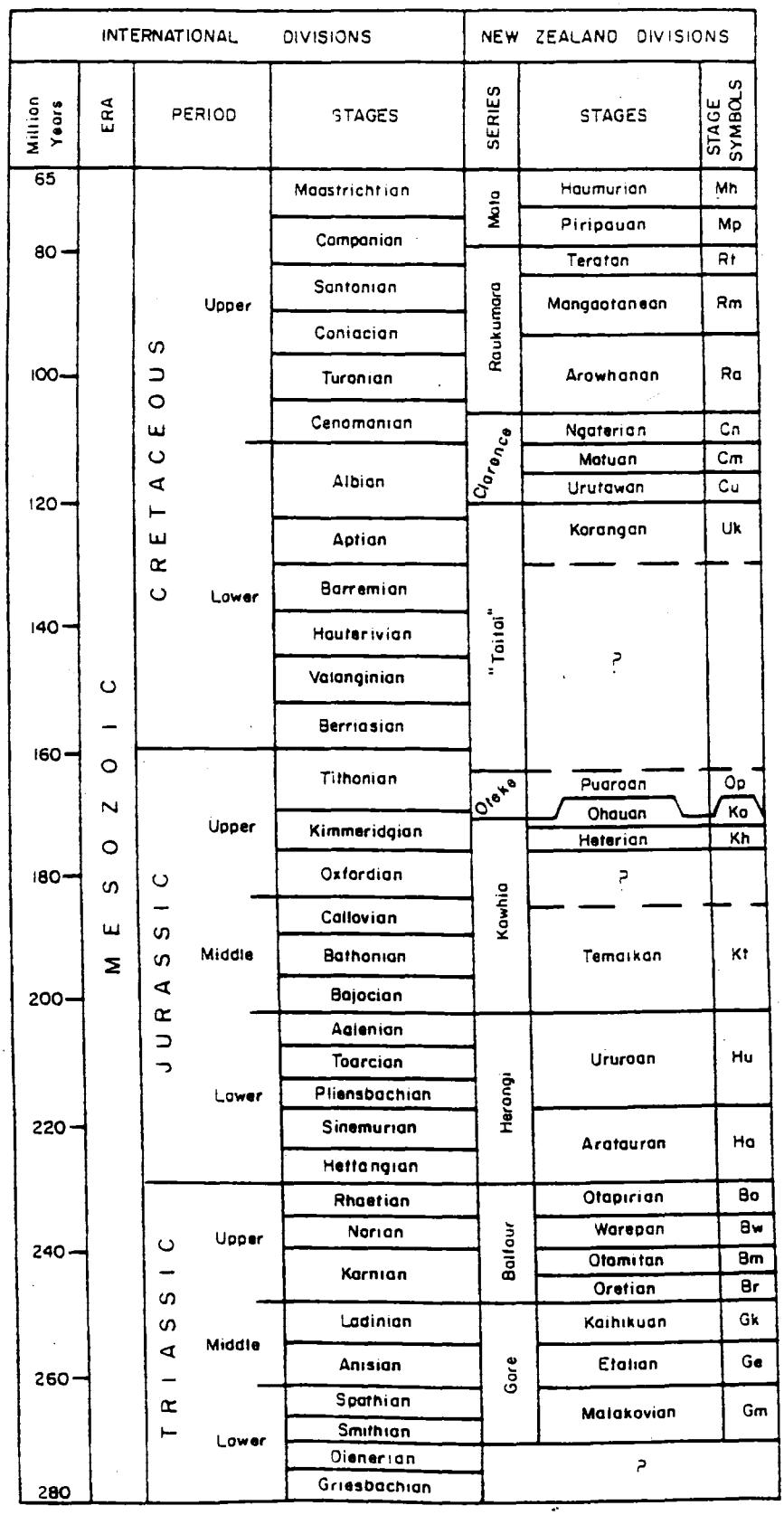

NEW ZEALAND GEOLOGICAL TIME SCALE WITH EQUIVALENT INTER - NATIONAL TIME UNITS - CENOZOIC

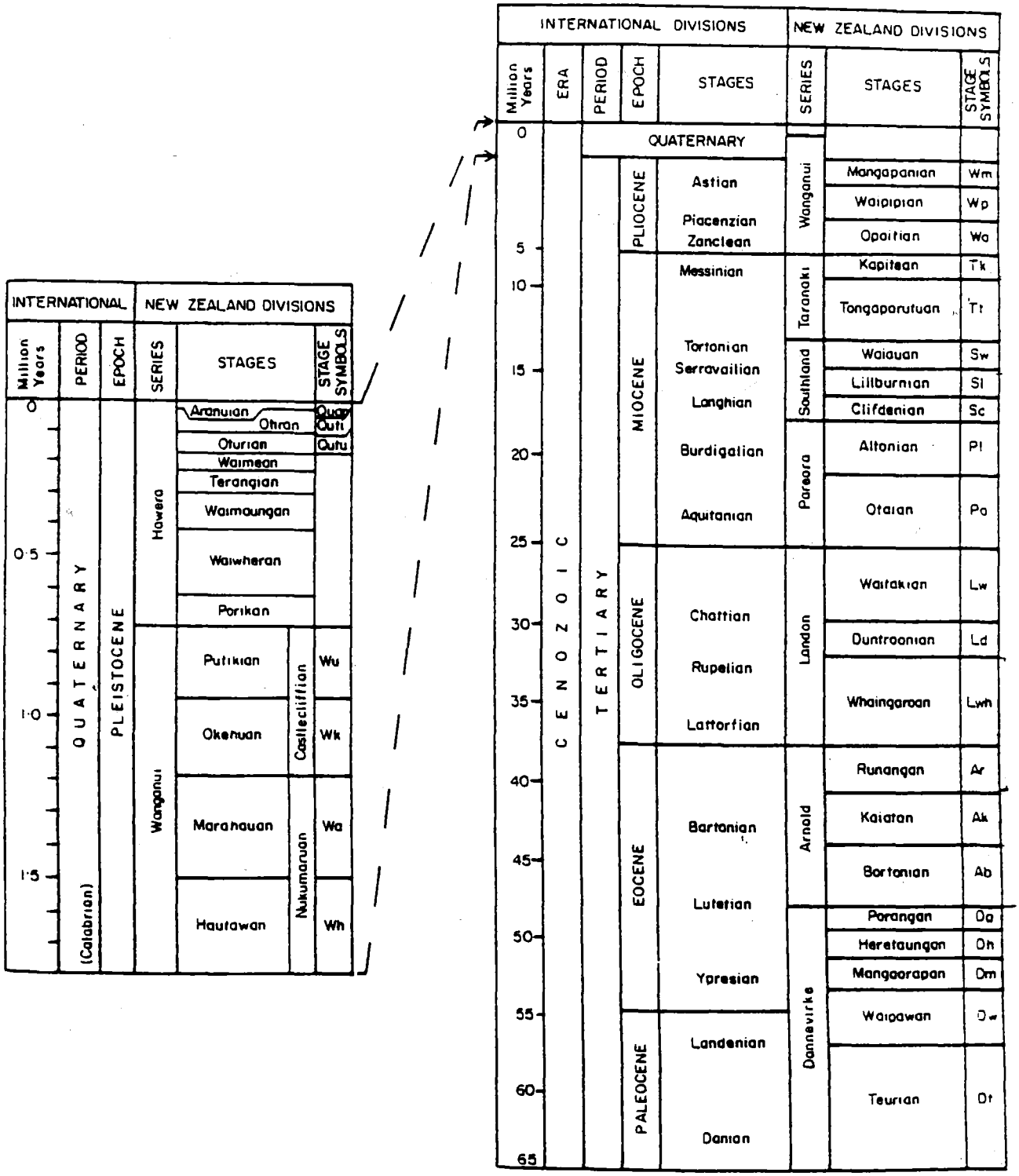

		SERIES	STAGES cold or glacial stages / temperate stages	GLACIATION
PLEISTOCENE	Late	HAWERA	ARANUIAN	
			OTIRAN	OTIRA
			OTURIAN	
			WAIMEAN	WAIMEA
			TERANGIAN	
	Middle		WAIMAUNGAN	WAIMAUNGA
			WAIWHERAN	
			PORIKAN	PORIKA
	Early	UPPER WANGANUI	CASTLECLIFFIAN	
			OKEHUAN	? part ROSS
			NUKUMARUAN	
			HAUTAWAN	ROSS
PLIOCENE		LOWER WANGANUI	WAITOTARAN OPOITIAN	

APPENDIX B

THE WAIKAWA BAY FAULT

B1 GEOPHYSICS

a) Transient Electromagnetism

b) Ground Penetrating Radar

B2 TRENCH LOGGING

B3 AUGER HOLE LOGGING

GEOPHYSICAL INVESTIGATIONS

A) TRANSIENT ELECTROMAGNETISM (TEM)

LOOP SIZES AND RAMP TIMES:

- WAIK100

  56m x109m loop size with 1amp current

  Ramp time 4.5 μs

  Between 6.8 μs to 696 μs

- WAIK200

  64m x 78m loop size with 1amp current

  Ramp time 4.5 μs

  Between 6.8μs to 262.8 μs

- WAIK300

  66m x 80m loop size with 1amp current

  Ramp time 4.5 μs

  Between 6.8 μs to 262.8 μs

- WAIK400

  80m x 80m loop size with 1amp current

  Ramp time 4.5 μs

  Between 6.8 μs and 262.8 μs

GEOPHYSICAL INVESTIGATIONS

B) GROUND PENETRATING RADAR

LINE 1: WAIMARAMA STREET

```
Waikawa Fault, Marlborough Sounds
Reeves (Sr.) property, next door to Campground
03/02/95
NUMBER OF TRACES    = 795
NUMBER OF PTS/TRC   = 500
TIMEZERO AT POINT   = 43
TOTAL TIME WINDOW   = 400
STARTING POSITION   = 0.000000
FINAL POSITION      = 159.000000
STEP SIZE USED      = 0.200000
POSITION UNITS      = metres
NOMINAL FREQUENCY   = 100.000000
ANTENNA SEPARATION  = 1.000000
PULSER VOLTAGE (V)  = 400
NUMBER OF STACKS    = 64
SURVEY MODE         = Reflection
SIGNAL SATURATION CORRECTION APPLIED
THIS FILE A MERGING OF \2 AND d:\gprdata\waikawa\sonz1x.
```

LINE 2: MAORI CEMETERY ROAD

```
Waikawa Fault, Marlborough Sounds
Maori cemetery road, centred on fault
03/02/95
NUMBER OF TRACES    = 501
NUMBER OF PTS/TRC   = 500
TIMEZERO AT POINT   = 51
TOTAL TIME WINDOW   = 400
STARTING POSITION   = 0.000000
FINAL POSITION      = 100.000000
STEP SIZE USED      = 0.200000
POSITION UNITS      = metres
NOMINAL FREQUENCY   = 100.000000
ANTENNA SEPARATION  = 1.000000
PULSER VOLTAGE (V)  = 400
NUMBER OF STACKS    = 64
SURVEY MODE         = Reflection
SOURCE DATA FILE    = C:\gprdata\waikawa\sonw2
FIRST BREAK POINT CORRECTED. THRESHOLD = -8000
FIRST BREAK SHIFT APPLIED.
SIGNAL SATURATION CORRECTION APPLIED
```

LINE 3: WAIKAWA SADDLE

```
Waikawa Fault, Marlborough Sounds
track depression
03/02/95
NUMBER OF TRACES    = 498
NUMBER OF PTS/TRC   = 500
TIMEZERO AT POINT   = 46
TOTAL TIME WINDOW   = 400
STARTING POSITION   = 0.600000
FINAL POSITION      = 100.000000
STEP SIZE USED      = 0.200000
POSITION UNITS      = metres
NOMINAL FREQUENCY   = 100.000000
ANTENNA SEPARATION = 1.000000
PULSER VOLTAGE (V) = 400
NUMBER OF STACKS    = 64
SURVEY MODE         = Reflection
THIS FILE A MERGING OF \2 AND C:\gprdata\waikawa\sonw3x.
SIGNAL SATURATION CORRECTION APPLIED
FIRST BREAK POINT CORRECTED. THRESHOLD = -8000
FIRST BREAK SHIFT APPLIED.
FIRST BREAK POINT CORRECTED. THRESHOLD = -4000
FIRST BREAK SHIFT APPLIED.
```

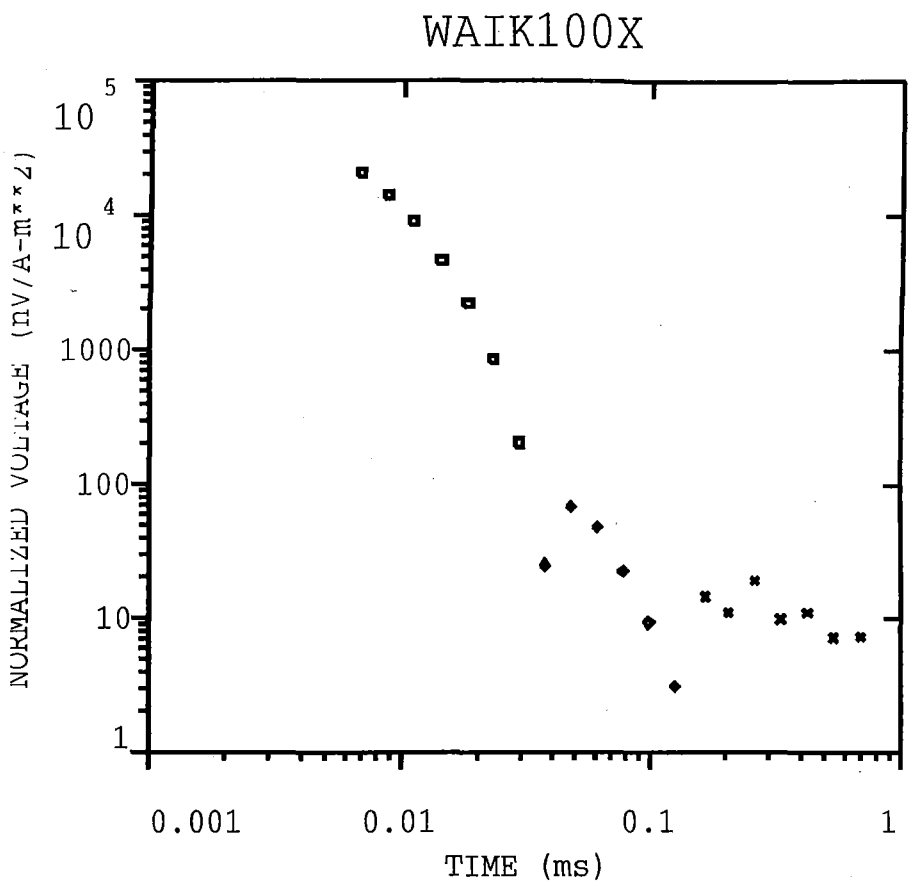
WAIK100X
NORMALIZED VOLTAGE (nV/A-m**2)
10^5
10^4
1000
100
10
1
0.001
0.01
0.1
1
TIME (ms)

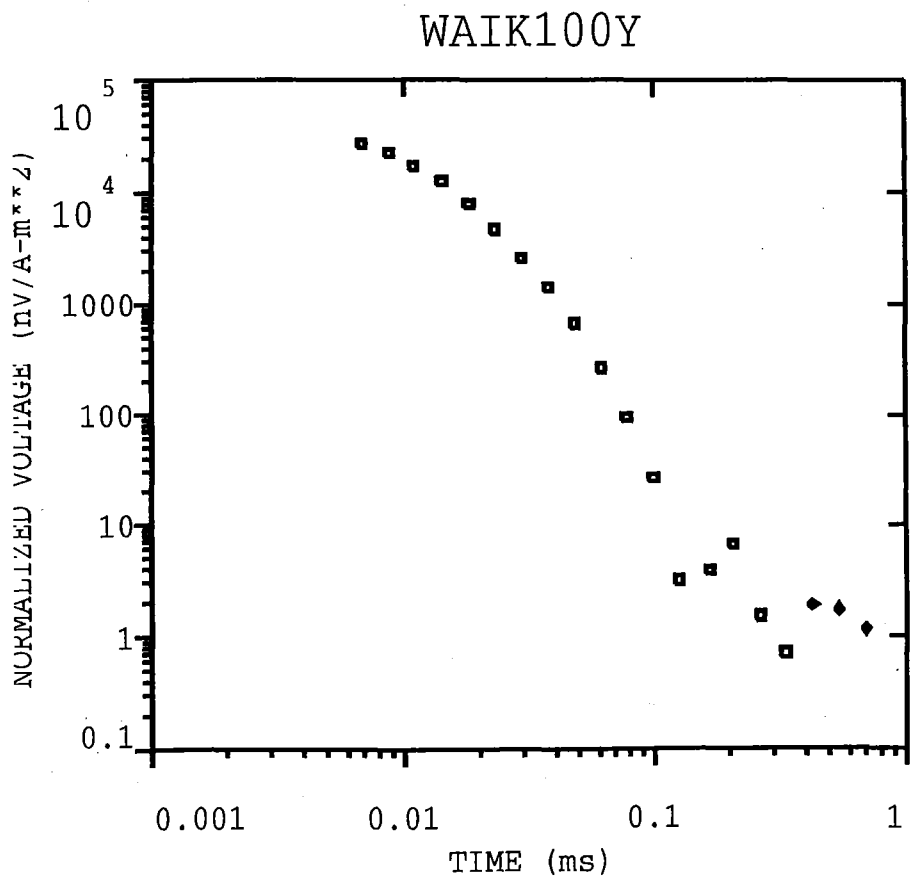
WAIK100Y
NORMALIZED VOLTAGE (nV/A-m**2)
10^5
10^4
1000
100
10
1
0.1
0.001
0.01
0.1
1
TIME (ms)

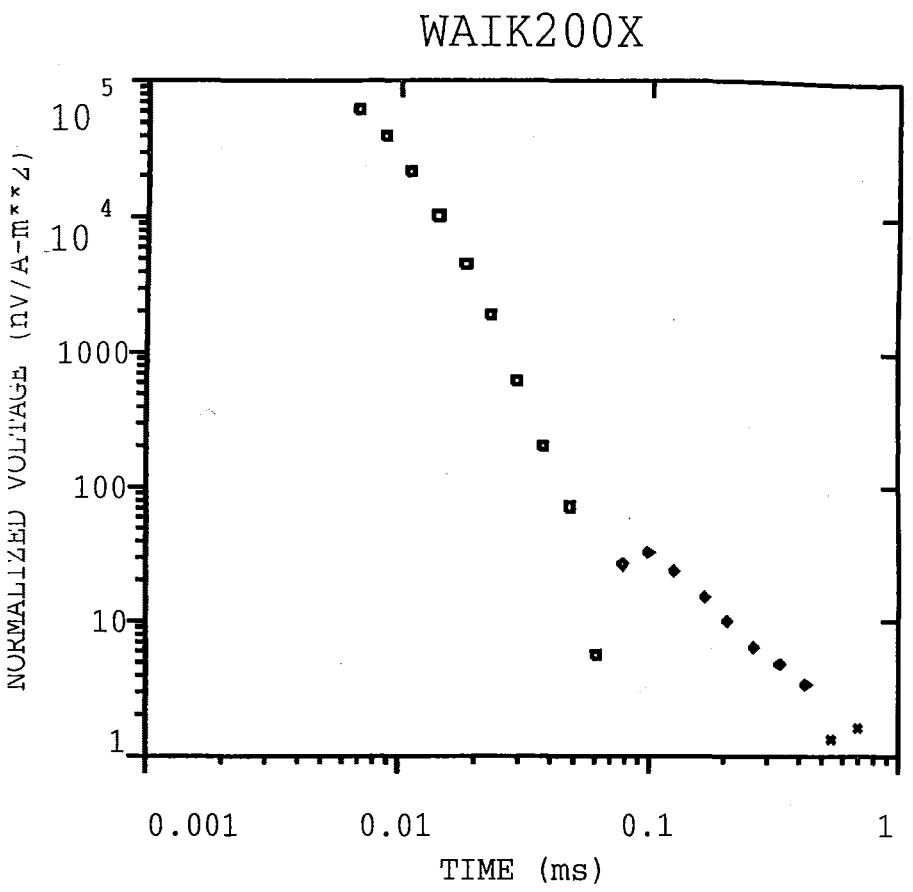
WAIK200X
NORMALIZED VOLTAGE (nV/A-m**4)
10^5
10^4
1000
100
10
1
0.001
0.01
0.1
1
TIME (ms)

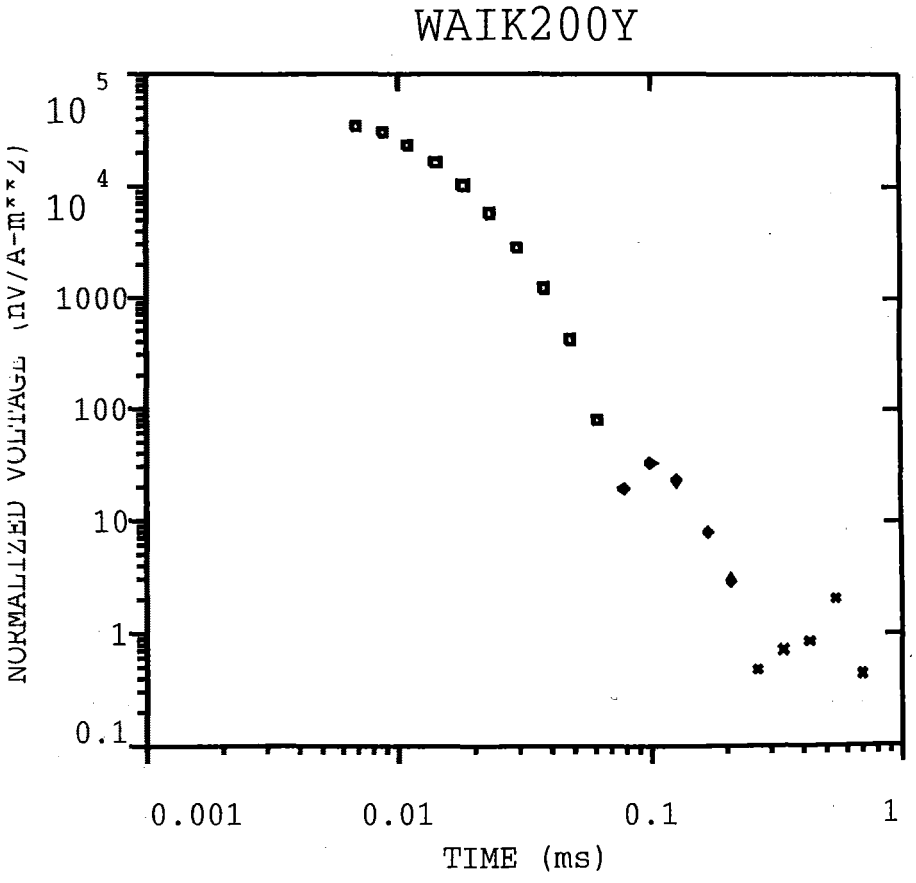
WAIK200Y
NORMALIZED VOLTAGE (nV/A-m**4)
10^5
10^4
1000
100
10
1
0.1
0.001
0.01
0.1
1
TIME (ms)

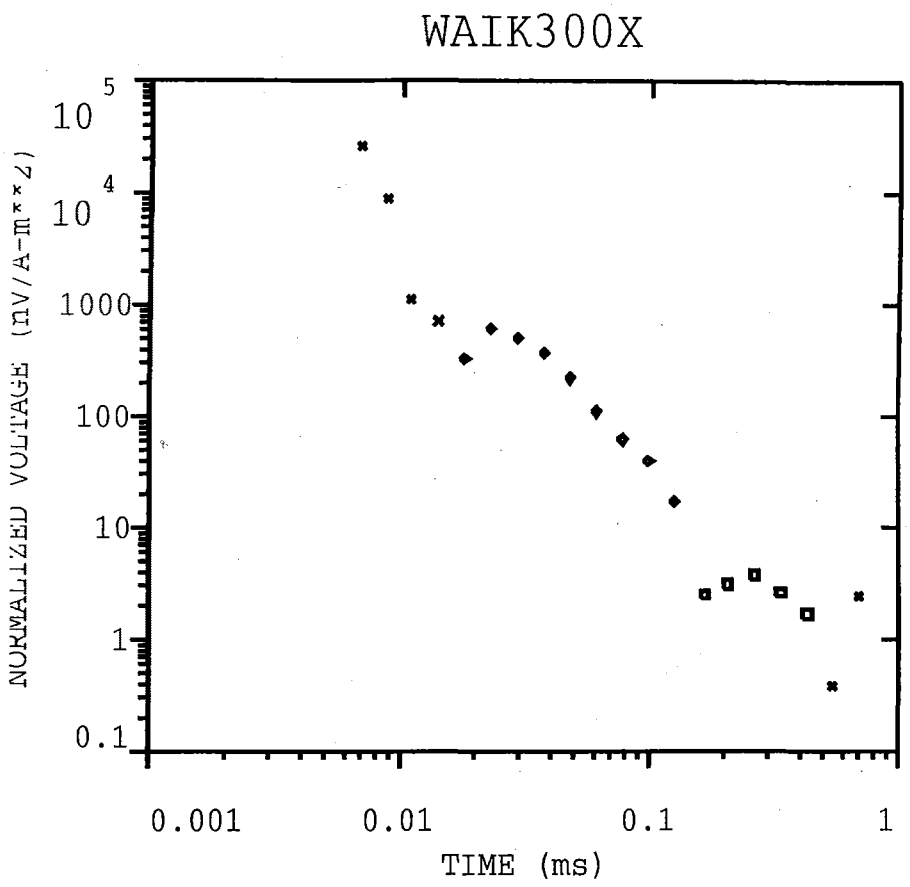
WAIK300X
NORMALIZED VOLTAGE (nV/A-m**2)
10^5
10^4
1000
100
10
1
0.1
0.001
0.01
0.1
1
TIME (ms)

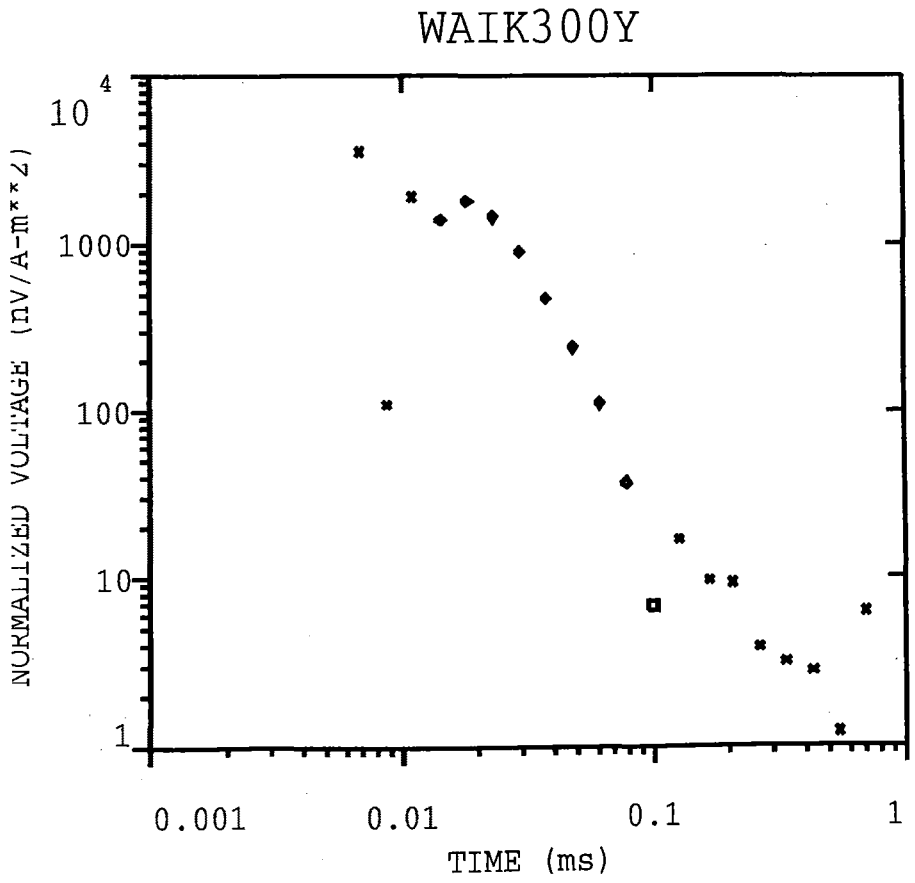
WAIK300Y
NORMALIZED VOLTAGE (nV/A-m**2)
10^4
1000
100
10
1
0.001
0.01
0.1
1
TIME (ms)

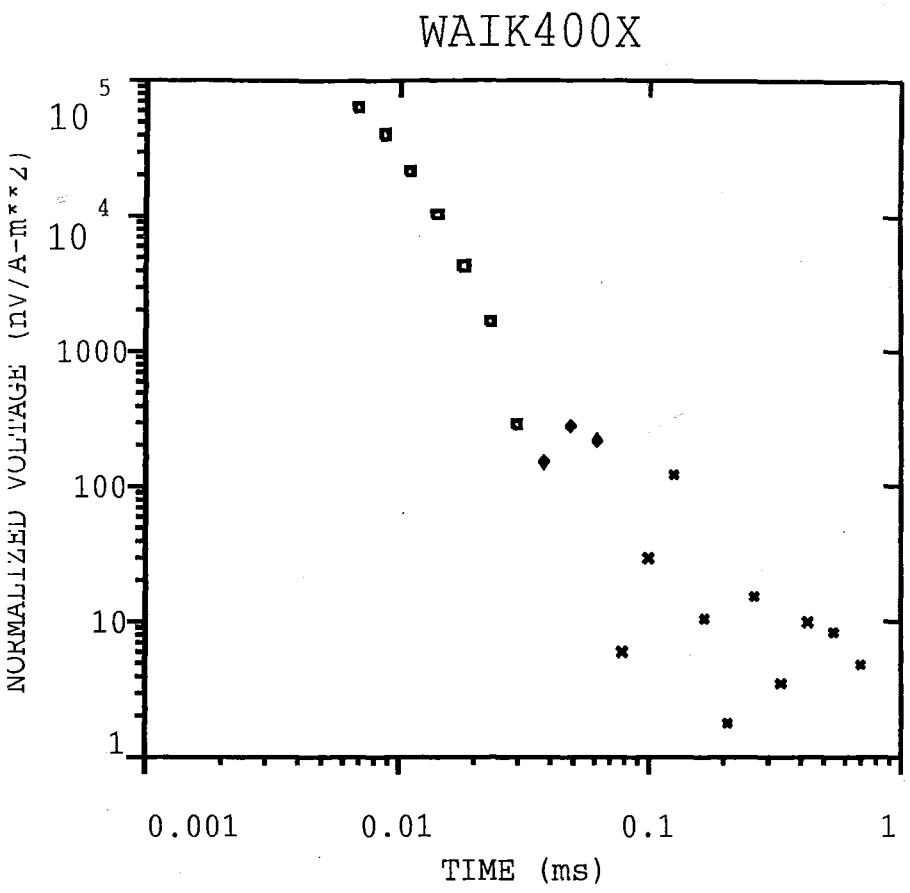
WAIK400X
NORMALIZED VOLTAGE (nV/A-m**4)
10^5
10^4
1000
100
10
1
0.001
0.01
0.1
1
TIME (ms)

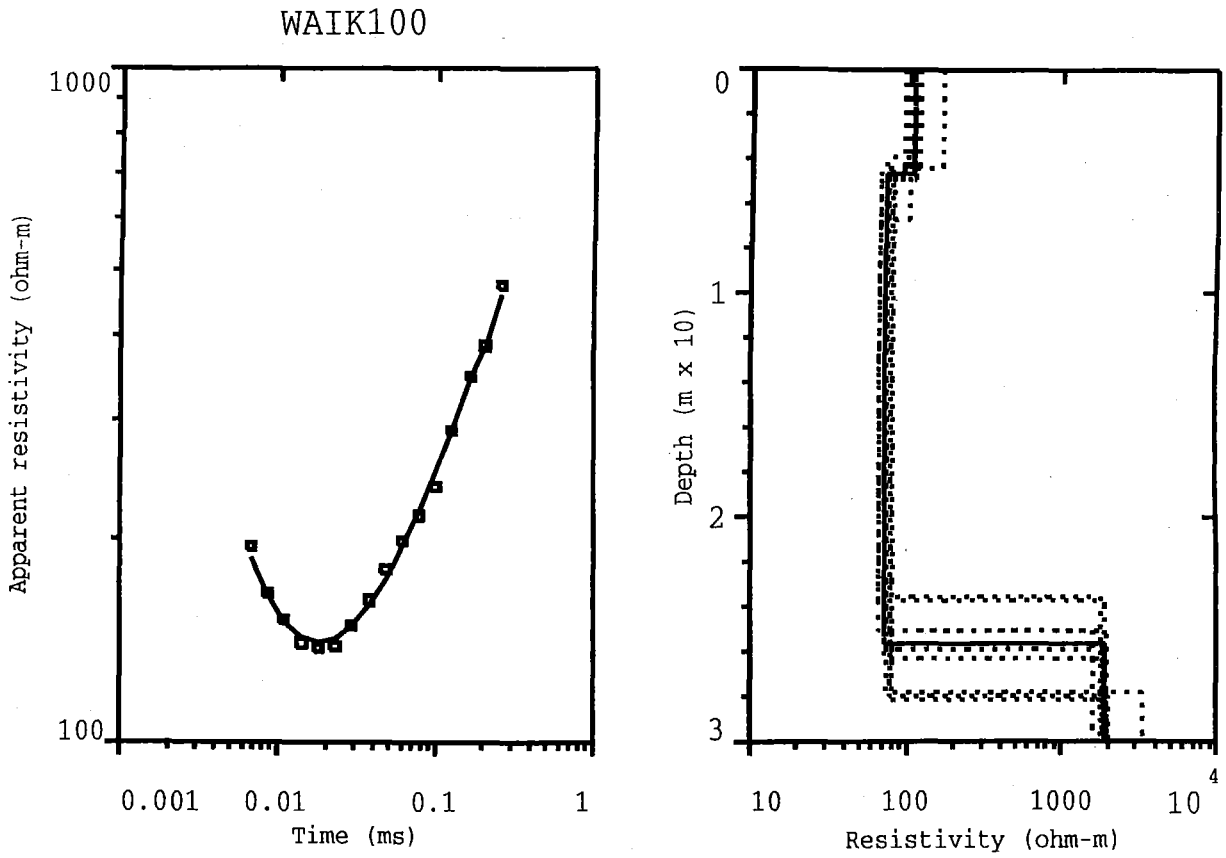
WAIK100
1000
100
Apparent resistivity (ohm-m)
0.001
0.01
0.1
1
Time (ms)
0
1
2
3
Depth (m x 10)
10
100
1000
10^4
Resistivity (ohm-m)

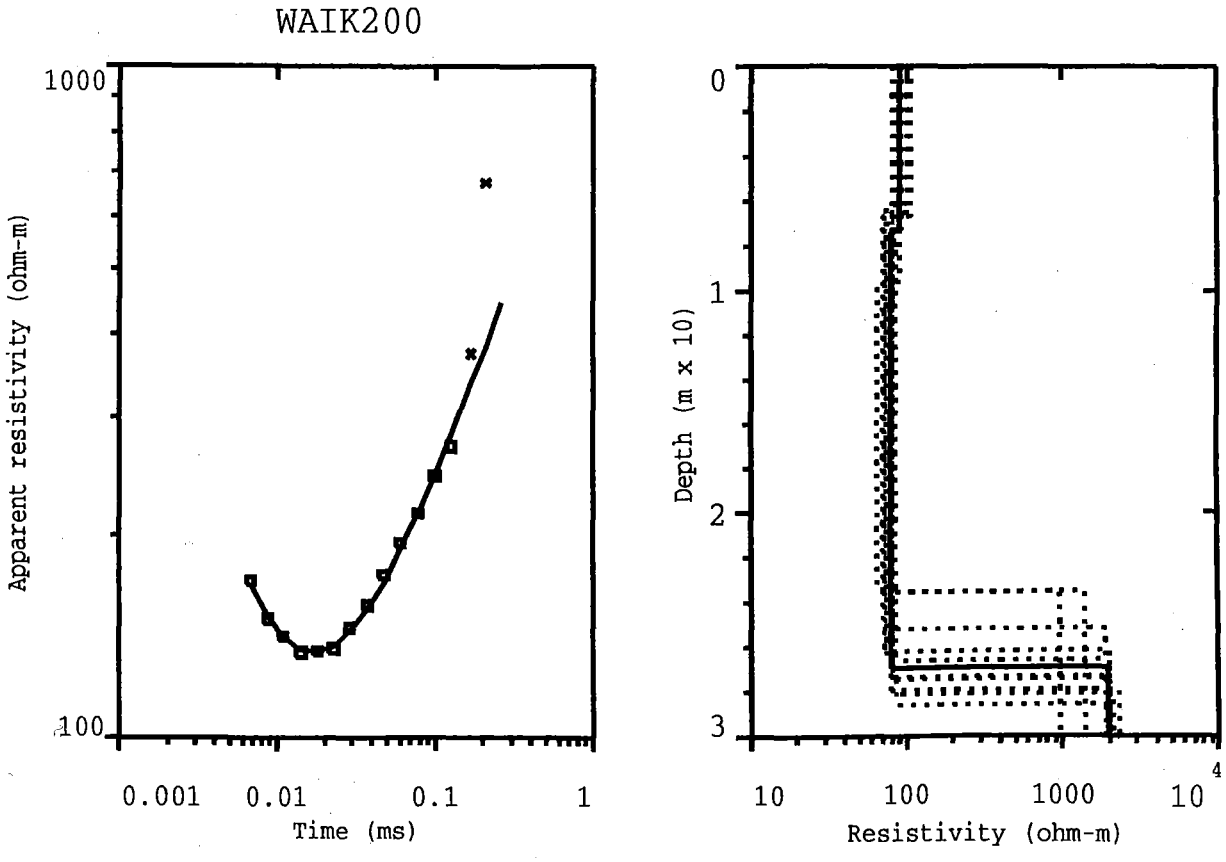
WAIK200
1000
100
Apparent resistivity (ohm-m)
0.001
0.01
0.1
1
Time (ms)
0
1
2
3
Depth (m x 10)
10
100
1000
10^4
Resistivity (ohm-m)

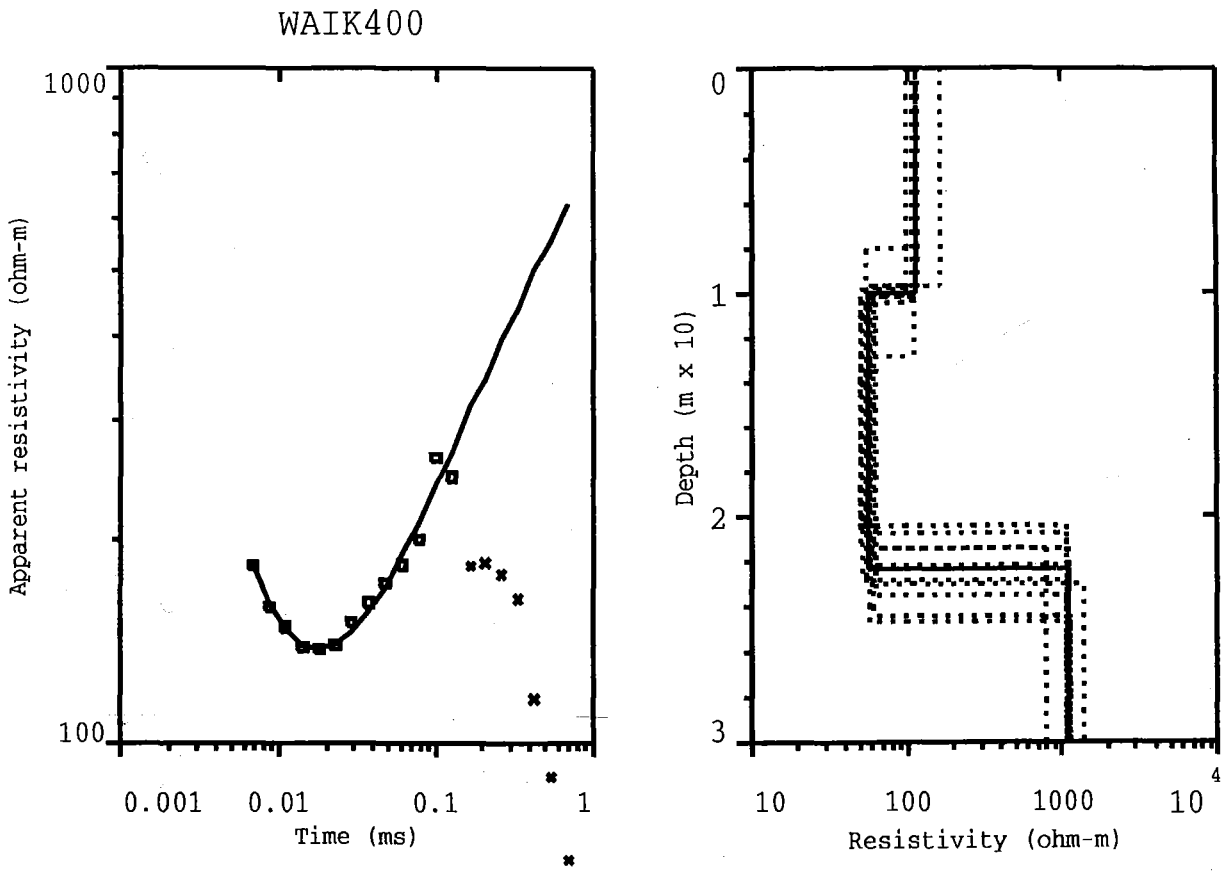
WAIK400
1000
100
Apparent resistivity (ohm-m)
0.001
0.01
0.1
1
Time (ms)
0
1
2
3
Depth (m x 10)
10
100
1000
10^4
Resistivity (ohm-m)

WAIK100

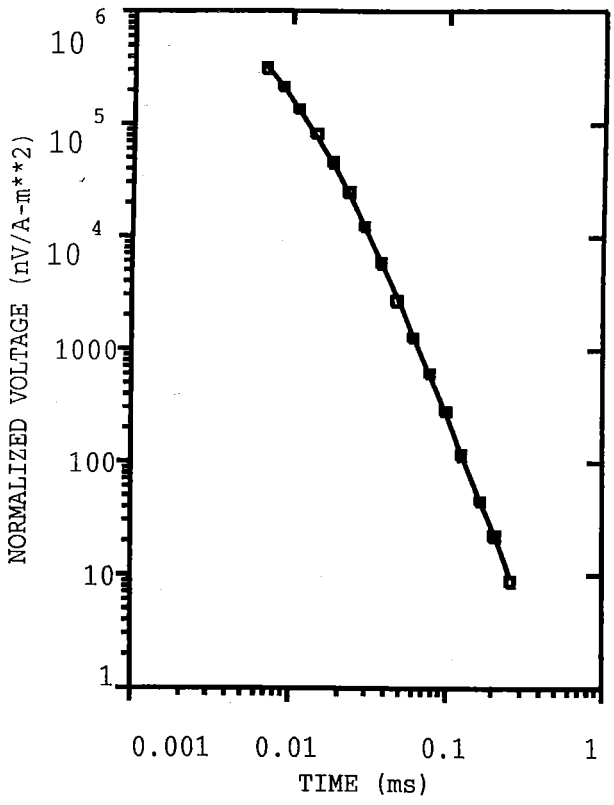

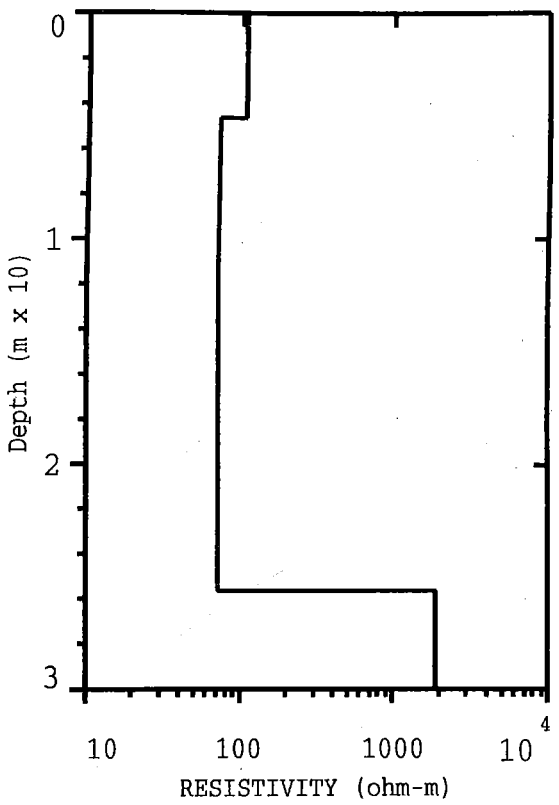

WAIK200

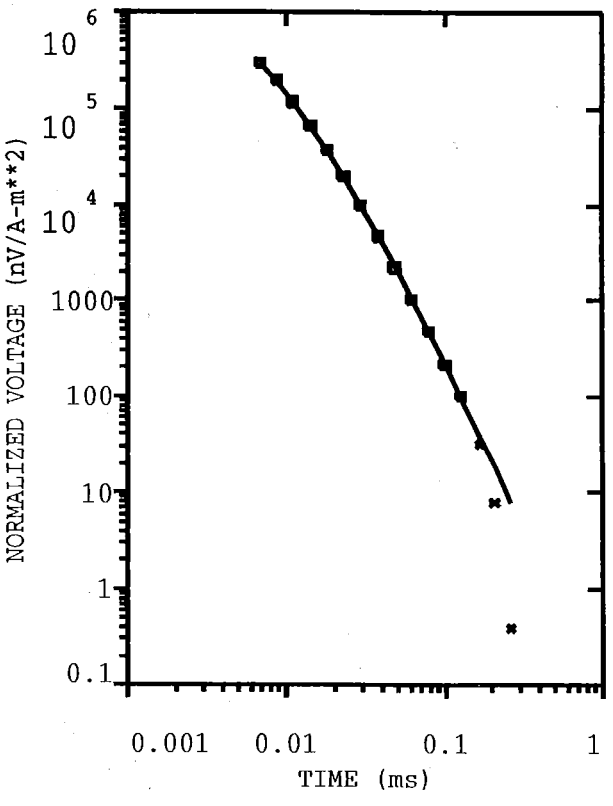

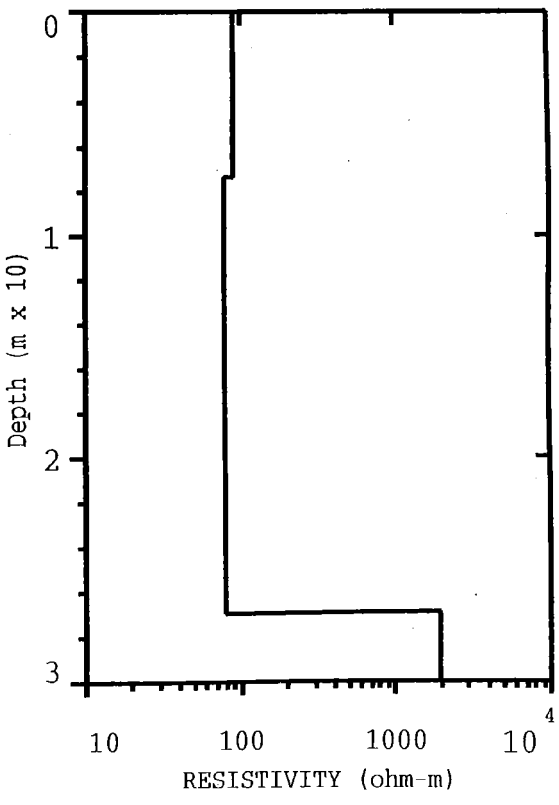

WAIK300

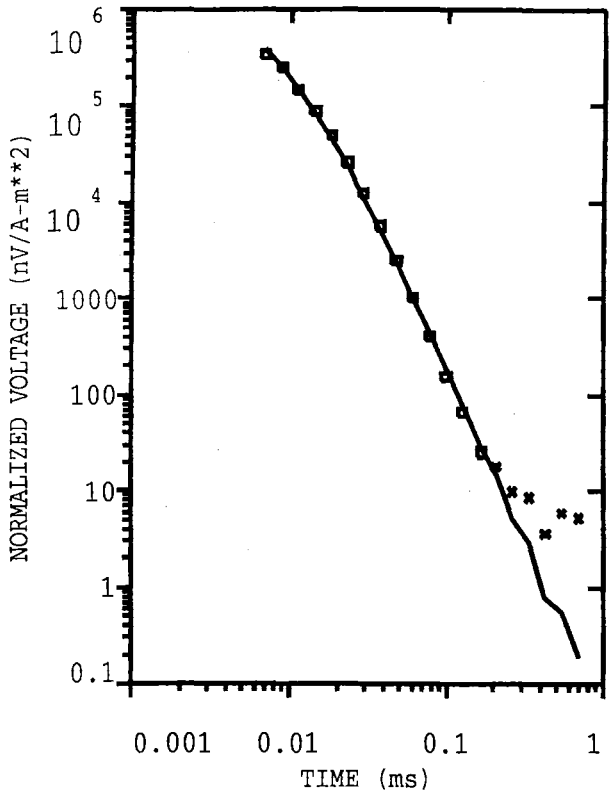

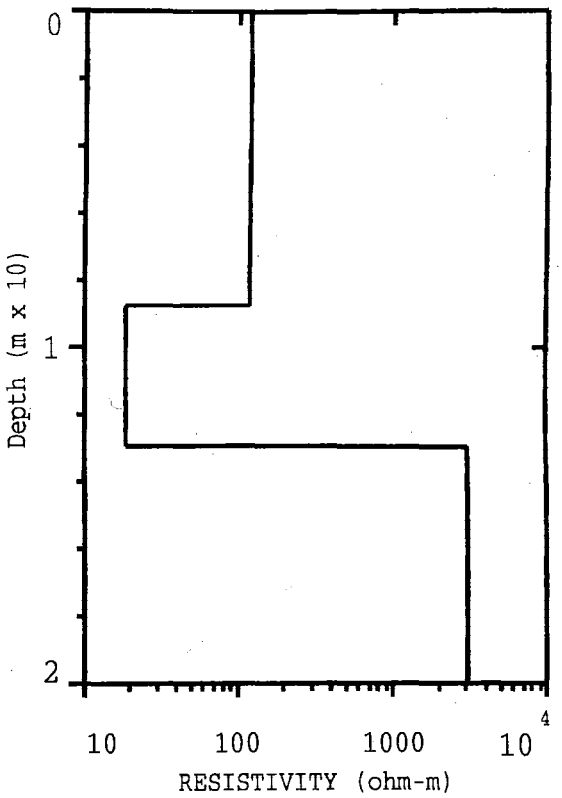

WAIK400

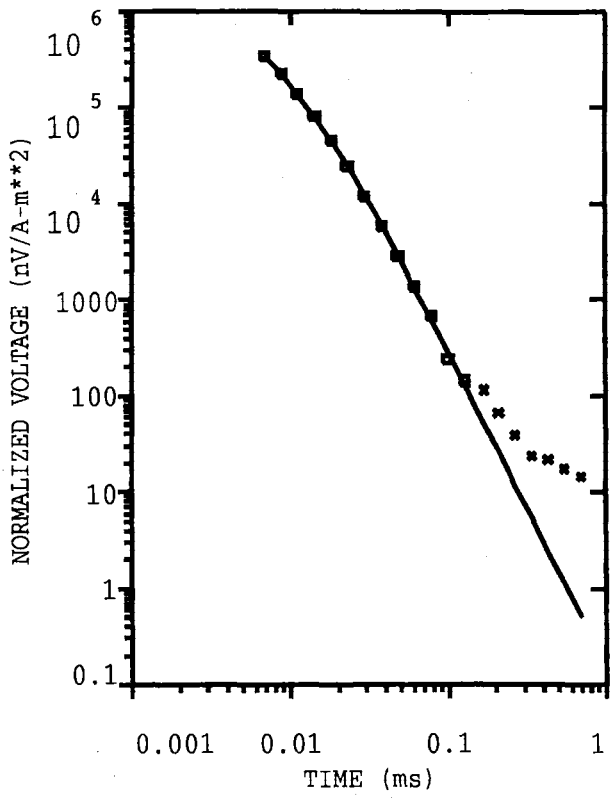

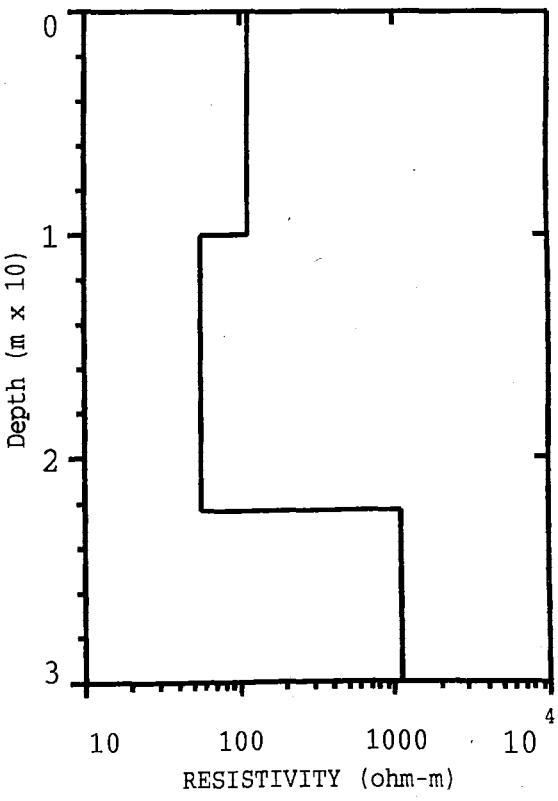

ENGINEERING GEOLOGY

TRENCH LOG

PROJECT:
B.Sc. Honours Project

EXCAVATION DETAILS:
Test Pit TP1

LOCALITY:
Smith Property, Moana View Rd.

LOGGED BY:
S.T. McManus

DATE:
February 8, 1994

SITE SKETCH

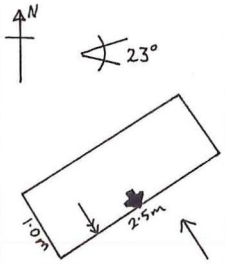

KEY

- Slope gradient
- Slope direction
- Face logged
- Photograph

DEPTH (M)	LOG	DESCRIPTION	SAMPLE
0		Dark brown/black organic rich topsoil	
		Greyish white gravely silt, wet, plastic, slightly stiff	
		Greywacke fragments up to 2.5cm	
0.5			
		Yellow gravely clay, moist, plastic, stiff-firm	
		Rare white veining present	
1.0			
		Yellow clay, moist, plastic, firm with some gravels present	
		White clay, very moist, plastic, stiff-firm	
1.5		Forms veins within the yellow clay	
2.0			
2.5			

LEGEND

- Organic material
- Silts
- Gravels
- Mottled clay
- Veined clay
- Seepage

NOTES

* Upslope face shows seepage
* Slumping of the upslope face 2 hrs after the excavation
* Slickenslides on the failure surface 345/32°NW
* Trench has 0.5m water in it 24 hrs after excavation

PROFILE

N/A

ENGINEERING GEOLOGY

TRENCH LOG

PROJECT:
B.Sc. Honours

EXCAVATION DETAILS:
Test Pit TP2

LOCALITY:
Smith Property, Moana View Rd.

LOGGED BY:
S.T.McManus

DATE:
February 8, 1994

SITE SKETCH

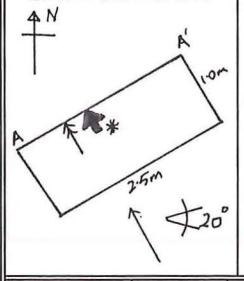

KEY

- Slope direction
- Slope gradient
- Face logged
- Photograph
- Sample

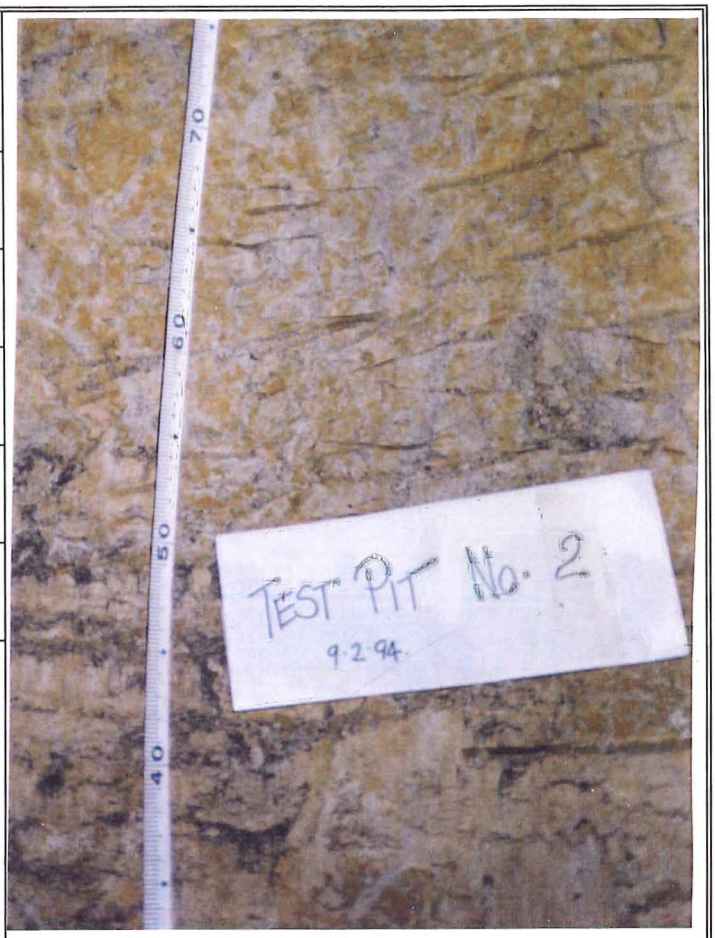

DEPTH (M)	LOG	DESCRIPTION	SAMPLE
0		Light greyish brown organic rich topsoil	
		Yellow/greyish white, very dry, friable, slightly plasticsilt with some lithics fragments up to 10mm	
0.5		Yellow/greyish white, soft, moist mod plastic, silty clay, some small white clay veins	
		Dark grey brown, moist, stiff, mod plastic, organic rich buried soil	
		Light grey/white, slightly moist, friable stiff sandy silt. Lithic fragments up to 5mm	
1.0		Yellow, moist, very plastic, stiff gravely clay	
		Completely weathered greywacke fragments up to 20mm and white clay veins	
1.5		Yellow, moist-wet, plastic, stiff gravely clay extensive white clay veining	
		Greywacke clasts up to 70mm	
2.0			
2.5			

LEGEND

- Organic material
- Silts
- Gravels
- Sands
- Mottled clay
- Veined Clay

NOTES

* WP11 Organic material 0.7m
* WP12 Bulk Sample of veined clay 1.65m
* Photograph of mottled clay

PROFILE

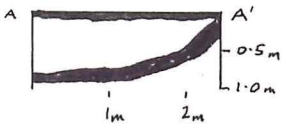

ENGINEERING GEOLOGY

TRENCH LOG

PROJECT:
B.Sc. Honours

EXCAVATION DETAILS:
Test Pit TP3

LOCALITY:
Smith Property, Moana View Rd.

LOGGED BY:
S.T.McManus

DATE:
February 8, 1994

SITE SKETCH

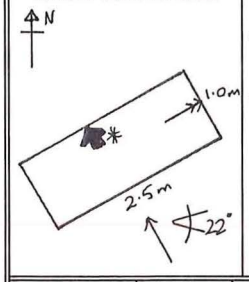

KEY

→ Slope direction

Slope gradient

Face logged

→→ Photograph

* Sample

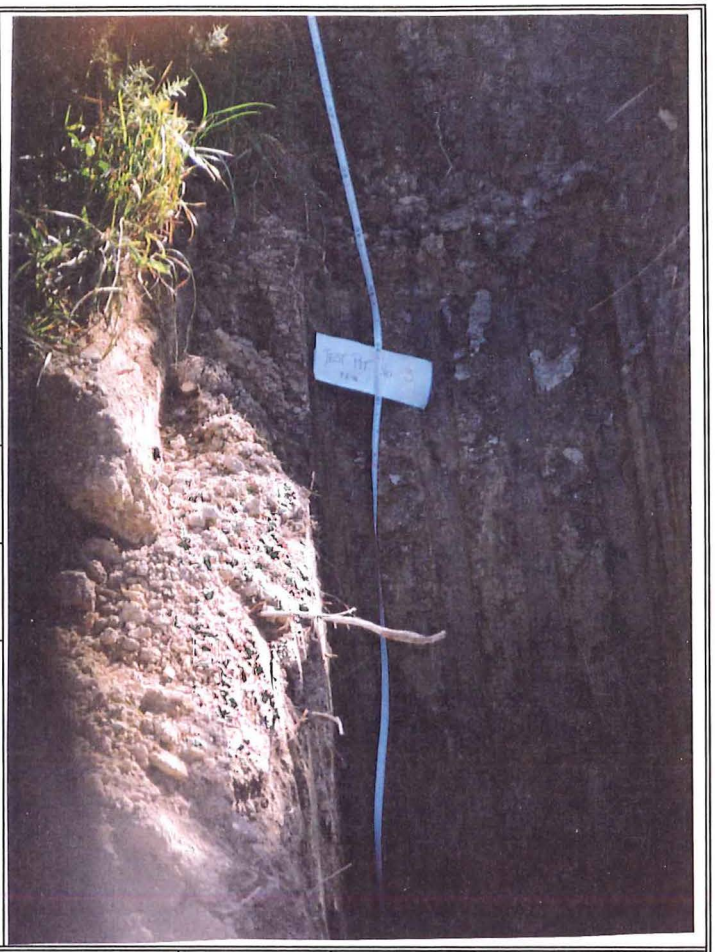

DEPTH (M)	LOG	DESCRIPTION	SAMPLE	LEGEND
0		Dark brown/black, organic rich topsoil		Organic Material
0.5		Yellow and white mottled clays, moist, plastic, stiff with lithic relics up to 10mm		Gravels Mottled clay Veined Clay
1.0				
1.5		Yellow and blue mottled clays, moist-wet, plastic, stiff-firm, with lithic fragments of schist up to 20mm, mod weathered	WP 13	NOTES * WP13 bulk sample of yellow and blue clays at 1.7m * Blue clays indicative of the water table * Trench assumed to be near/on fault trace
2.0				PROFILE N/A
2.5				

ENGINEERING GEOLOGY

TRENCH LOG

PROJECT:
B.Sc. Honours

EXCAVATION DETAILS:
Test Pit TP4

LOCALITY:
Smith Property, Moana View Rd.

LOGGED BY:
S.T.McManus

DATE:
February 8. 1994

SITE SKETCH

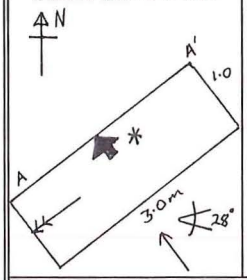

KEY

- Slope direction
- Slope gradient
- Face logged
- Photograph
- Sample

DEPTH (M)	LOG	DESCRIPTION	SAMPLE
0		Dark brown/black organic rich topsoil	
		Greyish white, dry, mod plastic, friable silty gravely clay with highly weathered greywacke and schist clasts up to 10mm	WP 14
0.5		Light yellow and white mottled moist, plastic, stiff gravely clay with lithic clasts up to 10mm forming lenses	
1.0		White veining of clays prominent	WP 15
1.5		Darker yellow gravely clay with less mottling and less veining	
2.0			
2.5			

LEGEND

- Organic material
- Silts
- Gravels
- Mottled clay
- Veined clay

NOTES

* WP14 Silty clay [loess] at 0.3m
* WP15 Clastic unit at 1.1m
* Potential failure surfaces in veined clay at 1.4m and 1.8m

PROFILE

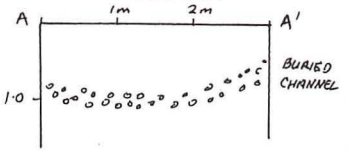

ENGINEERING GEOLOGY

TRENCH LOG

PROJECT:
B.Sc. Honours

EXCAVATION DETAILS:
Test Pit TP5

LOCALITY:
Smith Property, Moana View Rd.

LOGGED BY:
S.T.McManus

DATE:
February 8, 1994

SITE SKETCH

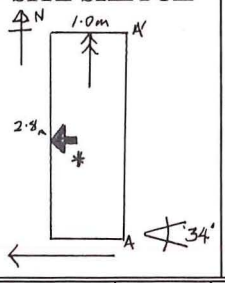

KEY

- Slope direction
- Slope gradient
- Face logged
- Photograph
- Sample

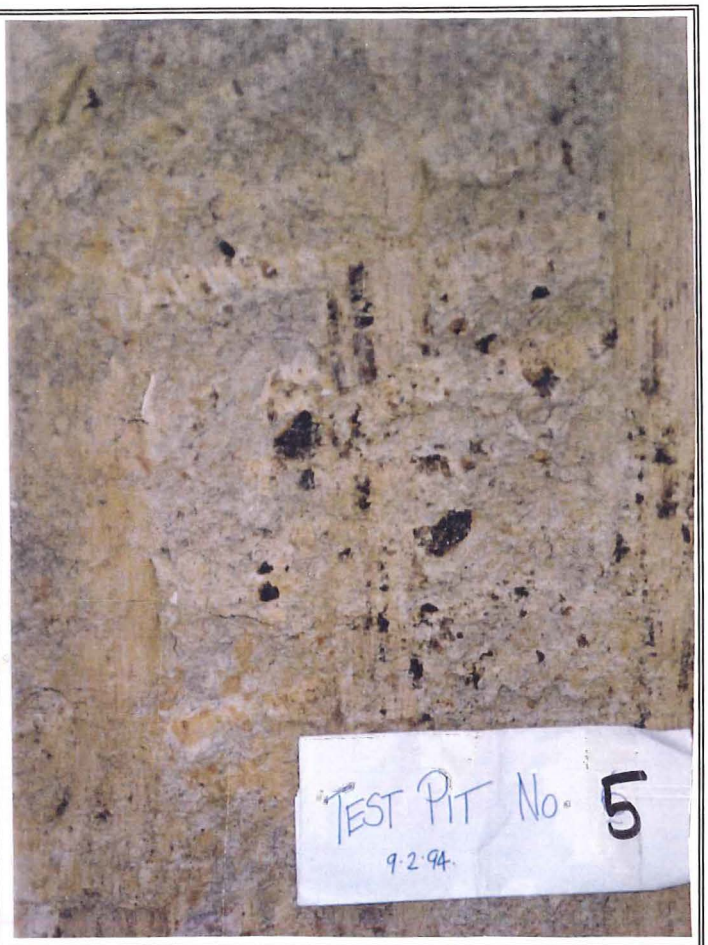

DEPTH (M)	LOG	DESCRIPTION	SAMPLE
0		Dark brown/black organic rich topsoil	
0.5		Yellow/greyish white dry-moist, mottled gravely clays. Random orientation of schist and greywacke clasts up to 1.5cm. White clay layering present	
1.0		Very coarse layer of greywacke clasts, mod weathered, 0.2-0.3cm Dark yellow/white sandy clay matrix	WP 16
1.5		Blue clay layer across trench face approx 3cm thick, orientated 180/13°N	
2.0		Dark yellow and blue/grey moist, plastic, firm mottled clay with greywacke clasts less than 5mm diameter	
2.5			

LEGEND

- Organic material
- Sands
- Gravels
- Mottled clay
- Blue/veined clay

NOTES

* WP16 Charcoal at 0.95m
* Blue clay layer at 1.5m
* Photograph of coarse clastic unit

PROFILE

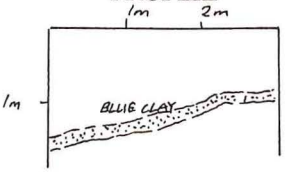

ENGINEERING GEOLOGY

TRENCH LOG

PROJECT:
B.Sc. Honours

EXCAVATION DETAILS:
Test Pit TP6

LOCALITY:
Smith Property, Moana View Rd.

LOGGED BY:
S.T.McManus

DATE:
February 8, 1994

SITE SKETCH

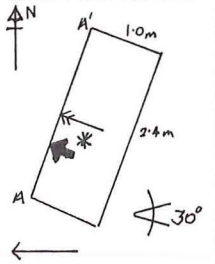

KEY

→ Slope direction

Slope gradient

Face logged

→→ Photograph

Sample

DEPTH (M)	LOG	DESCRIPTION	SAMPLE
0		Light brown/grey organic poor topsoil	
		Yellowish grey organic rich, sandy, non-plastic	
		Organic layer of wood and charcoal 2-3cm	WP18/19
		Yellow /grey very dry, non-plastic, friable,	
0.5		sandy gravel with schist clasts up to 5cm	
		Dark brown/grey organic rich soil with schist clasts up to 5mm	WP20
		Light grey/brown organic layer, moist, slightly	WP21
1.0		plastic silty clay. schist fragments, some charcoal within clay	
1.5		Yellow/white moist, mod plastic stiff mottled gravely clay with schist clasts up to 5mm	
2.0			
2.5			

LEGEND

Organic material

Silts

Sands

Gravels

Mottled clay

Charcoal

NOTES

* WP18 wood sample 0.3m
* WP19 charcoal 0.3m
* WP20 charcoal 0.6m
* WP21 charcoal 0.85m

PROFILE

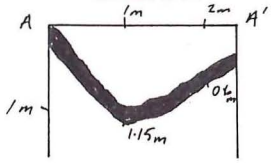

ENGINEERING GEOLOGY

TRENCH LOG

PROJECT:
B.Sc. Honours

EXCAVATION DETAILS:
Test Pit TP7a

LOCALITY:
Smith Property, Moana View Rd.

LOGGED BY:
S.T.McManus

DATE:
February 8, 1994

SITE SKETCH

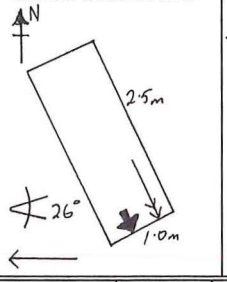

KEY

- Slope direction
- Slope gradient
- Face logged
- Photograph

DEPTH (M)	LOG	DESCRIPTION	SAMPLE
0		Light greyish brown, organic poor topsoil	
		Light brownish yellow, very dry, friable-mod stiff, slightly plastic, silty clay	
0.5		Yellow/white moist, plastic, stiff, mottled gravely clay with schist clasts up to 5mm	
1.0		Dark yellow, closely jointed, well indurated moist moderately weathered greywacke Oxidation of joint surfaces common	
1.5			
2.0			
2.5			

LEGEND

- Organic material
- Silts
- Gravels
- Mottled clay
- Bedrock

NOTES

* Bedrock surface represents failure surface
* Trench located 30m downslope of degraded major scarp

PROFILE

N/A

ENGINEERING GEOLOGY

TRENCH LOG

PROJECT:
B.Sc. Honours

EXCAVATION DETAILS:
Test Pit TP7b

LOCALITY:
Smith Property, Moana View Rd.

LOGGED BY:
S.T. McManus

DATE:
February 8, 1994

SITE SKETCH

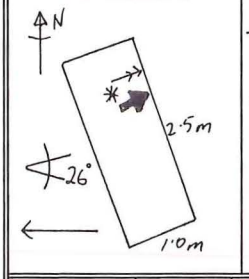

KEY

→ Slope direction

Slope gradient

Face logged

→→ Photograph

* Sample

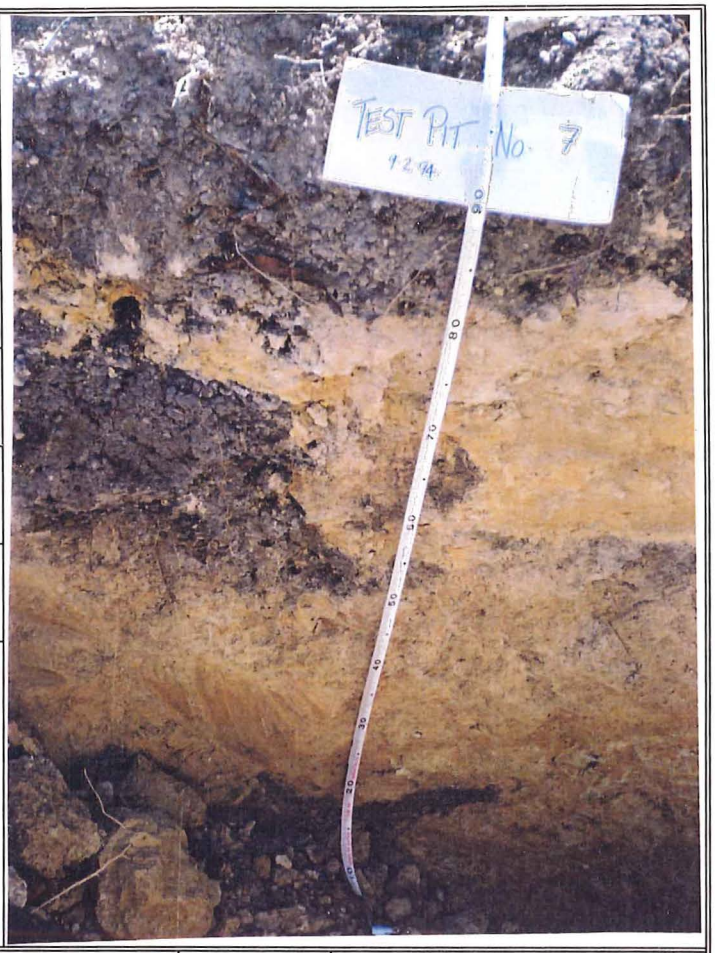

DEPTH (M)	LOG	DESCRIPTION	SAMPLE
0		Light greyish brown organic poor topsoil Some charcoal present	
0.5		Yellow/white moist, plastic, stiff mottled clay with schistose clasts up to 10mm	WP22
1.0		Yellow and white mottled gravely clay	
1.5		Organic soils	
2.0			
2.5			

LEGEND

Organic material

Gravels

Mottled clay

NOTES

* WP22 Organic material from buried soil

* Material represents shallow debris over the failure surface

PROFILE

N/A

ENGINEERING GEOLOGY

TRENCH LOG

PROJECT:
B.Sc. Honours

EXCAVATION DETAILS:
Test Pit TP8

LOCALITY:
Smith Property, Moana View Rd.

LOGGED BY:
S.T.McManus

DATE:
February 8, 1994

N/A

SITE SKETCH

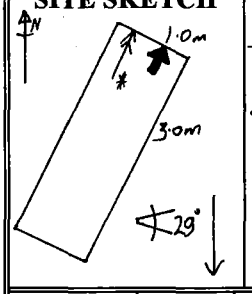

KEY

→ Slope direction

Slope gradient

Face logged

→→ Photograph

* Sample

DEPTH (M)	LOG	DESCRIPTION	SAMPLE
0		Dark brown organic rich topsoil Varying thickness 0.15-0.3m	
0.5		Light yellow and white moist, plastic, stiff mottled, very gravely clays. Greywacke and schist clasts up to 20mm	
1.0			
1.5		Dark yellow and grey mottled clays grading into moderately weathered greywacke bedrock. Oxidation along joint surfaces White clays forming in open joints, wet, very plastic, soft	WP23
2.0			
2.5			

LEGEND

Organic material

Gravels

Mottled clay

Bedrock

Seepage

NOTES

* WP23 Bulk bedrock sample
* Seepage from open joints
* White clay developing in open joints

PROFILE

N/A

ENGINEERING GEOLOGY

TRENCH LOG

PROJECT:
B.Sc. Honours

EXCAVATION DETAILS:
Test Pit TP9

LOCALITY:
Smith Property, Moana View Rd.

LOGGED BY:
S.T.McManus

DATE:
February 8, 1994

SITE SKETCH

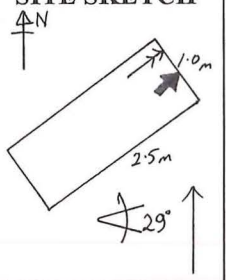

KEY

→ Slope direction

Slope gradient

Face logged

→→ Photograph

DEPTH (M)	LOG	DESCRIPTION	SAMPLE	LEGEND
0		Dark grey/brown organic rich topsoil		Organic material
0.5		Light yellow and white, moist, plastic, stiff finely mottled highly weathered greywacke bedrock		Mottled clay
1.0		Dark yellow/brown moderately weathered slightly mottled greywacke bedrock Wet white clays developing along open joint systems		Bedrock Seepage
1.5				NOTES * White clay developing in joints
2.0				PROFILE
2.5				N/A

ENGINEERING GEOLOGY

TRENCH LOG

PROJECT:
B.Sc. Honours

EXCAVATION DETAILS:
Test Pit TP10

LOCALITY:
Smith Property, Moana View Rd.

LOGGED BY:
S.T.McManus

DATE:
February 8, 1994

SITE SKETCH

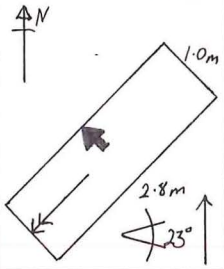

KEY

→ Slope direction

Slope gradient

Face logged

→→ Photograph

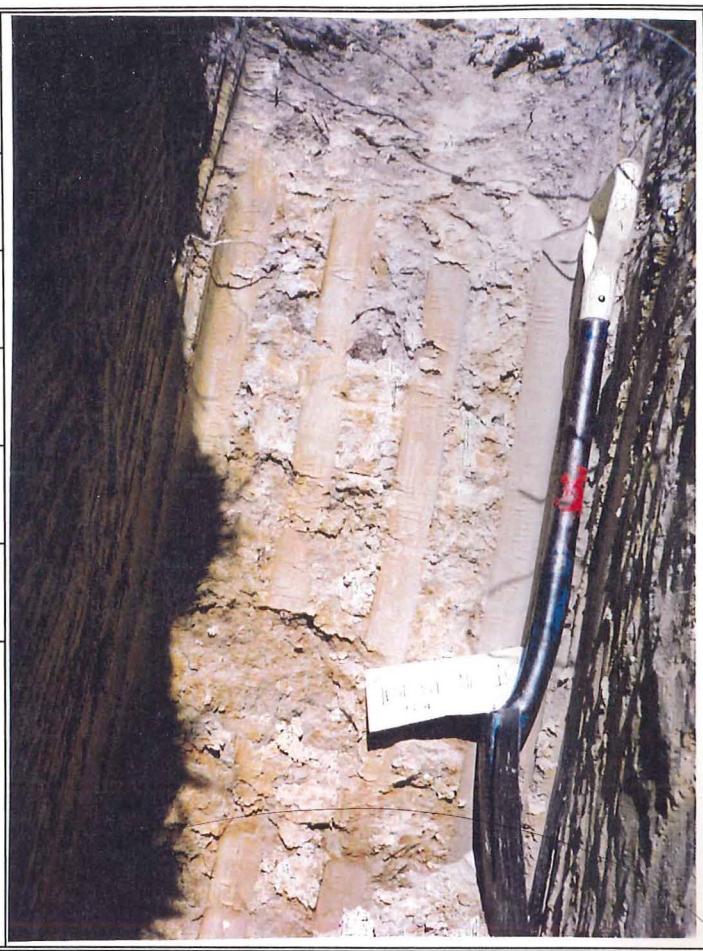

DEPTH (M)	LOG	DESCRIPTION	SAMPLE
0		Light greyish brown organic rich topsoil	
		Light greyish white dry, non-plastic, stiff-firm silty sand with rare highly weathered greywacke clasts	
0.5		Light yellow and white moist, plastic, firm, mottled gravely clays with greywacke clasts up to 5mm	
1.0		Dark yellow and white, moist, plastic, stiff gravely clays. 2-3cm angular greywacke clasts. Possible shear surfaces along white clay layers near base of trench	
1.5			
2.0			
2.5			

LEGEND

Organic material

Silts

Sands

Gravels

Mottled clay

Veined clay

NOTES

* Sandy material beneath topsoil is loess

PROFILE

N/A

ENGINEERING GEOLOGY

TRENCH LOG

PROJECT:
B.Sc. Honours

EXCAVATION DETAILS:
Test Pit TP11

LOCALITY:
Smith Property, Moana View Rd.

LOGGED BY:
S.T.McManus

DATE:
February 8, 1994

SITE SKETCH

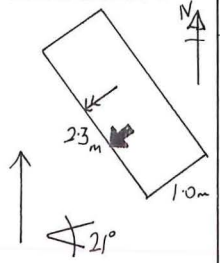

KEY

→ Slope direction

Slope gradient

Face logged

→» Photograph

DEPTH (M)	LOG	DESCRIPTION	SAMPLE
0		Dark brown/black organic rich, moist topsoil	
		Greyish white very dry, non-plastic, friable-stiff silty sand with highly weathered greywacke clasts	
0.5		Light yellow and white very moist-wet, highly plastic, mod stiff mottled clay with highly weathered greywacke clasts up to 5mm	
1.0		Dark yellow and grey moist-wet, highly plastic stiff clays with greywacke clasts up to 10mm Mottled clays grade into layered yellow and white clays	
1.5			
2.0			
2.5			

LEGEND

Organic material

Silts

Gravels

Sands

Mottled clay

Veined clay

NOTES

* Surrounding area is hummocky may represent past root raking

PROFILE

N/A

ENGINEERING GEOLOGY

TRENCH LOG

PROJECT:
B.Sc. Honours

EXCAVATION DETAILS:
Test Pit TP12

LOCALITY:
Windley Property, Moana View Rd.

LOGGED BY:
S.T.McManus

DATE:
February 10. 1994

SITE SKETCH

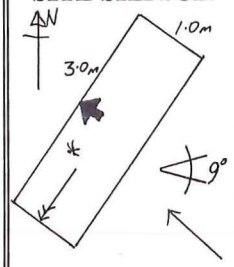

KEY

- Slope direction
- Slope gradient
- Face logged
- Photograph
- Sample

DEPTH (M)	LOG	DESCRIPTION	SAMPLE
0		Light grey brown organic topsoil	
		Yellow moist, plastic, stiff-firm, mottled clays Schistose clasts up to 10mm	
0.5		Yellow/white gravely clays with schist clasts Clays mottled and veined, very moist, very plastic, soft-mod stiff Clasts of schist up to 20mm	
1.0		Yellow/blue grey clays Weathered schist clasts up to 20mm	
1.5		Red weathered schist clast rich clays, very moist	WP28
		Yellow gravely clays	
2.0			
2.5			

LEGEND

- Organic material
- Gravels
- Mottled clay
- Veined clay

NOTES

* WP28 red weathered material at 1.5m

PROFILE

N/A

ENGINEERING GEOLOGY

TRENCH LOG

PROJECT:
B.Sc.Honours

EXCAVATION DETAILS:
Test Pit TP13

LOCALITY:
Miles and West, Moana View Rd.

LOGGED BY:
S.T.McManus

DATE:
February 10, 1994

SITE SKETCH

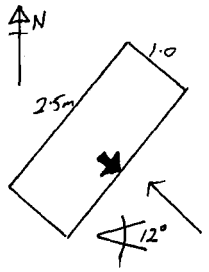

KEY

→ Slope direction

Slope gradient

Face logged

DEPTH (M)	LOG	DESCRIPTION	SAMPLE
0		Light brown organic topsoil	
		Dark yellow moist, plastic, stiff clay	
0.5			
		Dark yellow/white moist, plastic, firm veined clay. Oxidation on preserved joint surfaces	
1.0			
1.5		Yellow/white moist, plastic, firm clays with increasing white clay veining Oxidation increases along joint planes Highly weathered greywacke bedrock	
2.0			
2.5			

LEGEND

Organic material

Mottled clay

Veined clay

Bedrock

NOTES

PROFILE

N/A

ENGINEERING GEOLOGY

TRENCH LOG

PROJECT:
B.Sc. Honours

EXCAVATION DETAILS:
Test Pit TP14

LOCALITY:
Maori Cemetery debris Fans

LOGGED BY:
S.T.McManus

DATE:
February 10, 1994

SITE SKETCH

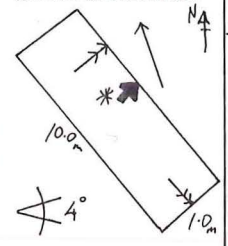

KEY

→ Slope direction

Slope gradient

Face logged

→→ Photograph

Sample

DEPTH (M)	LOG	DESCRIPTION	SAMPLE
0		Light grey/brown organic topsoil	
0.5			
1.0		Yellow/white moist, plastic, stiff silty clay matrix. Schist clasts, angular, matrix support Clasts between 10mm and 500mm	WP25 WP26 WP27
1.5			
2.0			
2.5			

LEGEND

Organic material

Gravels

Silts

Mottled clay

Veined clay

NOTES

* WP25 Fan matrix
* WP26 Fan gravels
* WP27 Fan gravels
* No evidence of disruption due to fault movement

PROFILE

N/A

HOLE A1

DEPTH	LOG	DETAIL
0	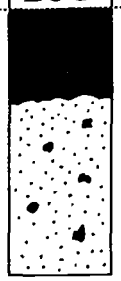	Dark grey/brown topsoil
		Silty clay, moist, v-plastic greywacke clasts
0.5		Base of hole 0.56m

HOLE A2

DEPTH	LOG	DETAIL
0		Organic rich topsoil
		Yellow/brown clay, moist v-plastic, greywacke clasts
0.5		Base of hole 0.6m

HOLE A3

DEPTH	LOG	DETAIL
0		Dark grey/brown organic topsoil
		Yellow/brown clay, v-plastic, stiff, weathered greywacke clasts
0.5		Base of hole 0.55m

HOLE A4

DEPTH	LOG	DETAIL
0	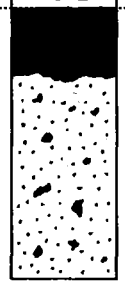	Dark brown/grey organic topsoil
		Dark yellow/brown silty clay greywacke clasts up to 10mm
0.5		Base of hole 0.55m

HOLE A5

DEPTH	LOG	DETAIL
0		Grey/brown topsoil
		Yellow /brown silty clay with schistose clasts
0.5		
1.0		Yellow clay with faint mottling
		Clastic rich material up to 2mm
		Base of hole 1.35m

HOLE A6

DEPTH	LOG	DETAIL
0	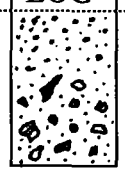	Yellow brown very dry sandy silt with coarse schist and greywacke gravels.
		Base of hole 0.30m

HOLE A7

DEPTH	LOG	DETAIL
0	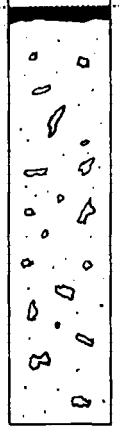	Topsoil thin, 0.05m
		Yellow and white mottled clay
		Schistose clasts highly weathered
0.5		
1.0		Base of hole 1.0m

HOLE A8

DEPTH	LOG	DETAIL
0	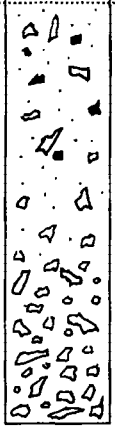	Yellow and white mottled clay
		Completely weathered schist
		and greywacke clasts
0.5		Yellow and white clay, v-wet
		Abundance of schistose clasts
		in a gravely clay
1.0		Base of hole 1.0m

HOLE A9

DEPTH	LOG	DETAIL
0	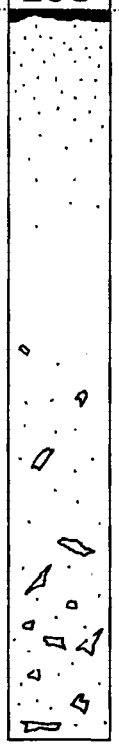	Very thin topsoil 0.05m
		Yellow/brown silty clay
		Yellow/white mottled clay
0.5		v-plastic, stiff, moist
1.0		Yellow/white veined clay
		slightly gravely, v-plastic, moist
1.5		Yellow/white veined clay
		gravely, with schist clasts 2mm
		Base of hole 1.8m

HOLE A10

DEPTH	LOG	DETAIL
0	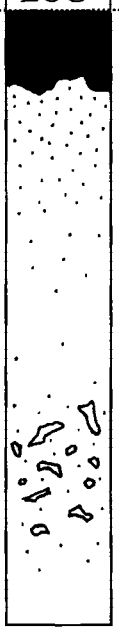	Topsoil 0.25m
		Light yellow/brown silty clay
		Yellow/white mottled clay
0.5		v-plastic, stiff, moist
		Yellow/white veined clay
1.0		Yellow /white veined clay
		Schist clasts up to 2mm
1.5		Yellow/white veined clay

HOLE A11

DEPTH	LOG	DETAIL
0	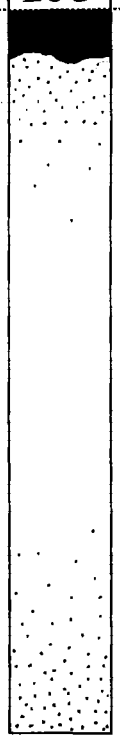	Organic topsoil
		Light yellow/brown silty clay
0.5		Yellow white mottled clay
		moist, plastic, stiff
1.0		Yellow/white veined clay
		slightly moist, plastic
1.5		Clay becoming more silty
		Base of hole 1.8m

HOLE A12

DEPTH	LOG	DETAIL
0	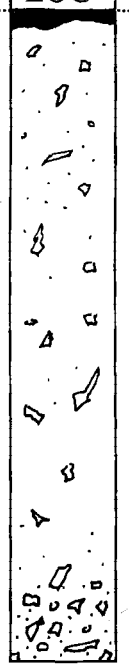	Thin grey/brown topsoil
		Yellow/brown mottled slightly
0.5		gravely clay, moist, plastic
		Yellow/white veined clay with
1.0		schistose gravel clasts 3mm
		White clay with some yellow
1.5		abundant schist clasts 3mm
		Base of hole 1.6m

HOLE A13

DEPTH	LOG	DETAIL
0	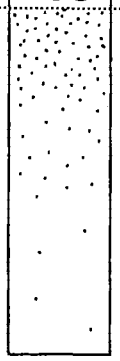	Light yellow/brown silty clay
0.5		Yellow/white mottled clay
		slightly moist, slightly plastic
		Base of hole 0.8m

HOLE A14

DEPTH	LOG	DETAIL
0	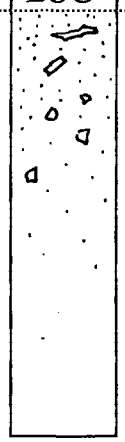	Light yellow/brown silty clay
		schist clasts up to 2mm
0.5		Yellow/white mottled clay
		slightly moist, soft, sl-plastic
		Yellow/white mottled clay
1.0		Base of hole 1.0m

HOLE A15

DEPTH	LOG	DETAIL
0		Organic topsoil
		Yellow/brown gravely clay
		Base of hole 0.35m
0.5		

HOLE A16

DEPTH	LOG	DETAIL
0	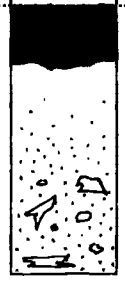	Organic topsoil
		Yellow/brown mottled clay
		Yellow/brown gravelly silt
		Schistose clasts present
0.5		Base of hole 0.55m

HOLE A17

DEPTH	LOG	DETAIL
0	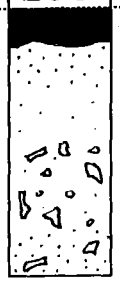	Organic topsoil
		Yellow /brown mottled silty clay
		Yellow gravely clay
		moist, plastic, schist up to 2mm
0.5		Base of hole 0.65m

HOLE A18

DEPTH	LOG	DETAIL
0	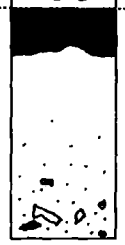	Organic topsoil
		Yellow clay, very plastic
		schist and greywacke clasts
0.5		Base of hole 0.5m

HOLE A19

DEPTH	LOG	DETAIL
0		Organic topsoil
		Yellow/white mottled gravely
		clay with clasts up to 2mm
		Organic layer with charcoal
0.5		Yellow/grey silty clay
		Yellow/white mottled gravely
		clay
1.0		Base of hole 1.25m

HOLE A20

DEPTH	LOG	DETAIL
0		Organic topsoil
0.5		White/grey sandy silt
		Yellow/white mottled clay
		some gravel clasts
1.0		Yellow/grey lithic rich layer
		Yellow/white veined clay
		wet, very plastic
1.5		Base of hole 0.65m

HOLE A21

DEPTH	LOG	DETAIL
0		Organic topsoil
		White/grey sandy silt
0.5		Yellow/white veined clays
		Greywacke clasts
		Moisture increases with depth
1.0		Base of hole 1.4m

HOLE A22

DEPTH	LOG	DETAIL
0	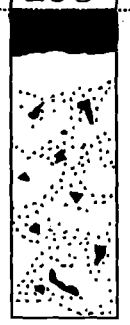	Organic rich topsoil
		Yellow/brown silty clay
0.5		some greywacke clasts
		Base of hole 0.7m

HOLE A23

DEPTH	LOG	DETAIL
0	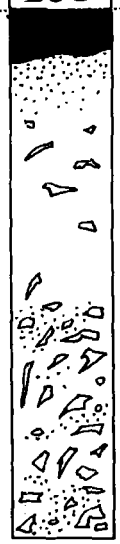	Dark brown organic topsoil
		White/grey silty sand
		Light yellow/white mottled clay
		schistose lithic fragments
0.5		
		Yellow/white mottled clay
		increasing moisture, schist clasts
1.0		
		Base of hole 1.3m

HOLE A24

DEPTH	LOG	DETAIL
0		Thin topsoil 0.07m
		White/grey sandy silt
0.5		Yellow clay, moist, plastic
		greywacke clasts 1-5mm
1.0		
		Base of Hole 1.4m

HOLE A25

DEPTH	LOG	DETAIL
0		Dark brown organic topsoil
		White/grey sandy silt
		Light yellow/white mottled clay
0.5		Plastic, soft-stiff
		moisture increases with depth
		Intense white clay veining
		Yellow clay, moist, plastic, stiff
		Base of hole 0.9m

HOLE A26

DEPTH	LOG	DETAIL
0	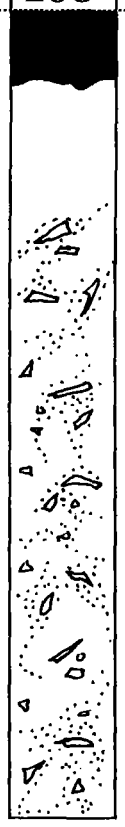	Grey/brown topsoil
0.5		Yellow/white mottled clay
		moisture increases with depth
		schist clasts increase with depth
1.0		Blue clay, schist clasts, moist
		Dark yellow gravely clay
		schistose clasts up to 5mm
1.5		Dark yellow gravely clay
		clasts become oxidised
2.0		Base of hole 2.0m

HOLE A27

DEPTH	LOG	DETAIL
0		Organic topsoil
		Dark yellow clay with some organics and gravels
0.5		Dark yellow gravely clay schistose clasts
		Some organics present
		Yellow/white veined clay
1.0		Yellow/white mottled clay abundant schistose clasts
1.5		Base of hole 1.55m

HOLE A28

DEPTH	LOG	DETAIL
0		Thin topsoil 0.07m
		Yellow clay, soft, plastic moisture increases with depth
0.5		Increasing greywacke clasts
1.0		
1.5		Base of hole 1.5m

HOLE A29

DEPTH	LOG	DETAIL
0		Organic topsoil
		Yellow/white mottled clay Greywacke clasts present
0.5		White clay later present
		White veining increases Moisture increases with depth
1.0		Base of hole 1.1m

HOLE A30

DEPTH	LOG	DETAIL
0	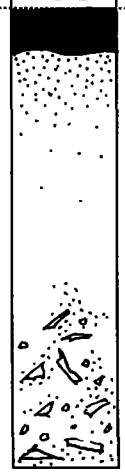	Grey/black topsoil
		White/grey sandy silt
		Yellow/white mottled clays
0.5		Yellow clays with some white mottling, moist, plastic Schist clasts up to 1mm
1.0		Base of hole 1.1m

HOLE A31

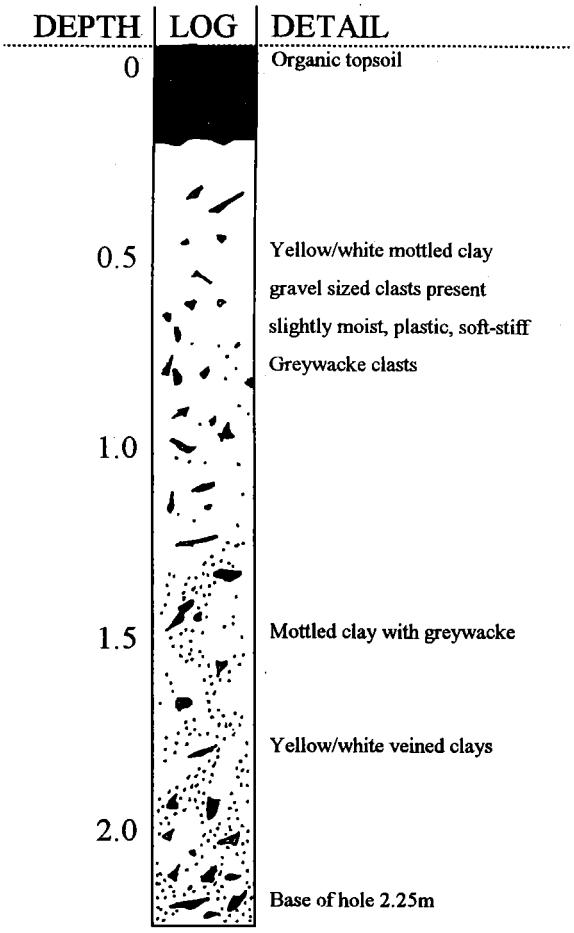

HOLE A32

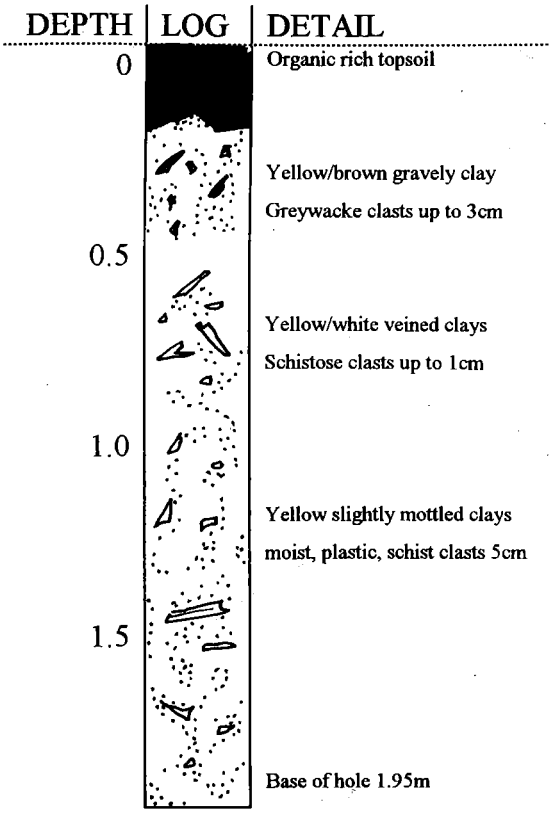

APPENDIX C

ROCK AND SOIL DEFINITIONS

C1 TERMINOLOGY

C2 FIELD DESCRIPTIONS FOR ROCK MATERIAL

C3 FIELD DESCRIPTIONS FOR SOIL MATERIAL

APPENDIX C1

ROCK AND SOIL TERMINOLOGY

(After McManus, 1994)

Geological Usage

The geological distinction between a rock and a soil is summarised by Bell and Pettinga (1983):-

ROCK

Any material below the depth of modern weathering, regardless of the degree of consolidation or cementation.

SOIL

Formed at the earth's surface by physical, chemical, and biological processes.

The geological classification for rocks is primarily dependent on a sedimentary, igneous or metamorphic origin and soils are either residual soils; insitu weathering, or transported by a particular geologic process.

Engineering Usage

Terminology for an engineering description differs from a geological classification by the different strength characteristics of the material. Engineering rocks and soils are defined as:-

ROCK

Hard and rigid, requiring blasting or some equivalent method for excavation. Not significantly affected by immersion in water.

SOIL

Loose or soft deposits that can be excavated by normal earth moving equipment. Either disagregates or becomes remouldable in water.

ENGINEERING GEOLOGICAL FIELD DESCRIPTION FOR ROCK MATERIAL

WEATHERING

	TERM	GRADE	ROCK DESCRIPTION
6.	* residual soil (RW)	VI	discolouration and complete transformation to soil; original fabric destroyed
5.	completely weathered (CW)	V	discolouration and transformation to soil; original fabric largely preserved
4.	highly weathered (HW)	IV	material pervasively altered with discolouration and loss of strength; fabric preserved; lithorelicts
3.	moderately weathered (MW)	III	penetrative discolouration and alteration of rock material, with some loss of strength
2.	slightly weathered (SW)	II	slight discolouration of rock fabric; no loss of material strength
1.	unweathered (UW)	I	no discolouration or loss of strength, or any other effects due to weathering

STRENGTH

	TERM	POINT LOAD STRENGTH INDEX $I_s(50)$	FIELD ESTIMATION OF STRENGTH
1.	extremely strong (ES)	more than 10	can only be chipped with geological hammer
2.	very strong (VS)	3 to 10	several hard blows required to break hand specimen
3.	strong (S)	1 to 3	few firm blows of hammer required to break specimen
4.	moderately strong (MS)	0·3 to 1	breaks readily with one blow of hammer
5.	moderately weak (MWk)	0·1 to 0·3	broken by hand only with difficulty; small thin pieces broken by finger pressure
6.	weak (Wk)	0·03 to 0·1	broken by hand; pieces 25 mm or more broken by finger pressure
7.	* very weak (VWk)	less than 0·03	crushed or remoulded by hand (grades into soil materials)

* may require description as soil material

GEOLOGICAL CLASSIFICATION

CRYSTAL OR GRAIN SIZE	SEDIMENTARY (1)		IGNEOUS (1)				METAMORPHIC (1)	
	CLASTIC	CHEM/ORGANIC		Silicic	Intermed	Mafic	Ultramaf	FOLIATED	MASSIVE
very coarse 64	CONGLOMERATE (1) AGGLOMERATE (2) BRECCIA (3)		PLUTONIC	(27) (28) GRANITE GRANODIORITE	(29) (30) SYENITE DIORITE	(31) GABBRO	(32) (33) PERIDOTITE DUNITE	GNEISS (34) SCHIST (35) PHYLLITE (36) SLATE (37) MYLONITE (38)	HORNFELS (39) MARBLE (40) QUARTZITE (41) AMPHIBOLITE (42)
coarse 2		Calcareous LIMESTONE (9)							
medium 0·06	SANDSTONE (4)	Siliceous CHERT (10) OTHER (11)							
fine	SILTSTONE (5)	Carbonaceous COAL (12) OTHER (13)	HYPABYSSAL	(19) (20) (21) RHYOLITE OBSIDIAN DACITE	(22) (23) TRACHYTE ANDESITE	(24) (25) DOLERITE BASALT	(26) SERPENTINITE		(1) OTHERS: Specify (43)
	MUDSTONE (6)	Ferruginous LATERITE (14) OTHER (15)							
very fine 0·002 (mm)	CLAYSTONE (8)	Saline ROCK SALT (16) GYPSITE (17) OTHER (18)	VOLCANIC						

Mode of Occurrence

WEATHERING TERM — STRENGTH TERM — COLOUR — FABRIC — ROCK NAME

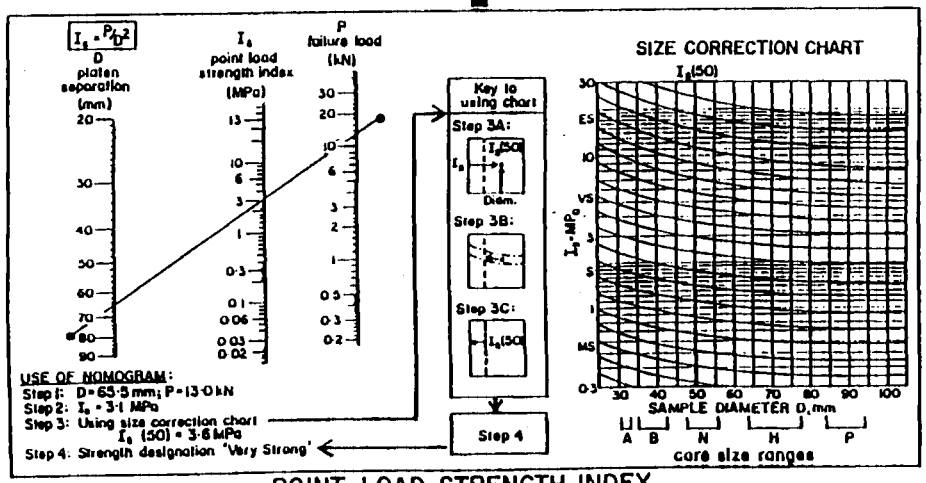

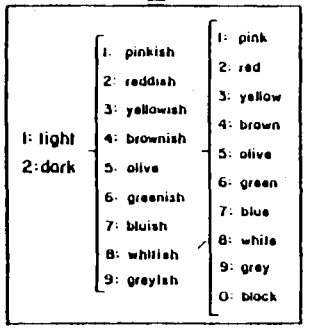

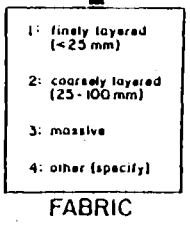

ENGINEERING GEOLOGICAL FIELD DESCRIPTION FOR ROCK MASS

FIELD SKETCH OR
ANNOTATED PHOTOGRAPH

SCALE:

ORIGINAL SCALE:
1:

SKETCH ORIENTATION:

GENERAL INFORMATION

PROJECT/AREA:
LOCALITY:
REFERENCE MAP:
COORDINATES:
ELEVATION:
GEOLOGY BY:
DATE:
CHECKED:
Sheet No.: of

SHEET REFERENCE

ADDITIONAL DATA

GRAPHIC SYMBOL	ROCK UNIT No.	ROCK MATERIAL DESCRIPTION				
		WEATHERING	STRENGTH	COLOUR	FABRIC	ROCK NAME
	1					
	2					
	3					
	4					
	5					
	6					
		OTHER MATERIAL DESCRIPTIONS: (specify)				
	7					
	8					
	9					

TERMINOLOGY FOR COMMON DEFECTS IN ROCK MASS

DEFECT TYPE	LAYERING (1)			FRACTURES AND FRACTURE ZONES (1)		WEAK SEAMS OR ZONES (1)		
	BEDDING (1)	FOLIATION (2)	CLEAVAGE (3)	JOINT / FAULT (4)	SHEARED ZONE (5)	CRUSHED (6)	DECOMPOSED (7)	INFILLED (8)
DESCRIPTION	i) Arrangement in layers of mineral grains or crystals of similar size or composition. ii) Arrangement of discontinuities or planes of mineral grains never parallel to one another and/or to the layers.			Single fracture across which rock has little tensile strength; planar, curved, or irregular; open, closed or occasionally; surface rough, smooth or slickensided.	Zone of multiple closely spaced (< 100 mm) fracture planes, with roughly parallel planar boundaries; blocks of intact material within zone typically lenticular or wedge shaped; fractures closed, open, weakly cemented or well-cemented.	Zone with roughly parallel planar boundaries:- i) Composed of disoriented, usually angular, rock fragments of variable size in a soil matrix. ii) Some weathering of fragments possible, with soils either cohesive or non-cohesive. iii) Lowest shear strength parallel to zone boundaries, which are commonly slickensided.	Zone of any shape, but commonly with roughly parallel planar boundaries:- i) Within zone rock moderately to completely weathered. ii) At margins gradation into fresher rock.	i) Composed of soil materials which may show layering roughly parallel to zone boundaries. ii) Rock fabric not present in infill zone. NOTE: materials forming zone require separate description as soil or rock mass
MAP SYMBOLS with strike and dip	075/73	60/064	37/Rx	'open' 27 'closed' 013/86	145/083	* Record width of zone as required.	78/072	20/069
								(1) OTHERS: Specify (9)

DEFECT DATA SUMMARY TABLE

ROCK UNIT No.	DEFECT SET No.	DEFECT TYPE	DEFECT SPACING	DEFECT PERSISTENCE	AV. UNIT BLOCK SIZE	DEFECT ORIENTATION: DIP DIRECTION	DEFECT ORIENTATION: DIP VALUE	GROUND-WATER	REMARKS
						±	±		
						±	±		
						±	±		
						±	±		
						±	±		
						±	±		
						±	±		
						±	±		
						±	±		
						±	±		

DEFECT ORIENTATION DIAGRAM

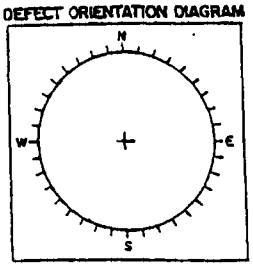

DEFECT SPACING

	TERM	SPACING (mm)
1	extremely wide	> 2000
2	very wide	600 — 2000
3	wide	200 — 600
4	moderate	100 — 200
5	close	25 — 100
6	very close	5 — 25
7	extremely close	< 5

DEFECT PERSISTENCE

	TERM	LENGTH (m)
1	very high	> 10
2	high	3 — 10
3	moderate	1 — 3
4	low	0.5 — 1
5	very low	< 0.5

AVERAGE UNIT BLOCK SIZE

	TERM	EQUIVALENT CUBE SIDE	APPROX. BLOCK VOLUME (m^3)
1	very large	1000 mm	> 1.0
2	large	500 mm	0.1 — 1.0
3	medium	100 mm	0.001 — 0.1
4	small	10 mm	< 0.001
5	very small		

GROUNDWATER

	TERM	FLOW RATE
1	dry	
2	seepage	< 1 l/min
3	very low flow	1 — 10 l/min
4	low flow	10 — 100 l/min
5	moderate flow	0.1 — 1 l/s
6	large flow	1 — 10 l/s
7	very large flow	> 10 l/s

ENGINEERING GEOLOGICAL FIELD DESCRIPTION FOR SOIL MATERIAL

WEATHERING

	TERM	GRADE	SOIL DESCRIPTION
5	Completely Weathered (CW)	V	completely discoloured and altered; no trace of original fabric
4	Highly Weathered (HW)	IV	mostly altered and weakened; little trace of original fabric
3	Moderately Weathered (MW)	III	large discoloured portions of original soil separated by more altered material, significantly weakened
2	Slightly Weathered (SW)	II	minor discolouration of some parts of the original soil, no loss of strength
1	Unweathered (UW)	I	original soil with NO discolouration, loss of strength or other effects due to weathering
0	NOTE * in coarse-grained soils record weathering grade of DOMINANT fraction here and qualify weathering grade of subordinate and/or minor fractions if appropriate		

STRENGTH

	TERM	FIELD CRITERIA
1	loose	can be removed from exposure in disaggregated form by hand
2	compact	only removed from exposure by implement; material readily disaggregated by physical means
3	+ cemented	only removed from exposure by implement; material does not disaggregate
4	hard	may be removed from exposure with difficulty by implement or hand; softened on immersion in water and may be remoulded
5	stiff	indented by thumb pressure, but not moulded by fingers; softened on immersion in water, and may be remoulded
6	firm	moulded or indented only by strong finger pressure, easily moulded after immersion in water
7	soft	easily indented or moulded by finger pressure
8	very soft	exudes between fingers when squeezed
9	spongy	readily compressed by finger pressure, but cannot be remoulded

+ may require description as rock material

UNIFIED SOIL CLASSIFICATION SYSTEM

			FIELD IDENTIFICATION	GROUP SYMBOL	TYPICAL NAMES
COARSE-GRAINED SOILS	GRAVELS (>50% larger than 2 mm)	clean gravels	wide range in grain size and substantial amounts of all interm. sizes	GW	well graded GRAVELS
			predom. one size or a range of sizes with some interm. sizes missing	GP	poorly graded GRAVELS
		gravels with fines	non-plastic fines (see ML below)	GM	poorly graded SILTY-GRAVELS
			plastic fines (see CL below)	GC	poorly graded CLAYEY-GRAVELS
	SANDS (<50% smaller than 2 mm)	clean sands	wide range in grain sizes and substantial amounts of all interm. sizes	SW	well graded SANDS
			predom. one size or a range of sizes with some interm. sizes missing	SP	poorly graded SANDS
		sands with fines	non-plastic fines (see ML below)	SM	poorly graded SILTY-SANDS
			plastic fines (see CL below)	SC	poorly graded CLAYEY-SANDS

			SHINE	DILATANCY (1)	TOUGHNESS (1)		
FINE-GRAINED SOIL	SILTS AND CLAYS	LIQUID LIMIT ≤50	none to very dull	quick to slow	none	ML	INORGANIC SILTS with slight plasticity
			moderate	none to very slow	medium	CL	INORGANIC CLAYS of low to medium plasticity
			none to very dull	slow	slight	OL	ORGANIC SILTS & CLAYS of low plasticity
		LIQUID LIMIT >50 A	dull	slow to none	slight to medium	MH	INORGANIC SILTS of high plasticity
			very glossy	none	high	CH	INORGANIC CLAYS of high plasticity
			moderate to v glossy	none to very slow	slight to medium	OH	ORGANIC CLAYS of medium to high plasticity
HIGHLY ORGANIC SOILS			identified by colour, odour, spongy feel and fibrous texture			Pt	PEAT and other highly organic soils

PROCEDURES FOR FINE-GRAINED SOILS OR FRACTIONS (1)

DILATANCY (reaction to shaking):-

1) Prepare pat of moist soil, adding water to make soft - but not sticky.

2) Place pat in palm of hand, shake horizontally by striking vigorously against other hand.

Positive Reaction: appearance of water on surface of pat, which becomes glossy. When squeezed between fingers, water and gloss disappear, pat stiffens and may crumble.

TOUGHNESS: (consistency near plastic limit):-

1) Mould sample to consistency of putty, adding water or air drying as required.

2) Roll to thin (3 mm) thread, fold and reroll repeatedly until thread crumbles at plastic limit.

3) Knead together and continue until lump crumbles.

Diagnosis: a tough thread and stiff lump indicate high plasticity; a weak thread and lump low plasticity clays.

GROUP SYMBOL CODINGS FOR USCS

COLUMN 1		COLUMN 2	
G:1	C:4	W:1	C:4
S:2	O:5	P:2	L:5
M:3	Pt:6	M:3	H:6

BOUNDARY CLASSIFICATIONS specify, enter 0.0

WEATHERING TERM | WATER CONTENT TERM | STRENGTH TERM | COLOUR | FABRIC | SOIL NAME | USCS SYMBOL

WATER CONTENT

	TERM	FIELD CRITERIA
1	Dry	looks and feels dry; fine-grained soils usually hard, powdery or friable; coarse-grained soils may run freely through hands
2	Moist	soil feels cool and may be darkened in colour; particles tend to adhere in coarse-grained materials, fine-grained soils may be softened
3	Wet	soils feel cold and are darkened in colour; free water forms on hands when sample is disturbed
4	Saturated	restricted to wet soils below the water table or the static water level in excavations or drill holes

COLOUR

	1	2	3	4	5	6	7	8	9	0
1: light	pinkish	reddish	yellowish	brownish	olive	greenish	bluish	whitish	greyish	
2: dark	pink	red	yellow	brown	olive	green	blue	white	grey	black

FABRIC

1: finely layered (<25 mm)
2: coarsely layered (25-100 mm)
3: massive
4: other (specify)

SOIL NAME

*SUBORDINATE FRACTION: 20-50% volume visual estimate

DOMINANT FRACTION: >50% volume visual estimate

* MINOR FRACTION: <20% volume visual estimate

1	coarse	gravelly
2	medium	
3	fine	
4	coarse	sandy
5	medium	
6	fine	
7	silty	
8	clayey	
9	peaty	

PARTICLE SIZE

	SOIL TYPE TERM		PARTICLE SIZE (mm)	GRAPHIC LOG
1	coarse	gravel	> 60	
2	medium		20-60	
3	fine		2-20	
4	coarse	sand	0·6-2·0	
5	medium		0·2-0·6	
6	fine		0·06-0·2	
7	silt		0·002-0·06	
8	clay		< 0·002	
9	peat		NA	

WITH SOME

1	coarse	gravel
2	medium	
3	fine	
4	coarse	sand
5	medium	
6	fine	
7	silt	
8	clay	
9	peat	

ENGINEERING GEOLOGICAL FIELD DESCRIPTION FOR SOIL MASS

FIELD SKETCH OR
ANNOTATED PHOTOGRAPH

SCALE: ORIGINAL SCALE: 1: SKETCH ORIENTATION

GENERAL INFORMATION

PROJECT/AREA:
LOCALITY:
REFERENCE MAP:
COORDINATES:
ELEVATION:
GEOLOGY BY:
DATE:
CHECKED:
Sheet No. of

SHEET REFERENCE:

ADDITIONAL DATA

GRAPHIC SYMBOL	SOIL UNIT No	SOIL MATERIAL DESCRIPTION: WEATHERING	WATER CONTENT	STRENGTH	COLOUR	FABRIC	SOIL NAME	USCS SYMBOL
	1							
	2							
	3							
	4							
	5							
	6							

		OTHER MATERIAL DESCRIPTIONS: (Specify)	
	7		
	8		
	9		

TERMINOLOGY FOR COMMON DEFECTS IN SOIL MASS

DEFECT TYPE	LAYERING (1) *		FRACTURES (1) *		CAVITIES (1) *	
	BEDDED/STRATIFIED (1)	LAYERED (2)(3)	JOINT/FISSURE (4)	SHEAR ZONE (5)	OPEN CAVITY (6)	INFILLED CAVITY (7)
DESCRIPTION	1) Arrangement in layers of soil particles of similar colour, size and composition 2) Arrangement of elongated or tabular particles or voids near parallel to one another or to the layers soil mass shows bedding or stratification with spacing > 100 mm	soil material is finely layered (<25 mm) or coarsely layered (25–100 mm)	Single fracture across which soil has little tensile strength; planar, curved or irregular; closed, open or partly infilled by soil or rock material; may be continuous over outcrop extent	Zone of multiple very closely spaced (<25 mm) fracture planes either irregular, or with roughly parallel planar boundaries that are smooth or slickensided; lens shaped blocks of soil within zone, which may be softened or vermed	Opening within soil mass, commonly tubular; may occur singly or as multiple, separate or interconnected tubes; may occur also as sheet or wall-like openings within soil mass; walls of cavity may be coated with clay/silt or organic matter	Open cavities that have been partly or completely infilled by collapsed or transported material; infilling material may be partly cemented, softened or wetted
	NOTE: Indicate bed or layer description and defect spacing as shown below				where cavities identified indicate origin (e.g. by piping)	
MAP SYMBOLS with strike and dip	068/21	32 1/016	'open' 090/27 'closed' 015/66	35 strike 012 W	W denotes presence of 'vermed' zone or margin	SKETCH AS APPROPRIATE
						(1) OTHERS (8): Specify

DEFECT DATA SUMMARY TABLE

SOIL UNIT No.	DEFECT SET No.	DEFECT TYPE	DESCRIPTION (1, III): LAYERING	DESCRIPTION (1, III): FRACTURE/CAVITY	DEFECT ORIENTATION: DIP DIRECTION	DEFECT ORIENTATION: DIP VALUE	GROUNDWATER	REMARKS
					±	±		
					±	±		
					±	±		
					±	±		
					±	±		
					±	±		
					±	±		
					±	±		

* NOTE I: Where softened or vermed zones occur adjacent to layering, fractures or cavities, indicate on sketch and in remarks column

NOTE II: Fracture/cavity description requires information on defect spacing, continuity and geometry. Sketch if appropriate

LAYERING DESCRIPTION

1: non-uniform
- 1: planar
- 2: curved
- 3: irregular
- 4: contorted
- 5: lenticular
- 6: gradational
- 7: other (specify)

2: uniform

DEFECT SPACING

	TERM	SPACING (mm)
1	extremely wide	> 2000
2	very wide	600–2000
3	wide	200–600
4	moderate	100–200
5	close	25–100
6	very close	5–25
7	extremely close	< 5

DEFECT CONTINUITY

	TERM	LENGTH (m)
1	very high	> 10
2	high	5–10
3	moderate	2–5
4	low	0.5–2
5	very low	< 0.5

GROUNDWATER

	TERM	FLOW RATE
1	dry	
2	seepage	< 1 ml s^{-1}
3	very low flow	1–10 ml s^{-1}
4	low flow	10–100 ml s^{-1}
5	moderate flow	0.1–1 l s^{-1}
6	large flow	1–10 l s^{-1}
7	very large flow	> 10 l s^{-1}

APPENDIX D

FIELD AND LABORATORY TESTING

D1 PERCOLATION DATA

D2 RAINFALL DATA, BOONS VALLEY

D3 STREAM FLOW DATA, GRAHAM RIVER

D4 GRAINSIZE ANALYSIS

D5 ATTERBERG LIMIT DATA

D6 SOIL EROSION TESTING

D7 POINT LOAD STRENGTH DATA

D8 CONE INDENTER STRENGTH DATA

D9 X-RAY DIFFRACTION ANALYSIS

D10 SCANNING ELECTRON MICROSCOPE

D11 RING SHEAR TESTING

APPENDIX D1

PERCOLATION DATA

Percolation Test (1979): Whatamango Bay, Section 21, Mr C.S. Speight						
Drop Time	HOLE 1	HOLE 2	HOLE 3	HOLE 4	HOLE 5	HOLE 6
1/2 hr	Empty	Empty	550	Empty	Empty	Empty
1.5 hrs	Empty	Empty	550	Empty	Empty	Empty
1.40 hrs	Empty	Empty	500	Empty	Empty	Empty
2.10 hrs	Empty	Empty	525	Empty	585	625
2.55 hrs	500	400	513	Empty	575	587
3.35 hrs	375	325	550	Empty	Empty	Empty
4.10 hrs	363	350	500	Empty	563	Empty
4.45 hrs	325	313	475	Empty	500	500

Percolation Test (1980): Whatamango Bay, Lot 9, DP 3341, Mr W.M. Gilbert						
TIME	HOLE 1	HOLE 2	HOLE 3	HOLE 4	HOLE 5	HOLE 6
0.30	17.5	17.5	0	17.5	0	0
1.00	0	0	0	17.5	0	0
1.30	0	0	0	17.5	0	0
2.00	0	0	0	17.5	0	0
2.30	0	0	0	0	0	0
3.00	0	0	0	0	0	0
3.30	0	0	0	0	0	0
4.00	0	0	0	0	0	0

Percolation Test (1978): Waikawa Bay, Lot 4A, DP 1123. P.E. Rothwell						
TIME	HOLE 1	HOLE 2	HOLE 3	HOLE 4	HOLE 5	HOLE 6
0.30	600	200	150	150	137	125
1.00	600	87	87	144	113	94
1.30	500	69	75	125	100	75
2.00	400	63	75	88	88	63
2.30	300	75	87	125	113	88
3.00	287	75	100	138	119	88
3.30	262	68	94	125	100	82
4.00	300	75	100	150	113	88

Percolation Test (1988): Wharetekura Bay, Lot 4, DP 1435, Mr R. Dudman						
TIME	HOLE 1	HOLE 2	HOLE 3	HOLE 4	HOLE 5	HOLE 6
0.30	140	135	135	138	140	136
1.00	115	120	123	120	124	126
1.30	110	115	115	116	118	116
2.00	110	107	108	110	115	110
2.30	110	110	115	110	112	110
3.00	107	110	118	112	110	108
3.30	103	105	115	108	105	108
4.00	103	105	110	106	105	106

Daily Rainfall Totals - Waikawa at Boons Valley												
Rainfall in mm - Day ends Midnight each Day												
Day	Jan	Feb	Mar	Apr	May	Jun	Jly	Aug	Sep	Oct	Nov	Dec
1	?	12	3	9	3	0	0	0	0	?	?	?
2	0	7	0	0	20	31	4	20	13	?	?	?
3	12	0	2	0	0	0	57	128	1	?	?	?
4	0	0	0	59	1	0	0	10	1	?	?	?
5	0	5	0	86	17	0	5	51	4	?	?	?
6	0	1	0	1	38	0	6	10	43	?	?	?
7	0	0	0	5	9	0	0	0	2	?	?	?
8	22	0	0	16	0	0	0	8	1	?	?	?
9	6	0	0	2	22	0	0	8	0	?	?	?
10	0	0	15	1	0	5	0	0	0	?	?	?
11	0	0	1	62	0	14	0	0	0	?	?	?
12	0	0	5	1	0	27	43	0	0	?	?	?
13	0	0	45	0	0	1	21	0	0	?	?	?
14	0	0	0	14	0	19	1	0	0	?	?	?
15	0	0	0	1	2	21	5	0	0	?	?	?
16	0	0	1	0	2	3	0	0	8	?	?	?
17	0	0	0	0	0	1	0	0	0	?	?	?
18	0	0	0	0	0	0	0	2	0	?	?	?
19	3	0	7	0	0	0	14	0	?	?	?	?
20	0	0	0	7	0	0	3	0	?	?	?	?
21	0	1	1	3	0	0	3	0	?	?	?	?
22	0	31	0	54	0	27	10	24	?	?	?	?
23	10	52	3	0	0	0	0	0	?	?	?	?
24	0	5	0	7	0	0	0	27	?	?	?	?
25	0	0	0	12	0	0	0	3	?	?	?	?
26	23	0	7	22	0	0	0	0	?	?	?	?
27	55	1	1	0	1	0	0	0	?	?	?	?
28	8	2	0	1	60	1	0	5	?	?	?	?
29	0		0	0	4	10	0	1	?	?	?	?
30	0		0	6	0	14	0	0	?	?	?	?
31	0		0		0		0	0		?		?

	Daily Mean Flow - Graham River at Whatamango											
	Litres/Second											
Day	Jan	Feb	Mar	Apr	May	Jun	Jly	Aug	Sep	Oct	Nov	Dec
1	?	?	?	27	45	35	31	8	16	?	?	?
2	?	?	?	28	62	66	21	7	42	?	?	?
3	?	?	?	25	53	113	404	524	46	?	?	?
4	?	?	?	64	43	58	166	415	29	?	?	?
5	?	?	?	1712	44	42	96	467	31	?	?	?
6	?	?	?	196	562	34	78	453	333	?	?	?
7	?	?	?	74	397	28	68	195	388	?	?	?
8	?	?	?	46	164	23	55	123	110	?	?	?
9	?	?	?	32	169	19	45	192	75	?	?	?
10	?	?	?	20	162	19	39	108	58	?	?	?
11	?	?	?	265	104	55	34	79	47	?	?	?
12	?	?	?	297	76	150	182	63	41	?	?	?
13	?	?	?	123	60	86	192	52	35	?	?	?
14	?	?	?	188	49	111	199	43	31	?	?	?
15	?	?	?	135	43	238	126	36	28	?	?	?
16	?	?	?	94	39	175	85	31	34	?	?	?
17	?	?	?	73	32	190	61	26	32	?	?	?
18	?	?	?	62	27	118	46	26	?	?	?	?
19	?	?	?	53	23	82	59	21	?	?	?	?
20	?	?	?	53	19	59	52	18	?	?	?	?
21	?	?	?	49	16	45	46	16	?	?	?	?
22	?	?	?	493	14	48	47	34	?	?	?	?
23	?	?	?	141	11	38	40	19	?	?	?	?
24	?	?	35	87	8	31	34	121	?	?	?	?
25	?	?	33	84	5	26	30	72	?	?	?	?
26	?	?	37	138	3	22	26	44	?	?	?	?
27	?	?	37	115	2	19	22	35	?	?	?	?
28	?	?	34	80	213	17	19	32	?	?	?	?
29	?		29	63	155	18	17	29	?	?	?	?
30	?		25	54	75	34	14	22	?	?	?	?
31	?		23		46		11	18		?		?

APPENDIX D4

GRAIN SIZE ANALYSIS

Twenty seven individual samples were analysed using the method sieve and pipette method presented in NZS 4402. Five separate soil types were represented; greywacke regolith, greywacke colluvium, schistose regolith, schistose colluvium and red weathered regolith.

All samples were disaggregated using a 10% solution of hydrogen peroxide and left for approximately one week each. Following disaggregation, preliminary wet seiving was performed using 1ϕ and 4ϕ sieves. The coarse fractions (<4ϕ) were then dried and subject to 30 minutes of dry seiving with sieve fractions of 1ϕ and ranging from 1ϕ to 4ϕ. The coarse fraction was then collected and weighed.

The mud fraction which passed through the 4ϕ sieve was also dried and weighed. Pipette analysis was then performed on the mud fraction with phi sizes determined up to 9ϕ; the engineering classification of clay.

Graphical representation of the results is presented on the following pages

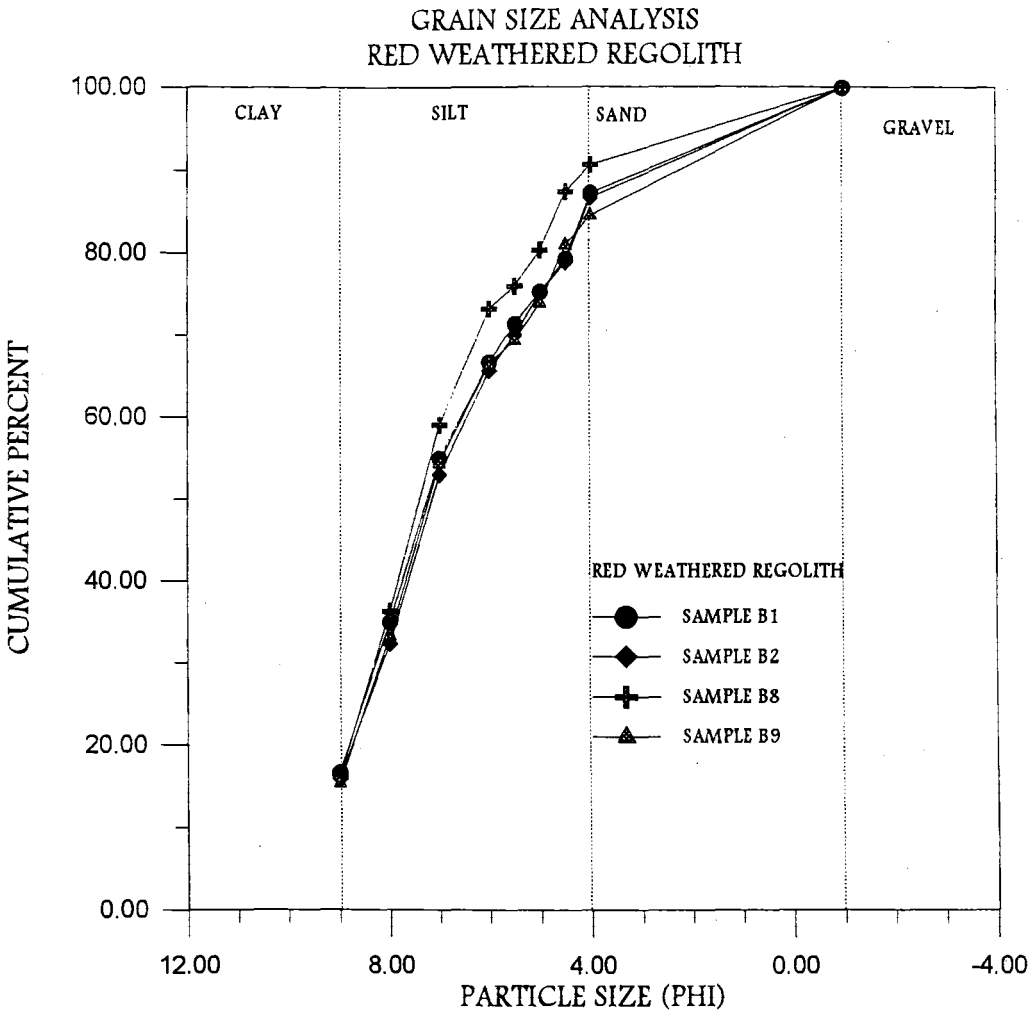
GRAIN SIZE ANALYSIS
RED WEATHERED REGOLITH
CLAY
SILT
SAND
GRAVEL
100.00
80.00
60.00
40.00
20.00
0.00
CUMULATIVE PERCENT
12.00
8.00
4.00
0.00
-4.00
PARTICLE SIZE (PHI)
RED WEATHERED REGOLITH
SAMPLE B1
SAMPLE B2
SAMPLE B8
SAMPLE B9

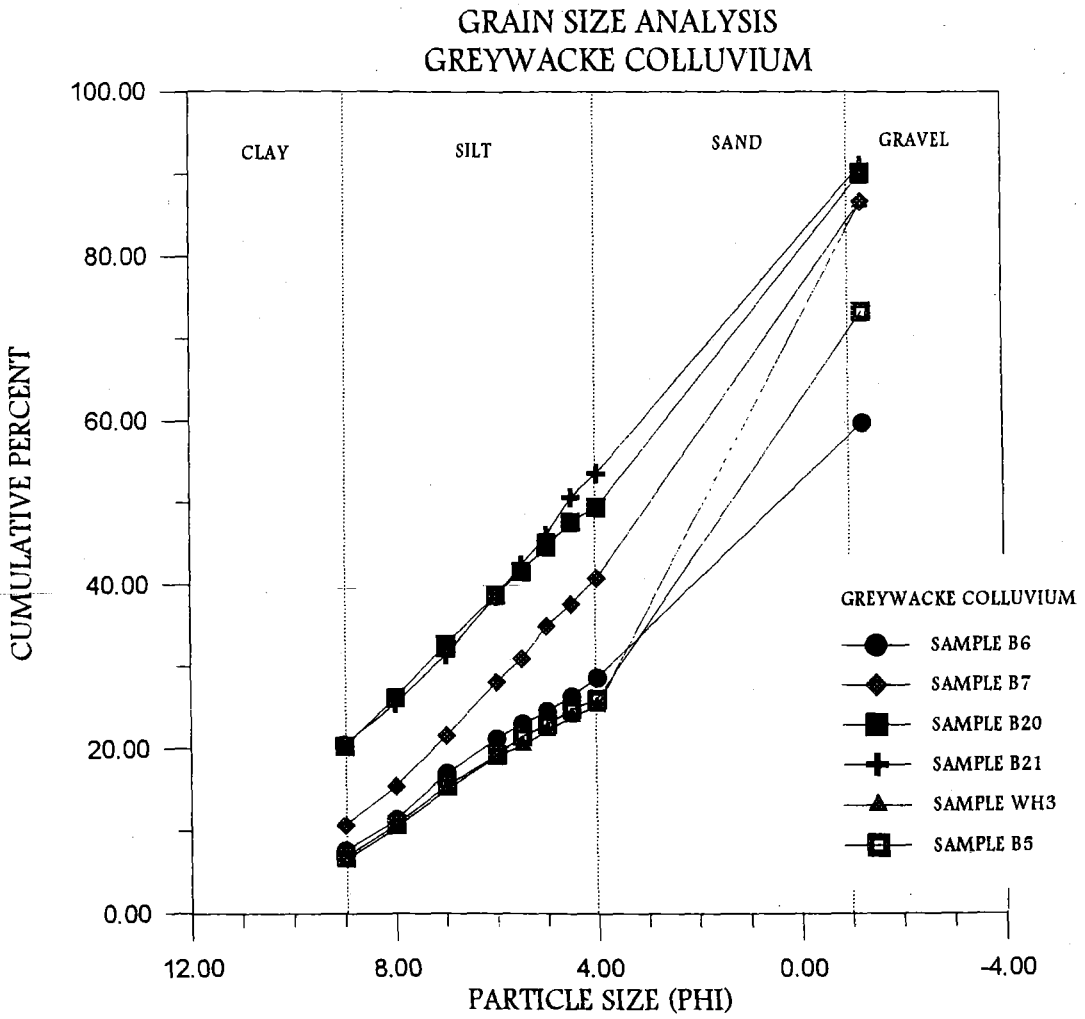
GRAIN SIZE ANALYSIS
GREYWACKE COLLUVIUM
CLAY
SILT
SAND
GRAVEL
100.00
80.00
60.00
40.00
20.00
0.00
CUMULATIVE PERCENT
12.00
8.00
4.00
0.00
-4.00
PARTICLE SIZE (PHI)
GREYWACKE COLLUVIUM
SAMPLE B6
SAMPLE B7
SAMPLE B20
SAMPLE B21
SAMPLE WH3
SAMPLE B5

GRAIN SIZE ANALYSIS
GREYWACKE REGOLITH

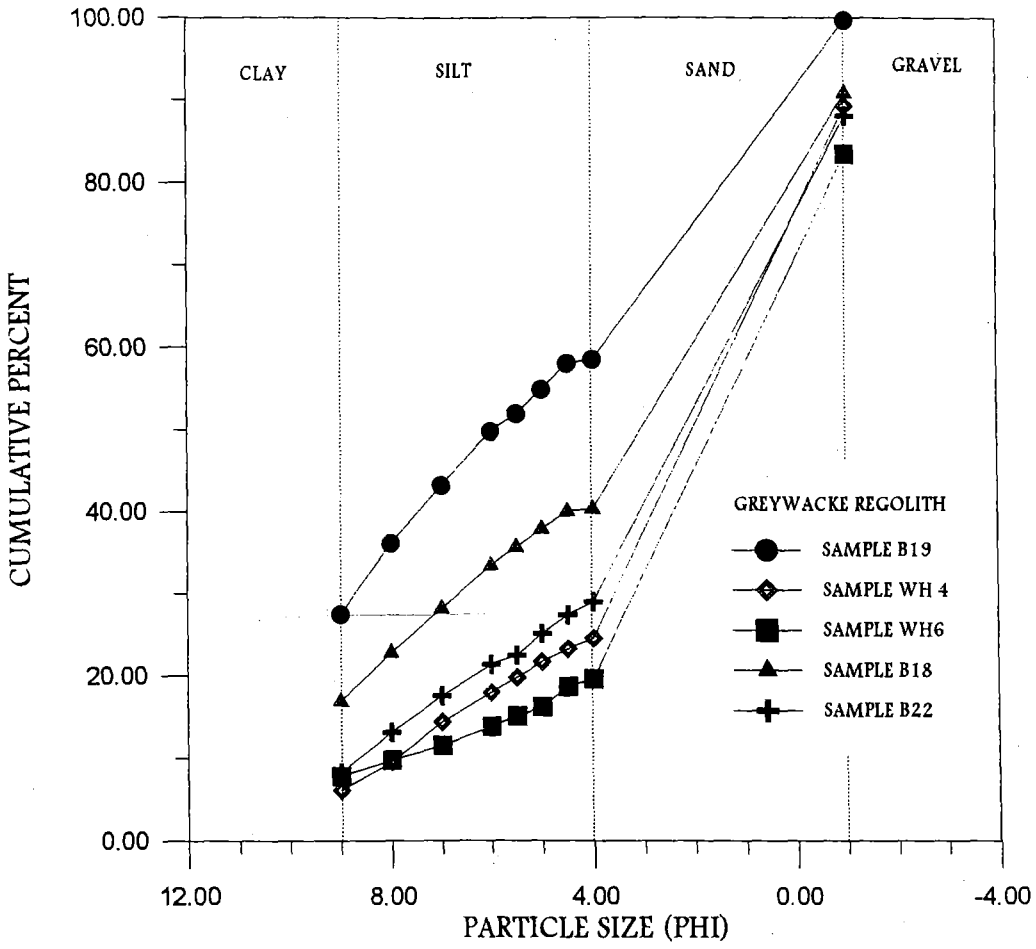

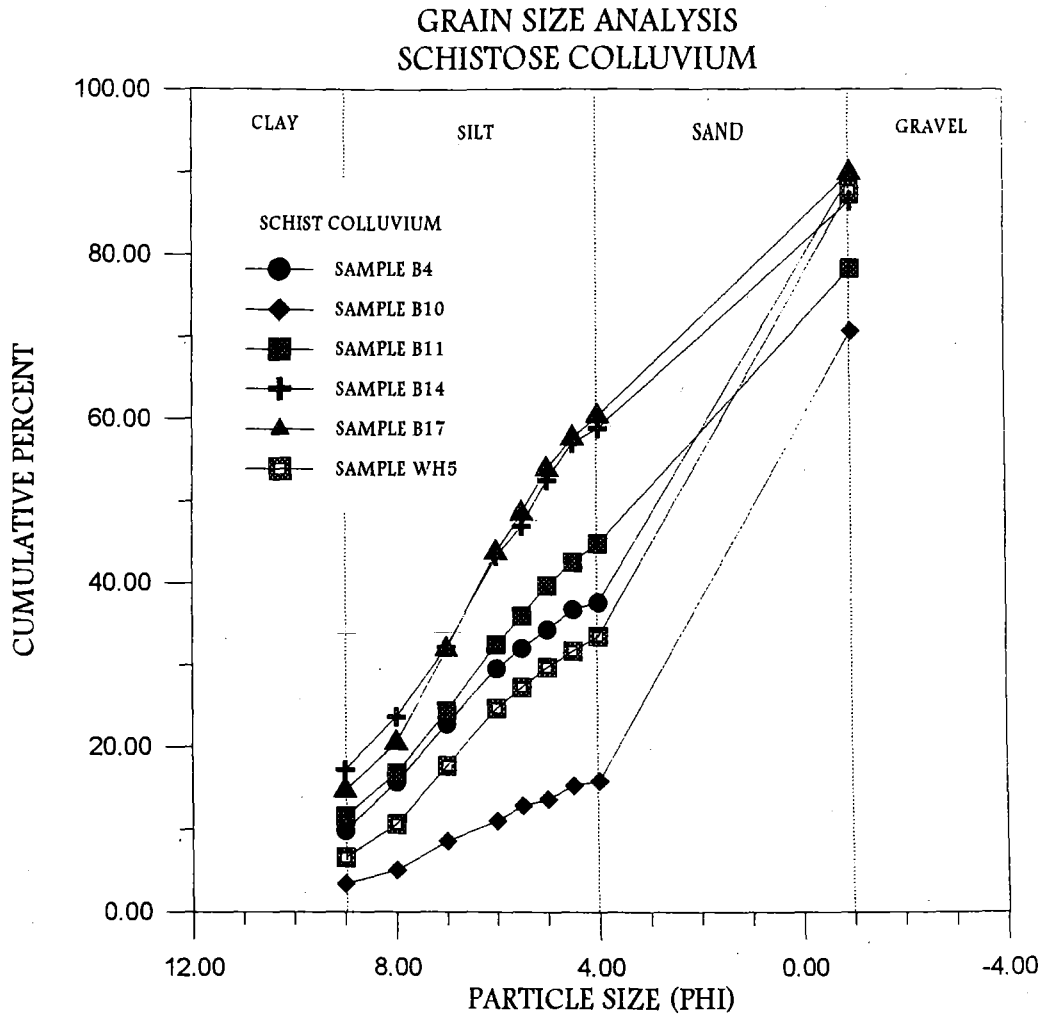
GRAIN SIZE ANALYSIS
SCHISTOSE COLLUVIUM
CLAY
SILT
SAND
GRAVEL
SCHIST COLLUVIUM
SAMPLE B4
SAMPLE B10
SAMPLE B11
SAMPLE B14
SAMPLE B17
SAMPLE WH5
CUMULATIVE PERCENT
100.00
80.00
60.00
40.00
20.00
0.00
12.00
8.00
4.00
0.00
-4.00
PARTICLE SIZE (PHI)

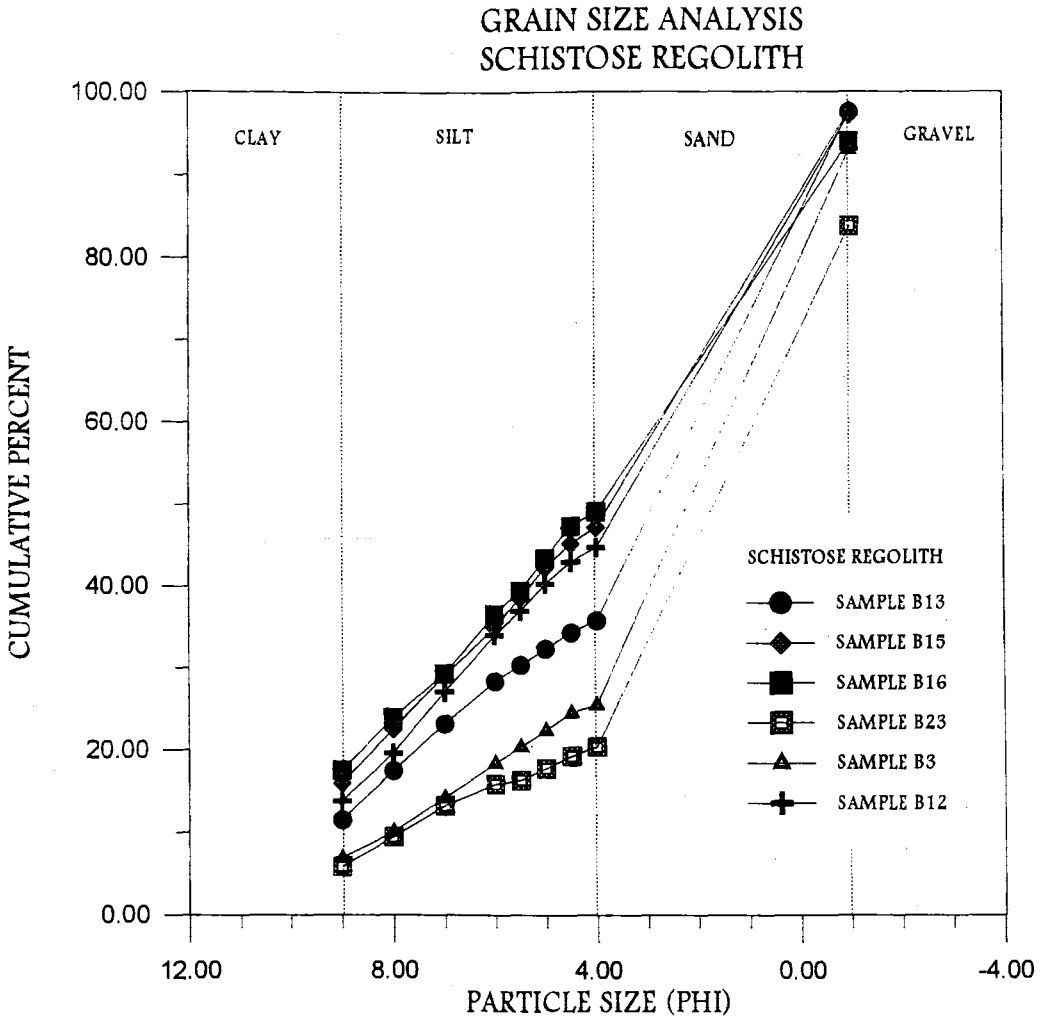
GRAIN SIZE ANALYSIS
SCHISTOSE REGOLITH
CLAY
SILT
SAND
GRAVEL
100.00
80.00
60.00
40.00
20.00
0.00
CUMULATIVE PERCENT
12.00
8.00
4.00
0.00
-4.00
PARTICLE SIZE (PHI)
SCHISTOSE REGOLITH
SAMPLE B13
SAMPLE B15
SAMPLE B16
SAMPLE B23
SAMPLE B3
SAMPLE B12

APPENDIX D5

ATTERBERG LIMITS

The same twenty seven samples used for grain size analysis were prepared for plastic and liquid limit determinations. The soils were again disaggregated in hydrogen peroxide and wet sieved through a 425μ sieve. Particles passing through the sieve were retained, waster was removed by decanting, and the samples then dried to just below their liquid limit.

LIQUID LIMIT: CONE PENETROMETER

The cone penetrometer consists of a 35mm long metal cone attached to a release system and a micrometre. The sample is placed in a 55mm diameter cup and the surface leveled off. The cone is lowered to the surface and the first micrometer reading taken. The cone is then released for 5±1 seconds into the sample and the second micrometer reading is taken. For two tests the difference must be <0.5mm and for three tests <10mm. A small sample is taken and water content determined. Distilled water is added to the sample and the test repeated. Four tests are performed on each sample ideally having a cone penetration between 15 and 25 mm.

The cone indenter number is that water content at 20mm penetration.

The results from each test are given overleaf with graphical presentation showing lines of best fit between points.

PLASTIC LIMIT

The samples from the cone penetration test are dried sufficiently that they may be handled without sticking to the hand. Samples are rolled into approximately 30g balls and retained for testing. Each ball is cut in half and each half then cut in quarters. Each half is tested independently. The quarters of clay are rolled using an even hand pressure, until a 3mm thread can be rolled which cracks longitudinally. The threads are collected and weighed to determine water content. The plastic limit of the soils is the average of these two water contents.

Results are presented in the text and the liquid limit presented data overleaf.

Additional parameters may be obtained from the Atterberg limits.

Plasticity index is obtained by subtracting the plastic limit from the liquid limit where:

$$I_p = W_L - W_P$$

Activity data can give an indication of the clay mineralogy within a sample

$$A_C = I_P / W\% \text{ Clay}$$

PLASTIC AND LIQUID LIMITS							
RED WEATHERED REGOLITH							
CONE PENETROMETER							
SAMPLE	*B9*						
TEST NO.	**AVG**	**Wet Wt.**	**Dry Wt**	**Beaker**	**water %**		
B9/1	10.4	41.89	39.77	34.666	41.53605		
B9/2	15.13	41.23	39.04	34.17	44.9692		
B9/3	18.41333	42.22	39.17	32.776	47.70097		
B9/4	24.175	20.73	17.13	10.113	51.30398		
SAMPLE	*B8*						
TEST NO.	**AVG**	**Wet Wt**	**Dry Wt**	**Beaker**	**Water %**		
B8/1	13.07667	31.62	29.54	24.89	44.73118		
B8/2	15.57	39.93	37.95	33.733	46.95281		
B8/3	20.06	34.91	32.47	27.764	51.8487		
B8/4	23.70333	35.65	32.79	27.41	53.15985		
SAMPLE	*B1*						
TEST NO.	**AVG**	**Wet Wt.**	**Dry Wt.**	**Beaker**	**Water %**		
B1/1	16.21	32.2	30.5	27.125	50.37037		
B1/2	20.26	33.54	31.14	26.508	51.81347		
B1/3	17.02	34.33	32.2	28.012	50.8596		
B1/4	24.345	39.34	36.42	31.074	54.62028		
SAMPLE	*B2*						
TEST NO.	**AVG**	**Wet Wt.**	**Dry Wt.**	**Beaker**	**Water %**		
B2/1	15.005	34.81	32.76	28.55	48.69359		
B2/2	19.69	33.28	31.35	27.638	51.99353		
B2/3	18.74	37.75	35.82	32.025	50.85639		
B2/4	22.60333	34.71	32.29	27.789	53.76583		
PLASTIC LIMIT							
SAMPLE	B1						
NUMBER	**BEAKER**	**Wet Wt.**	**Dry Wt.**	**Water %**			
B1/A	7.009	35.165	28.059	25.23796			
B1/B	7.616	33.498	27.2	24.33351			
SAMPLE	B2						
NUMBER	**BEAKER**	**Wet. Wt.**	**Dry Wt.**	**Water %**			
B2/A	27.678	48.508	43.222	25.37686			
B2/B	27.599	50.331	44.584	25.28154			
SAMPLE	B8						
NUMBER	**BEAKER**	**Wet Wt.**	**Dry Wt.**	**Water %**			
B8/A	27.437	45.065	40.912	23.55911			
B8/B	27.844	46.727	42.337	23.24842			
SAMPLE	B9						
NUMBER	**BEAKER**	**Wet Wt**	**Dry Wt.**	**Water %**			
B9/A	27.505	46.528	41.971	23.95521			
B9/B	27.174	46.062	41.526	24.01525			

LIQUID LIMIT SAMPLE B1

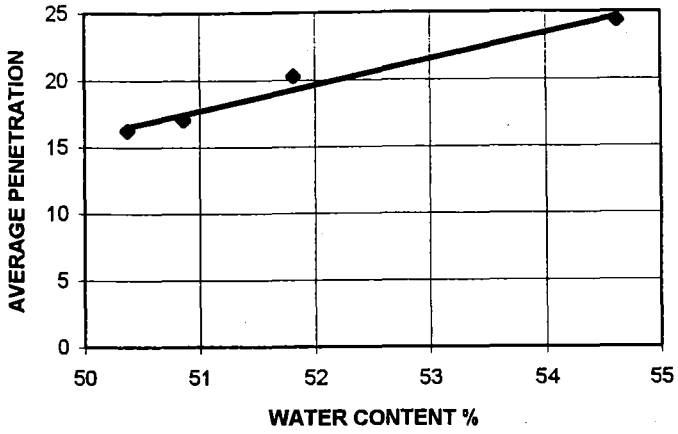

LIQUID LIMIT SAMPLE B2

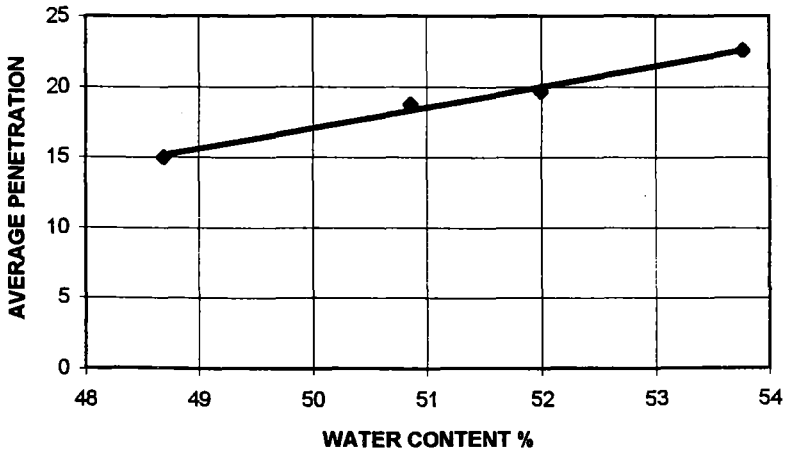

LIQUID LIMIT SAMPLE B8

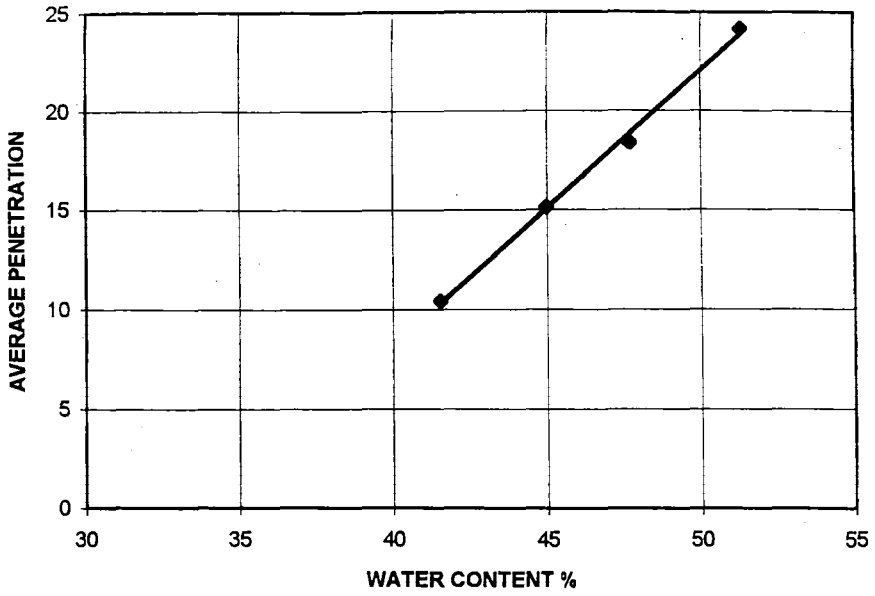

LIQUID LIMIT SAMPLE B9

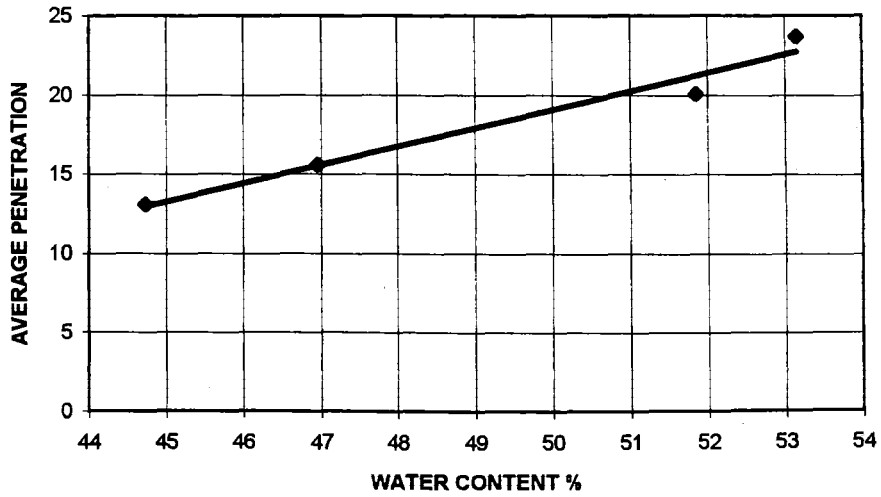

PLASTIC AND LIQUID LIMITS				Schist Regolith			
CONE PENETROMETER							
SAMPLE	*B3*						
TEST NO.	**AVG**	**Wet Wt.**	**Dry Wt**	**Beaker**	**water %**		
B3/1	8.695	32.55	31.291	27.4	24.4466		
B3/2	15.02	35.62	33.371	27.83	28.87035		
B3/3	18.035	35.24	32.892	27.69	31.09934		
B3/4	21.925	33.75	31.038	25.41	32.51799		
SAMPLE	*B12*						
TEST NO.	**AVG**	**Wet Wt.**	**Dry Wt**	**Beaker**	**water %**		
B12/1	12.41	32.02	30.357	25.68	35.55698		
B12/2	15.7	39.02	37.226	32.42	37.32834		
B12/3	20.94	36.22	33.67	27.47	41.12903		
B12/4	22.125	38.66	35.581	28.37	42.69865		
SAMPLE	*B23*						
TEST NO.	**AVG**	**Wet Wt.**	**Dry Wt**	**Beaker**	**water %**		
B23/1	16.65	31.15	29.171	24.89	46.22752		
B23/2	18.16	41.75	39.149	33.733	48.02437		
B23/3	21.74	39.61	35.677	27.784	49.82896		
B23/4	23.145	35.88	33.028	27.41	50.7654		
SAMPLE	*B15*						
TEST NO.	**AVG**	**Wet Wt.**	**Dry Wt**	**Beaker**	**water %**		
B15/1	13.4	38.7	36.235	28.55	32.07547		
B15/2	16.065	36.1	34.014	27.638	32.71644		
B15/3	18.23333	40.68	38.524	32.025	33.17433		
B15/4	22.10667	40.71	37.36	27.785	34.98695		
SAMPLE	*B16*						
TEST NO.	**AVG**	**Wet Wt.**	**Dry Wt**	**Beaker**	**water %**		
B16/1	11.46	42.5	40.627	34.666	31.4209		
B16/2	15.025	43.5	41.101	34.17	34.61261		
B16/3	21.535	45.51	42.003	32.776	38.00802		
B16/4	23.58	21.84	18.553	10.113	38.9455		
SAMPLE	*B13*						
TEST NO.	**AVG**	**Wet Wt.**	**Dry Wt**	**Beaker**	**water %**		
B13/1	10.78667	35.88	33.39	27.125	39.74461		
B13/2	17.975	34.86	32.304	26.508	44.09938		
B13/3	21.75333	35.3	33.014	28.012	45.70172		
B13/4	22.275	43.62	39.611	31.074	46.96029		
PLASTIC LIMIT							
SAMPLE	***TEST #***	***BEAKER***	***WET WT.***	***DRY WT.***	***WATER %***		
B3	a	5.496	34.744	28.603	26.57636		
	b	5.5	24.879	20.907	25.78049		
B12	a	7.083	26.373	22.483	25.25974		
	b	7.048	22.73	19.703	23.9194		
B13	a	5.717	28.839	23.975	26.64038		
	b	7.02	24.355	20.787	25.91705		
B15	a	7.226	25.621	22.306	21.98276		
	b	7.648	26.846	23.403	21.85338		
B16	a	7.622	27.042	23.465	22.57779		
	b	7.009	26.465	22.94	22.12667		
B23	a	7.236	26.82	22.573	27.6912		
	b	7.1	23.408	19.838	28.02638		

LIQUID LIMIT SAMPLE B3

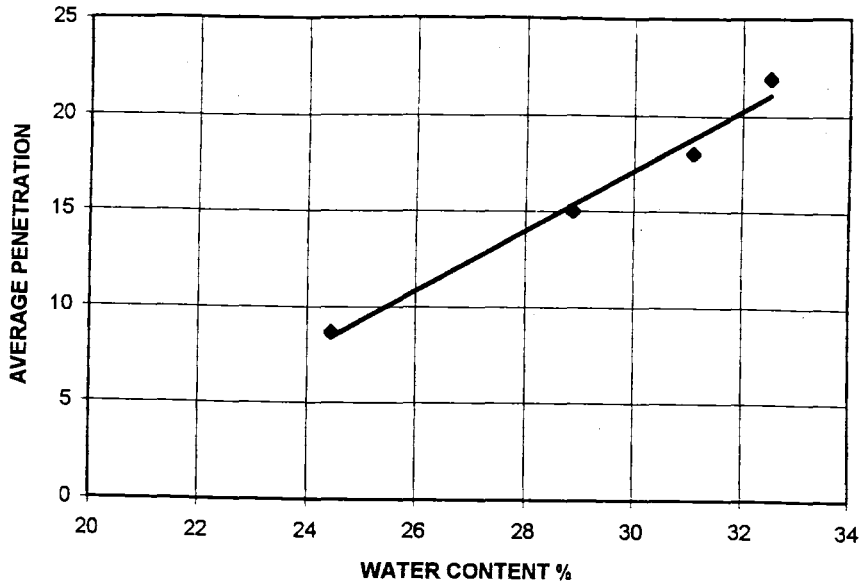

LIQUID LIMIT SAMPLE B12

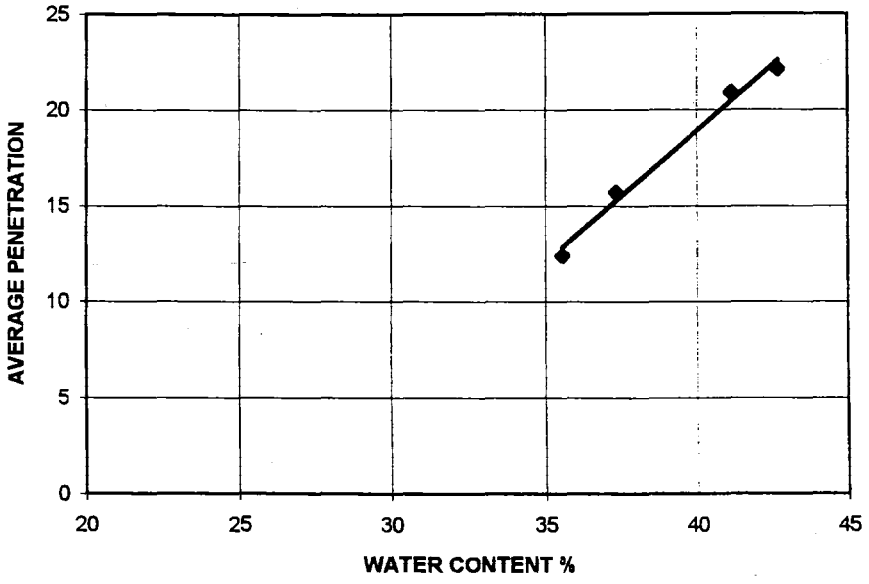

LIQUID LIMIT SAMPLE B13

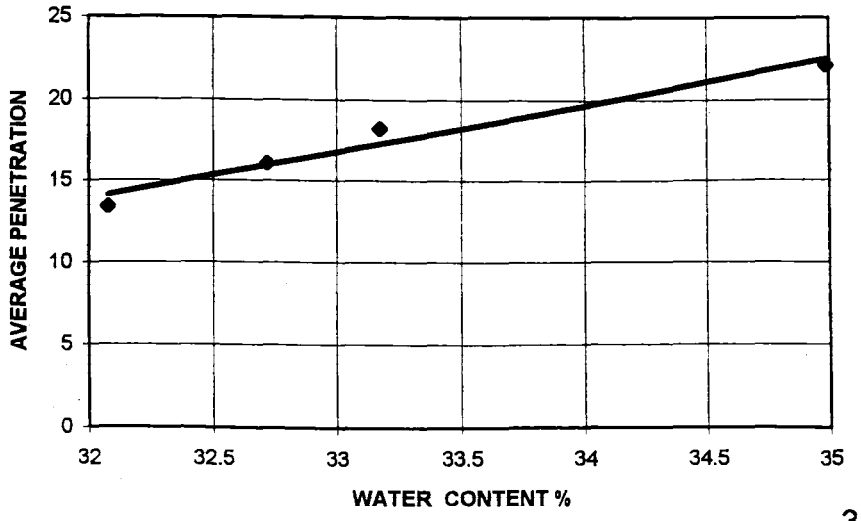

LIQUID LIMIT SAMPLE B15

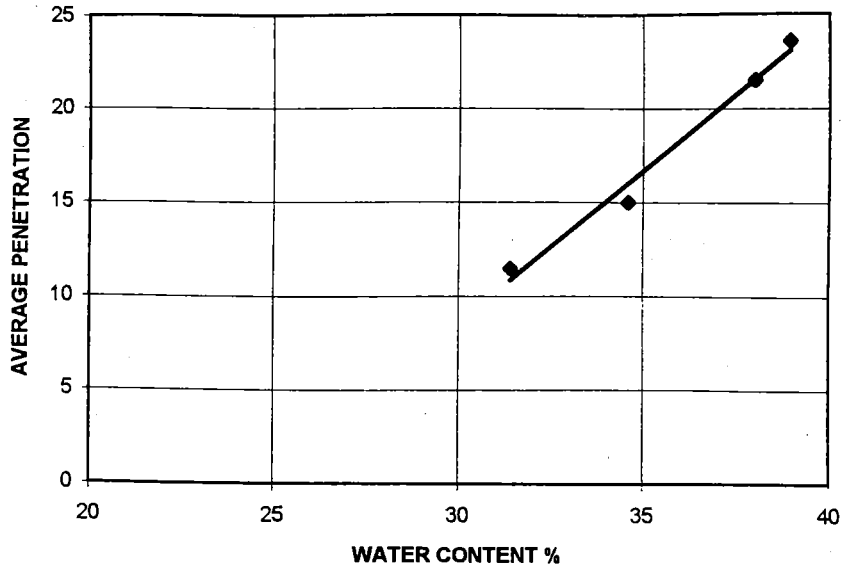

LIQUID LIMIT SAMPLE B16

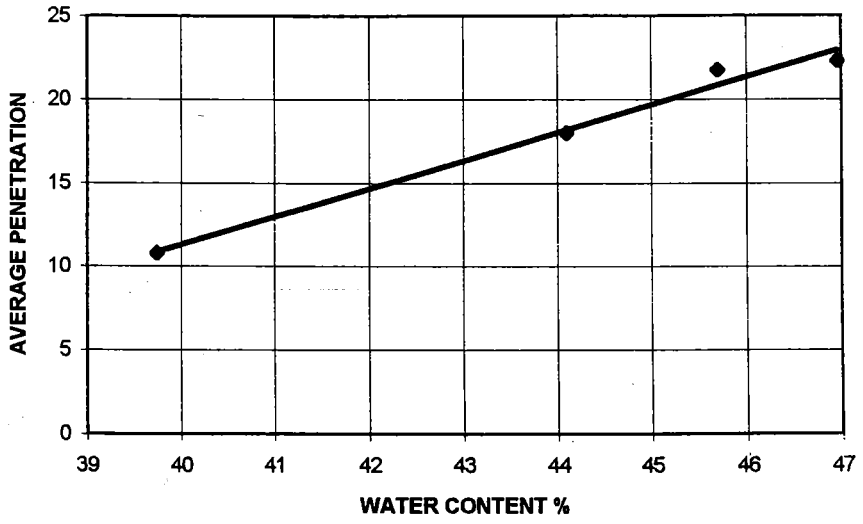

LIQUID LIMIT SAMPLE B23

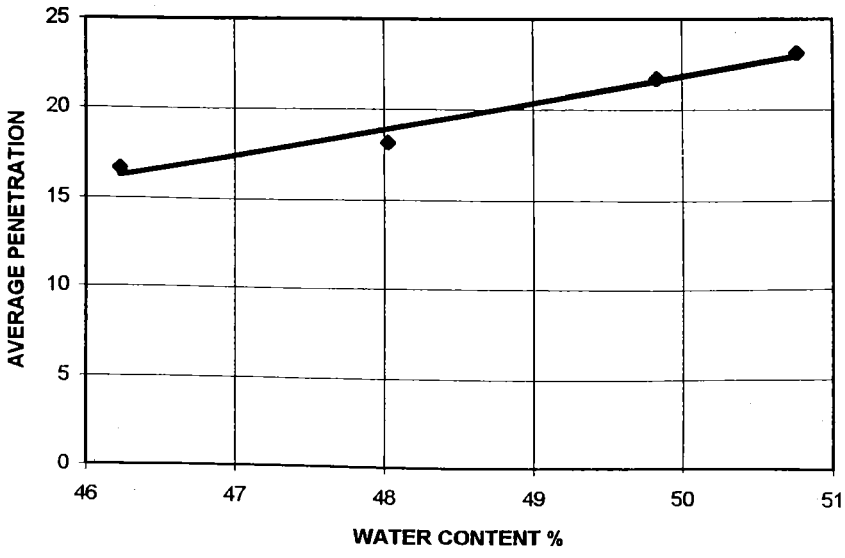

PLASTIC AND LIQUID LIMITS							
CONE PENETROMETER				Schist Colluvium			
SAMPLE	*B4*						
TEST NO.	**AVG**	**Wet Wt.**	**Dry Wt**	**Beaker**	**water %**		
B4/1	10.39	36.24	34.148	28.01	34.08276		
B4/2	17.89667	36.14	33.811	27.79	38.68128		
B4/3	19.69	36.73	34.051	27.18	38.98996		
B4/4	22.58333	39.49	36.108	27.83	40.85528		
SAMPLE	*B10*						
TEST NO.	**AVG**	**Wet Wt.**	**Dry Wt**	**Beaker**	**water %**		
B10/1	11.75333	17.71	15.338	7.59	30.61435		
B10/2	16.275	13.65	11.637	5.54	33.01624		
B10/3	20.04	15.66	13.478	7.22	34.86737		
B10/4	22.985	15.83	13.576	7.26	35.68714		
SAMPLE	*B11*						
TEST NO.	**AVG**	**Wet Wt.**	**Dry Wt**	**Beaker**	**water %**		
B11/1	14.765	35.92	33.932	27.66	31.69643		
B11/2	16.505	43.2	41.114	34.67	32.3712		
B11/3	19.915	32.76	30.774	24.91	33.86767		
B11/4	20.725	38.59	36.158	29.18	34.85239		
SAMPLE	*B14*						
TEST NO.	**AVG**	**Wet Wt.**	**Dry Wt**	**Beaker**	**water %**		
B14/1	13.86	43.59	41.248	32.77	27.62444		
B14/2	16.84	37.88	35.528	27.43	29.04421		
B14/3	19.005	39.36	36.609	27.61	30.57006		
B14/4	19.46	41.07	37.953	27.82	30.76088		
SAMPLE	*B17*						
TEST NO.	**AVG**	**Wet Wt.**	**Dry Wt**	**Beaker**	**water %**		
B17/1	13.185	36.99	34.974	27.81	28.1407		
B17/2	16.565	37.68	35.334	27.58	30.25535		
B17/3	18.955	38.48	36.094	28.34	30.77121		
B17/4	20.06	39.26	36.45	27.66	31.96815		
SAMPLE	*WH5*						
TEST NO.	**AVG**	**Wet Wt.**	**Dry Wt**	**Beaker**	**water %**		
WH5/1	13.91667	41.05	39.612	34.18	26.47275		
WH5/2	14.955	34.8	33.215	27.51	27.78265		
WH5/3	17.555	35.96	33.984	27.18	29.04174		
WH5/4	19.36667	39.09	36.02	27.5	36.03286		
PLASTIC LIMIT							
SAMPLE	***TEST #***	***BEAKER***	***WET WT.***	***DRY WT.***	***WATER %***		
B4	a	26.485	41.944	38.97	23.82058		
	b	27.851	42.151	39.094	27.19025		
B10	a	31.127	47.276	44.146	24.04179		
	b	27.445	44.213	41.791	16.88275		
B11	a	33.733	56.93	52.243	25.32145		
	b	27.732	45.559	41.987	25.05787		
B14	a	31.091	45.535	43.29	18.40315		
	b	33.758	48.993	46.664	18.04587		
B17	a	7.242	23.702	21.361	16.58049		
	b	7.658	25.439	22.85	17.04186		
WH5	a	27.81	42.775	40.445	18.44084		
	b	28.365	42.669	40.434	18.51852		

LIQUID LIMIT SAMPLE B4

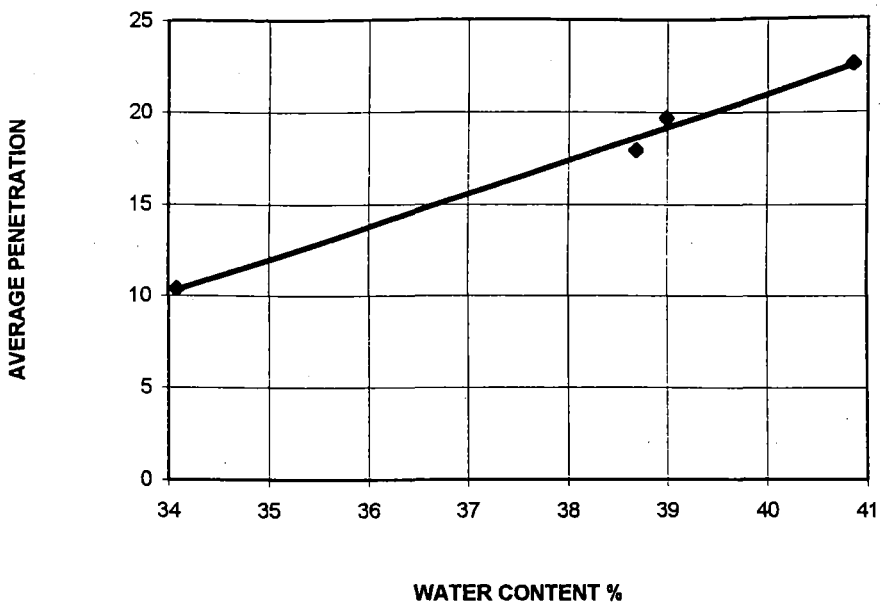

LIQUID LIMIT SAMPLE B10

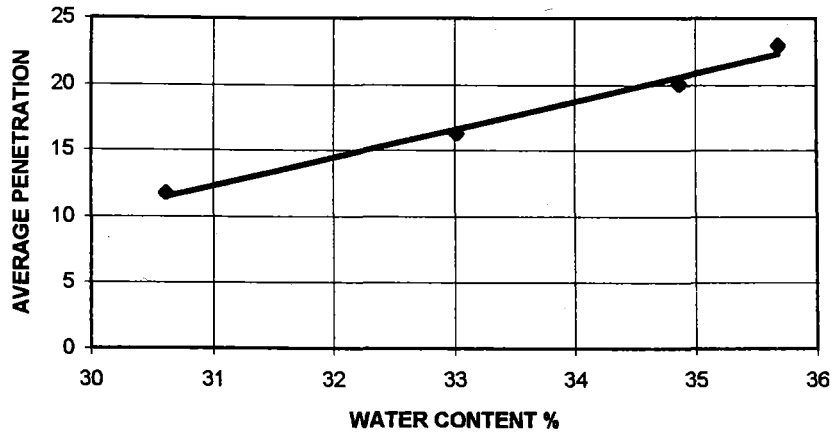

LIQUID LIMIT SAMPLE B11

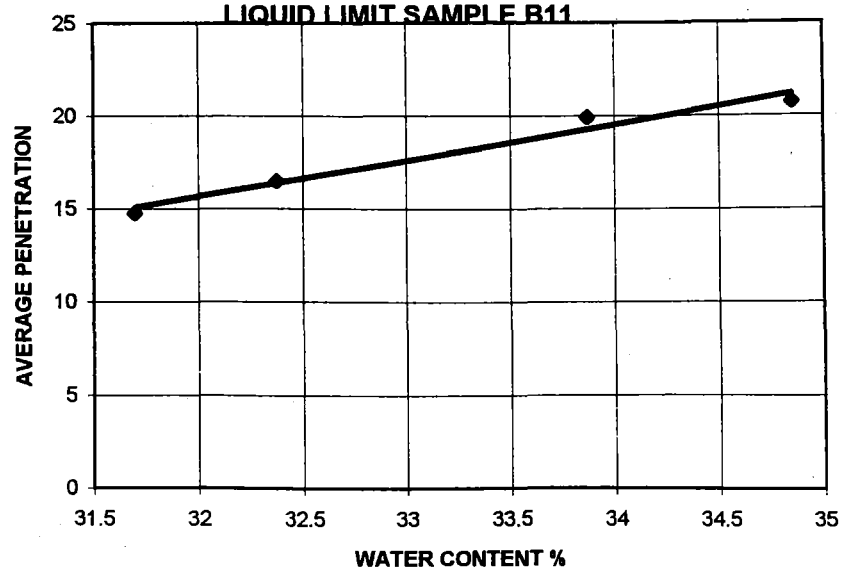

LIQUID LIMIT SAMPLE B17

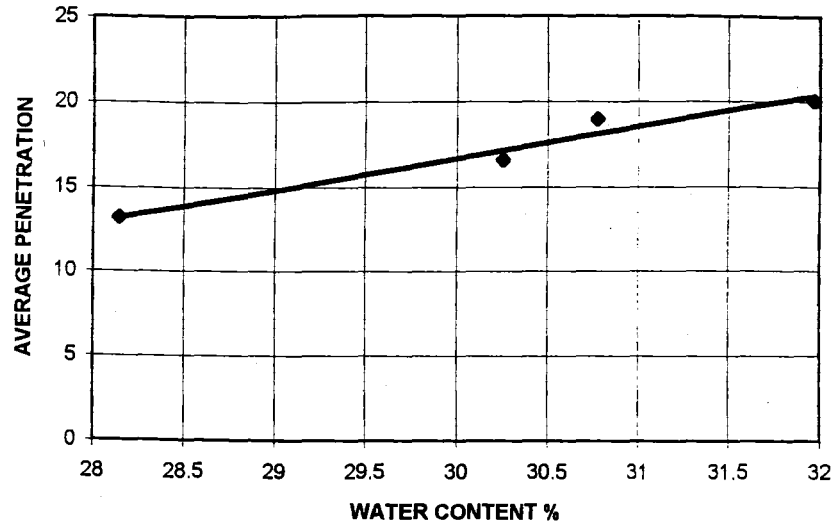

LIQUID LIMIT SAMPLE B14

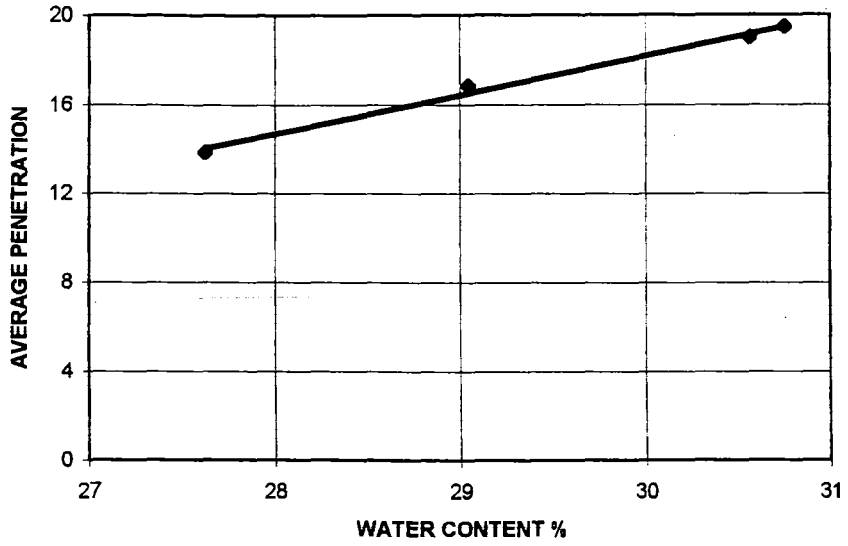

LIQUID LIMIT SAMPLE WH5

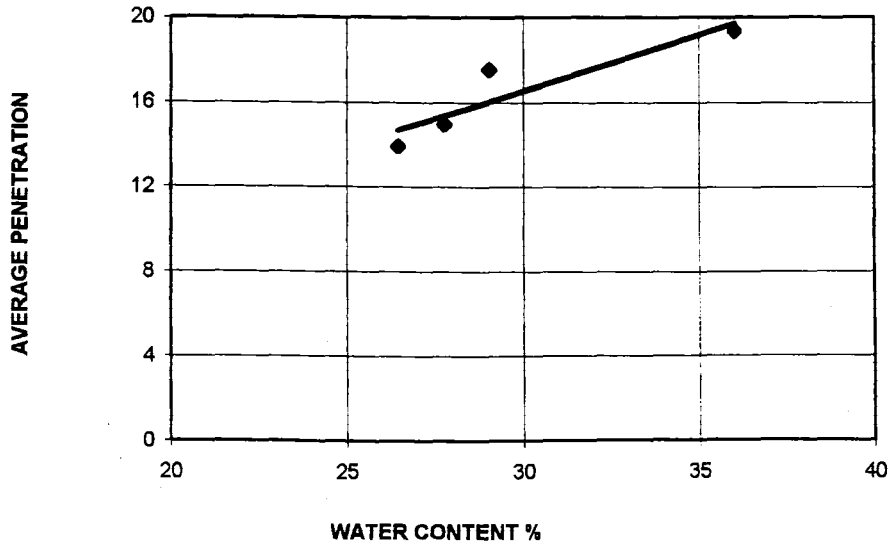

PLASTIC AND LIQUID LIMITS							
CONE PENETROMETER				Greywacke Colluvium			
SAMPLE	*WH3*						
TEST NO.	**AVG**	**Wet Wt.**	**Dry Wt**	**Beaker**	**water %**		
WH3/1	13.86	16.897	14.412	7.657	36.78756		
WH3/2	16.58333	16.163	13.658	7.062	37.97756		
WH3/3	18.535	17.252	14.394	7.054	38.93733		
WH3/4	23.065	19.665	16.202	7.618	40.3425		
SAMPLE	*B5*						
TEST NO.	**AVG**	**Wet Wt.**	**Dry Wt**	**Beaker**	**water %**		
B5/1	11.55667	16.041	13.591	5.509	30.31428		
B5/2	16.57	18.388	15.517	7.018	33.78044		
B5/3	18.515	16.118	13.436	5.703	34.68253		
B5/4	23.505	17.461	14.76	7.266	36.04217		
SAMPLE	*B6*						
TEST NO.	**AVG**	**Wet Wt.**	**Dry Wt**	**Beaker**	**water %**		
B6/1	10.74	18.118	15.427	7.023	32.02047		
B6/2	17.41667	20.884	17.468	7.667	34.85359		
B6/3	21.08333	18.06	15.117	7.141	36.89819		
B6/4	20.79	16.648	13.664	5.509	36.59105		
SAMPLE	*B7*						
TEST NO.	**AVG**	**Wet Wt.**	**Dry Wt**	**Beaker**	**water %**		
B7/1	15.60667	38.13	35.552	28.018	34.21821		
B7/2	16.335	35.51	32.79	24.882	34.39555		
B7/3	18.445	40.94	37.497	27.871	35.76771		
B7/4	22.25667	38.982	36.324	29.157	37.08665		
SAMPLE	*B20*						
TEST NO.	**AVG**	**Wet Wt.**	**Dry Wt**	**Beaker**	**water %**		
B20/1	10.075	17.958	15.425	7.284	31.11411		
B20/2	16.91	18.104	15.262	7.003	34.41095		
B20/3	17.88667	20.508	17.062	7.226	35.03457		
B20/4	22.195	19.538	16.262	7.26	36.39191		
SAMPLE	*B21*						
TEST NO.	**AVG**	**Wet Wt.**	**Dry Wt**	**Beaker**	**water %**		
B21/1	13.075	36.546	34.568	27.497	27.97341		
B21/2	14.765	41.062	38.109	28.611	31.09076		
B21/3	19.11	41.537	38.163	27.682	32.19158		
B21/4	19.99667	42.301	38.588	27.451	33.33932		
PLASTIC LIMIT							
SAMPLE	***TEST #***	***BEAKER***	***WET WT.***	***DRY WT.***	***WATER %***		
WH3	a	27.671	48.861	43.094	37.39221		
	b	26.55	45.444	41.741	24.37628		
B5	a	28.907	44.91	41.867	23.47994		
	b	27.957	39.555	37.37	23.21258		
B6	a	27.723	42.118	39.306	24.27696		
	b	27.439	44.85	41.443	24.32876		
B7	a	25.731	44.314	41.023	21.52106		
	b	32.065	48.999	46.029	21.26898		
B20	a	7.247	23.426	20.446	22.57747		
	b	7.29	26.281	22.77	22.68088		
B21	a	27.772	42.316	40.167	17.33764		
	b	27.177	40.212	38.335	16.82201		

LIQUID LIMIT SAMPLE B5

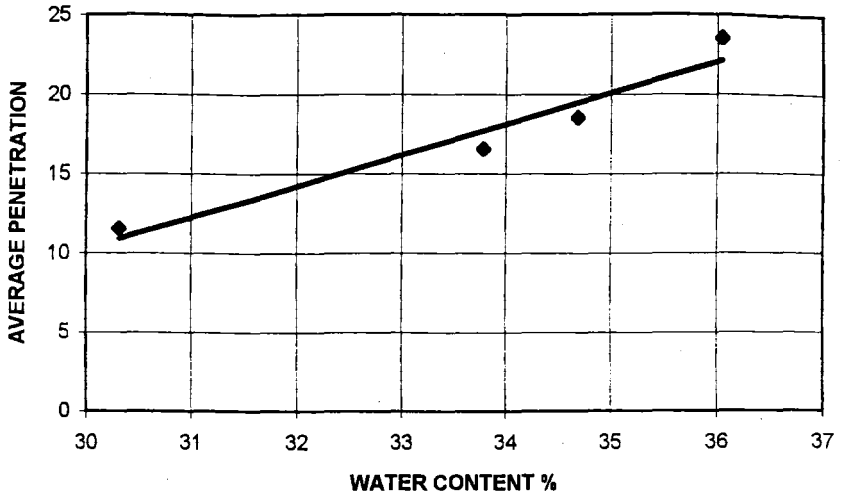

LIQUID LIMIT SAMPLE B6

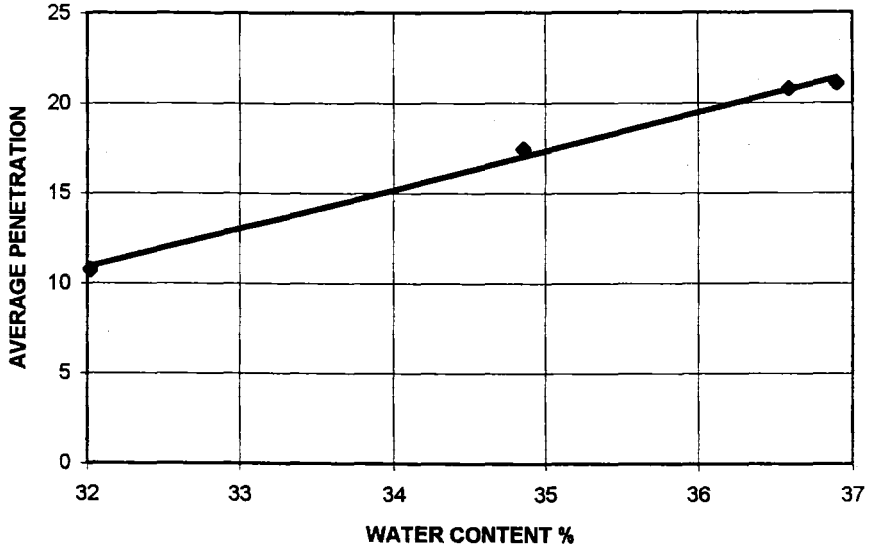

LIQUID LIMIT SAMPLE B7

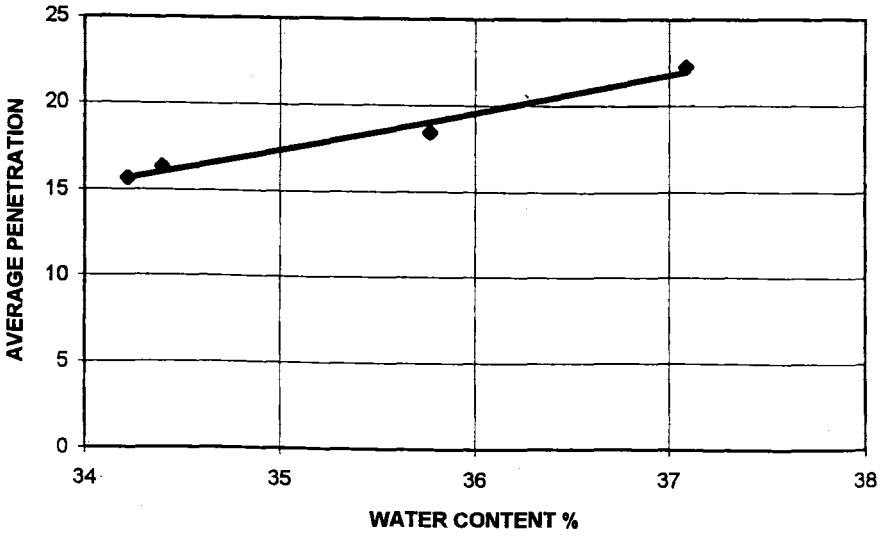

PLASTIC AND LIQUID LIMITS							
CONE PENETROMETER				Greywacke Regolith			
SAMPLE	*WH4*						
TEST NO.	**AVG**	**Wet Wt.**	**Dry Wt**	**Beaker**	**water %**		
WH4/1	14.235	17.74	14.966	7.688	38.11487		
WH4/2	17.235	19.629	16.187	7.235	38.44951		
WH4/3	19.24	19.391	15.441	5.53	39.85471		
WH4/4	23.05	19.533	15.97	7.272	40.96344		
SAMPLE	*WH6*						
TEST NO.	**AVG**	**Wet Wt.**	**Dry Wt**	**Beaker**	**water %**		
WH6/1	12.73667	37.78	35.098	28.59	41.21082		
WH6/2	13.865	43.45	40.075	32.43	44.1465		
WH6/3	17.55	42.14	38.95	32.06	46.29898		
WH6/4	20.9	34.71	31.692	25.71	50.45135		
SAMPLE	*B18*						
TEST NO.	**AVG**	**Wet Wt.**	**Dry Wt**	**Beaker**	**water %**		
B18/1	11.59	17.89	15.277	7.64	34.21501		
B18/2	19.37667	19.82	16.557	7.64	36.59302		
B18/3	20.13	18.24	15.232	7.28	37.82696		
B18/4	23.27	18.35	15.186	7.09	39.08103		
SAMPLE	*B19*						
TEST NO.	**AVG**	**Wet Wt.**	**Dry Wt**	**Beaker**	**water %**		
B19/1	11.595	16.6	14.239	7.27	33.87861		
B19/2	14.695	17.81	15.004	7.22	36.0483		
B19/3	18.73	15.88	12.999	5.53	38.57277		
B19/4	21.535	19.83	16.391	7.68	39.47882		
SAMPLE	*B22*						
TEST NO.	**AVG**	**Wet Wt.**	**Dry Wt**	**Beaker**	**water %**		
B22/1	10.82	37.22	35.347	27.873	25.06021		
B22/2	14.81667	39.984	37.446	27.88	26.53147		
B22/3	18.48667	42.423	39.186	27.616	27.97753		
B22/4	19.845	44.012	40.35	27.604	28.73058		
PLASTIC LIMIT							
SAMPLE	***TEST #***	***BEAKER***	***WET WT.***	***DRY WT.***	***WATER %***		
WH4	a	27.174	42.497	39.51	24.21368		
	b	34.676	48.767	46.058	23.80074		
WH6	a	7.673	24.325	20.931	25.59964		
	b	7.258	21.001	18.254	24.98181		
B18	a	7.239	27.665	23.759	23.64407		
	b	7.631	22.557	19.794	22.71644		
B19	a	7.23	27.753	23.735	24.34414		
	b	7.663	25.948	22.402	24.05862		
B22	a	32.424	52.014	48.873	19.09539		
	b	34.209	54.046	50.713	20.1951		

LIQUID LIMIT SAMPLE B20

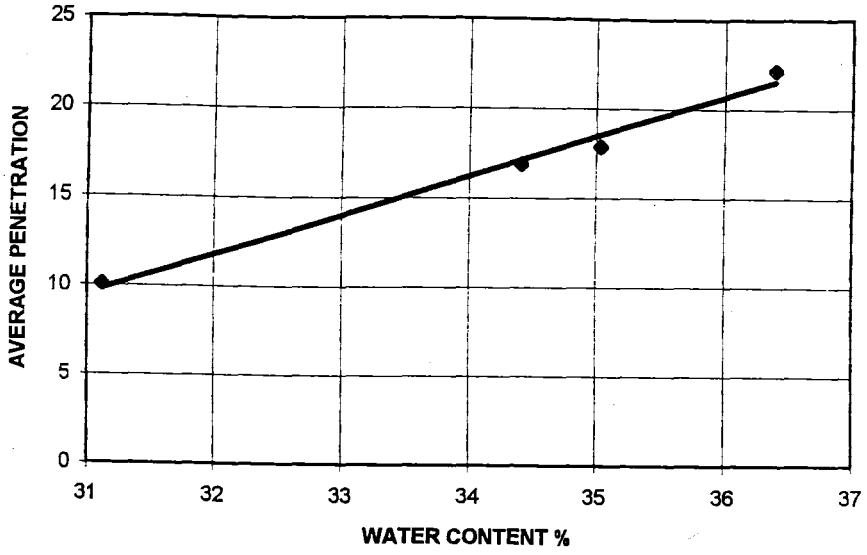

LIQUID LIMIT SAMPLE B21

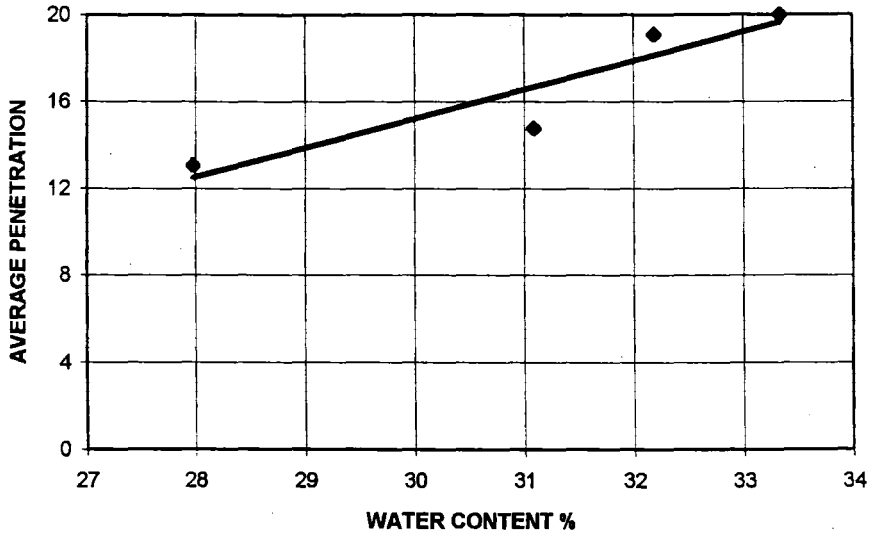

LIQUID LIMITS SAMPLE WH3

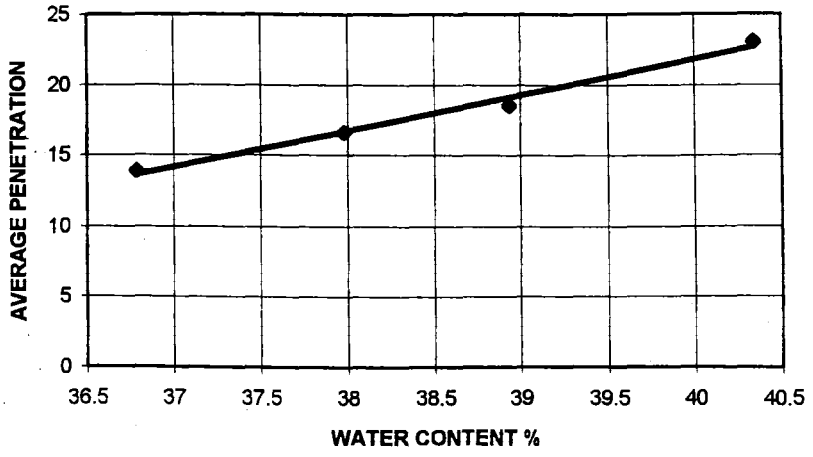

LIQUID LIMITS SAMPLE B18

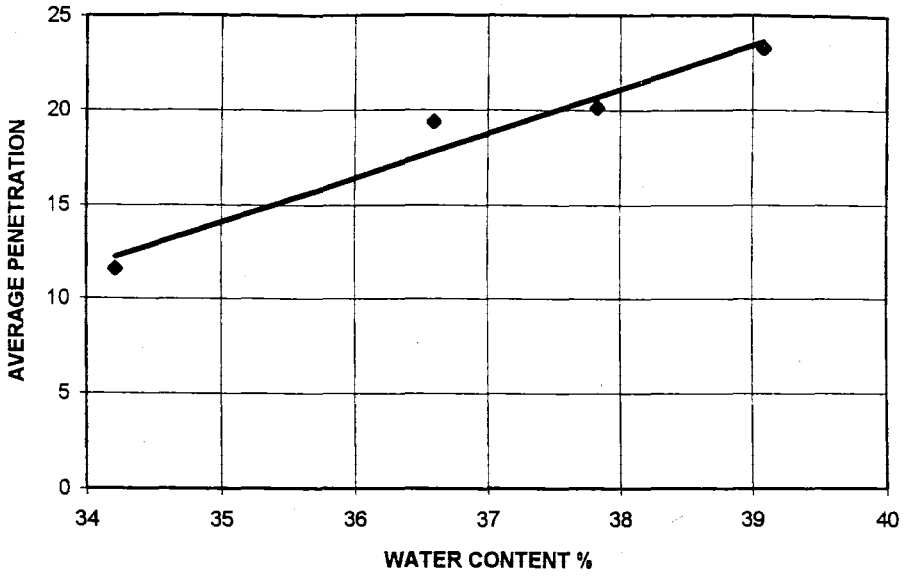

LIQUID LIMIT SAMPLE B19

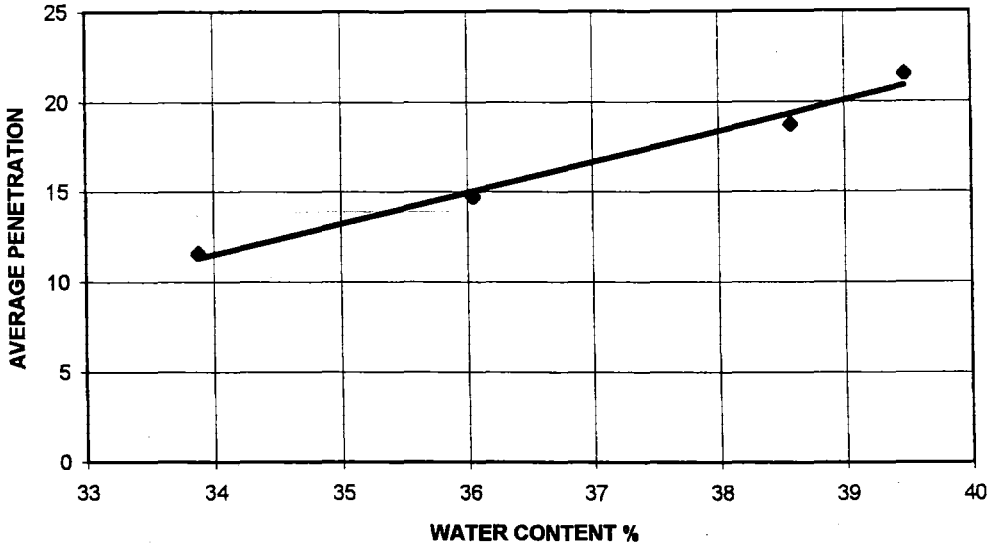

LIQUID LIMIT SAMPLE B22

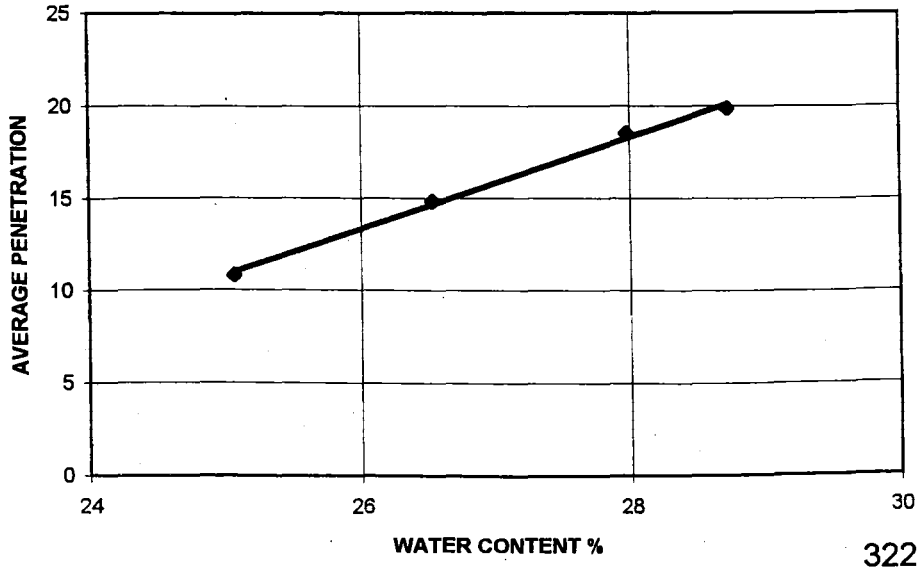

LIQUID LIMIT SAMPLE WH4

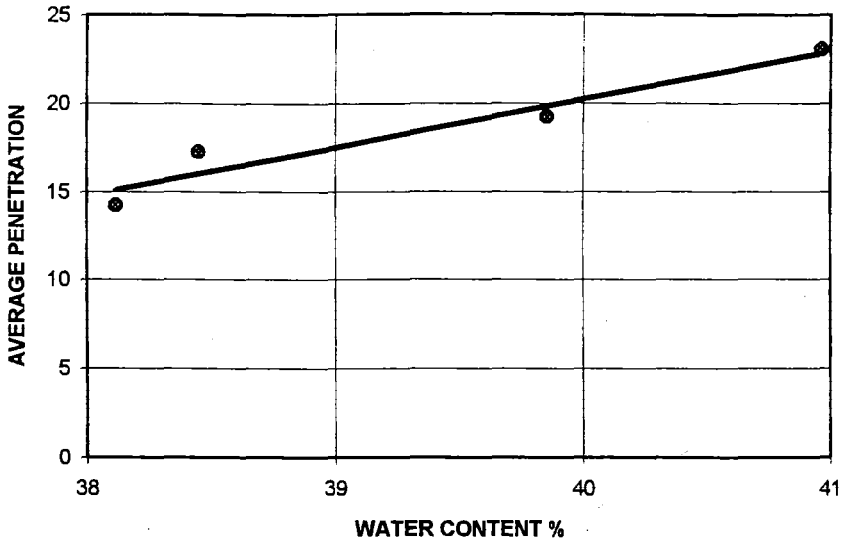

LIQUID LIMIT SAMPLE WH6

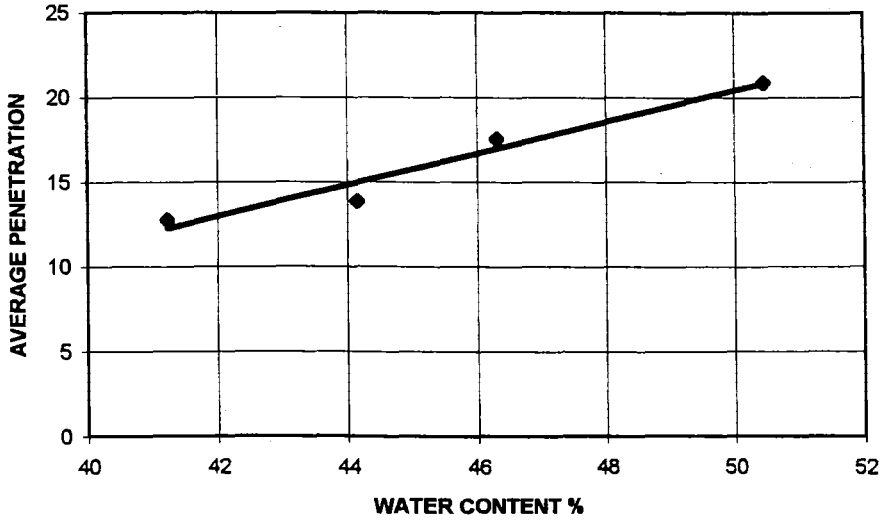

APPENDIX D6

EROSION TESTS

PIN HOLE EROSION TESTS

Using 35mm diameter insitu tube samples, the pin hole erosion test follows that in the NZS 4402. Eight 35mm diameter tube samples of 50mm length, representing four soil types (excluding red weathered regolith) were drilled through with a 1mm diameter needle. Each sample was then attached up to the pin hole device (Fig D4.1) with an initial head of 50mm. Water was then allowed to pass through the sample with the flow passing being collected. Flow rate was determined after ten minutes; a clear flow requiring an increased head to 180mm, 380mm, and 1020mm respectfully. A cloudy flow or higher flow rate led to the end of the test. Using the classification table presented in NZS 4402 the erodibility of the samples were determined and is presented in the text (Chapter 5).

CRUMB TEST

The Crumb test is a simple method for quickly analysing the erodibility of a particular soil. Small crumbs of soil (6mm-10mm diameter) are placed into a beaker with approximately 75ml of distilled water. The soil is then left for 5 or 10 minutes and observed.

The method of analysis follows the NZS 4402 whereby grade 1 and 2 soils are non-dispersive while grades 3 and 4 display increasing dispersion.

The results of the Crumb dispersion test are given in the text and compared to the results obtained using pin hole erosion testing in Chapter 5.

APPENDIX A5

POINT LOAD STRENGTH TEST

The Point Load test has generally been considered applicable only to core samples however, in the last 15 years the use of the test on irregular rock lumps has become more widely accepted. This study only had access to irregular lumps of rock obtained in the field and no core samples.

The Point Load test recognises that there is a direct relationship between the dimensions of the lump tested and the resulting strength obtained. For this reason the lumps used were within a chosen size range in accordance with ISRM (1985). Figure A4.1 shows the assumed relationship between the lump size and the equivalent core size. Dimensions of the lump require that samples are between 25mm and 85mm, the width and height approximately equal, and the length should be close to half the width.

Samples are then placed into the point load machine. The sample is placed between two metal conical platens which are then closed to hold the sample in place. Distance between the platens is recorded and hydraulic load is applied to the sample. Load is such that the sample should fail within 60 seconds, and the load at failure is recorded.

The anisotropic schistose rocks were tested parallel and perpendicular to the foliation in order to obtain maximum and minimum strength values for these rocks. The greywacke rock was tested without any particular orientation selected.

The calculations for the point load strength and the uniaxial compressive strength are as follows:

$$\textbf{Uncorrected Point Load Strength} = I_s = P/D_e^2$$

Where De = equivalent core diameter, and where $D_e = 4A/\pi$, and A = WD is the minimum cross sectional area of a plane through the platen contact points (ISRM, 1985).

The value for Is is then corrected to account for the irregular lump test and a standard 50mm diameter is used.

$$\text{Corrected Point Load Strength (MPa)} = Is_{(50)} = F \times Is$$

Where F = Size Correction Factor, and $F = (D_e/50)^{0.45}$

$$\text{Uniaxial Compressive Strength (MPa)} = UCS = 24Is_{(50)}$$

The results for the Point Load Strength test are given overleaf, and a summary and discussion of the results is presented in the text (Chapter 5).

POINT LOAD TEST		GREYWACKE, WEATHERING GRADE II									
Sample	Type	W (mm)	D (mm)	L (mm)	P (kN)	De^2 (mm^2)	De (mm)	Is	F	Is_{50}	UCS
1	WG II	57	29.9	49.5	17	2169.982	46.58307	7.834166	0.968648	7.588552	182.1252
2	WG II	49.5	44.3	80.7	12	2792.023	52.8396	4.297958	1.025169	4.406132	105.7472
3	WG II	39.3	26.3	52.8	1.5	1316.008	36.27682	1.139811	0.865559	0.986574	23.67777
4	WG II	58.9	43	66.6	7	3224.734	56.78674	2.170722	1.058948	2.298681	55.16835
5	WG II	77.7	50	71	8	4946.536	70.33161	1.617294	1.165954	1.885689	45.25654
6	WG II	55.3	43.9	117.7	7	3091.005	55.59681	2.264635	1.048904	2.375386	57.00927
7	WG II	67.2	29.5	98.6	1	2524.07	50.24012	0.396186	1.002158	0.397041	9.528974
8	WG II	43.5	34.5	93.3	2	1910.814	43.71286	1.046674	0.941321	0.985256	23.64615
9	WG II	57.3	32.6	107	1	2378.386	48.7687	0.420453	0.988842	0.415762	9.978285
10	WG II	70.4	39.3	124.2	10	3522.697	59.35232	2.838734	1.080216	3.066445	73.59467
11	WG II	64	27.9	83.2	7.5	2273.497	47.6812	3.298883	0.978858	3.229139	77.49933
12	WG II	58.6	29.6	79	1	2208.51	46.99479	0.452794	0.972492	0.440338	10.56812
13	WG II	34.1	40.1	83	1	1741.04	41.72578	0.574369	0.921819	0.529464	12.70714
14	WG II	73.9	48	77	11	4516.435	67.20443	2.435549	1.142333	2.782207	66.77297
15	WG II	34.9	31.3	60.8	0.5	1390.849	37.29408	0.359493	0.876398	0.315059	7.561411
16	WG II	64.5	43.9	151.6	19	3605.241	60.04366	5.270105	1.08586	5.722595	137.3423
17	WG II	48.4	23.3	86.9	12	1435.858	37.89271	8.357374	0.882701	7.377062	177.0495
18	WG II	40	20.7	63.7	6	1054.242	32.4691	5.691291	0.823427	4.686363	112.4727
19	WG II	33.4	25.1	51.4	8	1067.408	32.67121	7.494794	0.82573	6.188672	148.5281
20	WG II	38.7	25.8	49.7	11	1271.279	35.655	8.652705	0.858851	7.431382	178.3532
21	WG II	52	47	84.9	19	3111.797	55.78349	6.105796	1.050488	6.414065	153.9375
22	WG II	68.6	42.2	146.4	18	3685.927	60.71183	4.88344	1.091281	5.329204	127.9009
23	WG II	61.4	40.4	73	0.5	3158.347	56.19917	0.158311	1.054003	0.16686	4.004639
24	WG II	48.7	36	119.3	1	2232.244	47.24662	0.44798	0.974833	0.436706	10.48093
25	WG II	50.6	55.9	65.7	17.5	3601.409	60.01174	4.859209	1.0856	5.275157	126.6038
26	WG II	48.4	36	124	6	2218.493	47.10088	2.704539	0.973479	2.632812	63.18748
27	WG II	42.4	36.2	76	0.5	1954.27	44.20713	0.25585	0.946096	0.242059	5.809406
28	WG II	28.6	27	73	3	983.1956	31.35595	3.051275	0.810602	2.473368	59.36084
29	WG II	33.5	28.3	78.4	2	1207.095	34.74327	1.656871	0.848898	1.406514	33.75633
30	WG II	38.3	31	77	2	1511.717	38.88081	1.322999	0.892985	1.181419	28.35405
31	WG II	54	41.9	61.5	9	2880.832	53.67338	3.124098	1.032417	3.225371	77.4089
32	WG II	44.4	26.2	63.9	11	1481.134	38.48551	7.426741	0.888888	6.601544	158.4371
33	WG II	36.4	37.7	46	9	1747.241	41.80001	5.150978	0.922556	4.752067	114.0496
									SUM	103.2449	2477.879
									AVG	2.949855	70.79653

Sample	Type	W (mm)	D (mm)	L (mm)	P (kN)	De^2 (mm^2)	De (mm)	Is	F	Is_{50}	UCS(MPa)
1	WG III	51.6	25.3	63.1	0.5	1662.189	40.76995	0.300808	0.912256	0.274414	6.585936
2	WG III	29	19.9	58.4	0.3	734.7865	27.10695	0.408282	0.759189	0.309963	7.439112
3	WG III	52.5	32.8	61.5	0.6	2192.518	46.82434	0.273658	0.970903	0.265695	6.376685
4	WG III	48.3	29.7	71.5	0.4	1826.475	42.73728	0.219001	0.931808	0.204067	4.897609
5	WG III	42.2	27.4	95.9	0.5	1472.221	38.36954	0.339623	0.887682	0.301477	7.23545
6	WG III	54.5	36.4	90.4	0.5	2525.853	50.25786	0.197953	1.002317	0.198412	4.761881
7	WG III	49.8	25.8	111.9	0.5	1635.909	40.44637	0.30564	0.90899	0.277824	6.667782
8	WG III	62.1	29.8	82.9	0.5	2356.232	48.54103	0.212203	0.986762	0.209394	5.02546
9	WG III	50.2	34.5	119.2	0.8	2205.124	46.95874	0.362791	0.972156	0.35269	8.464556
10	WG III	43.7	40.5	105.8	0.5	2253.443	47.47044	0.221883	0.976909	0.216759	5.202219
11	WG III	65.4	39.8	100.4	2	3314.141	57.56857	0.603475	1.065484	0.642993	15.43182
12	WG III	38	37.9	84.5	1	1833.72	42.82195	0.54534	0.932639	0.508605	12.20652
13	WG III	35	27.4	81.7	0.5	1221.037	34.94334	0.409488	0.851094	0.348513	8.364307
14	WG III	46.5	42.3	57.7	0.8	2504.399	50.04397	0.319438	1.000396	0.319564	7.669544
15	WG III	49.5	41.5	55.2	0.2	2615.552	51.14247	0.076466	1.010218	0.077247	1.853929
16	WG III	50.8	31.9	79	1	2063.31	45.42367	0.484658	0.957724	0.464169	11.14005
17	WG III	49.7	25.8	93.5	0.5	1632.624	40.40574	0.306255	0.908579	0.278257	6.678177
18	WG III	44	29.6	88	0	1658.267	40.72183	0	0.911771	0	0
19	WG III	49.2	25.2	101.4	0.5	1578.613	39.73177	0.316734	0.901728	0.285608	6.854583
20	WG III	61.5	23.9	95.7	0.2	1871.471	43.2605	0.106868	0.936925	0.100127	2.40305
21	WG III	42.1	33.2	87.3	1	1779.632	42.18569	0.561914	0.926377	0.520544	12.49306
22	WG III	42.1	30.9	59.1	0.3	1656.345	40.69821	0.181122	0.911533	0.165098	3.962363
23	WG III	45.7	31.1	67.1	0.5	1809.617	42.5396	0.276302	0.929866	0.256923	6.166164
24	WG III	40.3	24.2	79.7	0	1241.74	35.23833	0	0.85432	0	0
25	WG III	49.8	38.1	67.1	1	2415.819	49.15098	0.413938	0.992323	0.41076	9.858249
26	WG III	55.5	24.4	72.9	1	1724.221	41.52374	0.579972	0.919807	0.533463	12.8031
27	WG III	29.7	31.8	46.9	0.5	1202.524	34.67743	0.415792	0.848173	0.352664	8.463931
28	WG III	36.9	23.4	67.5	0.5	1099.391	33.15707	0.454797	0.831233	0.378042	9.073016
29	WG III	33.3	34.1	62.3	1	1445.802	38.0237	0.691658	0.884073	0.611476	14.67542
30	WG III	50	23.6	55.6	0.5	1502.423	38.7611	0.332796	0.891747	0.29677	7.122474
31	WG III	38.6	25	53.3	0.5	1228.676	35.05248	0.406942	0.852289	0.346832	8.323974
32	WG III	49	20	58.6	0.3	1247.775	35.32386	0.240428	0.855252	0.205627	4.935037
33	WG III	44	23.2	56.3	0	1299.723	36.05167	0	0.863137	0	0
									SUM	9.713977	233.1355
									AVG	0.294363	7.064711

Sample	Type	W (mm)	D (mm)	L (mm)	P (kN)	De^2 (mm^2)	De (mm)	Is	F	Is_{50}	UCS
1	WG IV	51.9	23.8	78.4	0.2	1572.731	39.65767	0.127167	0.900971	0.114574	2.749777
2	WG IV	55.3	33.5	82.4	0.2	2358.74	48.56686	0.084791	0.986999	0.083689	2.008527
3	WG IV	46.5	28.7	103	0.3	1699.202	41.22138	0.176553	0.916787	0.161862	3.884688
4	WG IV	67	56.4	111	0.2	4811.318	69.36366	0.041569	1.158705	0.048166	1.155979
5	WG IV	51.1	33.4	108.1	0.2	2173.089	46.6164	0.092035	0.96896	0.089178	2.140276
6	WG IV	61.9	30.4	104.2	0.1	2395.931	48.94825	0.041737	0.990479	0.04134	0.992161
7	WG IV	84.3	34.1	94.1	0.4	3660.093	60.4987	0.109287	1.089555	0.119074	2.857777
8	WG IV	27.9	30.8	62.3	0.1	1094.12	33.07749	0.091398	0.830335	0.075891	1.821375
9	WG IV	27.9	25.4	91.4	.	902.2939	30.03821	#VALUE!	0.795091	#VALUE!	#VALUE!
10	WG IV	54.3	30.3	82.5	0.2	2094.848	45.76951	0.095472	0.960999	0.091749	2.20197
11	WG IV	77.9	34.6	85.7	0.4	3431.813	58.58168	0.116556	1.073881	0.125168	3.004027
12	WG IV	54.8	52.6	95.6	0.5	3670.088	60.58125	0.136237	1.090224	0.148528	3.56468
13	WG IV	41.3	29.6	93	0.3	1556.51	39.45263	0.192739	0.898872	0.173248	4.157941
14	WG IV	57.2	35	80	.	2549.026	50.48788	#VALUE!	1.004379	#VALUE!	#VALUE!
15	WG IV	44.2	35.7	101	0.4	2009.096	44.82294	0.199095	0.952004	0.189539	4.54893
16	WG IV	50.1	33.5	78.9	0.1	2136.942	46.22707	0.046796	0.96531	0.045173	1.08414
17	WG IV	55.3	42.6	104.4	0.3	2999.472	54.76744	0.100018	1.041834	0.104202	2.500842
18	WG IV	34	31.1	85	0.2	1346.323	36.69228	0.148553	0.870006	0.129242	3.101801
19	WG IV	40.4	26.4	51.6	0.3	1357.986	36.85087	0.220915	0.871696	0.192571	4.621703
20	WG IV	49	26.3	80.4	0.2	1640.824	40.50708	0.12189	0.909604	0.110872	2.660919
21	WG IV	29.1	39.7	50	0.3	1470.935	38.35278	0.203952	0.887508	0.181009	4.344211
22	WG IV	56.2	37.6	71.2	0.5	2690.508	51.87011	0.185839	1.016661	0.188935	4.534435
23	WG IV	46	37.2	78.7	0.2	2178.768	46.67727	0.091795	0.969529	0.088998	2.135951
24	WG IV	24.6	23.4	74.8	0.3	732.9276	27.07264	0.409317	0.758756	0.310572	7.45373
25	WG IV	46.3	35.8	80.4	0.2	2110.445	45.93959	0.094767	0.962604	0.091223	2.189348
26	WG IV	31.9	32	107.7	0.3	1299.723	36.05167	0.230818	0.863137	0.199228	4.781472
27	WG IV	37.7	27.5	78.2	0.1	1320.031	36.33223	0.075756	0.866154	0.065616	1.574788
28	WG IV	64	30.5	93.5	0.2	2485.364	49.85342	0.080471	0.99868	0.080365	1.928757
29	WG IV	39.4	29.5	110.7	0.3	1479.886	38.46929	0.202718	0.88872	0.18016	4.323834
30	WG IV	33.5	48.5	62.3	0.3	2068.696	45.48292	0.145019	0.958286	0.13897	3.335271
31	WG IV	50.6	31.6	72.7	0.3	2035.859	45.1205	0.147358	0.954842	0.140704	3.376887
32	WG IV	37.7	26.5	71.7	0.2	1272.03	35.66553	0.157229	0.858965	0.135054	3.2413
33	WG IV	29.7	41.7	71.3	0.1	1576.894	39.71013	0.063416	0.901507	0.05717	1.372075
									SUM	2.6296	63.11039
									AVG	0.079685	1.912436

Sample	Type	W (mm)	D (mm)	L (mm)	P (kN)	De^2 (mm^2)	De (mm)	Is	F	Is_{50}	UCS
1	WSII PER	45.3	40	103.6	7	2307.11	48.03239	3.034099	0.982096	2.979776	71.51462
2	WSII PER	34.3	28.7	86	3	1253.39	35.40324	2.393509	0.856117	2.049123	49.17895
3	WSII PER	67.4	48.4	79.3	1	4153.511	64.44774	0.24076	1.121003	0.269893	6.477431
4	WSII PER	77.9	34.4	107.1	7.5	3411.976	58.41213	2.198139	1.072482	2.357464	56.57914
5	WSII PER	82.4	71.3	139.2	4	7480.435	86.48951	0.534728	1.279667	0.684274	16.42258
6	WSII PER	52	34.9	111.6	2	2310.675	48.06948	0.865548	0.982437	0.850346	20.40831
7	WSII PER	42.4	34.3	81.4	4.5	1851.698	43.03136	2.430202	0.934688	2.271481	54.51555
8	WSII PER	61.1	50.9	122.6	8	3959.762	62.92664	2.020323	1.109019	2.240577	53.77385
9	WSII PER	47.4	44.1	71.7	1	2661.504	51.58976	0.375727	1.014185	0.381057	9.14537
10	WSII PER	51.6	25.9	78.5	3	1701.608	41.25055	1.763038	0.917079	1.616846	38.8043
11	WSII PER	45	24.1	44.4	1.2	1380.828	37.1595	0.869044	0.874974	0.76039	18.24936
12	WSII PER	55.3	24.1	83.6	3.7	1696.885	41.19326	2.180467	0.916506	1.99841	47.96185
13	WSII PER	43.5	31.1	75.3	4.15	1722.502	41.50304	2.409286	0.919601	2.215582	53.17396
14	WSII PER	48.2	23.4	53.6	4.8	1436.061	37.8954	3.342475	0.882729	2.9505	70.812
15	WSII PER	59	30	80.9	4.6	2253.634	47.47246	2.041148	0.976927	1.994053	47.85727
16	WSII PER	56.9	41.5	93.3	10	3006.564	54.83215	3.326056	1.042388	3.46704	83.20896
17	WSII PER	31.8	31.3	85.4	3.3	1267.306	35.59925	2.603948	0.858246	2.234829	53.63589
18	WSII PER	57.8	40.5	66.7	4.7	2980.526	54.5942	1.576903	1.04035	1.64053	39.37273
19	WSII PER	55.9	40.5	65.2	6	2882.551	53.68939	2.08149	1.032555	2.149253	51.58208
20	WSII PER	54	30.8	83.6	5.2	2117.652	46.01795	2.45555	0.963343	2.365536	56.77286
21	WSII PER	28.4	28.7	81	3.2	1037.792	32.21478	3.083469	0.820518	2.530043	60.72104
22	WSII PER	33.9	33.8	52.8	2.4	1458.903	38.19559	1.645071	0.885869	1.457318	34.97562
23	WSII PER	29.8	31.6	47.1	2.3	1198.984	34.62635	1.91829	0.847611	1.625964	39.02313
24	WSII PER	29.8	19	63.2	2.7	720.9082	26.84973	3.745276	0.755939	2.831198	67.94876
25	WSII PER	24.7	23.4	45.5	2.6	735.907	27.12761	3.533055	0.759449	2.683175	64.39621
26	WSII PER	39.3	25.6	70.4	2.6	1280.981	35.79079	2.029695	0.860321	1.746189	41.90854
27	WSII PER	47.7	25.2	48	3.5	1530.485	39.12141	2.286857	0.895468	2.047807	49.14737
28	WSII PER	28	22.2	41.3	2.2	791.4457	28.13264	2.779723	0.771984	2.145902	51.50164
29	WSII PER	28.5	32.8	59.9	2.2	1190.224	34.49963	1.848391	0.846214	1.564134	37.53921
30	WSII PER	39.9	38	50.7	1.3	1930.486	43.93729	0.673406	0.943493	0.635353	15.24848
31	WSII PER								SUM	56.74404	1361.857
32	WSII PER								AVG	1.891468	45.39524
33	WSII PER										

Sample	Type	W (mm)	D (mm)	L (mm)	P (kN)	De^2 (mm^2)	De (mm)	Is	F	Is_{50}	UCS
1	WS II PL	50.7	36.7	116	2	2369.104	48.67344	0.844201	0.987973	0.834047	20.01714
2	WS II PL	33.7	23.1	45.7	1	991.1788	31.48299	1.0089	0.812078	0.819305	19.66332
3	WS II PL	38.9	42.3	59	1	2095.077	45.77202	0.477309	0.961022	0.458705	11.00892
4	WS II PL	55	30.3	84.4	1	2121.854	46.06358	0.471286	0.963772	0.454212	10.9011
5	WS II PL	39.7	27	87.2	1	1364.785	36.943	0.732716	0.872676	0.639424	15.34616
6	WS II PL	27.6	28.1	103.5	2.2	987.4737	31.42409	2.227908	0.811394	1.807711	43.38505
7	WS II PL	24.5	35.9	73.3	1.95	1119.878	33.46458	1.741261	0.834693	1.453419	34.88206
8	WS II PL					0	0	#DIV/0!	0	#DIV/0!	#DIV/0!
9	WS II PL	20	25.2	93.4	0.7	641.7127	25.33205	1.090831	0.736402	0.80329	19.27897
10	WS II PL	18.8	28.7	54.8	1	686.9891	26.21048	1.455627	0.747786	1.088497	26.12394
11	WS II PL	28.6	20.5	51.7	0.5	746.5003	27.32216	0.669792	0.761895	0.510311	12.24747
12	WS II PL	17.1	24.1	73.2	0.6	524.7147	22.90665	1.143478	0.703795	0.804775	19.31459
13	WS II PL	33.7	28.3	42.7	1.6	1214.301	34.84683	1.31763	0.850035	1.120032	26.88077
14	WS II PL	28.3	29.8	77.7	2.8	1073.774	32.76849	2.607625	0.826835	2.156076	51.74583
15	WS II PL	25.2	19.3	69	0.01	619.2528	24.88479	0.016148	0.730523	0.011797	0.283124
16	WS II PL	33	28.7	54	3.4	1205.885	34.72586	2.819506	0.848706	2.392932	57.43036
17	WS II PL	31	42.5	86.8	4.1	1677.493	40.95721	2.444123	0.914139	2.234268	53.62243
18	WS II PL	16.4	26.8	52.1	0.4	559.6142	23.65617	0.714778	0.714066	0.510399	12.24957
19	WS II PL	25.9	42.2	51.9	2.3	1391.625	37.3045	1.652744	0.876508	1.448644	34.76744
20	WS II PL	24.8	40.5	65	5.8	1278.842	35.7609	4.535354	0.859998	3.900394	93.60945
21	WS II PL	33.2	47.6	95.6	3.2	2012.126	44.85673	1.590358	0.952327	1.51454	36.34896
22	WS II PL	21.1	37.9	85.9	1	1018.197	31.9092	0.982128	0.817007	0.802405	19.25773
23	WS II PL	58	50.4	84.8	3.3	3721.934	61.00765	0.886636	1.09367	0.969687	23.2725
24	WS II PL	17.6	25.2	62.1	0.9	564.7072	23.76357	1.593746	0.715523	1.140363	27.3687
25	WS II PL	31.3	32.1	82.5	5.8	1279.262	35.76677	4.533864	0.860061	3.899401	93.58562
26	WS II PL	30	47.3	65	0.5	1806.727	42.50561	0.276744	0.929532	0.257242	6.173807
27	WS II PL	25.3	29.6	76.4	0.6	953.5036	30.87885	0.629258	0.805028	0.506571	12.15769
28	WS II PL	19.4	37.3	91	6	921.3416	30.35361	6.512243	0.798837	5.20222	124.8533
29	WS II PL	26.1	40.9	74.5	1.8	1359.17	36.86693	1.324337	0.871867	1.154646	27.71149
30	WS II PL								SUM	32.42849	778.2837
31	WS II PL								AVG	1.118224	26.83737
32	WS II PL										
33	WS II PL										

Sample	Type	W (mm)	D (mm)	L (mm)	P (kN)	De^2 (mm^2)	De (mm)	Is	F	Is_{50}	UCS
1	WSIII per	40.12	40.76	62.86	4.4	2082.117	45.63022	2.113233	0.959682	2.028031	48.67275
2	WSIII per	43.71	40.91	73.72	0.6	2276.777	47.71558	0.26353	0.979176	0.258043	6.193023
3	WSIII per	50.28	26.45	86.72	1.5	1693.289	41.14959	0.88585	0.916069	0.811499	19.47598
4	WSIII per	40.08	35.48	66.03	0.85	1810.596	42.55109	0.469459	0.929979	0.436587	10.47809
5	WSIII per	45.85	35.79	95.54	1.6	2089.35	45.70941	0.765788	0.960431	0.735487	17.65168
6	WSIII per	49.85	36.7	99.1	1.3	2329.385	48.26371	0.558087	0.984221	0.549281	13.18275
7	WSIII per	53.85	51.51	78.17	1.2	3531.729	59.42835	0.339777	1.080838	0.367244	8.813852
8	WSIII per	42.09	31.9	71.51	1.6	1709.542	41.34661	0.935923	0.91804	0.859215	20.62115
9	WSIII per	48.86	28.34	94.23	2.2	1763.045	41.98863	1.247841	0.924427	1.153538	27.68492
10	WSIII per	24.52	20.22	46.38	0.7	631.265	25.12499	1.108884	0.733688	0.813575	19.52579
11	WSIII per	25.12	20.15	56.05	0.6	644.4731	25.38648	0.930993	0.737114	0.686248	16.46995
12	WSIII per	30.96	31.57	57.23	1	1244.473	35.2771	0.803553	0.854742	0.686831	16.48393
13	WSIII per	28.27	20.01	66.21	2	720.2496	26.83747	2.776815	0.755783	2.09867	50.36808
14	WSIII per	53.55	56.22	66.4	0.55	3833.191	61.91277	0.143484	1.100942	0.157967	3.791212
15	WSIII per	38.67	29.61	62.18	0.5	1457.883	38.18224	0.342963	0.885729	0.303772	7.290539
16	WSIII per	26.72	18.86	39.97	0.6	641.6353	25.33052	0.935111	0.736382	0.688599	16.52637
17	WSIII per	43.22	26.43	64	2.2	1454.427	38.13696	1.512623	0.885257	1.339059	32.13743
18	WSIII per	50.02	25.25	78.91	2.1	1608.108	40.10122	1.305883	0.905492	1.182466	28.37917
19	WSIII per	41.97	32.86	61.55	0.5	1755.968	41.90427	0.284743	0.923591	0.262986	6.311671
20	WSIII per	25.42	18.19	42.6	0.9	588.733	24.26382	1.528707	0.722263	1.104128	26.49906
21	WSIII per	25.27	31.34	56.92	0.4	1008.357	31.75464	0.396685	0.815224	0.323387	7.761285
22	WSIII per	25.4	23.99	48.53	0.9	775.8434	27.85397	1.160028	0.768533	0.89152	21.39648
23	WSIII per	36.69	18.14	45.66	0.9	847.413	29.11036	1.062056	0.783944	0.832592	19.98221
24	WSIII per	37.24	21.66	41.92	0.5	1027.018	32.04713	0.486846	0.818594	0.398529	9.564706
25	WSIII per	33.14	23.12	58.05	0.7	975.5521	31.23383	0.717542	0.809179	0.580621	13.93489
26	WSIII per	28.56	24.03	55	1.1	873.8202	29.56045	1.25884	0.789375	0.993697	23.84873
27	WSIII per	31.57	27	57.67	0.6	1085.297	32.94384	0.552844	0.828823	0.45821	10.99704
28	WSIII per	32.71	28.58	54.79	2.2	1190.29	34.50058	1.848289	0.846224	1.564066	37.53759
29	WSIII per	31.88	28.38	44.69	0.85	1151.969	33.94067	0.737867	0.840016	0.61982	14.87569
30	WSIII per	31.04	24.05	54.62	1	950.4886	30.83	1.05209	0.804455	0.846359	20.31262
31	WSIII per	35.59	29.85	39.89	2	1352.641	36.77826	1.478589	0.870923	1.287737	30.90568
32	WSIII per	40.3	17.59	42.76	0.85	902.5702	30.04281	0.941755	0.795146	0.748832	17.97198
33	WSIII per								SUM	26.0686	625.6463
									AVG	0.789957	19.55145

Sample	Type	W (mm)	D (mm)	L (mm)	P (kN)	De^2 (mm^2)	De (mm)	Is	F	Is_{50}	UCS		
1	WSIII PL	33.05	20.41	49.81	0.2	858.8644	29.30639	0.232866	0.786315	0.183106	4.394538		
2	WSIII PL	27.43	31.21	61.05	1	1090.008	33.01527	0.917424	0.829631	0.761124	18.26698		
3	WSIII PL	27.42	27.36	58.95	0	955.1986	30.90629	0	0.80535	0	0		
4	WSIII PL	30.6	26.98	59.91	0.5	1051.171	32.42177	0.47566	0.822887	0.391414	9.39394		
5	WSIII PL	30.35	22.22	57.81	0.3	858.6435	29.30262	0.349388	0.786269	0.274713	6.593121		
6	WSIII PL	28.31	30.63	46.99	0.25	1104.071	33.22756	0.226435	0.832028	0.1884	4.521599		
7	WSIII PL	30.84	33.03	32.58	0.5	1296.979	36.0136	0.385511	0.862727	0.332591	7.982182		
8	WSIII PL	33.12	28.68	49	0.3	1209.427	34.77681	0.248051	0.849266	0.210662	5.055881		
9	WSIII PL	29.42	27.79	63.74	0.2	1040.977	32.26418	0.192127	0.821084	0.157753	3.786062		
10	WSIII PL	29.66	28.42	57.23	0.15	1073.261	32.76066	0.139761	0.826746	0.115547	2.773124		
11	WSIII PL	31.36	25.68	46.1	0.1	1025.371	32.02142	0.097526	0.818299	0.079805	1.915322		
12	WSIII PL	33.5	30.29	67.69	0.35	1291.975	35.94406	0.270903	0.861977	0.233512	5.604292		
13	WSIII PL	37.58	29.22	64.54	0.1	1398.129	37.39156	0.071524	0.877428	0.062757	1.506176		
14	WSIII PL	34.63	27.75	60.59	0.2	1223.561	34.97944	0.163457	0.851489	0.139182	3.340372		
15	WSIII PL	46.62	35.45	44.79	0.5	2104.256	45.87217	0.237614	0.961968	0.228577	5.485842		
16	WSIII PL	47.18	30.59	58.99	0.5	1837.585	42.86707	0.272096	0.933081	0.253888	6.093305		
17	WSIII PL	46.05	30.28	44.54	0.35	1775.398	42.13547	0.197139	0.925881	0.182527	4.380651		
18	WSIII PL								SUM	3.795558	91.09339		
19	WSIII PL								AVG	0.223268	5.358435		
20	WSIII PL												
21	WSIII PL												
22	WSIII PL												
23	WSIII PL												
24	WSIII PL												
25	WSIII PL												
26	WSIII PL												
27	WSIII PL												
28	WSIII PL												
29	WSIII PL												
30	WSIII PL												
31	WSIII PL												
32	WSIII PL												
33	WSIII PL												

Sample	Type	W (mm)	D (mm)	L (mm)	P (kN)	De^2 (mm^2)	De (mm)	Is	F	Is_{50}	UCS	
1	SG IV	70.94	44.62	90.27	2	4030.24	63.48417	0.496248	1.11343	0.552538	13.26091	
2	SG IV	42.06	35.35	88.26	0.7	1893.079	43.50953	0.369768	0.939348	0.347341	8.336178	
3	SG IV	50.86	36.19	77.73	1	2343.554	48.41027	0.426702	0.985565	0.420543	10.09303	
4	SG IV	45.66	42.04	68.84	1.6	2444.042	49.43726	0.654653	0.99492	0.651327	15.63185	
5	SG IV	48.66	33.46	90.24	0.75	2073.042	45.53067	0.361787	0.958739	0.346859	8.324625	
6	SG IV	42.83	25.02	57.92	0.85	1364.412	36.93795	0.622979	0.872622	0.543625	13.04701	
7	SG IV	47.22	52.27	70.35	1.55	3142.596	56.05887	0.493223	1.052818	0.519274	12.46257	
8	SG IV	53.44	34.83	71.91	0.8	2369.9	48.68162	0.337567	0.988047	0.333532	8.004772	
9	SG IV	52.07	31.09	81.36	0.95	2061.192	45.40035	0.460898	0.957503	0.441312	10.59148	
10	SG IV	47.26	30.78	78.77	0.8	1852.134	43.03643	0.431934	0.934738	0.403745	9.689884	
11	SG IV	48.31	36.44	69.46	0.8	2241.432	47.34376	0.356915	0.975735	0.348254	8.358098	
12	SG IV	44.46	34.77	60.16	1	1968.268	44.36517	0.508061	0.947616	0.481447	11.55472	
13	SG IV	40.77	37	66.83	0.8	1920.669	43.82544	0.416522	0.942411	0.392534	9.420826	
14	SG IV	49.95	37.07	71.52	0.9	2357.59	48.55502	0.381746	0.98689	0.376741	9.04179	
15	SG IV	36.49	31.43	47.93	0.5	1460.254	38.21327	0.342406	0.886053	0.30339	7.281364	
16	SG IV	44.53	39.95	68.28	0.3	2265.059	47.59264	0.132447	0.97804	0.129538	3.108918	
17	SG IV	39.73	42.8	57.08	0.6	2165.073	46.53034	0.277127	0.968155	0.268302	6.439243	
18	SG IV	57.31	43.47	56.82	0.25	3171.978	56.32032	0.078815	1.055025	0.083152	1.995648	
19	SG IV	35.38	39.19	42.24	0.4	1765.4	42.01667	0.226578	0.924705	0.209517	5.028417	
20	SG IV	42.75	50.36	62.76	0.7	2741.145	52.35594	0.255368	1.020935	0.260714	6.257135	
21	SG IV	48.66	34.68	72.52	0.5	2148.628	46.3533	0.232707	0.966495	0.22491	5.397837	
22	SG IV	44.16	36.38	82.97	0.6	2045.511	45.22733	0.293325	0.955859	0.280378	6.729062	
23	SG IV	41.33	34.6	64.62	0.5	1820.755	42.67031	0.274611	0.931151	0.255705	6.13691	
24	SG IV	57.1	34.03	55.3	0.6	2474.048	49.73981	0.242517	0.997655	0.241949	5.80677	
25	SG IV	35.08	31.02	63.66	0.5	1385.516	37.22252	0.360876	0.875641	0.315998	7.583957	
26	SG IV	44.12	32.99	65.31	1	1853.224	43.04909	0.5396	0.934862	0.504451	12.10683	
27	SG IV	37.16	41.19	62.55	0.85	1948.846	44.14574	0.436155	0.945504	0.412387	9.897284	
28	SG IV	34.21	33.09	68.82	0.5	1441.318	37.9647	0.346905	0.883455	0.306475	7.355391	
29	SG IV	32.25	22.45	52.79	0.2	921.8413	30.36184	0.216957	0.798934	0.173334	4.160027	
30	SG IV	24.38	22.83	36.6	0.55	708.6793	26.62103	0.776092	0.753034	0.584423	14.02616	
31	SG IV								SUM	10.7137	257.1287	
32	SG IV								AVG	0.324657	8.570957	
33	SG IV											

Sample	Type	W (mm)	D (mm)	L (mm)	P (kN)	D_e^2 (mm^2)	D_e (mm)	Is	F	$Is_{(50)}$	UCS	
1	SG IV PL	30	39.41	58.69	0	1505.351	38.79885	0	0.892138	0	0	
2	SG IV PL	32.35	31.53	57.1	0.2	1298.699	36.03746	0.154	0.862984	0.1329	3.189596	
3	SG IV PL	31.5	30.21	46.31	0	1211.634	34.80853	0	0.849615	0	0	
4	SG IV PL	31.37	33.83	38.21	0.25	1351.222	36.75897	0.185018	0.870717	0.161098	3.866354	
5	SG IV PL	24.94	23.37	49.96	0.1	742.1049	27.2416	0.134752	0.760884	0.10253	2.460731	
6	SG IV PL	26.13	23.89	41.57	0	794.8143	28.19245	0	0.772722	0	0	
7	SG IV PL	25.45	21.14	41.42	0.15	685.0194	26.17288	0.218972	0.747303	0.163638	3.92732	
8	SG IV PL	28.28	25.34	34.19	0	912.4228	30.20634	0	0.79709	0	0	
9	SG IV PL	25.83	35.35	41.53	0.05	1162.583	34.09667	0.043008	0.841751	0.036202	0.868843	
10	SG IV PL	29.75	34.13	47.4	0	1292.806	35.95561	0	0.862102	0	0	
11	SG IV PL	25.7	33.52	62.13	0	1096.85	33.11873	0	0.8308	0	0	
12	SG IV PL	29.86	46.68	41.87	0	1774.724	42.12747	0	0.925802	0	0	
13	SG IV PL	35.49	38.25	42.1	0	1728.413	41.57419	0	0.92031	0	0	
14	SG IV PL	20.82	27.62	35.59	0	732.1744	27.05872	0	0.758581	0	0	
15	SG IV PL	17.98	26.2	39.03	0	599.7926	24.49066	0	0.725293	0	0	
16	SG IV PL	25.29	28.22	46.6	0	908.6904	30.14449	0	0.796356	0	0	
17	SG IV PL	21.14	25.48	36.19	0	685.8269	26.1883	0	0.747501	0	0	
18	SG IV PL	24.19	35.6	34.56	0.05	1096.468	33.11296	0.045601	0.830735	0.037882	0.909176	
19	SG IV PL	36.91	35.99	35.57	0	1691.36	41.12615	0	0.915834	0	0	
20	SG IV PL	34.16	35.99	40.2	0	1565.344	39.56443	0	0.900017	0	0	
21	SG IV PL	21.59	25.02	28.65	0	687.7808	26.22558	0	0.74798	0	0	
22	SG IV PL	19.33	32.61	36.48	0.05	802.5882	28.32999	0.062298	0.774416	0.048245	1.157878	
23	SG IV PL	23.66	33.16	48.74	0	998.9399	31.60601	0	0.813504	0	0	
24	SG IV PL	32.33	35.81	47.16	0	1474.077	38.39371	0	0.887934	0	0	
25	SG IV PL	27.53	33.92	40.9	0	1188.973	34.48149	0	0.846013	0	0	
26	SG IV PL	21.29	30.03	41.46	0	814.0313	28.53123	0	0.776887	0	0	
27	SG IV PL	17.79	35.74	35.92	0	809.5443	28.45249	0	0.775921	0	0	
28	SG IV PL	22.22	27.08	48.14	0	766.1306	27.67907	0	0.766358	0	0	
29	SG IV PL	20.92	33.37	33.44	0	888.849	29.81357	0	0.79241	0	0	
30	SG IV PL	26.2	36.93	48.15	0	1231.943	35.09905	0	0.852798	0	0	
									SUM	0.682496	16.3799	
									AVG	0.02275	0.528384	

APPENDIX A6

NCB CONE INDENTER

The cone indenter is a device for measuring the strength of rock material using resistance to indentation of a tungsten carbide platen into a particular sample. The steel frame holds a metal strip attached to a dial gauge measuring the amount of plate movement The sample is placed onto the metal strip and held gently in place by the platen. The stem of the platen is calibrated as a micrometer to measure the amount of indentation (Figure 5.17.).

For the purpose of this study dealing with weak weathered rocks, the cone indenter number for weak rocks was used. The weak rock indenter number requires that the micrometer on the stem be turned until the dial reads 0.23mm which is approximately equal to a load of 12 N.

Calculations for the cone indenter are:

$$\textbf{Penetration} = P_W = (M_3 - M_0) - D_3 \textbf{ (mm)}$$

Where M_3 = Micrometer reading at 0.23mm (12N)

M_o = Micrometer reading at 0mm (initial reading)

D_3 = Spring deflection for weak rocks 0.23mm

$$\textbf{Cone indenter number} = I_W = 0.23/P_W$$

Unconfined Compressive Strength

$$\textbf{UCS} = I_W \textbf{ x 16.5 (MPa)}$$

The data for unconfined compressive strength using the cone indenter are presented following while comparisons with point load results are reproduced in the text (Chapter 5)

CONE INDENTER TESTS			Greywacke weathering grade II			
SAMPLE	Mo	M3	D3 (kN)	Pw	Iw	UCS(MPa)
1	3.775	4.055	0.23	0.05	4.6	75.9
2	7.45	8.775	0.23	1.095	0.210046	3.465753
3	2.575	3.855	0.23	1.05	0.219048	3.614286
4	8.725	9.125	0.23	0.17	1.352941	22.32353
5	0.275	0.67	0.23	0.165	1.393939	23
6	0.41	1.75	0.23	1.11	0.207207	3.418919
7	0.72	2.175	0.23	1.225	0.187755	3.097959
8	1.75	2.1	0.23	0.12	1.916667	31.625
9	3.375	3.7	0.23	0.095	2.421053	39.94737
10	4.865	5.85	0.23	0.755	0.304636	5.02649
11	6.3	6.84	0.23	0.31	0.741935	12.24194
12	4.4	4.75	0.23	0.12	1.916667	31.625
13	7.825	8.19	0.23	0.135	1.703704	28.11111
14	4.92	5.65	0.23	0.5	0.46	7.59
15	2.575	2.985	0.23	0.18	1.277778	21.08333
16	1.15	1.395	0.23	0.015	15.33333	253
17	5.23	5.515	0.23	0.055	4.181818	69
18	6.35	6.7	0.23	0.12	1.916667	31.625
19	4.65	4.91	0.23	0.03	7.666667	126.5
20	3.745	4.025	0.23	0.05	4.6	75.9
21	2.99	3.3	0.23	0.08	2.875	47.4375
22	2.75	3.425	0.23	0.445	0.516854	8.52809
23	4.175	4.456	0.23	0.051	4.509804	74.41176
24	1.175	1.48	0.23	0.075	3.066667	50.6
25	1.97	2.235	0.23	0.035	6.571429	108.4286
26	5.575	5.89	0.23	0.085	2.705882	44.64706
27	1.875	2.13	0.23	0.025	9.2	151.8
28	3.87	4.135	0.23	0.035	6.571429	108.4286
29	3.7	4.025	0.23	0.095	2.421053	39.94737
30	4.345	5.24	0.23	0.665	0.345865	5.706767
31	8.47	8.925	0.23	0.225	1.022222	16.86667
32	8.42	8.7	0.23	0.05	4.6	75.9
33	4.9	5.17	0.23	0.04	5.75	94.875
34	1.345	1.65	0.23	0.075	3.066667	50.6
35	1.37	1.645	0.23	0.045	5.111111	84.33333
				SUM	110.9458	1830.606
	KEY			AVG	3.169881	52.30304
	Pw = (M3-Mo)-D3					
	(cone penetration)					
	Iw = 0.23/Pw					
	(Weak rock cone indenter number)					

			Weathered greywacke grade III			
SAMPLE	Mo	M3	D3 (kN)	Pw	Iw	UCS(MPa)
1	2.9	3.2	0.23	0.07	3.285714	54.21429
2	4.135	4.74	0.23	0.375	0.613333	10.12
3	2.76	3.19	0.23	0.2	1.15	18.975
4	7.125	7.425	0.23	0.07	3.285714	54.21429
5	4.41	4.68	0.23	0.04	5.75	94.875
6	4.66	5.15	0.23	0.26	0.884615	14.59615
7	4.965	5.24	0.23	0.045	5.111111	84.33333
8	9.15	9.48	0.23	0.1	2.3	37.95
9	3.385	3.775	0.23	0.16	1.4375	23.71875
10	7.595	8.015	0.23	0.19	1.210526	19.97368
11	4.6	5.06	0.23	0.23	1	16.5
12	6.485	6.775	0.23	0.06	3.833333	63.25
13	8.25	8.525	0.23	0.045	5.111111	84.33333
14	7.425	8	0.23	0.345	0.666667	11
15	5.95	6.255	0.23	0.075	3.066667	50.6
16	5.25	5.595	0.23	0.115	2	33
17	6.7	7.025	0.23	0.095	2.421053	39.94737
18	7.49	8.29	0.23	0.57	0.403509	6.657895
19	8.255	8.55	0.23	0.065	3.538462	58.38462
20	6.555	6.845	0.23	0.06	3.833333	63.25
21	6.635	7.08	0.23	0.215	1.069767	17.65116
22	2.92	3.34	0.23	0.19	1.210526	19.97368
23	6.35	6.75	0.23	0.17	1.352941	22.32353
24	3.25	3.65	0.23	0.17	1.352941	22.32353
25	6.115	6.575	0.23	0.23	1	16.5
26	9.475	9.935	0.23	0.23	1	16.5
27	9.225	9.81	0.23	0.355	0.647887	10.69014
28	8.275	FAILED	0.23	#VALUE!	0	0
29	5.57	5.87	0.23	0.07	3.285714	54.21429
30	6.915	7.525	0.23	0.38	0.605263	9.986842
31	6.575	6.88	0.23	0.075	3.066667	50.6
32	5.46	6.395	0.23	0.705	0.326241	5.382979
33	3.815	4.12	0.23	0.075	3.066667	50.6
34	2.245	2.975	0.23	0.5	0.46	7.59
35	2.955	3.715	0.23	0.53	0.433962	7.160377
				SUM	69.78123	1151.39
				AVG	1.993749	32.89686
	KEY					
	Pw = (M3-Mo)-D3					
	(cone penetration)					
	Iw = 0.23/Pw					
	(Weak rock cone indenter number)					

CONE INDENTER TESTS			Greywacke weathering grade IV			
SAMPLE	Mo	M3	D3 (kN)	Pw	Iw	UCS(MPa)
1	3.925	4.495	0.23	0.34	0.676471	11.16176
2	0.8	FAILED	0.23	#VALUE!	0	0
3	3.32	4.565	0.23	1.015	0.226601	3.738916
4	5.675	FAILED	0.23	#VALUE!	0	0
5	3.485	3.62	0.23	-0.095	-2.42105	-39.9474
6	2.845	3.73	0.23	0.655	0.351145	5.793893
7	3.51	3.8	0.23	0.06	3.833333	63.25
8	2.11	3.155	0.23	0.815	0.282209	4.656442
9	3.97	FAILED	0.23	#VALUE!	0	0
10	3.665	3.96	0.23	0.065	3.538462	58.38462
11	5.85	6.5	0.23	0.42	0.547619	9.035714
12	6.975	7.075	0.23	-0.13	-1.76923	-29.1923
13	2.555	3	0.23	0.215	1.069767	17.65116
14	3.7	4.565	0.23	0.635	0.362205	5.976378
15	2.8	3.3	0.23	0.27	0.851852	14.05556
16	4.135	FAILED	0.23	#VALUE!	0	0
17	5.945	6.4	0.23	0.225	1.022222	16.86667
18	5.595	6.075	0.23	0.25	0.92	15.18
19	2.525	4.125	0.23	1.37	0.167883	2.770073
20	4.85	5.475	0.23	0.395	0.582278	9.607595
21	6.44	6.89	0.23	0.22	1.045455	17.25
22	7.015	7.775	0.23	0.53	0.433962	7.160377
23	7.075	7.375	0.23	0.07	3.285714	54.21429
24	6.9	7.36	0.23	0.23	1	16.5
25	5.51	6.075	0.23	0.335	0.686567	11.32836
26	4.11	4.9	0.23	0.56	0.410714	6.776786
27	5.75	FAILED	0.23	#VALUE!	0	0
28	4.125	4.375	0.23	0.02	11.5	189.75
29	7.335	8.08	0.23	0.515	0.446602	7.368932
30	4.775	5.59	0.23	0.585	0.393162	6.487179
31	7.575	FAILED	0.23	#VALUE!	0	0
32	4.11	4.855	0.23	0.515	0.446602	7.368932
33	5.65	6.35	0.23	0.47	0.489362	8.074468
34	6.43	6.675	0.23	0.015	15.33333	253
35	2.815	3.735	0.23	0.69	0.333333	5.5
				SUM	46.04657	759.7684
KEY				AVE	1.315616	21.70767
Pw = (M3-Mo)-D3						
(cone penetration)						
Iw = 0.23/Pw						
(Weak rock cone indenter number)						

CONE INDENTER TESTS			Schist weathering grade II			
SAMPLE	Mo	M3	D3 (MM)	Pw	Iw	UCS(MPa)
1	3.75	4.76	0.23	0.78	0.294872	4.865385
2	2.25	2.96	0.23	0.48	0.479167	7.90625
3	0.495	1.58	0.23	0.855	0.269006	4.438596
4	3.63	failed	0.23	#VALUE!	0	0
5	4.425	7.1	0.23	2.445	0.09407	1.552147
6	3.68	3.99	0.23	0.08	2.875	47.4375
7	7.98	8.335	0.23	0.125	1.84	30.36
8	8.12	9.89	0.23	1.54	0.149351	2.464286
9	4.5	4.875	0.23	0.145	1.586207	26.17241
10	1.545	2.075	0.23	0.3	0.766667	12.65
11	3.775	failed	0.23	#VALUE!	0	0
12	2.6	3.785	0.23	0.955	0.240838	3.973822
13	4.825	5.945	0.23	0.89	0.258427	4.264045
14			0.23			0
15	failed	15.79	0.23	#VALUE!	0	0
16	16.95	17.34	0.23	0.16	1.4375	23.71875
17	16.59	16.83	0.23	0.01	23	379.5
18	14.42	16.25	0.23	1.6	0.14375	2.371875
19	16.8	17.21	0.23	0.18	1.277778	21.08333
20	failed	16.7	0.23	#VALUE!	0	0
21	15.84	16.28	0.23	0.21	1.095238	18.07143
22	21.75	22.05	0.23	0.07	3.285714	54.21429
23	failed	15.83	0.23	#VALUE!	0	0
24	19.21	19.48	0.23	0.04	5.75	94.875
25	15.7	15.95	0.23	0.02	11.5	189.75
26	14.75	15.14	0.23	0.16	1.4375	23.71875
27	failed	16.04	0.23	#VALUE!	0	0
28	16.72	17.09	0.23	0.14	1.642857	27.10714
29	15.67	16.26	0.23	0.36	0.638889	10.54167
30	failed	21.84	0.23	#VALUE!	0	0
31				SUM	51.20923	991.0367
32		KEY		AVERAGE	1.765835	34.17368
33		Pw = (M3-Mo)-D3				
34		(cone penetration)				
35		Iw = 0.23/Pw				
36		(Weak rock cone indenter number)				
37						

CONE INDENTER TESTS			Schist weathering grade III			
SAMPLE	Mo	M3	D3 (MM)	Pw	Iw	UCS(MPa)
1	21.61	21.97	0.23	0.13	1.769231	29.19231
2	18.62	19.05	0.23	0.2	1.15	18.975
3	17.53	17.91	0.23	0.15	1.533333	25.3
4	21.57	21.88	0.23	0.08	2.875	47.4375
5	19.64	19.92	0.23	0.05	4.6	75.9
6	21.73	22.17	0.23	0.21	1.095238	18.07143
7	25.09	25.51	0.23	0.19	1.210526	19.97368
8	17.49	17.94	0.23	0.22	1.045455	17.25
9	failed	18.89	0.23	#VALUE!	0	0
10	18.73	19.02	0.23	0.06	3.833333	63.25
11	17.65	17.99	0.23	0.11	2.090909	34.5
12	16.79	18.15	0.23	1.13	0.20354	3.358407
13	21.64	22.06	0.23	0.19	1.210526	19.97368
14	21.7	22.18	0.23	0.25	0.92	15.18
15	19.67	20.06	0.23	0.16	1.4375	23.71875
16	18.8	19.44	0.23	0.41	0.560976	9.256098
17	24.22	24.87	0.23	0.42	0.547619	9.035714
18	17.4	17.7	0.23	0.07	3.285714	54.21429
19	17.68	18.01	0.23	0.1	2.3	37.95
20	17.2	17.57	0.23	0.14	1.642857	27.10714
21						0
22						0
23						0
24						0
25						0
26						0
27				SUM	18.03297	549.644
28		**KEY**		AVERAGE	0.693576	21.14015
29		Pw = (M3-Mo)-D3				
30		(cone penetration)				
31		Iw = 0.23/Pw				
32		(Weak rock cone indenter number)				
33						
34						
35						
36						
37						

CONE INDENTER TESTS			Schist weathering grade IV			
SAMPLE	Mo	M3	D3 (MM)	Pw	Iw	UCS(MPa)
1	18.83	19.39	0.23	0.33	0.69697	11.5
2	failed	17.76	0.23	#VALUE!	0	0
3	21.07	21.55	0.23	0.25	0.92	15.18
4	failed	19.03	0.23	#VALUE!	0	0
5	failed	19.77	0.23	#VALUE!	0	0
6	failed	17.07	0.23	#VALUE!	0	0
7	18.89	19.31	0.23	0.19	1.210526	19.97368
8	failed	17.97	0.23	#VALUE!	0	0
9	failed	20.09	0.23	#VALUE!	0	0
10	16.83	17.33	0.23	0.27	0.851852	14.05556
11	16.88	17.31	0.23	0.2	1.15	18.975
12	18.12	18.67	0.23	0.32	0.71875	11.85938
13	failed	17.33	0.23	#VALUE!	0	0
14	19.37	19.7	0.23	0.1	2.3	37.95
15	failed	17.14	0.23	#VALUE!	0	0
16	failed	17.8	0.23	#VALUE!	0	0
17	16.82	17.23	0.23	0.18	1.277778	21.08333
18	failed	17.83	0.23	#VALUE!	0	0
19	18.12	18.61	0.23	0.26	0.884615	14.59615
20	21.27	21.65	0.23	0.15	1.533333	25.3
21	18.88	19.3	0.23	0.19	1.210526	19.97368
22	failed	20.97	0.23	#VALUE!	0	0
23	20.96	21.38	0.23	0.19	1.210526	19.97368
24	18.25	18.71	0.23	0.23	1	16.5
25	17.78	18.67	0.23	0.66	0.348485	5.75
26				SUM	15.31336	252.6705
27				AVERAGE	0.612534	10.10682
28	**KEY**					
29	Pw = (M3-Mo)-D3					
30	(cone penetration)					
31	Iw = 0.23/Pw					
32	(Weak rock cone indenter number)					
33						
34						
35						
36						
37						

APPENDIX D9

X-RAY DIFFRACTION

The identification of clay minerals is an important feature of an engineering geological soil stability study. X-ray diffraction (XRD) is one of the more accurate methods for mineral identification, particularly for clay minerals. The method involves the diffraction of x-rays off a sample; all crystalline minerals have specific atomic layer spacings and therefore may be distinguished. The samples in this study were analysed using a Phillips PW 1729 x-ray generator and a Philips PW 1710 diffractometer control. The scanning speed was 0.2°2θ per second and the Cu $_{k\alpha}$ wavelength was 1.5418 A°.

The clay samples were collected from grain size analysis at 9ϕ, and placed on a glass slide. The suspension was allowed to settle and dry to obtain an oriented sample of clays. Treatment of the clay slides was threefold. Firstly the samples were analysed in their natural state. Then the samples are exposed to an atmosphere of ethelene glycole in order to expand the swelling clays, and finally samples are fired at 580° C to collapse certain clays such as kaolinite.

Whole rock analyses were performed on samples of schist and greywacke at varying weathering grades. The samples were ground up using a mortar and pestle with ethanol and then allowed to settle onto glass slides. Treatment of the whole rock samples was considerably more simple than for clays; diffractograms only required on the samples in their natural state.

The diffractograms obtained and identification of the peaks are presented on the following pages. Representative diffractograms and analyses are given in the text (Chapter 5).

RED WEATHERED REGOLITH
SAMPLE B9

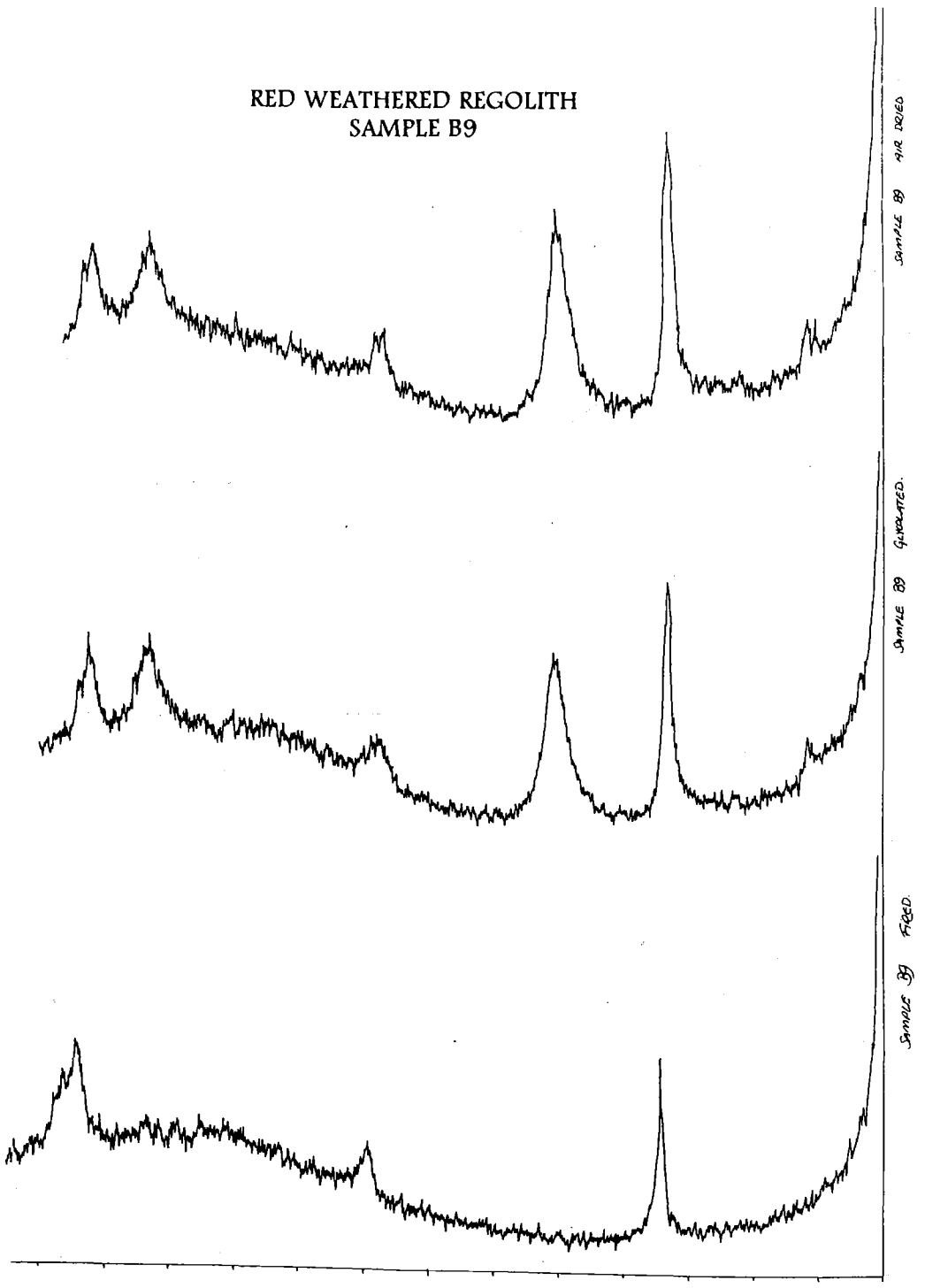

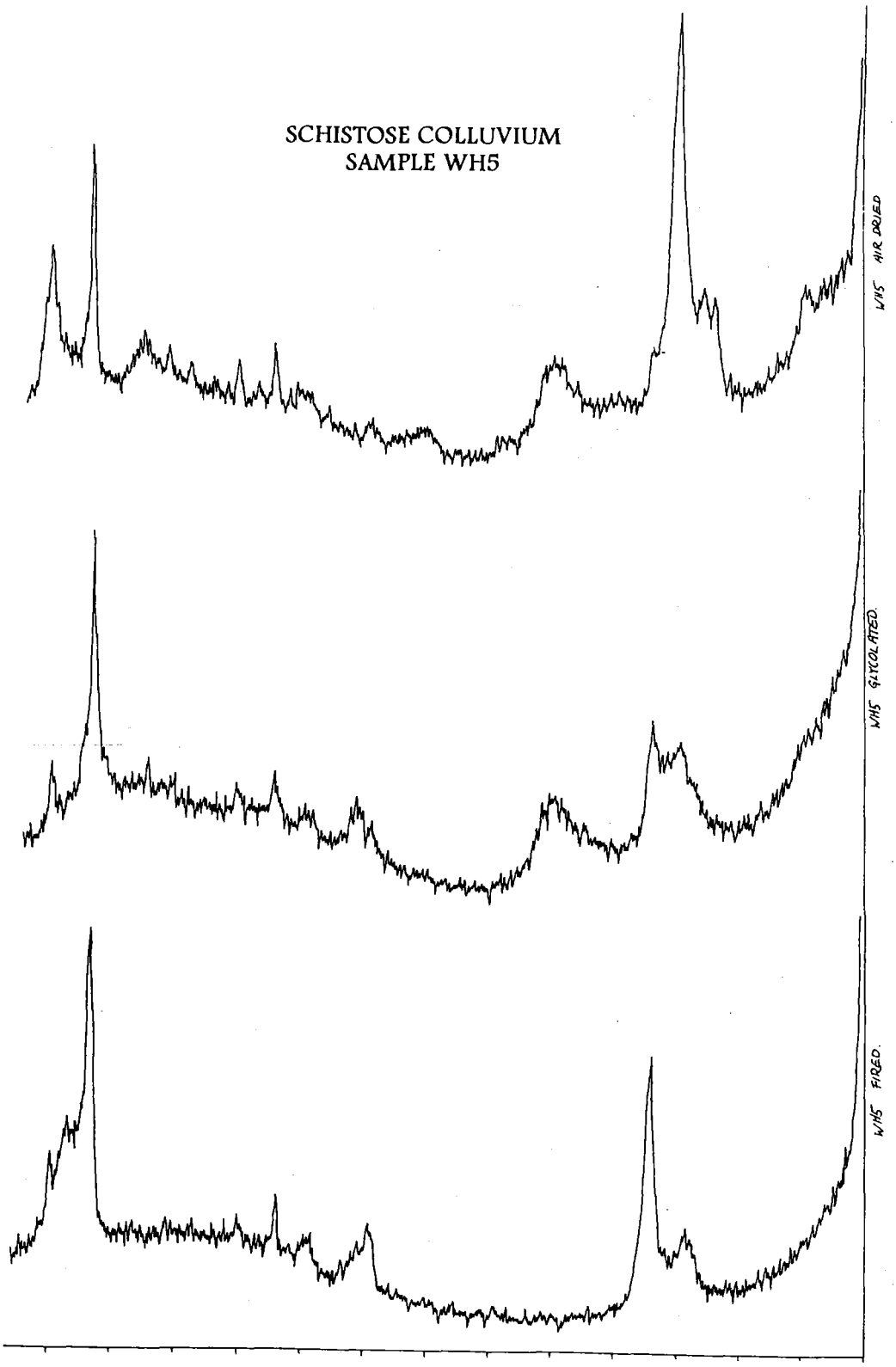
SCHISTOSE COLLUVIUM
SAMPLE WH5
WH5 AIR DRIED
WH5 GLYCOLATED.
WH5 FIRED.

SCHISTOSE REGOLITH
SAMPLE B12

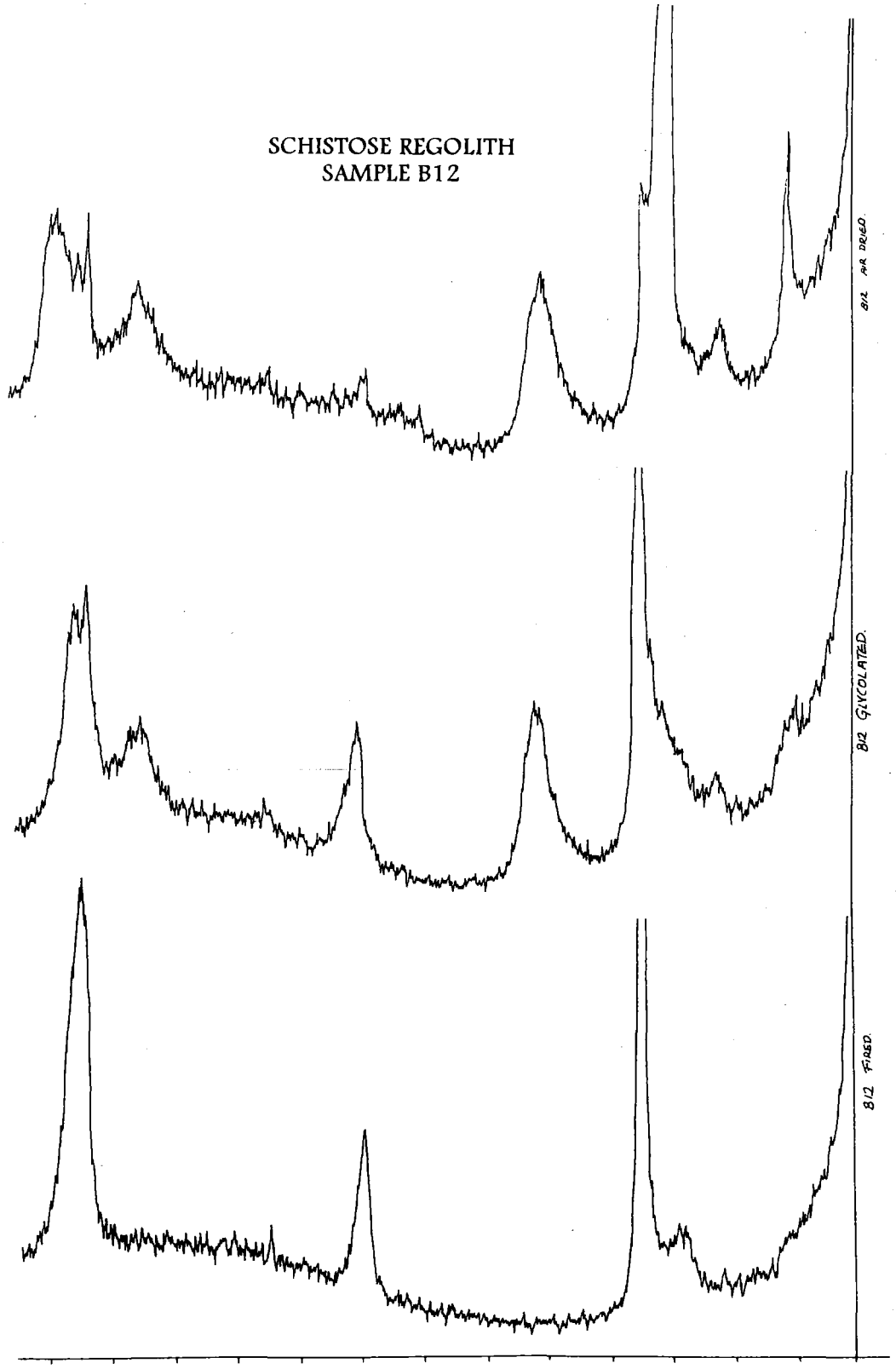

GREYWACKE REGOLITH
SAMPLE B18

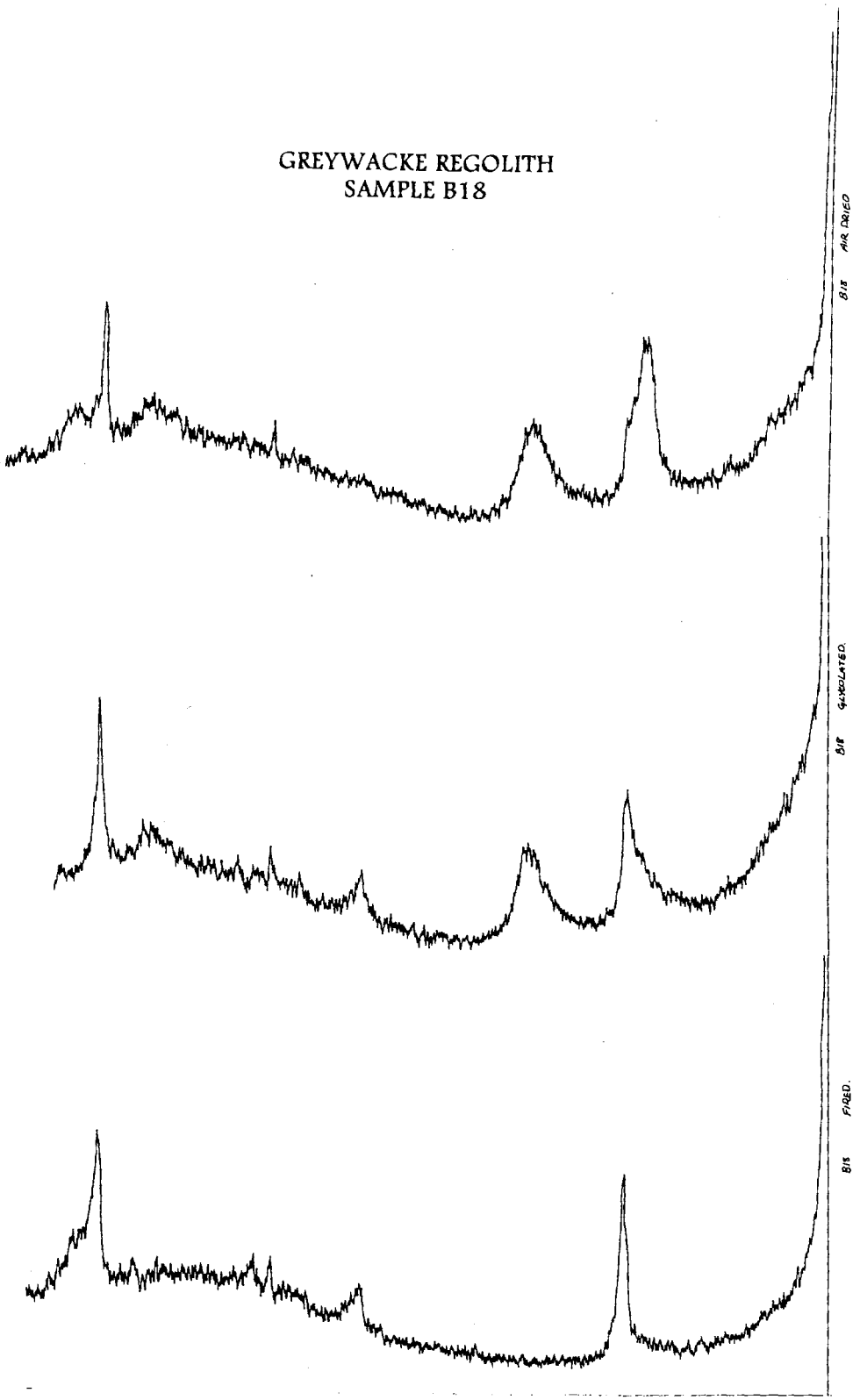

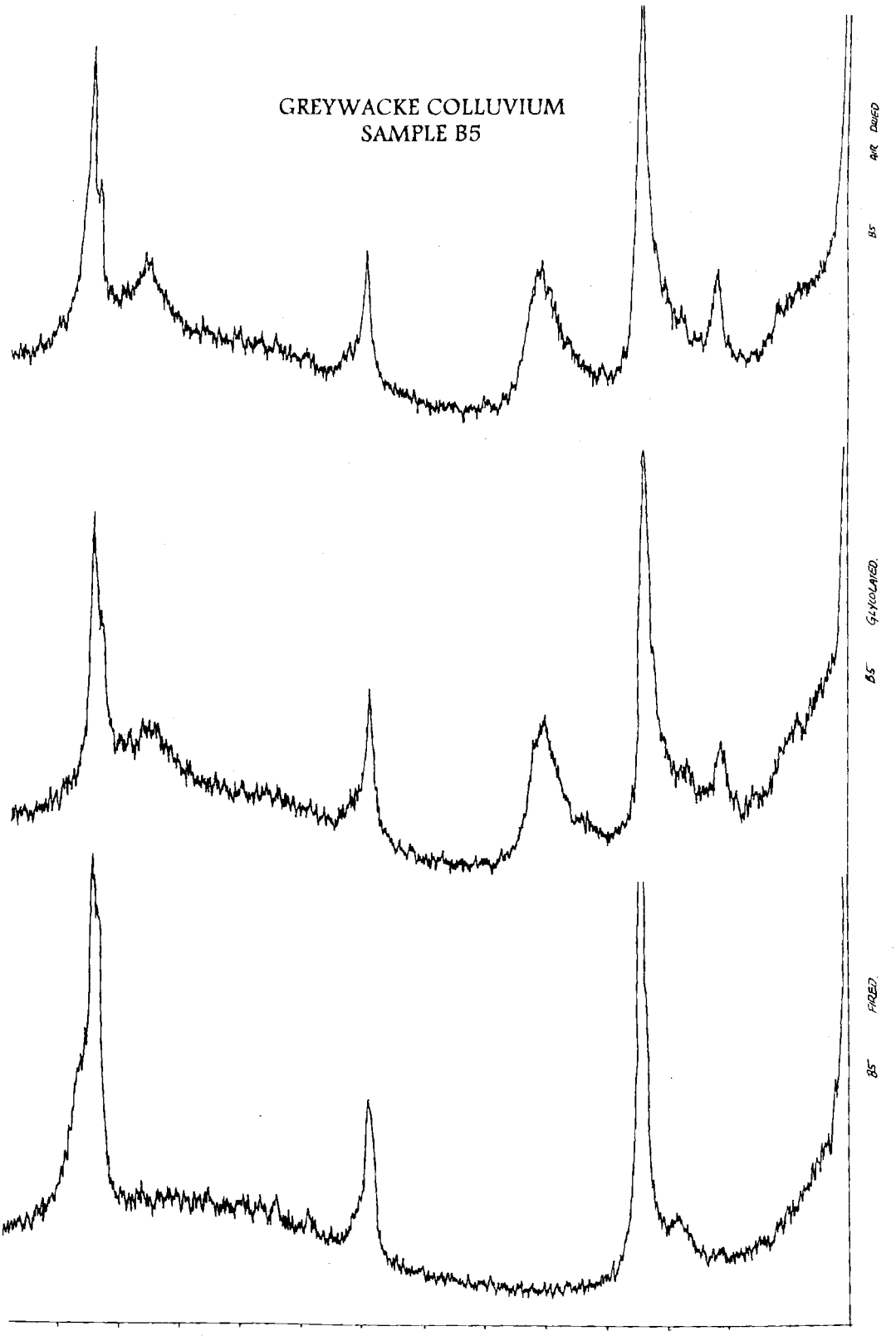
GREYWACKE COLLUVIUM
SAMPLE B5
B5 AIR DRIED
B5 GLYCOLATED
B5 FIRED

APPENDIX D10

SCANNING ELECTRON MICROSCOPE

The scanning electron microscope (SEM) allows the magnification of individual samples in excess of 20,000 times. The SEM involves the production of a primary electron beam which is focused onto the sample located in the evacuated optics column. The interaction of the primary beam with the sample produces a number of different types of radiation, most useful being the secondary electrons used for SEM and the characteristic x-rays. The x-rays which occur are analysed separately as energy dispersive x-rays (EDX spectrums).

SAMPLE PREPARATION

Clay minerals were sampled and allowed to settle into a preferred orientation on a glass slide mounted on a metal stub. All samples were initially coated with a thin carbon coating (200A) for EDX analysis, and then coated again with a thin layer of gold to accentuate the photographic quality of the sample. Both stubs and sample were kept clean and dry in order to negate any contamination; finger print oil will degrade the SEM image due to the release of gas in the SEM sample chamber.

EDX ANALYSIS

In order to validate the visual identification of minerals and the XRD analyses, an EDX identification of each clay sample was performed. All samples were coated with carbon being more accurate for EDX than gold because it has a lighter atomic weight. The stage height was lowered from 11mm for SEM analysis so that the focus was at 25mm. The lower stage height allowed for a more optimum angle between the primary beam and secondary x-rays; approximately 30°. Magnification for the minerals selected was at 10,000 times. Each element has a unique energy level which can be interpreted from individual peaks on the EDX graph. Mineral identification was compared with those presented in the SEM petrography atlas (Welton, 1984).

SEM SAMPLING PROGRAM

The sampling and identification of minerals using SEM and EDX followed several stages.

a) sample collection from grain size analysis and preparation by sample settling onto glass slides mounted onto metal stubs.

b) coating of the samples in carbon for EDX analysis,

c) further coating with a thin layer of gold for photographic collection of mineral images

e) data manipulation and printing of the EDX graphs.

f) data interpretation and comparison with XRD information.

EDX graphs and their associated SEM images are presented in the following pages and discussed in Chapter 5.

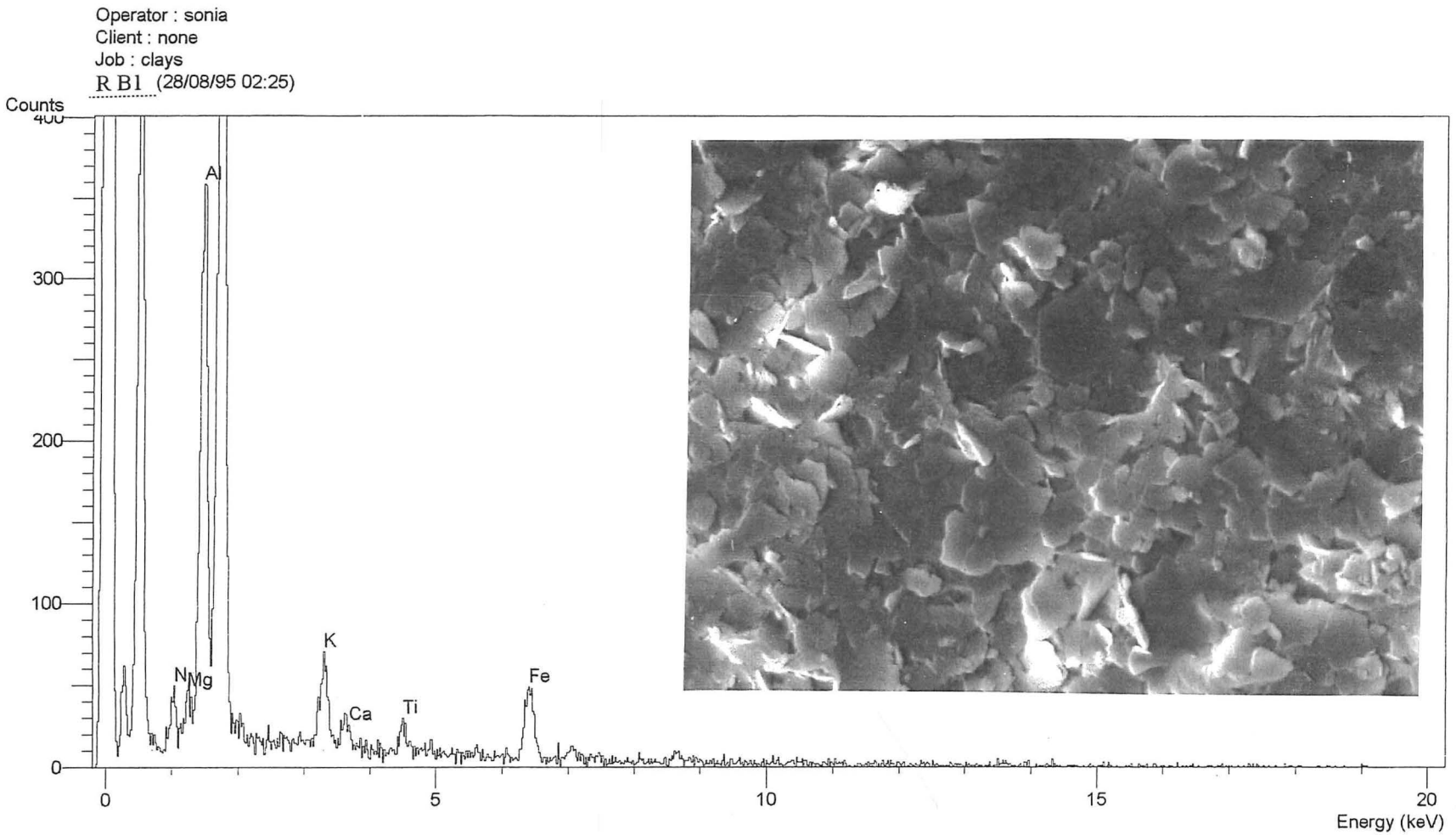
Operator : sonia
Client : none
Job : clays
R B1 (28/08/95 02:25)
Counts
400
300
200
100
0
Al
N
Mg
K
Ca
Ti
Fe
0
5
10
15
20
Energy (keV)

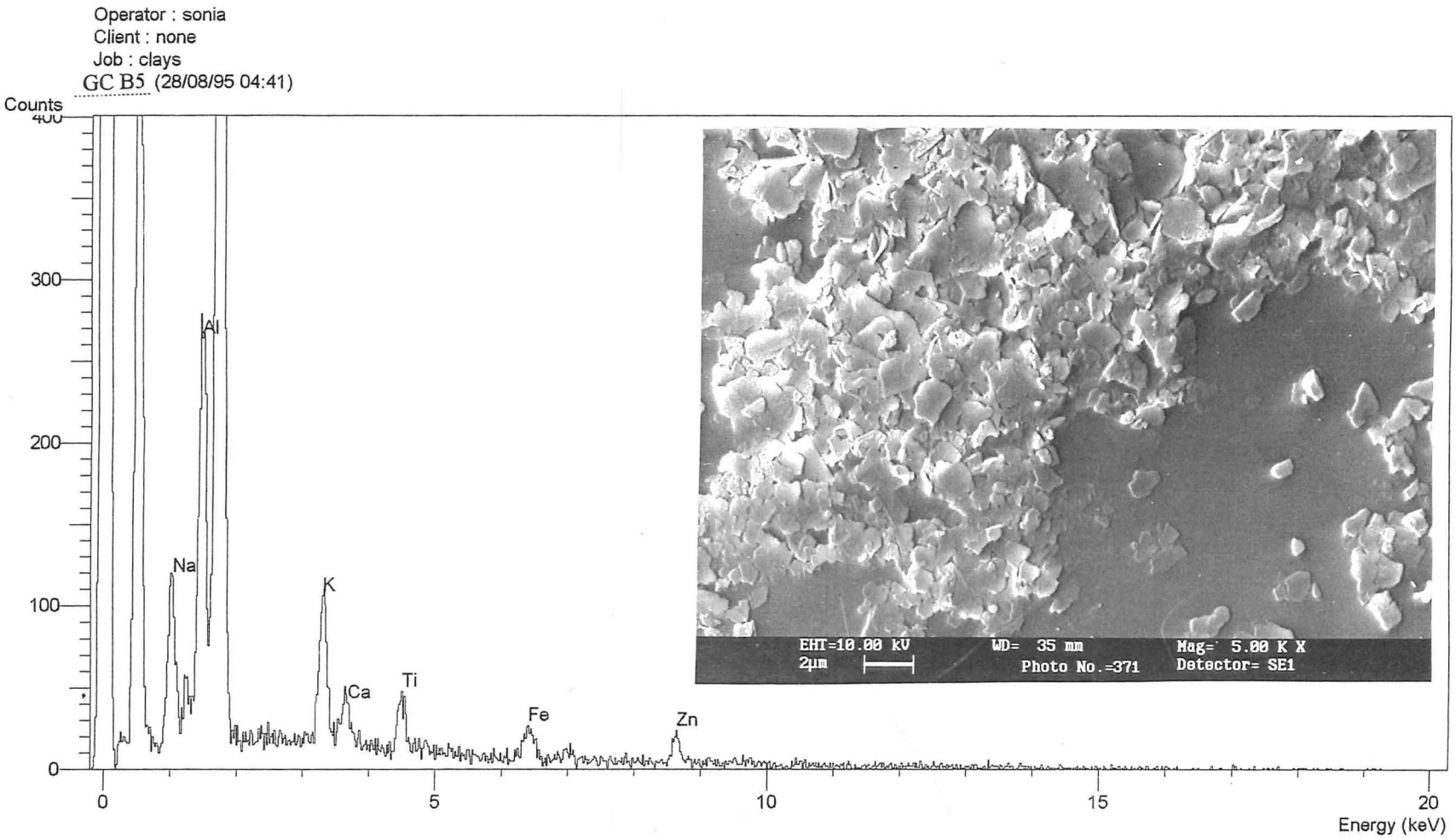
Operator : sonia
Client : none
Job : clays
GC B5 (28/08/95 04:41)
Counts
400
300
200
100
0
Na
Al
K
Ca
Ti
Fe
Zn
0
5
10
15
20
Energy (keV)
EHT=10.00 kV
2µm
WD= 35 mm
Photo No.=371
Mag= 5.00 K X
Detector= SE1

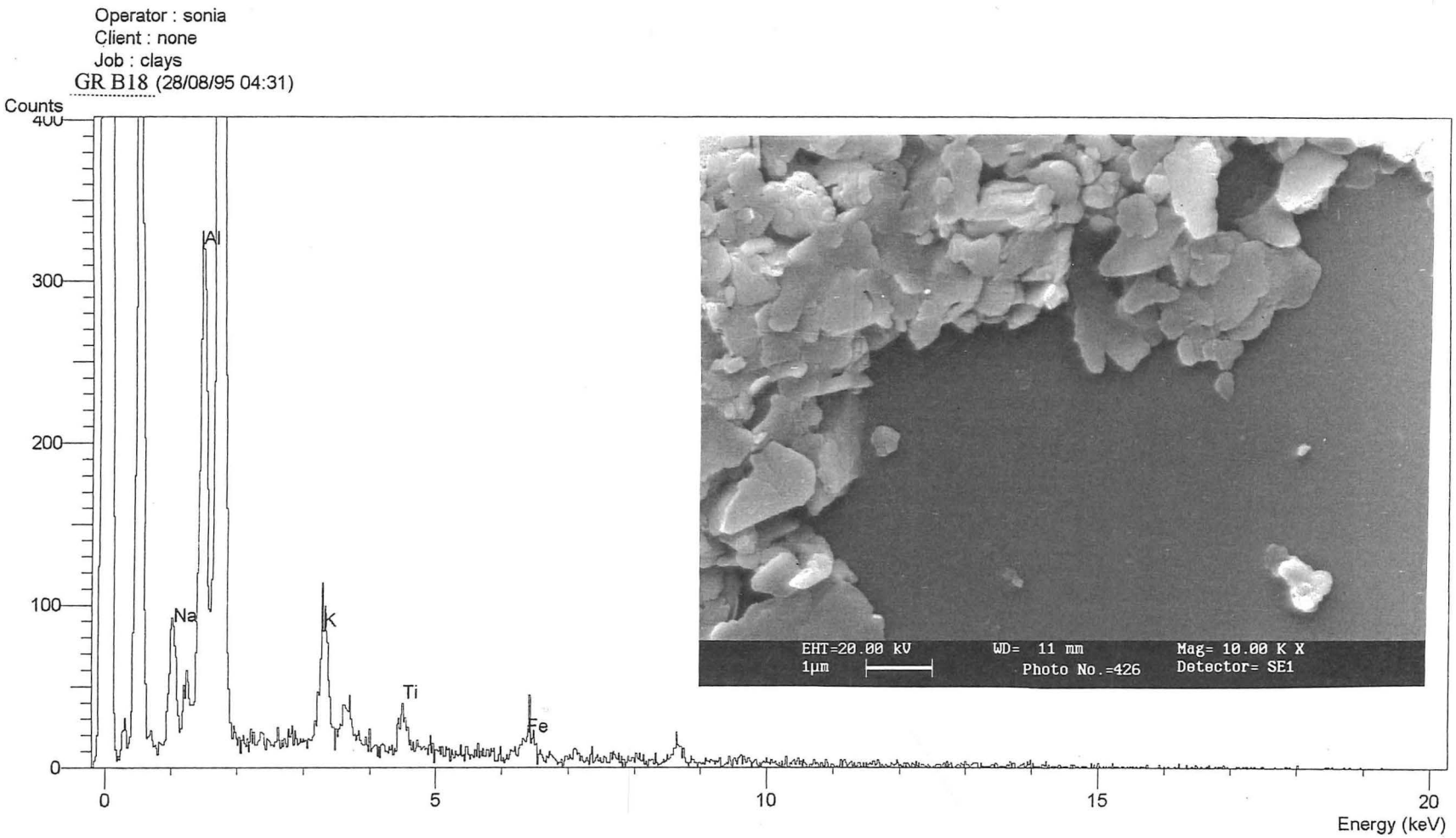
Operator : sonia
Client : none
Job : clays
GR B18 (28/08/95 04:31)
Counts
400
300
200
100
0
Al
Na
K
Ti
Fe
0
5
10
15
20
Energy (keV)
EHT=20.00 kV
WD= 11 mm
Mag= 10.00 K X
1µm
Photo No.=426
Detector= SE1

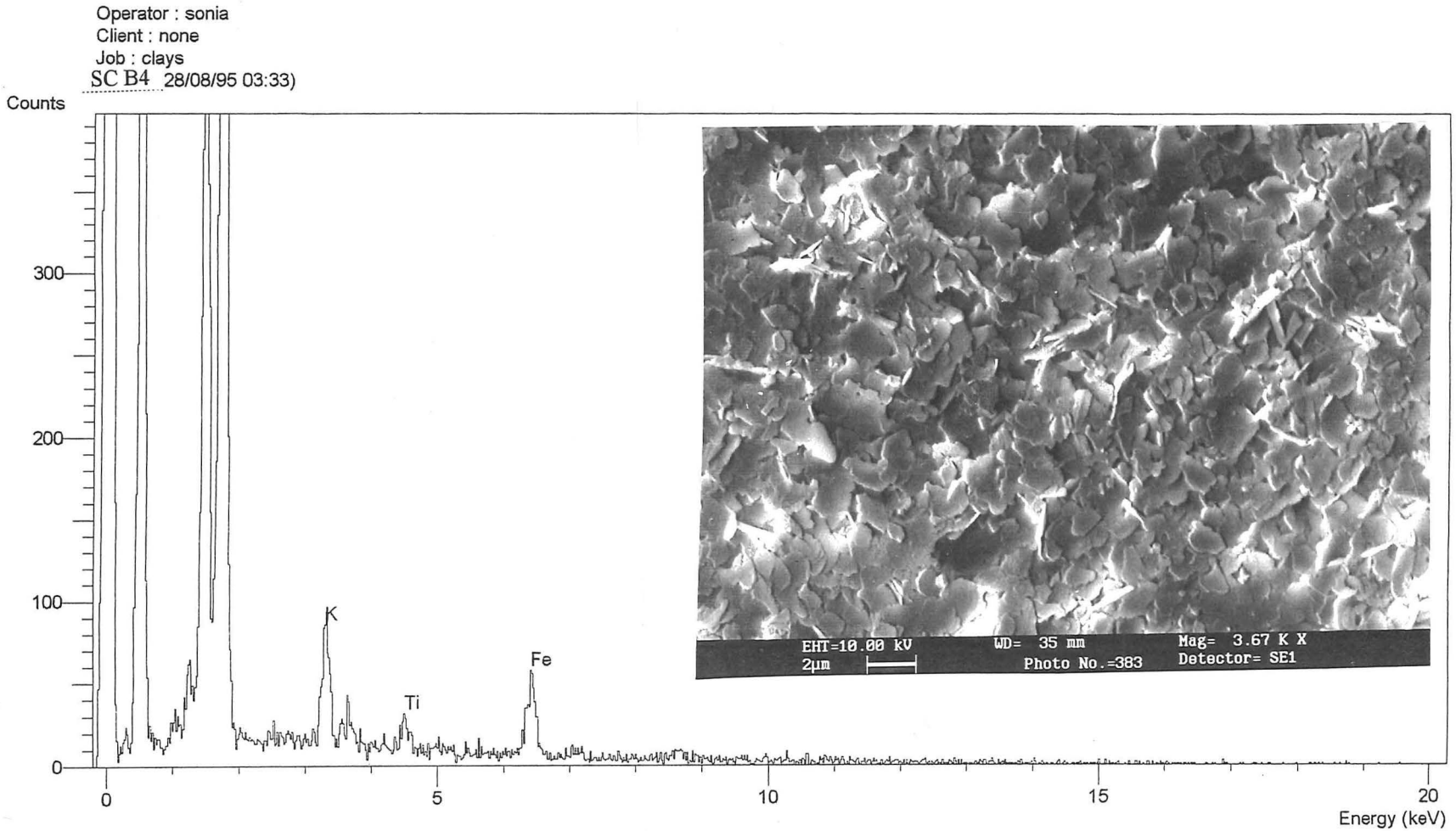
Operator : sonia
Client : none
Job : clays
SC B4 28/08/95 03:33)
Counts
300
200
100
0
K
Ti
Fe
0
5
10
15
20
Energy (keV)
EHT=10.00 kV
WD= 35 mm
Mag= 3.67 K X
2µm
Photo No.=383
Detector= SE1

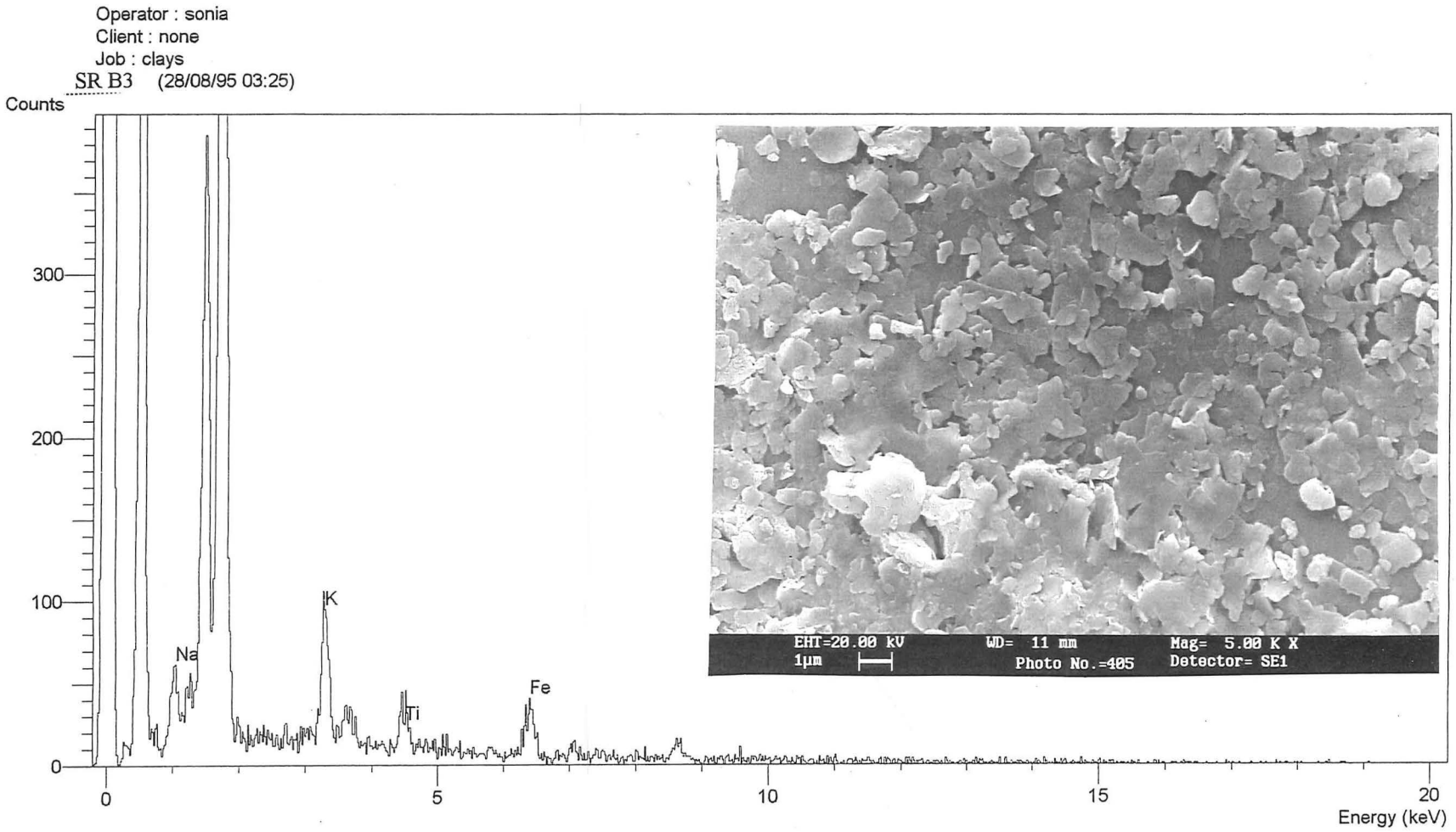
Operator : sonia
Client : none
Job : clays
SR B3 (28/08/95 03:25)
Counts
300
200
100
0
Na
K
Ti
Fe
0
5
10
15
20
Energy (keV)
EHT=20.00 kV
WD= 11 mm
Mag= 5.00 K X
1µm
Photo No.=405
Detector= SE1

APPENDIX D11

RING SHEAR TESTING

The shear strength behavior of a soil is of paramount importance in assessing the stability of a particular soil in the field. The ring shear test requires an annular soil sample of 5mm thickness to be subjected to a rotational shear stress while under the influence of a confining stress normal to the failure plane. The vertical stress represents the depth of burial of the shear plane.

CONSOLIDATION STAGE

The sample chosen is completely remolded and all particles greater than 2mm are removed. Once prepared the sample is pressed into the circular mold of the lower confining ring and leveled off to the top of the ring. The upper confining ring is replaced and the loading yoke is placed on top. The dial gauge is lowered to touch the yoke, and an initial measurement is taken. A vertical force is then applied to the loading arm causing the specimen to undergo consolidation. The weight applied to the loading arm is calculated as follows:

$$\text{Normal Stress} = \frac{(\text{Torque arm mass} = (\text{Hanger mass} \times 10)}{\text{Sample area} \times 1000} \times G \ (kN/m^2)$$

Where: Torque arm mass = 1.143 kg

Sample area = 40.07×10^{-4} m^2

Gravitational constant = G = 9.81 m/s^{-2}

Leverage of the loading arm = 10 times

For this study a hanger mass of 1kg-6kg was applied:

$$\text{Normal stress} = \frac{(1.143 + (1 \times 10)) \times 9.81}{(40.07 \times 10^{-4}) \times 1000} = 27.27 \ kN/m^2$$

Therefore, for soils with a calculated unit weight of 13.0 kN/m^3, and a hanger mass of 1kg, a normal stress of 27.27 kN/m^2 is the equivalent of 2m overburden.

The time taken for the sample to consolidate and the amount of consolidation are recorded to calculate the strain rate.

The graphical results of the ring shear testing in this study are reproduced and discussed in the text (Chapter 5).

WATER CONTENT

All of the soils tested in this study were at water contents slightly above their Plastic Limits.

APPENDIX E

GEOLOGICAL HAZARDS AND DEVELOPMENT CONSTRAINTS

E1 DEFINITIONS OF HAZARD AND RISK

E2 RESOURCE MANAGEMENT ACT 1991

E3 BUILDING ACT 1991

APPENDIX

DEFINITIONS OF HAZARD AND RISK

INTRODUCTION

The purpose of this review is the critically analyse the concepts of 'natural hazard' and 'risk' as expressed in current literature. The concepts of hazard and risk are closely related and often linked such that overlap and confusion of definitions is common. This review attempts to clarify the confusion and synthesise the information presented as applied to natural phenomena.

THE PHILOSOPHY OF NATURAL HAZARDS

The philosophy of designing a definition for natural hazards must be approached from two directions. Firstly, one must be specific in describing hazards dealing with natural phenomena as opposed to human phenomena. Secondly, to define the term hazard, its scope and concepts. However, there are a number of problems inherent in making these definitions and these will be analysed in the following section.

The Oxford Dictionary of Current English (Allen, 1985) defines a hazard as 'a danger or risk - the source of this'. Such a definition is extremely broad and may include industrial, chemical, or biological hazards for example. Therefore for the purposes of this review, hazards must be further categorised as geological or natural hazards.

Bell (1987) states that geological hazards 'all originate either directly from material properties or from some externally generated (ie. geological) processes acting on the local rock or soil materials'. However, Bell neglects to define the term 'geological processes'. Arnould (1976) in his assessment of geological hazards considered meteorological events as separate from geological processes. But even this subdivision is inadequate as Bell (1990) indicates. Storm events, which are inherently a meteorological phenomenon, often induce a series of potentially hazardous geological processes such as landsliding and flooding.

Coates (1981) defines geological hazards a 'a phenomenon associated with geologic processes that can product disaster when a critical threshold is exceeded and can result in significant loss in life or property'. Once again, as with Bell (1987), the term geologic process is not defined. An important item of note in Coates' definition is that a 'critical threshold' must be exceeded by the geologic process before the hazard is recognised. This threshold will vary considerably for each hazard and each locality of concern. Coates goes on to say that a geological hazard 'is distinguished by its short duration'. This is an important notion to consider as certain events, such as landslides, floods and earthquakes may be extremely sudden, however, this is not true

for hazards such as soil creep, coastal erosion and other processes which have a cumulative effect on the environment. Excess rainfall over a long duration increases the hazard potential of landslide-prone slopes and, although the final event may be sudden, the geologic processes causing the landsliding occur over a long period of time. Consequently the concept of hazard uncovers another important factor that natural hazards do not occur independently of one another and they are all intrinsically linked.

The term geological hazard may include a human influence in addition to the natural geological process. Costa and Baker (1981) define a geologic hazard as 'a naturally occurring or man-made geologic condition or phenomenon that presents a risk or potential danger to life and property'. Although natural and 'man-made' hazards may be differentiated, they both may be involved in the development of natural hazards at any given location.

Rahn (1986) states that 'earthquakes, floods etc. are natural phenomena, and as such are not hazards at all'. He goes on to say that they become hazardous only when humans ignore the natural processes and phenomena in operation and develop an area for their own needs. Therefore, it is difficult to separate 'natural' hazards from 'man-made' hazards when a hazard is recognised only when there is a human influence. Tanaka (Rahn, 1986) also recognises this concept; 'an earthquake in the wilderness is a seismic event. When humans clear the land and build by the fault and over the swamp, they have created a seismic hazard. When the earthquake happens and buildings are destroyed and people are killed, a seismic disaster has taken place'.

The Resource Management Act 1991 of New Zealand defines natural hazard as the following:

'Any atmospheric or earth or water related occurrence* the action of which adversely affects or may adversely affect human life, property or other aspects of the environment.

*Earthquakes, tsunami, erosion, volcanism and geothermal activity, landslip, subsidence, sedimentation, wind, drought, fire, or flooding'.

It should be noted that this particular definition neglects the influence of natural leechates and avalanches. The main problem with this legal definition of hazard is that a landslide, for example, may be caused by human intervention either at the foot or headscarp of the area. Therefore, as such, can a hazard event which has been induced by the actions of humans be rightly called a natural hazard under the Resource Management Act 1991?

The definition of hazard must be considered 'in the context of the community which it affects' (Stillwell, 1992). Stillwell also considers a natural hazard to involve 'the potential for damage or loss in the presence of a vulnerable human community ...

and can also be dependent on the organisation and values of society which control the degree to which risk may be reduced'. Therefore, each individual society may consider identical hazardous events with varying degrees of danger or risk.

The notion of hazard potential versus hazard event as introduced by Stillwell (1992) is echoed by IPENZ (1983) which consider a hazard as 'a condition or situation which has the potential to create or increase harm to people, property or the environment'. Such a definition distinguishes between the hazard's potential to cause harm, which may be defined by the occurrence of a previous hazard event. Thus the potential and occurrence of a hazard are intrinsically linked.

Varnes, (1984) defines hazard as 'the probability of occurrence of a potentially damaging phenomenon within a specified time period and area'. Varnes (1984) correctly identifies the need for a return period estimation in a hazard assessment which accounts for the phenomenon occurring within a specified time frame and also the area which is at risk (See following RISK section).

Gardenier (1991) indicates that 'hazard normally refers to the magnitude or the loss or harm'. Therefore, the return period of a particular hazard is dependent on the size and potential damage of that event at a particular time. For example, the formulation of return periods for flooding hazards is based on events of various magnitude ie. 100 year floods versus 10 year floods which are of a lesser magnitude.

THE PHILOSOPHY OF RISK

'RISK: the chance or possibility of loss or bad consequence' (Allen, 1985).

The concept of risk is linked closely to the philosophy behind hazard definition however, there are some aspects of risk which may be defined independently of hazard. A risk cannot be a risk without the influence of a natural hazard. Varnes (1984) illustrates this point by saying that total risk 'is the expected number of lives lost, persons injured, damage to property or the disruption of economic activity due to a particular natural phenomena'. Varnes also introduces the notion of risk as an expected or probable consequence. Gardenier (1991) expands this idea saying ' Risk has a consequence component and a probability component therefore a risk increases with increasing consequence and probability'.

Consequence and probability of risk are important for a definition of risk and are extensively analysed throughout the relevant literature. Gardenier goes on to identify layers of risk which should be considered.

1. The risk or an incident occurring at a source some distance away.
2. The risk of the effect of that incident reaching a certain feature at a certain place.

3. The risk that this would have a negative consequence for that feature.

In Gardenier's definition the relationship between risk probability and risk consequence is stated and the definition relates to the probability of the risk consequence occurring.

Sutherland et.al. (1992) state that 'risk probability is the consequence of an event having an impact on human activity', which again demonstrates the relationship of probability and consequence.

An interesting procedure for the recognition of risk is described in detail by Einstein (1988). He describes risk as 'the product of the hazard times the potential worth of loss where loss includes death or injury, capital losses and non-monetary environmental effects'. Einstein also presents a flow chart which shows the importance of risk determination, and therefore definition in a formal risk assessment procedure (Figure E1.1). The determination of Probabilities at level 3 on the flow diagram (Figure E1.1) comes from a step by step procedure.

1. Prior probabilities, which is the historical and general existing knowledge of dangers and hazards in a given area.
2. Indicators, which may be a surface expression of a particular hazard combined with the likelihood function, which is the reliability of these indicators.
3. Posterior probabilities, which combines both 1. and 2. above.

For Risk Determination (Level 4, Figure E1.1) Einstein observes that a 'particular danger (hazard) can have different consequences' depending on the particular land usage of the area at risk, for example agricultural land versus urban developed land.

In addition, Einstein claims that any area may be subject to risks from a number of different hazards, which have a cumulative effect on the risk probability and consequence for that area. However, Einstein rightly indicates that, for the purposes of land use planning, the concept of risk should be applied to each hazardous process rather than as a whole.

Risk must also be considered relative to the magnitude of a particular hazard. For any hazard, the areas, people and communities potentially at risk will increase with increasing magnitude of an event. Therefore, when producing a risk assessment of an area using Einstein's flow chart method, one must incorporate a specific magnitude at Level 3 (Figure E1.1) which will be recognised within the Risk Determination at Level 4.

Thus, returning to Gardenier's definition of risk, 'Risk increases with an increasing consequence and probability'. Therefore, risk is the 'probability of an event occurring times the magnitude' and similarly, Lowrance (1976) defines risk as 'a measure of the probability and severity of adverse effects'.

Finally, a definition and assessment of risk cannot be complete without recognising that the perception of risk at any particular location and point in time

will vary from individual to individual and community to community. This perception of risk is never static and is merely a function of necessity and immediacy. For any individual or community the risk of a particular hazard being recognised lessens with increasing duration between hazardous events. Therefore, if a major event such as a flood or an earthquake has not caused any substantial damage or loss of life within the life span of one generation, the perceived risk decreases. However, if an event occurs which does cause widespread destruction and disruption to the normal societal pattern, the perceived risk greatly increases for events of smaller magnitude.

DEFINITIONS

NATURAL HAZARD: One or more natural or human induced landscape modification processes* of varying duration, which have potential to cause loss of life, injury, or property/infrastructure damage within or adjacent to, a given human community. Natural hazards have a specified magnitude, return period and affected area.

* Earthquakes, tsunami, erosion, volcanism and geothermal activity, landslip, subsidence, sedimentation, wind, drought, fire, flooding, rock fall, and avalanche.

RISK: The probability of a natural hazard occurring and having a negative consequence on aspects of the environment considered valuable to human communities and/or individuals, relative to the magnitude and return period of the natural hazard event.

APPENDIX E1

DEFINITIONS OF HAZARD AND RISK

HAZARD DEFINITIONS

Coates, 1981	A process or locality that has the potential for producing a disaster.
Costa and Baker, 1981	A naturally occurring, or man made geologic condition or phenomenon that presents a risk or potential danger to life and property.
Einstein, 1988	The probability that a particular danger occurs within a specified period of time.
Gardenier, 1991	Hazard normally refers to the magnitude or the loss or harm.
IPENZ, 1989	A condition or situation which has the potential to create or increase harm to people, property, or the environment.
Resource Management Act, 1991	Any atmospheric or earth or water related occurrence* the action of which adversely affects or may adversely affect human life, property or other aspects of the environment. * Earthquakes, tsunami, erosion, volcanism and geothermal activity, landslip, subsidence, sedimentation, wind, drought, fire or flooding.
Stillwell, 1992	The potential for damage or loss in the presence of a vulnerable human community and can also be dependent on the organisation and values of society which control the degree to which risk may be reduced.

Tanaka, 1981	An earthquake in the wilderness is a seismic event. When humans clear the land and build by the fault and over a swamp, they have created a seismic hazard. When the earthquake happens and buildings are destroyed and people killed, a seismic disaster has taken place.
Varnes, 1984	The probability of occurrence of a potentially damaging phenomenon within a specified time period and area.

RISK DEFINITIONS

Einstein, 1988	The product of the hazard, time potential worth of loss, where loss includes death or injury, capital losses, and non-monetary environmental effects.
Gardenier, 1991	Risk has a consequence component and a probability component, therefore a risk increases with increasing consequence and probability.
Gardenier and Keey, 1992	The probability of a specified hazard, loss or detrimental outcome happening within a defined period of time.
IPENZ, 1983	The probability that a potential hazard will be realised and the probability of the harm itself.
Sutherland et al, 1992	Risk probability is the consequence of an event having an impact on human activity.

APPENDIX E2

THE RESOURCE MANAGEMENT ACT

Introduction

The Resource Management Act (RMA) was introduced in 1991 and effectively replaced the Town and Country Planning Act (1977). The RMA is primarily concerned with the management of environmental resources, both natural and physical (Bell et al, 1992). Furthermore, the RMA makes Council's responsible for the effects which management policies may have on the environment. With respect to natural processes, development options may be restricted due to the hazard imposed by the process on any potential development. For this reason, the approach advocated by this study is to identify the natural hazards affecting the area prior to any development proposals.

The Functions of Local Authorities

Under Section 30 and 31 of the RMA, the functions powers and duties of the local authorities are expressed. With respect to natural hazards, those functions are as follows:

30 (1) a) The establishment, implementation and review of objectives, policies and methods to achieve integrated management of the natural and physical resources of the region.

b) Preparation of policies in relation to any actual or potential effects of the use, development, or protection of land which are of regional significance.

c) The control of the use of land for the purpose of:

i) Soil conservation

ii)The maintenance and enhancement of the quality of water in water bodies and coastal water.

iv) The avoidance or mitigation of natural hazards.

d) In respect of any coastal marine area in the region, the control (in conjunction with the minister of Conservation) of

v) Any actual or potential effects of the use, development, or protection of land, including the avoidance or mitigation of natural hazards and the prevention or mitigation of any adverse effects of the storage, use, disposal, or transportation of hazardous substances.

Section 31. Every territorial authority shall have the following functions for the purpose of giving effect to this Act in its district:

b) The control of any actual or potential effects of the use, implementation of rules for the avoidance or mitigation of natural hazards and the prevention and mitigation of any adverse effects of the storage, use, disposal, or transportation of hazardous substances.

Hazard Information Register

Additionally, the RMA requires that the local authorities identify and collate information relating to areas prone to hazardous processes under Section 35.

Section 35. Duty to gather information, monitor and keep records -

1) Every local authority shall gather such information, and undertake or commission such research, as is necessary to carry out effectively its functions under this Act.

2) Every local authority shall monitor:

a) The state of the whole or any part of the environment of its region or district to the extent that is appropriate to enable the local authority to effectively carry out it functions under this Act;

b) The suitability and effectiveness of any policy statement or plan for its region or district;

d) The exercise of the resource consents that have effect in its region or district, as the case may be, and take appropriate action...where this is shown to be necessary.

3) Every local authority shall keep reasonably available at its principal office, information which is relevant to the administration of policy statements and plans, the monitoring of resource consents, and current issues relating to the environment of the area the enable the public -

a)To be better informed of their duties and of the functions, powers, and duties of the local authority.

5) The information to be kept by a local authority under subsection 3) shall include:

j) Records of natural hazards to the extent that the local authority considers appropriate for the effective discharge of its functions.

Regional and District Plans

The preparation of Regional and District plans must be considered where the conditions outlined under Section 65 and Section 76 of the RMA.

Section 65 3) Without limiting the power of a regional council to prepare a regional plan at any time, a regional council shall consider the desirability of preparing a regional plan whenever any of the following circumstances or considerations arise or are likely to arise:

a) Any significant conflict between the use, development , or protection of natural and physical resources or the avoidance or mitigation of such conflict.

b)Any significant need or demand for the protection of natural and physical resources or of any site, feature, place or area of regional significance.

c) Any threat from natural hazards or any actual or potential effects of the storage, use, disposal, or transportation of hazardous substances which may be avoided or mitigated.

d)Any foreseeable demand for or on natural and physical resources.

f) The restoration or enhancement of any natural and physical resources in a deteriorated state or the avoidance or mitigation of any such deterioration.

h) Any use of land or water that has actual or potential adverse effects on soil conservation or air quality or water quality.

Section 76 3) In making a rule, the territorial authority shall have regard to the actual or potential effect on the environment of activities including, in particular, any adverse effect; and rules may

accordingly specify permitted activities, controlled activities, discretionary activities, non-complying activities, and prohibited activities.

Resource Consents

The RMA deals with the identification, control and mitigation of natural hazards when issuing resource consents. Resource consents include Land Use consents, subdivision consents, coastal permits, water permits and discharge permits. Section 88 outlines the requirements for making an application for a resource consent.

Section 88 (4) An application for a resource consent shall be in the prescribed form and shall include:

b) An assessment of any actual or potential effects that the activity may have on the environment, and the ways in which any adverse effects may be mitigated.

Subdivision consents are dealt with separately in the RMA and include strict regulations concerning natural hazards.

Section 106: Subdivision consent not to be granted in certain circumstances

1) A consent authority shall not grant a subdivision consent if it considers that either:

a) Any land in respect of which a consent is sought, or any structure on that land, is or is likely to be subject to material damage by erosion, falling debris, subsidence, slippage or inundation from any source; or

b) Any subsequent use that is likely to be made of the land is likely to accelerate, worsen, or result in material damage to that land, other land, or structure, by erosion, falling debris, subsidence, slippage or inundation from any source -

unless the consent authority is satisfied that sufficient provision has been made or will be made in accordance with subsection 2)

2) A consent authority may grant a subdivision consent if it is satisfied that the effects described in subsection 1) will be avoided, remedied, or mitigated by one or more of the following:

a) Rules in the district plan

b) Conditions of a resource consent...

c) Other matters, including works.

As with the preceding legislation, there are no statutory requirements under the RMA for geotechnical or engineering geological investigations in relation to natural hazards and resource consents. Any such information is provided at the discretion of each council or regional authority.

APPENDIX E3

THE BUILDING ACT

Introduction

The Building Act, also introduced in 1991, is seen to compliment the RMA at the scale of building construction. Therefore the requirements of the Building Act, with regard to the environment and natural hazards, are similar to those of the RMA.

Building Consents

The most important information in the Building Act for land use planning purposes is that contained in Section 36; limitations and restrictions on Building Consents.

36(1) [Building consent refused]

Except as provided for in subsection (2) of this section, a territorial authority shall refuse to grant a building consent involving construction of a building or major alterations to a building if -

a) The land on which the building work is to take place is subject to, or is likely to be subject to, erosion, avulsion, alluvion, falling debris, subsidence, inundation or slippage, or

b) The building work itself is likely to accelerate, worsen, or result in erosion, avulsion, alluvion, falling debris, subsidence, inundation, or slippage of that land or any other property -

Unless the territorial authority is satisfied that adequate provision has been or will be made to -

c) Protect the land or building work or that other property concerned from erosion, avulsion, alluvion, falling debris, subsidence, inundation, or slippage; or

d) Restore any damage to the land or that other property concerned as a result of the building work.

36 (2) [Where building work will not worsen erosion]

Where a building consent is applied for and the territorial authority considers that -

a) The building work itself will not accelerate, worsen, or result in erosion, avulsion, alluvion, falling debris, subsidence, inundation, or slippage of that land or any other property; but

b) The land on which the building work is to take place is subject to, or is likely to be subject to, erosion, avulsion, alluvion, falling debris, subsidence, inundation or slippage.

Project Information Memoranda

The project information memoranda (PIM) required in the Building Act parallels the hazard register as required by the RMA Section 35.

Section 30 (1) [Application]

An owner who is contemplating undertaking any building work for which a building consent is required may, without applying for a building consent under section 33 of this Act, apply to the territorial authority for a project information memorandum in respect of the work.

Section 31 (1) [Contents]

Every project information memorandum shall include -

a) Information identifying each (if any) special feature of the land concerned, including (but not limited to) potential erosion, avulsion, falling debris, subsidence, slippage, alluvion, or inundation, or the likely presence of hazardous contaminants, being a feature or characteristic that -

i) Is likely to be relevant to the design and construction or alteration of the building or proposed building.

APPENDIX F

SAMPLE LOCATIONS

APPENDIX F.

SAMPLE LOCATIONS			
SAMPLE NUMBER	GRID LOCATION	SAMPLE TYPE	LOCATION
WH 1	P27 2599845 589335	Colluvium, mixed greywacke and schist	Port Underwood Road, Waikawa
WH 2	P27 259945 589340	Greywacke regolith	Forestry track, Whatamango Bay
S 2	P27 259950 589370	Greywacke bedrock joint surface	Forestry track, Whatamango Bay
WH 3	P27 259955 589380	Greywacke Colluvium	Forestry track, Whatamango Bay
WH 4	P27 259935 589375	Greywacke Regolith	Forestry track, Whatamango Bay
WH 5	P27 259835 589315	Schistose Colluvium	Port Underwood Road, Waikawa
WH 6	P27 259895 599350	Greywacke Regolith	Sunshine Heights
WH 7	P27 269925 599350	Pink schistose mudstone	Ridge tops
WH 8	P27 260035 599260	Debris Slide material	Graham River flood plane
WH 9	P27 260050 599260	Older Debris Fan	Graham River flood plane
WH 10	P27260010 599200	Post glacial weathered loess	Graham River aggradation terrace
WH 11	P27 259975 599350	Buried soil in colluvium	Whatamango Bay, western side
WH 12	P27 259975 599350	Faulted organic rich horizon	Whatamango Bay, western side
	P27		
	P27		
WH 15	P27260130 599500	Quartz Vein material	Green Bay
WH 16	P27 260115 599510	Iron stained sedimentary structures	Green Bay
WH 17	P27 0004 9204	Charred Wood sample	Graham River degradation terrace, 400 mm from top
WH 18	P27 0004 9204	Charcoal horizon	Graham River degradation Terrace, 900 mm from top
B1	P27 0031 9237	Red Weathered Regolith	Port Underwood Road, Whatamango Bay
B2	P27 0031 9237	Red Weathered Regolith	Port Underwood Road, Whatamango Bay
GWIV	P27 9986 9256	Greywacke Weathering Grade IV	Whatamango Bay
T1 A	P27 9955 9336	35mm Schistose Regolith	Forestry Track, Whatamango
T1 B	P27 9955 9336	35mm Schistose Regolith	Forestry Track, Whatamango
T1 C	P27 9955 9336	100mm Schistose Regolith	Forestry Track, Whatamango
T1 D	P27 9955 9336	35mm Schistose Regolith	Waipuna Lodge
B3	P27 9955 9336	Schistose Regolith	Forestry Track, Whatamango
T2 A	P27 9967 9327	35mm Schistose Colluvium	Forestry Track, Whatamango
T2 B	P27 9967 9327	35mm Schistose Colluvium	Forestry Track, Whatamango
T2 C	P27 9967 9327	35mm Schistose Colluvium	Wharetukura Bay
B4	P27 9967 9327	Schistose Colluvium	Forestry Track, Whatamango
GWIII	P27 9986 9256	Greywacke, Weathering Grade III	Whatamango Bay
B5	P27 9986 9256	Greywacke Colluvium	Whatamango Bay
B6	P27 9986 9256	Greywacke Colluvium	Whatamango Bay
T3 A	P27 9986 9256	Greywacke Colluvium	Whatamango Bay
T3 B	P27 9986 9256	Greywacke Colluvium	Whatamango Bay
T3 C	P27 9986 9256	Greywacke Colluvium	Whatamango Bay

GWII	P27 9986 9256	Greywacke Weathering Grade II	Whatamango Bay
B7	P27 9986 9256	Greywacke Colluvium	Whatamango Bay
B8	P27 0028 9217	Red weathering regolith	Forestry Track east of Graham River
B9	P27 0028 9217	Red weathering regolith	Forestry Track east of Graham River
B10	P27 9945 9380	Schistose Colluvium	East of Karaka Point
B11	P27 9945 9380	Schistose Colluvium	East of Karaka Point
B12	P27 9975 9345	Schistose Regolith	Waipuna Lodge
B13	P27 9975 9345	Schistose Regolith	Waipuna Lodge
B14	P27 9839 9328	Schistose Colluvium	115-119 Wharetukura Bay
B15	P27 9839 9328	Schistose Regolith	Wharetukura Bay
B16	P27 9839 9328	Schistose Regolith	Wharetukura Bay
B17	P27 9835 9314	Schistose Colluvium	Wharetukura Bay
T4 A	P27 9817 9320	35mm Greywacke Regolith	Wharetukura Bay
T4 B	P27 9817 9320	35mm Greywacke Regolith	Wharetukura Bay
T4 C	P27 9817 9320	35mm Greywacke Regolith	Wharetukura Bay
B18	P27 9817 9320	Greywacke Regolith	Wharetukura Bay
B19	P27 9817 9320	Greywacke Regolith	Wharetukura Bay
B20	P27 9814 9320	Greywacke Colluvium	Wharetukura Bay
B21	P27 9785 9305	Greywacke Colluvium	Jeffcot Subdivision
B22	P27 9785 9305	Greywacke Regolith	Jeffcot Subdivision
SWGIV	P27 9889 9365	Schist Weathering Grade IV	Sunshine Bay
SWGIII	P27 9889 9365	Schist Weathering Grade III	Sunshine Bay
SWGII	P27 9933 9387	Schist Weathering Grade II	Near Karaka Point
B23	P27 9975 9345	Schistose Regolith	Waipuna Lodge